GEORGIA INSTITUTE OF TECHNOLOGY
OFFICE OF CONTRACT ADMINISTRATION
SPONSORED PROJECT INITIATION

Date: 11/26/79

Project Title: Parametric Investigation of Randome Analysis Methods

Project No: E-21-605 and B-494-004 (Co-projects) (Continuation of E-21-612/E-21-636 and B-494-000/001/002/003)

Co-Project Director: Dr. Gene K. Huddleston and Mr. Harold L. Bassett

Sponsor: Air Force Office of Scientific Research

Agreement Period: From 9/30/79 Until 9/29/80 (Grant Period)

Type Agreement: Grant No. AFOSR-77-3469, Amendment "B"

Amount:	EE	RAIL/MAD	TOTAL
	AFOSR $30,510 (E-21-605)	$28,727 (B-494-004)	$59,237
	GIT 2,197 (E-21-350)	2,368 (E-702-400)	4,565
	TOTAL $32,707	$31,095	$63,802

Reports Required: Annual Technical Report
Final Technical Report

Sponsor Contact Person (s):

Technical Matters

William J. Best
Program Manager
AFOSR (NP)
Bolling AFB, DC 20332

Contractual Matters
(thru OCA)

Jeffrey P. Parsons
Buyer
AFOSR (PKZ)
Bolling AFB, DC 20332
202/767-4959

R.K. Gillispie
Contracting Officer

Defense Priority Rating:

Assigned to: Electrical Engineering and Radar & Instrumentation Laboratory/MAD

COPIES TO:

- Project Director
- Division Chief (EES)
- School/Laboratory Director
- Dean/Director–EES
- Accounting Office
- Procurement Office
- Security Coordinator (OCA)
- Reports Coordinator (OCA)
- Library, Technical Reports Section
- EES Information Office
- EES Reports & Procedures
- Project File (OCA)
- Project Code (GTRI)
- Other Mr. H.L. Bassett/RAIL/MAD
  Dr. E.K. Reedy/RAIL

GEORGIA INSTITUTE OF TECHNOLOGY
OFFICE OF CONTRACT ADMINISTRATION

SPONSORED PROJECT TERMINATION

Date: May 4, 1981

Project Title: Parametric Investigation of Randome Analysis Methods

Project No: E-21-605 and B-494-004 (Co-projects) (Continuation of E-21-612/E-21-636 and B-494-000/001/002/003)

Project Director: Dr. Gene K. Huddleston and Mr. Harold L. Bassett

Sponsor: Air Force Office of Scientific Research

Effective Termination Date: 12/31/80

Clearance of Accounting Charges: 12/31/80

Grant/Contract Closeout Actions Remaining:

- X Final Invoice and Closing Documents
- X Final Fiscal Report
- X Final Report of Inventions
- X Govt. Property Inventory & Related Certificate
- _ Classified Material Certificate
- _ Other _____

Assigned to: EE and RAIL (School/Laboratory)

COPIES TO:

Administrative Coordinator
Research Property Management
Accounting Office
Procurement Office/EES Supply Services
Research Security Services
Reports Coordinator (OCA)

Legal Services (OCA)
Library, Technical Reports
EES Research Public Relations (2)
Project File (OCA)
Other: _____

SECURITY CLASSIFICATION OF THIS PAGE *(When Data Entered)*

REPORT DOCUMENTATION PAGE

READ INSTRUCTIONS BEFORE COMPLETING FORM

1. REPORT NUMBER	2. GOVT ACCESSION NO. / 3. RECIPIENT'S CATALOG NUMBER
4. TITLE *(and Subtitle)* Parametric Investigation of Radome Analysis Methods	5. TYPE OF REPORT & PERIOD COVERED Annual Technical Report October 1, 1977 to Sept. 30, 1978 6. PERFORMING ORG. REPORT NUMBER
7. AUTHOR(s) G. K. Huddleston, H. L. Bassett, and J. N. Newton	8. CONTRACT OR GRANT NUMBER(s) AFOSR-77-3469
9. PERFORMING ORGANIZATION NAME AND ADDRESS Georgia Institute of Technoloby School of Electrical Engineering Atlanta, Georgia 30332	10. PROGRAM ELEMENT, PROJECT, TASK AREA & WORK UNIT NUMBERS
11. CONTROLLING OFFICE NAME AND ADDRESS Air Force Office of Scientific Research Directorate of Physics (Code NP-77-148) Bolling Air Force Base, D.C. 20332	12. REPORT DATE November 30, 1978 13. NUMBER OF PAGES 40
14. MONITORING AGENCY NAME & ADDRESS*(if different from Controlling Office)*	15. SECURITY CLASS. *(of this report)* Unclassified 15a. DECLASSIFICATION/DOWNGRADING SCHEDULE

16. DISTRIBUTION STATEMENT *(of this Report)*

17. DISTRIBUTION STATEMENT *(of the abstract entered in Block 20, if different from Report)*

18. SUPPLEMENTARY NOTES

19. KEY WORDS *(Continue on reverse side if necessary and identify by block number)*

Radome Analysis
Millimeter Wave Radomes

20. ABSTRACT *(Continue on reverse side if necessary and identify by block number)*

The status is described of a research program whose objective is to determine the accuracies of various methods of radome analysis as functions of antenna size and placement, radome size and shape, and wavelength. The analytical methods used and the experimental program to establish true data are described concisely.

DD FORM 1 JAN 73 1473 EDITION OF 1 NOV 65 IS OBSOLETE

SECURITY CLASSIFICATION OF THIS PAGE *(When Data Entered)*

PARAMETRIC INVESTIGATION

OF

RADOME ANALYSIS METHODS

by

G. K. Huddleston, H. L. Bassett, and J. N. Newton

for

Air Force Office of Scientific Research
Bolling Air Force Base, D.C. 20332

Under

Grant AFOSR-77-3469
October 1, 1977 - September 30, 1978

School of Electrical Engineering
and
Engineering Experiment Station

Georgia Institute of Technology
Atlanta, Georgia 30332

November 1978

TABLE OF CONTENTS

LIST OF ILLUSTRATIONS

LIST OF TABLES

PARAMETRIC INVESTIGATION OF RADOME ANALYSIS METHODS

I. Introduction and Summary

The overall objective of this research is to develop a general theory of radome analysis and to determine the accuracies of various radome analysis methods under controlled conditions of antenna size and placement, wavelength, and radome size and shape. Experimental measurements on selected antenna/radome combinations at 35 GHz will be used as true data in the assessment of accuracy.

During the first year, which this report covers, a general theory of analysis has been developed based on the Lorentz reciprocity theorem and on the Huygens-Fresnel principle. Computer-aided methods of analysis based on these principles have been formulated and programmed. Three monopulse antennas have been designed and fabricated for use in carrying out the measurements at 35 GHz. Three radomes have been designed and fabricated for use in the experimental program. A mechanical fixture has been fabricated which will allow accurate positioning of the antenna with respect to the radome and with respect to the reference system used for pattern measurements. A detailed discussion of the progress in the first year is presented in Section II below.

During the second year, the initiation efforts of the first year's work will come to fruition through concentrated experimental and analytical efforts to gather true and calculated data which will serve as the basis for realizing the overall research objective. Extensive pattern measurements will be made for nine of the fifteen antenna/radome combinations

available. These experimental efforts will be paralleled by computer-aided analyses of the same combinations for comparison purposes. In addition, techniques to account for the effects of metal tips will be incorporated into the analysis methods for use during the third and final phase of the research.

In the third year, it is anticipated that measurements will be carried out on radomes to which metal tips have been added, and comparisons to theoretical predictions will be made. In addition, antenna/radome configurations which lend themselves to exact analysis using boundary-valued approaches and variational and relaxation techniques will be investigated.

Two publications and three presentations concerning this research have resulted. They are described in Section III along with papers planned for submission to technical journals.

The professional personnel associated with the research effort are listed in Section IV.

Appendix A contains copies of the two papers presented at symposia.

II. Progress to Date

Efforts during the first year's work have been devoted to developing the general theory of radome analysis, formulating the radome analysis methods, implementing the methods in digital computer software, designing and building three monopulse antennas, designing five suitable radomes, and designing and fabricating a test fixture for positioning the antenna/radome combinations in the measurement environment. These efforts have

been carried out to prepare for the extensive measurements and analytical efforts planned for Phase II.

The general theory of radome analysis is based on the Lorentz reciprocity theorem [1] and the Huygens-Fresnel principle [2] as described in the papers included in Appendix A. Briefly, the reciprocity theorem serves as the basis for all receiving formulations of radome analysis; i.e., the response of the antenna inside the radome to a plane wave incident on the radome is the desired analysis objective. The Huygens-Fresnel principle serves as the basis for all rigorous transmitting formulations; i.e., the Fraunhofer fields are determined for the case when the radome-enclosed antenna is radiating by performing integrations of the tangential electric and magnetic fields over a surface which encloses the sources. Since a homogeneous medium is required by the theory in the region not containing the sources, the radome must also be enclosed by the surface. The third facet of the general theory makes use again of the reciprocity theorem for widely separated antennas to provide the unifying connection between the response of an antenna to a plane wave of specified polarization and direction of arrival and the vector far fields of the antenna.

Analytical efforts thus far have concentrated on formulating and implementing both receiving and transmitting formulations which require integration of the fields over the outer surface of the radome. Upon examination of the role of the field scattered by the radome when a plane wave is incident, it has been established that the scattered field contributes nothing to the antenna response and, therefore, can be neglected in the computations. The equivalence of the transmitting and receiving

formulations has also been rigorously established for the first time, the import of which is that intermediate calculations of the vector far field as required in the transmitting case can be avoided in many cases of practical importance.

Attention has also been directed toward sampling of the electromagnetic fields on the surface of the radome as required in the surface integrations. Two methods have been considered. In the first, the radome surface is partitioned into elemental areas by dividing the axis of symmetry (z_R-axis) into equal linear increments; in the circumferential direction, equal angular segments are used. In the second method, equal angular increments are used in the longitudinal (θ) direction so that the length of the elemental area is the same regardless of location on the surface. Angular increments are also used in the circumferential (ϕ) direction and are adjusted so that at the center of the elemental area, the arc distance is approximately constant. In both methods, the field values are computed at the center of each elemental area.

The surface integration method has been implemented in computer software (Fortran IV) and is currently being tested for accuracy and speed of computation. A simple method has been devised to do this as follows. A tangent ogive radome shape having zero wall thickness represents the surface of integration. The tangential components of a source field $\underline{E}_s$, $\underline{H}_s$ are specified over the circular region or aperture at the base of the radome. A plane wave relationship is assumed between $\underline{E}_s$ and $\underline{H}_s$, where the direction of propagation is normal to the circular region; i.e., parallel to the axis of symmetry of the radome. A plane wave having specified polarization and direction of arrival is assumed

incident on the circular aperture and, simultaneously, on the tangent ogive surface. The reaction integral [2] is proportional to the voltage received by the circular aperture antenna and is easily computed for the circular aperture to yield an exact result. The computation of the same received voltage is carried out using the computer-aided techniques for various tangent ogive surfaces.

Table I shows some salient results obtained with the computer-aided surface integration method. Five radome shapes (sizes) as explained below were used. The results shown were obtained using the second method of sampling described above. Sample distances (equal in θ and ϕ) of $\lambda/6$ to λ were used, where λ is the free space wavelength. The total number of samples depends on the sample increment and radome size as shown in column four of the table. Comparison of the true and computed values of received voltage shows excellent agreement. Examination of the entries in the last column of Table I shows the dramatic influence of the number of samples on computation time.

It can be concluded at this point that the surface integration may be practical for small radomes but perhaps not so practical for larger radomes, assuming that a fixed sample size which yields consistently accurate results can be established. But this trend is neither unexpected nor catatrophic from a practical standpoint. It is expected that the other computational methods under investigation will yield acceptably accurate results for large radomes and will require much less computation time; in fact, the larger the radome and antenna, the more accurate will be the computed result. The question addressed by this research concerns, of course, the establishment of the ranges of validities of these various

Table I. Accuracy and Computation Time for Surface Integration Method

Radome ID				Received Voltage		
Diameter (λ)	Length (λ)	Sample Size	Number of Samples	True	Computed	Computation Time (sec)
20.49	19.93	λ/6	35157	-1.28355	-1.28355	61.11
20.49	19.93	λ/3	8718	-1.28355	-1.28362	13.05
20.49	19.93	λ/2	3869	-1.28355	-1.28373	7.00
20.49	19.93	λ	967	-1.28355	-1.28431	1.64
11.86	22.30	λ/6	20716	-0.43011	-0.43011	31.68
11.86	22.30	λ/3	5167	-0.43011	-0.43013	7.95
11.86	22.30	λ/2	2262	-0.43011	-0.43017	4.05
11.86	22.30	λ	571	-0.43011	-0.43037	.86
11.86	16.78	λ/6	15929	-0.43011	-0.43011	24.68
11.86	16.78	λ/3	3973	-0.43011	-0.43015	6.77
11.86	16.78	λ/2	1769	-0.43011	-0.43021	2.59
11.86	16.78	λ	442	-0.43011	-0.43054	.82
11.86	11.30	λ/6	11554	-0.43011	-0.43012	19.69
11.86	11.30	λ/3	2846	-0.43011	-0.43019	5.31
11.86	11.30	λ/2	1265	-0.43011	-0.43031	2.31
11.86	11.30	λ	319	-0.43011	-0.43092	.61
7.56	6.97	λ/6	4560	-0.17480	-0.17482	7.11
7.56	6.97	λ/3	1115	-0.17480	-0.17489	2.37
7.56	6.97	λ/2	498	-0.17480	-0.17502	1.06
7.56	6.97	λ	127	-0.17480	-0.17567	.25

methods.

One of the speedier radome analysis methods under investigation uses a receiving formulation as described earlier [3]. The method is illustrated in Figure 1. The plane wave $\underline{E}_i$, $\underline{H}_i$ is incident on the radome with direction of arrival $\hat{k}_a$. A ray is traced backwards from each aperture point (x,y,o) in the direction $\hat{k}_a$ to find the intersection with the radome wall and the unit normal vector $\hat{\eta}_R$ at the intersection point. From $\hat{k}_a$, $\hat{\eta}_R$, and $\underline{E}'_i$, the field $\underline{E}'_R$ produced on the antenna aperture can be found, where the components of $\underline{E}_i$ parallel and perpendicular to the plane of incidence are properly weighted by the complex transmission coefficients $T_\perp$, $T_{\parallel}$ as illustrated in Figure 2.

The transmission coefficients used are those which apply to an infinite plane dielectric sheet [4]. This approximate method of transforming the fields on one side of the radome wall to the other side appears to be a common feature of all radome analysis methods except that described by Van Doeren [5]. Use of this method precludes the computation of surface (trapped) wave effects and may represent the single most significant deficiency in all of these methods.

Another computationally fast method under investigation utilizes a transmitting formulation and makes extensive use of the Fast Fourier Transform (FFT) to enhance the computational speed [6]. Briefly, the radiation from the antenna is characterized by using the plane wave spectrum (PWS) representation (a modal expansion) [7]. The antenna aperture is sampled at an array of equally spaced points in x and y. From each point in the aperture there emanates a spectrum of plane waves, obtained very simply as the (inverse) FFT of the tangential electric

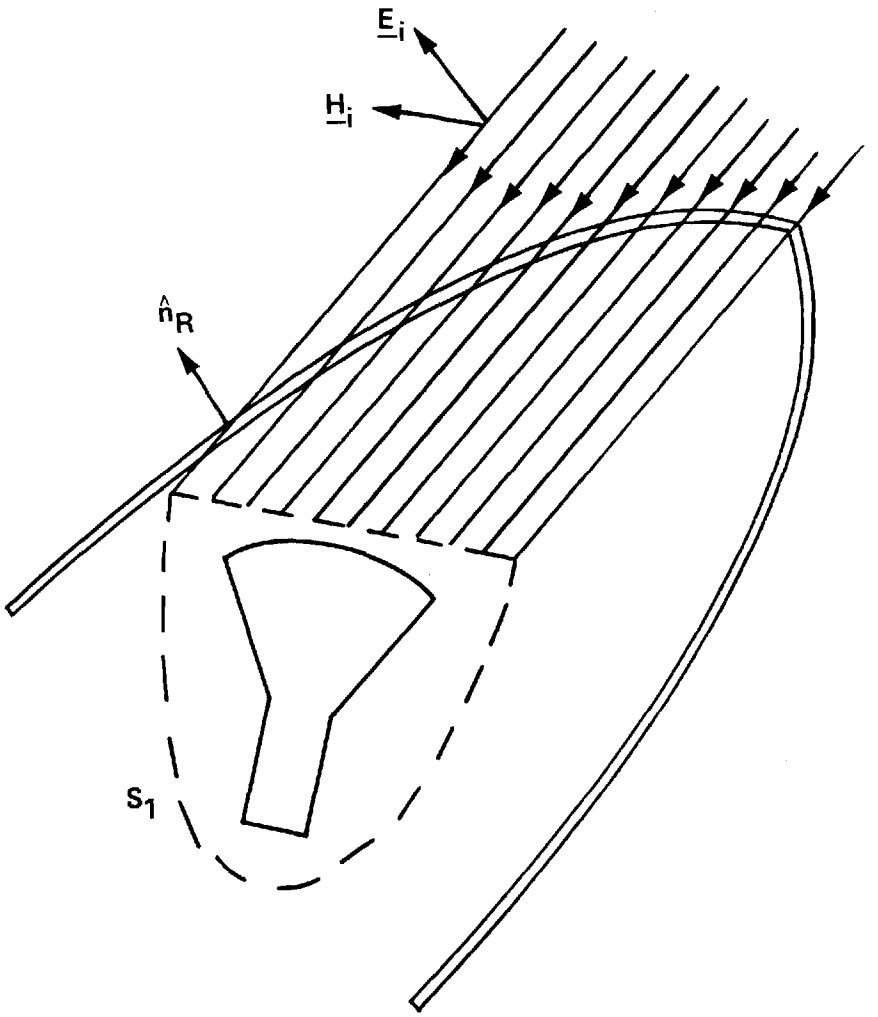

Figure 1. Illustration of the Fast Receiving Method of Radome Analysis

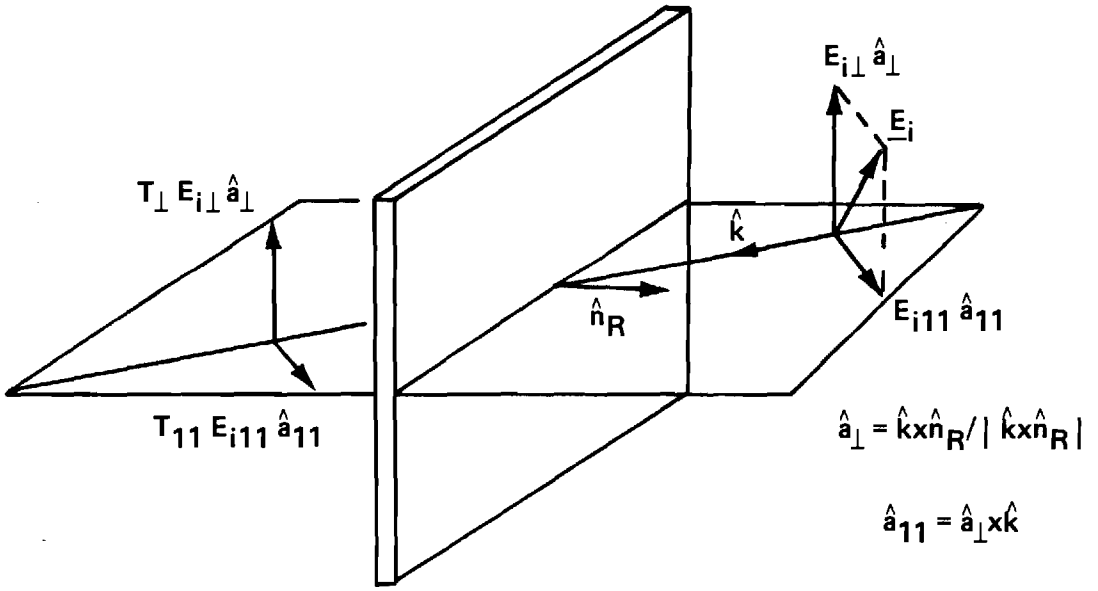

Figure 2. Plane Wave Propagation Through an Infinite Plane Sheet

field in the aperture. Rays are traced to each point to find their intersections with the inside surface of the radome. The plane wave field $\underline{e}$, $\underline{h}$ associated with each ray is weighted by the transmission coefficients $T_{\perp}$, T_{11} as depicted in Figure 2. The modified plane wave $\underline{e}'$, $\underline{h}'$ is then included in the summation of all such contributions to produce modified aperture fields $\underline{E}_s'$, $\underline{H}_s'$ at the specified point. The procedure is repeated for each aperture point, resulting in a modified aperture field which is assumed to correctly embody the effects of the radome. Further computations are then performed using the modified fields. This method is recognized to be an intuitive method of analysis based on the ideas presented earlier by Kilkoyne in his equivalent aperture approach [8].

The time to compute a single value of received voltage is independent of the size of the radome for the two methods just described. The time depends, instead, on the number of sample points used in the aperture. For the case of a square array of 256 sample points (16 x 16), the computation time for one value of received voltage for the fast transmitting case is approximately one minute. The fast receiving method requires 1.5 seconds. No account is made here of the core memory requirements.

Some analytical work and associated computer implementation remains to be done. An additional receiving formulation method of analysis will be implemented wherein integration over the inner surface of the radome will be done to determine if any computational advantages are realized. Antenna characterization routines which utilize theoretical representation and measured data also being implemented. Of future interest is the spherical wave expansion described by Ludwig [9] where

limited measured far-field data are used to generate coefficients in the expansion so that radiation from the antenna can be more accurately described analytically. Presently, the PWS formulation is being used to characterize radiation from the antenna. Also, the effects of reflected waves are also to be included in the analysis using the Huygens-Fresnel formulation embodied in Equations (108) and (109) of Silver [2]. Finally, a method of comparison of analysis methods is being developed which includes both computation time and memory requirements so that fair comparisons can be made.

Five radomes have been designed for fabrication and use during the experimental program. All five radomes have the tangent ogive shape. Three radomes have 1:1 fineness ratios (length/diameter) and have dimensions to yield a small, medium, and large radome in terms of base diameter in wavelengths. Two other radomes have the medium-size base diameter but fineness ratios of 1.5:1 and 2:1.

The geometry and dimensions of the radomes showing the orientations of the antennas to be used with them are illustrated in Figures 3, 4, and 5. The radius of the generating arc is shown in each figure as R_{is}. The antenna is shown pivoted about a gimbal point to look in a direction that is 15° from the axis of symmetry of the radome. The dimension of a wavelength is indicated by λ in each figure for convenient reference. Table II presents the radome dimensions in terms of wavelengths at this frequency.

Two radomes have been fabricated using Rexolite ($\epsilon_r = 2.52$). A full-wavelength wall thickness for this material at 35 GHz is approximately 0.25 inch. A full-wavelength thickness has been selected to

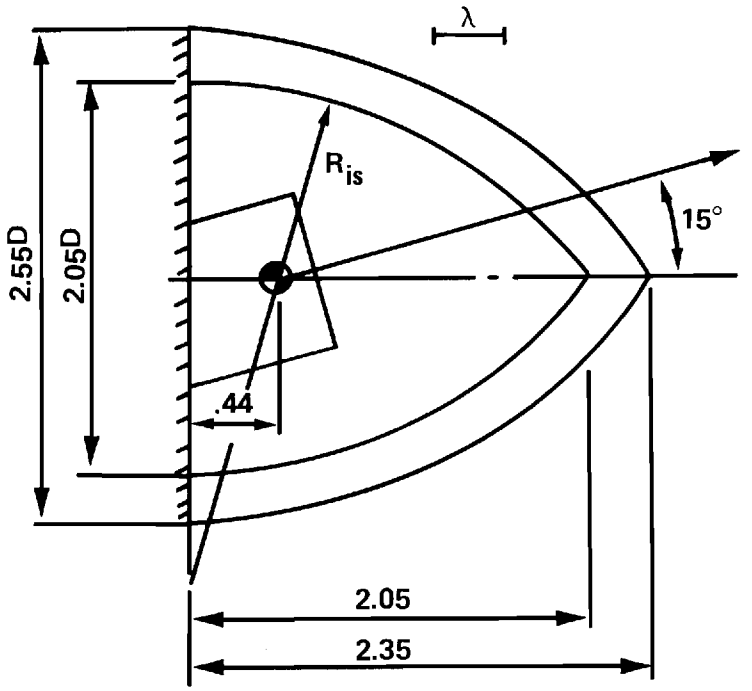

Figure 3. Geometry and Dimensions of Small Radome Showing Orientation of Small Antenna

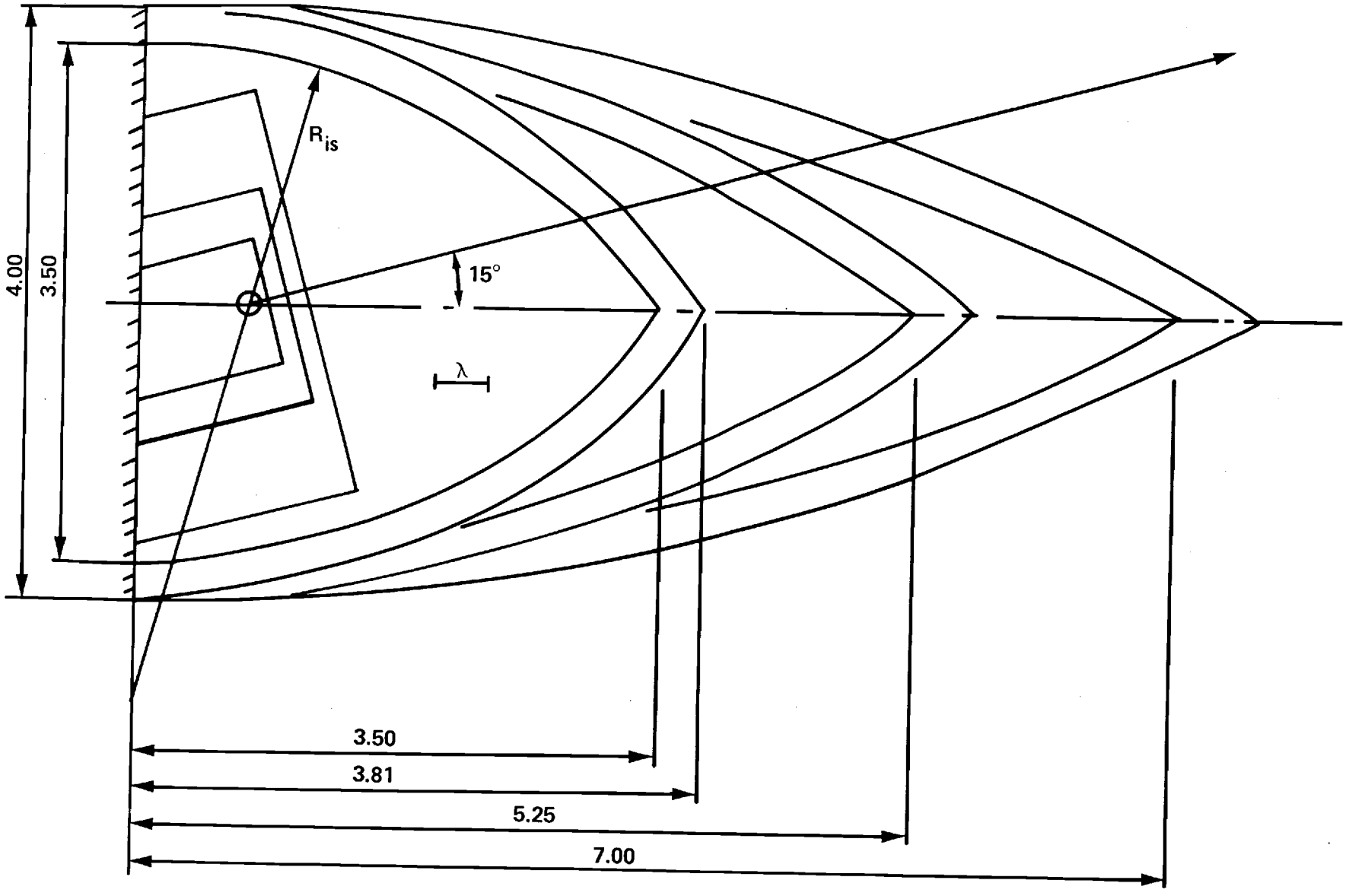

Figure 4. Geometry and Dimensions of Medium Size Radomes Having Fineness Ratios of 1:1, 1.5:1, and 2:1 Showing Small, Medium, and Large Antennas

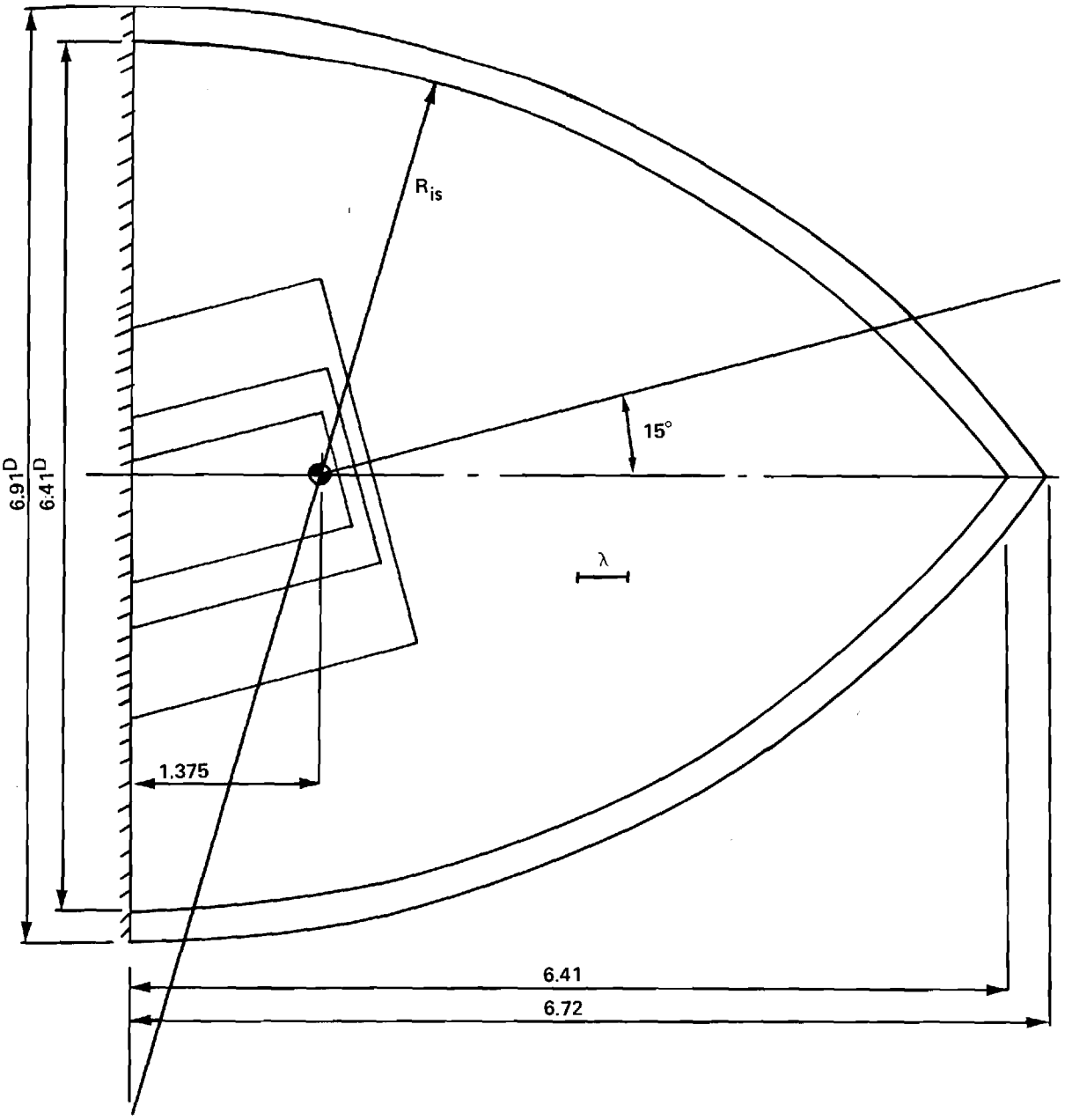

Figure 5. Geometry and Dimensions of Large Radome Showing Orientations of Small, Medium, and Large Antennas

Table II. Radome Dimensional Data in Wavelengths

	Inside Diameter	Inside Length	Outside Diameter	Outside Length
Small (F=1)	6.08	6.08	7.56	6.97
Medium (F=1)	10.38	10.38	11.86	11.30
Medium (F=1.5)	10.38	15.57	11.86	16.78
Medium (F=2.0)	10.38	20.76	11.86	22.30
Large (F=1)	19.01	19.01	20.49	19.93

provide adequate strength and rigidity for the larger radomes and to provide consistent effects for all sizes. Rexolite has excellent electromagnetic and machining properties. Photographs of the two radomes are shown in Figure 6.

Three four-horn monopulse antennas, representing a small, medium, and large antenna, have been designed and fabricated for use alone and with the five radomes. Each antenna is connected through a circular-to-rectangular waveguide transition and adapter network to a monopulse comparator which forms sum, elevation difference, and azimuth difference channels as required in monopulse tracking. The waveguide transitions and adapter networks have been fabricated in the main campus machine shop. The four-horn configurations have been built and their aperture dimensions are illustrated in Figure 7. These antennas are designed to provide sum pattern beamwidths of 8°, 15°, and 30°.

A mechanical fixture to position the radome with respect to the antenna and to position the combination in the pattern range coordinate system has also been built. Basically, a simple fixture is used which mounts on the azimuth positioner turntable and holds the antenna in a horizontal position. The antenna is mounted in a horizontal bushing so that accurate rotation of the antenna about its longitudinal axis is provided. If this axis is designated as the z-axis of the antenna, then rotation of the antenna about the z-axis selects a ϕ = constant plane in the associated spherical coordinate system. Rotation of the entire assembly about the vertical axis of the positioner turntable corresponds to movement in the θ direction of the spherical system. Vertical polarization corresponds to E_θ, horizontal polarization corresponds to E_ϕ.

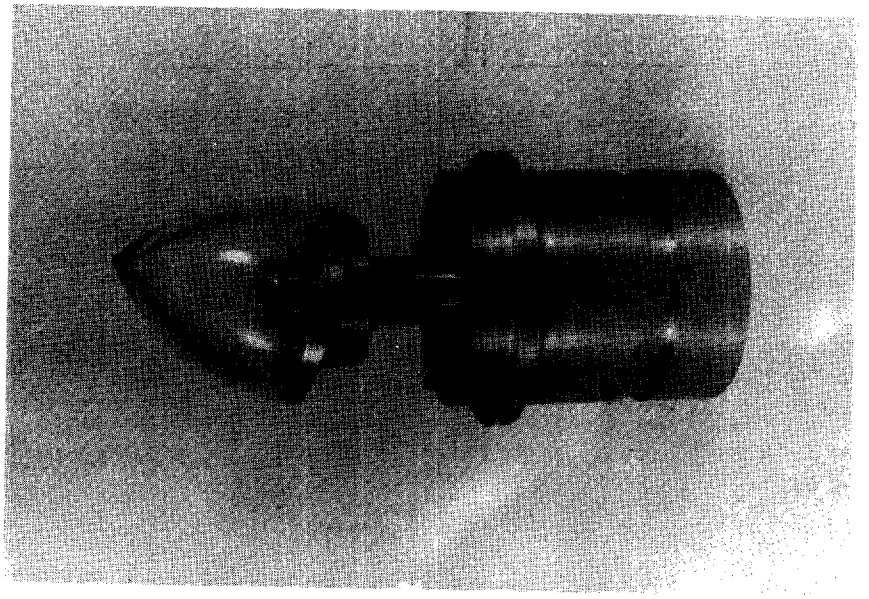

(a) Small Radome

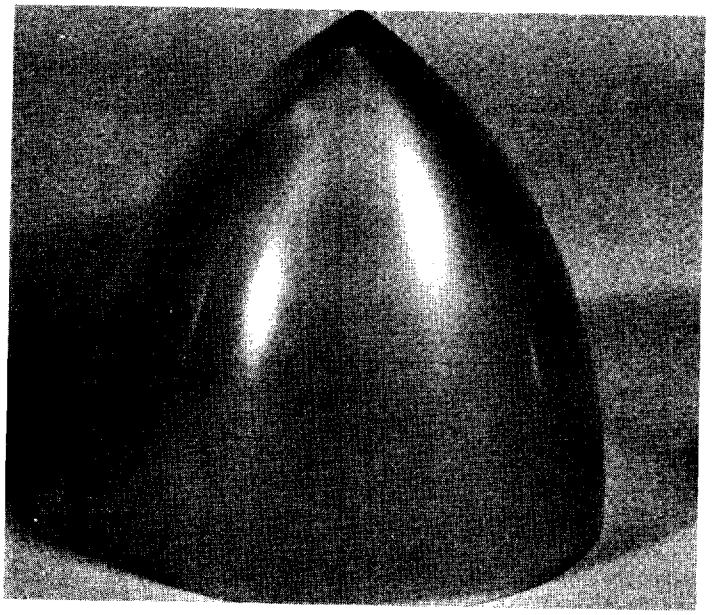

(b) Medium Radome

Figure 6. Photographs of Two Rexolite Radomes Having Fineness Ratio of 1:1

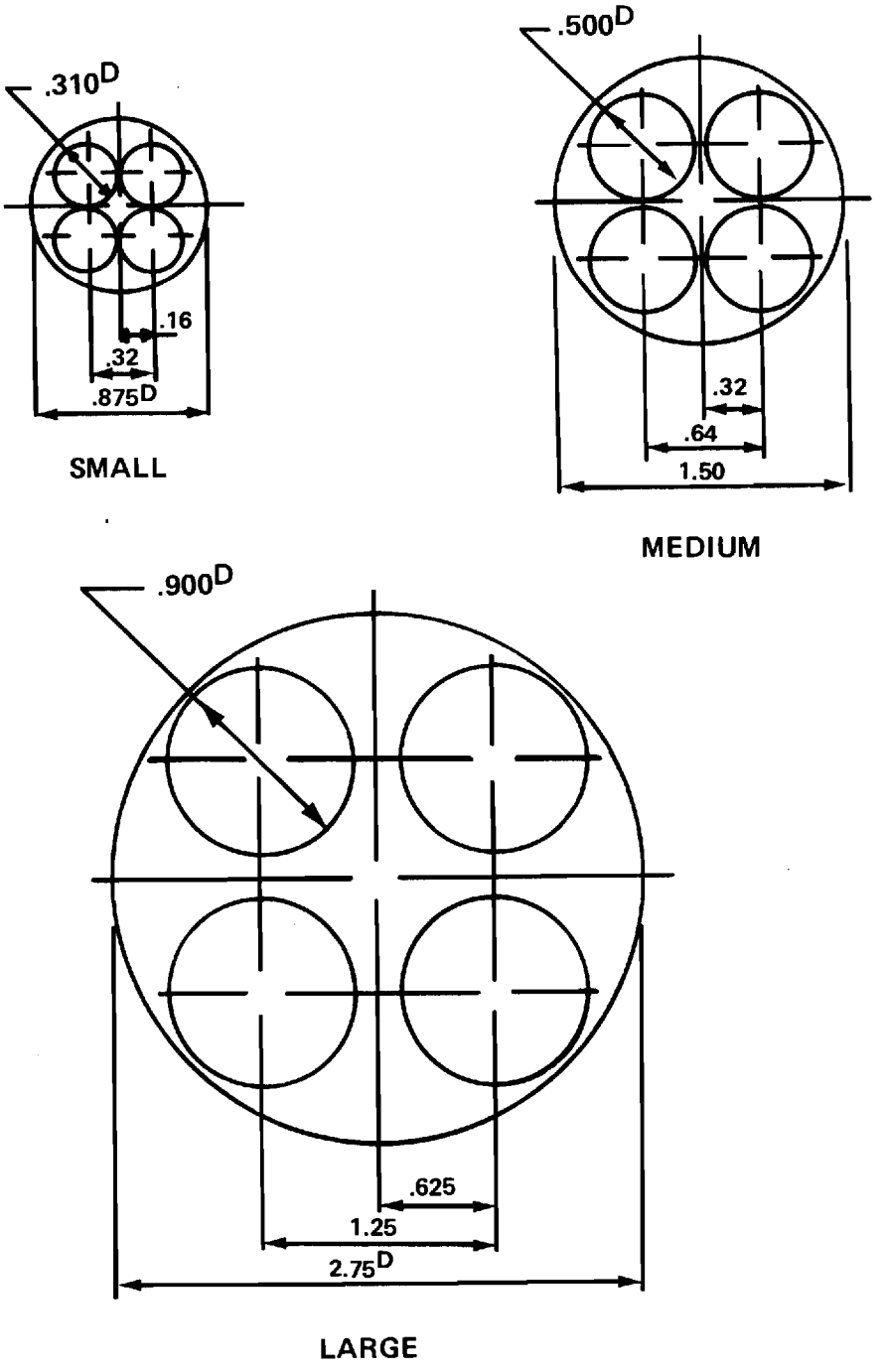

Figure 7. Geometry and Dimensions of Three Monopulse Antennas for Use at 35 GHz

The radome is positioned with respect to the antenna by a circular base plate to which the radome will be mounted. A circular hole has been accurately bored in the base plate which allows insertion onto the corresponding diameter antenna and which provides a very accurate, single angular orientation of the antenna z-axis with respect to the axis of symmetry of the radome. Rotation of the radome and base plate about the antenna z-axis provides selection of any desired plane of radome scan. Each antenna requires a different diameter base plate for each different radome with which the antenna is to be used; however, only nine such base plates are required and each base plate is very inexpensive to fabricate. Although this method of orienting the radome with respect to the antenna does not allow complete degrees of freedom, its low cost and high accuracy make it a very attractive method for this particular research program. Photographs of two antennas and the mounting fixture are shown in Figure 8.

Table III shows the specific combinations of antennas and radomes for which measured and analytical data will be obtained. Each entry in the table is the ratio of inside base diameter of the radome to the diameter of antenna aperture. Entries are made only for the nine combinations of interest. The results for the three entries of 2.33 for which F=1 are expected to show the effects of the size of the antenna/radome combination in wavelengths on the accuracy of the analysis methods. Results for the other entries of 2.33 and F=1 will provide information on the accuracy of the methods as a function of the relative size of antenna and radome. The entries of 2.33 for medium size radomes indicate those combinations which will provide information concerning the effects of

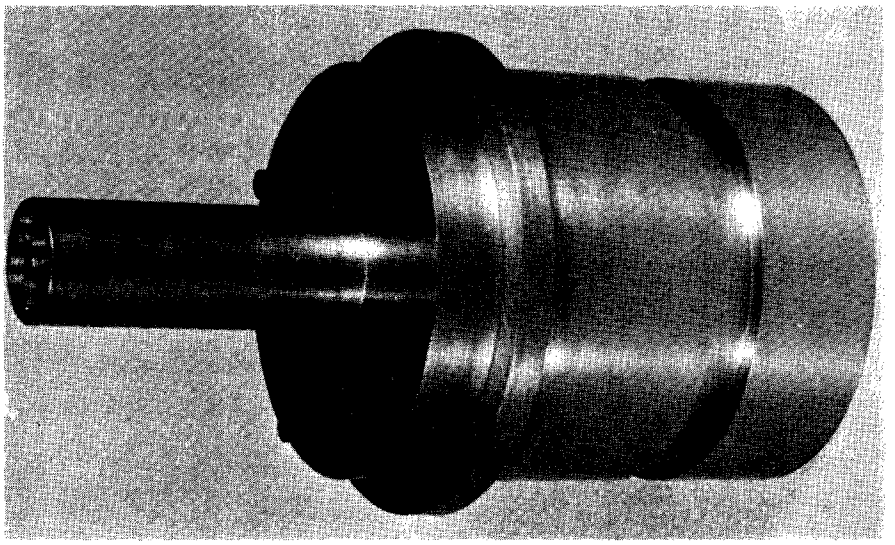

(a) Small Antenna

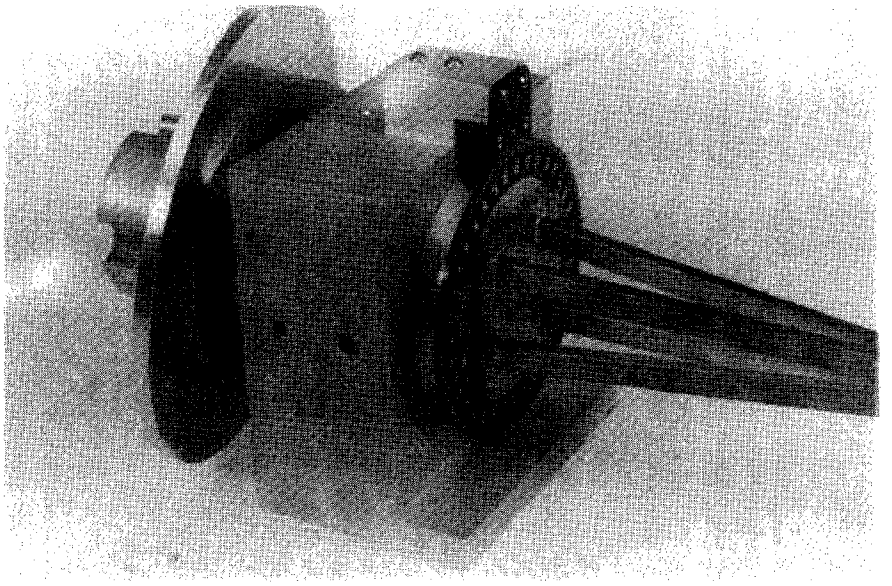

(b) Large Antenna

Figure 8. Photographs of Antennas and Mounting Fixture

Table III. Ratios of D_{is}/D_{ap} for Selected Antennas and Radomes.

Radome	Antenna		
	Small	Medium	Large
Small (F=1)	2.33	--	--
Medium (F=1)	3.98	2.33	1.27
Medium (F=1.5)	--	2.33	--
Medium (F=2.0)	--	2.33	--
Large (F=1)	7.28	4.27	2.33

fineness ratio on accuracy.

III. Presentations and Publications

G. K. Huddleston, H. L. Bassett, and J. N. Newton, "Parametric Investigation of Radome Analysis Methods," presented at and published in the Proceedings of the 1978 International IEEE AP-S Symposium, pp. 199-202, May 1978; also presented at and published in the Proceedings of the Fourteenth Symposium on Electromagnetic Windows, pp. 53-55, June 1978, (Copies included in Appendix A).

G. K. Huddleston, "Radome Analysis," invited presentation to Atlanta Chapter of IEEE, AP-S/MTT Group, September 26, 1978.

G. K. Huddleston, "A General Theory of Radome Analysis," a paper planned for submission to IEEE Transactions on Antennas and Propagation, January 1979.

IV. Personnel and Interactions

The following professional personnel are actively engaged in this research program:

G. K. Huddleston	Assistant Professor	School of Electrical Engineering
H. L. Bassett	Senior Research Engineer	Engineering Experiment Station
J. N. Newton	Research Engineer	Engineering Experiment Station

Dr. Huddleston and Mr. Bassett serve as co-principal investigators. Dr. Huddleston directs the analytical efforts while Mr. Bassett directs the experimental work. Mr. Jason Rusodimos, a graduate student in the School of Electrical Engineering works with Dr. Huddleston on the computer implementation of various analysis methods.

No specific interactions have taken place with other laboratories or DOD agencies; however, tentative plans have been made with Eglin Air Force Base (Dr. Ralph Calhoun, AFATL/DLMP) for the transfer of the analytical technology developed during this research.

V. References

1. R. E. Collin and F. J. Zucker, "Antenna Theory, Part 1," Sections 4.2 and 4.5, McGraw-Hill, New York, 1969.

2. Samuel Silver, ed., Microwave Antenna Theory and Design, Section 3-8, McGraw-Hill, New York, 1949.

3. G. K. Huddleston and E. B. Joy, "Development of Fabrication and Processing Techniques for Laser Hardened Missile Radomes: Radome Electrical Design Analysis," Technical Report for Martin-Marietta Aerospace, April 1977.

4. J. H. Richmond, "Calculation of Transmission and Surface Wave Data for Plane Multilayer and Inhomogeneous Plane Layers," Air Force Contract No. AF 33(615)-1081, Antenna Laboratory, Ohio State University, Columbus, Ohio, October 1963.

5. R. E. Van Doeren, "Application of the Integral Equation Method to Scattering from Dielectric Rings," Contract N62269-C-0582, Naval Air Development Center, Johnsville, PA, April 1968.

6. E. B. Joy and G. K. Huddleston, "Radome Effects on Ground Mapping Radar," Contract DAAH01-72-C-0598, U.S. Army Missile Command, March 1973.

7. Collin and Zucker, Ch. 3.

8. N. R. Kilcoyne, "An Approximate Calculation of Radome Boresight Error," Proceedings of the USAF/Georgia Tech Symposium on Electromagnetic Windows, pp. 91-111, June 1968.

9. A. C. Ludwig, "Near-Field Far-Field Transformations Using Spherical Wave Expansions," IEEE Transactions, AP-19, No. 2, pp. 214-220, March 1971.

APPENDIX A

Copies of Papers Presented

at

1978 International IEEE AP-S Symposium

and

Fourteenth Symposium on Electromagnetic Windows

PARAMETRIC INVESTIGATION OF RADOME ANALYSIS METHODS

Presented at

1978 International IEEE AP-S Symposium
University of Maryland
College Park, Maryland
May 1978

G. K. Huddleston, H. L. Bassett, and J. M. Newton
Georgia Institute of Technology
School of Electrical Engineering and Engineering Experiment Station
Atlanta, Georgia 30332

Numerous methods of radome analysis have been developed, and some comparisons of theoretical and measured results have been made for specific radome/antenna combinations; however, no attempt has been made to define the ranges of antenna and radome parameters over which any given method of analysis yields acceptably accurate results. This paper describes some early results of an investigation recently undertaken to determine the accuracies of various radome analysis methods under controlled conditions of antenna size and placement, wavelength, and radome size and shape. A fundamental theory of radome analysis has been developed and is presented below. Comparisons of computed results obtained for two methods of analysis are also presented. No experimental results are available at this time, but rather extensive measurements involving antennas and radomes of various sizes are planned.

Theory

The Lorentz reciprocity theorem [1] is a starting point for the formulation of a basic theory of radome analysis. Field equivalence principles [2] are also important in suggesting approximate methods of obtaining the fields called for in the reciprocity theorem; more importantly, such theory is needed to obtain the transmitting formulation for radome analysis.

Consider the antenna/radome combination shown in Figure 1 where the surface S encloses the antenna. Let a plane wave be incident on the radome from the direction $\hat{K}_A$ expressed in the antenna coordinate system (X,Y,Z). Then application of the reciprocity theorem results in the following expression for the voltage produced at the antenna terminals by the incident field:

$$V_R(\hat{K}_A) = C \iint_S (\underline{E}_T \times \underline{H}_R - \underline{E}_R \times \underline{H}_T) \cdot \hat{n} da \qquad (1)$$

where C is a complex constant and where

$\underline{E}_T, \underline{H}_T$ = the electric and magnetic fields produced on S when the antenna is transmitting (and no fields are incident on the radome from the outside)

$\underline{E}_R, \underline{H}_R$ = the electric and magnetic fields produced on S when the plane wave is incident (and the antenna is passive or in the receive mode)

$\hat{n}$ = unit vector pointing out of the volume V enclosed by S

da = element of area on the surface S

The fields $(\underline{E}_R, \underline{H}_R)$ and $(\underline{E}_T, \underline{H}_T)$ are the total fields produced in each case and would correctly include incident and all scattered components. The voltage given by Equation (1) is exact and serves as a basic tenet of radome analysis theory. The surface S may be any conveniently chosen closed surface. Linear, homogenous, isotropic media are assumed. Time variations of the form $e^{j\omega t}$ are understood and suppressed.

A second generalized approach to radome analysis uses a transmitting formulation which does not consider explicitly the fields produced by an incident plane wave. Instead, the tangential fields produced by the antenna on a closed surface outside the radome are used to determine the fields anywhere in the unbounded, homogeneous medium outside this surface. Equations (108) and (109) of [3] are the basic equations which apply, where the point P is at a great distance from S so that $\underline{E}_p, \underline{H}_p$ become the far zone fields $\underline{E}_{Tff}, \underline{H}_{Tff}$ radiated by the antenna in the presence of the radome. Selection of the surface S are the parameters which, again, differentiate the various methods of radome analysis based on a transmitting formulation.

The voltage that would be received by the antenna which produces far zone fields $\underline{E}_{Tff}$, $\underline{H}_{Tff}$ is given by [4]

$$V_R(\hat{K}_A) = C\, \underline{E}_{Tff} \cdot \hat{n}_b \qquad (2)$$

where C is a complex constant and $\hat{n}_b$ is a generally complex vector which describes the orientation and polarization of an infinitesimal current element located in the direction (with respect to the antenna) given by $\hat{K}_A$. Equation (2) provides the connection between the receiving and transmitting formulations and is the third facet of a basic theory of radome analysis.

Application

A computationally fast method of radome analysis based on a receiving formulation results when the surface S in Equation (1) is chosen to coincide with the planar aperture of the antenna whose radiating characteristics are represented using the plane wave spectrum formulation. The receiving pattern (difference channel) in the azimuth plane for a vertically polarized antenna with square aperture (corners removed) of dimensions $4.3\lambda \times 4.3\lambda$ is shown in Figure 2 for the case of a Pyroceram radome of wall thickness $d = .22\lambda$. The tangent ogive radome with fineness ratio $L/D = 2.25$ is gimballed so that its tip is positioned at $+12^{o}$ in the azimuth plane of the antenna. Execution time to generate this pattern and three others like it was 104 seconds (CDC Cyber 70).

For comparison, the pattern obtained for the same values of radome and antenna parameters when a transmitting formulation is used is shown in Figure 3. In this method, a PWS representation is used to describe the antenna, and rays representing each plane wave are used to construct an equivalent aperture which includes the effects of the radome on each plane wave in the spectrum. The execution time to generate this pattern and three others was 60 seconds on the same computing system.

Other methods of analysis which utilize integration on the surface of the radome for both receiving and transmitting formulations are currently being implemented. Computed results obtained using these methods will be presented at the symposium. The experimental procedures being used will also be described.

Acknowledgement

This research is sponsored by the Air Force Office of Scientific Research, Air Force Systems Command, USAF, under Grant No. AFOSR-77-3469. The United States Government is authorized to reproduce and distribute reprints for governmental purposes notwithstanding any copyright notation hereon.

References

1. R. E. Collin and F. J. Zucker, "Antenna Theory, Part 1," Section 4.2, McGraw-Hill, New York, 1969.

2. Ibid., Section 3.3.

3. S. Silver, ed., "Microwave Antenna Theory and Design," Section 3-8, McGraw-Hill, New York, 1949.

4. Collin and Zucker, op. cit., Section 4.5.

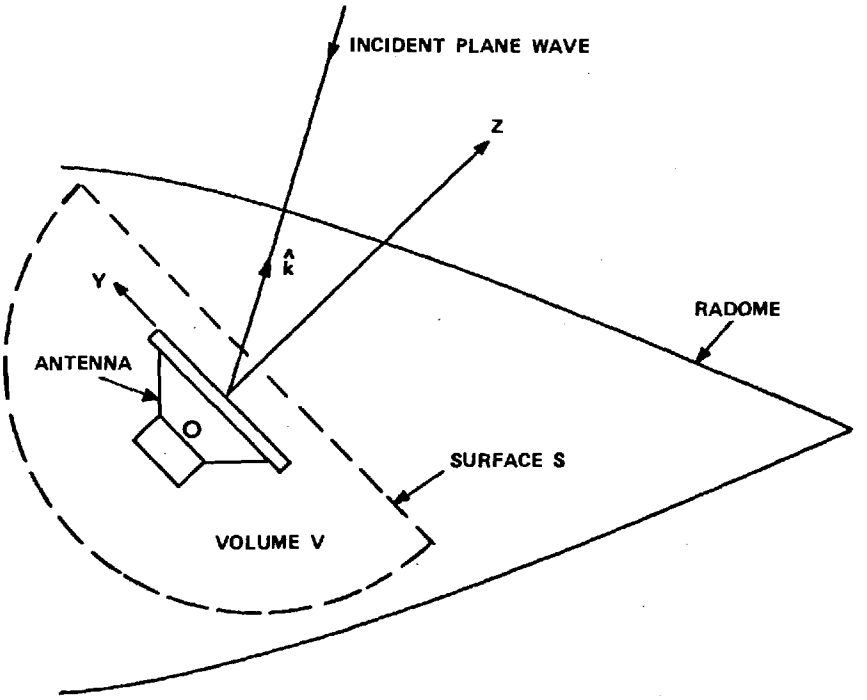

FIGURE 1. ANTENNA/RADOME GEOMETRY FOR ANALYSIS.

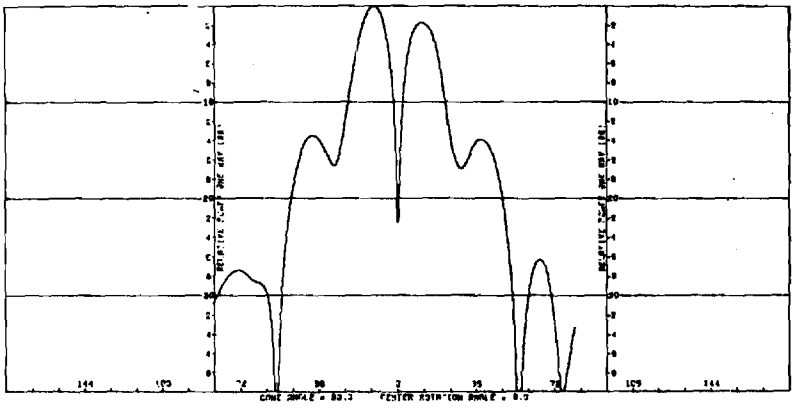

FIGURE 2. AZIMUTH PATTERN FOR RECEIVING FORMULATION.

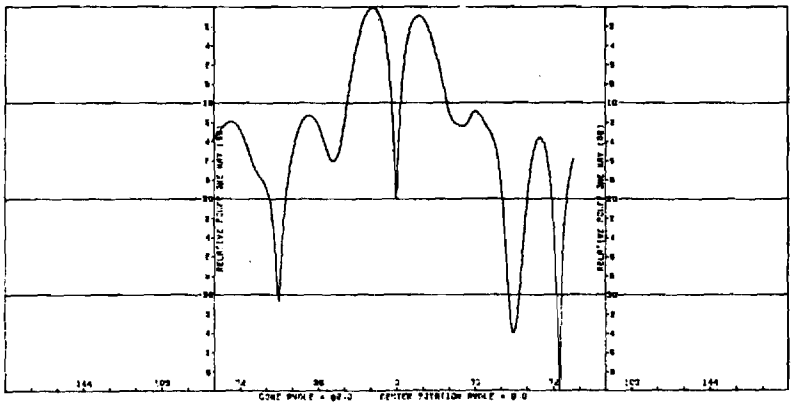

FIGURE 3. AZIMUTH PATTERN FOR TRANSMITTING FORMULATION.

PARAMETRIC INVESTIGATION OF RADOME ANALYSIS METHODS

Presented at
Fourteenth Electromagnetic Window Symposium
Georgia Institute of Technology
Atlanta, Georgia
June 1978

G. K. Huddleston, H. L. Bassett, and J. M. Newton
Georgia Institute of Technology
School of Electrical Engineering and Engineering Experiment Station
Atlanta, Georgia 30332

Numerous methods of radome analysis have been developed [1-9], and some comparisons of theoretical and measured results have been made for specific radome/antenna combinations [2,5,7,8]; however, no attempt has been made to define the ranges of antenna and radome parameters over which any given method of analysis yields acceptably accurate results.

This paper describes some early results of an investigation recently undertaken to determine the accuracies of various radome analysis methods under controlled conditions of antenna size and placement, wavelength, and radome size and shape. To carry out valid comparisons of various methods, a fundamental theory of radome analysis has been developed and is presented below. All existing methods, as well as some new ones, can be formulated in terms of the basic theory. Comparisons of computed results obtained for two methods of analysis are also presented. No experimental results are available at this time, but rather extensive measurements involving antennas and radomes of various sizes are planned.

Theory

The Lorentz reciprocity theorem [11] is a starting point for the formulation of a basic theory of radome analysis. Field equivalence principles [12] are also important in suggesting approximate methods of obtaining the fields called for in the reciprocity theorem; more importantly, such theory is needed to obtain the transmitting formulation for radome analysis.

Consider the antenna/radome combination shown in Figure 1 where the surface S encloses the antenna. Let a plane wave be incident on the radome from the direction K_A expressed in the antenna coordinate system (X,Y,Z). Then application of the reciprocity theorem results in the following expression for the voltage produced at the antenna terminals by the incident field:

$$V_R(\hat{K}_A) = C \int\int_S (\underline{E}_T \times \underline{H}_R - \underline{E}_R \times \underline{H}_T) \cdot \hat{n}\, da \qquad (1)$$

where C is a complex constant and where

$\underline{E}_T, \underline{H}_T$ = the electric and magnetic fields produced on S when the antenna is transmitting (and no fields are incident on the radome from the outside)

E_R, H_R = the electric and magnetic fields produced on S when the plane wave is incident (and the antenna is passive or in the receive mode)

$\hat{n}$ = unit vector pointing out of the volume V enclosed by S

da = element of area on the surface S

The fields $(\underline{E}_R, \underline{H}_R)$ and $(\underline{E}_T, \underline{H}_T)$ are the total fields produced in each case and would correctly include incident and all scattered components. The voltage given by Equation (1) is exact and serves as a basic tenet of radome analysis theory. The surface S may be any conveniently chosen closed surface. Linear, homogenous, isotropic media are assumed. Time variations of the form $e^{j\omega t}$ are understood and suppressed.

The selection of the surface S and the approximations used to determine the fields $(\underline{E}_T, \underline{H}_T)$ and $(\underline{E}_R, \underline{H}_R)$ on this surface are the parameters which differentiate the various methods of radome analysis which are based on a receiving formulation. For example, Tricoles [5] and Huddleston and Joy [10] chose a planar surface coinciding with the antenna aperture for the surface S, ignoring the contribution of that portion of the surface needed to completely enclose the antenna. Huddleston and Joy used ray tracing to approximate the fields $(\underline{E}_R, \underline{H}_R)$ on S. Tricoles used field equivalence and induction theorems to determine these fields on S. Huddleston and Joy used the primary transmitting fields of the antenna to approximate $(\underline{E}_T, \underline{H}_T)$. Tricoles used measured values of antenna response.

Other approximate methods based on the receiving formulation in Equation (1) are obvious. Consider the surface S which coincides with the inner surface of the radome. The fields $(\underline{E}_T, \underline{H}_T)$ on S may be approximated using modal expansions such as the PWS [8], a spherical wave expansion [13], or from theoretical analysis [14]. These fields should correctly contain reflected components which may be approximated using plane sheet transmission coefficients and Poynting's vector. The fields $(\underline{E}_R, \underline{H}_R)$ on S may be approximated using plane sheet transmission coefficients and ray tracing. The voltage received could then be obtained by performing the surface integration over the inside surface of the radome indicated by Equation (1).

The effects of reflections may also be included in the analysis. Let $(\underline{E}_T', \underline{H}_T')$ represent the transmitting fields on the surface S which coincides with the inner radome surface. Then at a point P on the inner surface, the fields at all other points contribute components due to reflections given by [15]

$$\underline{E}p = \frac{1}{4\pi} \iint_S [-j\omega\mu\ \psi\ (\hat{n} \times \underline{H}_T') + (\hat{n} \times \underline{E}_T') \times \nabla\psi + (\hat{n} \cdot \underline{E}_T')\nabla\psi\ ]dS \qquad (2)$$

$$\underline{H}p = \frac{1}{4\pi} \iint_S [j\omega\varepsilon(\hat{n} \times \underline{E}_T')\psi + (\hat{n} \times \underline{H}_T') \times \nabla\psi + (\hat{n} \cdot \underline{H}_T')\nabla\psi\ )]dS \qquad (3)$$

where

$$\psi = \frac{e^{-jkr}}{r} \qquad (4)$$

and where r is the distance from P to any other point on S. The importance of the contributions of first and higher order reflections has not been established.

A second generalized approach to radome analysis uses a transmitting formulation which does not consider explicitly the fields produced by an incident plane wave. Instead, the tangential fields produced by the antenna on a closed surface outside the radome are used to determine the fields anywhere in the unbounded, homogenous medium outside this surface. Equations (2) and (3) are the basic equations which apply, where the point P is at a great distance from S so that $\underline{E}_p, \underline{H}_p$ become the far zone fields $\underline{E}_{Tff}, \underline{H}_{Tff}$ radiated by the antenna in the presence of the radome. Selection of the surface S and the approximations used to find the fields $(\underline{E}_T, H_T)$ on S are the parameters which, again, differentiate the various methods of radome analysis based on a transmitting formulation.

The voltage that would be received by the antenna which produces far zone fields $\underline{E}_{Tff}, \underline{H}_{Tff}$ is given by [23]

$$V_R(\hat{K}_A) = C\ \underline{E}_{Tff} \cdot \hat{n}_b \qquad (5)$$

where C is a complex constant and $\hat{n}_b$ is a generally complex vector which describes the orientation and polarization of an infinitesimal current element located in the direction given by $\hat{K}_A$. Note that the current element would produce an

incident plane wave on the radome having the same polarization as that indicated by $\hat{n}_b$; hence, Equation (5) provides the connection between the receiving and transmitting formulations and is a third facet of a basic theory of radome analysis.

The above equations combine to form a fundamental theory of radome analysis. All existing analysis methods, as well as some new ones, can be cast in terms of this theory. The theory provides a rigorous framework in which the approximations which may be used in any analysis method can be clearly seen and their effects on predicted results assessed. Comparisons of the various methods in terms of speed of computations and accuracy can also be made.

All radome analysis methods of practical interest entail approximations of one form or another. Consequently, the only satisfactory way to determine the accuracy of any method is by comparison with experimental data. To cover the broad range of parameters that may be encountered in practice, combinations of radomes and antennas of various sizes should be carefully selected for measurement to yield the most useful true data for assessing the accuracies of different methods of analysis.

Application

A computationally fast method of radome analysis based on a receiving formulation [10] results when the surface S in Equation (1) is chosen to coincide with the planar aperture of the antenna whose radiating characteristics are represented using the plane wave spectrum formulation [17]. The difference receiving pattern in the azimuth plane for a vertically polarized monopulse antenna with square aperture (corners removed) of dimensions $4.3\lambda \times 4.3\lambda$ is shown in Figure 2 for the case of a Pyroceram radome of wall thickness $d = .22\lambda$. The tangent ogive radome with fineness ratio $L/D = 2.25$ gimballed so that its tip is positioned at $+12^{\circ}$ in the azimuth plane of the antenna. Execution time to generate this pattern and three others like it was 104 seconds (CDC Cyber 70).

For comparison, the pattern obtained for the same values of radome and antenna parameters when a transmitting formulation [9] is used is shown in Figure 3. In this method, a PWS representation is used to describe the antenna, and rays representing each plane wave are used to construct an equivalent aperture which includes the effects of the radome on each plane wave in the spectrum. The execution time to generate this pattern and three others was 60 seconds on the same computing system.

Other methods of analysis which utilize integration on the surface of the radome for both receiving and transmitting formulations are currently being implemented. Computed results obtained using these methods will be presented at the symposium. The

experimental procedures being used will also be described.

Summary

A fundamental theory of radome analysis, which embodies all existing methods as well as some new ones, is presented. Computed results using two different methods of analysis have been obtained as preliminary data. Computed results obtained using additional methods of analysis will be presented at the symposium.

Acknowledgement

This research is sponsored by the Air Force Office of Scientific Research, Air Force Systems Command, USAF, under Grant No. AFOSR-77-3469. The United States Government is authorized to reproduce and distribute reprints for governmental purposes notwithstanding any copyright notation hereon.

References

1. "Microwave Antenna Theory and Design," edited by Samuel Silver, McGraw-Hill Book Company, Chapter 14, 1949.

2. N. R. Kilcoyne, "An Approximate Calculation of Radome Boresight Error," Proceedings of the USAF/Georgia Institute of Technology Symposium on Electromagnetic Windows, pp. 91-111, June 1968.

3. O. Snow, "Discussion of Ellipticity Produced by Radomes and Its Effects on Crossover Point Position for Conically Scanning Antennas," U. S. Naval Air Development Center, Report E15108, 1951.

4. P. I. Pressel, "Boresight Prediction Technique," Proceedings OSU-WADC Radome Symposium, 1956.

5. G. Tricoles, "Radiation Patterns and Boresight Error of a Microwave Antenna Enclosed in an Axially Symmetric Dielectric Shell," J. Optical Soc. of America, 54, No. 9, pp. 1094-1101, September 1964.

6. M. Tavis, "A Three-Dimensional Ray Tracing Method for the Calculation of Radome Boresight Error and Antenna Pattern Distortion," Report No. TOR-0059(56860)-2, Air Force Systems Command, May 1971.

7. D. T. Paris, "Computer-Aided Radome Analysis," IEEE Transactions, AP-18, No. 1, pp. 7-15, January 1970.

8. D. C. F. Wu and R. C. Rudduck, "Application of Plane Wave Spectrum Representation to Radome Analysis," Proceedings of the Tenth Symposium on Electromagnetic Windows, pp. 46-49, July 1970; also Final Technical Report 2969-4 (AD 722 634), March 1971.

9. E. B. Joy and G. K. Huddleston, "Radome Effects on Ground Mapping Radar," Contract DAAH01-72-C-0598, U. S. Army Missile Command, March 1973.

10. G. K. Huddleston and E. B. Joy, "Development of Fabrication and Processing Techniques for Laser Hardened Missile Radomes: Radome Electrical Design Analysis," MMC Purchase Agreement No. 573712, Martin Marietta Aerospace, March 1977.

11. R. E. Collin and F. J. Zucker, "Antenna Theory, Part 1," Section 4.2, McGraw-Hill Book Company, New York, 1969.

12. Ibid., Section 3-3.

13. A. C. Ludwig, "Near-Field Far-Field Transformations Using Sperical Wave Expansions," IEEE Transactions, AP-19, No. 2, pp. 214-220, March 1971.

14. D. T. Paris, "Digital Computer Analysis of Aperture Antennas," IEEE Transactions, AP-16, pp. 262-264, March 1968.

15. Silver, op. cit., Section 3-8, Equations (108)-(109).

16. Collin and Zucker, op.cit., Section 4.5.

17. H. G. Booker and P. C. Clemmow, "The Concept of an Angular Spectrum of Plane Waves, etc.," Proceedings IEE, 97, Part III, p. 11-17, 1950.

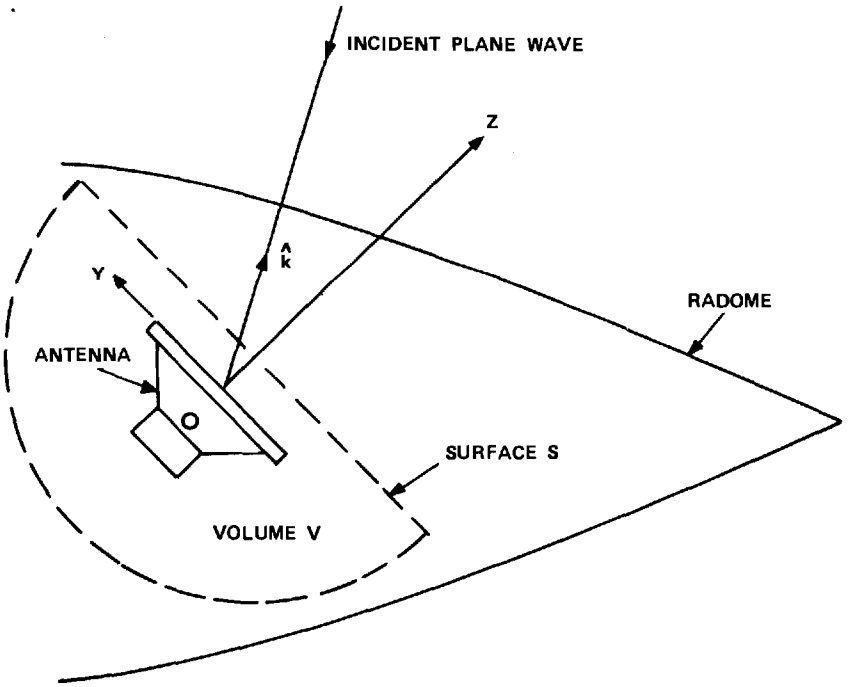

FIGURE 1. ANTENNA/RADOME GEOMETRY FOR ANALYSIS.

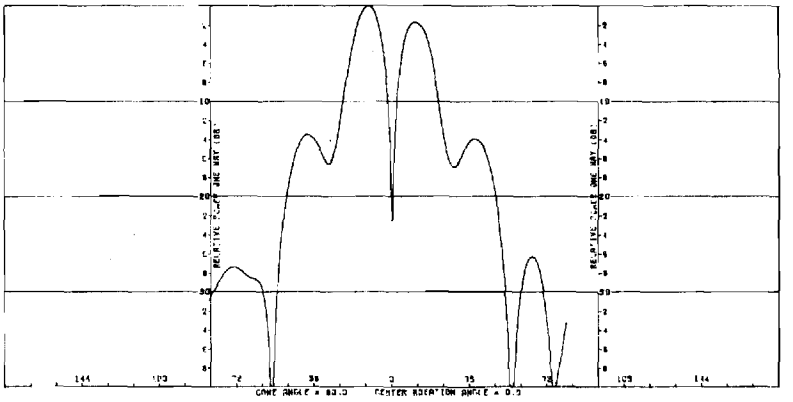

FIGURE 2. AZIMUTH PATTERN FOR RECEIVING FORMULATION.

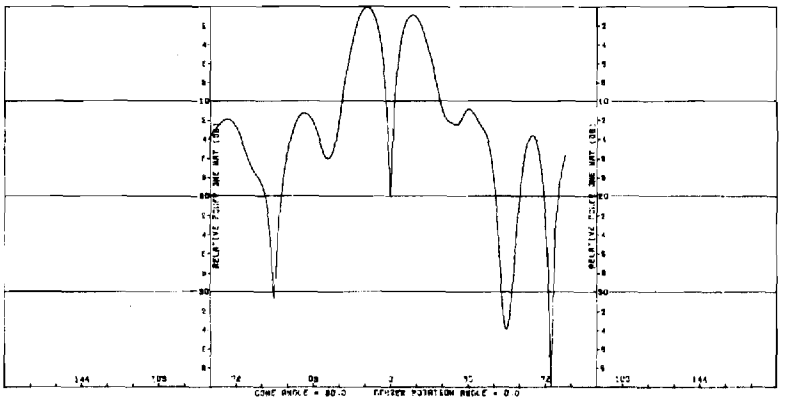

FIGURE 3. AZIMUTH PATTERN FOR TRANSMITTING FORMULATION.

PARAMETRIC INVESTIGATION OF RADOME ANALYSIS METHODS:

SALIENT RESULTS

By

G. K. Huddleston, H. L. Bassett, & J. M. Newton

Prepared for

AIR FORCE OFFICE OF SCIENTIFIC RESEARCH (AFSC)
BOLLING AIR FORCE BASE, D. C. 20332

FINAL TECHNICAL REPORT, VOLUME I OF IV
GRANT AFOSR–77–3469
30 September 1977 – 31 December 1980

February 1981

GEORGIA INSTITUTE OF TECHNOLOGY
SCHOOL OF ELECTRICAL ENGINEERING &
Engineering Experiment Station
Atlanta, Georgia 30332

UNCLASSIFIED

SECURITY CLASSIFICATION OF THIS PAGE *(When Data Entered)*

REPORT DOCUMENTATION PAGE		READ INSTRUCTIONS BEFORE COMPLETING FORM
1. REPORT NUMBER	2. GOVT ACCESSION NO.	3. RECIPIENT'S CATALOG NUMBER
4. TITLE *(and Subtitle)* PARAMETRIC INVESTIGATION OF RADOME ANALYSIS METHODS: SALIENT RESULTS		5. TYPE OF REPORT & PERIOD COVERED Final Technical Report, Vol. 1 of 4, 30 Sept. '77- 31 Dec. '80 6. PERFORMING ORG. REPORT NUMBER
7. AUTHOR(s) G. K. Huddleston, H. L. Bassett, & J. M. Newton		8. CONTRACT OR GRANT NUMBER(s) AFOSR-77-3469
9. PERFORMING ORGANIZATION NAME AND ADDRESS Georgia Institute of Technology School of Electrical Engineering & Engineering Experiment Station, Atlanta, GA 30332		10. PROGRAM ELEMENT, PROJECT, TASK AREA & WORK UNIT NUMBERS 61102F 2301/A6
11. CONTROLLING OFFICE NAME AND ADDRESS Air Force Office of Scientific Research Physics Directorate (Code NP-77-148) Bolling Air Force Base, D. C. 20332		12. REPORT DATE February 1981 13. NUMBER OF PAGES 92
14. MONITORING AGENCY NAME & ADDRESS*(if different from Controlling Office)*		15. SECURITY CLASS. *(of this report)* UNCLASSIFIED 15a. DECLASSIFICATION/DOWNGRADING SCHEDULE

16. DISTRIBUTION STATEMENT *(of this Report)*

Approved for public release; distribution unlimited.

17. DISTRIBUTION STATEMENT *(of the abstract entered in Block 20, if different from Report)*

18. SUPPLEMENTARY NOTES

19. KEY WORDS *(Continue on reverse side if necessary and identify by block number)*

Radome Analysis
Electromagnetic Analysis
Boresight Error

20. ABSTRACT *(Continue on reverse side if necessary and identify by block number)*

The salient results, conclusions, and recommendations are presented for a three-year program of research to assess the accuracies and ranges of validities of computer-aided methods of radome analysis.

DD FORM 1 JAN 73 1473

UNCLASSIFIED

SECURITY CLASSIFICATION OF THIS PAGE

PARAMETRIC INVESTIGATION OF RADOME ANALYSIS METHODS:

SALIENT RESULTS

by

G. K. Huddleston, H. L. Bassett, & J. M. Newton
School of Electrical Engineering &
Engineering Experiment Station
Georgia Institute of Technology
Atlanta, Georgia 30332

Final Technical Report, Volume I of IV

for

Air Force Office of Scientific Research (AFSC)
Physics Directorate (Code NP-77-148)
Bolling Air Force Base, D. C. 20332

under

Grant AFOSR-77-3469
30 September 1977 - 31 December 1980

February 1981

Table of Contents

PARAMETRIC INVESTIGATION OF RADOME ANALYSIS METHODS: SALIENT RESULTS

I. Introduction

The final technical report on this three-year radome research program consists of four volumes. This report, Volume I, presents the salient results conclusions, and recommendations of this research whose objective was to develop a general theory of radome analysis and to determine the accuracies and ranges of validity of three particular computer-aided radome analysis methods. The results are presented in appendices as copies of papers prepared for publication as summarized in the main body of this report.

Volume II documents the analytical method and Fortran computer code used to analyze the antenna/radome combinations using a fast receiving formulation based on Lorentz reciprocity and geometrical optics. Volume III documents the analytical method and additional Fortran software required for radome analysis based on the Huygens-Fresnel principle or surface integration. Volume IV documents the pattern and boresight error measurements made on eight combinations of three monopulse antennas and five tangent ogive radomes at 35 GHz.

Measured data is used as true data in assessing the accuracies of the computer codes. It is expected that the measured data obtained will be used in the future for similar purposes. It is also expected that the documented computer codes will serve as part of a technology base for use by researchers and practitioners in the radome technical community.

II. Results

Appendix A presents a paper which describes the theory of radome analysis developed during this investigation. The theory is simply an application

of the Huygens-Fresnel principle and Lorentz reciprocity to the radome problem. All methods of radome analysis appearing in the literature are embodied in this general theory. It provides the correct framework in which to think about radome analysis and to make objective comparisons between the various methods of analysis.

Appendix B presents a paper describing some antenna synthesis work that was undertaken during this research. A procedure is described whereby the aperture fields of the four-horn monopulse antenna without radome can be synthesized from measured, amplitude-only, far-field, principal plane patterns. A priori information about the geometry and excitation of the actual antenna is used to find a credible solution to an inverse source problem for which there would otherwise be no unique solution. In the absence of the radome, each analysis method accurately predicts the measured patterns.

Appendix C presents comparisons of measured and computed boresight errors and radome losses for four of the eight antenna/radome combinations considered. The antennas and radomes used are briefly described. (More detailed descriptions are presented in Volume IV.) Qualitative conclusions about the accuracies of the methods can be made from the data presented; in addition, recommendations for future work are brought to light.

III. Conclusions and Recommendations

From the data presented in Appendix C, it is concluded that none of the computer aided radome analysis methods investigated consistently and accurately predicted the boresight errors and losses of the various antenna/radome combinations used. For moderate size antennas and radomes (as defined in Appendix C), the fast receiving method predicts boresight errors reasonably accurately and is perhaps the fastest method available anywhere; however, for

small radomes and large radomes, the accuracy of the error predictions is not as good.

The surface integration method was not completely assessed for predictive accuracy because of unresolved problems with the code. A large part of the problem with the development of the code was the relatively long execution times required on the Cyber 70 system used. It is clear that because of the long execution times, use of the surface integration method will be restricted to the analysis of small radomes.

It is recommended that some "fine tuning" be done on the fast receiving method to improve its predictive accuracy over a larger range of antenna/radome parameters. Specifically, the ray tracing procedure should be modified to account for refractive effects and propagation of the fields along the rays. The expected improvement in accuracy, coupled with the inherent practicality of this code, make this recommended endeavor worthwhile.

It is also recommended that work be continued on the development of the surface integration method of analysis so that its predictive accuracy can be clearly established. A dedicated, small computer system (32-bit word length) is recommended for this work to avoid the anticipated high costs associated with very heavy use of a time-share system such as the Cyber 70 at Georgia Institue of Technology.

It is recommended that exact solutions of carefully selected antenna/radome configurations be obtained for use as true data in the assessment of the accuracies of various computer-aided radome analysis methods. Configurations used must conform to those expected in the applications. The accuracies of the solutions and the solutions themselves must be impeccable. Until such time as this recommendation is carried out, measured data must continue to be used as true data.

As a parallel approach to exact solutions, it is recommended that numerical solutions be obtained on practical configurations of interest using modern numerical methods such as method of moments and integral equation formulations. The use of specialized computing structures for dedicated application to such electromagnetic radiation and scattering problems should be investigated.

Finally, it is recommended that experimental techniques be developed to help isolate deficiencies in the methods of analysis. The usual measurements of patterns and boresight errors simply do not provide the necessary information to pinpoint invalid assumptions and poor approximations in any analysis procedure. New experimental methods which make use of automated measurements and near-field/far-field transformations need to be developed.

APPENDIX A

"Theory of Radome Analysis"

Submitted for Review for Publication

in

IEEE Transactions of the Antennas and Propagation Society

November 1980

THEORY OF RADOME ANALYSIS

G. K. Huddleston
School of Electrical Engineering
Georgia Institute of Technology
Atlanta, Georgia 30332

Abstract

A basic theory of radome analysis is presented based on the reciprocity theorem and the Huygens-Fresnel principle. Receiving and transmitting formulations are developed. Techniques of analysis are presented to distinguish the salient features of radome analysis and to show the relationships between the theory and some existing methods of analysis. The equivalence between the receiving and transmitting cases is also established, both in general and explicitly for the far-field case.

I. INTRODUCTION

Radome analysis is the application of electromagnetic theory to determine the effects of protective dielectric structures on the electrical characteristics of antennas enclosed by them. Numerous methods of analysis have been developed for the prediction of radome effects; however, no unified theory has been advanced to provide a common basis of understanding of the various approaches taken and the approximations used therein. Furthermore, no comprehensive measurements have been reported which provide true data in determining the accuracies of the various methods when parameters such as antenna size, wavelength, radome size and shape are considered over the ranges that they are likely to assume in the applications.

This paper presents a theory of radome analysis which embodies known methods of analysis that have appeared in the literature. The theory is based on the reciprocity theorem [1] and the Huygens-Fresnel principle for electromagnetic fields [2,3] both of which are derivable from Maxwell's equations via the divergence theorem and the vector Green's theorem. The reciprocity theorem serves as the basis for the receiving formulation of radome analysis, and the Huygens-Fresnel principle is the basis for the transmitting formulation as seen in what follows. The equivalences of the two formulations are also established. Some approximations and techniques used in implementing the analyses are presented along with discussions which clarify the justifications for the approaches used in practice.

The development and presentation of this theory of radome analysis is motivated by an on-going parametric investigation of radome analysis methods [4]. Measured pattern data and boresight error data for three antenna sizes combined in fifteen combinations with five radomes have been obtained to serve as true data in determining the accuracies and ranges of validities of three common computer-aided analyses. Great care has been taken to ensure accurate modeling of the antennas such that, in the absence of a radome, each computer code accurately predicts the measured radiation patterns [5]. The theory provides the framework in which the methods can be compared, especially in regard to the approximations used, the validity of various assumptions made, and the equivalence of different computational procedures which yield, or should yield, the same result. The theory also provides the basis for developing test cases to verify the computer codes.

Development of radome analysis methods have paralleled the development of airborne radar systems whose complexities have increased over the years. Silver [6] illustrates the geometrical optics approaches taken up to 1949 and which were developed during the previous war years. Kilcoyne [7] presented a two-dimensional ray tracing method for analyzing radomes which utilized the digital computer, and is an extension of work done earlier by Snow [8] and by Pressel [9]. A more rigorous method of analysis was introduced in the same year by Van Doeren [10] using an integral equation to compute fields inside the radome caused by an incident plane wave. Tricoles [11] formulated a three-dimensional method of radome analysis based on Shelkunoff's induction and equivalence theorems. Tavis [12] describes a three-dimensional ray tracing technique to find the fields on an equivalent aperture external to an axially symmetric radome.

Paris [13] describes a three-dimensional radome analysis wherein the tangential fields on the outside surface of the radome due to the horn antenna radiating inside the radome are found. Wu and Rudduck [14] describe a three-dimensional method which uses the plane wave spectrum representation to characterize the antenna. Joy and Huddleston [15] describe a computationally fast, three-dimensional radome analysis which utilizes the plane wave spectrum (PWS) representation and exploits the Fast Fourier Transform (FFT) to speed up the computer calculations. Chesnut [16] has combined the program of Wu and Rudduck with the work of Paris to form a three-dimensional radome analysis method. Huddleston [17] has recently developed a three-dimensional radome analysis method which uses a general formulation based on the Lorentz reciprocity theorem. Siwiak, et al., [18] have recently applied the reaction theorem to the analysis of a tangent ogive radome at X-band frequencies to determine boresight error. Hayward, et al., [19] have compared the accuracies of two methods of analysis in the cases of large and small radomes to show that ray tracing does not accurately predict wavefront distortion in the case of small radomes.

II. RECEIVING FORMULATION

The reciprocity theorem is a starting point for the formulation of a unified theory of radome analysis. The general reciprocity theorem [1] states that

$$\oint_S (\underline{E}_a \times \underline{H}_b - \underline{E}_b \times \underline{H}_a)\cdot\hat{n}\, da = \int_V (\underline{E}_b \cdot \underline{J}_a - \underline{E}_a \cdot \underline{J}_b - \underline{H}_b \cdot \underline{J}^m_a + \underline{H}_a \cdot \underline{J}^m_b)\cdot dV \tag{1}$$

where the surface S encloses the volume V containing two sets of electric and magnetic sources ($\underline{J}_a$, $\underline{J}_a^m$), ($\underline{J}_b$, $\underline{J}_b^m$) which give rise to electromagnetic fields ($\underline{E}_a$, $\underline{H}_a$), ($\underline{E}_b$, $\underline{H}_b$), respectively. (Time variations of the form $e^{j\omega t}$ are understood and suppressed).

Figure 1 illustrates a typical radome analysis situation where it is desired to determine the response V_a of Antenna "a" to fields produced by Antenna "b". The closed surface S in the reciprocity theorem is chosen to be $S_0 + S_1$ so that the volume V is the source-free region lying between Antenna "a" and the inner surface of the dielectric enclosure depicted in Figure 1. In this case, the right side of Equation (1) equates to zero (Lorentz reciprocity theorem), and the left side can be separated into two surface integrals as

$$- \int_{S_0} (\underline{E}_a \times \underline{H}_b - \underline{E}_b \times \underline{H}_a) \cdot \hat{n} \, da = \int_{S_1} (\underline{E}_a \times \underline{H}_b - \underline{E}_b \times \underline{H}_a) \cdot \hat{n} \, da \qquad (2)$$

where $\hat{n}$ is the unit normal to the surface and is directed positively out of the volume V. The fields $\underline{E}_a$, $\underline{H}_a$ are those produced on S_1 and S_0 by Antenna "a" when it is activated (transmitting); $\underline{E}_b$, $\underline{H}_b$ are the fields produced on S_1 and S_0 when Antenna "b" is activated (and Antenna "a" is passive or receiving).

Let surface S_0 be divided into two parts: S_0' consisting of that portion of S_0 across the waveguiding structure connecting the generator of Antenna "a" to the radiating structure; S_o'' consisting of the remainder of S_0 and which coincides with the conducting surface of the antenna as indicated in the figure. The integral of the fields over S_0'' is identically zero [20] so that the left side of Equation (2) reduces to the integration over S_0'. Now, in the many practical cases of interest, there exists a dominant mode of propagation over S_0' (e.g., TE_{10}

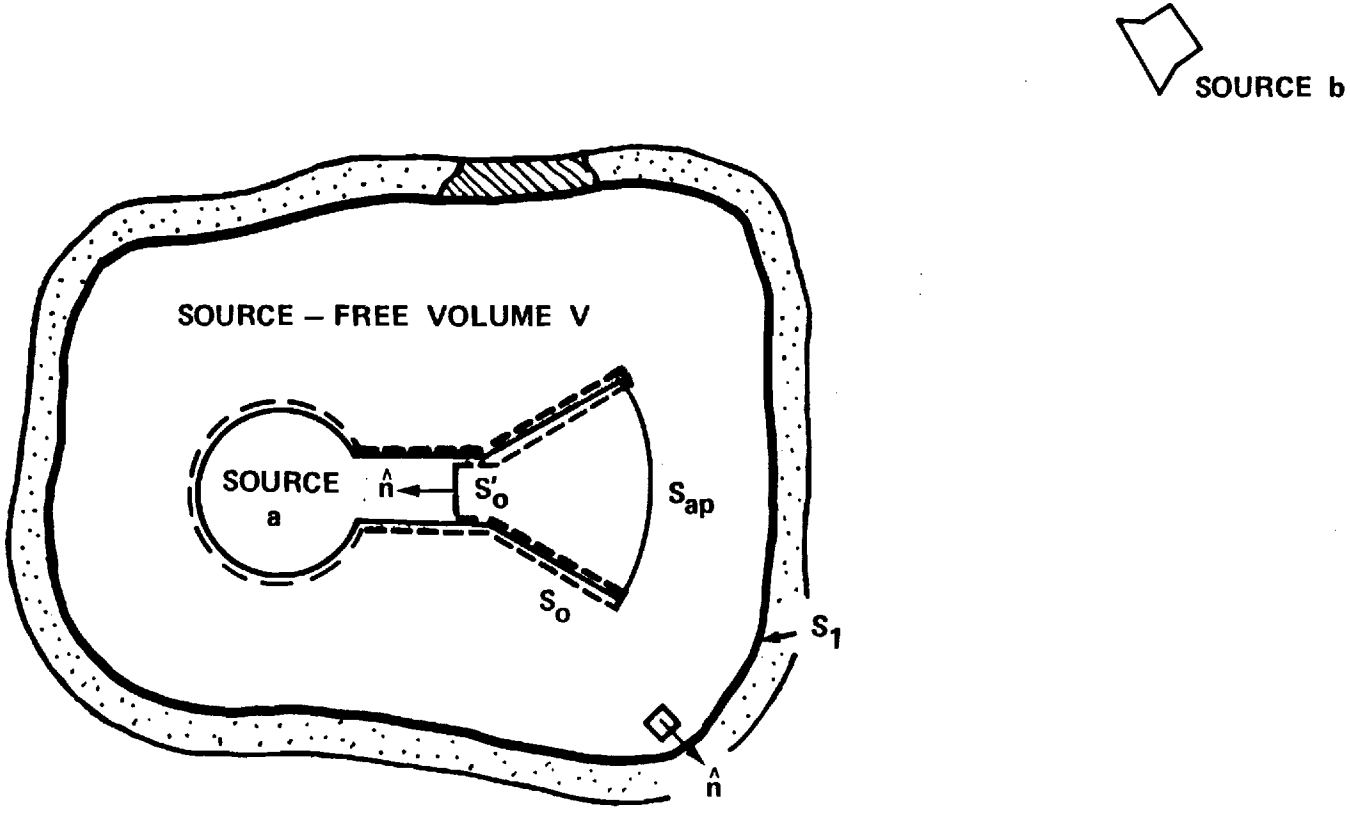

FIGURE 1. GEOMETRY FOR RECEIVING FORMULATION USING RECIPROCITY THEOREM.

mode in rectangular waveguide) so that currents and voltages can be defined at this terminal plane so that there results

$$V_a I_b + V_b I_a = - \int_{S_0'} (\underline{E}_a \times \underline{H}_b - \underline{E}_b \times \underline{H}_a) \cdot \hat{n} \, da \tag{3}$$

The currents and voltages are defined for the two cases of interest in Figure 2:

V_a, I_a - Voltage and current produced at S_0' by generator "a" when generator "b" is passive;

V_b, I_b - Voltage and current produced at S_0' by generator "b" when generator "a" is passive.

Linear impedance relationships can also be defined as indicated in Figure 2 such that (using $Y = 1/Z$)

$$V_a I_b + V_b I_a = V_a(V_b Y_a) + V_b(V_a Y_1) \tag{4}$$

Equating Equation (4) to Equation (2) and solving for the received voltage V_b results in

$$V_b = \frac{V_{REC}}{V_a(Y_a+Y_1)} = \frac{1}{V_a(Y_a+Y_1)} \int_{S_1} (\underline{E}_a \times \underline{H}_b - \underline{E}_b \times \underline{H}_a) \cdot \hat{n} \, da \tag{5}$$

where V_{REC} has been defined for convenience. This is one desired result.

In most analysis situations, Antenna "a" and the dielectric enclosure comprise the antenna/radome combination. The separation of this combination and Antenna "b" can be made very large so that the fields of "b" are those of a transverse electromagnetic plane wave incident on the radome. In radar applications, the distant target is illuminated either

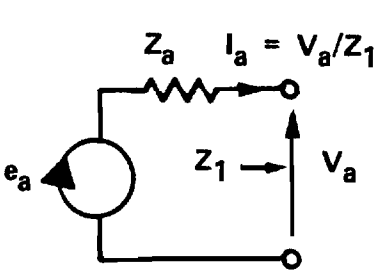

(a) Source "a" active,

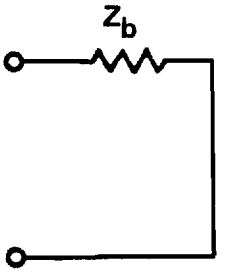

Source "b" passive

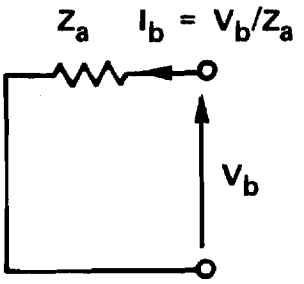

(b) Source "a" passive,

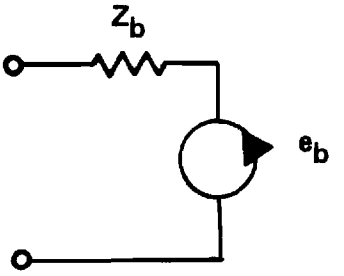

Source "b" active

FIGURE 2. DEFINITIONS OF CIRCUIT PARAMETERS OF THE ANTENNAS.

by Antenna "a" or another antenna not shown in Figure 1. The reflection from the target comprises Antenna "b" in the analysis and, for large separation, arrives, again, as an incident plane wave on the radome. Note, however, that the receiving formulation embodied in Equation (5) is valid for either the near-field (small separation) or far-field (large) case. Also, superposition applies so that multiple targets or sources can be accommodated as linear combinations comprising the fields $\underline{E}_b$, $\underline{H}_b$ in Equation (5).

Equation (5) is exact; however, in the evaluation of the integral, approximations to the actual fields on S_1 may be introduced so that inaccuracies in the computation of the received voltage may result. To see the effects of certain approximations, it is advantageous to make the following definitions of primary and scattered fields:

$$\underline{E}_a = \underline{E}^i_{ao} + \underline{E}_{as} + \underline{E}'_{as} \tag{6}$$

$$\underline{H}_a = \underline{H}^i_{ao} + \underline{H}_{as} + \underline{H}'_{as} \tag{7}$$

where

$\underline{E}^i_{ao}$, $\underline{H}^i_{ao}$ - Fields on S_1 due to Antenna "a" which contain no scattered field components; i.e., the fields that would exist on S_1 in the absence of the dielectric.

$\underline{E}_{as}$, $\underline{H}_{as}$ - First order scattered fields on S_1 due to Antenna "a"; i.e., fields reflected only once from material media outside S_1 and from Antenna "b".

$\underline{E}'_{as}$, $\underline{H}'_{as}$ - Higher order scattered fields on S_1 due to Antenna "a"; i.e., components caused by multiple scattering

between Antenna "a" and surrounding media, including Antenna "b".

Similar definitions can be made for Antenna "b" with respect to the surface S_1 as follows:

$$\underline{E}_b = \underline{E}^t_{bo} + \underline{E}_{bs} + \underline{E}'_{bs} \tag{8}$$

$$\underline{H}_b = \underline{H}^t_{bo} + \underline{H}_{bs} + \underline{H}'_{bs} \tag{9}$$

where $\underline{E}^t_{bo}$, $\underline{H}^t_{bo}$ are the fields on S_1 due to Antenna "b" and which contain no scattered components due to material media inside S_1, including Antenna "a". The fields $\underline{E}_{bs}$, $\underline{H}_{bs}$ are first order scattered fields on S_1 due to a single scattering from Antenna "a". The fields $\underline{E}'_{bs}$, $\underline{H}'_{bs}$ are the higher order scattered fields. When these definitions are substituted into Equation (5) and the vector cross products evaluated, there results

$$\begin{aligned} V_{REC} = & \int_{S_1} (\underline{E}^i_{ao} \times \underline{H}^t_{bo} - \underline{E}^t_{bo} \times \underline{H}^i_{ao}) \cdot \hat{n} \, da \\ & + \int_{S_1} (\underline{E}^i_{ao} \times \underline{H}_{bs} - \underline{E}_{bs} \times \underline{H}^i_{ao}) \cdot \hat{n} \, da \\ & + \int_{S_1} (\underline{E}_{as} \times \underline{H}^t_{bo} - \underline{E}^t_{bo} \times \underline{H}_{as}) \cdot \hat{n} \, da \\ & + \int_{S_1} (\underline{E}_{as} \times \underline{H}_{bs} - \underline{E}_{bs} \times \underline{H}_{as}) \cdot \hat{n} \, da \\ & + \text{Terms involving higher order scattered fields} \end{aligned} \tag{10}$$

The first integral on the right side of Equation (10) provides the primary contribution to the received voltage for those cases of interest where the dielectric is somewhat transparent to the incident fields $\underline{E}^i_{bo}$, $\underline{H}^i_{bo}$ of Antenna "b". The second and third integrals are each identically zero by virtue of the definitions of the scattered fields and the general reciprocity theorem as applied to the source-free volume $\overline{V}$ consisting of the region outside S_1; i.e., since there are no sources of the defined fields in this region, the right side of Equation (1) and, hence, the second integral of Equation (10), are both zero. A similar argument holds for the third integral when the general reciprocity theorem is applied to the source-free region V enclosed by S_1.

The contribution of the fourth integral in Equation (10) depends on the scattering properties of Antenna "a" as well as on the reflective properties of the dielectric enclosure with respect to the incident fields $\underline{E}^i_{ao}$, $\underline{H}^i_{ao}$. It is difficult to assess the significance of these contributions and those of the integrals involving higher order scattered fields. At any rate, it is impractical in current computer-aided analyses to include scattering from the antenna inside the enclosure; hence, only the first term in Equation (10) is usually retained. The objective of practical radome analysis then centers on the determination of the fields in the integral

$$V_{REC} \approx \int_{S_1} (\underline{E}^i_{ao} \times \underline{H}^t_{bo} - \underline{E}^t_{bo} \times \underline{H}^i_{ao}) \cdot \hat{n} \, da \qquad (11)$$

and on the evaluation of the integral itself.

Surfaces other than the inside surface S_1 of the dielectric of Figure 1 can also be selected for the evaluation of the received voltage

via Equation (10) or (11). For example, choose S_0 as before and choose S_1 to also coincide with the outer surface of Antenna "a", including the radiating aperture portion S_{ap}. Apply Lorentz reciprocity to the source-free volume contained between the antenna aperture and S_0' to yield

$$V_{REC} \approx \int_{S_{ap}} (\underline{E}^i_{ao} \times \underline{H}^t_{bo} - \underline{E}^t_{bo} \times \underline{H}^i_{ao}) \cdot \hat{n} \, da \tag{12}$$

The fields $\underline{E}^i_{ao}$, $\underline{H}^i_{ao}$ are the aperture fields of Antenna "a" when it is transmitting in the absence of the dielectric and are often known or specified for analysis purposes. The real difficulty arises in the determination of the fields $\underline{E}^t_{bo}$, $\underline{H}^t_{bo}$ on the chosen surface S_1. And it is the choice of the surface S_1 and the approximations used to find the fields on it which distinguish the various methods of analysis based on the receiving formulation. More will be said concerning the determination of these fields in the next section.

Another choice of the surface of integration consists of the outer surface S_3 of the dielectric enclosure of Figure 1. First apply Equation (1) to the source-free region consisting of the dielectric itself as enclosed by its inner surface S_1 and its outer surface S_3; i.e., $S = S_1 + S_3$. Since the right side of Equation (1) is zero, and since the positive direction of $\hat{n}$ is out of V, it is seen from Equation (5) that

$$V_{REC} = \int_{S_3} (\underline{E}_a \times \underline{H}_b - \underline{E}_b \times \underline{H}_a) \cdot \hat{n} \, da \tag{13}$$

where $\hat{n}$ is the unit outward normal to the outer surface of the dielectric. It will be shown in a later section that Equation (13) is equivalent to the transmitting formulation to be discussed next.

III. TRANSMITTING FORMULATION

A second generalized approach to radome analysis uses a transmitting formulation which does not explicitly consider the fields produced by the incident fields of a source outside the dielectric structure. Instead, the equivalence and uniqueness theorems of electromagnetics [21] are invoked to establish the result that the fields radiated by Antenna "a" into the unbounded, homogeneous region outside the dielectric enclosure can be found from knowledge of the tangential electric and magnetic fields on the outer surface of the dielectric. Moreover, there exists an integral formula for the actual computation of these fields.

After Stratton and Chu [2], Silver [3] derives the general solution for the time-harmonic electromagnetic fields in a homogeneous medium which arise from a prescribed set of sources, including magnetic (equivalent) charges and currents. The derivation is based on Maxwell's equations (including the equations of continuity for charges and currents), a vector Green's theorem, and the free-space Green's function $\psi = e^{-jkr}$. The results, Equations (3.108) and (3.109) of Silver, are called the Huygens-Fresnel principle (also called Kirchhoff-Huygens principle) and are repeated here for convenience:

$$\underline{E}(x',y',z') = + \frac{T}{4\pi} \int_S [-j\omega\mu\psi(\hat{n} \times \underline{E}) + (\hat{n} \times \underline{E}) \times \nabla\psi + (\hat{n}\cdot\underline{E})\nabla\psi] \, dS \qquad (14)$$

$$\underline{H}(x',y',z') = \frac{T}{4\pi} \int_S [j\omega\varepsilon(\hat{n} \times \underline{E})\psi + (\hat{n} \times \underline{H}) \times \nabla\psi + (\hat{n}\cdot\underline{H})\nabla\psi] \, dS \qquad (15)$$

where $\hat{n}$ is the unit normal to S which points into the source-free medium as indicated in Figure 3.

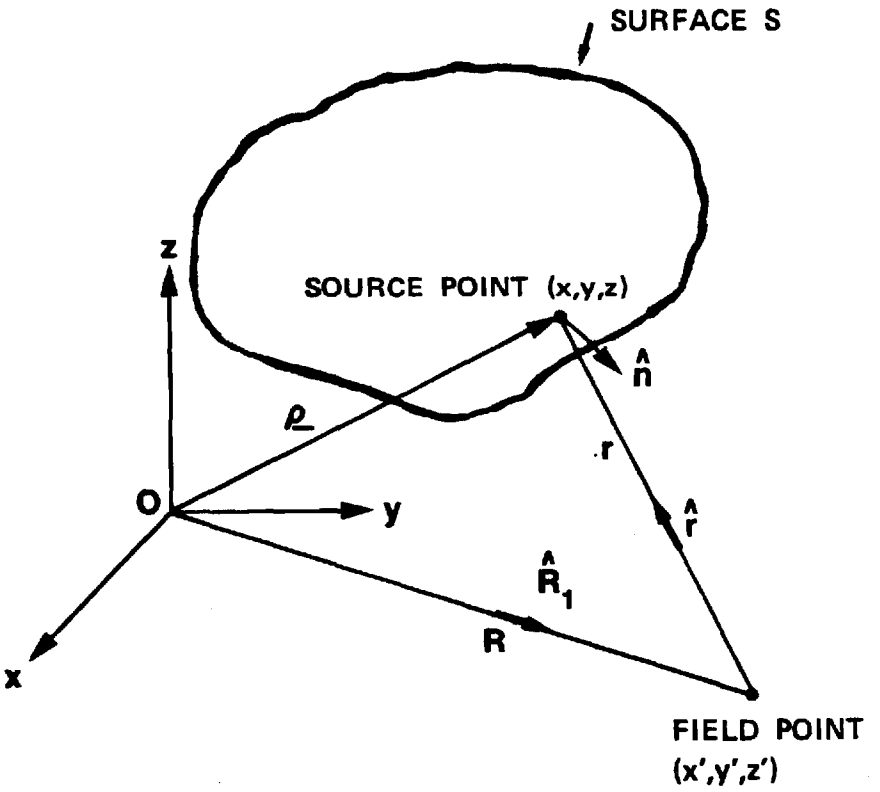

FIGURE 3. GEOMETRY FOR HUYGENS–FRESNEL PRINCIPLE.

In the above equations, primed variables are the coordinates of the point at which the field is to be computed, and unprimed coordinates are used to designate the source coordinates lying on the surface S. The distance r is measured from the field point (x',y',z') to the source point (x,y,z) so that

$$r = \sqrt{(x-x')^2 + (y-y')^2 + (z-z')^2} \tag{16}$$

and

$$\nabla\psi = -\left(jk + \frac{1}{r}\right)\psi\,\hat{r} = \left(jk + \frac{1}{r}\right)\psi\,\hat{r}_1 \tag{17}$$

where $r = -r_1$ is a unit vector directed along r from the field point to the source point. The variable T is adopted from the notation of Poggio and Miller [22] so that the fields at points on S can also be included; it is given by

$$T = \frac{1}{1-\Omega/4\pi} = \begin{cases} 1 & \text{if } \Omega=0,\ (x',y',z') \text{ not on S} \\ 2 & \text{if } \Omega=2\pi,\ (x',y',z') \text{ on S} \end{cases} \tag{18}$$

The terms $(\hat{n} \times \underline{E})$, $(\hat{n} \times \underline{H})$ in Equations (14) and (15) can be considered as equivalent magnetic and electric surface current densities

$$\underline{K} = \hat{n} \times \underline{H} \tag{19}$$

$$\underline{K}_m = -(\hat{n} \times \underline{E}) \tag{20}$$

with corresponding equivalent surface charge densities

$$\eta = (\hat{n} \cdot \underline{E}) \tag{21}$$

$$\eta_m = (\hat{n} \cdot \underline{H}) \tag{22}$$

These equivalent currents and charges are the sources of the fields $\underline{E}$, $\underline{H}$ in the region outside the dielectric enclosure. Using the equation of continuity for surface currents and charges [23].

$$\nabla_S \cdot \underline{K} + \frac{\partial \eta}{\partial t} = 0 \tag{23}$$

the terms in Equations (14) and (15) involving normal field components may be rewritten for the time-harmonic case as

$$\hat{n} \cdot \underline{E} = \frac{j}{\omega\varepsilon} \nabla_S \cdot (\hat{n} \times \underline{H}) \tag{24}$$

$$\hat{n} \cdot \underline{H} = \frac{j}{\omega\mu} \nabla_S \cdot (\underline{E} \times \hat{n}) \tag{25}$$

where $\nabla_S \cdot$ is the "surface divergence". Thus, the fields $\underline{E}$, $\underline{H}$ in V are expressible entirely in terms of the tangential fields on S as is in keeping with the uniqueness theorem. (Note, however, that the surface divergence involves first order partial derivatives whose numerical computation may not be desirable.)

Implicit in the application of equivalent surface charges and currents is Love's equivalence principle [24]. It is a special case of the general field equivalence principle [25] in that a null field is postuated inside the surface S, and the charges and currents of Equations (19)-(22)

are required on S to maintain the original field $\underline{E}$, $\underline{H}$ outside S. Hence, an application of the Huygens-Fresnel integrals using these surface currents to find the fields at a point inside S would necessarily yield a null result. This observation is important when applying the Huygens-Fresnel integrals to find specially defined fields inside the radome as discussed below.

The integral representations in Equations (14) and (15) for the fields radiated by Antenna "a" into the homogeneous, unbounded medium outside the radome are exact for points up to and including the surface S; however, the difficulty in analysis is the accurate determination of fields $\underline{E}$, $\underline{H}$ on S. To gain further insight into this problem, consider the geometry of Figure 4. Define primary and scattered fields of the antenna with respect to surfaces S_1 and S_2 as was done in Equations (6) and (7) of the previous section. Let the primary fields $\underline{E}_{ao}$, $\underline{H}_{ao}$ on S_2 be known. Then the primary fields incident on surface S_1 can be found via Equations (14) and (15) above where the surface of integration is now S_2 of Figure 4; i.e.,

$$\underline{E}_{ao}(S_1) = \frac{1}{4\pi} \int_{S_2} H_F\{\hat{n}, \underline{E}_{ao}, \underline{H}_{ao}\}dS \tag{26}$$

where the Huygens-Fresnel operator $H_F\{\ \}$ is defined here to be the integrand of Equation (14). A similar expression holds for the magnetic field intensity $\underline{H}_{ao}$. By definition, the fields $\underline{E}_{ao}$, $\underline{H}_{ao}$ are those that would exist at S_1 in the absence of the dielectric.

The first-order scattered fields $\underline{E}_{as}$, $\underline{H}_{as}$ on S_1 are those caused by the boundary S_1 and the media outside S_1. A very common approximation for this complicated scattering process utilizes the results

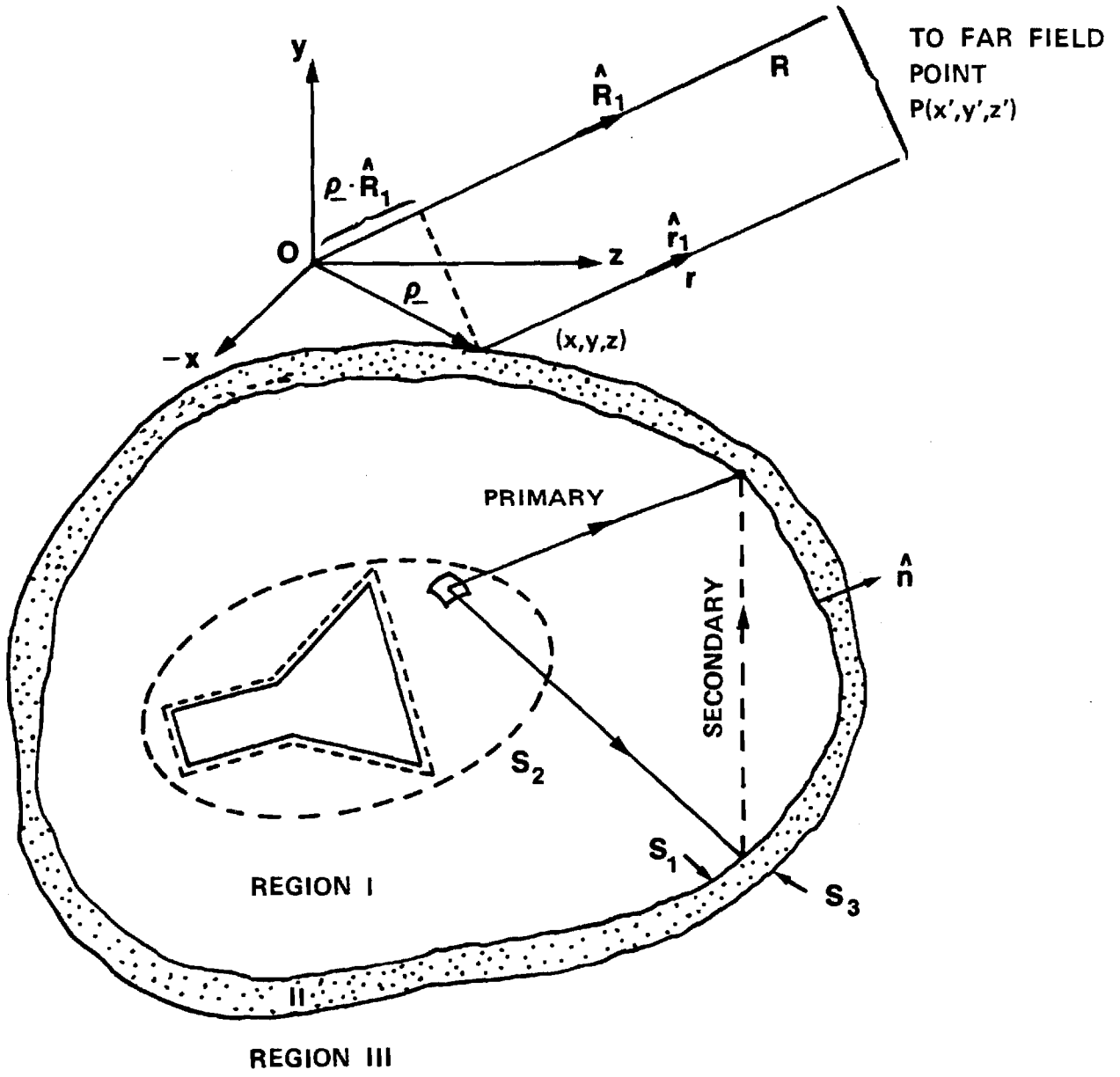

FIGURE 4. GEOMETRY USED TO COMPUTE FIELDS ON SURFACES OF RADOME AND TO COMPUTE FAR FIELDS.

of plane wave interaction with a dielectric interface: at each point on S_1, the incident fields $\underline{E}_{ao}$, $\underline{H}_{ao}$ are approximated locally as a plane wave, and the dielectric is assumed to have the same effect as a plane dielectric panel. The normal to the dielectric surface and the direction of propagation of the incident fields define the plane of incidence and the angle of incidence. The incident electric field is resolved into components perpendicular to and parallel to the plane of incidence as illustrated in Figure 5. The flat panel reflection coefficients $R_\perp$, $R_{||}$ are then applied to the incident fields to find estimates of the first-order scattered fields; i.e.

$$\underline{E}_{as} \approx \hat{a}_\perp(\underline{E}_{ao} \cdot \hat{a}_\perp)R_\perp + \hat{a}_{||}(\underline{E}_{ao} \cdot \hat{a}_{||})R_{||} \triangleq \underline{E}_{ao} \cdot \underline{\underline{R}} \tag{27}$$

where the dyadic $\underline{\underline{R}}$ is defined.

The flat panel transmission coefficients $T_\perp$, $T_{||}$ may also be used to estimate the fields transmitted to the outside surface; i.e.,

$$\underline{E}_{ao}^{t} \approx \hat{a}_\perp(\underline{E}_{ao} \cdot \hat{a}_\perp)\, T_\perp + \hat{a}_{||}(\underline{E}_{ao} \cdot \hat{a}_{||})\, T_{||} \triangleq \underline{E}_{ao} \cdot \underline{\underline{T}} \tag{28}$$

$$\underline{H}_{ao}^{t} = \hat{a}_\perp(\underline{H}_{ao} \cdot \hat{a}_\perp)\, T_{||} + \hat{a}_{||}(\underline{H}_{ao} \cdot \hat{a}_{||})T_\perp \triangleq \underline{H}_{ao} \cdot \underline{\underline{T}}' \tag{29}$$

When $\underline{E}_{ao}^{t}$, $\underline{H}_{ao}^{t}$ are used in Equations (14) and (15), a first-order approximation to the radiated fields outside the dielectric is obtained.

The procedure just described is that used earlier by Paris [13] and emulated by Wu and Rudduck [14] and Chesnut [16]. The direction of propagation $\hat{k}$ of the incident field was taken to be that of the Poynting

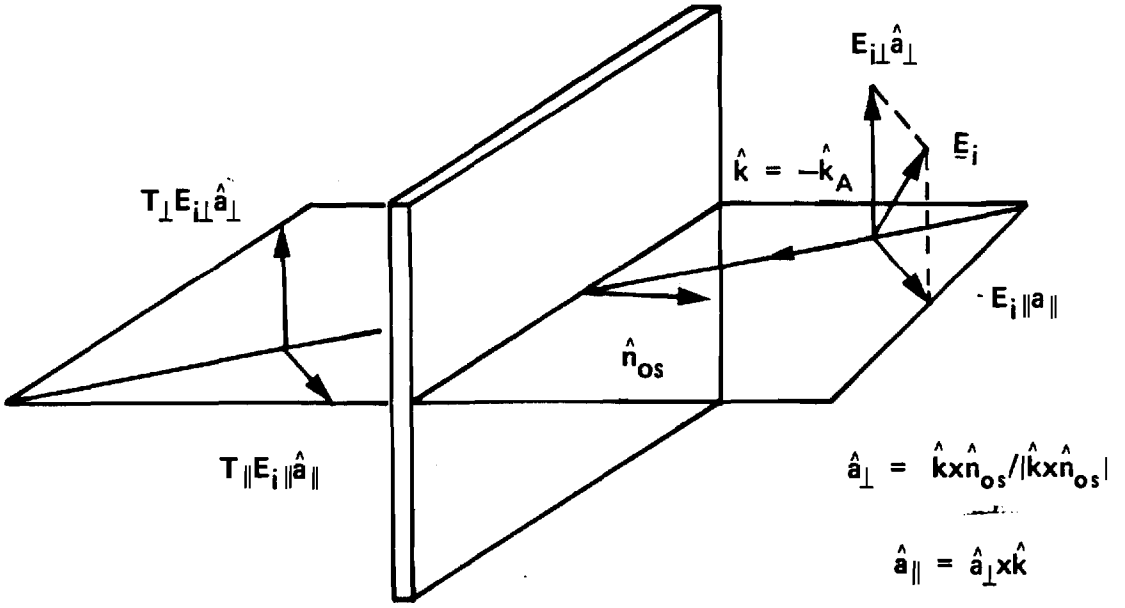

FIGURE 5. PLANE WAVE PROPAGATION THROUGH AN INFINITE PLANE SHEET.

vector or real power flow. Also, since only far-field patterns were of interest, the usual simplifying approximations were applied to Equations (14) and (15) to obtain the following far-field approximations

$$\underline{E}_{ff}(R\hat{R}_1) = \frac{-j\omega\mu}{4\pi R} e^{-jkR} \int_{S_3} [\hat{n}x\underline{H} - ((\hat{n}x\underline{H})\cdot\hat{R}_1)\hat{R}_1 + \frac{(\underline{E}x\hat{n})x\hat{R}_1}{\eta_o}] e^{jk\underline{\rho}\cdot\hat{R}_1} dv \quad (30)$$

$$\underline{H}_{ff}(R\hat{R}_1) = \frac{\hat{R}_1 \times \underline{E}_{ff}}{\eta_o} \quad (31)$$

where $\eta_o = \sqrt{\mu/\epsilon}$ is the characteristic impedance of free space and where the geometry variables are defined in Figure 4. Note that the second term in the integrand of Equation (30) is the radial component of $\hat{n} \times \underline{H}$ which is subtracted to ensure that only transverse (to $\hat{R}_1$) components of the fields are found in the far zone. Paris used the fields given by Equations (28) and (29) in the integrand of Equation (30).

The first-order scattered fields $\underline{E}_{as}$, $\underline{H}_{as}$ on surface S_1 also contribute to the incident fields at the surface S_1 as indicated by the dashed secondary ray in Figure 4. To formulate this contribution, consider the computation of the field $\underline{E}_{as}$ at an interior point P of the volume enclosed by S_1. Since all sources of $\underline{E}_{as}$, $\underline{H}_{as}$ are outside S_1,

$$\underline{E}_{as}(P) = \frac{T}{4\pi} \int_{S_1} H_F\{-\hat{n}, \underline{E}_{as}, \underline{H}_{as}\} dS \quad (32)$$

where $-\hat{n}$ is the unit inward normal to S_1 and T=1. On surface S_1 write $\underline{E}_{as}$, $\underline{H}_{as}$ as

$$\underline{E}_{as}(S_1) = \underline{E}_{ao} \cdot \underline{\underline{R}} + \underline{E}''_{as} \quad (33)$$

$$\underline{H}_{as}(S_1) = \underline{H}_{ao} \cdot \underline{\underline{R}}' + \underline{H}''_{as} \quad (34)$$

where $\underline{\underline{R}}$, $\underline{\underline{R}}'$ are flat panel reflection dyadics already defined, and where $\underline{E}''_{as}$, $\underline{H}''_{as}$ represent the contributions to $\underline{E}_{as}$, $\underline{H}_{as}$ at each point on S_1 from radiation by the fields at every other point. Substitute Equations (33) and (34) into Equation (32) with T = 2 for P on S_1 to yield

$$\underline{E}_{as}(S_1) = \frac{1}{2\pi} \int_{S_1} H_F\{-\hat{n}, \underline{E}_{ao} \cdot \underline{\underline{R}} + \underline{E}''_{as}, \underline{H}_{ao} \cdot \underline{\underline{R}}' + \underline{H}''_{as}\}dS \qquad (35)$$

Carry out the integration on the directly reflected terms to yield

$$\underline{E}_{as}(S_1) = \underline{E}_{ao} \cdot \underline{\underline{R}} + \frac{1}{2\pi} \int_{S_1'} H_F\{-\hat{n}, \underline{E}''_{as}, \underline{H}''_{as}\}dS \qquad (36)$$

where S_1' is surface S_1 with the point of interest excluded.

The fields $\underline{E}''_{as}$, $\underline{H}''_{as}$ are, of course, unknown; however, a first-order approximation to $\underline{E}''_{as}$ at a point P on S_1 is

$$\underline{E}''_{as}(S_1) \approx \frac{1}{2\pi} \int_{S_1'} H_F\{-\hat{n}, \underline{E}_{ao} \cdot \underline{\underline{R}}, \underline{H}_{ao} \cdot \underline{\underline{R}}'\}dS \qquad (37)$$

That is, the directly reflected fields at every other point on S_1 are used to determine $\underline{E}''_{as}$ at the point of interest on S_1. The fields $\underline{E}''_{as}$, $\underline{H}''_{as}$ at each point on S_1 should then be added to incident fields $\underline{E}_{ao}$, $\underline{H}_{ao}$ to produce a second order estimate to the fields on the outside surface of the dielectric via Equations (28) and (29). Hence, an approximate, iterative procedure to compute the effects of the first-order scattered fields on the final radiated fields is formulated.

An important hypothesis for the validity of Equations (14) and (15) is that the fields $\underline{E}$, $\underline{H}$ on S satisfy Maxwell's equations, including the equations of continuity. If this hypothesis is not met, the fields

computed at points not on S will still satisfy Maxwell's equations provided only that the equations of continuity are satisfied on S; e.g., if surface currents are terminated abruptly, then a line of surface charge must be explicitly included in the field expressions [26]. If the hypothesis that $\underline{E}$, $\underline{H}$ on S satisfy Maxwell's equations is met, then the equations of continuity are automatically satisfied; moreover, the expressions in Equations (14) and (15) are valid for points on surface S as well as for points outside. Now, the fields given by Equations (26), (33), (34), and (37) do satisfy Maxwell's equations; however, when the approximation in Equation (37) is substituted into Equation (33), the latter may no longer satisfy Maxwell's equations on S_1 because of the first term. Hence, a number of iterations may be required before the true values of $\underline{E}_{as}$, $\underline{H}_{as}$ on S_1 are found.

Other approaches to the determination of the first-order scattered fields $\underline{E}_{as}$, $\underline{H}_{as}$ include the integral equation formulation discussed by Poggio and Miller [22] for scattering from dielectric bodies. In this approach for the geometry of Figure 4, integral expressions are written in each region for the electric and magnetic fields in terms of the equivalent surface currents and charges via Equations (14) and (15). In Region I there are added terms $\underline{TE}_{ao}$, $\underline{TH}_{ao}$ in the integral expressions due to the incident fields. The boundary conditions at each material interface are then written using the integral expressions, resulting in a system of integral equations in the unknown surface charges and currents. In principle, the equations can be solved by the method of moments [27] or by iterative methods such as discussed above. The radiation fields in Region III could then be found directly from the solutions for the surface currents and charges on S_3 via Equations (14) and (15); however,

the contributions of the higher order scattered fields would not be included.

The techniques discussed in this section for the determination of the fields on a specified surface are directly applicable to the receiving formulation of the previous section. Most notably, in Equation (12), it is necessary to find the fields $\underline{E}^t_{bo}$, $\underline{H}^t_{bo}$ of Antenna "b" on the surface S_{ap} which coincides with the radiating aperture of Antenna "a". When Antenna "b" is greatly removed, the fields incident on the outside of the dielectric are those of an infinite plane wave. Appropriate adaptations of Equations (28) and (29) could be used to estimate the fields $\underline{E}^t_{bo}$, $\underline{H}^t_{bo}$ on the inner surface of the dielectric enclosure. The Huygens-Fresnel integrals of Equations (14) and (15) could then be applied to transform these fields to the surface S_{ap}. This approach is essentially that developed by Tricoles [28]. An integral equation approach could also be used, including the one described by Van Doeren [10].

IV. EQUIVALENCE OF FORMULATIONS

It is well known that the receiving and transmitting patterns of an antenna in free space are identical. In this section, it is theoretically demonstrated that the receiving and transmitting patterns for an antenna enclosed by a dielectric radome as in Figure 1 are also identical, and that the receiving and transmitting formulations of radome analysis lead to identical results. Establishment of the equivalence yields insight into the computational advantages of one formulation over the other and provides a means to compare numerical results obtained using the two approaches.

Consider the geometry of Figure 6 where $\hat{n}_b$ represents an infinitesimal electric current source of strength I_b, length $\Delta\ell$, and orientation $\hat{n}_b$ located at the point (x',y',z') which is a great distance R from the origin of coordinates. For definiteness, $\hat{n}_b$ is transverse to $\hat{R}_1$, which is the orientation that would normally be assigned for the measurement of the radiation pattern of Antenna "a" enclosed by the surface S_3. The fields $\underline{E}$, $\underline{H}$ at (x',y',z') due to Antenna "a" are given by Equations (14) and (15). For clarity, let $\underline{E}_T$, $\underline{H}_T$ represent the fields on S_3 produced by Antenna "a" when it is transmitting.

Let $\underline{E}_R$, $\underline{H}_R$ be the fields produced on S_3 by the current element $\hat{n}_b$. An application of the general reciprocity theorem to the unbounded region yields

$$\int_{S_3} (\underline{E}_T \times \underline{H}_R - \underline{E}_R \times \underline{H}_T) \cdot \hat{n}\, dS = - \underline{E} \cdot \hat{n}_b I_b \Delta\ell \tag{38}$$

A second application of the reciprocity theorem to Antenna "a" inside the surface S_3 as was done in the discussion leading up to Equation (13) yields the result that the complex voltage response of Antenna "a" to the fields $\underline{E}_R$, $\underline{H}_R$ incident on S_3 is proportional to the integral in Equation (38); hence,

$$V_R = I_b \Delta\ell\, \underline{E} \cdot \hat{n}_b = C \int_{S_3} (\underline{E}_T \times \underline{H}_R - \underline{E}_R \times \underline{H}_T) \cdot \hat{n}\, dS \tag{39}$$

where C is a complex constant.

Equation (39) provides the connection between the receiving and transmitting formulations and, as such, represents the third facet of

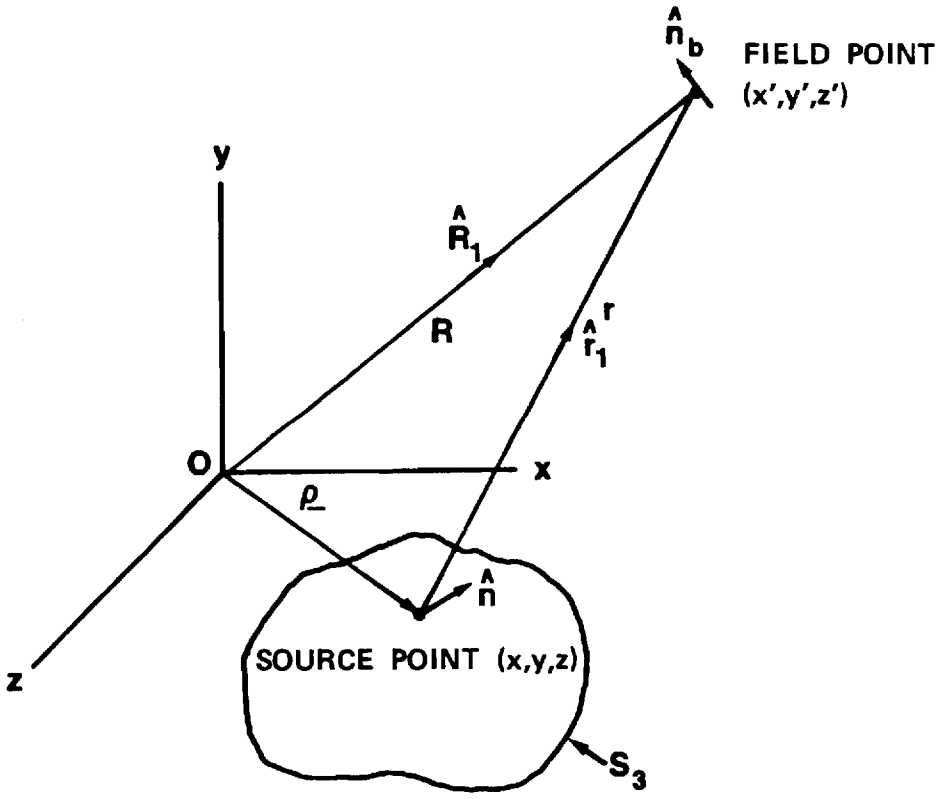

FIGURE 6. GEOMETRY USED TO ESTABLISH EQUIVALENCE BETWEEN THE RECEIVING AND TRANSMITTING FORMULATIONS OF RADOME ANALYSIS.

the theory of radome analysis. Basically, it states that if $\underline{E}$, $\underline{H}$ are the fields of Antenna "a" at (x',y',z') as determined via the Huygens-Fresnel principle, then the voltage response of Antenna "a" (when receiving) to an elementary current source at (x',y',z') is given succinctly by Equation (39) as $I_b \, \Delta\ell \, \underline{E} \cdot \hat{n}_b$. An antenna more complicated than the elementary current source could be assumed for Antenna "b": for the far-zone case, the same results would be obtained since the radiation and reception properties of the antenna can be embodied in a complex effective vector length $\hat{h}$ which is entirely analogous to $\hat{n}_b$ [29]; for the near-field case, the approach described by Paris et al. [30] would be required.

Even though Equation (39) is valid regardless of the separation and orientation of the elementary source, it is desired here to explicitly establish the second equality in that equation for the far-zone case. To this end, it is noted that the fields $\underline{E}^i_R$, $\underline{H}^i_R$ on S_3 are those of a plane electromagnetic wave propagating in the $\hat{k} = -\hat{R}_1$ direction with polarization properties given by $\hat{n}_b$ according to

$$\underline{E}^i_R = j\omega\mu \, \frac{e^{-jkR}}{R} \, \hat{n}_b \, e^{jk\hat{k}\cdot\underline{\rho}} \tag{40}$$

$$\underline{H}^i_R = \frac{\hat{k} \times \underline{E}_R}{\eta_o} = jk \, \frac{e^{-jkR}}{R} \, e^{jk\hat{k}\cdot\underline{\rho}} \, (\hat{n}_b \times \hat{R}_1) \tag{41}$$

where $k = \omega\mu/\eta_o = 2\pi/\lambda$ and where $\underline{\rho}$ is the position vector from the origin of coordinates to the source point on S_3 as indicated in Figure 6. The constant C in Equation (39) will be chosen to conform to these explicit expressions for the incident plane wave. When Equation (14) is substituted for $\underline{E}$ in $I_b \, \Delta\ell \, \underline{E} \cdot \hat{n}_b$, there results

$$V_R = \frac{I_b \Delta \ell}{4\pi} \int_S [-j\omega\mu \frac{e^{-jkR}}{R} e^{jk\hat{k}\cdot\underline{\rho}} \hat{n}_b \cdot (\hat{n} \times \underline{H}_T) + \hat{n}_b \cdot \Big((\hat{n} \times \underline{E}_T) \tag{42}$$

$$\times R_1 \frac{jke^{-jkR}}{R} e^{jk\hat{k}\cdot\underline{\rho}}\Big) + \hat{n}_b \cdot \nabla\psi_{ff}(\hat{n}\cdot\underline{E}_T)]dS$$

where the following asymptotic relations have been used:

$$r \sim R - \underline{R}_1 \cdot \underline{\rho} \tag{43}$$

$$\frac{e^{-jkr}}{r} \sim \frac{e^{-jkR}}{R} e^{jk\hat{k}\cdot\underline{\rho}} \tag{44}$$

$$\underline{\nabla\psi} \sim \underline{\nabla\psi}_{ff} = \hat{R}_1 jk \frac{e^{-jkR}}{R} e^{jk\hat{k}\cdot\underline{\rho}} \tag{45}$$

Applying the vector identity $\underline{a} \cdot \underline{b} \times \underline{c} = \underline{b} \cdot \underline{c} \times \underline{a}$ to the first term in the integrand of Equation (42) yields

$$-j\omega\mu \frac{e^{-jkR}}{R} e^{jk\hat{k}\cdot\underline{\rho}} \hat{n}_b \cdot (\hat{n} \times \underline{H}_T) = -j\omega\mu \frac{e^{-jkR}}{R} \hat{n} \cdot \underline{H}_T \times \hat{n}_b e^{jk\hat{k}\cdot\underline{\rho}} \tag{46}$$

$$= \underline{E}_R^i \times \underline{H}_T \cdot \hat{n} \tag{47}$$

i.e., it is equal to the negative of the second term of the integrand in Equation (39). Repeated application of the same vector identity to the second term in the integrand of Equation (42) yields

$$\hat{n}_b \cdot \Big((\hat{n} \times \underline{E}_T) \times \hat{R}_1 \frac{jke^{-jkR}}{R} e^{jk\hat{k}\cdot\underline{\rho}}\Big) = \hat{n} \cdot \Big(\underline{E}_T \times (jk \frac{e^{-jkR}}{R} e^{jk\hat{k}\cdot\underline{\rho}} \hat{R}_1 \times \hat{n}_b)\Big) \tag{48}$$

$$= - \underline{E}_T \times \underline{H}_R^i \tag{49}$$

i.e., it is equal to the negative of the first term in the integrand of Equation (39). The third term in the integrand of Equation (42) is identically zero since $\hat{n}_b$ is perpendicular to $\underline{\nabla}\psi_{ff}$. Collecting results yields the final desired result where the complex constant C is chosen to be

$$C = - \frac{I_b \, \Delta\ell}{4\pi} \tag{50}$$

to ensure equality.

A concise application of the foregoing analysis is to show that the response of Antenna "a" to the incident plane wave depends only on the incident fields $\underline{E}_R^i$, $\underline{H}_R^i$ and not on the scattered fields $\underline{E}_{RS}$, $\underline{H}_{RS}$. Direct examination of the first equality in Equation (39), as well as examination of Equations (47) and (49), revelas that this is indeed the case. The total fields $\underline{E}_R$, $\underline{H}_R$ on S_3 are given by the superposition of the incident and the scattered fields as

$$\underline{E}_R = \underline{E}_R^i + \underline{E}_{RS} \tag{51}$$

$$\underline{H}_R = \underline{H}_R^i + \underline{H}_{RS} \tag{52}$$

Substituting into the reciprocity integral of Equation (39) yields

$$V_R = C \int_{S_3} (\underline{E}_T \times \underline{H}_R^i - \underline{E}_R^i \times \underline{H}_T) \cdot \hat{n} \, dS + C \int_{S_3} (\underline{E}_T \times \underline{H}_{RS} - \underline{E}_{RS} \times \underline{H}_T) \cdot \hat{n} \, dS \tag{53}$$

The second integral must be identically zero because of the equivalence established explicitly above; also, it must be zero by virtue of the

reciprocity theorem itself as discussed in Section II above following Equation (10).

V. CONCLUSIONS

The theory of radome analysis is based entirely on the reciprocity theorem and the Huygens-Fresnel (or Kirchoff-Huygens) principle, both of which are derivable from Maxwell's equations via a vector Green's theorem and the divergence theorem (Gauss' Law). All methods of radome analysis can be cast in terms of the theory presented to provide a common basis of understanding, to clarify any approximations, and to provide a basis of comparison for the procedures used and numerical results obtained.

The theory presented provides the correct framework in which to think about radome analysis. Its understanding is of paramount importance to the correct development of new analysis methods which may utilize modern numerical methods such as method of moments, GTD, and hybrids of the two. The theory provides the basis for the development of even newer methods of analysis which may rely on special computer architectures or networks. Its presentation here provides a solid theoretical foundation for future thrusts in this important area.

ACKNOWLEDGMENTS

This research was sponsored by the Air Force Office of Scientific Research under Grant AFOSR-77-3469. The United States Government is authorized to reproduce and distribute reprints for governmental purposes notwithstanding any copyright notation hereon.

REFERENCES

1. R. F. Harrington and A. T. Villeneuve, "Reciprocal relations for gyrotropic media", IRE Trans., Vol. MMT-6, pp. 308-310, July 1958.

2. J. A. Stratton and L. J. Chu, "Diffraction theory of electromagnetic waves", Physical Review, Vol. 56, pp. 99-107, July 1939.

3. S. Silver, Microwave Antenna Theory and Design, New York: McGraw-Hill, 1949, pp. 80-84.

4. G. K. Huddleston, "Aperture synthesis of monopulse antenna for radome analysis using limited measured pattern data", submitted to IEEE Trans., AP, September 1980.

5. G. K. Huddleston, H. L. Bassett, and J. M. Newton, "Parametric investigation of radome analysis methods", 1978 IEEE AP-S Symposium Digest, pp. 199-201, 1978.

6. S. Silver, ibid., pp. 522-542.

7. N. R. Kilcoyne, "An approximate calculation of radome boresight error", Proc. USAF/Georgia Inst. of Tech. Symp. on Electromagnetic Windows, pp. 91-111, June 1968.

8. O. Snow, "Discussion of ellipticity produced by radomes and its effects on crossover point position for conically scanning antennas", U. S. Naval Air Development Center, Rpt. E15108, 1951.

9. P. I. Pressel, "Boresight prediction technique", Proc. OSU-WADC Radome Symposium, 1956.

10. R. E. VanDoeren, "Application of an integral equation method to scattering from dielectric rings", Proc. of the Symposium on Electromagnetic Windows, pp. 113-127, June 1968.

11. G. Tricoles, "Radiation patterns and boresight error of a microwave antenna enclosed in an axially symmetric dielectric shall", J. Opt. Soc. of Amer., 54, No. 9, pp. 1094-1101, Sept. 1964.

12. M. Tavis, "A three-dimensional ray tracing method for the calculation of radome boresight error and antenna pattern distortion", Report No. TOR-0059(56860)-2, Air Force Systems Command, May 1971.

13. D. T. Paris, "Computer-aided radome analysis", IEEE Trans., AP-18, No. 1, pp. 7-15, Jan. 1970.

14. D.C.F. Wu and R. C. Rudduck, "Application of plane wave spectrum representation to radome analysis", Proc. of the Tenth Symposium on Electromagnetic Windows, pp. 46-49, July 1970; also Final Report 2969-4 (AD 722 634), March 1971.

15. E. B. Joy and G. K. Huddleston, "Radome effects on ground mapping radar", Contract DAAH01-72-C-0598, U. S. Army Missile Command, March 1973.

16. Robert Chesnut, "LAMPS radome design", Proc. of the Thirteenth Symposium on Electromagnetic Windows, pp. 73-78, Sept. 1976.

17. G. K. Huddleston and E. B. Joy, "Development of fabrication and processing techniques for laser hardened missile radomes: radome electrical design analysis", MMC Purchase Agreement No. 573712, Martin-Marietta Aerospace, March 1977.

18. K. Siwiak, T. Dowling, L. R. Lewis, "The reaction approach to radome induced boresight error analysis", 1978 Inter. IEEE Symp. Digest, Antennas and Prop., pp. 203-205, May 1978.

19. R. A. Hayward, E. L. Rope, and G. P. Tricoles, "Accuracy of two methods for numerical analysis of radome electromagnetic effects", Proc. of the Fourteenth Symp. on Electromagnetic Windows, pp. 53-55, June 1978.

20. R. E. Collin and F. J. Zucker, Antenna Theory, Part 1, New York: McGraw-Hill, 1961, pp. 94-98.

21. R. F. Harrington, Time-Harmonic Electromagnetic Fields, New York: McGraw-Hill, 1961, pp. 100-110.

22. A. J. Poggio and E. K. Miller, "Integral equation solutions of three-dimensional scattering problems", in Computer Techniques for Electromagnetics, R. Mittra, Ed., New York: Pergamon, 1973, Ch. 4.

23. S. Silver, ibid., p. 63.

24. A.E.H. Love, "The integration of the equations of propagation of electric waves", Philosophical Transactions of the Royal Society of London, Vol. 197-A.287, pp. 1-45, February 1901.

25. R. F. Harrington, ibid., pp. 106-110.

26. S. Silver, ibid., pp. 146-149.

27. R. F. Harrington, Field Computation by Moment Methods, New York: McMillan, 1968.

28. R. A. Hayward, E. L. Rope, and G. Tricoles, "Radome boresight error and its relation to wavefront distortion", Proceedings of 13th Symposium on Electromagnetic Windows, Atlanta, Georgia, pp. 87-91, September 1976.

29. Collin and Zucker, ibid., p. 105.

30. D. T. Paris, E. B. Joy, W. M. Leach, and G. P. Rodrigue, "Basic theory of probe-compensated near-field measurements", IEEE Trans., Vol. AP-26, No. 3, pp. 373-379, May 1978.

APPENDIX B

"Aperture Synthesis of Monopulse Antenna for
Radome Analysis Using Limited Measured Pattern Data"

Submitted for Review for Publication

in

IEEE Transactions of the Antennas and Propagation Society

September 1980

Aperture Synthesis of Monopulse Antenna For Radome Analysis Using Limited Measured Pattern Data

G. K. Huddleston
School of Electrical Engineering
Georgia Institute of Technology
Atlanta, Georgia 30332
404-894-2928

Abstract

A planar aperture synthesis procedure which predicts measured radiation pattern data accurately and which exploits known physical parameters of the actual antenna is described for use in computer-aided radome analysis. The plane wave spectrum (PWS) representation, with the geometrical optics approximation, is used to characterize radiation from the array of four identical, discrete, conical horn elements that was studied. Solutions for the PWS of each element from measured array patterns over the visible region are presented, and a digital signal processing algorithm is described for extrapolating the aperture-limited PWS into the evanescent region as required to determine the near field of each element. The element near fields, having bounded support, are combined to produce a near field for the complete array. The array near field is used in a computer-aided radome analysis to demonstrate the accuracy to which the measured antenna patterns are predicted for the case of a free space radome. For completeness, comparisons of measured and computed patterns for a tangent ogive Rexolite ($\varepsilon_r = 2.54$) radome are presented.

INTRODUCTION

Valid comparisons of the accuracies of radome analysis methods using measured radiation patterns as true data [1] require that each method under consideration be capable of predicting accurately from a suitable antenna near field the antenna patterns measured in the absence of the radome; otherwise, any differences between measured and calculated patterns with the radome in place would be as attributable to the inadequacy of the antenna model as to the radome analysis method itself.

When the measured amplitude and phase of the antenna fields are known over a complete sphere enclosing the antenna, a complete aperture synthesis method such as that described by Ludwig can be used [2]. But when, as in many cases of practical importance, the measured pattern data is limited to amplitude-only, principal plane patterns, a different approach and one which exploits all available information about the antenna being modelled must be used.

Such a method of planar aperture synthesis for the four-horn monopulse antenna of Figure 1 using measured principal plane amplitude patterns of the sum, elevation difference, and azimuth difference channels is described in what follows. The radius ($a = .74\lambda$) and element half-spacing ($d_x = d_y = .95\lambda$) of each vertically (y) polarized conical horn element (10° flare angle) are used in the antenna model to describe radiation from it in the sinusoidal steady state (time variations of the form $e^{j\omega t}$ and suppressed). The aperture fields of each identical element in the four-horn array are

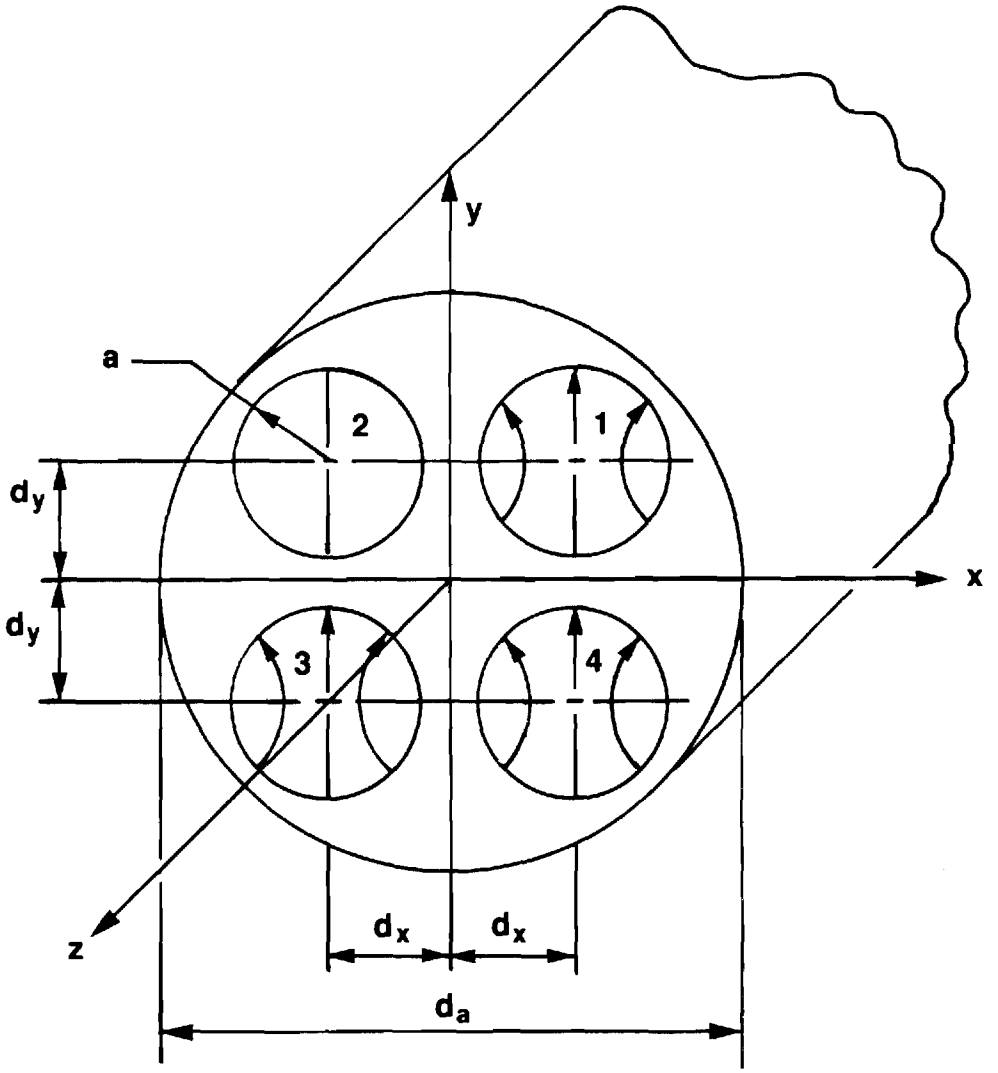

Figure 1. Geometry of Four–Horn Monopulse Antenna.

represented by their plane wave spectra [3] as determined in the principal planes from the measured patterns and the above physical parameters of the actual antenna. The two-dimensional plane wave spectra in the other radiating portions of the wavenumber $k_x k_y$-plane are determined according to a mathematical model deemed characteristic of the actual element and which utilizes principal plane spectra only; e.g., separable spectra, circularly symmetric spectra, etc. The element plane wave spectra in the non-radiating or evanescent region of the wavenumber plane are found by extrapolating the aperture-limited spectra from the visible to the invisible region using an algorithm described by Papoulis for one-dimensional band-limited functions [4]. The element plane wave spectra so found are then recombined with the array factor to produce the spectra for the complete antenna which, upon Fourier transformation, yields a near field for the antenna which accomplishes the desired result.

This antenna synthesis problem is motivated by an on-going parametric investigation of radome analysis methods [1]. A general theory has been developed, based on the Huygens-Fresnel principle and Lorentz reciprocity, which embodies the various methods of radome analysis [e.g., 5-10]. Computer codes for three typical methods have been implemented. Measured pattern data and boresight error data for three antenna sizes (small, medium, and large) combined in fifteen combinations with five radomes have been obtained to serve as true data in determining the accuracies and ranges of validity of the three methods of analysis. The particular monopulse antenna configuration [11] in Figure 1 was chosen for its ruggedness, ease of fabrication, and ease of duplication in the different physical sizes. Since the perturbations in the patterns and boresight errors caused by the radome are small, it is essential to the success of the research that the actual antennas be accurately modelled in the analyses so that

valid comparisons of the methods can be made. The synthesis procedure was developed specifically for this purpose and for this antenna configuration, but it has wider application and is applicable to more general configurations.

The plane wave spectrum representation of the antenna fields is well suited to the radome analysis application because of the computational efficiency which can accrue as a result of the Fourier transform relationship between the aperture fields and the plane wave spectra/far fields. And because of the asympototic relationships between the far fields and the plane wave spectra, the latter can be mathematically determined from the former, at least over the visible region corresponding to the hemisphere $z>0$. But before the desired near fields can be determined, it is necessary to assign values to the spectra corresponding to the evanescent or non-radiating modes. Failure to do so may result in a near field which, because it contains only radiating modes, may be too spread out to fit within the confines of the radome for analysis purposes.

In the synthesis procedure here, values are assigned to the evanescent modes by extrapolating the plane wave spectra from the known visible region into the evanescent region. Such extrapolation is valid only for an aperture-limited spectrum; i.e., a spectrum which is the Fourier transform (or inverse transform) of an aperture field which has bounded support. Such a spectrum is an entire function [12] of the (complex) wavenumbers k_x, k_y whose value in one region of the complex k_x and k_y planes can, in principle, be determined by analytic continuation from a known region [13]. The algorithm described by Papoulis provides a practical, computer-aided procedure for implementing the extrapolation; it is also computationally efficient since the Fast Fourier Transform (FFT) algorithm can be exploited.

This synthesis problem is actually an inverse source problem such as that described by Schmidt-Weinmar and Baltes [14] in which prior knowledge about the source plays an important role. It is well known that such problems involve the mathematical questions of existence, uniqueness, and stability of the solution. Small errors in the experimental data, (errors and noise are inevitably present) can lead to large errors in the solution unless suitable stabilizing constraints are imposed; i.e., unless additional prior knowledge can be taken for granted or known to be fact. The procedure described here utilizes a novel combination of known and assumed data, the sum of which provides enough information to produce a stable solution to the inverse problem which fits all the prescribed known data -- but which may not be unique. The question of uniqueness and the amount of information, both prior knowledge and measured data, needed to ensure uniqueness is the subject of a current investigation.

This paper presents the solution for the plane wave spectra of the antenna in terms of the measured patterns and the physical parameters of the antenna. Spectrum functions separable in rectangular and in polar coordinates are presented which permit the specification of the complete radiating spectrum from knowledge of it in only the principal planes. The extrapolation procedure in both one dimension and in two dimensions is detailed and used to effect solutions for a theoretical antenna, whose solution is known exactly for verification purposes, and for the actual antenna. Computer generated results are presented in the forms of radiation pattern comparisons and three-dimensional plots of the near fields and plane wave spectra. To demonstrate applicability and for completeness, some radome analysis results are presented.

THEORETICAL DERIVATIONS

The synthesis procedure is carried out independently in the two principal planes to determine the plane wave spectra $A_{xe}(k_x,k_y)$, A_{ye}, and aperture fields $E_{xe}(x,y)$, E_{ye} of each identical element in the four-horn array of Figure 1. The general expression for the radiation field of the array may be written as a product of the element field and the array factor as

$$\underline{E}_{ff}(k_x,k_y) = \underline{E}_{eff}(k_x,k_y)\,[a_1\, e^{jk_o(d_x k_x + d_y k_y)} + a_2\, e^{jk_o(-d_x k_x + d_y k_y)} + a_3\, e^{jk_o(-d_x k_x - d_y k_y)} + a_4\, e^{jk_o(d_x k_x - d_y k_y)}] \quad (1)$$

where $k_o=2\pi/\lambda$, $j=\sqrt{-1}$, the a_i's are the complex excitation coefficients of the elements numbered and spaced as shown in Figure 1, $\underline{E}_{eff}$ is the radiation (electric) field of the element, and the normalized wavenumbers k_x, k_y are related to spherical angles θ, ϕ of Figure 2 by

$$k_x = \sin\theta \cos\phi \quad (2)$$

$$k_y = \sin\theta \sin\phi\ , \quad (3)$$

at least for the visible region defined by $\sqrt{k_x^2+k_y^2} \leq 1$

The three monopulse channels of the antenna are formed by phasing the elements appropriately. In the ideal case, $|a_i|=1$ for i=1-4. For the sum (Σ) channel, all elements are assigned equal phase. For the elevation difference (Δ_{EL}) channel, $a_1=a_2=-a_3=-a_4$. For the azimuth difference (Δ_{AZ}) channel, $a_1=a_4=-a_2=-a_3$. For perfect assignment of the excitation coefficients, there results

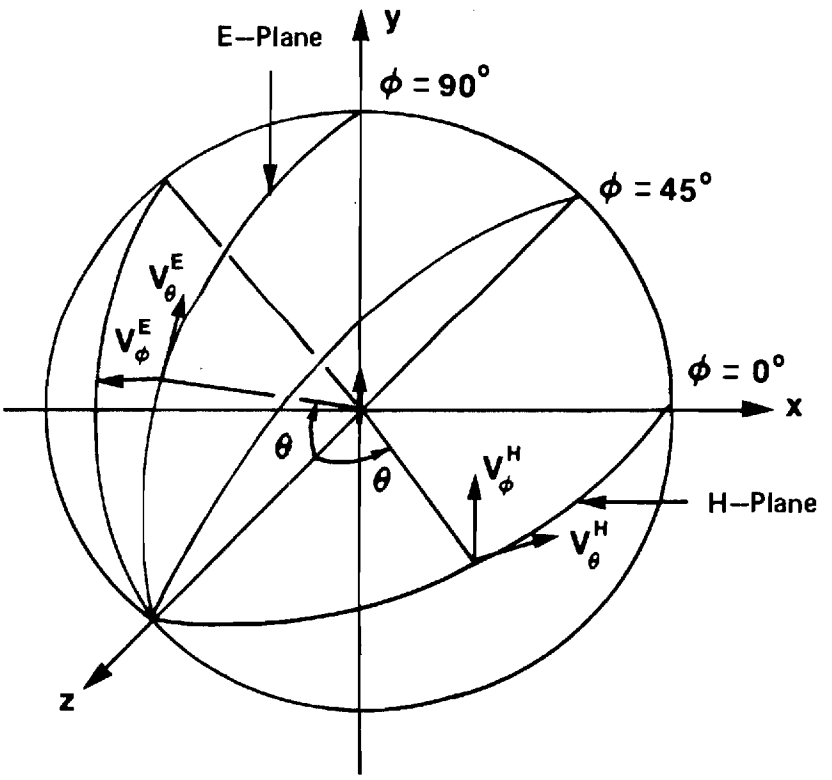

FIGURE 2. COORDINATE SYSTEM FOR ANTENNA PATTERN MEASUREMENTS ON VERTICALLY POLARIZED ANTENNA.

$$\underline{E}_{ff\Sigma} = \underline{E}_{eff}(k_x,k_y)(4 \cos k_o d_x k_x \cos k_o d_y k_y) \tag{4}$$

$$\underline{E}_{ff\Delta EL} = \underline{E}_{eff}(k_x,k_y)(j\ 4 \cos k_o d_x k_x \sin k_o d_y k_y) \tag{5}$$

$$\underline{E}_{ff\Delta AZ} = \underline{E}_{eff}(k_x,k_y)(j\ 4 \sin k_o d_x k_x \cos k_o d_y k_y) \tag{6}$$

In the non-ideal case encountered in practice, the excitation coefficient values may vary somewhat from the ideal values so that the complex array factor of Equation (1) must be used in solving for the element field and plane wave spectra of measured sum and difference patterns.

The radiation field of the element is related to its plane wave spectra according to [15]

$$\begin{aligned}\underline{E}_{eff}(k_x k_y) = \quad & \hat{x}[(1+k_z-k_x^2)\ A_{xe} - k_x k_y\ A_{ye}] \\ & + \hat{y}[-k_x k_y\ A_{xe} + (1+k_z-k_y^2)\ A_{ye}] \\ & + \hat{z}[-k_x(1+k_z)A_{xe} - k_y(1+k_z)\ A_{ye}]\end{aligned} \tag{7}$$

where $k_z=\sqrt{1-k_x^2-k_y^2}$. The geometrical optics approximation [16] has been assumed for the aperture fields in the conical horn element; viz.,

$$\underline{H}_{ap} = \frac{\hat{z} \times \underline{E}_{ap}}{\eta} \tag{8}$$

where $\hat{x}$, $\hat{y}$, $\hat{z}$ are unit vectors in the rectangular coordinate system of Figure 2 and η is the wave impedance. In Equation (7), the radiation factor of the form e^{-jkr}/r has been suppressed where r is the radial

distance from the origin of antenna coordinates to the far-field measurement sphere of Figure 2.

Equation (7) may also be written in terms of the transverse spherical components as

$$\underline{E}_{eff}(k_x,k_y) = \frac{(1+k_z)}{\sqrt{k_x^2+k_y^2}} [\hat{\theta}(k_x A_{xe} + k_y A_{ye}) + \hat{\phi}(-k_y A_{xe} + k_x A_{ye})] \qquad (9)$$

which is a form more suitable to solution for A_{xe}, A_{ye} in terms of the measured transverse components E_θ, E_ϕ or the related measured quantities V_θ, V_ϕ defined by

$$V_\theta = \begin{cases} E_\theta , & k_x > 0 \\ -E_\theta , & k_x < 0 \end{cases}$$

$$V_\phi = \begin{cases} E_\phi , & k_x \quad 0 \\ -E_\phi , & k_x \quad 0 \end{cases} \qquad (11)$$

For k_x=0 (E-plane), the definitions above apply when k_y is substituted for k_x. Let AF_i, i=1,2,3, denote the array factors associated with the Σ, Δ_{EL}, Δ_{AZ} channels, respectively, modelled in Equation (1). Then the solutions for the element spectra are given by

$$A_{xe}(k_x,k_y) = \frac{k_x V_{\theta i} - k_y V_{\phi i}}{(1+k_z)\sqrt{k_x^2+k_y^2}\, AF_i} \qquad (12)$$

$$A_{ye}(k_x,k_y) = \frac{k_y V_{\theta i} + k_x V_{\phi i}}{(1+k_z)\sqrt{k_x^2+k_y^2} AF_i} \qquad (13)$$

for all k_x, k_y such that $0 \leq k_z < 1$. At the pole, $k_z = 1$ and the spectra may be found from the sum channel measured voltages as

$$A_{xe}(0,0) = V^{H}_{\theta 1}(0,0) = -V^{E}_{\phi 1}(0,0) \tag{14}$$

$$A_{ye}(0,0) = V^{H}_{\phi 1}(0,0) = V^{E}_{\theta 1}(0,0) \tag{15}$$

where the superscripts denote the conventional E and H planes [17]. The general expressions in Equations (12) and (13) can be specialized to these principal planes as follows:

H-Plane ($k_y = 0$):

$$A_{xe}(k_x,0) = \frac{V^{H}_{\theta i}(k_x)}{(1+\sqrt{1-k_x^2})AF_i} \tag{16}$$

$$A_{ye}(k_x,0) = \frac{V^{H}_{\phi i}(k_x)}{(1+\sqrt{1-k_x^2})AF_i} \tag{17}$$

E-Plane ($k_x = 0$):

$$A_{xe}(0,k_y) = \frac{-V^{E}_{\phi i}(k_y)}{(1+\sqrt{1-k_y^2})AF_i} \tag{18}$$

$$A_{ye}(0,k_y) = \frac{V^{E}_{\theta i}(k_y)}{(1+\sqrt{1-ky^2})AF_i} \tag{19}$$

When numerically evaluating Equations (16)-(19), the channel index i is chosen on the basis of highest signal level. For example, the Σ channel (i=1) provides the best data for small $|k_x|$ in the H-plane; however, as $|k_x|$ increases, the sum channel amplitude decreases toward the first null in the array factor AF_1 while the Δ_{AZ} channel amplitude increases toward its peak at $k_x \approx \pm\sin^{-1}((4d_x/\lambda)^{-1})$. When alternating between the data sets, it is important to ensure that the measured difference channel data is correctly normalized with respect to the sum data as dictated by the model in Equation (1). For ideal excitation coefficients, the ratio of difference channel response to sum channel response is given in each principal plane by

H-Plane:

$$\frac{\Delta_{AZ}(k_x,0)}{\Sigma\ (k_x,0)} = j\ \tan\ k_o d_x k_x \tag{20}$$

E-Plane:

$$\frac{\Delta_{EL}(0,k_y)}{\Sigma\ (0,k_y)} = j\ \tan\ k_o\ d_y k_y \tag{21}$$

These relationships can be used to adjust the measured data for consistent solutions of the element spectra.

The measured quantities $V_{\theta i}$, $V_{\phi i}$ in Equations (16)-(19) are complex quantities usually measured using a phase/amplitude receiver. In those myriad cases where far-field phase data are not valid due to range imperfections, unstable microwave sources, etc., some assumption must be made in assigning phase values to the measured amplitude data at each angular direction. In this investigation, phase data were assigned as dictated by the array factor for each channel. The phase of the

element was assumed constant. The phase reconstruction problem [18] was beyond the scope of the present work.

In practice, the excitation coefficients a_i will differ from their ideal values to produce asymmetries in the measured patterns. Values of the excitation coefficients based on the asymmetries in the sum patterns may be found, in paired combinations, as

$$a_{14} = (a_1 + a_4) = \frac{8(e^{j\psi} V^H_{\phi 1}(k_x) - e^{-j\psi} V^H_{\phi 1}(-k_x))}{(e^{j2\psi} - e^{-j2\psi})(1 + k_z)A_{ye}(k_x,0)} \tag{22}$$

$$a_{23} = (a_2 + a_3) = \frac{8(e^{j\psi} V^H_{\phi 1}(-k_x) - e^{-j\psi} V^H_{\phi 1}(k_x))}{(e^{j2\psi} - e^{-j2\psi})(1 + k_z)A_{ye}(-k_x,0)} \tag{23}$$

$$a_{12} = (a_1 + a_2) = \frac{8(e^{j\psi} V^E_{\theta 1}(k_x) - e^{-j\psi} V^E_{\theta 1}(-k_x))}{(e^{j2\psi} - e^{-j2\psi})(1 + k_z)A_{ye}(0,k_x)} \tag{24}$$

$$a_{34} = (a_3 + a_4) = \frac{8(e^{j\psi} V^E_{\theta 1}(-k_x) - e^{-j\psi} V^E_{\theta 1}(k_x))}{(e^{j2\psi} - e^{-j2\psi})(1 + k_z)A_{ye}(0,-k_x)} \tag{25}$$

where

$$\psi = k_o d_x k_x = k_o d_y k_x \tag{26}$$

$$k_z = \sqrt{1 - k_x^2} \tag{27}$$

and where k_x=sinθ is a conveniently chosen point in the sum pattern principal planes, such as the angle corresponding to the peak of the first sidelobe. It is noted that the values of A_{ye} appearing in Equations (22)-

(25) depend on the excitation coefficients; hence, an iterative procedure is indicated. The individual excitation coefficients can then be found, to within a constant, from the four above equations. For definiteness, a value of (1+j0) may be assigned to a_1. The solutions for the other coefficients follow as:

$$a_2 = a_{12} - 1 \tag{28}$$

$$a_3 = a_{34} - a_{14} + 1 \tag{29}$$

$$a_4 = a_{14} - 1 \tag{30}$$

The near fields of the element can be found from the principal plane PWS via Fourier transformation only for the special case of rectangularly separable spectra; i.e.,

$$A_{xe}(k_x,k_y) = p_x(k_x)\ q_x(k_y) \tag{31}$$

$$A_{ye}(k_x,k_y) = p_y(k_x)\ q_y(k_y) \tag{32}$$

In such case, the near fields are also separable and given by

$$c_1 E_{xenf}(x,y) = c_1\ P_x(x)\ Q_x(y) = q_x(0)\ p_x(0)\ F\{p_x(k_x)\}\ F\{q_x(k_y)\} \tag{33}$$

$$c_2 E_{yenf}(x,y) = c_2\ P_y(x)\ Q_y(y) = q_y(0)\ p_y(0)\ F\{p_y(k_x)\}\ F\{q_y(k_y)\} \tag{34}$$

where F{ } denotes Fourier transform and where constants c_1 and c_2 are given by

$$c_1 = p_x(0)\ q_x(0) = \frac{V^H_{\theta 1}(0)}{8} \tag{35}$$

$$c_2 = p_y(0)\ q_y(0) = \frac{V^H_{\phi 1}(0)}{8} \tag{36}$$

The Fourier transformation above implies that the spectra are known for all k_x (k_y) on the real line; however, Equations (16)-(19) produce solutions only in the visible region $|k_x| \leq 1$, $|k_y| \leq 1$ of the principal planes. The extrapolation technique for assigning values to the spectra outside the visible region will be deferred until after the discussion immediately below concerning another type of separability for spectra and near fields which will be applied during the synthesis procedure.

The TE_{11} circular waveguide mode (y-polarized) provides a model for an element near field that is separable in cylindrical coordinates ρ and ϕ, and which depends only on knowledge of the principal plane PWS. Assume that the element near field can be written as

$$\underline{E}_{nf}(\rho,\phi) = \hat{\rho}\ f_\rho(\rho)\ g_\rho(\phi) + \hat{\phi}\ f_\phi(\rho)\ g_\phi(\phi) \tag{37}$$

Convert to rectangular coordinates and assume, as in the case of the TE_{11} waveguide mode, that

$$g_\rho(\phi) = \sin\phi \tag{38}$$

$$g_\phi(\phi) = \cos\phi \tag{39}$$

The element (tangential) near field can then be expressed in rectangular coordinates as

$$\underline{E}_{nf}(x,y) = \hat{x}\ \frac{f_\rho - f_\phi}{2} \sin 2\phi + \hat{y}\ \left(\frac{f_\rho + f_\phi}{2} - \frac{f_\rho - f_\phi}{2} \cos 2\phi\right) \tag{40}$$

where $x=\rho\cos\phi$, $y=\rho\sin\phi$ as usual. Inverse Fourier transform these rectangular components to yield integrals

$$A_x(k_x,k_y) = \int_0^a \frac{f_\rho - f_\phi}{2}\, \rho d\rho \int_0^{2\pi} \sin 2\phi\ e^{j2\pi\rho\, k_\rho \cos(\phi-\xi)} d\phi \tag{41}$$

$$A_y(k_x,k_y) = \int_0^a \frac{f_\rho + f_\phi}{2}\, \rho d\rho \int_0^{2\pi} e^{j2\pi\rho k_\rho \cos(\phi-\xi)} d\phi \tag{42}$$

$$- \int \frac{f_\rho - f_\phi}{2}\, \rho d\rho \int_0^{2\pi} \cos 2\phi\ e^{j2\pi\rho\, k_\rho \cos(\phi-\xi)} d\phi$$

Carry out the integrations in ϕ [19] to obtain

$$A_x(k_x,k_y) = -2\pi \frac{k_x k_y}{k_\rho^2} H_0(k_\rho) \tag{43}$$

$$A_y(k_x,k_y) = \pi H_0(k_\rho) + \pi \frac{k_x^2 - k_y^2}{k_\rho^2} H_2(k_\rho) \tag{44}$$

where $k_\rho = \sqrt{k_x^2 + k_y^2}$ and where the Hankel transforms H_0, H_2 are defined by [20]

$$H_0(k_\rho) \triangleq \int_0^a (f_\rho + f_\phi)\, J_0(k_\rho \rho)\, \rho d\rho \tag{45}$$

$$H_2(k_\rho) \triangleq \int_0^a (f_\rho - f_\phi)\, J_2(k_\rho \rho)\, \rho d\rho \tag{46}$$

Specialize Equations (43) and (44) to the principal planes, and solve the resulting system of equations for H_0, H_2 to yield

$$H_0(k_\rho) = \frac{A_y(k_\rho,0) + A_y(0,k_\rho)}{2\pi} \tag{47}$$

$$H_2(k_\rho) = \frac{A_y(k_\rho,0) - A_y(0,k_\rho)}{2\pi} \tag{48}$$

Thus, the two-dimensional plane wave spectra A_x, A_y are expressible in terms of only the principal plane spectra via Equations (43)-(48).

Since the assumed trigonometric variations of g_ρ, g_ϕ in Equations (38) and (39) do not produce any x-component of near field along x=0 or y=0, a similar analysis can be carried out for an orthogonal TE-type mode which will account for the presence of such cross-polarized components. Write the total element fields as the sum of two components

$$\underline{E}_{enf} = \hat{\rho}\,(E_\rho + E'_\rho) + \hat{\phi}\,(E_\phi + E'_\phi) \tag{49}$$

where E_ρ, E_ϕ are given in Equation (37) and where

$$E'_\rho = f'_\rho(\rho)\, g'_\rho(\phi) = f'_\rho \cos\phi \tag{50}$$

$$E'_\phi = f'_\phi(\rho)\, g'_\phi(\phi) = f'_\phi \sin\phi \tag{51}$$

Follow through with the analysis and define Hankel transforms G_0, G_2 by

$$G_0(k_\rho) = \int_0^a (f'_\rho - f'_\phi)\, J_0(k_\rho \rho)\, \rho d\rho \tag{52}$$

$$G_2(k_\rho) = \int_0^a (f'_\rho + f'_\phi)\, J_2(k_\rho \rho)\, \rho d\rho \tag{53}$$

Combine all results for the two orthogonal modes to yield the following expressions for the element plane wave spectra in terms of the principal plane spectra $A^H_{xe}(k_\rho)$, $A^E_{xe}(k_\rho)$, $A^H_{ye}(k_\rho)$, $A^E_{ye}(k_\rho)$:

$$A_{xe}(k_x,k_y) = \frac{A^H_{xe}+A^E_{xe}}{2} + \frac{k_x^2-k_y^2}{k_\rho^2}\left(\frac{A^H_{xe}-A^E_{xe}}{2}\right) + \frac{k_x k_y}{k_\rho^2}\,(A^E_{ye}-A^H_{ye}) \tag{54}$$

$$A_{ye}(k_x,k_y) = \frac{A^H_{ye}+A^E_{ye}}{2} + \frac{k_x^2-k_y^2}{k_\rho^2}\left(\frac{A^H_{ye}-A^E_{ye}}{2}\right) + \frac{k_x k_y}{k_\rho^2}\,(A^H_{xe}-A^E_{xe}) \tag{55}$$

The above two equations constitute a reasonable model for the plane wave spectra of a circular element such as that shown in Figure 1. The principal plane spectra in these equations are found from measured principal plane patterns via Equations (16)-(19). Note that the above equations reduce identically to the measured spectra in the principal planes. Note also that the model is based on the characteristic modes of a circular aperture geometry and, in the absence of complete measured data which could perhaps determine exactly the plane wave spectra off the principal planes, this model is more suitable for the antenna described than is the model of Equations (31)-(32) which assumes rectangular

separability. Strictly speaking, the latter would more suitable for use with a rectangular element geometry, but does find application in the extrapolation procedure described next.

EXTRAPOLATION PROCEDURE

The extrapolation procedure is best explained in one dimension before extending it to the two-dimensional case. The objective of the procedure is to assign values to the evanescent modes in the plane wave spectrum of the element such that the known spectrum in the visible region is preserved and such that the near field of the element is restricted to a finite portion of the xy-plane. Results are presented in this section which demonstrate the algorithm for both an ideal case and a case which uses measured data.

The flow chart in Figure 3 summarizes the extrapolation procedure for the case of plane wave spectrum $A_x(k_x)$ and its corresponding near field $E_x(x)=F\{A_x(k_x)\}$. The zeroeth estimate to the actual spectrum is the portion known only over radiating wavenumbers as defined by

$$A_{xo}(k_x) = \begin{cases} A_x(k_x) & , \quad |k_x| \leq 1 \\ 0 & , \quad \text{elsewhere} \end{cases} \tag{56}$$

The known length 2a of the interval over which the near field is non-zero, and a lower bound $1-\varepsilon$ on the fraction of energy in the near field which must be contained in this interval for an acceptable solution, constitute the remaining elements of input data.

The first estimate E'_{xo} of the near field is found by Fourier transformation of A_{xo}. Due to the lack of radiating modes in the spectra, the near field will be spread out in x. That portion lying

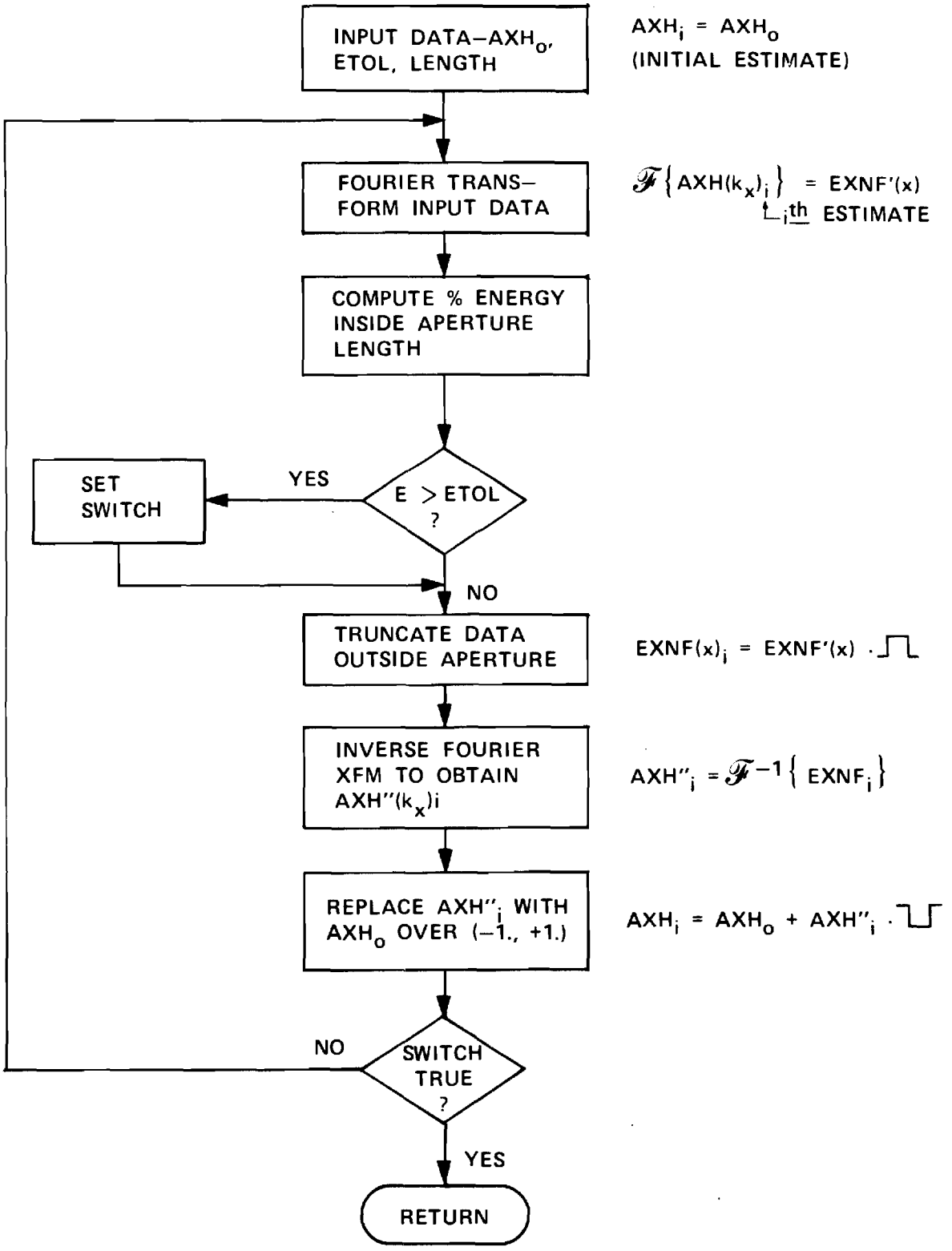

FIGURE 3. FLOW CHART FOR EXTRAPOLATION ALGORITHM.

outside $|x| \leq a$ is then truncated so that $E_{xo} = E'_{xo}\, p_a(x)$ results, where $p_a(x)$ is the rectangular function whose value is unity for $|x| \leq a$ and zero elsewhere. The resulting near field E_{xo} is inverse Fourier transformed to produce the spectrum $A'_{x1}(k_x)$ which does contain non-zero evanescent modes due to the bounded support of E_{xo}. The evanescent modes of A'_{x1} are added to the radiating modes A_{xo} to produce the first-order spectrum $A_{x1} = A_{xo} + A'_{x1}\, \bar{p}_1(k_x)$ where $\bar{p}_1(k_x)$ is the complement of the rectangular function whose value is unity for $|x| > a$ and zero for $|x| \leq a$. The process is repeated until the fraction of energy in the near field $E_{xi}(x)$ on the interval $|x| \leq a$ exceeds the lower bound specified. The FFT algorithm is used to effect the Fourier transformations.

The algorithm was first tested on an ideal four-horn monopulse array (Figure 1) where a TE_{11} circular waveguide mode was assumed present in each element. The mode was y-polarized but then rotated by $\alpha = 5°$ counterclockwise so that a small x-component of radiated field would be present. The far fields of the array were computed at 2° increments in the principal planes for all three channels over a dynamic range of 40 decibels. These data were used as the "measured" data $V_{\theta i}$, $V_{\phi i}$ in Equations (16)-(19) to produce element spectra $A^H_{xe}(k_x)$, $A^H_{ye}(k_x)$, $A^E_{xe}(k_y)$, $A^E_{ye}(k_y)$ over the visible region in each plane at 2° increments in polar angle θ. Since the discrete Fourier transform relationship between spectrum and near field requires samples of the spectra at equal increments in wavenumber $k_x = \sin\theta$, a Whittaker-Shannon expansion [21] was used to Fourier interpolate the spectrum samples at equal angle; i.e.,

$$A(\theta) = \sum_{m=1}^{N} A(\theta_m)\, \frac{\sin\left(\pi N \dfrac{\theta - \theta_m}{2\,\theta_{max}}\right)}{\pi N \dfrac{\theta - \theta_m}{2\,\theta_{max}}} \tag{57}$$

where $\theta=\sin^{-1} k_x$, N = number of angular samples (91), and θ_{max} = angle corresponding to the Nth sample (90°). The interpolated spectra were then operated on in turn by the extrapolation algorithm.

Some computed results are shown in Figure 4 where comparisons of the true and synthesized near fields of the element in the x=0 plane are presented. The true x and y field components are simply those of the rotated TE_{11} mode. After twenty-one iterations of the extrapolation algorithm, the concentration factors for the x and y components were $\varepsilon_x^E = .013$ and $\varepsilon_y^E = .330 \times 10^{-4}$, respectively. (In the y=0 plane, slightly better results were obtained; i.e., $\varepsilon_x^H = .0153$, $\varepsilon_y^H = .982 \times 10^{-5}$). The half-length of the interval occupied by the element was $a=.74136\lambda$. The algorithm was quite successful in concentrating the near field into the desired interval and in predicting the spatial variation of the near field reasonably well. The sample spacing in the near field was $\Delta y=\lambda/8$.

The element near fields in Figure 4 were (inverse) Fourier transformed to produce the corresponding spectra at equal wavenumber over the range $|k_y| \le k_{ymax}=(2\ \Delta y/\lambda)^{-1}=4$. The spectra were then Fourier interpolated, to produce their values at 2° increments over the range $|\theta| \le 90°$ according to

$$A(k_y) = \sum_{m=1}^{N} A(k_{ym}) \frac{\sin\left(\pi N \frac{k_y - k_{ym}}{2\ k_{ymax}}\right)}{\pi N \frac{k_y - k_{ym}}{2\ k_{ymax}}} \tag{58}$$

The interpolated values were used in the antenna model of Equation (1) to produce the sum channel E-plane patterns shown in Figure 5. Differences between the true and synthesized primary E_θ^E components are hardly

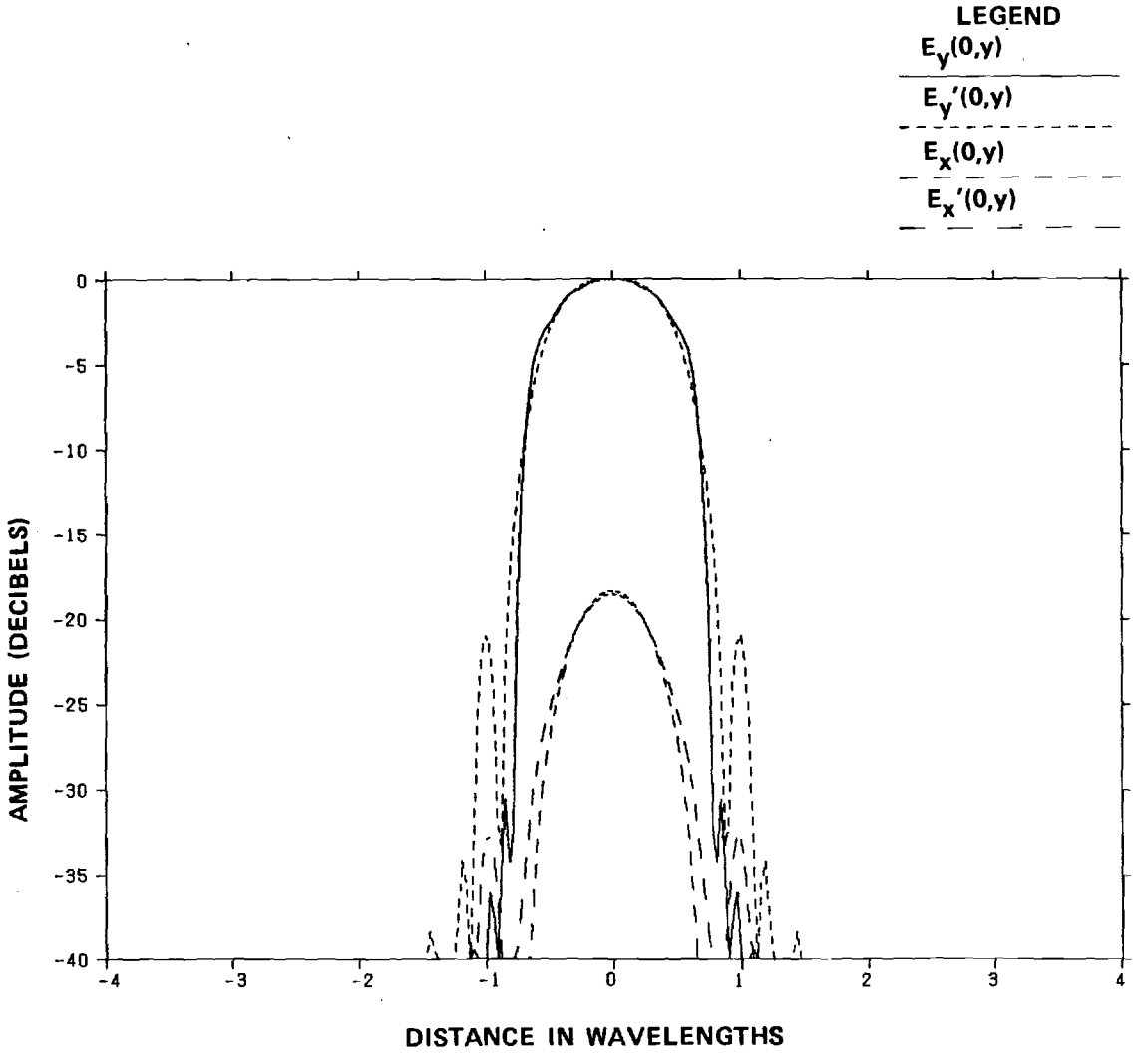

FIGURE 4. COMPARISONS OF TRUE AND SYNTHESIZED (') NEAR FIELDS OF THEORETICAL FOUR–HORN MONOPULSE ANTENNA ELEMENT ($\alpha = 5^{o}$).

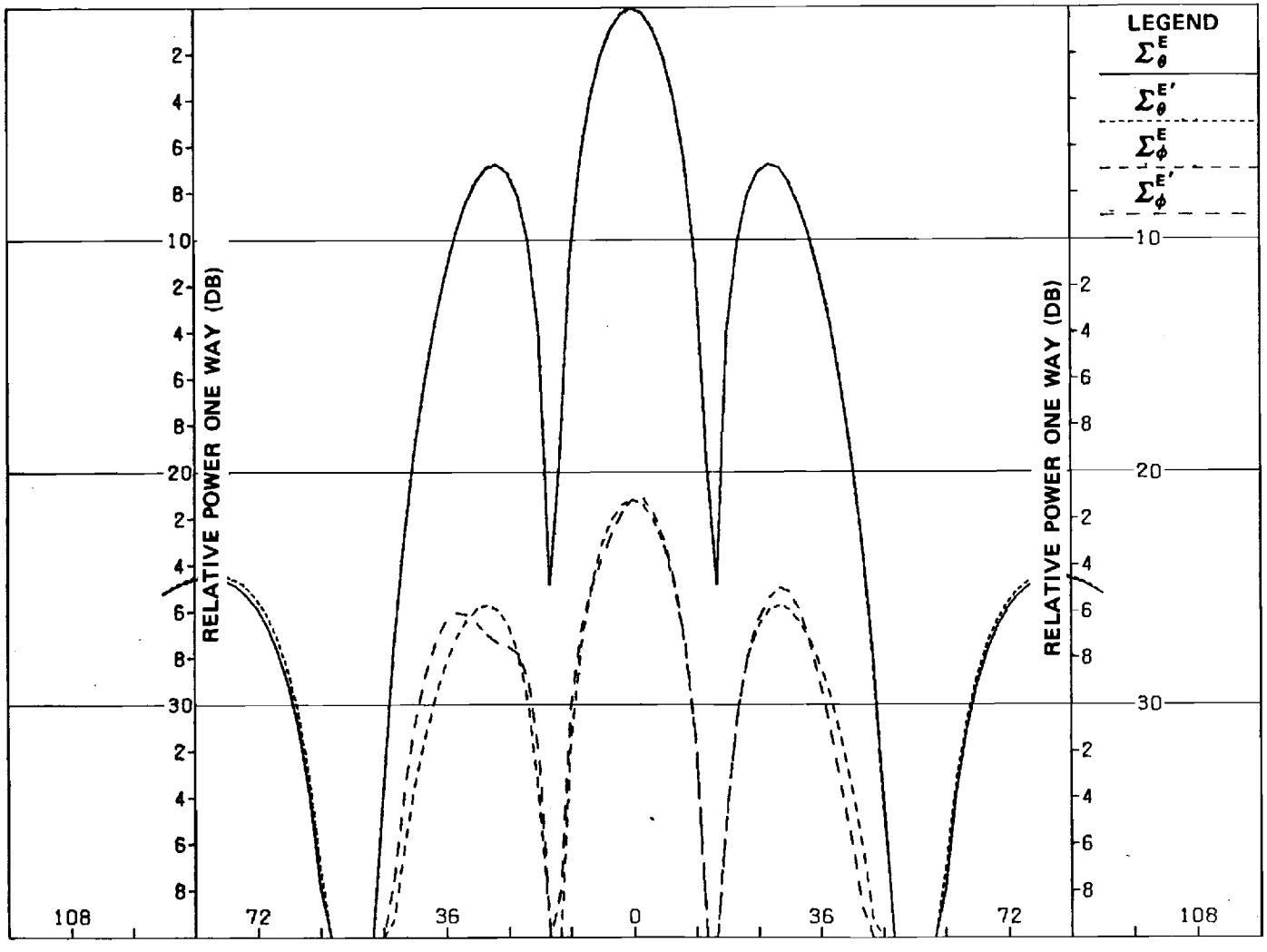

FIGURE 5. COMPARISONS OF TRUE AND SYNTHESIZED (') E–PLANE SUM PATTERNS OF THEORETICAL FOUR–HORN MONOPULSE ANTENNA ($a = 5^o$).

discernable except at very wide angles. Good agreement is obtained for the cross E_{ϕ}^{E} component where all amplitude levels are less than -20 dB. Similar results were obtained in the H-plane and for the other two channels. In conclusion, the synthesis procedure works quite well in one dimension for theoretical data having a dynamic range of 40 decibels.

The one-dimensional synthesis procedure was next tested using principal plane patterns obtained at 35 GHz for the actual antenna of Figure 1. Figure 6 shows the first and final estimates of the element near field in the x=0 plane. After 51 iterations of the extrapolation algorithm, the E-plane concentration factors were ε_x^E=.069 and ε_y^E=.38 x 10^{-3}. (The H-plane concentration factors were ε_x^H=.508 and ε_y^H=.494 x 10^{-2}.) The sample spacing was $\Delta y=.025\lambda$, yielding a maximum wavenumber $k_{ymax}=20$ for N=256 samples over the total interval of 6.4λ. Referring to Figure 6, it is seen that the algorithm successfully concentrated the near field into the interval $|y| \leq a=.74136\lambda$ as desired.

Figure 7 shows comparisons of the measured patterns with those synthesized from the extrapolated element spectra as explained above for the ideal array. The agreement is quite good in the E-plane. Similar results were obtained for the H-plane and for the other two channels. In conclusion, the synthesis procedure works well for measured, one-dimensional data having a 40-dB dynamic range.

TWO DIMENSIONAL EXTRAPOLATION

The one dimensional results could be used through Equations (31) and (32) to generate two-dimensional spectra and near fields; however, if the $\rho\phi$-separability model is used as preferred, then the extrapolation

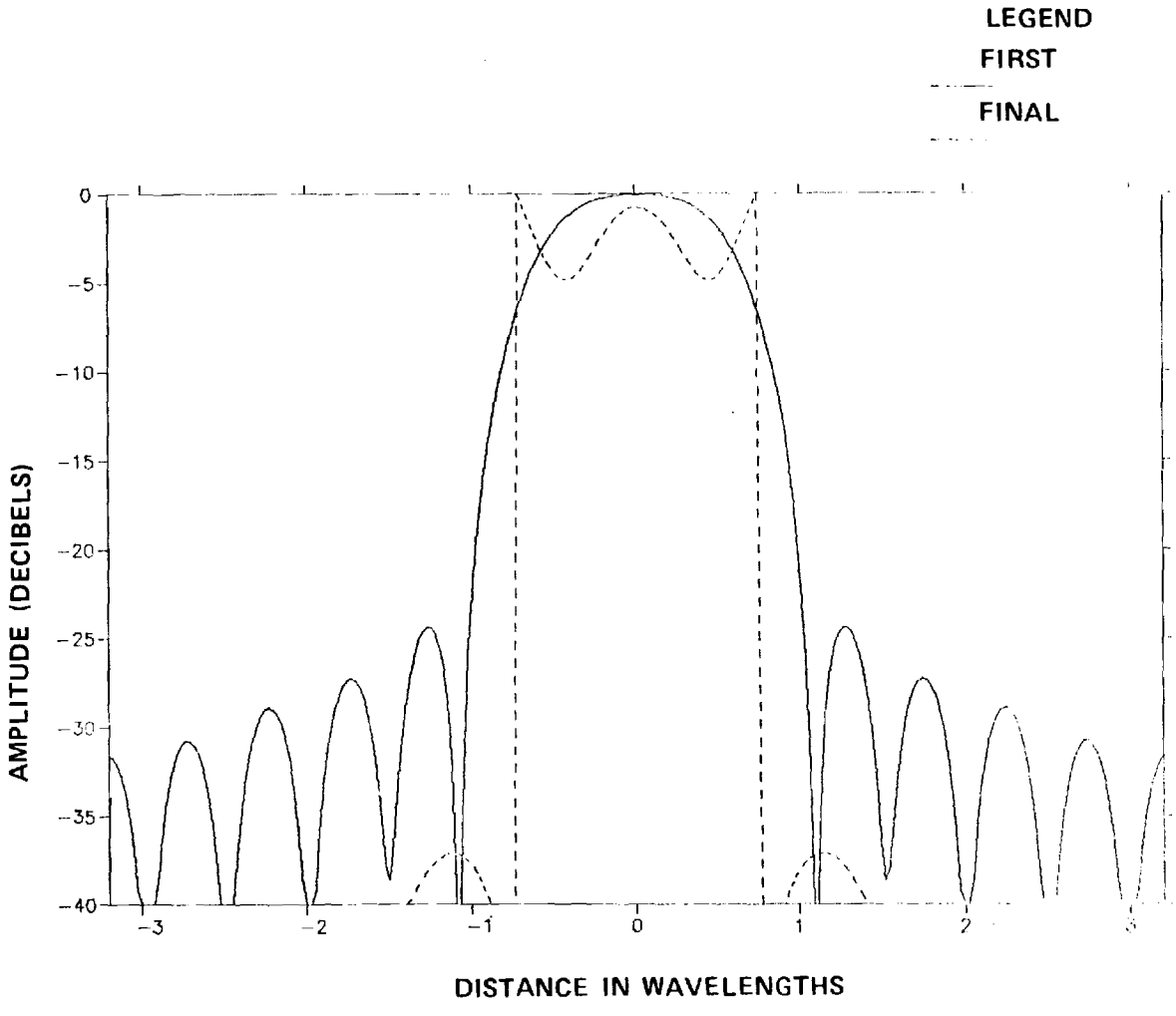

FIGURE 6. FIRST AND FINAL ESTIMATES OF APERTURE FIELD OF ACTUAL ELEMENT IN E–PLANE.

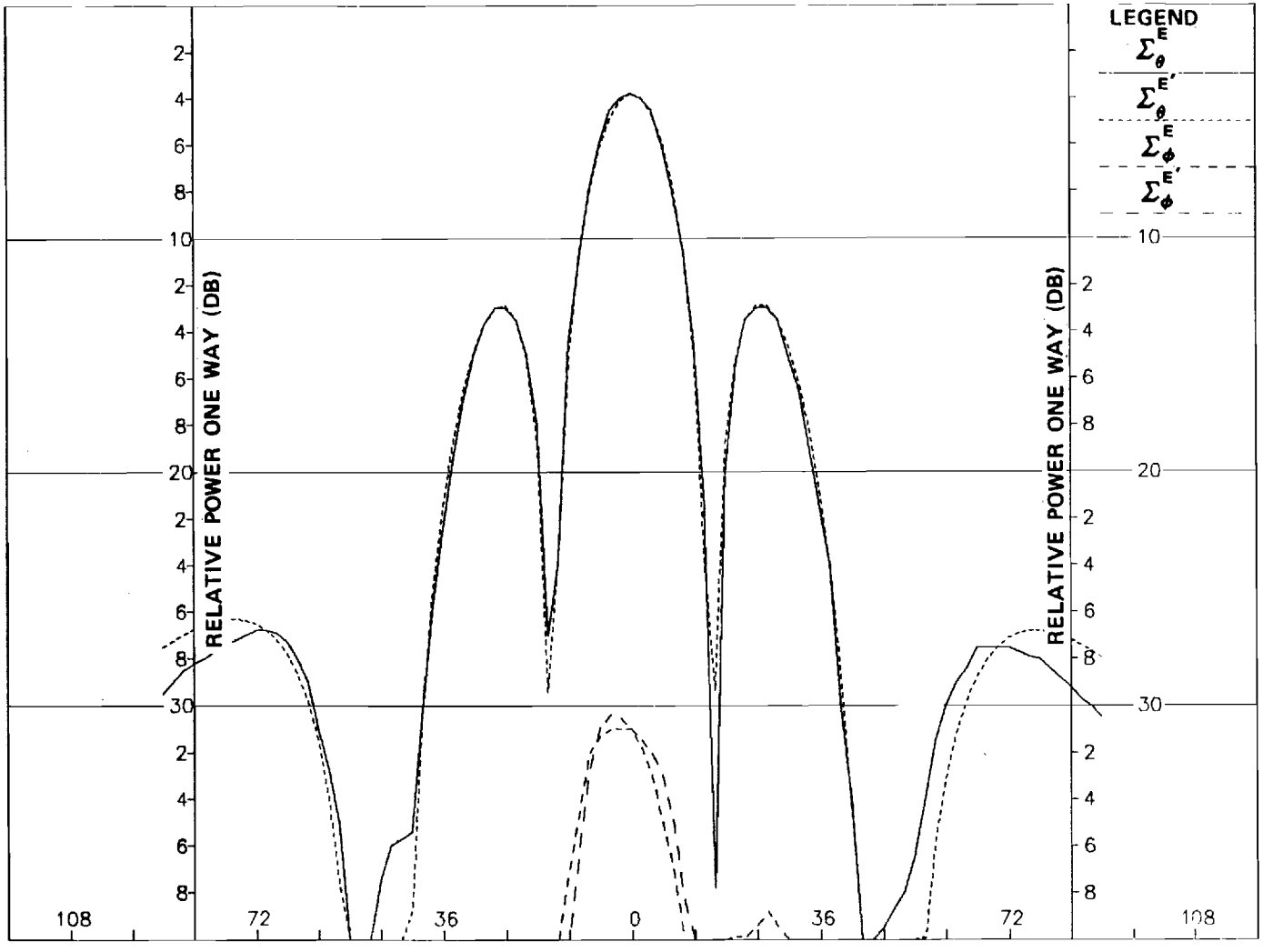

FIGURE 7. COMPARISONS OF MEASURED AND SYNTHESIZED (') E–PLANE SUM PATTERNS OF ACTUAL FOUR–HORN MONOPULSE ANTENNA.

procedure must be carried out in two dimensions.* This section presents results of two-dimensional synthesis of the element spectra and fields of the antenna in Figure 1 using measured principal plane patterns.

Figure 8 shows the element near field $E_{ye}(x,y)$ and the corresponding plane wave spectrum $A_{ye}(k_x,k_y)$ obtained using the 2-D extrapolation algorithm. The element principal plane spectra were first determined via Equations (16)-(19) from the measured data. These results were then used in Equations (54) and (55) to generate the 2-D plane wave spectra over the visible region $k_x^2+k_y^2\leq 1$. The extrapolation algorithm was then applied to each 2D spectrum in turn using a 2-D Fast Fourier Transform. After eleven iterations, the concentration factors were $\varepsilon_x=.065$ and $\varepsilon_y=.028$; i.e,, for the y-component $E_{ye}(x,y)$, 98.2% of the near-field energy was concentrated in the circular element region of radius $a=.74316\lambda$. A square array of 64 x 64 samples spaced at $\Delta x=\Delta y=.07031\lambda$ and resulting in $k_{xmax}=k_{ymax}=7.11$ was used for each component. An exponential window was used to limit the near fields to the circular region.

The resulting element spectra were next combined via Equations (1) and (9) to produce the 2D plane wave spectra for the three monopulse channels. Each spectra was then Fourier transformed to obtain the corresponding near fields. Some results for the sum channel are presented in Figure 9. The PWS $A_y^{\Sigma}(k_x,k_y)$ shown in Figure 9(a) has maximum wavenumbers $k_{xmax}=k_{ymax}=3.56$. Although no extrapolation was applied to the PWS containing the array factor, the actual measured spectra in the principal planes were inserted directly into the final PWS to guarantee close agreement with measured patterns as extracted from the 2-D PWS.

*One-dimensional extrapolation could possibly be used by utilizing the Hankel transform in place of the Fourier transform.

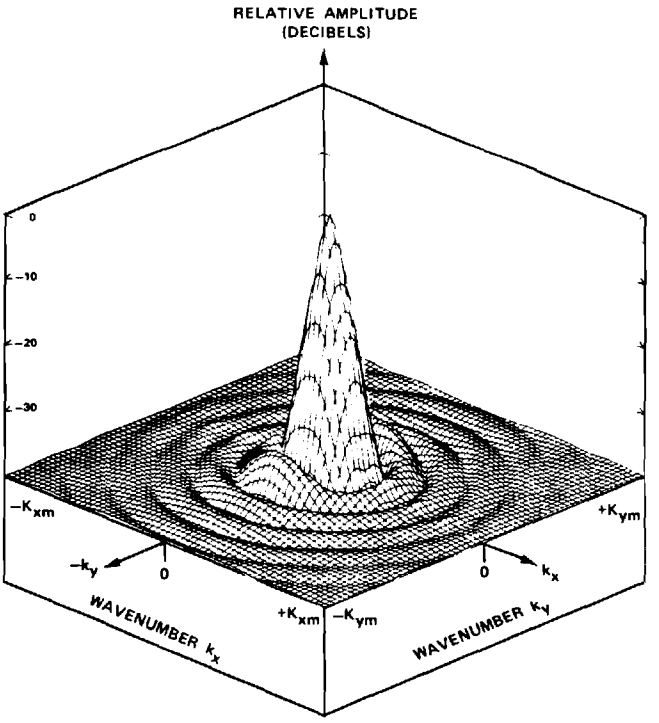

(a) Plane Wave Spectrum.

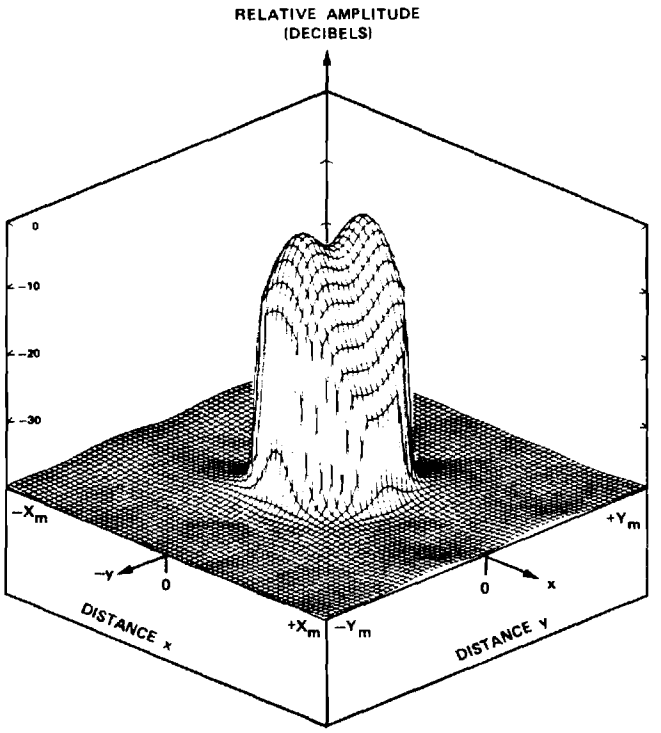

(b) Near Field.

FIGURE 8. PLANE WAVE SPECTRUM Ay (kx,ky) AND NEAR FIELD Eynf (x,y) OF ELEMENT.

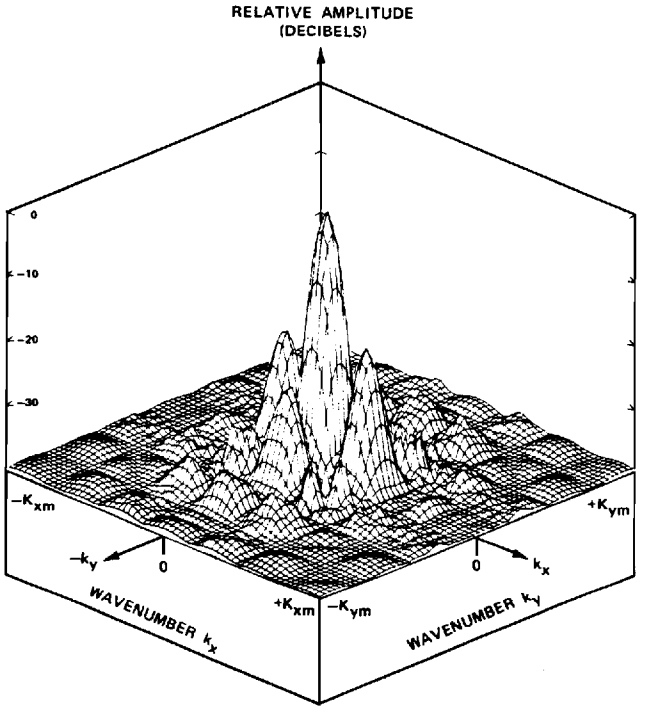

(a) Plane Wave Spectrum.

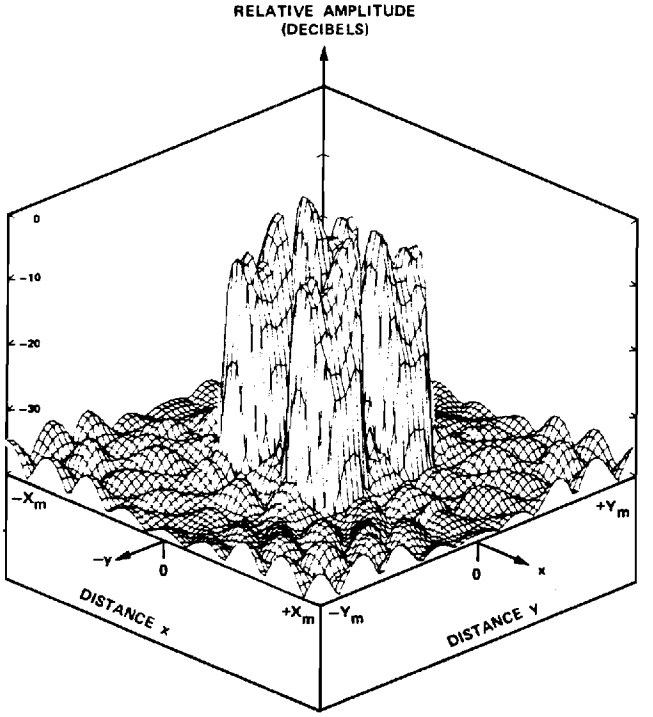

(b) Near Field.

FIGURE 9. PLANE WAVE SPECTRUM AND NEAR FIELD OF Y–COMPONENT OF FOUR–HORN MONOPULSE ARRAY.

Figure 9(b) shows the y-component of the synthesized near field of the four-horn monopulse antenna at 64 x 64 samples spaced at $\Delta x=\Delta y=.14045\lambda$. The near fields of the four circular elements are clearly visible, and the vast majority of the near-field energy is concentrated in the central portion of the array.

When selected cuts were extracted from the 2-D phase wave spectra of the sum channel and used in Equation (9), the patterns of Figure 10 resulted. Agreement between the measured and synthesized E-plane sum patterns shown in Figure 10(a) is excellent. But perhaps more importantly, the agreement in the $\phi=45°$ plane is also excellent as shown in Figure 10(b) -- facts which attest to the apparent correctaness of the underlying assumptions used throughout the synthesis procedure. Similar results were obtained for the other planes and other channels.

RADOME ANALYSIS EXAMPLE

The motivation for the antenna synthesis procedure described above is to ensure the valid assessment of the accuracies of various computer-aided radome analysis techniques [1], one of which is described in this section.

A computationally fast receiving formulation for radome analysis [9] is illustrated in Figure 11. The antenna near fields $\underline{E}_{Ti}$, $\underline{H}_{Ti}$ are represented by a uniform grid of sample points on a finite planar aperture surface S_{ap} placed on or just in front of the radiating portion of the actual antenna. The near fields are assumed to be the same as those produced by the antenna when transmitting in the absence of the radome. Rays representing the incident plane wave (target return) are traced from each point in the aperture in the direction $\hat{k}$ to the radome wall. The electromagnetic field associated with each ray is weighted by the insertion

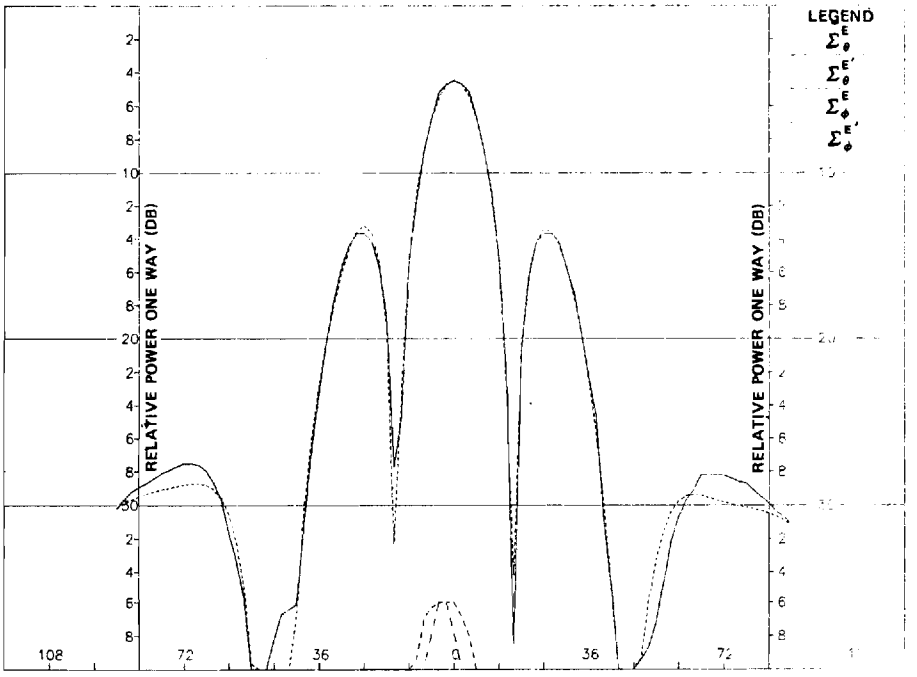

(a) E–Plane Patterns.

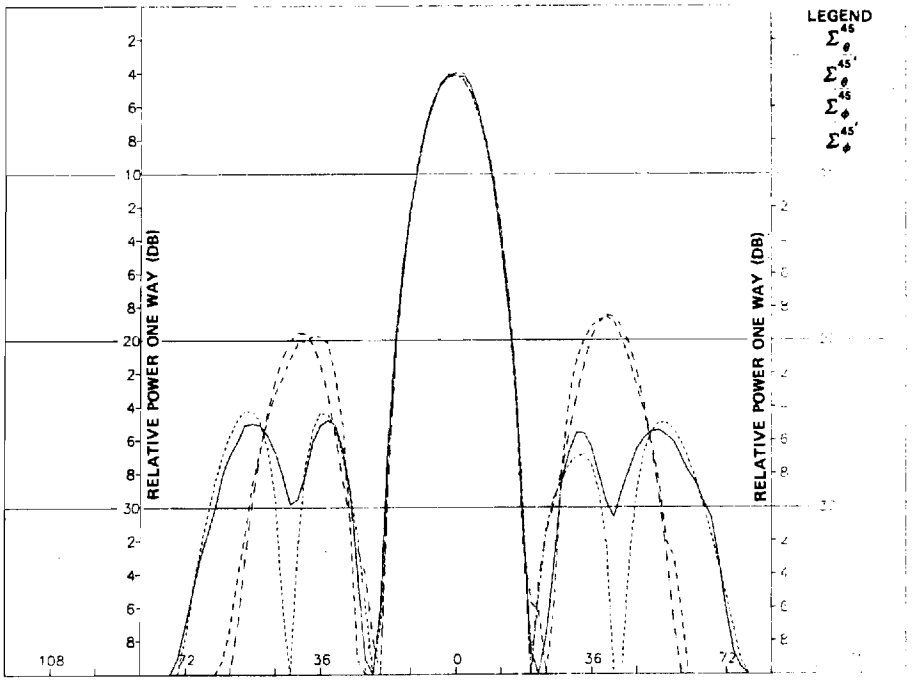

(b) Patterns in $\phi = 45^\circ$ Plane.

FIGURE 10. COMPARISONS OF MEASURED AND SYNTHESIZED (') SUM PATTERNS OF ACTUAL ANTENNA USING 2–D EXTRAPOLATION.

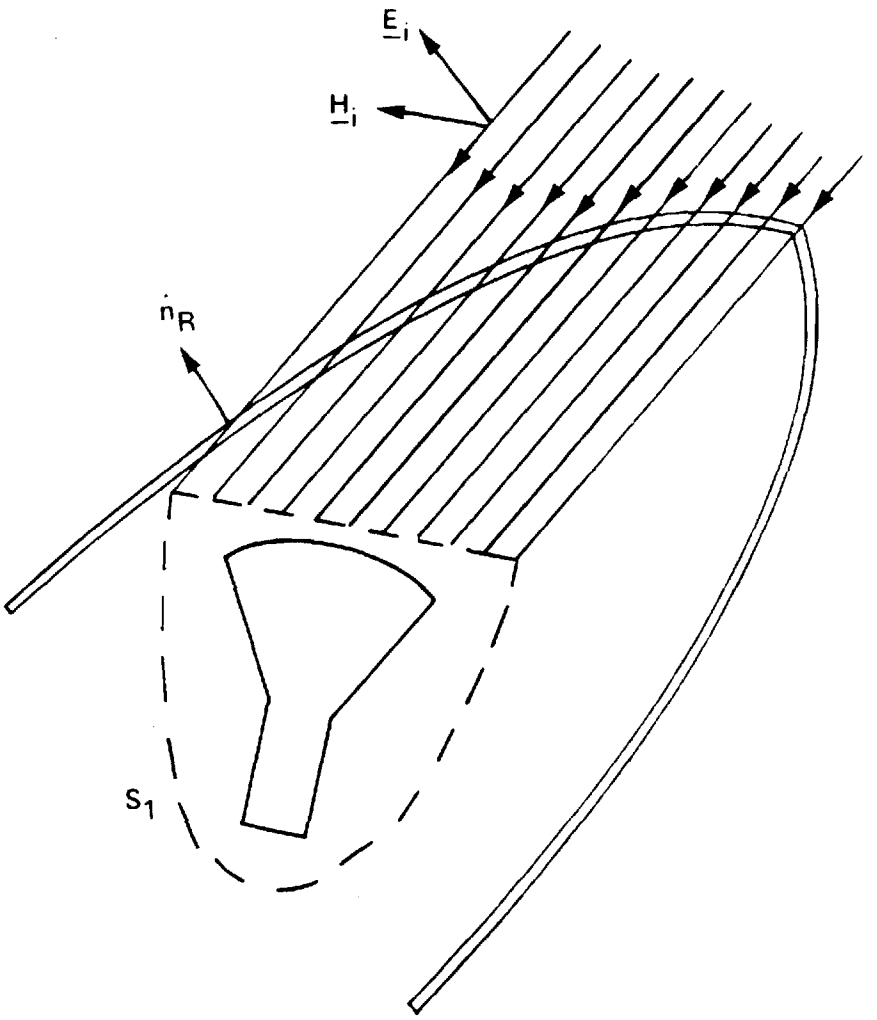

Figure 11. Illustration of the Fast Receiving Method of Radome Analysis

transmission coefficients for field components parallel and perpendicular to the plane of incidence at each point on the radome wall. The response V_R of the antenna is obtained by summing up the contributions of the received fields $\underline{E}_R$, $\underline{H}_R$ as specified by Lorentz reciprocity; viz.,

$$V_{Ri}(\hat{k}) = C \int_{S_{ap}} (\underline{E}_{Ti} \times \underline{H}_R - \underline{E}_R \times \underline{H}_{Ti}) \cdot \hat{n} \, da \qquad (59)$$

The subscript i=1,2,3 specifies the antenna near fields for the Σ, Δ_{EL}, and Δ_{AZ} channels, respectively. Antenna patterns can be computed by controlling the direction of arrival and polarization of the incident plane wave. Boresight errors in the two monopulse planes can also be computed for specified antenna/radome orientations by determining the direction of arrival which produces the difference pattern nulls.

The 64 x 64 sample array of Figure 9(b) representing the near field of the antenna was actually too large to fit into the 10.38λ-diameter, 10.38λ length, tangent ogive, Rexolite (ε_r=2.54, tan δ=.002) radome used in the analysis and measurement. Also, since six such complex arrays are used in the program for the three antenna channels, core memory storage was a consideration. Consequently, only the central 49 x 49 sample points of the near fields were actually used in the radome computations.

Comparisons of the E-plane Δ_{EL} patterns, measured without the radome and computed using a free space radome, are shown in Figure 12 to demonstrate the adequacy of the synthesis technique and the small effects of the near-field truncation. The pattern in Figure 12 was computed as the response of the antenna to plane waves arriving from 65 directions in the E-plane, equally spaced in k_y=sinθ over the visible region $|k_y| \leq 1$. The

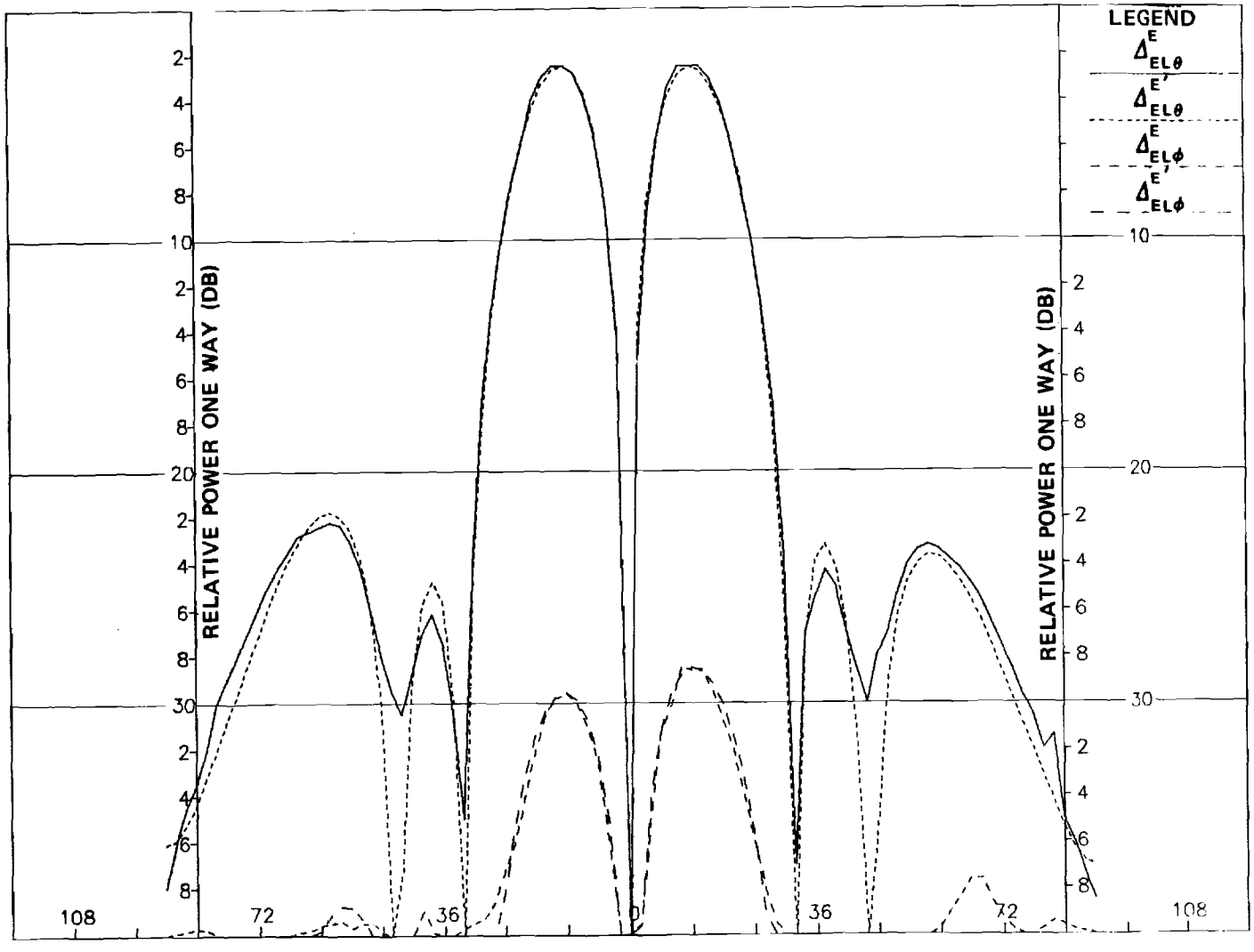

FIGURE 12. COMPARISONS OF MEASURED AND COMPUTED (') E–PLANE DIFFERENCE PATTERNS FOR FREE SPACE RADOME.

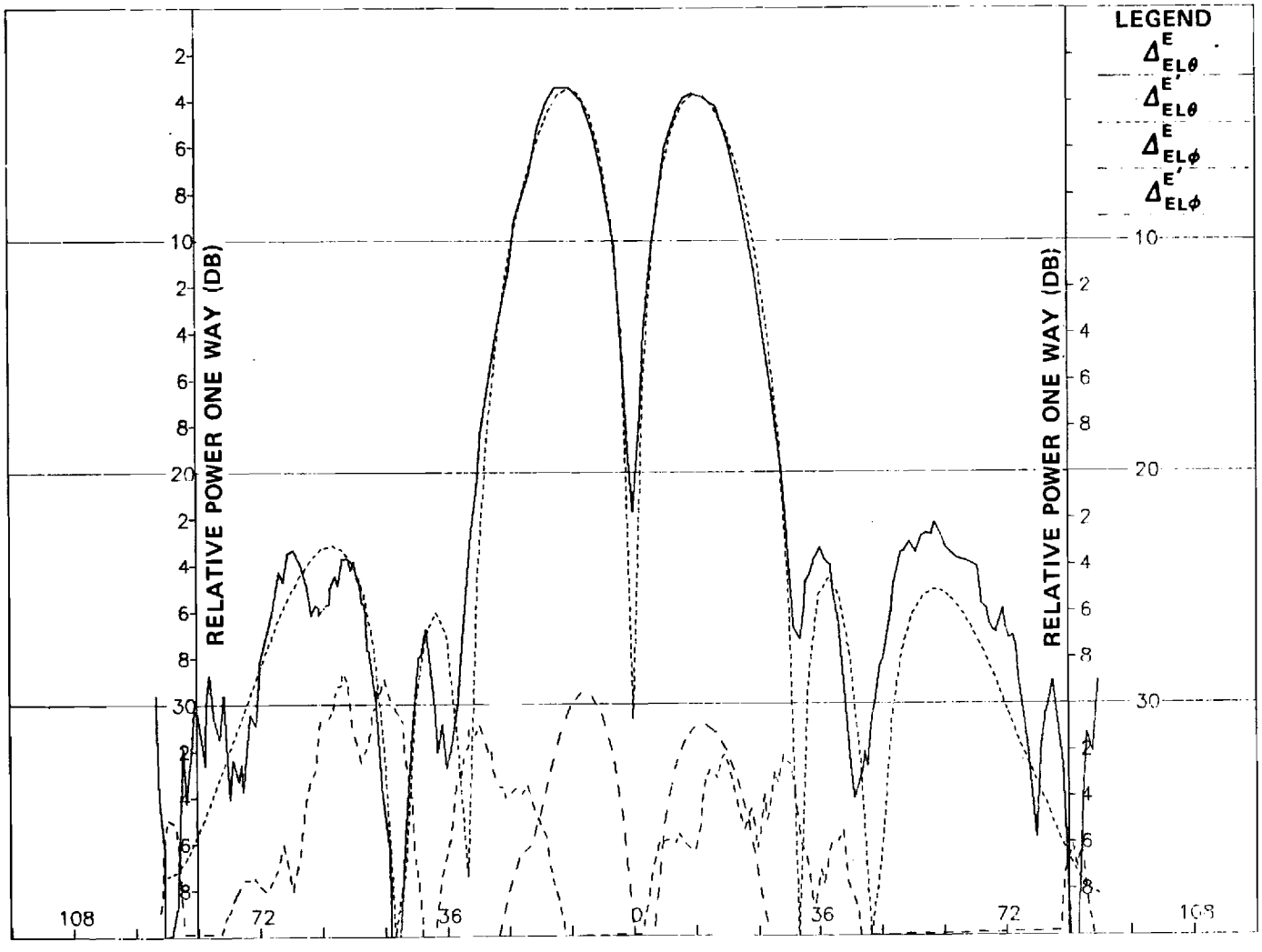

FIGURE 13. COMPARISONS OF MEASURED AND COMPUTED (') E–PLANE DIFFERENCE PATTERNS FOR REXOLITE RADOME.

computed patterns were then Fourier interpolated via Equation (58) to produce sample points at 2° increments over the angular range $|\theta| \leq 90°$.

The computer-aided analysis was repeated using the Rexolite radome, and Δ_{EL} E-plane patterns were computed and interpolated as before. The results are graphed in Figure 13 and compared to the measured patterns with the actual radome in place. The radome was oriented with respect to the antenna such that the radome axis of symmetry made an angle of 15° with respect to the antenna z-axis, and the tip of the radome was located in the $\phi=-45°$ plane of the antenna (Figure 2). Agreement is good for the primary $\Delta^{E}_{EL\theta}$ component over the range $|\theta| \leq 36°$; the discrepancies outside this range of angles are attributed to reflections not accounted for in the analysis. The poor agreement between the cross-polarized $\Delta^{E}_{EL\phi}$ components in Figure 13 is attributed to deficiencies in the analysis, particularly the absence of any accounting for reflections inside the radome.

DISCUSSION

It is important to distinguish the band-limited or aperture-limited nature of the plane wave spectra of each element at z=0 from the unlimited nature of the PWS of the four-horn array of elements at z>0. Each element has finite size; hence, it is a source whose aperture fields have bounded support. It follows that the PWS is not limited in extent in the wavenumber plane since a function and its Fourier transform cannot both have finite support [22]. The unlimited nature of the element plane wave spectra must be taken into consideration when implementing the extrapolation algorithm to minimize the effects of aliasing.

The near field of the four-horn array can be synthesized from the element near field or from its plane wave spectra. The results presented above utilized the latter method, and since no windowing function was applied to the plane wave spectra of the four-horn array, the resulting near fields are theoretically those right at the z=0 plane where the elements are located. It is well known that the planar near field changes as a function of z[3]; viz., the plane wave spectrum is modified by the exponential function $e^{-jk_o k_z z}$ so that $E_{nf}(x,y,z)=F\{A(k_x,k_y)e^{jk_o k_z z}\}$. For values of z of only a few wavelengths, the effect of the exponential function is to drastically attenuate the evanescent modes of the spectra and to cause the planar near field to spread out. Thus, what was a near field having bounded support at z=0 becomes a Fresnel field of unlimited extent with increasing z; concurrently, the initial spectra having unlimited extent become limited. In the limit of very large z, the spectra have bounded support on the region $\sqrt{k_x^2+k_y^2}\leq 1$. This interchangeability of the roles of aperture-limited PWS, and wavenumber-limited near fields, is not always fully appreciated.

The synthesis procedure described above also allows for the inclusion of virtually any amount of additional measured pattern data. The additional data form added constraints on the near-field solutions finally obtained in the same way that the principal plane data have worked here.

CONCLUSIONS AND RECOMMENDATIONS

The aperture synthesis procedure described has been demonstrated to yield excellent results, both in terms of the measured versus synthesized patterns and in the reasonableness of the near fields produced. The procedure is specifically applicable to computer-aided radome analysis,

especially in regard to verification of computed results by comparison to measured pattern data.

It is recommended that additional work be carried out to determine the applicability of the method to source synthesis using complete amplitude and phase data, both near-field and far-field. Additional source geometries should be included in the source specification to ensure close conformance with physical fact. It is anticipated that the actual fields of a number of common source geometries can be determined quite accurately from measured radiation data using the general procedure described here.

ACKNOWLEDGMENTS

This research was sponsored by the Air Force Office of Scientific Research under Grant AFOSR-77-3469. The United States Government is authorized to reproduce and distribute reprints for governmental purposes notwithstanding any copyright notation hereon.

The help of Professor R. W. Schafer in defining the extrapolation algorithm is gratefully acknowledged.

REFERENCES

1. G. K. Huddleston, H. L. Bassett, and J. M. Newton, "Parametric Investigation of Radome Analysis Methods," in 1978 IEEE AP-S Symposium Digest, 1978, pp. 199-201.

2. A. C. Ludwig, "Radiation Pattern Synthesis for Circular Aperture Horn Antennas," IEEE Trans., AP-14, No. 4, pp. 434-440, July 1966.

3. P. C. Clemmow, The Plane Wave Spectrum Representation of Electromagnetic Fields, Pergamon Press, Oxford, 1966.

4. A. Papoulis, "A New Algorithm in Spectral Analysis and Band-Limited Extrapolation," IEEE Trans., CAS-22, No. 9, pp. 1299-1306, September 1975.

5. G. Tricoles, "Radiation Patterns and Boresight Error of a Microwave Antenna Enclosed in an Axially Symmetric Dielectric Shell," J. Optical Soc. of America, Vol. 54, No. 9, pp. 1094-1101, September 1964.

6. D. T. Paris, "Computer-Aided Radome Analysis," IEEE Trans., AP-18, No. 1, pp. 7-15, January 1970.

7. D.C.F. Wu and R. C. Rudduck, "Application of Plane Wave Spectrum Representation to Radome Analysis," in Proc. of the Tenth Symposium on Electromagnetic Windows, July 1970, pp. 46-49.

8. E. B. Joy and G. K. Huddleston, "Radome Effects on Ground Mapping Radar," Technical Report for U. S. Army Missile Command, AD-778 203, March 1973.

9. G. K. Huddleston, "Radome Analysis Computer Program: Ray Tracing Formulation," Technical Report for Johns Hopkins University Applied Physics Laboratory, November 1979.

10. K. Siawak, T. B. Dowling, and L. R. Lewis, "Boresight Errors Induced by Missile Radomes," IEEE Trans., AP-27, No. 6, pp, 832-841, November 1979.

11. L. G. Bulluck, G. R. Oeh, and J. J. Sparagna, "An Analysis of Wide-Band Microwave Monopulse Direction-Finding Techniques," IEEE Trans., AES-7, No. 1, pp. 188-202, January 1971.

12. J. Arsac, Fourier Transforms and the Theory of Distributions, Prentice-Hall, Inc., Englewood Cliffs, N.J., 1966, Ch. 5.

13. D. R. Rhodes, Synthesis of Planar Antenna Sources, Oxford University Press, London, 1974.

14. H. G. Schmidt-Weinmar, "Spatial Resolution of Subwavelength Sources from Optical Far Zone Data," Chapter 4 of Inverse Source Problems in Optics, H. P. Baltes, editor, Springer-Verlag, Berlin, 1978.

15. G. K. Huddleston, "Optimum Probes for Near-Field Antenna Measurements on a Plane," Ph.D. Dissertation, Georgia Institute of Technology, Atlanta, Gerogia, 1978, Ch. 3.

16. S. Silver (ed.), Microwave Antenna Theory and Design, McGraw-Hill New York, 1949, pp. 161-162.

17. J. D. Kraus, Antennas, McGraw-Hill, New York, 1950, Ch. 15.

18. H. A. Ferwerda, "The Phase Reconstruction Problem for Wave Amplitudes and Coherence Functions," Chapter 2 of Inverse Source Problems in Optics, H. P. Baltes, editor, Springer-Verlag, Berlin, 1978.

19. S. Silver, op. cit., p. 337.

20. Ian N. Sneddon, Fourier Transforms, McGraw-Hill, New York, 1951, Ch. 2.

21. J. W. Goodman, Fourier Optics, McGraw-Hill, New York, 1968, p. 25.

22. H. J. Landau and H. O. Pollak, "Prolate Spheroidal Wave Functions, Fourier Analysis and Uncertainty - I," BSTJ, 40, pp. 43-64, January 1961.

APPENDIX C

"Comparative Accuracies of Radome Analysis Methods"

Accepted for Publication

in

Proceedings of the Fourth International Conference
on Electromagnetic Windows

Toulon, France

June 10-12, 1981

COMPARATIVE ACCURACIES OF RADOME ANALYSIS METHODS

G. K. Huddleston
School of Electrical Engineering

and

H. L. Bassett and M. J. Hadsell
Engineering Experiment Station (RAIL)

Georgia Institute of Technology
Atlanta, Georgia 30332

INTRODUCTION

This paper presents the salient results of a parametric investigation of radome analysis methods [1]. Three methods of analysis were investigated as described below. Measured boresight error data obtained at 35 GHz on eight combinations of three, four-horn monopulse antennas and five polystyrene, tangent ogive radomes are used as true data in assessing the speeds, accuracies, and ranges of validity of the three methods of analysis.

METHODS OF ANALYSIS

Three computer-aided methods of radome analysis were investigated. The theoretical bases for all three methods are the Huygens-Fresnel principle, Lorentz reciprocity, and geometrical optics [2]. The first method, called herein the fast receiving method, uses geometrical optics (ray tracing) to find the fields incident on the aperture of a monopulse antenna enclosed by the radome due to a TEM wave incident on the radome from a specified direction $\hat{k}$ [3]. The insertion voltage transmission coefficients of flat panel theory for parallel and perpendicular polarization are used to transform the plane wave fields associated with each ray from their values at the incident point on the outside surface of the radome to their values $\underline{E}_R$, $\underline{H}_R$ at the sample point in the aperture. The voltage received by each channel (Σ, Δ_{EL}, Δ_{AZ}) of the monopulse antenna is obtained according to the reciprocity integral

$$V_{REC}(\hat{k}) = \int_S (\underline{E}_T \times \underline{H}_R - \underline{E}_R \times \underline{H}_T) \cdot \underline{n} \; da \qquad (1)$$

where $\underline{E}_T$, $\underline{H}_T$ are the aperture fields of the antenna when transmitting, and where S is the aperture surface.

The second method of analysis, referred to herein as the fast transmitting method, uses a transmitting formulation based on the plane wave spectrum (PWS) representation of the antenna aperture fields and an equivalent aperture approach [4]. The aperture fields are represented by their samples at MN equally spaced increments in x and y. The two-dimensional Fourier transform of the aperture fields yield the corresponding plane wave spectra. From each sample point, there emanate MN plane waves.

Each plane wave is traced to an incident point on the inner surface of the radome and weighted by the insertion voltage transmission coefficients. The modified fields of each plane wave are then added together at each sample point to produce modified aperture fields which embody the effects of the radome. The voltages received by the radome-enclosed antenna are then calculated according to Equation (1), where $\underline{E}_T$, $\underline{H}_T$ are the modified aperture fields.

The third method of analysis is referred to as the surface integration method [5]. The voltage received by the antenna enclosed by the radome is again given by Equation (1), where S is now the inside surface of the radome, $\underline{E}_T$, $\underline{H}_T$ are the radiated fields of the antenna on S, and $\underline{E}_R$, $\underline{H}_R$ are the fields of the incident plane wave on S as transformed from their values on the outside surface using the insertion voltage transmission coefficients. For some directions of arrival k, portions of the inner radome surface are "shadowed" by other portions; the fields on the shadowed portions are approximated by ray tracing as described above for the fast receiving case. Aperture integration is used to calculate the fields of the antenna at each point on the radome surface from the specied aperture values.

All three methods were implemented in Fortran for execution on the Cyber 70 computing system at Georgia Tech. Maximum use was made of features and software common to all three codes.

ANTENNA/RADOME DESCRIPTIONS

Three, four-horn monopulse antennas were designed and fabricated exclusively for use in this research, corresponding to small (BW_{3dB}=30°), medium (15°), and large (8°) sizes. The conical horn elements of each antenna were machined into a single piece of aluminum. The salient dimensions of the antennas are given in Figure 1 and Table 1. More details are given in Reference 6. The elements were y-polarized.

Five, tangent ogive radomes having dimensions given in Figure 1 and Table 2 were machined from cylinders of polystyrene (ε_r=2.54, tanδ=.002), corresponding to small, medium, and large radome sizes. A fineness ratio of 1.0 was used for each size; in addition, for the medium size, fineness ratios of 1.5 and 2.0 were used. All five radomes had a wall thickness of 0.25 inch, corresponding to a full wavelength in the dielectric at 35 GHz and a design angle of approximately 60 degrees.

The antenna and radome were used together in eight different combinations for measurement and analysis purposes. The intent here was to obtain true data from measurements for comparison to the predicted results over ranges of parameters which would help clarify any deficiencies in the three methods of analysis.

RESULTS

Comparisons of measured and computed boresight error data for five antenna/radome combinations are presented in Figures 2 through 5. Boresight errors in both the elevation difference channel (BSEEL) and azimuth difference channel (BSEAZ) are shown in each graph as functions of the

radome orientation angle α. The antenna and radome were mounted together such that the radome axis of symmetry passed through the antenna axis of symmetry at the gimbal point (Figure 1b) at an angle of 15 degrees. The radome could then be rotated about the antenna axis of symmetry through the angle α indicated in Figure 1a, thereby placing the tip of the radome in any desired plane of scan. For example, $\alpha=0$ corresponds to the radome tip being in the azimuth plane (+xz-plane) of the monopulse antenna; $\alpha=-90°$ places the tip in the elevation plane (-yz-plane in Figure 1a).

In Figures 2 through 5, α varies from zero to -90 degrees. For $\alpha=0$, symmetry dictates that there should be no boresight error in elevation, and the azimuth boresight error should be nonzero. For $\alpha=-90°$, azimuth boresight error should be zero, and elevation boresight error should be nonzero. The boresight errors are defined here as the true direction to the target in the antenna coordinate system of Figure 1a; e.g., positive boresight error in azimuth (elevation) means that the target lies in the +xz (+yz) plane.

Figure 2 compares the computed results for all three methods with the measured boresight error data. In carrying out the computations for the fast receiving case, it was found that only four points were needed in the antenna aperture, located at the center of each element, to obtain essentially the same results as were computed using a 49 X 49 point representation of the aperture fields [7]. The same four-point representation was also used in the other two computer codes because the enormous computation times required using the 49 X 49 point representation were prohibitive. Even using the four-point representation, the surface integration required such long run times that only the small radome could be adequately analyzed on the Cyber system.

Examination of Figure 2 shows that none of the three methods of analysis accurately predicts the measured boresight errors in the case of the small antenna with small radome, especially for the elevation channel. The fast receiving method tends to overestimate the error while the fast transmitting method underestimates it. The surface integration method does the best job for the azimuth error. All three methods predict the correct sign of the error for most of the range of α considered. Deficiencies in the methods of analysis to account for the lack of agreement with measured results cannot be isolated on the basis of the data.

Figures 3 and 4 present results for the medium antenna and medium radomes having two different fineness ratios. The fast receiving method predicts the measured errors most accurately, though not as accurately as desired. The fast transmitting method underestimates the errors. Unstable results were obtained with the surface integration method as indicated in Figure 3, indicating unresolved problems with the computer code. The two fast methods accurately predict the sign of the error, and the fast receiving method does predict accurately an increase in errors with increasing fineness ratio as expected.

Figure 5 presents the results for the medium antenna and large radome. Neither of the two fast methods predicts the elevation error very accurately. Better predicted results are obtained in the azimuth error, with the fast transmitting being more accurate than the fast receiving method.

The computation times and core storage requirements for the three methods of analysis are presented in Table 3 for comparison purposes. For the fast methods of analysis, these two parameters are independent of the radome size, but do depend on the number of points in the antenna aperture: for the fast receiving method, computation time increases directly with the number of points; for the fast transmitting method, the logarithm (base 2) of the computation time increases in the same manner.

The computation time of the surface integration method depends on both the number of points in the aperture and the number of points used to represent the fields on the radome surface. In Figure 2, four points were used for the aperture fields, and 781 points (spaced $\lambda/3$ apart) were used on the radome surface. In Figure 3, 2291 points at $\lambda/3$ spacing were used on the radome surface, and four points were used for the aperture fields.

Comparisons of measured and computed values of on-axis sum channel gain loss relative to the case of no radome are shown in Table 4 for three positions of the radome tip. For the small losses encountered, no method consistently predicted the measured radome losses.

CONCLUSIONS AND RECOMMENDATIONS

The main conclusion to be made from the data presented is that there is room for improvement in the predictive accuracies of the computer codes used with respect to the important parameters of boresight error and radome loss. This conclusion is especially true for the case of small antennas and radomes where the effects of antenna/radome interactions are not properly included. For the case of moderate sized antennas and radomes, the fast receiving method is attractive because of the fast computation time and reasonably accurate results. The surface integration code used requires additional development before any valid conclusions can be drawn about its predictive accuracy; however, it is clear that its applicability will be restricted to small radomes because of the relatively large computation times required.

It is recommended that the fast receiving method be modified so that refractive effects and ray spreading are more accurately accounted for in the ray tracing procedure. It is also recommended that the surface integration method be further developed, even to include first-order reflected fields. Additionally, it is recommended that new experimental techniques be developed which will allow the determination of radome fields close to the dielectric so that deficiencies in the analytical methods can be isolated and corrected.

ACKNOWLEDGMENT

This research was sponsored by the Air Forec Office of Scientific Research under grant AFOSR-77-3469. The United State Government is authorized to reproduce and distribute reprints for governmental purposes notwithstanding any copyright notation hereon.

REFERENCES

1. G. K. Huddleston, H. L. Bassett, & J. M. Newton, "Parametric Investigation of Radome Analysis Methods", Annual Report, Grant AFOSR-77-3469, November 1978.

2. G. K. Huddleston, "Theory of Radome Analysis", submitted to IEEE AP-S Transactions, November 1980.

3. G. K. Huddleston, H. L. Bassett, & J. M. Newton, "Parametric Investigation of Radome Analysis Methods: Computed-Aided Analysis Using Geometrical Optics and Lorentz Reciprocity", Final Technical Report, Vol. 2 of 4, Grant AFOSR-77-3469, February 1981.

4. E. B. Joy & G. K. Huddleston, "Radome Effects on the Performance of Ground Mapping Radar", Final Technical Report, U. S. Army Missile Command, DAAH01-72-C-0598, March 1972.

5. G. K. Huddleston, H. L. Bassett, & J. M. Newton, "Parametric Investigation of Radome Analysis Methods: Computer-Aided Radome Analysis Using the Huygens-Fresnel Principle and Lorentz Reciprocity", Final Technical Report, Vol. 3 of 4, Grant AFOSR-77-3469, February 1981.

6. H. L. Bassett, J. M. Newton, et al., "Parametric Investigation of Radome Analysis Methods: Experimental Results", Final Technical Report, Vol. 4 of 4, Grant AFOSR-77-3469, February 1981.

7. G. K. Huddleston, "Aperture Synthesis of Monopulse Antenna for Radome Analysis Using Limited Measured Pattern Data", Proceedings Southeastcon '81, April 1981.

Table 1. Dimensions in Inches of Antennas. (See Figure 1(a)).

Antenna Identification	R_A	Element Diameter A	Element Half-Spacing C	Overall Diameter B
Small	.1875	.310	.160	.875
Medium	.250	.620	.320	1.540
Large	.375	1.225	.878	3.040

Table 2. Dimensions in Inches of Radomes. (See Figure 1(b)).

Radome Identification	Outside Diameter D	Outside Length C	Inside Diameter E	Inside Length B	R_R
Small (F=1.0)	2.55	2.35	2.05	2.05	.4375
Medium (F=1.0)	4.00	3.81	3.50	3.50	.75
Medium (F=1.5)	4.00	5.66	3.50	5.25	.75
Medium (F=2.0)	4.00	7.52	3.50	7.00	.75
Large (F=1.0)	6.91	6.72	6.41	6.41	.375

Table 3. Computation Time and Core Storage Requirements.

Case	Computation Time*(sec.)/Core Storage (octal) Fast Receiving	Fast Transmitting	Surface Integration
Small Antenna, Small Radome	.24/67100	.62/77300	34.0/135300
Medium Antenna, Medium (F=1.0)	.25/67100	.62/77300	44.0/135300

*Per look angle.

Table 4. Radome Loss Comparisons.

Antenna	Radome	Alpha (Deg.)	Loss (dB) Measured	Fast Revg	Fast Xmtg	Surface Integration
Small	Small	0	0.4	0.5	0.5	1.9
"	"	-45	0.7	0.5	0.4	1.7
"	"	-90	0.6	0.3	0.3	1.9
Medium	Medium (F=1.0)	0	1.4	0.4	0.6	1.2
"	" "	-45	1.4	0.4	0.5	1.2
"	" "	-90	0.8	0.3	0.4	1.2
Medium	Medium (F=2.0)	0	0.2	0.1	0.6	-
"	" "	-45	0.5	0.1	0.4	-
"	" "	-90	0.6	0.1	0.2	-

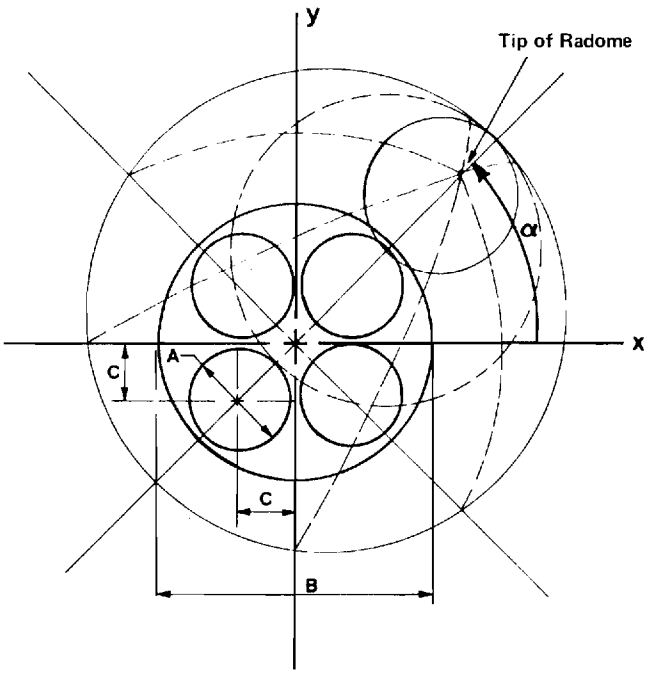

(a) Antenna Geometry Showing Radome Orientation

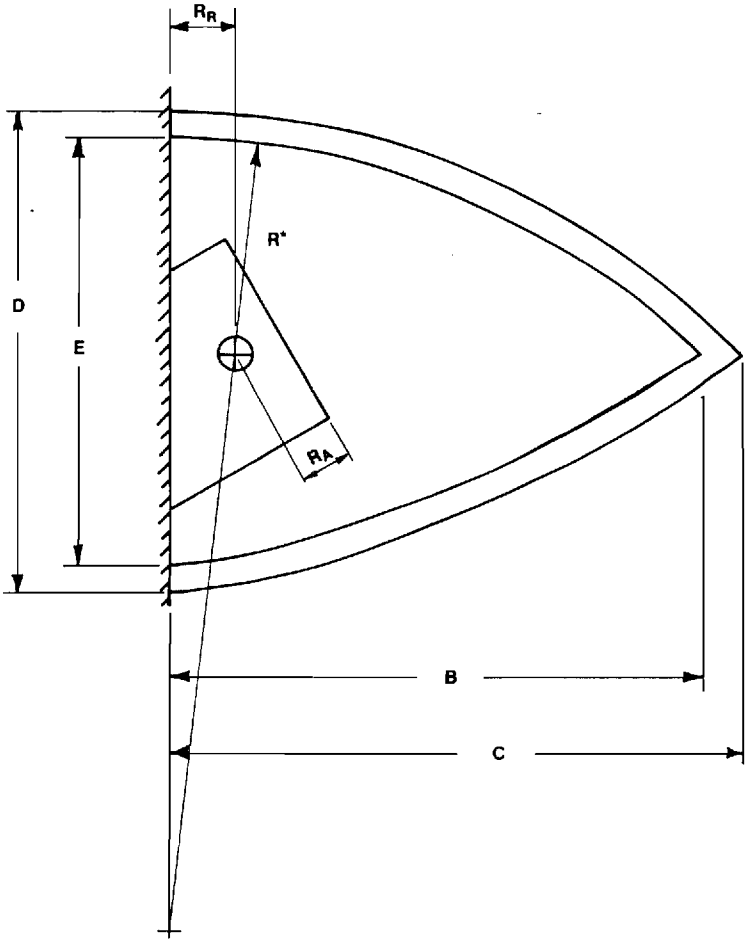

(b) Radome Geometry

Figure 1. Antenna and Radome Geometries as Dimensioned in Tables 1 and 2.

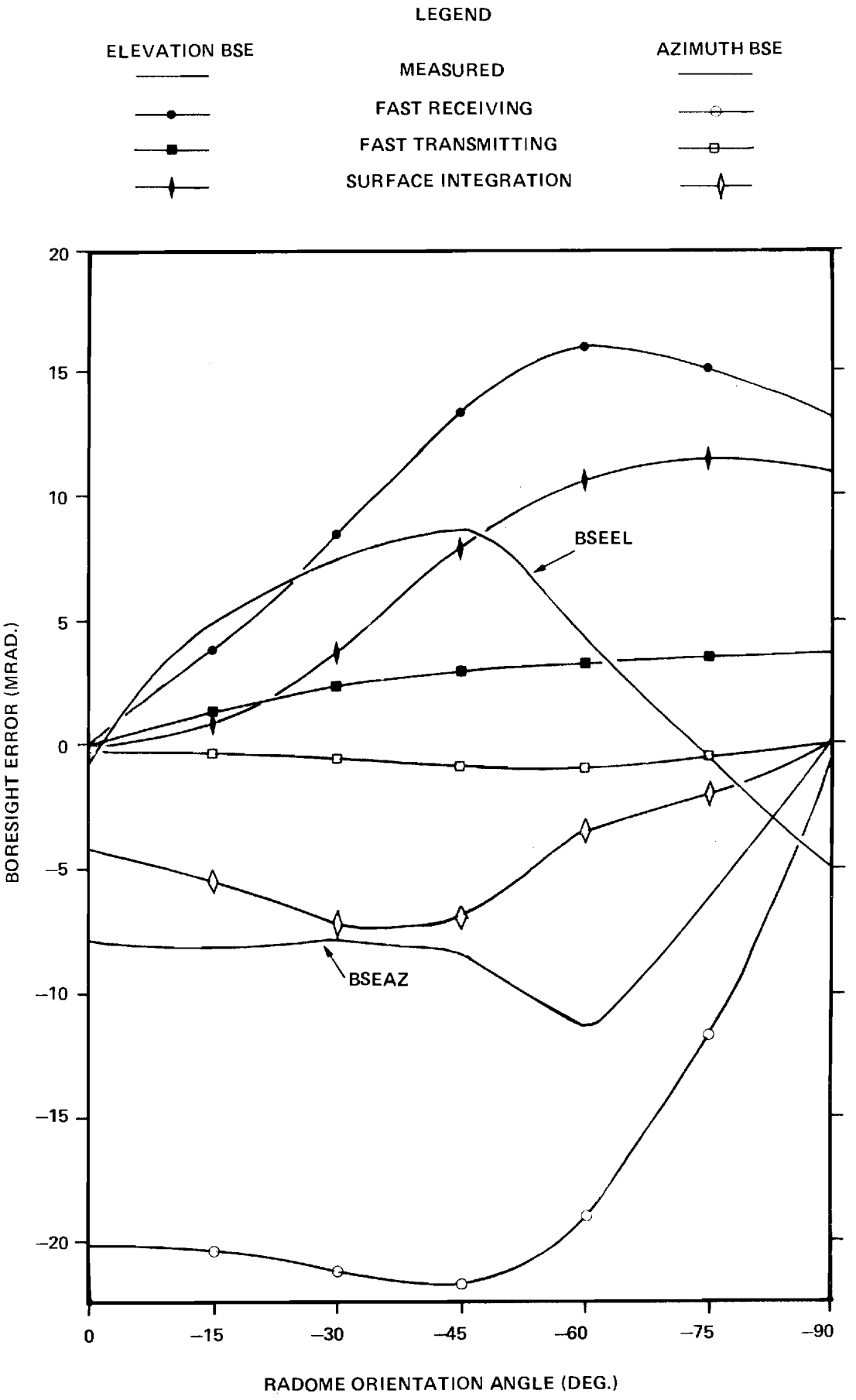

Figure 2. Comparisons of Measured and Computed Boresight Errors for Small Antenna, Small (F = 1.0) Radome.

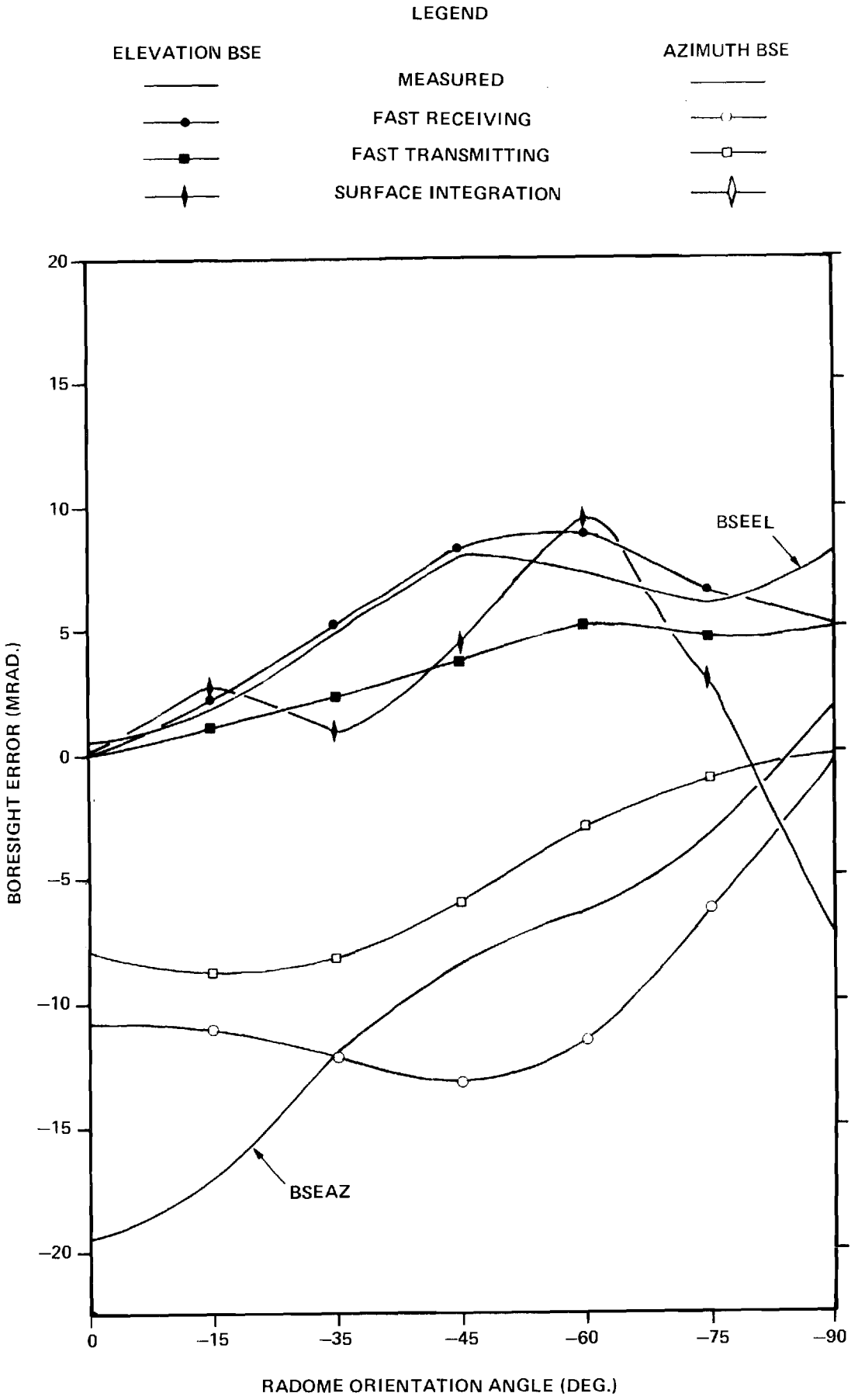

Figure 3. Comparisons of Measured and Computed Boresight Errors for Medium Antenna, Medium (F = 1.0) Radome.

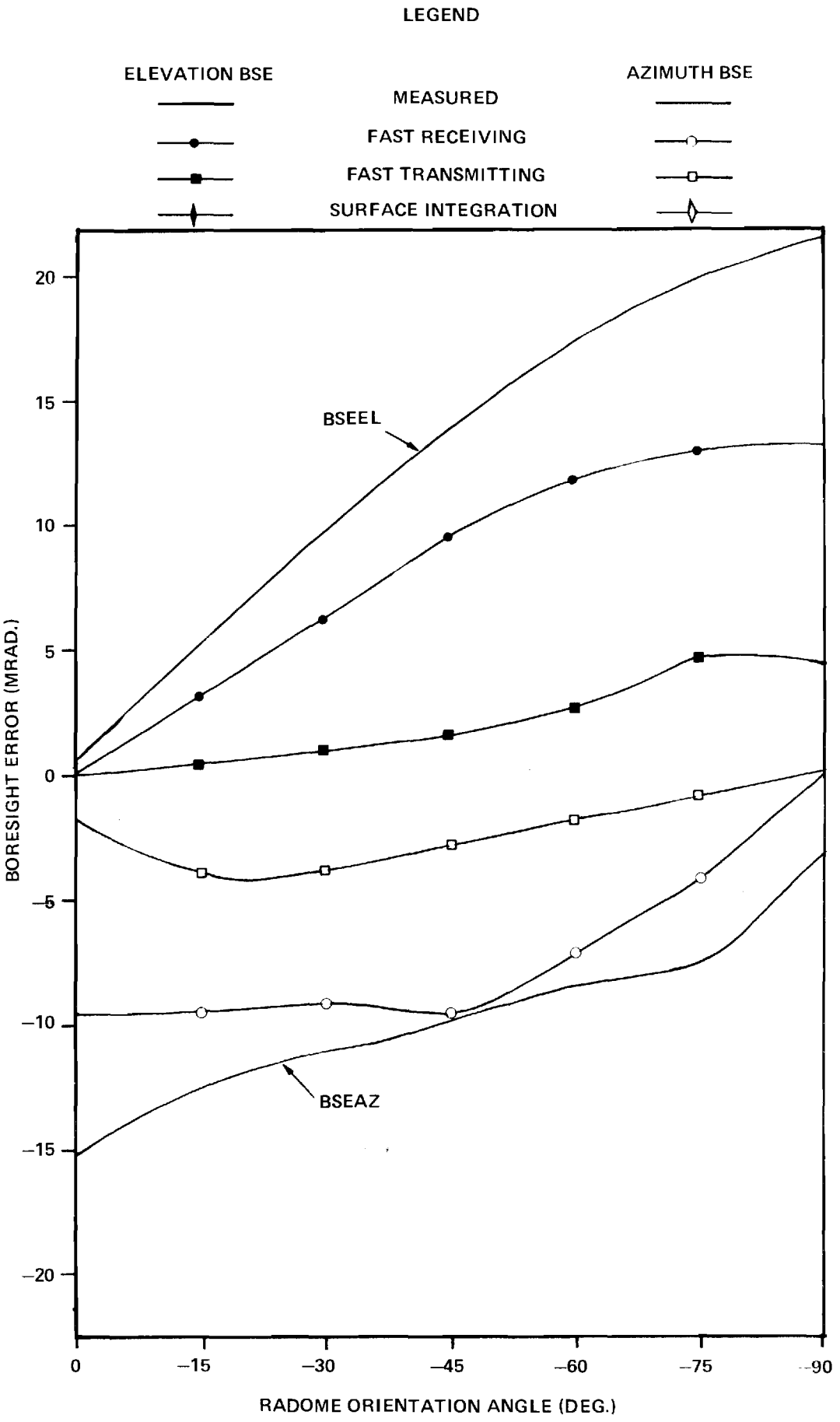

Figure 4. Comparisons of Measured and Computed Boresight Errors for Medium Antenna, Medium (F = 2.0) Radome.

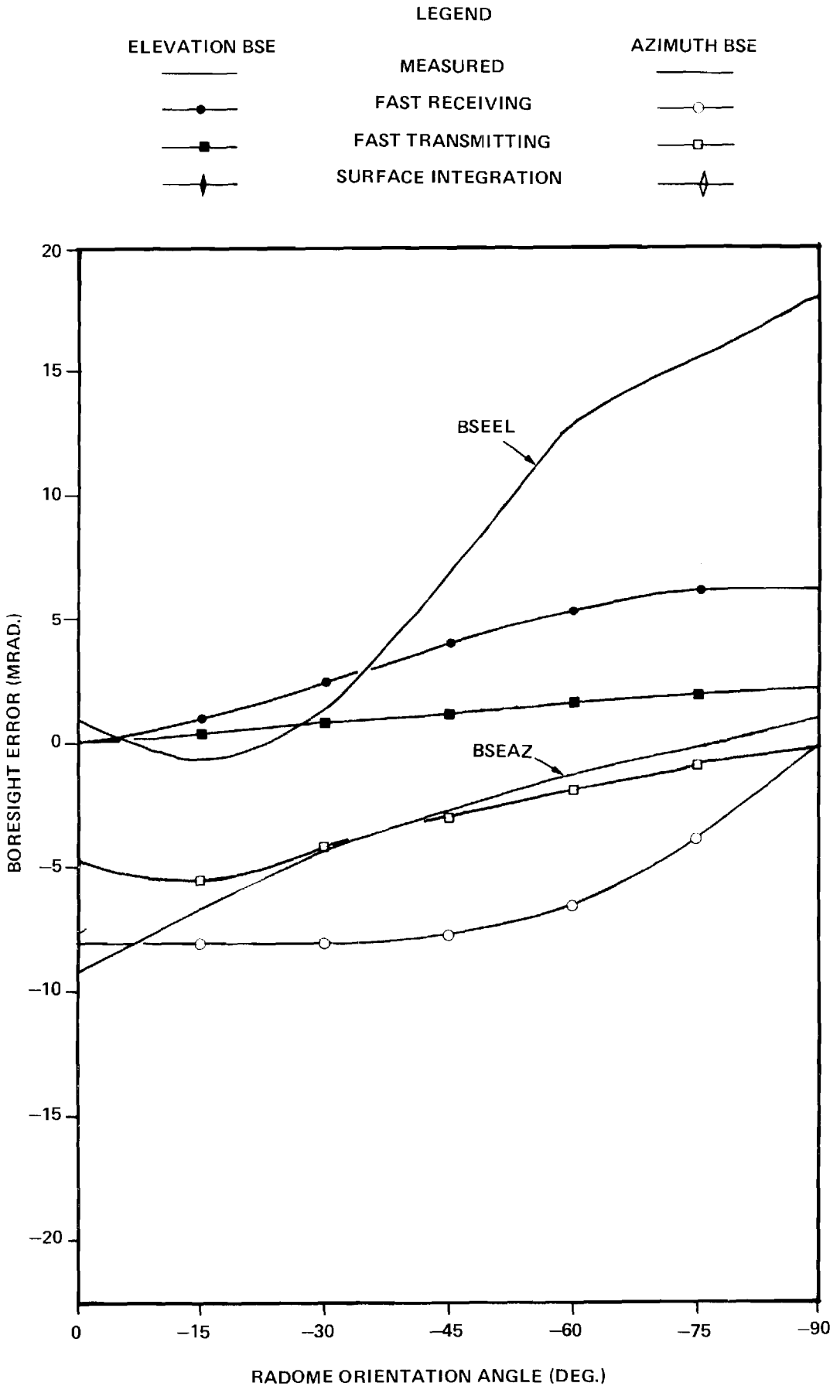

Figure 5. Comparisons of Measured and Computed Boresight Errors for Medium Antenna, Large (F = 1.0) Radome.

E21-603

PARAMETRIC INVESTIGATION OF RADOME ANALYSIS METHODS:

COMPUTER–AIDED RADOME ANALYSIS USING GEOMETRICAL OPTICS AND LORENTZ RECIPROCITY

By

G. K. Huddleston, H. L. Bassett, & J. M. Newton

Prepared for

AIR FORCE OFFICE OF SCIENTIFIC RESEARCH (AFSC)
BOLLING AIR FORCE BASE, D. C. 20332

FINAL TECHNICAL REPORT, VOLUME II OF IV
GRANT AFOSR–77–3469
30 September 1977 – 31 December 1980

February 1981

GEORGIA INSTITUTE OF TECHNOLOGY
SCHOOL OF ELECTRICAL ENGINEERING &
Engineering Experiment Station
Atlanta, Georgia 30332

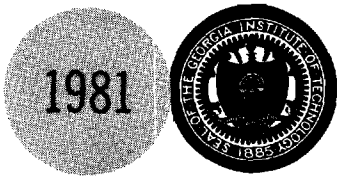

UNCLASSIFIED

SECURITY CLASSIFICATION OF THIS PAGE *(When Data Entered)*

REPORT DOCUMENTATION PAGE

READ INSTRUCTIONS BEFORE COMPLETING FORM

1. REPORT NUMBER	2. GOVT ACCESSION NO. / 3. RECIPIENT'S CATALOG NUMBER
4. TITLE *(and Subtitle)* PARAMETRIC INVESTIGATION OF RADOME ANALYSIS METHODS: COMPUTER-AIDED RADOME ANALYSIS USING GEOMETRICAL OPTICS AND LORENTZ RECIPROCITY	5. TYPE OF REPORT & PERIOD COVERED Final Technical Report, Vol. 2 of 4 30 Sept. 1977-31 Dec. 1980 6. PERFORMING ORG. REPORT NUMBER
7. AUTHOR(s) G. K. Huddleston, H. L. Bassett, & J. M. Newton	8. CONTRACT OR GRANT NUMBER(s) AFOSR-77-3469
9. PERFORMING ORGANIZATION NAME AND ADDRESS Georgia Institute of Technology School of Electrical Engineering & Engineering Experiment Station Atlanta, Georgia 30332	10. PROGRAM ELEMENT, PROJECT, TASK AREA & WORK UNIT NUMBERS 61102F 2301/A6
11. CONTROLLING OFFICE NAME AND ADDRESS Air Force Office of Scientific Research Physics Directorate (Code NP-77-148) Bolling Air Force Base, D. C. 20332	12. REPORT DATE February 1981 13. NUMBER OF PAGES 338
14. MONITORING AGENCY NAME & ADDRESS*(if different from Controlling Office)*	15. SECURITY CLASS. *(of this report)* UNCLASSIFIED 15a. DECLASSIFICATION/DOWNGRADING SCHEDULE

16. DISTRIBUTION STATEMENT *(of this Report)*

Approved for public release; distribution unlimited.

17. DISTRIBUTION STATEMENT *(of the abstract entered in Block 20, if different from Report)*

18. SUPPLEMENTARY NOTES

19. KEY WORDS *(Continue on reverse side if necessary and identify by block number)*

Radome Analysis
Electromagnetic Analysis
Lorentz Reciprocity
Geometrical Optics

20. ABSTRACT *(Continue on reverse side if necessary and identify by block number)*

A Fortran computer program is described for computing the effects of a tangent ogive radome on the receiving patterns and boresight directions of a monopulse antenna. The analytical method based on ray tracing, main program, and 34 subroutines are thoroughly documented. Four test cases and their results in the form of printouts, pattern plots, and near-field graphs are presented.

DD FORM 1 JAN 73 1473 EDITION OF 1 NOV 65 IS OBSOLETE

UNCLASSIFIED

SECURITY CLASSIFICATION OF THIS PAGE *(When Data Entered)*

PARAMETRIC INVESTIGATION OF

RADOME ANALYSIS METHODS:

COMPUTER-AIDED RADOME ANALYSIS USING

GEOMETRICAL OPTICS AND LORENTZ RECIPROCITY

by

G. K. Huddleston, H. L. Bassett, & J. M. Newton
School of Electrical Engineering &
Engineering Experiment Station
Georgia Institute of Technology
Atlanta, Georgia 30332

Final Technical Report, Volume II of IV

for

Air Force Office of Scientific Researhc (AFSC)
Physics Directorate (Code NP-77-148)
Bolling Air Force Base, D. C. 20332

under

Grant AFOSR-77-3469
30 September 1977 - 31 December 1980

February 1981

TABLE OF CONTENTS

CHAPTER PAGE

LIST OF ILLUSTRATIONS

LIST OF TABLES

Chapter 1

INTRODUCTION AND SUMMARY

1-1. Introduction

This Volume II of this final technical report of four volumes documents a ray tracing radome analysis computer program written in Fortran IV for use on the Cyber 70/74 computing system at Georgia Institute of Technology and the IBM 3033 computing system at Johns Hopkins University Applied Physics Laboratory. The program was developed at Georgia Institute of Technology over the past four years; however, considerable development work in computer aided radome analysis has taken place here prior to that time [1-7].

This analysis package was used during the research carried out under this grant to analyze the antennas and radomes using the fast receiving formulation as described in Volume I. Its documentation was done in conjunction with the on-going radome technology program at JHU/APL under the cognizance of R. C. Mallalieu (APL Contract 601053). It is intended to serve as part of a technology base for the radome technical community.

The report is organized by chapters according to the approximate order in which the subprograms are called, and each chapter describes one subprogram. Each chapter is essentially self-contained since it is meant to serve as the complete documentation on a single subroutine. References are provided at the end of each chapter. In some cases, figures are duplicated in different chapters for completeness. Each chapter is terminated with the listing of the subroutine.

Chapter 2 describes the main program and instructions for its use. Chapters 3 through 28 describe the thirty four subroutines required for execution, including those for producing Calcomp pattern plots and three-dimensional plots. Appendices A through D present computed results for four test cases for use in verifying correct operation on other systems. These results were obtained on the Cyber 70/74 computing system at Georgia Tech. The remaining part of this chapter describes background of the program development and summarizes the features of the computer analysis.

This report comprises Volume II of four volumes. Volume I describes the salient results of this overall investigation to determine the accuracies and ranges of validity of various analysis methods. Volume III documents the additional software required to analyze radomes using a surface integration method. Volume IV presents the experimental results obtained and is meant to serve as a data base for other investigators seeking to verify the accuracy of their computer codes.

1-2. Background

Development of the radome analysis computer program (RACP) was initiated in 1971 in an effort to include the effects of the radome on a ground mapping radar [1]. A three-dimension geometry and vector field formulation were used. A plane wave spectrum (PWS) representation of the radiation from the antenna greatly facilitated the computations since the Fast Fourier Transform (FFT) could be used. The program was used to compute power patterns on the ground for many different cases of antenna/missile orientations. From these data, the effects of the radome on pattern shape, power loss and VSWR were determined.

Monopulse tracking antennas were next introduced into the computer analysis to evaluate radome materials and shapes for seeker systems in the 8-18 GHz band [2]. Tangent ogive shapes of various fineness ratios were analyzed. Monolithic and multilayer wall structures were used. Algorithms were developed to compute boresight errors from the sampled data difference patterns in two orthogonal planes. A modification of this program was also used to conduct a trade-off and development study for the Multipurpose Missile (MPM), later known as ASALM [3].

The next step in the development of RACP came in 1977 with the introduction of a conical scan tracking antenna into the analysis [4]. This antenna necessitated a reformulation of the analysis from the transmitting formulation used earlier to a receiving formulation. The big advantage offered by the latter is that the antenna response can be calculated for only one direction of arrival of the target return (plane wave). In the former, the FFT automatically computes "responses" for many directions of arrival and, hence, is computationally slower. Subsequent versions of the program have used the same receiving formulation with monopulse and other types of antenna models.

The computed results obtained with the receiving and transmitting formulations are not always the same [5]. A computed-aided analysis which utilizes the Huygens-Fresnel principle [6, 7] is generally considered to be more accurate than the two methods already mentioned, but requires considerably more computation time that may not be warranted in all cases. A research program is now underway at Georgia Tech whose objective is to establish the accuracies and ranges of validity of these three methods of radome analysis [5].

1-3. Description of the Analysis

The current version of the ray tracing analysis computer program utilizes a receiving formulation based on the Lorentz reciprocity theorem [5]. A plane wave of selectable linear or circular polarization is assumed incident on the outside of the radome and is represented by a system of parallel rays. There is one ray for each sample data point in the antenna aperture inside the radome. Each ray is traced from the point where it impinges on the outside surface to the corresponding aperture point. The electric and magnetic fields $\underline{E}_i$, $\underline{H}_i$ associated with each ray are weighted by the flat panel transmission coefficients $T_\perp$, $T_{||}$ as determined by the unit normal $\hat{n}$, the direction of propagation $\hat{k}$, and the dielectric properties of the radome wall. The weighted incident fields $\underline{E}_i'$, $\underline{H}_i'$ at each aperture point are then used in the following integral to obtain the complex voltage response V_r of the antenna as

$$V_r = C \iint_S (\underline{E}_T \times \underline{H}_i' - \underline{E}_i' \times \underline{H}_T) \cdot \hat{z} \, dxdy \qquad (1)$$

where $\underline{E}_T$, H_T are the aperture fields when the antenna is transmitting, C is a complex constant, and $\hat{z}$ is the unit vector normal to the xy (aperture) plane. For digital computer implementation, the integral in Equation (1) reduces to a double summation, and the equal-area elements dxdy become $\Delta x \Delta y$ and can be absorbed into the constant C.

In its present form, the program accommodates only one radome shape; viz., the tangent ogive. The length, diameter and fineness ratio are, of course, all variable in the input data. Monolithic and multilayer wall configurations can be analyzed; however, only uniform wall configurations whose properties do not vary from point to point on the

wall can be handled. Provisions are made to allow for a metal tip on the radome whose effect is aperture blockage.

The geometry subroutines provide for three separate coordinate systems and the point and vector transformations among them. A reference coordinate system is provided to orient the antenna/radome combination with respect to other bodies. The coordinate systems for the antenna and the radome comprise the other two systems. Boresight error and pattern computations are carried out and expressed in the antenna coordinate system.

The primary outputs of the program are boresight error (mrad.), boresight error slope (deg./deg.), gain loss, and when selected, principal plane patterns. Outputs include both printing and plotting (Calcomp). Plotting options allow for selection of aperture fields with and without the radome. A feature is also provided to either obtain or suppress intermediate calculated results for debugging purposes.

Boresight error calculations for monopulse antennas are carried out by setting the first target return at a known direction within a few degrees of true boresight. The responses in the two difference channels and the sum channel are then computed and stored. Another set of responses for a return 180° away from the first is computed next. The two sets of data are then used to construct a linear tracking model in the two orthogonal planes, and the process is repeated until a boresight null is indicated. The true direction of arrival of the plane wave at this point represents the boresight error directly.

The current subroutine used to characterize the antenna permits selection of various polarizations and two aperture distributions. A uniform, circular aperture distribution having vertical, horizontal or

circular (LHR or RHC) polarizations is one combination. The second distribution is a tapered rectangular distribution having vertical polarization as found in flat plate antennas. This basic subroutine would not be difficult to modify to accommodate other distributions, such as rectangular aperture with cosine taper.

Computation time is independent of radome size but depends on the number of samples used in the aperture. For 256 sample points (16 X 16 array), the time to compute the received voltages in the three channels is 1.5 seconds.

The program is organized as a main program and a number of supporting subroutines, all written in Fortran IV. The complete program, including plotting software, contains thirty four subroutines. The core storage required for the complete program, including all library and system I/O routines, is just over 46,000 (decimal) words. Integer, real and complex variables and arrays are utilized. Single, double and three-dimensional data arrays are present. Only single precision variables and computations are required with the 60-bit word available on the Cyber 70 at Georgia Tech.

1-4. References

1. E. B. Joy and G. K. Huddleston, "Radome Effects on Ground Mapping Radar", Contract DAAH01-72-C-0598, U. S. Army Missile Command, March 1973.

2. E. B. Joy, G. K. Huddleston, H. L. Bassett and C. L. Gorton, "Analysis and Evaluation of Radome Materials and Configurations for Advanced rf Seekers", Contract DAAH01-73-C-0769, December 1973.

3. E. B. Joy, G. K. Huddleston and H. L. Bassett, "Multi-Purpose Missile (MPM) High Performance Radome Trade-Off and Development Study", Martin Marietta Aerospace, April 1975.

4. G. K. Huddleston and E. B. Joy, "Development of Fabrication and Processing Techniques for Laser-Hardened Missile Radomes; Radome Electrical Design Analysis", Martin Marietta Aerospace, April 1977.

5. G. K. Huddleston, H. L. Bassett and J. M. Newton, "Parametric Investigation of Radome Analysis Methods", 1978 IEEE AP-S Symposium Digest, pp. 199-202, May 1978.

6. S. Silver, Microwave Antenna Theory and Design, New York, New York: McGraw-Hill Book Company, 1949.

7. D. T. Paris, "Computer-Aided Radome Analysis", IEEE Transactions, AP-18, no. 1, pp. 7-15, January 1970.

8. G. K. Huddleston, H. L. Bassett, & J. M. Newton, "Parametric Investigation of Radome Analysis Methods: Salient Results", Final Technical Report, Volume I of IV, Grant AFOSR-77-3469, February 1981.

9. G. K. Huddleston, H. L. Bassett, & J. M. Newton, "Parametric Investigation of Radome Analysis Methods: Computed-aided Radome Analyis Using the Huygens-Fresnel Principle and Lorentz Reciprocity", Final Technical Report, Volume III of IV, Grant AFOSR-77-3469, February 1981.

10. H. L. Bassett, J. M. Newton, W. Adams, J. S. Ussailis, M. J. Hadsell, and G. K. Huddleston, "Parametric Investigation of Radome Analysis Methods: Experimental Results", Final Technical Report, Volume IV of IV, Grant AFOSR-77-3469, February 1981.

Chapter 2

PROGRAM RTFRACP

2-1. Purpose: RTFRACP is a Fortran computer program used to analyze the effects of a tangent ogive radome on the performance of a monopulse aperture antenna. It consists of a main program and 34 subroutines. It uses complex arithmetic and requires 57121 octal words of core memory for execution on the CDC Cyber 70 system (60-bit words) at Georgia Institute of Technology. Execution time to compute boresight error on the Cyber 70 is approximately two seconds per look direction when the antenna aperture is represented by 16 x 16 = 256 sample data points. Execution time to compute transmitting and receiving patterns and aperture near fields, and to compute the necessary Calcomp commands for two- and three-dimensional plotting, is approximately 35 seconds for one look direction.

The computer-aided radome analysis uses a receiving formulation based on the Lorentz reciprocity theorem as described earlier [1,2]. The voltage produced at the terminals of a linear antenna by an incident plane wave is given by

$$V_R(\hat{k}) = \oint\!\!\oint (\underline{E}_T \times \underline{H}_R - \underline{E}_R \times \underline{H}_T) \cdot \hat{n}\, da \qquad (1)$$

where $\underline{E}_T$, $\underline{H}_T$ are the fields produced on the surface S enclosing the antenna when the antenna is transmitting; $\underline{E}_R$, $\underline{H}_R$ are the incident fields produced on S by the incident plane wave or perturbations thereof; $\hat{k}$ is a unit vector which points from the antenna toward the direction from which the plane wave arrives; and $\hat{n}$ is a unit vector normal to the surface S and pointing

outward. The fields $\underline{E}_T$, $\underline{H}_T$ are taken to be those produced in the planar aperture when the antenna is transmitting in the absence of the radome. The geometrical optics approximation

$$\underline{H}_T = \frac{\hat{n} \times \underline{E}_T}{\eta} \tag{2}$$

is used to generate the magnetic field in the aperture from the aperture illumination specified by $\underline{E}_T$. Rays are traced from each sample point in the aperture in the direction $\hat{k}$ to the inner radome wall. The plane wave fields associated with each ray are weighted with the flat panel insertion voltage transmission coefficients as determined by the radome wall configuration, the angle of incidence, and the plane of incidence. The individual contributions are summed up as indicated in Equation (1).

The parameters of the tangent ogive radome are indicated in Figure 2-1. The outside base diameter D_{os} and fineness ratio F_{os} determine the outside length according to

$$F_{os} = L_{os}/D_{os} \tag{3}$$

A similar relation holds for the inside dimensions; viz.,

$$F_{is} = L_{is}/D_{is} \tag{4}$$

The radius of curvature of the outside wall R_{os} is given by

$$R_{os} = F_{os}\, D_{os} \,/\, \sin\left(\pi - 2\, \mathrm{Tan}^{-1}(2F_{os})\right) \tag{5}$$

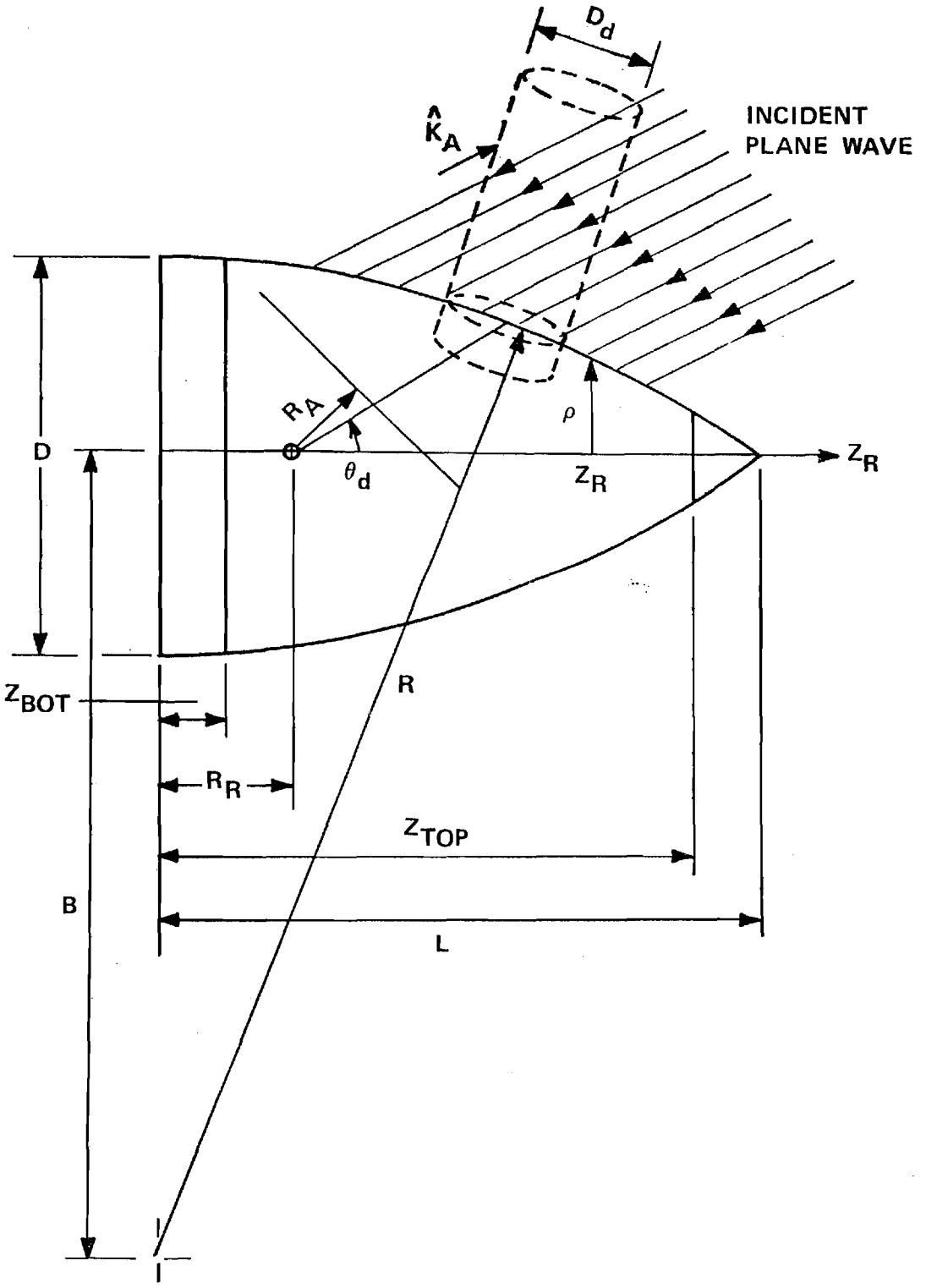

Figure 2-1. Tangent Ogive Radome Geometry.

and the dimension B is given by

$$B = R_{os} - D_{os}/2 \tag{6}$$

The placements of a bulkhead (bottom disk) and metal tip (top disk) can be specified by Z_{BOT} and Z_{TOP}, respectively. The thickness, dielectric constant, and loss tangent of the wall may also be specified for up to N=5 layers. The radome is assumed to be a body of revolution with uniform wall dimensions independent of location. The dashed cylindrical shape of a diameter D_d in Figure 2-1 was used earlier to simulate a laser-induced defect and is not pertinent here.

The subroutine which generates the antenna aperture fields represents two types of antennas: circular aperture with uniform illumination and any one of four polarizations (vertical, horizontal, RHC, LHC); flat plate antenna with tapered illumination and vertical polarization. For either antenna, the fields are computed for one of three selected channels: sum, azimuth difference, elevation difference. Inputs include the number of samples N_X, N_Y and the aperture diameter D_{AP}/λ in wavelengths.

The antenna/radome orientation is specified according to the parameters defined in Figure 2-2. The angle ϕ_p selects the plane of scan of the radome tip with respect to the antenna coordinate system: $\phi_p = 0°$ selects the azimuth plane; $\phi_p = 90°$ selects the elevation plane. The angle θ_L scans the tip in the selected plane.

The program computes boresight errors in the azimuth and elevation planes of the antenna. The radome orientation is specified by ϕ_p and ϕ_L. The first target return (plane wave) is made to arrive from the direction

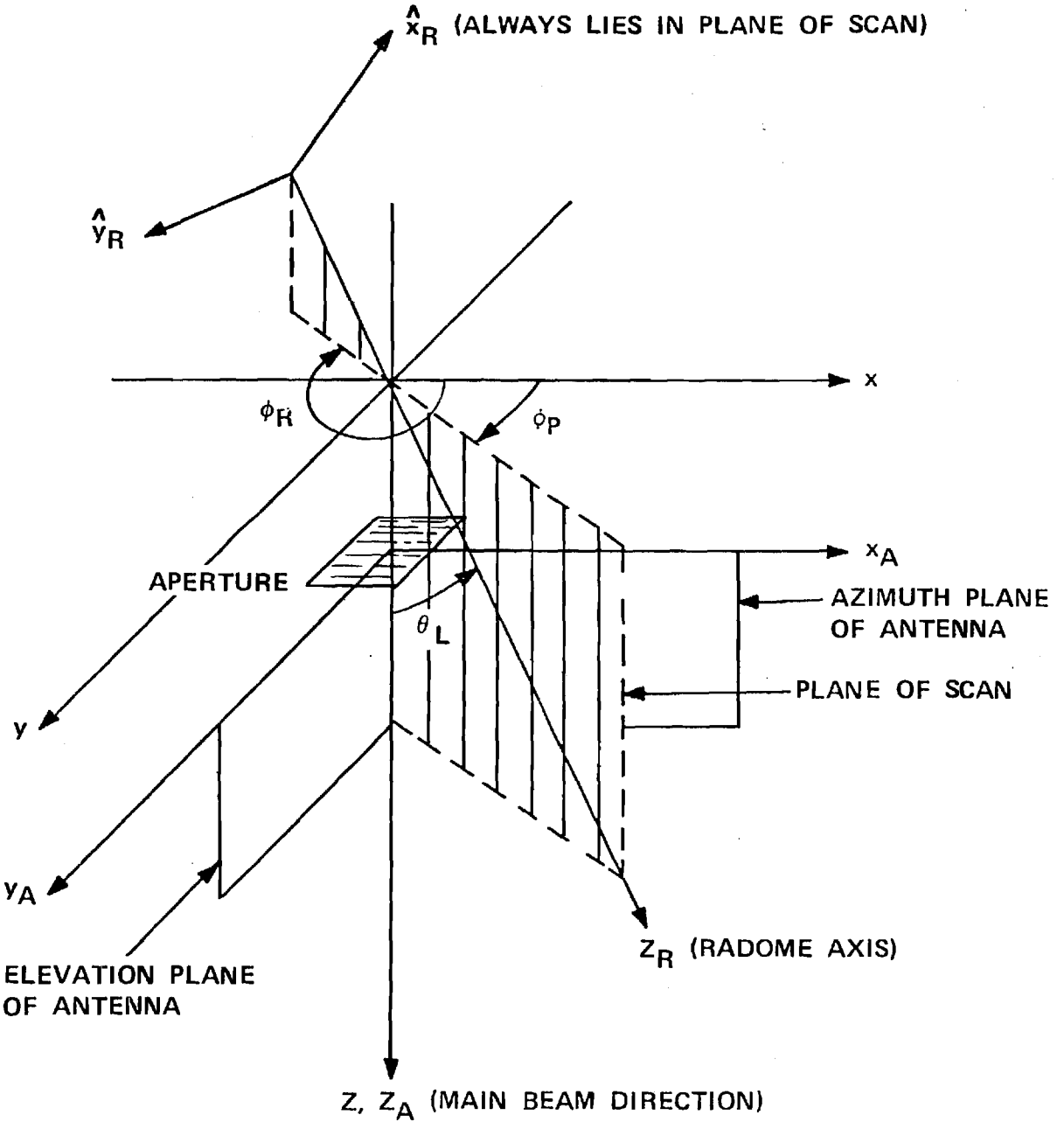

Figure 2-2. Coordinate Systems Used in Radome Analysis.

$$\hat{k}_1 = \hat{x}_A \sin \theta_{os} + \hat{y}_A \sin \theta_{os} + \hat{z}_A \sqrt{1 - 2 \sin^2 \theta_{os}} \qquad (7)$$

where θ_{os} is the initial specified offset angle; e.g., 2°. The voltage received by each channel is computed and stored. The second return is made to arrive from

$$\hat{k}_2 = \hat{x}_A(-\sin \theta_{os}) + \hat{y}_A(-\sin \theta_{os}) + \hat{z}_A \sqrt{1 - 2 \sin^2 \theta_{os}} \qquad (8)$$

and the voltages are again computed. The data from these two points are used to construct a linear tracking model in the two planes, and a direction of arrival $\hat{k}$ is predicted which will yield null indications in both planes. The process is repeated until a desired error tolerance is satisfied or a maximum number of iterations is exceeded. Upon completion, the output $\hat{k}$ indicates the direction from which the plane arrives which yields an electrical boresight indication. If α and β represent the boresight error angles in the azimuth and elevation planes, respectively, then they are related to the direction $\hat{k} = \hat{x}_A k_x + \hat{y}_A k_y + \hat{z}_A k_z$ by

$$\sin \alpha = \frac{k_x}{\sqrt{1 - k_y^2}} \qquad (9)$$

$$\sin \beta = \frac{k_y}{\sqrt{1 - k_x^2}} \qquad (10)$$

where

$$k_z = \sqrt{1 - k_x^2 - k_y^2} \quad . \qquad (11)$$

Options are also provided whereby principal plane patterns as shown in Figure 2-3 and additional outputs around boresight can be computed and printed. These options are useful when preparing software for a new type of antenna and to ensure correct operation whenever curious results are obtained.

2-2. Usage:

	Line No.
DATA APIN/0./	47
DATA ZBOTIN/0.00/	49
DATA RADIUS/1E0/	52
DATA THETAA, PHIA, AGAM3A/0.0,90.0,0.0/	53
DATA NX, NY, NXE, NYE, NXY/16,16,256,1,512/	56
DATA NREC, NS, MX, MY/32,16,16,1/	57
READ (5,6) TITLE	62
READ (5,*) GRAF3D, GRAFSA, GRAFTR, GRAFRV, SUPPRS, IPENCD	65
READ (5,*) NFINE, NPHI, NTHE, DIAOS, RA, RR, ZTOPIN, FREQ, OSANG	67
READ (5,*) LMAX, DMRAD, IOPT, RAPMAX, VAIRM, IPOL, ICASE, N, IPWR	76
READ (5,*) DIN(I), ER(I), TD(I) (I=1,N)	108
READ (5,*) FINR(I) (I=1,NFINE)	117
READ (5,*) PHI(I) (I=1, NPHI)	120
READ (5,*) THETA(I) (I=1,NTHE)	122

2-3. Arguments

a. Inputs. Units of arguments on input are distances in inches, angles in degrees, and frequency in gigahertz, unless otherwise noted. Units of arguments passed to subroutines are centimeters, radians, and

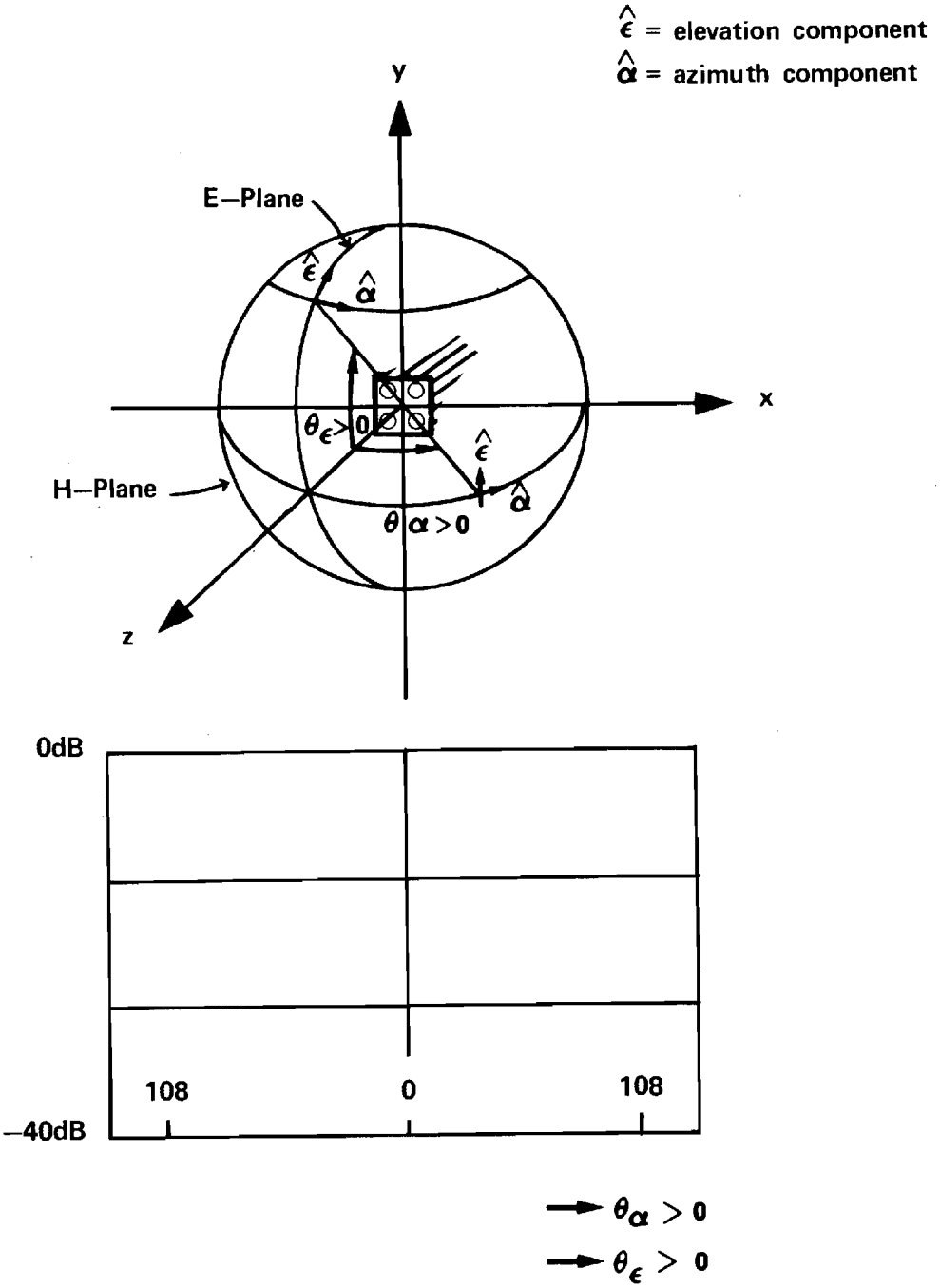

Figure 2.3 Coordinate System for Far Field Patterns

gigahertz. An asterisk is used to denote those DATA arguments that do not normally need to be changed by the user.

APIN* - Height of a cylindrical base section of the tangent ogive radome. It is no longer included in the ray tracing algorithms and should not be changed from its zero value.

ZBOTIN - Distance from base of tangent ogive radome to missile bulkhead (Figure 2-1).

RADIUS* - The radius R used in the far field factor e^{-jkR}/R by Subroutine FAR. Do not change.

THETAA* - Angle θ_a between z-axis and the position vector $\underline{r}_a$ to the antenna origin. This angle was used in earlier work to locate the antenna origin in the reference system using spherical coordinates (r_a, θ_a, ϕ_a). Do not change. See Chapter 7.

PHIA* - Angle ϕ_a between the projection of z_A axis onto the xy-plane and the x-axis. Do not change.

AGAM3A* - Angle between z_A-axis and z-axis in Figure 2-2. Do not change.

NX,NY - Integer powers of two equal to the number of sample points in the antenna aperture; e.g., 16, 32, 64, etc. Changing NX and NY necessitates compatible changes in Lines 16-18.

NXE,NYE - Integer powers of two which specify the expanded number of sample points desired when computing the transmitting patterns of the antenna by inverse Fourier transforming the aperture fields.

Subroutine JOYFFT provides this capability of increased resolution in one or both dimensions. Changes in NXE, NYE necessitate compatible changes in Lines 16, 20, 22, and 23. Note that NXE*NYE≤NX*NY and either NXE≤NX or NYE≤NY.

NXY - Integer power of two used by Subroutine JOYFFT for dimension of complex working array XYFFT. Note that MX*NX≤NXY and MY*NY≤NXY. See below for MX and MY.

NREC - Integer power of two equal to the number of points at which to compute the receiving pattern in either principal plane. The received voltage is computed at points θ_i equally spaced in $\sin\theta$, where θ is the angle measured from the z_A-axis as indicated in Figure 2-3, where $\sin\theta_i = -KMAX + (I-1)*2*KMAX/NREC$, and where $KMAX = \sin\theta_{max} < 1.0$.

NS - Not used. It was originally used by Subroutine RECBS. Do not remove.

MX,MY - Integer powers of two equal to the magnification factors desired in the k_x and k_y (E-plane) directions, respectively, of the transmitting antenna patterns. Note that the restrictions MX*NY≤NXY and MY*NY≤NXY must be observed. The data cited above indicated increased resolutions in the NX direction of MX=16 and no magnification (MY=1) in the NY direction. Consequently, note that NXE=MX*NX=256.

TITLE - A Hollerith string of up to 72 characters which describes briefly the analysis being done. A format of 18A4 is specified and should work for machines with word length greater than or equal to 32 bits. The dimension of TITLE (Line 31) should be at least 18.

GRAF3D - A logical variable used to control the plotting of the incident fields on the antenna aperture. This feature has been removed from the program, and GRAF3D should always be FALSE.

GRAFSA - A logical variable which (if TRUE) controls the plotting of the transmitting power patterns of the antenna as follows: E-plane sum, E-plane difference equation (Δ_{EL}), H-plane sum, and H-plane difference azimuth(Δ_{AZ}). The radome is absent.

GRAFTR - A logical variable which controls the plotting of the amplitude and phase of the antenna aperture fields in the following order:

$E_{X\Sigma}$, $E_{Y\Sigma}$, $E_{X\Delta EL}$, $E_{Y\Delta EL}$, $E_{X\Delta AZ}$, $E_{Y\Delta AZ}$.

GRAFRV - A logical variable which controls the plotting of the receiving patterns of the antenna with radome in the same order as specified under GRAFSA above.

SUPPRS - A logical variable which controls the printing of numerous results as illustrated in the test data in Section 2-6 below. When TRUE, the printing of these numerous results are suppressed. This feature

is convenient to aid in debugging new portions of software prior to making production runs.

IPENCD - An integer variable which selects pen and paper for the Calcomp. This variable may be system dependent. For the Cyber 70, IPENCD=00 yields ballpoint pen and 11" wide plain paper; IPENCD=40 yields a heavier ink pen and the same paper.

NFINE - Integer variable equal to the number of fineness ratios to be considered for the tangent ogive radome; e.g., NFINE=1.

NPHI - Integer variable equal to the number of scan planes; e.g., NPHI=2.

NTHE - Integer variable equal to the number of angles in each scan plane at which to compute boresight errors, etc. Note: The program is set up to iterate on fineness ratio, scan plane, and scan angle as outer loop, middle loop, and inner loop, respectively. Therefore, for each of NFINE fineness ratios, the analysis will be done for NTHE scan angles in NPHI different scan planes.

DIAOS - Real variable equal to the outside base diameter (in.) of the radome. See Figure 2-1.

RA - Real variable equal to the distance (in.) from the gimbal point to the antenna aperture.

RR - Real variable equal to the distance (in.) from the gimbal point to the base of the radome.

ZTOPIN - Real variable equal to the distance (in.) from the base of the radome to the face of a metal tip on the radome.

FREQ - Real variable equal to the frequency of operation in gigahertz.

OSANG - Real variable equal to the offset angle in degrees at which the first target return is to arrive on the antenna; e.g., OSANG=3.0.

LMAX - Integer variable equal to the maximum number of iterations allowed by Subroutine RECBS in computing boresight error; e.g., LMAX=5.

DMRAD - Real variable equal to the tolerance in milliradians allowed on computing boresight error; e.g., DMRAD=0.1.

IOPT - Integer variable which selects the polarization of the incident plane wave as follows:

1. Linear, elevation component
2. Linear, azimuth component
3. Right hand circular
4. Left hand circular

RAPMAX - Real variable equal to the maximum radius (in.) of the antenna aperture. See Figure 3-1.

VAIRM - Real variable equal to the maximum amplitude of sum channel received voltage without radome. Any real value can be entered for this variable since a subsequent program modification (Lines 326-328) causes VAIRM to be computed automatically.

IPOL - Integer variable which selects the polarization of the antenna when ICASE=1 according to the

same code as used above for IOPT.

ICASE - Integer variable which selects one of two types of antenna apertures for the analysis: ICASE=1 or 2 selects a circular aperture with uniform illumination; ICASE=3 selects a flat plate antenna with programmed illumination. See Subroutine HACNF in Chapter 3.

N - Integer variable equal to the number of layers (up to 5) in the radome wall. For cases where more than 5 layers are required, the dimensional arrays on Line 37 must be changed to NN=N+1.

IPWR - Integer variable which selects the component for which to compute the transmitting power patterns as follows:

1. Elevation Component
2. Azimuth Component
3. Total power

DIN,ER,TD - Subscripted real variables equal to the thickness (in.), dielectric constant (ε_r), and loss tangent (tan δ) of each layer of the radome wall. I=1 corresponds to the first layer and is the layer on the exit side of the wall. Layer N is the first layer encountered by the incident plane wave. See Subroutine WALL.

FINR - Subscripted real variable equal to NFINE fineness ratios.

PHI - Subscripted real variable equal to NPHI angles (degrees) which specify the scan planes.

THETA - Subscripted real variable equal to NTHE angles (degrees) which specify the scan angles in the scan plane.

b. Outputs. The parameters of analysis which are computed and and outputted by the program depend on whether SUPPRS is true. In what follows, it is assumed that SUPPRS=FALSE so that all possible outputs are obtained. Since many of the original input parameters are printed directly, only those parameters not already explained above will be included below. Additional clarification may be found in Section 2-6.

TABLE - Logical variable which, if TRUE, causes a look-up table to be used in computing transmission coefficients. When SUPPRS=FALSE, an abbreviated table of transmission coefficients of the radome wall is printed by Subroutine WALL with variables as explained immediately below.

ANGLE - Real variable equal to the angle of incidence (degrees) of the plane wave on a plane sheet of infinite extent having the layered configuration specified for the radome wall. The entries in the table are computed at 250 equal increments in sin θ_i, but only every fifth result is printed.

TPERI,TPARI- Complex variables equal to the voltage insertion transmission coefficients of the sheet for the two cases of $\underline{E}_i$ perpendicular to the plane of incidence ($T_\perp$) and $\underline{E}_i$ parallel to the plane of incidence ($T_{||}$). In the printed table, the power transmission coefficients $|T_\perp|^2$ are

$|T_{||}|^2$ are printed; adjacent to each, the phases of $T_\perp$ and $T_{||}$ are also printed.

RPERI,RPARI- Complex variables equal to the reflection coefficients $R_\perp$, $R_{||}$ of the plane dielectric sheet. Actually, $|R_\perp|^2$ and $|R_{||}|^2$ are printed, accompanied by the phases $R_\perp$ and $R_{||}$.

KXMAX - Real variable equal to the folding wavenumber associated with sampling the aperture fields according to KXMAX = 1./(2($\Delta x/\lambda$), where Δx is the distance between samples. See Subroutines HACNF and FFTA.

DXWL - Real variable equal to $\Delta x/\lambda$.

KXM,KYM - Real variables equal to the folding wavenumbers of the principal plane patterns after magnification for increased resolution. KXM=KYMAX*NXE/(MX*NX) and applies to the H-plane. KYM=KYMAX*NYE/(MY*NY) and applies to the E-plane. Usually, the expanded dimension NXE and magnification factor MX are selected so that KXM=KXMAX. Also, NYE and MY are usually selected so that KYM<<KYMAX.

MIN,MAX Real variables equal to the minimum and maximum values of the amplitude of the complex arrays containing the aperture fields as processed by Subroutine NORMH in preparation for 3D plotting by Subroutine PLT3DH.

ROS - Real variable equal to the radius of curvature of the outside shape of the tangent ogive radome.

BOS - Real variable equal to the distance B in inches defined in Figure 2-1.

FINOS - Real variable equal to the fineness ratio of the radome as based on the outside dimensions.

FINIS - Real variable equal to the fineness ratio of the radome as based on the inside dimensions.

The following variables are printed when the receiving patterns are computed and printed:

ICUT - Integer variable which defines the E-plane (ICUT=1) or H-plane (ICUT=2) pattern. See Figure 2-3.

ICOMP - Integer variable which defines the field component of the plane wave incident on the receiving antenna: ICOMP=1 for elevation component; ICOMP=2 for azimuth component.

KMAX - Real variable equal to the sine of the maximum angle off broadside for which the received voltage is computed.

NREC - Integer variable (power of 2) equal to the number of points at which the receiving pattern is computed. The pattern is computed at NREC points spaced equally in $k_{xy}=\sin\theta$ according to $\Delta k_{xy}=$ 2 KMAX/NREC.

DK - Real variable equal to 2*KMAX/NREC.

ANGMAX - Real variable equal to $\sin^{-1}$(KMAX).

The receiving pattern is computed at NREC points and magnified using Subroutine MAGFFT to 256 points equally spaced in sin θ over the range (-KMAX, KMAX-DK). Three parameters are printed: angle in degrees, amplitude in decibels, and phase in degrees. Only every fourth point in the 256 points is printed. The receiving patterns are printed in the following order:

E-Plane: Σ_{EL}, Δ_{EL}

H-Plane: Σ_{AZ}, Δ_{AZ}

Subroutine RECM maintains a count NRAY of the number of rays actually traced from points in the aperture to the radome wall. When SUPPRS=FALSE, this number will be printed.

Subroutine RECBS computes the boresight error of the antenna as produced by the radome. When SUPPRS=FALSE, the following parameters are printed:

K1, K2 - Real subscripted variables containing the direction cosines (k_{xi},k_{yi},k_{zi}) of the last and next to last true directions to the target. One of these variables is equal to K, the subscripted variable containing the direction cosines of the last target return.

AZTM,ELTM - Real variables equal to the boresight error in the H-plane and E-plane associated with the last target return (k_x,k_y,k_z). Expressed in milliradians, these errors are computed according to

$$AZTM = \sin^{-1}(k_x/\sqrt{1-k_y^2})*1000.$$

$$ELTM = \sin^{-1}(k^y/\sqrt{1-k_x^2})*1000.$$

Let $\hat{k} = \hat{x}_A k_x + \hat{y}_A k_y + \hat{z}_A k_z$. Then AZTM is the angle between the z_A-axis and the projection of $\hat{k}$ onto the $x_A z_A$ (azimuth) plane. ELTM is the angle between the z_A-axis and the projection of $\hat{k}$ onto the $y_A z_A$ (elevation) plane.

MESAZ,MESEL- Real variables equal to the monopulse error slopes in the azimuth and elevation channels expressed in units of volts per degree, where the maximum signal received by the sum channel is considered to be one volt.

UAZ,UEL - Real subscripted variables equal to the received tracking functions $I_{mag}\{\Delta/\Sigma\}$ corresponding to the target returns K1 and K2 above; e.g., UAZ(1) = $I_{mag}\{\Delta_{AZ}/\Sigma_{AZ}\}$ for K1.

SMAX - Real variable equal to the maximum amplitude of the received sum channel voltage.

LCTR - Integer variable equal to the number of iterations (target returns) used by Subroutine RECBS to compute boresight error.

Subroutine RECBS also computes and prints six additional monopulse outputs around the apparent boresight direction $\hat{k}_o$. The directions $\hat{k}$ chosen lie in the plane $k_x = k_y$ and are spaced one milliradian apart over the range ±3 mrad and centered on the direction $\hat{k}_o$. The variables printed are as follows:

ANG - Real variable equal to the angle in milliradians between $\hat{k}_o$ and $\hat{k}$.

VRAZ,VREL - Real variables equal to $I_{mag}\{\Delta/\Sigma\}$ for the target return from direction $\hat{k}$ for the azimuth and elevation channels, respectively.

DAZ,DEL - Amplitude and phase (degrees) of the complex voltages received on the Δ_{AZ} and Δ_{EL} channels, respectively, for target return $\hat{k}$.

SLPAZ,SLPEL- Average values of the monopulse error slopes (volts/degree) in the azimuth and elevation channels, respectively, obtained by a linear approximation of the tracking functions based on their values at ANG = ±3 mrad. For example,

SLPAZ = [VRAZ(3 mrad) - VRAZ(-3 mrad)]/(.006*57.3)

The main program always prints the boresight error in azimuth (BSEAZ) and elevation (BSEEL), and the values printed are identical to AZTM and ELTM defined above. Main also computes the gain of the antenna in decibels with the radome in place according to

GAIN = 20. * ALOG1Ø(SMAX/VAIRM)

For other than an "air radome", GAIN is negative and indicates a loss in antenna maximum gain due to radome reflections and ohmic ($\tan\delta$) losses. The amplitude of received sum voltage, VAIRM, is always printed as the last item prior to termination of the program.

2-4. Comments and Method

a. Method. The method of analysis has been presented in Section 2.1. Additional details of analysis are presented in the descriptions of each subroutine.

b. Supporting Subroutines. Thirty four supporting subroutines are required by RTFRACP. The purpose of each one is briefly described below.

(1) HACNF--Computes complex vector aperture electric fields of antenna for all three monopulse channels at NX x NY sample points.

(2) ORIENT--Computes matrices ROTATE and TRANSLate used for coordinate transformations by Subroutines POINT and VECTOR.

(3) POINT--Transforms a point $P(x_A, y_A, z_A)$ in antenna system to the same point $P(x_R, y_R, z_R)$ in radome coordinate system, and vice versa.

(4) VECTOR--Transforms a vector from radome to antenna coordinate system, and vice versa.

(5) INCPW--Computes the rectangular electric field components of a plane wave incident from the direction $\hat{k}_A$ in antenna coordinates. The power density of the plane wave is unity.

(6) RECM--Computes the voltage received by each channel of the antenna for a plane wave $PWI(E_x, E_y, E_z)$ incident on the radome from the direction $KA(k_x, k_y, k_z)$. Subroutine RECM calls the following subroutines:
VECTOR, POINT, TRACE, RXMIT, CAXB.

(7) TRACE--Directs the ray tracing process and calls Subroutines OGIVE, OGIVEN, TDISK, TDISKN, BDISK, BDISKN, SQR, CBRT, and XY.

(8) RXMIT--Computes the transmitted electric fields of the plane wave traveling in direction $-\hat{k}$ and incident on a flat

dielectric wall with unit inner normal $\hat{n}$. The unit vectors $\hat{k}$, $\hat{n}$ are used to resolve the incident plane wave into vector components perpendicular and parallel to the plane of incidence, and to determine the angle of incidence. RXMIT calls Subroutines WALL and AMPHS.

(9) WALL--Computes the voltage insertion transmission coefficients of flat panel model of the radome wall as function of the sine of the incidence angle.

(10) AXB--Computes real vector cross product $\underline{C} = \underline{A} \times \underline{B}$.

(11) CAXB--Computes the complex vector cross product $\underline{C} = \underline{A} \times \underline{B}$.

(12) RECBS--Computes boresight errors of antenna enclosed by the radome for the specified orientation, fineness ratio, etc. RECBS calls Subroutines INCPW, RECM, and AMPHS.

(13) RECPTN--Computes receiving patterns of all three channels. RECPTN calls Subroutines INCPW and RECM.

(14) OGIVE--Computes point of intersection of ray and ogive by solving a quartic equation. OGIVE calls Subroutines CBRT, SQR, and XY.

(15) CBRT--Computes cube root.

(16) SQR--Computes square root with test for negative argument.

(17) OGIVEN--Computes the unit inward normal vector to the ogive surface at the point $P(x_R, y_R, z_R)$.

(18) XY--Used by Subroutine OGIVE to compute the x_R and y_R components of the point of intersection of a ray on the inner radome surface.

(19) BDISK--Computes the point of intersection of a ray and planar bottom disk representing the bulkhead inside the radome.

(20) BDISKN--Computes unit normal vector to bulkhead ($\hat{n} = +\hat{z}_R$).

(21) TDISK--Computes the point of intersection of a ray and the base of the metal tip on the radome.

(22) TDISKN--Computes unit normal vector to metal tip ($\hat{n} = -\hat{z}_R$)

(23) FAR--Computes the amplitude of the power pattern from the complex plane wave spectra $A_x(k_x,k_y)$, $A_y(k_x,k_y)$ of an antenna.

(24) AMPHS--Converts a complex number from rectangular to polar form. This subroutine utilizes the intrinsic function ATAN2. The amplitude produced is linear (not decibels), and the phase is in degrees on the range (-180, 180).

(25) DBPV--Converts a real, two-dimensional array from linear to logarithmic values in decibels on the range 0 to -40 dB.

(26) NORMH--Normalizes a two-dimensional real array to values between 0 and 1.

(27) CNPLTH--Plots single dimensional far field patterns on axes patterned after standard pattern recorder paper. CNPLTH calls Subroutine PSI in addition to the usual Calcomp subroutines.

(28) PSI--Used by Subroutine CNPLTH to compute the azimuthal angle ψ.

(29) PLT3DH--Yields three-dimensional plots of the data in the two-dimensional real array FIELD. PLT3DH calls Subroutines PLTT, NORMH as well as the usual Calcomp subroutines.

(30) PLTT--Used by Subroutine PLT3DH to eliminate moving the pen for hidden lines.

(31) FFTA--Computes the Fast Fourier Transform of a one-dimensional complex array having 2**IEXP elements. Proper operation is machine dependent.

(32) MAGFFT--Provides increased resolution of a sampled function using FFT and Discrete Fourier Transform techniques.

(33) JOYFFT--Provides increased resolution of selected portions of a two-dimensional Fourier transform. JOYFFT calls Subroutines FFTA and PWRTWO.

(34) PWRTWO--Used by Subroutine JOYFFT to ensure that a given integer is a power of 2.

2-5. Program Flow

For the following, refer to the program listing in Section 2-8 and the line numbers shown on the right-hand margin of that listing.

Line Nos.	Explanation
Line 15:	All variables beginning with the letter K in the main program are real.
Lines 16-32:	Declare variables and array dimensions. Note equivalence statements in Lines 24-26. The dimension of IBUF in Line 29 may be computer system dependent. Note in Line 32 that only twenty fineness ratios, scan planes, and scan angles can be accommodated.
Lines 34-38:	Label common is used as a convenient means to transmit variables to subroutines not directly called by MAIN. The labels are generated from the names of the subroutines which receive the variables, and each label is terminated with the letter C to denote common; e.g., TDISKC denotes variables common to MAIN and Subroutine TDISK.

Lines 40-42: Declare namelists for printing data. These namelists are no longer used except for occasional debugging purposes.

Lines 43-57: Set data in DATA statements as described above in Section 2-3.

Lines 61-62: Set SMAX and VMAX to unity to prevent division by zero.

Lines 63-64: Read and write TITLE according to 18A4 format.

Lines 65-67: Read input data using free-field format.

Line 68: Compute sine of the offset angle θ_{OS}.

Line 69: Set TABLE=FALSE so that normalizing factor VAIRM can be computed (Lines 319-329) via a call to Subroutines RECM and RXMIT. In the latter, TABLE= FALSE causes $T_{\perp}$, $T_{||}$ to be set to unity as in the case of no radome.

Lines 71-75: Write input data.

Lines 76-77: Read input data and set VAIRM needlessly.

Lines 78-104: Comments explaining input variables.

Line 105: Set NN=N+1= Number of wall layers plus one.

Line 106: Initialize DINCH= total thickness of radome wall in inches.

Lines 107-109: Read wall data and compute total thickness.

Line 110: Compute DIAIN= inside base diameter of the radome in inches.

Lines 111-112: Compute indices of the center element of near-field arrays corresponding to $x_A=y_A=0$.

Lines 113-114: Write array dimensional data.

Lines 115-122: Read fineness ratios, scan planes, and scan angles.

Lines 123-126: Compute wavelength in inches and centimeters. Compute $\beta=2\pi/\lambda_{cm}$.

Lines 127-128: Call RXMIT and compute table of transmission coefficients versus sine of incidence angle. The first call to RXMIT builds the table. Subsequent calls use the table if TABLE=TRUE.

Line 129: Compute DAPWL= diameter of antenna aperture in wavelengths.

Lines 130-139: Convert variables in inches to centimeters for input to subroutines. Some variables are multiply defined to avoid conflicts in labeled common; e.g., ZBOT and Z1. Note that DIACM is the inside diameter of the radome in centimeters.

Lines 140-144: Convert angles from degrees to radians using RAD=π/180.

Lines 145-151: Compute near fields of three channel monopulse antenna using Subroutine HACNF.

Lines 152-158: Set KYMAX=KXMAX, compute magnified folding wavenumbers KXM, KYM, and print results.

Lines 159-177: Initialize Calcomp plotter, if required. The commented initialization (Lines 164-174) applies to the IBM 3033 system at JHU/APL.

Note: Lines 178-258 are used to plot the near fields of the antenna and/or the transmitting principal plane power patterns.

Lines 178-179: Initialize the maximum values FMXEL, FMXDAZ of the E- and H-plane patterns so that when used initially as inputs to Subroutine FAR, the resulting pattern will be normalized with respect to its own maximum and FMXEL and FMXDAZ will be set equal to these respective maxima. On subsequent calls to FAR, the resulting patterns will be normalized with respect to FMXEL and FMXDAZ. Hence, the relative gain of the difference and sum patterns will be correctly displayed in the graphs.

Line 180: Iterate for each of three monopulse antenna channels.

Lines 181-190: Equate complex arrays EXT, EYT to the selected near field and compute the amplitude NF of EXT.

Line 191: Assume transmitting near fields are to be plotted (GRAFTR=T).

Line 193: Call Subroutine PLT3DH to plot the amplitude of EXT. The inputs XSIZE=6., YSIZE=2.5, HEIGHT=2.5 yield a 3D plot that will fit on a 8½" x 11" report page. The inputs NF, NX, NY specify the real array to be plotted and its dimensions. The input NMZ=.TRUE. directs the subroutine to normalize NF so that its values be between 0 and 1. The input LDB=.FALSE indicates that the array NF contains linear values rather than logarithmic values (decibels).

Lines 194-201: Compute and plot phase of EXT on a scale of -180 degrees to +180 degrees. Note that Line 199 ensures that the real array NF contains these phase values scaled to the required 0 to 1 range.

Lines 202-215: Repeat amplitude and phase 3D plots for EYT.

Line 216: Assume GFAFSA=T so that principal plane patterns are plotted.

Line 219: If IP=3, go to Line 243 and plot H-plane patterns; otherwise, plot E-plane patterns.

Line 222: Call Subroutine JOYFFT to calculate the inverse Fourier transform of the x_A-component of near field EXT to produce the plane wave spectrum XEEL from which the radiation field can be computed. In the process of computing the transform, provide increased resolution from NX x NY points to NYE x NXE points through the point (NXC,NYC) in the array EXT. In the k_x direction, the plane wave spectrum is magnified by MY; it is magnified by MX in the k_y direction. The array FFTXY is a working array.

Line 223: Repeat for EYT to produce the plane wave spectrum YEEL for the y_A-component of field.

Line 224: Call Subroutine FAR to calculate the E-plane elevation (IPWR=3) power pattern FFSEL of the near field at equal samples in $\sin\theta$ over the range (-KXM, KXM $-\Delta$K). If FMXEL$\leq$0 (and it is for IP=1), normalize FFSEL with respect to its own maximum.

Line 226: Call Subroutine DBPV and convert the power pattern to decibels on a scale of 0 to -40 dB.

Lines 227-230: Scale the values in FFSEL to the range of 0 to 1 for plotting.

Line 231: Call Subroutine CNPLTH and plot the power pattern. If KXM<1, the pattern is plotted over the angular range corresponding to $\sin^{-1}$(KXM); if KXM≥1, the angular angle is (-90°, 90°). Subroutine CNPLTH actually plots conical cuts corresponding to k_x = constant or k_y = constant as specified by inputs KXC, KYC. In the call here, KXC=KYC=0 so that a principal pattern is produced.

Lines 232-236: Write a figure title for the plot and establish a new origin for the next plot.

Line 237: If IP=2, the E-plane patterns are finished.

Lines 238-242: Since JOYFFT changes the input arrays EXT,EYT, it is necessary to recompute them so that increased resolution can be obtained in the plane wave spectra in the H-plane.

Lines 243-258: Repeat computation and plotting for H-plane power patterns.

Line 260: Iterate the radome analysis for NFINE fineness ratios.

Line 261: Set FINE = outside fineness ratio.

Lines 262-266: Calculate and write R_{OS}, B, F_{OS}, F_{IS} as defined in Figure 2-1 for the radome geometry.

Line 267: Compute RDML = distance from the base of the radome to the theoretical tip on the inside of the radome.

Lines 268-272: If ZTOPIN<RDML, the radome has a metal tip, and a message is written to that effect.

Lines 273-283: Compute parameters needed by Subroutine OGIVE to describe the radome shape. R and B are in centimeters

and apply to the inside dimensions. AP, the height of the cylinder in centimeters, is not used. RTSQ= square of the radius of the top disk. RBSQ= square of the radius of the bottom disk (bulkhead). The other variables, BSQ, RINV, RSQ1, RP, and RP2, are precalculated here to speed later computations in OGIVE.

Line 285: Compute conversion factor DPMR for converting milliradians to degrees.

Lines 286-288: Initialize the "last" values of boresight error in azimuth (AZL) and elevation (ELL) and the "last" value THL of scan angle. These variables are used later to compute boresight error slope in degrees per degree from the present and last values of boresight error.

Lines 289-290: Write title for analysis results.

Lines 291-293: Write parameters of radome wall.

Lines 294-296: Write heading for table of boresight error and gain data.

Lines 297-301: Write this same data to logical unit 7 for subsequent storage as a disk file, if desired.

Line 309: Iterate the radome analysis for NPHI scan planes.

Lines 310-312: Compute ϕ_r in radians as required by Subroutine ORIENT.

Line 313: Iterate the analysis for NTHE scan angles in each scan plane.

Lines 314-316: Compute θ_r in radians as required by Subroutine ORIENT.

Line 317: Call Subroutine ORIENT and compute the rotation matrix ROTATE and translation matrix TRANSL required for coordinate transformations using Subroutines POINT and VECTOR.

Line 318: On the first iteration, TABLE is false so that the maximum amplitude of the received voltage on the sum channel is computed without the radome.

Line 319-322: Set the direction cosines of the incident plane wave so that it arrives from the $\hat{z}_A$ direction.

Line 323: Call Subroutine INCPW and compute the rectangular components PWI of the incident plane wave having polarization specified by IOPT.

Lines 324-325: Set TSUP=T and TABLE=F so that an air radome wall be used and so that printing by Subroutines RXMIT and RECM will be suppressed.

Lines 326-327: Call Subroutine RECM and compute the complex voltages VR received on the sum, difference elevation, and difference azimuth channels, respectively, corresponding to VR(I), I=1,3.

Line 328: Compute VAIRM=$|$VR(1)$|$.

Line 329: Set TABLE=T so that on subsequent iterations VAIRM will not be recomputed, and so that the table of transmission coefficients will be utilized when RXMIT is called.

Line 330: If SUPPRS=F, compute and print the E-plane and H-plane receiving power patterns of the antenna with the radome in place.

Lines 333-334: Iterate in J for E-plane (ICUT=1) and H-plane (ICUT=2) patterns.

Line 335: Set the desired far field component.

Lines 336-337: Set KMAX=$\sin^{-1}(\theta_{max})$=.996. If KXMAX, as computed by HACNF, is less than KMAX, then use the smaller as the maximum angle in the principal plane at which to compute the pattern.

Line 338: Set the temporary logical variable TSUP=T so that printing will be suppressed.

Lines 339-340: Call Subroutine RECPTN and compute the complex received voltages on each of three channels at NREC points over the range (-KMAX, KMAX - DK).

Lines 341-344: Increase the resolution and print results for all three channels. Do not print results that are known to be identically zero.

Lines 345-346: Transfer the received voltage into a one-dimensional array VREC.

Line 347: If NREC>NXE, there is no need to increase the resolution.

Line 348: Call Subroutine MAGFFT to increase the resolution of VREC from NREC points to NXE points. The result is contained in complex array XYFFT on output.

Lines 349-353: Compute linear power pattern.

Line 354: Select NXX=larger of NXE and NREC.

Lines 355-356: Write heading for printed results from Subroutine NORMH.

Line 357: Call Subroutine NORMH to normalize the NXX values in real array MVREC to be between zero and one. The input argument LDB=.FALSE. since the values are not in decibels.

Line 358: Call Subroutine DBPV to convert the power pattern in MVREC to decibels.

Lines 359-360: Write correct heading for E-plane or H-plane.

Line 361: Compute the increment in sinθ at which the power pattern has been computed and resolved.

Lines 362-368: Scale the power pattern to have values between 0 and 1. If SUPPRS=F, compute the angle θ=ANG and the phase of the pattern, and print the results for every fourth angle.

Line 372: If GRAFRV=T, plot the receiving power patterns.

Lines 373-378: Call Subroutine CNPLTH and plot the receiving patterns in turn. Write an appropriate figure title following each pattern plot. Re-origin the plotter pen for subsequent plots. The result of Lines 330-383 is four principal plane patterns: E-plane sum, E-plane Δ_{EL}, H-plane sum, H-plane Δ_{AZ}.

Lines 384-386: Call Subroutine RECBS and compute the boresight errors AZT, ELT in the azimuth and elevation planes of the antenna as caused by the radome. On output, the real array KA contains the direction cosines of the last target return and, hence, gives the true direction to the target at the time that the tracking functions in the azimuth and elevation planes indicated the electrical boresight direction.

Line 387: If this is the first iteration in scan angle, do not attempt to compute boresight error slope.

Lines 388-389: Compute boresight error slope (degrees/degree) in azimuth and elevation channels.

Lines 390-392: Set the "last" values of boresight errors and scan angle to the current values in preparation for next iteration.

Line 393: Compute loss in maximum gain of the antenna sum channel due to the radome.

Lines 349-395: Write results to logical units 6 and 7.

Lines 399-400: Write maximum amplitude of received sum voltage VAIRM without radome.

Line 401: Terminate plotting software.

STOP

END

2-6. Test Cases

Four test cases are presented in Appendices A, B, C, and D to demonstrate correct operation of the radome analysis computer program RTFRACP.

Appendices A and B present the test data and results for a circularly (RHC) polarized antenna and five-layer tangent ogive radome at a frequency of 11.80285GHz (λ=1.0 inch). The diameter of the aperture is 11.84λ. The outside diameter of the radome is 16.267 inches. The fineness ratio is 3.00. In Appendix A, the program is exercised without plotting, and printing is minimized. In Appendix B, all plotting and printing options are exercised.

Appendices C and D present the test data and results for a vertically polarized flat plate antenna of diameter 5.1992λ. All other parameters of the analysis are the same as in Appendices A and B. Appendix C contains the

case of no plotting and minimum printing. Appendix D contains the results for all plotting and printing options.

The first page in each appendix presents the test data as actually read in by the program except that line numbers have been added along the right-hand margin. The second and succeeding pages of each appendix contain the printed output as produced by the program. Line numbers have been added along the right-hand margin.

In Appendices B and D, the plots produced by the program are presented immediately after the printed output. The plots are presented in the order that they were produced by the program. Captions have been added for clarity. In addition, axes have been provided for the three-dimensional plots.

Referring to Appendix A, Lines 32-40 of the output listing, it is seen that a circularly polarized antenna produces boresight errors in both planes even though the scan of the radome tip is confined to a single plane. Comparison of these results to those in Appendix C (Lines 32-40) indicate that for a linearly polarized antenna, boresight errors are produced only in the plane of scan as would be expected from symmetry considerations. Further detailed consideration of the circularly polarized antenna shows that depolarization of the incident plane wave by the radome produces additive errors, and the results shown are according to expectations.

The transmitting and receiving patterns in Appendix B (and D) are not in agreement contrary to expectations. The discrepancy is due to the fact that the receiving patterns have a $(1 + \cos\theta)$ variation characteristic of the geometrical optics approximation used for $\underline{H}_T$. On the other hand, the transmitting patterns have a $\cos\theta$ variation as characteristic of an assumption of only magnetic current sources in the aperture. The disagreement is significant only for angles away from boresight.

The total computation time required for each test case on the Cyber 70 system at Georgia Institute of Technology was as follows:

Test Case	Appendix	Time (sec.)	No. of Scan Angles
1	A	17.52	10
2	B	36.844	1
3	C	20.369	10
4	D	34.678	1

In all four cases NX=NY=16, NXE=256, MX=16, and the incident plane wave contained only an elevation component. Variances in execution time are due to time-share nature of the computing system used.

2-7. References

1. G. K. Huddleston and E. B. Joy, "Development of Fabrication and Processing Techniques for Laser Hardened Missile Radomes: Radome Electrical Design Analysis", Martin Marietta Purchase Agreement 573712, April 1977.
2. G. K. Huddleston, H. L. Bassett, and J. M. Newton, "Parametric Investigation of Radome Analysis Methods", IEEE AP-S Symposium Digest, pp. 199-202, May 1978; also, Proc. Fourteenth Symposium on Electromagnetic Windows, pp. 21-28, June 1978.
3. E. B. Joy and G. K. Huddleston, "Radome Effects on the Performance of Ground Mapping Radar," U.S. Army Missile Command, DAAH-01-72-C-0598, March 1973.

2-8. Program Listing: See following pages.

```
C   THIS RAY TRACING FORMULATION RADOME ANALYSIS COMPUTER PROGRAM,                1
C   RTFRACP, USES GEOMETRICAL OPTICS AND LORENTZ RECIPROCITY                      2
C   TO COMPUTE THE RESPONSES AND BORESIGHT ERRORS OF A MONOPULSE                  3
C   ANTENNA INSIDE A TANGENT OGIVE RADOME TO AN INCIDENT PLANE                    4
C   ELECTROMAGNETIC WAVE OF SPECIFIED POLARIZATION (TARGET RETURN).               5
C                                                                                 6
C   RTFRACP WAS DEVELOPED AT GEORGIA INSTITUTE OF TECHNOLOGY, ATLANTA             7
C   GEORGIA, PRIMARILY UNDER GRANT AFOSR-77-3469 (PHYSICS DIRECTORATE)            8
C   AND DOCUMENTED UNDER JHU/APL CONTRACT NO. 601053 (ROBERT C.                   9
C   MALLALIEU) FOR USE ON A SIGNIFICANT RADOME TECHNOLOGY PROGRAM                10
C   FOR THE DEPARTMENT OF THE NAVY.                                              11
C                                                                                12
C   THIS VERSION IS FOR EXECUTION ON CYBER 70/74.  WITH ONLY MINOR               13
C   SYNTAX CHANGES,  IT HAS BEEN IMPLEMENTED ON THE IBM 3033 AT JHU/APL.         14
C                                                                                15
      PROGRAM RTFRACP(INPUT,OUTPUT,TAPE5=INPUT,TAPE6=OUTPUT,TAPE7)               16
      IMPLICIT REAL(K)                                                           17
      REAL NF(16,16),MVREC(256),KA(3)                                            18
      COMPLEX SUMX(16,16),SUMY(16,16),DELX(16,16),DELY(16,16)                    19
      COMPLEX DAZX(16,16),DAZY(16,16),EXT(16,16),EYT(16,16)                      20
      COMPLEX VR(16),VREC3(32,3),VREC(32)                                        21
      REAL FFS(256,1),FFSEL(1,256),NORM(3),P1(3)                                 22
      COMPLEX PWT(3),PWI(3)                                                      23
      COMPLEX XE(256,1),YE(256,1),XYFFT(512)                                     24
      COMPLEX XEEL(1,256),YEEL(1,256)                                            25
      EQUIVALENCE(XE(1,1),XEEL(1,1))                                             26
      EQUIVALENCE(YE(1,1),YEEL(1,1))                                             27
      EQUIVALENCE(FFS(1,1),MVREC(1),FFSEL(1,1))                                  28
      LOGICAL GRAF3D,GRAFSA,GRAFTR,GRAFRV,TABLE,SUPPRS,TSUP                      29
      INTEGER IBUF(512)                                                          30
      REAL ROTATE(3,3),TRANSL(3),TITLE(18)                                       31
      REAL FINR(20),PHI(20),THETA(20)                                            32
C                                                                                33
      COMMON/TDISKC/ZTOP,RTSQ                                                    34
      COMMON/TRACC/Z2,Z1                                                         35
      COMMON/BDISKC/ZBOT,RBSQ                                                    36
      COMMON/TRANSC/DIN(6),ER(6),TD(6),TZ,WALTOL,N,NN,D(6),ZB,TK                 37
      COMMON/CGIVC/PP,BSQ,AP,PINV,B,RSQ1,RP2                                     38
```

```
C                                                                       39
      NAMELIST/GEOM/RR,RA,APIN,ZBOTIN,NX,NY,NXE,NYE,NXY,MX,MY,NXC,NYC  40
      NAMELIST/KDATA/KXMAX,KYMAX,KXM,KYM                                41
      NAMELIST/NEW/LMAX,DMRAD,IOPT,RAPMAX,VAIRM                         42
C  BOUNDARY VALUES NEEDED BY SUBR TRACE (INCHES, CONVERT TO CM BELOW)   43
C Z1=ZR COORDINATE OF BOTTOM DISK                                       44
C Z2=ZR COORDINATE OF TOP DISK (Z1,Z2 IN CM)                            45
C  APIN IS HEIGHT OF CYLINDER IN INCHES, CONVERT TO CM BELOW            46
      DATA APIN/0./                                                     47
C  ZBOTIN IS ZR COORD OF BOTTOM DISK (BULKHEAD) IN RADOME COORD IN INCHE 48
      DATA ZBOTIN/0.00/                                                 49
C  KXMAX,KYMAX ARE OUTPUTS OF NEAR FIELD SUBR                           50
C  INITIALIZE CONSTANTS                                                 51
      DATA RADIUS/1E0/                                                  52
      DATA THETAA,PHIA,AGAM3A/0.0,90.0,0.0/                             53
      DATA PI/3.14159265358 98/                                         54
C************                                                           55
      DATA NX,NY,NXE,NYE,NXY/16,16,256,1,512/                           56
      DATA NREC,NS,MX,MY/32,16,16,1/                                    57
C************                                                           58
C                                                                       59
C  READ IN DESCRIPTION OF RADOME WALL                                   60
      SMAX=1.0                                                          61
      VMAX=1.0                                                          62
      READ(5,6)TITLE                                                    63
      WRITE(6,6) TITLE                                                  64
      READ(5,*) GRAF3D,GRAFSA,GRAFTR,GRAFRV,SUPPRS,IPENCD               65
  260 FORMAT(4L6)                                                       66
      READ(5,*) NFINE,NPHI,NTHE,DIAOS,RA,RR,ZTOPIN,FREQ,OSANG           67
      SINOS=SIN(CSANG*PI/180.)                                          68
      TABLE=.FALSE.                                                     69
C  TABLE IS SET FALSE SO THAT NORMALIZING FACTOR CAN BE COMPUTED.       70
      WRITE(6,265) GRAF3D,GRAFSA,GRAFTR,GRAFRV,TABLE                    71
  265 FORMAT(" GRAF3D=",L2," GRAFSA=",L2," GRAFTR=",L2," GRAFRV=",L2,   72
     $ "  TABLE=",L2)                                                   73
      WRITE(6,270) NFINE,NPHI,NTHE,OSANG                                74
  270 FORMAT(/" NFINE=",I5," NPHI=",I3,"  NTHETA=",I3,"  OSANG= ",F5.2/) 75
      READ(5,*) LMAX,DMRAD,IOPT,RAPMAX,VAIRM,IPOL,ICASE,N,IPWR          76
```

```
      IF (VAIRM.LE.0.) VAIRM=1.0                                          77
C DIACS=OUTSIDE DIAMETER OF BASE OF TANGENT OGIVE RADOME                  78
C VAIR=MAXIMUM REC'D VOLTAGE W/O RADOME AT KX=0.,KY=0.                    79
C NFINE=NO. OF FINENESS RATIOS                                            80
C  NPHI=NUMBER OF SCAN PLANES                                             81
C  NTHE=NUMBER OF ANGLES IN EACH SCAN PLANE                               82
C DIAIN=INSIDE BASE DIAMETER OF RADOME IN INCHES                          83
C ZTOPIN=ZR COORD (IN) OF TOP DISK (METAL TIP)                            84
C FREQ=FREQUENCY IN GHZ                                                   85
C GRAF3D=.TRUE. GIVES 3D PLOTS OF INCIDENT FIELDS ON APERTURE (DELETED)   86
C GRAFRV=.TRUE. GIVES SA PLOTS OF RECEIVING PATTERNS (AZ & EL)            87
C GRAFSA=.TRUE. GIVES SA PLOTS OF TRANSMITTING PATTERN WITHOUT RADOME     88
C SUPPRS=.TRUE. SUPPRESSES THE PRINTING OF NUMEROUS RESULTS               89
C RAPMAX=MAX RADIUS OF ANTENNA APERTURE IN INCHES.                        90
C  IOPT SELECTS POLARIZATION OF INCIDENT PLANE WAVE:                      91
C      =1 ELEV (VERTICAL)                                                 92
C      =2 AZIMUUTH (HORIZONTAL)                                           93
C      =3 RHC                                                             94
C      =4 LHC                                                             95
C  IPOL SELECTS POLARIZATION OF ANTENNA WHEN ICASE=1:                     96
C      = SAME CODE AS FOR IOPT                                            97
C  ICASE=1 OR 2 FOR CIRC APERTURE, UNIFORM ILLUMINATION                   98
C       =3 FOR FLAT PLATE WITH SPECIFIED ILLUM, VERT POL (CASE III)       99
C  N=NUMBER OF LAYERS IN RADOME WALL                                     100
C  OSANG=ANGLE IN DEG IN 45 PLANE OFF BORESIGHT OF FIRST TARGET RETURN   101
C       USED BY SUBR RECBS IN GETTING INITIAL DATA.                      102
C  IPWR=1 FOR POWER IN ELEV COMP OF FAR FIELD PATTERN                    103
C      =2 FOR AZIMUTH COMP,=3 FOR TOTAL POWER.                           104
      NN=N+1                                                            105
      DINCH=0.                                                          106
      DO 5 I=1,N                                                        107
      READ(5,*) DIN(I),ER(I),TD(I)                                      108
    5 DINCH=DIN(I)+DINCH                                                109
      DIAIN=DIAOS-DINCH*2.                                              110
      NXC=NX/2+1                                                        111
      NYC=NY/2+1                                                        112
      WRITE(6,4) NX,NY,NXE,NYE,NXY,MX,MY                                113
    4 FORMAT(" NX,NY,NXE,NYE,NXY,MX,MY:",7I4)                           114
```

```
C READ FINENESS RATIOS FOR THIS RUN--BASED ON OUTSIDE DIMENSIONS          115
      DO 13 I=1,NFINE                                                    116
   13 READ(5,*) FINR(I)                                                  117
C READ ORIENTATIONS FOR THIS RUN (DEGREES)                               118
      DO 14 I=1,NPHI                                                     119
   14 READ(5,*) PHI(I)                                                   120
      DO 15 I=1,NTHE                                                     121
   15 READ(5,*) THETA(I)                                                 122
C  COMPUTE WAVELENGTH:                                                   123
      WLIN=29.97925/(FREQ*2.54)                                          124
      WLCM=WLIN*2.54                                                     125
      BETA=2.*PI/WLCM                                                    126
C  INITIALIZE TABLE OF XMN COEFFICIENTS:                                 127
      CALL RXMIT(FWI,FWT,KA,NORM,P1,TABLE,SUPPRS,BETA)                   128
      DAPWL=2.*RAPMAX/WLIN                                               129
C  CONVERT TO CENTIMETER AND RADIANS                                     130
      ZBOT=ZBOTIN*2.54                                                   131
      Z1=ZBOT                                                            132
      RSQMAX=(2.54*RAPMAX)**2                                            133
      ZTOP=ZTOPIN*2.54                                                   134
      ZB=ZTOP                                                            135
      Z2=ZTOP                                                            136
      RA=RA*2.54                                                         137
      RR=RR*2.54                                                         138
      DIACM=DIAIN*2.54                                                   139
      RAD=PI/180.0                                                       140
    6 FORMAT(18A4)                                                       141
      THETAA=THETAA*RAD                                                  142
      PHIA=PHIA*RAD                                                      143
      AGAM3A=AGAM3A*RAD                                                  144
C  COMPUTE FIELDS OF ANTENNA WHEN XMITTING:                              145
      CALL HACNF(SUMX,NX,NY,1,IPOL,1,DAPWL,DXWL,KXMAX,ICASE)             146
      CALL HACNF(SUMY,NX,NY,1,IPOL,2,DAPWL,DXWL,KXMAX,ICASE)             147
      CALL HACNF(DELX,NX,NY,2,IPOL,1,DAPWL,DXWL,KXMAX,ICASE)             148
      CALL HACNF(DELY,NX,NY,2,IPOL,2,DAPWL,DXWL,KXMAX,ICASE)             149
      CALL HACNF(DAZX,NX,NY,3,IPOL,1,DAPWL,DXWL,KXMAX,ICASE)             150
      CALL HACNF(DAZY,NX,NY,3,IPOL,2,DAPWL,DXWL,KXMAX,ICASE)             151
      KYMAX=KXMAX                                                        152
```

```
      KXM=KXMAX*NXE/MX/NX                                                153
      KYM=KYMAX*NYE/MY/NY                                                154
      WRITE(6,3) KXMAX,DXWL,KXM,KYM                                      155
    3 FORMAT(" KXMAX=KYMAX=",F8.5,"  XY SPACING=",                       156
     $F8.5," WAVELENGTHS"/"  KXM=",F8.5,"  KYM=",F8.5)                   157
C                                                                        158
C  INITIALIZE PLOTTER SOFTWARE                                           159
      IF (GRAF3D.OR.GRAFSA.OR.GRAFTR.OR.GRAFRV) GO TO 200                160
      GO TO 205                                                          161
  200 CONTINUE                                                           162
C                                                                        163
C------------------- CALCOMP INITIALIZATION --------------------------  164
C                                                                        165
C     CALL TITL36("RADOME ANALYSIS COMPUTER PROGRAM",                    166
C    *            "          G.K. HUDDLESTON       ",                   167
C    *            " GEORGIA INSTITUTE OF TECHNOLOGY"  )                 168
C     CALL INIT36( MDAY )                                                169
CC                                                                       170
C     CALL PLOT(0.,-3.,-3)                                               171
      CALL PLOTS(IBUF,512,3,IPENCD)                                      172
C                                                                        173
C------------------------------------------------------------------------174
C                                                                        175
      IF (GRAFTR.OR.GRAFSA) GO TO 201                                    176
      GO TO 205                                                          177
  201 FMXEL=0.                                                           178
      FMXDAZ=0.                                                          179
      DO 30 IP=1,3                                                       180
      DO 35 I=1,NX                                                       181
      DO 35 J=1,NY                                                       182
      IF (IP.EQ.1) EXT(I,J)=SUMX(I,J)                                    183
      IF (IP.EQ.1) EYT(I,J)=SUMY(I,J)                                    184
      IF (IP.EQ.2) EXT(I,J)=DELX(I,J)                                    185
      IF (IP.EQ.2)EYT(I,J)=DELY(I,J)                                     186
      IF (IP.EQ.3) EXT(I,J)=DAZX(I,J)                                    187
      IF (IP.EQ.3) EYT(I,J)=DAZY(I,J)                                    188
      NF(I,J)=CABS(EXT(I,J))                                             189
   35 CONTINUE                                                           190
```

```
      IF (.NOT.GRAFTR) GO TO 215                                          191
C PLOT 3D NEAR FIELDS X-COMPONENTS                                        192
      CALL PLT3DH(6.,2.5,2.5,NF,NX,NY,.TRUE.,.FALSE.)                     193
C  PLOT PHASE ALSO                                                        194
      DO 40 I=1,NX                                                        195
      DO 40 J=1,NY                                                        196
      NF(I,J)=0.                                                          197
      CALL AMPHS(EXT(I,J),RLF,AIF)                                        198
      NF(I,J)=(AIF+180.)/360.                                             199
   40 CONTINUE                                                            200
      CALL PLT3DH(6.,2.5,2.5,NF,NX,NY,.FALSE.,.FALSE.)                    201
C PLOT 3D NEAR FIELDS Y-COMPONENTS                                        202
      DO 45 I=1,NX                                                        203
      DO 45 J=1,NY                                                        204
      NF(I,J)=CABS(EYT(I,J))                                              205
   45 CONTINUE                                                            206
      CALL PLT3DH(6.,2.5,2.5,NF,NX,NY,.TRUE.,.FALSE.)                     207
C  PLOT PHASE ALSO                                                        208
      DO 50 I=1,NX                                                        209
      DO 50 J=1,NY                                                        210
      NF(I,J)=0.                                                          211
      CALL AMPHS(EYT(I,J),RLF,AIF)                                        212
      NF(I,J)=(AIF+180.)/360.                                             213
   50 CONTINUE                                                            214
      CALL PLT3DH(6.,2.5,2.5,NF,NX,NY,.FALSE.,.FALSE.)                    215
      IF (GRAFSA) GO TO 215                                               216
      GO TO 30                                                            217
  215 CONTINUE                                                            218
      IF (IP.EQ.3) GO TO 220                                              219
C CALC EL CUT OF SUM                                                      220
C  NOTE THAT  JCYFFT CHANGES EXT,EYT.                                     221
      CALL JOYFFT(EXT,NX,NY,MY,MX,NXC,NYC,XEEL,NYE,NXE,XYFFT,NXY,3)       222
      CALL JOYFFT(EYT,NX,NY,MY,MX,NXC,NYC,YEEL,NYE,NXE,XYFFT,NXY,3)       223
      CALL FAR(FFSEL,XEEL,YEEL,NYE,NXE,FREQ,KYM,KXM,RADIUS,IPWR,FMXEL)    224
C SA PLOTS OF ELEVATION RESULTS                                           225
      CALL DBPV(FFSEL,NYE,NXE,1)                                          226
      DO 216 I=1,NYE                                                      227
      DO 216 J=1,NXE                                                      228
```

```
      FFSEL(I,J)=1.0+FFSEL(I,J)/40.                                          229
  216 CONTINUE                                                               230
      CALL CNPLTH(FFSEL,NXE,KXM,0.,0.)                                       231
      CALL SYMBOL(.5,6.5,.140000,39HFIGURE      TRANSMITTING ELEVATION PO    232
     $WER,0.,39)                                                             233
      RPWR=FLOAT(IPWR)                                                       234
      CALL NUMBER(999.,999.,.14,RPWR,0.,0)                                   235
      CALL PLOT(8.5,0.,-3)                                                   236
      IF (IP.EQ.2) GO TO 30                                                  237
C  RECOMPUTE SUMX,SUMY FOR JOYFFT:                                           238
      CALL HACNF(EXT,NX,NY,1,IPOL,1,DAPWL,DXWL,KXMAX,ICASE)                  239
      WRITE(6,219) IPWR                                                      240
  219 FORMAT(" IPOWER OF PATTERN=",I2)                                       241
      CALL HACNF(EYT,NX,NY,1,IPOL,2,DAPWL,DXWL,KXMAX,ICASE)                  242
  220 CALL JOYFFT(EXT,NX,NY,MX,MY,NXC,NYC,YE,NXE,NYE,XYFFT,NXY,3)            243
      CALL JOYFFT(EYT,NX,NY,MX,MY,NXC,NYC,YE,NXE,NYE,XYFFT,NXY,3)            244
      CALL FAR(FFS,XE,YE,NXE,NYE,FREQ,KXM,KYM,RADIUS,IPWR,FMXDAZ)            245
C SA PLOTS OF AZIMUTH RESULTS                                                246
      CALL DBPV(FFS,NXE,NYE,1)                                               247
      DO 10 I=1,NXE,1                                                        248
      DO 10 J=1,NYE                                                          249
      FFS(I,J)=1.0+FFS(I,J)/40.0                                             250
   10 CONTINUE                                                               251
      CALL CNPLTH(FFS,NXE,KXM,0.,0.)                                         252
  226 CALL SYMBOL(.5,6.5,.14000,37HFIGURE      TRANSMITTING AZIMUTH POWER    253
     $,0.,37)                                                                254
      CALL NUMBER(999.,999.,.14,RPWR,0.,0)                                   255
      CALL PLOT(8.5,0.,-3)                                                   256
   30 CONTINUE                                                               257
  205 CONTINUE                                                               258
C                                                                            259
      DO 100 NG=1,NFINE                                                      260
      FINE=FINR(NG)                                                          261
C CALCULATE INSIDE FINENESS RATIO                                            262
      RIN=FINE*DIAOS/(SIN(PI-2.*ATAN(2.*FINE)))                              263
      BIN=RIN-DIAOS/2.                                                       264
      FINE=SQRT((RIN-DINCH)**2-BIN**2)/DIAIN                                 265
      WRITE(6,20) RIN,BIN,FINR(NG),FINE                                      266
```

```
      RDML=FINE*DIAIN+APIN                                                  267
      IF (ZTOPIN.LT.RDML) WRITE(6,25) ZTOPIN                                268
   20 FORMAT(" TANGENT OGIVE PARAMETERS: ","  ROS(IN)="                     269
     $ ,F9.5," BOS(IN)=",F9.5,/26X," FINOS=",F5.3,                          270
     $ " FINIS=",F8.5)                                                      271
   25 FORMAT(/" THIS RADOME HAS A TOP DISK AT ZTOPIN= ",E12.5/)              272
C  COMPUTE PARAMETERS NEEDED BY SUBR OGIVE                                  273
      R=FINE*DIACM/(SIN(PI-2.*ATAN(2.*FINE)))                               274
      B=R-DIACM/2.                                                          275
      AP=APIN*2.54                                                          276
      RTSQ=(SQRT(R**2-(ZTOP-AP)**2)-B)**2                                   277
      RBSQ=(SQRT(R**2-(ZBOT-AP)**2)-B)**2                                   278
      BSQ=B**2                                                              279
      RINV=1./R                                                             280
      RSQ1=R**2                                                             281
      RP=RSQ1-BSQ                                                           282
      RP2=RSQ1+BSQ                                                          283
C                                                                           284
      DPMR=180./(PI*1000.)                                                  285
      AZL=0.                                                                286
      ELL=0.                                                                287
      THL=0.                                                                288
      WRITE(6,2) TITLE,FINR(NG),DIAOS,ZTOPIN,FREQ,RA,RR,DAPWL,IPOL,         289
     $ICASE,IOPT                                                            290
      DO 8 I=1,N                                                            291
    8 WRITE(6,7) I,DIN(I),ER(I),TD(I)                                       292
    7 FORMAT(2X,I3,F13.5,F10.3,F9.4)                                        293
      WRITE(6,9)                                                            294
    9 FORMAT(//"  PHI   THETA  BSEEL   BSEAZ   SLPEL     SLPAZ     GAIN"/   295
     $       " (DEG) (DEG)  (MRAD)  (MRAD) (DEG/DEG) (DEG/DEG)  (DB)"//)   296
      WRITE(7,2) TITLE,FINR(NG),DIAOS,ZTOPIN,FREQ,RA,RR,DAPWL,IPOL,         297
     $ICASE,IOPT                                                            298
      DO 18 I=1,N                                                           299
   18 WRITE(7,7) I,DIN(I),ER(I),TD(I)                                       300
      WRITE(7,9)                                                            301
    2 FORMAT(1H1,5X," RESULTS OF RADOME ANALYSIS"/                          302
     1 18A4/" FINENESS RATIO=",F6.2,2X,                                     303
     2"DIAMETER=",F8.5," IN.  LENGTH=",F8.5," IN."/" FREQUENCY=",           304
```

```
     3F7.3," GHZ "/                                                          305
     4" RA=",F8.5," IN.  RR=",F8.5," IN.  ANTENNA D=",F8.4,                  306
     5" WAVELENGTHS"/" IPOL=",I2,"  ICASE=",I2,"  IOPT=",I2//                307
     6" LAYER  THICKNESS(IN.)   ER      TAND"/)                              308
      DO 100 IPHI=1,NPHI                                                     309
      PHIP=PHI(IPHI)                                                         310
      PHIR=PHIP+180.                                                         311
      PHIR=PHIR*RAD                                                          312
      DO 100 ITHE=1,NTHE                                                     313
      THETAL=THETA(ITHE)                                                     314
      THETAR=180.-THETAL                                                     315
      THETAR=THETAR*RAD                                                      316
      CALL ORIENT(RA,THETAA,PHIA,RR,THETAR,PHIR,AGAM3A,ROTATE,TRANSL)        317
      IF (TABLE) GO TO 23                                                    318
C   COMPUTE NORMALIZING FACTOR:                                              319
      KA(1)=0.                                                               320
      KA(2)=0.                                                               321
      KA(3)=1.                                                               322
      CALL INCPW(KA,PWI,ICPT)                                                323
      TSUP=.TRUE.                                                            324
      TABLE=.FALSE.                                                          325
      CALL RECM(PWI,KA,NX,NY,KXMAX,KYMAX,FREQ,ROTATE,TRANSL,                 326
     $SUMX,SUMY,DELX,DELY,DAZX,DAZY,VR,TABLE,TSUP,RSQMAX)                    327
      VAIRM=CABS(VR(1))                                                      328
      TABLE=.TRUE.                                                           329
   23 IF (.NOT.SUPPRS) GO TO 24                                              330
      GO TO 350                                                              331
   24 CONTINUE                                                               332
      DO 320 J=1,2                                                           333
      ICUT=J                                                                 334
      ICOMP=IOPT                                                             335
      KMAX=.996                                                              336
      IF (KMAX.GT.KXMAX) KMAX=KXMAX                                          337
      TSUP=.TRUE.                                                            338
      CALL RECPTN(SUMX,SUMY,DELX,DELY,DAZX,DAZY,NX,NY,ICUT,ICOMP,KMAX,       339
     $NREC,VREC3,KXMAX,KYMAX,FREQ,ROTATE,TRANSL,TABLE,TSUP,RSQMAX)           340
      DO 325 MM=1,3                                                          341
      ICHAN=MM                                                               342
```

```
      IF ((ICUT.EG.1).AND.(ICHAN.EQ.3)) GC TO 325                          343
      IF ((ICUT.EQ.2).AND.(ICHAN.EQ.2)) GO TO 325                          344
      DO 26 I=1,NREC                                                       345
   26 VREC(I)=VREC3(I,ICHAN)                                               346
      IF (NREC.GT.NXE) GO TO 31                                            347
      CALL MAGFFT(VREC,NREC,XYFFT,NXE)                                     348
      DO 305 I=1,NXE                                                       349
  305 MVREC(I)=CABS(XYFFT(I))**2                                           350
      GO TO 33                                                             351
   31 DO 32 I=1,NREC                                                       352
   32 MVREC(I)=CABS(VREC(I))**2                                            353
   33 NXX=MAX0(NXE,NREC)                                                   354
      WRITE(6,306)                                                         355
  306 FORMAT(/" MIN AND MAX VALUES OF REC""G PATTERN: "/)                   356
      CALL NORMH(MVREC,NXX,1,.FALSE.)                                      357
      CALL DBPV(MVREC,NXX,1,1)                                             358
      IF (J.EQ.1) WRITE(6,308)                                             359
      IF (J.EQ.2) WRITE(6,309)                                             360
      DK=2.*KMAX/NXX                                                       361
      DO 307 I=1,NXX,1                                                     362
      IF (SUPPRS) GO TO307                                                 363
      ANG=ASIN(-KMAX+(I-1)*DK)*180./PI                                     364
      CALL AMPHS(XYFFT(I),AMP,PHS)                                         365
      IF (NREC.GE.NXE) CALL AMPHS(VREC(I),AMP,PHS)                         366
      IF (MOD(I,4).EQ.0) WRITE(6,310) ANG,MVREC(I),PHS                     367
  307 MVREC(I)=1.0+MVREC(I)/40.                                            368
  308 FORMAT(/" REC""G PATTERN, EL CUT, EL COMP (DB): "/)                  369
  309 FORMAT(/" REC""G PATTERN, AZ CUT,EL COMP (DB): "/)                   370
  310 FORMAT(F9.1,5X,F8.3,3X,F6.1)                                         371
      IF (.NOT.GRAFRV) GO TO 320                                           372
      CALL CNPLTH(MVREC,NXX,KMAX,0.,0.)                                    373
      IF (J.EQ.1) CALL SYMBOL(.5,6.5,.140,43HFIGURE       RECVG POWER PA   374
     $TTERN-ELEV PLANE,0.,43)                                              375
      IF (J.EQ.2) CALL SYMBOL(.5,6.5,.140,41HFIGURE       RECVG POWER PA   376
     $TTERN-AZ PLANE,0.,41)                                                377
      CALL PLOT(8.5,0.,-3)                                                 378
  325 CONTINUE                                                             379
  320 CONTINUE                                                             380
```

```
  350 CONTINUE                                                          381
C COMPUTE BORESIGHT ERROR                                               382
  275 CONTINUE                                                          383
      CALL RECBS(SUMX,SUMY,DELX,DELY,DAZX,DAZY,NX,NY,                   384
     $ LMAX,NS,ICPT,VR,DMRAD,ROTATE,TRANSL,FREQ,KXMAX,KYMAX,            385
     $ TABLE,SINOS,KA,AZT,ELT,RSQMAX,VMAX,SMAX,SUPPRS)                  386
      IF (ITHE.EQ.1) GO TO 300                                          387
      SLPAZ=(AZT-AZL)*DPMR/(THETAL-THL)                                 388
      SLPEL=(ELT-ELL)*DPMR/(THETAL-THL)                                 389
  300 AZL=AZT                                                           390
      ELL=ELT                                                           391
      THL=THETAL                                                        392
      GAINM=20.*ALOG10(SMAX/VAIRM)                                      393
      WRITE(6,11) PHIP,THETAL,ELT,AZT,SLPEL,SLPAZ,GAINM                 394
      WRITE(7,11) PHIP,THETAL,ELT,AZT,SLPEL,SLPAZ,GAINM                 395
   11 FORMAT(1X,F5.1,F6.1,F8.2,F8.2,F9.4,F10.4,F7.1)                    396
C  GRAF3D OPTION HAS BEEN REMOVED.                                      397
  100 CONTINUE                                                          398
      WRITE(6,105) VAIRM                                                399
  105 FORMAT(//" RECEIVED SUM VOLTAGE WITHOUT RADOME=",E12.5//)         400
      IF (GRAF3D.OR.GRAFSA.OR.GRAFTR.OR.GRAFRV) CALL PLOT(0.,0.,999)    401
      STOP                                                              402
      END                                                               403
```

```
      BLOCK DATA                                                        1
C                                                                       2
      COMMON/TRANSC/DIN(6),ER(6),TO(6),TZ,WALTOL,N,NN,D(6),ZB,TK        3
C                                                                       4
      DATA WALTOL,TK,TZ/0.,0.,0./                                       5
C                                                                       6
      END                                                               7
```

Chapter 3

SUBROUTINE HACNF

3-1. Purpose: To compute near-field aperture distributions for two types of three-channel monopulse antennas: (1) circular aperture with uniform amplitude and phase distributions; (2) flat plate antenna with a programmed amplitude distribution and uniform phase. Four polarizations can be selected for the circular aperture. The flat plate antenna is vertically ($\hat{y}_A$) polarized only.

3-2. Usage: CALL HACNF (E, NX, NY, ICHAN, IPOL, IXY, DAPWL, DXWL, KXMAX, ICASE)

3-3. Arguments

E - Complex array of NX by NY elements which, on output, contains the values of the specified (IXY) rectangular component ($\hat{x}_A$ or $\hat{y}_A$) of the electric field distribution over the specified (ICASE) antenna aperture having the specified (IPOL) polarization for the specified (ICHAN) channel of a three-channel monopulse antenna.

NX,NY - Even integer number of points in a rectangular array at which the aperture distribution is computed in the x_A and y_A directions, respectively. The point I=NX/2 + 1, J=NY/2 + 1 corresponds to $x_A=0$, $y_A=0$.

ICHAN - Integer control variable with values 1, 2, or 3 which selects the sum, elevation difference, or azimuth difference channel, respectively.

IPOL - Integer control variable which selects the antenna polarization as follows:

1 - Vertical ($\hat{y}_A$) polarization

2 - Horizontal ($\hat{x}_A$) "

3 - Right-hand circular "

4 - Left-hand circular "

IXY - Integer control variable having values 1 or 2 to select the x_A or y_A component of aperture electric field.

DAPWL - Diameter, in wavelengths, of the antenna aperture.

DXWL - Spacing, in wavelengths, between samples in aperture in x_A and y_A directions (output).

KMAX - Maximum value of normalized wavenumber corresponding to KMAX = 1./(2.*DXWL) (output).

ICASE - Integer control variable having values 1 or 2 to specify a circular aperture antenna with uniform amplitude and phase. If ICASE=3, a flat plate antenna having a programmed amplitude distribution (see Table 3-2) with vertical polarization is selected.

3-4. Comments and Method

a. The integers NX,NY must each be equal to each other and to an integer power of two; e.g., NX=NY=16. In addition, when ICASE=3 (flat plate antenna), NX and NY must equal 16.

b. The actual shape of the circular aperture, as approximated by a rectangular array of sample points, is shown in Figure 3-1 for the case of NX=NY=16. Row 1 and Column 1 of the array contain null elements. The elements inside and on the boundary of the aperture may contain non-zero values as shown in Table 3-1 for the various cases when ICHAN=1 (sum channel). Note that specification of D_{AP} in Figure 3-1 determines the sample spacings according to

$$\Delta x_A = \Delta y_A = \frac{D_{Ap}\cos\alpha}{(N_x-2)} = \frac{D_{Ap}\cos\alpha}{(N_y-2)} \qquad (1)$$

where $\alpha = \mathrm{Tan}^{-1}(2/7)$.

The aperture distributions for three monopulse channels are formed by phasing the elements in the four quadrants of the aperture appropriately. The sum channel distribution is formed by assigning equal phases to all elements. The azimuth difference channel is formed by multiplying all elements in Quadrants II and III of the sum distribution by minus one and by zeroing all elements along x_A=0. For the elevation difference channel, Quadrants III and IV are negated, and all elements along the line y_A=0 are made zero for symmetry reasons.

The phasing chosen models a tracking antenna and provides outputs in two orthogonal channels from which the direction of arrival of a target return can be mathematically determined. Let $\hat{k}$ be a unit vector which points from the antenna origin toward the direction from whence the plane wave (target return) emanates; i.e.,

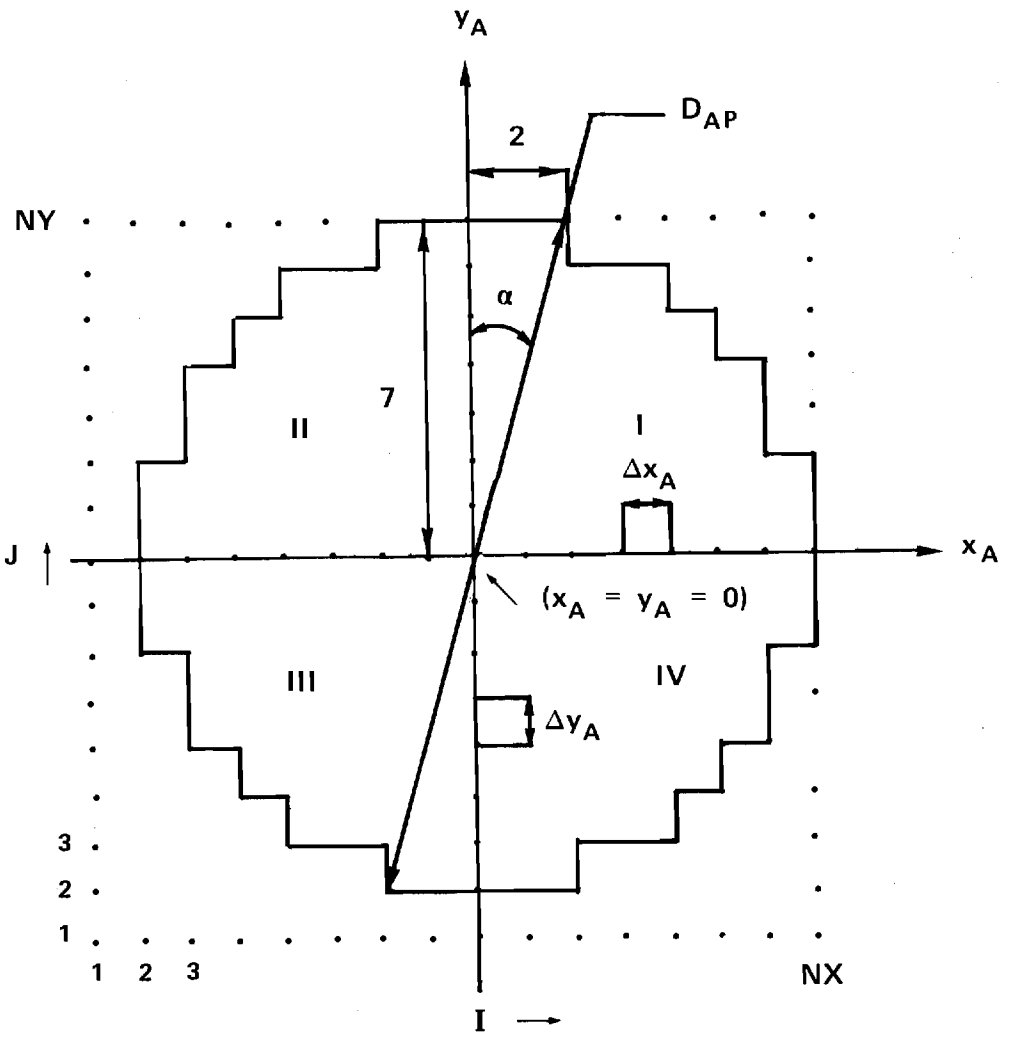

FIGURE 3–1. APPROXIMATION OF CIRCULAR APERTURE BY RECTANGULAR GRID OF SAMPLE POINTS.

Table 3-1. Values of Non-Zero Elements in Circular Aperture (ICHAN=1, ICASE=1 or 2)

IPOL	IXY	Value	Polarization Type
1	1	(0 + j0)	Vertical
1	2	(1 + j0)	"
2	1	(1 + j0)	Horizontal
2	2	(0 + j0)	"
3	1	(0 + j1)	RHC
3	2	(1 + j0)	"
4	1	(0 - j1)	LHC
4	2	(1 + j0)	"

$$\hat{k} = \hat{x}_A k_x + \hat{y}_A k_y + \hat{z}_A k_z \qquad (2)$$

Define the tracking functions for this plane wave as

$$f_i(k_x,k_y) = \frac{\Delta_i(k_x,k_y)}{\Sigma(k_x,k_y)} \qquad (3)$$

where Δ_i represents the output of the elevation (ε) or azimuth (α) difference channel and Σ represents the sum channel output. Then for small $k_x>0$, the phase of f_α is + $\pi/2$; for small $k_x<0$, the phase of f_α is $-\pi/2$. Similarly, for small $k_y>0$, arg (f_ε) = $\pi/2$; for small $k_y<0$, arg (f_ε) = $-\pi/2$. Hence, the change in phase by π in either channel represents the boresight direction of the antenna, and tracking is done using the imaginary parts of the tracking functions rather than their real parts.

c. The shape and sampling grid used to model the flat plate antenna are shown in Figure 3-2. In Subroutine HACNF, the integers NX and NY must both equal 16, and only linear polarization ($\hat{y}_A$) is applicable to the flat plate antenna (ICASE=3). The phasing of the four quadrants is done as described above to model the three monopulse channels so that tracking can be simulated. Note that specification of D_{Ap} determines the sample spacing according to

$$\Delta x_A = \Delta y_A = \frac{D_{Ap}\cos\alpha}{N_x\left(\frac{x}{2} - 2\right)} \qquad (4)$$

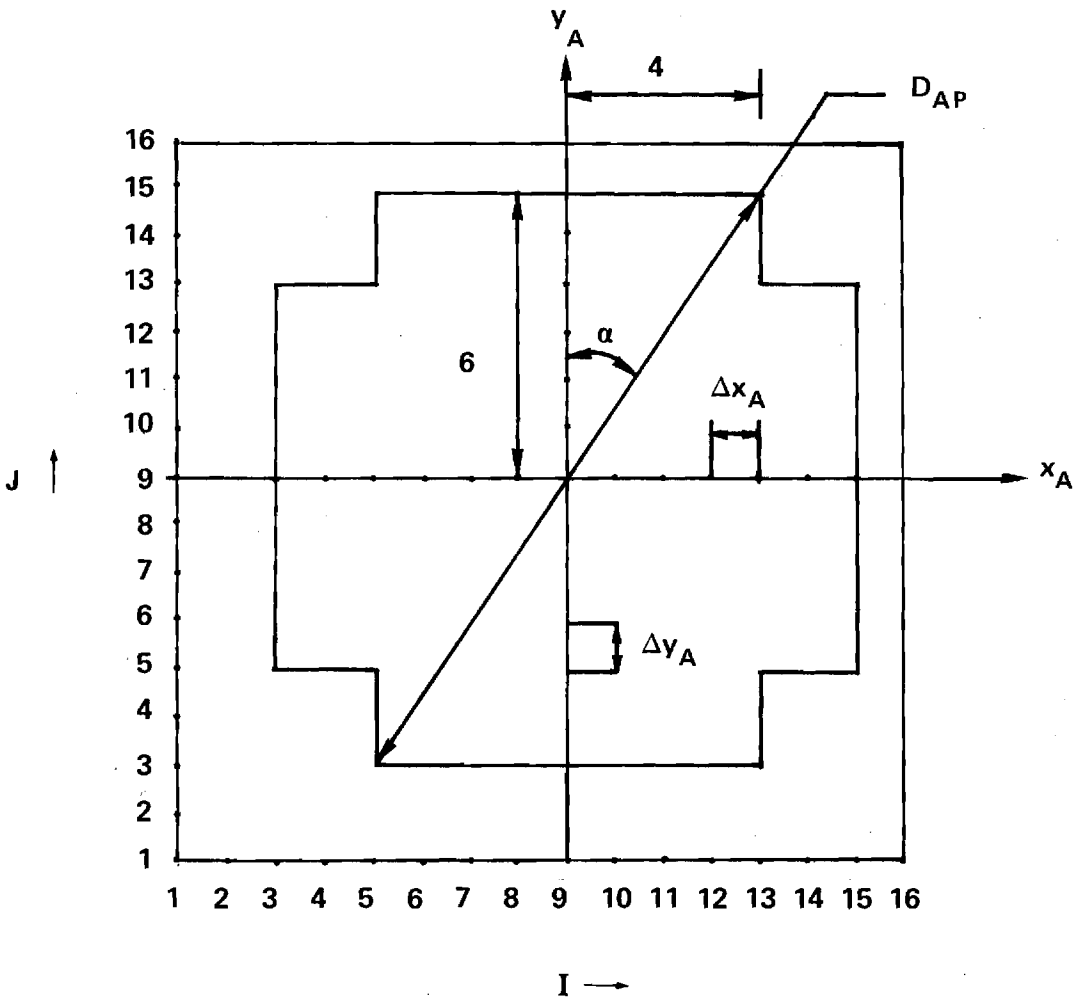

FIGURE 3–2. GEOMETRY OF FLAT PLATE ANTENNA.

where $\alpha = \text{Tan}^{-1}$ (4/6).

The phase of each sample point in Figure 3-2 for the sum channel is made equal, but the amplitudes are tapered in the x_A and y_A directions as shown in Table 3-2. The amplitude distribution is separable and symmetrical so that

$$E_{yA}(x_A,y_A) = g(x_A)h(y_A) = E_{yA}(-x_A,y_Z) = E_{yA}(x_A,-y_A) \qquad (5)$$

It is noted that samples 10, 12, 14, and 16 are actually specified in the program, and samples 9, 11, 13, and 15 are obtained from them by averaging.

3-5. Program Flow

Line 16: Assign complex values to CFAC to use in generating vertical, horizontal, RHC, and LHC polarization according to IPOL.

Lines 17-19: Compute the angle α and the upper bound R_{max} of the radius of the circular aperture.

Lines 20-21: Ensure that IPOL has correct values of 1, 2, 3, or 4.

Line 22: If NX≠NY, write error message and stop the program.

Line 23: Ensure that IXY=1 or 2.

Line 24: If NX and NY are not even, stop the program.

Line 25: Test value of ICASE: if ICASE=3 generate fields of flat plate antenna (Lines 47-83); otherwise, generate fields of circular aperture (Lines 26-43).

Lines 26-41: Assign complex field value to each sample point $(x_A,y_A,0)$ in the aperture according to the values shown in Table 3-1. If $\sqrt{x_A^2 + y_A^2} > R_{max}$, make the

Table 3-2. Symmetrical Amplitude Distribution for Flat Plate Antenna

Sample No.	x_A	Amplitude	y_A	Amplitude
9	0	1.0280	0	1.0280
10	Δx	1.0280	Δy	1.0280
11	$2\Delta x$	.9120	$2\Delta y$	.9170
12	$3\Delta x$	.7959	$3\Delta y$	.8060
13	$4\Delta x$	.6077	$4\Delta y$	.6155
14	$5\Delta x$	.4194	$5\Delta y$	.4250
15	$6\Delta x$	.2097	$6\Delta y$	.2125
16	$7\Delta x$	0.0	$7\Delta y$	0.0

field value zero (Line 40). Multiply the non-zero elements by CFAC(IPOL) to generate the correct polarization (Line 38).

Lines 42-43: Compute sample spacing $\Delta x_A/\lambda$ and go to statement 60.

Lines 44-46: Error message and STOP.

Line 47-48: Flat plate antenna-- if NX≠16, write error message and STOP (Lines 109-111).

Line 49: Compute sample spacing $\Delta x_A/\lambda$.

Line 50: Ensure NX=NY

Lines 51-54: Zero all elements in the aperture. If IXY=1 (x_A-component), go to statement 60.

Lines 55-62: Assign tapered amplitude values to eight "even" elements in Quadrant III.

Lines 63-71: Compute amplitude values for the "odd" elements in Quadrant III.

Lines 72-75: Compute amplitude values for elements 3-9 along $y_A=0$ line and along $x_A=0$ line.

Lines 76-79: Generate symmetrical amplitude values in Quadrant IV.

Lines 80-83: Generate symmetrical amplitude values in Quadrants I and II.

Line 84: Compute k_{xmax}.

Lines 85-89: Test to determine if the sum channel data generated should be phased to produce the aperture distribution for a specified difference channel (ICHAN).

Lines 90-98: Form aperture distribution for difference elevation channel by zeroing all elements along $y_A=0$ and negating all elements for $y_A<0$. RETURN.

Lines 99-107: Form aperture distribution for difference azimuth channel by zeroing all elements along $x_A=0$ and negating all elements for $x_A<0$. RETURN.

Lines 108-112: Error message for ICASE=3 and NX≠16. Comment of DAPWL=5.047 applies to the test described in Chapter 2. END

3-6. Test Case: See discussion in Chapter 2.

3-7. References

1. D. R. Rhodes, Introduction to Monopulse, McGraw Hill, New York, 1959.

3-8. Program Listing: See following pages.

```
      SUBROUTINE HACNF(E,NX,NY,ICHAN,IPCL,IXY,DAPWL,DXWL,KXMAX,ICASE)
C SUBR HACNF COMPUTES ELECTRIC FIELDCOMPONENTS OVER A CIRCULAR APERTURE
C OF RADIUS RMAX=(NX/2-1)/COS(ATAN(2/7)) AND RETURNS SAME IN E(NX,NY).
C NX MUST EQUAL NY AND MUST BE EVEN.
C  ICHAN=1 FOR SUM CHANNEL   IPOL=1 FOR VERT-Y POL.   IXY=1 FOR X-COMP.
C       =2 FOR ELEV DIFF          =2 FOR HORIZ-X POL      =2 FOR Y-COMP.
C       =3 FOR AZ DIFF            =3 FOR RHC POL
C       =                         =4 FOR LHC POL
C DAPWL=DIAMETER OF APERTURE IN WAVELENGTHS (INPUT)
C  DXWL=SAMPLE SPACING IN APERTURE (OUTPUT)
C KXMAX=MAXIMUM WAVENUMBER (OUTPUT)
C  ICASE=1 OR 2 FOR UNIFORM, CIRCULAR APERTURE (CASE I AND II)
C       =3 FOR FLAT-PLATE ANTENNA, VERTICAL POL (CASE III).
      COMPLEX E(NX,NY),CFAC(4)
      REAL KXMAX
      DATA CFAC/(1.,0.),(1.,0.),(0.,+1.),(0.,-1.)/
      ANG=ATAN(2./7.)
      IF (ICASE.EQ.3) ANG=ATAN(4./6.)
      RMAX=(NX/2-1)/COS(ANG)+.001
      IF (IPOL.GT.4) IPCL=4
      IF (IPOL.LT.1) IPOL=1
      IF (NX.NE.NY) GO TO 15
      IF ((IXY.LT.1).OR.(IXY.GT.2)) IXY=2
      IF (MOD(NX,2).NE.0) GO TO 15
      IF (ICASE.EQ.3) GO TO 25
      DO 10 I=1,NX
      X=FLOAT(-(NX/2)+I-1)
      DO 10 J=1,NY
      Y=FLOAT(-(NY/2)+J-1)
      R=SQRT(X**2+Y**2)
      IF (R.GT.RMAX) GO TO 9
      IF ((IPOL.EQ.1).AND.(IXY.EQ.1)) GO TO 9
      IF ((IPOL.EQ.2).AND.(IXY.EQ.2)) GO TO 9
C  IF RHC, EY=(1,0), EX=(0,1)  I.E., EX LEADS EY BY 90 DEG.
C  IF LHC,EY=(1,0), EX=(0,-1)  I.E., EX LAGS EY BY 90 DEG.
      E(I,J)=(1.,0.)
      IF ((IPOL.LT.3).OR.(IXY.EQ.2)) GO TO 10
      E(I,J)=E(I,J)*CFAC(IPOL)
```

```
      GO TO 10                                                          39
    9 E(I,J)=(0.,0.)                                                    40
   10 CONTINUE                                                          41
      DXWL=(DAPWL/2.)*COS(ANG)/(NX/2-1)                                 42
      GO TO 60                                                          43
   15 WRITE(6,20)                                                       44
   20 FORMAT(//" NX.NE.NY OR NX NOT EVENIN SUBR HACNF"//)               45
      STOP                                                              46
C THE FOLLOWING IS FOR CASE III (ICASE=2):                              47
   25 IF (NX.NE.16) GO TO 90                                            48
      DXWL=(DAPWL/2.)*COS(ANG)/(NX/2-2)                                 49
      NY=NX                                                             50
      DO 26 I=1,NX                                                      51
      DO 26 J=1,NY                                                      52
   26 E(I,J)=(0.,0.)                                                    53
      IF (IXY.EQ.1) GO TO 60                                            54
      E(6,4)=(.2824,0.)                                                 55
      E(8,4)=(.4250,0.)                                                 56
      E(4,6)=(.2888,0.)                                                 57
      E(6,6)=(.5218,0.)                                                 58
      E(8,6)=(.8060,0.)                                                 59
      E(4,8)=(.4194,0.)                                                 60
      E(6,8)=(.7959,0.)                                                 61
      E(8,8)=(1.028,0.)                                                 62
      DO 30 J=4,8,2                                                     63
      DO 30 I=3,8,1                                                     64
      IF ((MOD(J,2).EQ.0).AND.(MOD(I,2).EQ.0)) GOTO 30                  65
      E(I,J)=(E(I-1,J)+E(I+1,J))/2.                                     66
   30 CONTINUE                                                          67
      DO 35 I=3,8,1                                                     68
      DO 35 J=3,8,2                                                     69
      E(I,J)=(E(I,J-1)+E(I,J+1))/2.                                     70
   35 CONTINUE                                                          71
      DO 40 I=3,9                                                       72
   40 E(I,J)=E(I,8)                                                     73
      DO 45 J=3,9                                                       74
   45 E(9,J)=E(8,J)                                                     75
      DO 50 J=3,9                                                       76
```

```
      DO 50 I=1,6                                                          77
      E(9+I,J)=E(9-I,J)                                                    78
   50 CONTINUE                                                             79
      DO 55 I=3,15                                                         80
      DO 55 J=1,6                                                          81
      E(I,9+J)=E(I,9-J)                                                    82
   55 CONTINUE                                                             83
   60 KXMAX=1./(2.*CXWL)                                                   84
      IF (ICHAN.EQ.1) RETURN                                               85
      IF ((IXY.EQ.1).AND.(ICASE.EQ.3)) RETURN                              86
      IF ((IXY.EQ.1).AND.(IPOL.EQ.1)) RETURN                               87
      IF ((IXY.EQ.2).AND.(IPOL.EQ.2)) RETURN                               88
      IF (ICHAN.EQ.3) GO TO 75                                             89
C  LOAD ELEVATION DIFFERENCE CHANNEL:                                       90
      J=NY/2+1                                                             91
      DO 65 I=1,NX                                                         92
   65 E(I,J)=(0.,0.)                                                       93
      JMAX=NY/2                                                            94
      DO 70 J=1,JMAX                                                       95
      DO 70 I=1,NX                                                         96
   70 E(I,J)=-E(I,J)                                                       97
      RETURN                                                               98
C  LOAD AZIMUTH DIFFERENCE CHANNEL:                                        99
   75 I=NX/2+1                                                            100
      DO 80 J=1,NY                                                        101
   80 E(I,J)=(0.,0.)                                                      102
      IMAX=NX/2                                                           103
      DO 85 I=1,IMAX                                                      104
      DO 85 J=1,NY                                                        105
   85 E(I,J)=-E(I,J)                                                      106
      RETURN                                                              107
C  DAPWL=5.047 FOR CASE III                                               108
   90 WRITE(6,95)                                                         109
   95 FORMAT(//"***ERROR EXIT! NX NOT EQUAL TO 16 IN SUBR HACNF***"//)    110
      STOP                                                                111
      END                                                                 112
```

Chapter 4

SUBROUTINE ORIENT

4-1. Purpose: To compute the rotational matrix of direction cosines ROTATE and the translational matrix TRANSL required to carry out coordinate and vector transformations between antenna coordinate system (x_A, y_A, z_A) and radome coordinate system (x_R, y_R, z_R).

4-2. Usage: CALL ORIENT (RA, THETA, PHIA, RR, THETAR, PHIR, AGAM3A, ROTATE, TRANSL)

4-3. Arguments

RA, THETA, PHIA - Spherical coordinates (cm, radians) of the origin of the antenna coordinate system with respect to the reference coordinate system (x,y,z) as indicated in Figure 4-1. Note that the origin of the reference system coincides with the gimbal point, which is located on the axis of symmetry z_R of the radome.

RR, THETAR, PHIR - Spherical coordinates (cm, radians) of the origin of the radome coordinate system with respect to the reference system.

AGAM3A - Angle (radians) between the z_A and z axes.

ROTATE - Real array of 3 x 3 elements which contains on output the matrix of direction cosines $[R_{ij}]$ explained below.

TRANSL - Real array of three elements which contains on output the translation matrix T_i as explained below.

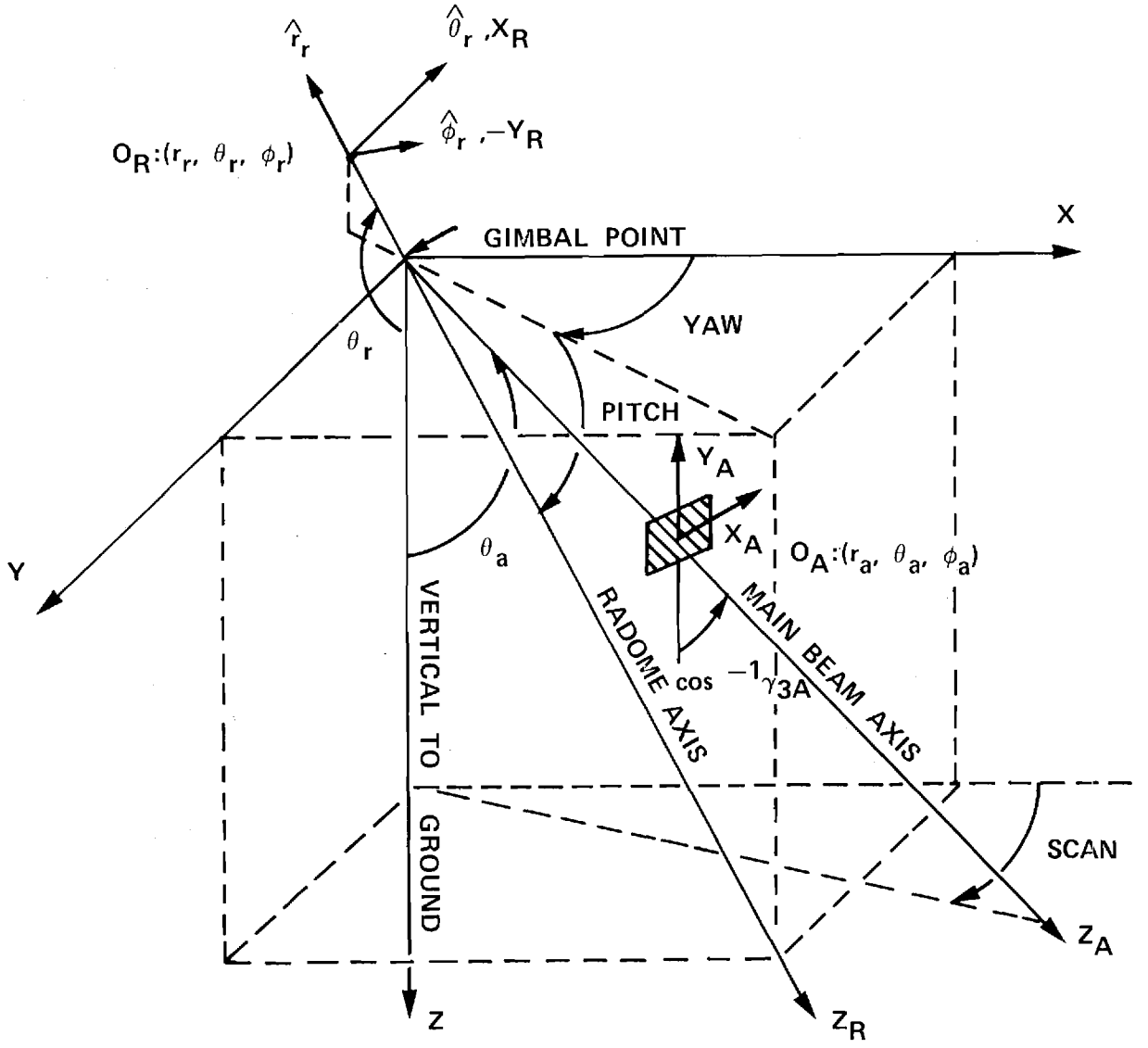

Figure 4–1. Coordinate Systems Used in Radome Analysis.

Reference System: (X, Y, Z)

Antenna System: (X_A, Y_A, Z_A)

Radome System: (X_R, Y_R, Z_R)

4-4. Comments and Method

a. The coordinate systems of Figure 2-2 are obtained from those shown in Figure 4-1 by setting THETAA = 0, PHIA = $\pi/2$, and AGAM3A = 0. When this is done, the z and z_A axes coincide, the x and x_A axes are parallel, and the y and y_A axes are parallel. The angles ϕ_p and θ_L in Figure 2-2 are related to θ_r and ϕ_r as

$$\phi_r = \phi_p + \pi \tag{1}$$

$$\theta_r = \pi - \theta_L \tag{2}$$

The unit vectors $\hat{x}_R$, $\hat{y}_R$, $\hat{z}_R$ were chosen to coincide with the spherical coordinate unit vectors $\hat{r}_r$, $\hat{\theta}_r$, $\hat{\phi}_r$ associated with the point O_R: (r_r, θ_r, ϕ_r); hence, $\hat{x}_R$ always lies in the plane of scan as indicated in Figure 4-2. This observation is important if the properties of the radome wall are not symmetric with respect to rotation about the z_R-axis, such as in the case of circumferential variations in wall thickness, nonuniform heating, etc.

b. The details of the coordinate system transformations are described in Reference 1 and summarized below. The transformation of the point P in antenna coordinates (x_A, y_A, z_A) to radome coordinates (x_R, y_R, z_R) is given by

$$\begin{bmatrix} x_R \\ y_R \\ z_R \end{bmatrix} = \begin{bmatrix} R_{ij} \end{bmatrix} \begin{bmatrix} x_A \\ y_A \\ z_A \end{bmatrix} + \begin{bmatrix} T_x \\ T_y \\ T_z \end{bmatrix} \tag{3}$$

The transformation of a vector

$$\underline{F} = \hat{x}_A F_{xA} + \hat{y}_A F_{yA} + \hat{z}_A F_{zA} = \hat{x}_R F_{xR} + \hat{y}_R F_{yR} + \hat{z}_R F_{zR} \tag{4}$$

is given by

$$\begin{bmatrix} F_{xR} \\ F_{yR} \\ F_{zR} \end{bmatrix} = \begin{bmatrix} R_{ij} \end{bmatrix} \begin{bmatrix} F_{xA} \\ F_{yA} \\ F_{zA} \end{bmatrix} \tag{5}$$

In the above, $[R_{ij}]$ is the matrix of direction cosines which describes the rotation of the radome coordinate system with respect to the antenna system; $[T_i]$ describes the translation of the radome origin O_r with respect to the origin O_a of the antenna system. In fact, setting ($x_A = 0$, $y_A = 0$, $z_A = 0$) in Equation (3) shows that (T_x, T_y, T_z) represents the location, in radome coordinates, of the antenna origin.

The matrix $[R_{ij}]$ can be expanded and written explicitly as

$$\begin{bmatrix} R_{ij} \end{bmatrix} = \begin{bmatrix} \cos\alpha_1 & \cos\beta_1 & \cos\gamma_1 \\ \cos\alpha_2 & \cos\beta_2 & \cos\gamma_2 \\ \cos\alpha_3 & \cos\beta_3 & \cos\gamma_3 \end{bmatrix} \tag{6}$$

where

$$\alpha_1 = \text{angle between } x_A \text{ and } x_R = \angle x_A, x_R \tag{7a}$$

$$\alpha_2 = \angle x_A, y_R \tag{7b}$$

$$\alpha_3 = \angle x_A, z_R \tag{7c}$$

$$\beta_1 = \angle y_A, x_R \tag{7d}$$

$$\beta_2 = \angle y_A, y_R \tag{7e}$$

$$\beta_3 = \angle y_A, z_R \tag{7f}$$

$$\gamma_1 = \angle z_A, x_R \tag{7g}$$

$$\gamma_2 = \angle z_A, y_R \tag{7h}$$

$$\gamma_3 = \angle z_A, z_R \tag{7i}$$

The inverse transformations are given by

$$\begin{bmatrix} x_A \\ y_A \\ z_A \end{bmatrix} = \begin{bmatrix} R_{ij} \end{bmatrix}^T \left\{ \begin{bmatrix} x_R \\ y_R \\ z_R \end{bmatrix} - \begin{bmatrix} T_x \\ T_y \\ T_z \end{bmatrix} \right\} \tag{8}$$

$$\begin{bmatrix} F_{xA} \\ F_{yA} \\ F_{zA} \end{bmatrix} = \left[R_{ij}\right]^T \begin{bmatrix} F_{xR} \\ F_{yR} \\ F_{zR} \end{bmatrix} \tag{9}$$

where $[R_{ij}]^T$ denotes the transpose of $[R_{ij}]$; i.e., $[R_{ij}]^T = [R_{ji}]$ since rows and columns are interchanged. Also, since $[R_{ij}]$ is a unitary matrix, its inverse is equal to its transpose.

To facilitate the specification of a particular antenna/radome orientation, the reference coordinate system (x, y, z) is used. Transformations from the reference system to the antenna system are described by

$$\begin{bmatrix} x_A \\ y_A \\ z_A \end{bmatrix} = \left[\gamma_{ij}\right] \begin{bmatrix} x - r_a \sin\theta_a \cos\phi_a \\ y - r_a \sin\theta_a \sin\phi_a \\ z - r_a \cos\theta_a \end{bmatrix} \tag{10}$$

while transformations from reference system to radome system are described by

$$\begin{bmatrix} x_R \\ y_R \\ z_R \end{bmatrix} = \left[\rho_{ij}\right] \begin{bmatrix} x - r_r \sin\theta_r \cos\phi_r \\ y - r_r \sin\theta_r \sin\phi_r \\ z - r_r \cos\theta_r \end{bmatrix} \tag{11}$$

where $[\gamma_{ij}]$ and $[\rho_{ij}]$ represent the rotations of the two systems with respect to the reference system. When these two separate transformations

are combined, there results

$$\begin{bmatrix} R_{ij} \end{bmatrix} = \begin{bmatrix} \rho_{ij} \end{bmatrix} \quad \begin{bmatrix} \gamma_{ij} \end{bmatrix}^T \tag{12}$$

$$\begin{bmatrix} T_x \\ T_y \\ T_z \end{bmatrix} = \begin{bmatrix} \rho_{ij} \end{bmatrix} \quad \begin{bmatrix} X_a - X_r \\ Y_a - Y_r \\ Z_a - Z_r \end{bmatrix} \tag{13}$$

where X_a, Y_a, etc., are defined in Equations (10) and (11); e.g., $X_a = r_a \sin\theta_a \cos\phi_a$.

4-5. Program Flow: See listing below and compare directly to method described above. Note that in GAM(I,J), the index I represents the row number in $[\gamma_{ij}]$, and index J represents the column number.

4-6. Test Case: See discussion in Chapter 2.

4-7. Reference

1. E. B. Joy and G. K. Huddleston, "Radome Effects on the Performance of Ground Mapping Radar," Technical Report, Contract DAAH01-72-C-0598, U. S. Army Missile Command, March 1973.

4-8. Program Listing: See following pages.

```
      SUBROUTINE ORIENT(RA,THETAA,PHIA,RR,THETAR,PHIR,AGAM3A,                1
     -   ROTATE,TRANSL)                                                      2
      DIMENSION              ROTATE(3,3),        TRANSL(3)                  3
      REAL   GAM(3,3),RHO(3,3)                                              4
      DIMENSION T(3)                                                        5
      PSI=THETAA-AGAM3A                                                     6
      GAM(1,1)=SIN(PHIA)                                                    7
      GAM(1,2)=-COS(PHIA)                                                   8
      GAM(1,3)=0.                                                           9
      GAM(2,1)=SIN(PSI)*SIN(THETAA)*COS(PHIA)+COS(PSI)*COS(THETAA)          10
     -   *COS(PHIA)                                                        11
      GAM(2,2)=SIN(PSI)*SIN(THETAA)*SIN(PHIA)+COS(PSI)*COS(THETAA)          12
     -   *SIN(PHIA)                                                        13
      GAM(2,3)=SIN(PSI)*COS(THETAA)-COS(PSI)*SIN(THETAA)                    14
      GAM(3,1)=COS(PSI)*SIN(THETAA)*COS(PHIA)-SIN(PSI)*COS(THETAA)          15
     -   *COS(PHIA)                                                        16
      GAM(3,2)=COS(PSI)*SIN(THETAA)*SIN(PHIA)-SIN(PSI)*COS(THETAA)          17
     -   *SIN(PHIA)                                                        18
      GAM(3,3)=COS(AGAM3A)                                                  19
      RHO(1,1)=COS(THETAR)*COS(PHIR)                                        20
      RHO(1,2)=COS(THETAR)*SIN(PHIR)                                        21
      RHO(1,3)=-SIN(THETAR)                                                 22
      RHO(2,1)=SIN(PHIR)                                                    23
      RHO(2,2)=-COS(PHIR)                                                   24
      RHO(2,3)=0.                                                           25
      RHO(3,1)=-SIN(THETAR)*COS(PHIR)                                       26
      RHO(3,2)=-SIN(THETAR)*SIN(PHIR)                                       27
      RHO(3,3)=-COS(THETAR)                                                 28
      XA=RA*SIN(THETAA)*COS(PHIA)                                           29
      YA=RA*SIN(THETAA)*SIN(PHIA)                                           30
      ZA=RA*COS(THETAA)                                                     31
      XR=RR*SIN(THETAR)*COS(PHIR)                                           32
      YR=RR*SIN(THETAR)*SIN(PHIR)                                           33
      ZR=RR*COS(THETAR)                                                     34
C          COMPUTE THE ROTATE ARRAY BY MULTIPLYING THE RHO ARRAY            35
C              AND THE TRANSPOSE OF THE GAM ARRAY.                          36
      DO 2 I=1,3                                                            37
      DO 2 J=1,3                                                            38
```

```
      ROTATE(I,J)=0.                                                    39
      DO 2 K=1,3                                                        40
      ROTATE(I,J)=ROTATE(I,J)+RHO(I,K)*GAM(J,K)                         41
    2 CONTINUE                                                          42
C          COMPUTE TRANSL ARRAY                                         43
      T(1)=XA-XR                                                        44
      T(2)=YA-YR                                                        45
      T(3)=ZA-ZR                                                        46
      DO 10 I=1,3                                                       47
      TRANSL(I)=0.0                                                     48
      DO 10 J=1,3                                                       49
      TRANSL(I)=TRANSL(I)+RHO(I,J)*T(J)                                 50
   10 CONTINUE                                                          51
      RETURN                                                            52
      END                                                               53
```

Chapter 5

SUBROUTINE POINT

5-1. Purpose: To transform a point P in antenna coordinates (x_A, y_A, z_A) to radome coordinates (x_R, y_R, z_R), and vice versa.

5-2. Usage: CALL POINT (P, PT, ATOR, T, PO)

5-3. Arguments

P - Real (input) array of three elements representing the Cartesian coordinates (cm) of the point to be transformed; e.g., P(1) = x_A, P(2) = y_A, P(3) = z_A.

PT - Real (output) array of three elements representing the Cartesian coordinates (cm) in the other coordinate system; e.g., PT(1) = x_R, etc.

ATOR - Logical input variable which controls direction of transformation: ATOR =.TRUE. for antenna-to-radome (see Equation (4-3)); ATOR = .FALSE. for radome-to-antenna coordinate transformation (Equation (4-8)).

T - Real (input) array of 3 x 3 elements representing the ROTATE array computed by Subroutine ORIENT.

PO - Real (input) array of three elements representing the TRANSL array computed by Subroutine ORIENT.

5-4. Comments and Method

a. Subroutines required: Subroutine ORIENT must be called prior to the first call to POINT so that T and PO are available.

b. For method, see Subroutine ORIENT in Chapter 4.

5-5. Program Flow: Compare listing below directly to Equations (4-3) and (4-8).

5-6. Test Case: See Chapter 2.

5-7. Reference: See Chapter 4.

5-8. Program Listing: See following page.

```
      SUBROUTINE POINT(P,PT,ATOR,T,PO)                                  1
C                                                                       2
C   THIS SUBROUTINE TRANSFORMS A POINT P GIVEN IN ONE COORDINATE SYSTEM  3
C   TO THE SAME POINT GIVEN IN ANOTHER COORDINATE SYSTEM, PT.           4
C   THE TRANSFORMATION IS ACCOMPLISHED USING THE TRANSFORM MATRIX T     5
C   THE LOGICAL VARIABLE ATOR DIRECTS WHICH TRANSFORM IS TO BE MADE     6
C   IF ATOR IS TRUE THE TRANSFORM IS FROM ANTENNA COORDINATES TO        7
C   RADOME COORDINATES.  IF ATOR IS FALSE THE OPPOSITE TRANSFORM IS MADE 8
C   T IS THE MATRIX OF DIRECTION COSINES WHICH DESCRIBE THE ROTATION    9
C   OF THE RADOME COORDIANTE SYSTEM WITH RESPECT TO THE ANTENNA        10
C   COORDINATE SYSTEM, PO IS THE ORIGIN OF THE RADOME COORDINATE       11
C   SYSTEM IN ANTENNA COORDINATES                                      12
C                                                                      13
      REAL P(3),PT(3),T(3,3),PS(3),PO(3)                               14
      LOGICAL ATOR                                                     15
      IF(ATOR) GO TO 1                                                 16
C                                                                      17
C   CONVERSION FROM RADOME TO ANTENNA COORDINATES                      18
C                                                                      19
      PS(1)=P(1)-PO(1)                                                 20
      PS(2)=P(2)-PO(2)                                                 21
      PS(3)=P(3)-PO(3)                                                 22
      PT(1)=T(1,1)*PS(1)+T(2,1)*PS(2)+T(3,1)*PS(3)                     23
      PT(2)=T(1,2)*PS(1)+T(2,2)*PS(2)+T(3,2)*PS(3)                     24
      PT(3)=T(1,3)*PS(1)+T(2,3)*PS(2)+T(3,3)*PS(3)                     25
      RETURN                                                           26
    1 CONTINUE                                                         27
C                                                                      28
C    CONVERSION FROM ANTENNA TO RADOME COORDINATES                     29
C                                                                      30
      PT(1)=T(1,1)*P(1)+T(1,2)*P(2)+T(1,3)*P(3)+PO(1)                  31
      PT(2)=T(2,1)*P(1)+T(2,2)*P(2)+T(2,3)*P(3)+PO(2)                  32
      PT(3)=T(3,1)*P(1)+T(3,2)*P(2)+T(3,3)*P(3)+PO(3)                  33
      RETURN                                                           34
      END                                                              35
```

Chapter 6

SUBROUTINE VECTOR

6-1. Purpose: To transform a vector $\underline{F}$ in antenna coordinates to radome coordinates, and vice versa.

6-2. Usage: CALL VECTOR (V, VT, ATOR, T)

6-3. Arguments

V - Real (input) array of three elements representing the rectangular components of the vector to be transformed; e.g., V(1) = F_{xA}, V(2) = F_{yA}, V(3) = F_{zA}.

VT - Real (output) array of three elements representing the rectangular components of the vector in the other coordinate system; e.g., VT(1) = F_{xR}, etc.

ATOR - Logical input variable which controls the direction of the transformation: ATOR = .TRUE. for antenna-to-radome (Equation (4-5)); ATOR = .FALSE. for radome-to-antenna (Equation (4-9)).

T - Matrix ROTATE described in Chapter 4 as computed by Subroutine ORIENT.

6-4. Comments and Method

a. Subroutines required: Subroutine ORIENT must be called prior to the first call to VECTOR so that T will be available.

b. For method, see Subroutine ORIENT in Chapter 4.

6-5. Program Flow: Compare listing below directly to Equations (4-5) and (4-9).

6-6. Test Case: See Chapter 2.

6-7. References: See Chapter 4.

6-8. Program Listing: See following page.

```
      SUBROUTINE VECTOR(V,VT,ATOR,T)                                    1
C                                                                       2
C   THIS SUBROUTINE TRANSFORMS A VECTOR V GIVEN IN ONE COORDINATE SYSTEM  3
C   TO THE SAME VECTOR GIVEN IN ANOTHER COORDINATE SYSTEM, VT.          4
C   THE TRANSFORMATION IS ACCOMPLISHED USING THE TRANSFORM MATRIX T     5
C   THE LOGICAL VARIABLE ATOR DIRECTS WHICH TRANSFORM IS TO BE MADE     6
C   IF ATOR IS TRUE THE TRANSFORM IS FROM ANTENNA COORDINATES TO        7
C   RADOME COORDINATES.  IF ATOR IS FALSE THE OPPOSITE TRANSFORM IS MADE 8
C   T IS THE MATRIX OF DIRECTION COSINES WHICH DESCRIBE THE ROTATION    9
C   OF THE RADOME COORDIANTE SYSTEM WITH RESPECT TO THE ANTENNA        10
C   COORDINATE SYSTEM.                                                 11
C                                                                      12
      REAL V(3),VT(3),T(3,3)                                           13
      LOGICAL ATOR                                                     14
      IF(ATOR) GO TO 1                                                 15
C                                                                      16
C   CONVERSION FROM RADOME TO ANTENNA COORDINATES                      17
C                                                                      18
      VT(1)=T(1,1)*V(1)+T(2,1)*V(2)+T(3,1)*V(3)                        19
      VT(2)=T(1,2)*V(1)+T(2,2)*V(2)+T(3,2)*V(3)                        20
      VT(3)=T(1,3)*V(1)+T(2,3)*V(2)+T(3,3)*V(3)                        21
      RETURN                                                           22
    1 CONTINUE                                                         23
C                                                                      24
C    CONVERSION FROM ANTENNA TO RADOME COORDINATES                     25
C                                                                      26
      VT(1)=T(1,1)*V(1)+T(1,2)*V(2)+T(1,3)*V(3)                        27
      VT(2)=T(2,1)*V(1)+T(2,2)*V(2)+T(2,3)*V(3)                        28
      VT(3)=T(3,1)*V(1)+T(3,2)*V(2)+T(3,3)*V(3)                        29
      RETURN                                                           30
      END                                                              31
```

Chapter 7

SUBROUTINE INCPW

7-1. Purpose: To compute the rectangular vector components of the electric field of a plane electromagnetic wave propagating in the direction $-\hat{k}_A$ and incident on the z_A=0 plane of the antenna coordinate system, where (x_A=0, y_A=0, z_A=0) is used as the phase origin.

7-2. Usage: CALL INCPW (KA, EI, IOPT)

7-3. Arguments

KA - Real input array of three elements containing the direction cosines of the direction $\hat{k}_A$ from whence the plane wave emanates; e.g., KA(1) = k_{xA}, KA(2) = k_{yA}, KA(3) = k_{zA} where $\hat{k}_A = \hat{x}_A\, k_{xA} + \hat{y}_A\, k_{yA} \hat{z}\, k_{zA}$.

EI - Complex output array of three elements containing the complex rectangular components of the electric field $\underline{E}$, normalized such that $|\underline{E}| = 1$.

IOPT - Integer input variable which selects one of four polarizations (see Figure 7.1):

IOPT = 1 Elevation component only: $\underline{E} = \hat{\varepsilon}$

IOPT = 2 Azimuth component only: $\underline{E} = \hat{\alpha}$

IOPT = 3 Right hand circular: $\underline{E} = (\hat{\alpha}\, 1 + \hat{\varepsilon}\, e^{j\frac{\pi}{2}})/\sqrt{2}$

IOPT = 4 Left hand circular: $\underline{E} = (\hat{\alpha}\, 1 + \hat{\varepsilon}\, e^{-j\frac{\pi}{2}})/\sqrt{2}$

7-4. Comments and Method

a. Circular polarization is defined with respect to the direction of propagation $-\hat{k}_A$: looking in the direction of propagation, the observer

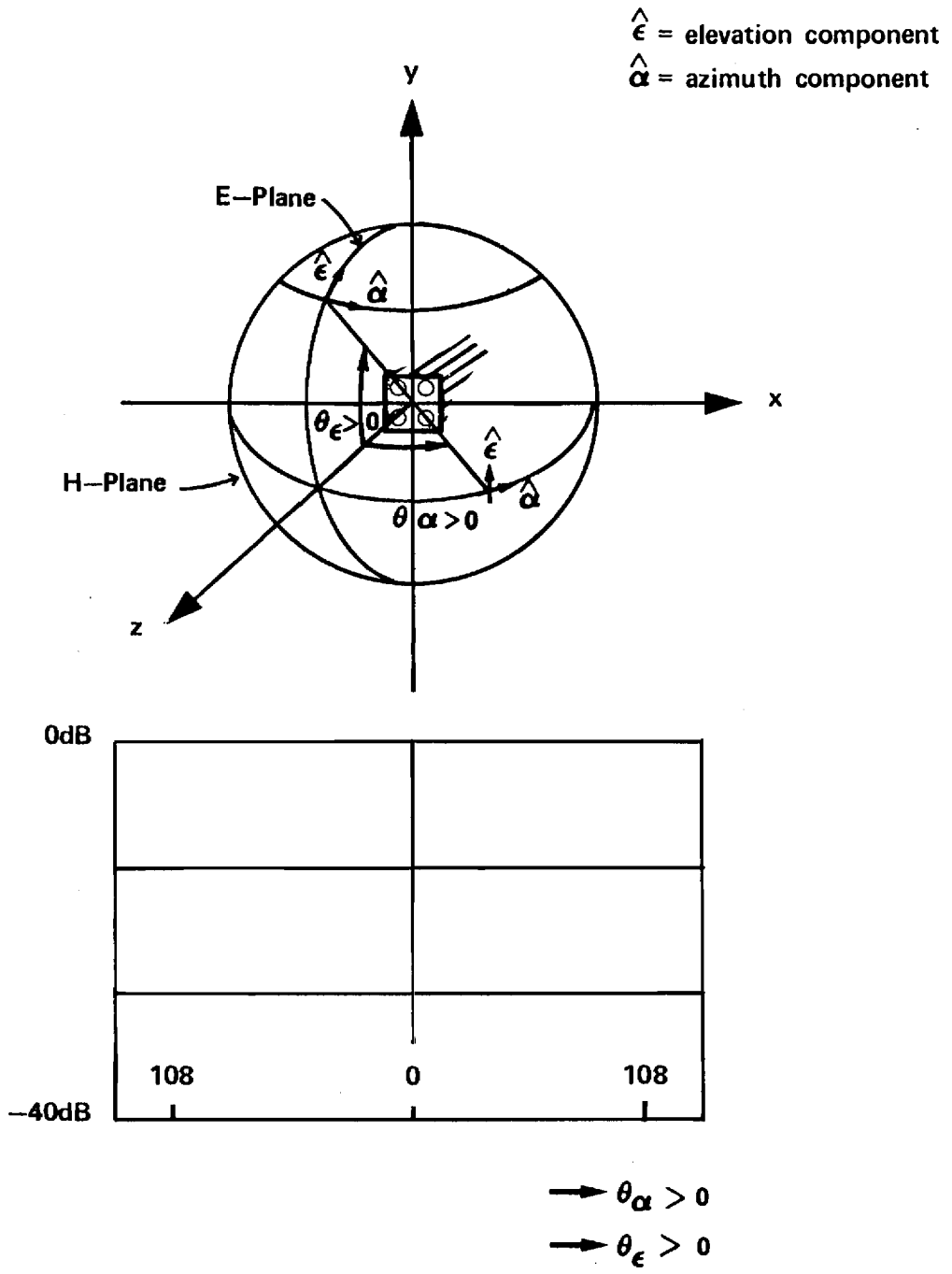

Figure 7-1. Coordinate System for Far Field Patterns

will see the tip of the $\underline{E}$ vector trace out a circle in a plane of equal phase, with the direction of rotation being clockwise for right-hand circular and counterclockwise for left-hand circular.

b. Spherical to rectangular coordinate transformations [1] are used to define the rectangular vector components E_x, E_y, E_z in terms of the transverse spherical components E_ε, E_α. Let $\hat{r} = \hat{k} = \hat{x}\,k_x + \hat{y}\,k_y + \hat{z}\,k_z$ represent the direction from whence the plane wave emanates, where k_x, k_y, k_z are the direction cosines of $\hat{r} = \hat{k}$. Then, with reference to Figure 7-1, there results

$$\hat{\varepsilon} = \hat{x}\,\frac{-k_x k_y}{\sqrt{1 - k_y^2}} + \hat{y}\sqrt{1 - k_y^2} + \hat{z}\,\frac{-k_y k_z}{\sqrt{1 - k_y^2}} \tag{1}$$

$$\hat{\alpha} = \hat{x}\,\frac{k_z}{\sqrt{1 - k_y^2}} + \hat{y}(0) + \hat{z}\,\frac{-k_x}{\sqrt{1 - k_y^2}} \tag{2}$$

except at $k_y = \pm 1$, where these equations reduce to

$$\hat{\varepsilon} = -\hat{z} \tag{3}$$

$$\hat{\alpha} = \hat{x} \tag{4}$$

The expressions for the field components for the four cases of interest are summarized in Table 7-1. The corresponding magnetic field can be obtained from

$$\underline{H} = (\underline{E} \times \hat{k})/\eta \tag{5}$$

7-5. Program Flow: Compare expressions in Table 7-1 directly to the program listing below.

Table 7-1. Rectangular Components for Four Cases of Plane Waves

IOPT	E_x	E_y	E_z
1	$-k_x k_y / \sqrt{1-k_y^2}$	$\sqrt{1-k_y^2}$	$-k_y k_z / \sqrt{1-k_y^2}$
2	$k_z / \sqrt{1-k_y^2}$	0	$-k_x / \sqrt{1-k_y^2}$
3	$(k_z - k_x k_y e^{j\frac{\pi}{2}}) / \sqrt{2(1-k_y^2)}$	$e^{j\frac{\pi}{2}} \sqrt{1-k_y^2} / \sqrt{2}$	$(-k_x - k_y k_z e^{j\frac{\pi}{2}}) / \sqrt{2(1-k_y^2)}$
4	$(k_z - k_x k_y e^{-j\frac{\pi}{2}}) / \sqrt{2(1-k_y^2)}$	$e^{-j\frac{\pi}{2}} \sqrt{1-k_y^2} / \sqrt{2}$	$(-k_x - k_y k_z e^{-j\frac{\pi}{2}}) / \sqrt{2(1-k_y^2)}$

7-6. Test Case: See Chapter 2.

7-7. References

1. D. T. Paris and F. K. Hurd, Basic Electromagnetic Theory, McGraw-Hill, New York, 1969, pp. 8-9.

7-8. Program Listing: See following pages.

```
      SUBROUTINE INCPW(KA,EI,IOPT)                                      1
C KA=NEGATIVE OF DIR OF PROP"N OF INCIDENT PLANE WAVE (ANT COORD)       2
C EI= ELECTRIC FIELD VECTOR OF INCIDENT PLANE WAVE (OUTPUT)             3
C IOPT=1 MAKES EI ELEVATION COMPONENT ONLY                              4
C     =2 MAKES EI AZIMUTH COMPONENT ONLY                                5
C     =3 FOR RHC POLARIZATION (DEFINED WRT DIR OF PROP OF INC WAVE)     6
C     *4 FOR LHC                                                        7
C POWER OF INCIDENT WAVE IS UNITY.                                      8
      COMPLEX EI(3),CIA                                                 9
      REAL KA(3),IE,IA                                                 10
    1 FORMAT(/" ERROR IN SUBR INCPW  IOPT= ",I3//)                     11
C COMPUTE ELEVATION COMPONENT ONLY:                                     12
      R=1.-KA(3)**2                                                    13
      IF (R.LT.0.) R=0.                                                14
      R=SQRT(R)                                                        15
      RY=1.-KA(2)**2                                                   16
      IF (RY.GT.0.) GO TO 5                                            17
      GO TO 40                                                         18
    5 RY=SQRT(RY)                                                      19
      GO TO (10,20,30,30),IOPT                                         20
C CORRECTIONS TO LOCPS 10,20,30,40 MADE JAN 78 BY GKH.                  21
   10 IE=1.                                                            22
      EI(1)=-KA(2)*KA(1)*IE/RY                                         23
      EI(2)=RY*IE                                                      24
      EI(3)=-KA(2)*KA(3)*IE/RY                                         25
      RETURN                                                           26
C COMPUTE AZIMUTH COMPONENT ONLY:                                       27
   20 IA=1.                                                            28
      EI(1)=+KA(3)*IA/RY                                               29
      EI(2)=CMPLX(0.,0.)                                               30
      EI(3)=-IA*KA(1)/RY                                               31
      RETURN                                                           32
C COMPUTE RHC:                                                          33
   30 IE=.707                                                          34
      CIA=CMPLX(0.,1.)*IE                                              35
      IF (ICPT.EQ.4) CIA=CMPLX(0.,-1.)*IE                              36
      EI(1)=(-KA(2)*KA(1)*CIA-KA(3)*IE)/RY                             37
      EI(2)=CIA*RY                                                     38
```

```
      EI(3)=(-KA(2)*KA(3)*CIA-IE*KA(1))/RY                              39
      RETURN                                                            40
   40 GO TO (50,60,70,70),ICPT                                          41
   50 EI(1)=(0.,0.)                                                     42
      EI(2)=(0.,0.)                                                     43
      EI(3)=-KA(2)                                                      44
      RETURN                                                            45
   60 EI(1)=(1.,0.)                                                     46
      EI(2)=(0.,0.)                                                     47
      EI(3)=(0.,0.)                                                     48
   70 IE=.707                                                           49
      CIA=CMPLX(0.,1.)*IE                                               50
      IF (IOPT.EQ.4) CIA=CMPLX(0.,-1.)*IE                               51
      EI(1)=IE                                                          52
      EI(2)=(0.,0.)                                                     53
      EI(3)=-KA(2)*CIA                                                  54
      RETURN                                                            55
      END                                                               56
```

Chapter 8

SUBROUTINE RECM

8-1. Purpose: To compute the complex voltages produced at the terminals of the three channels of a radome enclosed monopulse antenna by a plane wave of specified polarization and direction of arrival.

8-2. Usage: CALL RECM (PWI, KA, NX, NY, KXMAX, KYMAX, FGHZ, ROTATE, TRANSL, SUMX, SUMY, DELX, DELY, VR, TABLE, SUPPRS, RSQMAX)

8-3. Arguments

PWI - A complex array of three elements containing E_x, E_y, E_z of the incident plane wave. See Subroutine INCPW.

KA - A real array of three elements containing the direction cosines k_{xA}, k_{yA}, k_{zA} of the unit vector $\hat{k}_A$ which points from the antenna origin in the direction from whence the plane wave emanates.

NX,NY - The even integer number of sample points in x_A and y_A directions used to represent the antenna aperture fields.

KXMAX,KYMAX- Real variables which represent the normalized folding wavenumbers corresponding to the sample distances Δx_A, Δy_A according to $\Delta x_A = \lambda/(2*KXMAX)$, $\Delta y_A = \lambda/(2*KYMAX)$, where λ is the free space wavelength.

FGHZ - Frequency in gigahertz of the monochromatic plane wave.

ROTATE,TRANSL- Real matrices of direction cosines and translation distances used to carry out coordinate transformations of points and vectors from antenna to radome coordinate systems, and vice versa. See Subroutine ORIENT.

SUMX,SUMY - Two dimensional (NX X NY) complex arrays of the x and y vector components of the antenna aperture fields for the sum channel of a three-channel monopulse antenna. The element at I=NX/2+1, J=NY/2+1, corresponds to that at x_A=0, y_A=0 in the aperture. The general correspondence is given by

$$x_A = - x_{max} + (I-1)*\Delta x_A = (I-MIDNX)*\Delta x_A$$

$$y_A = - y_{max} + (J-1)*\Delta y_A = (J-MIDNY)*\Delta y_A$$

where $x_{max} = \Delta x_A*NX/2$ and $y_{max} = \Delta y_A*NY/2$.

Also see Subroutine HACNF.

DELX,DELY - Antenna aperture fields for the difference elevation channel.

DAZX,DAZY - Antenna aperture fields for the difference azimuth channel.

VR - Complex array of three elements which on output contains the complex terminal voltage of the antenna for the sum, elevation difference, and azimuth difference channels, respectively.

TABLE - Logical variable required by Subroutine RXMIT: if TRUE, a look-up table is used to calculate the transmission coefficients of the radome wall; if FALSE, these coefficients are calculated exactly for each angle of incidence specified.

SUPPRS - Logical variable used to control the printing of results from Subroutine RXMIT: if FALSE, a table of power transmission and reflection coefficients for equal increments in the sine of the incidence angle is printed. The phases of the complex voltage transmission and reflection coefficients of the radome wall are also printed.

RSQMAX - Real variable denoting the maximum radius of the antenna aperture such that any point $(x_A^2+y_A^2)>$RSQMAX is omitted from the ray tracing and summation procedure used to compute the received voltages VR.

8-4. Comments and Method

a. Subroutines Required: TRACE, VECTOR, POINT, RXMIT, CAXB.

b. Method: The voltage V_R induced at the terminals of a linear antenna by a "received" electromagnetic plane wave $\underline{E}_R$, $\underline{H}_R$ is given by the Lorentz reciprocity theorem as [1]

$$V_R(\hat{k}) = C \oint_S (\underline{E}_T \times \underline{H}_R - \underline{E}_R \times \underline{H}_T) \cdot \hat{n} da \qquad (1)$$

where $\hat{k}$ is the unit vector which points in the direction from whence the plane wave emanates and where $\underline{E}_T$, $\underline{H}_T$ are the electromagnetic fields of

the antenna as produced on the closed surface S which surrounds the antenna when it is transmitting. The unit vector $\hat{n}$ is the normal to S pointing into the region not containing the antenna, and C is a complex constant.

When the closed surface S is the $z_A=0$ plane, $\hat{n}=\hat{z}_A$, $da=dx_A dy_A \tilde{\Delta} x_A \Delta y_A$ and the integral in (1) can be approximated by

$$V_R(\hat{k}) = C\Delta x_A \Delta y_A \sum_l \sum_m (E_{Tx} H_{Ry} - E_{Ty} H_{Rx} - E_{Rx} H_{Ty} + E_{Ry} H_{Tx}) \quad (2)$$

where Δx_A, Δy_A are equal sample distances in x_A and y_A and where the rectangular vector components of the fields on the $z_A=0$ plane are given generically by

$$\underline{E}_T = \hat{x}_A E_{Tx} + \hat{y}_A E_{Ty} + \hat{Z}_A E_{Tz} \quad (3)$$

It is assumed that the fields $\underline{E}_T$, $\underline{H}_T$ on S with the radome in place are unperturbed by the radome. Also, $\underline{E}_T$ is specified according to the aperture distribution and polarization desired as is usually done in antenna analysis. The corresponding magnetic field $\underline{H}_T$, however, presents something of a vexation in that a non-Maxwellian aperture field can result if $\underline{H}_T$ is specified independently of $\underline{E}_T$ and Maxwell's equation $\underline{H}_T=\nabla x\underline{E}_T/-j\omega\mu$. On the other hand, specification of $\underline{H}_T$ independently of $\underline{E}_T$ is tantamount to specifying magnetic and electric current sheets in the antenna aperture which produce two independent solutions to Maxwell's equations whose sum yields the total fields. This latter approach is

taken here when the geometrical optics approximation

$$\underline{H}_T = \frac{\hat{z}_A \times \underline{E}_T}{\eta} \tag{4}$$

is utilized, where $\eta=\sqrt{\mu/\varepsilon} \approx 377$ ohms. Also, the magnetic field $\underline{H}_R$ is given by a similar formula

$$\underline{H}_R = \frac{-\hat{k} \times \underline{E}_R}{\eta} \tag{5}$$

where $-\hat{k}$ is the direction of propagation of the incident plane wave.

Combining the results of Equations (4) and (5) into (2), and designating the origin $x_A=y_A=z_A=0$ as the phase reference for the complex fields, there results

$$V_R(\hat{k}) = C' \sum_l \sum_m \{[(E_{Tx} E_{Rx} + E_{Ty} E_{Ry})(1 + k_{zA}) - (k_{xA} E_{Tx} + k_{yA} E_{Ty})E_{Rz}]. \\ e^{j \frac{2\pi}{\lambda} (k_{xA} x_A + k_{yA} y_A)}\} \tag{6}$$

where

$$\hat{k} = \hat{x}_A k_{xA} + \hat{y}_A k_{yA} + \hat{z}_A k_{zA} \tag{7}$$

$$k_{xA}^2 + k_{yA}^2 + k_{zA}^2 = 1 \tag{8}$$

and where the exponential factor accounts for the phase of the incident wave. It is noted that k_{xA}, k_{yA}, k_{zA} are direction cosines of $\hat{k}$; hence, $k_{zA}=\cos\theta$, where θ is the polar angle measured from the z_A-axis in the usual spherical coordinate system. The $(1+\cos\theta)$ term in Equation (6) is characteristic of the geometrical optics approximation of Equation (4) [2]. The other factors have been absorbed into complex constant C'.

The effects of the radome on the received voltage given by Equation (6) are accounted for by tracing a ray from each aperture element $\Delta x_A \Delta y_A$ in the direction $\hat{k}$ and weighting the field $\underline{E}_R$ associated with the ray by the complex insertion transmission coefficients $T_\perp$, $T_{||}$ of the radome wall as shown in Figure 8-1. These coefficients depend on the incidence angle θ_i and the plane of incidence defined by $\hat{k}$ and the unit inward normal $\hat{n}_R$ to the radome wall at each point of incidence for each ray as illustrated in Figure 8-2. The ray tracing is carried out in the direction $\hat{k}$, and the direction of propagation of each ray is assumed to be the same on both sides of the wall, an assumption that mandates use of the insertion transmission coefficients defined for an infinite sheet by

$$T_\perp = \frac{E_\perp\ (P)}{E_{\perp i}\ (P)} \tag{9}$$

$$T_{||} = \frac{E_{||}\ (P)}{E_{||\ i}\ (P)} \tag{10}$$

where the numerator in each case is the field at point P with the sheet in place and the denominator is the field at the same point with the sheet removed.

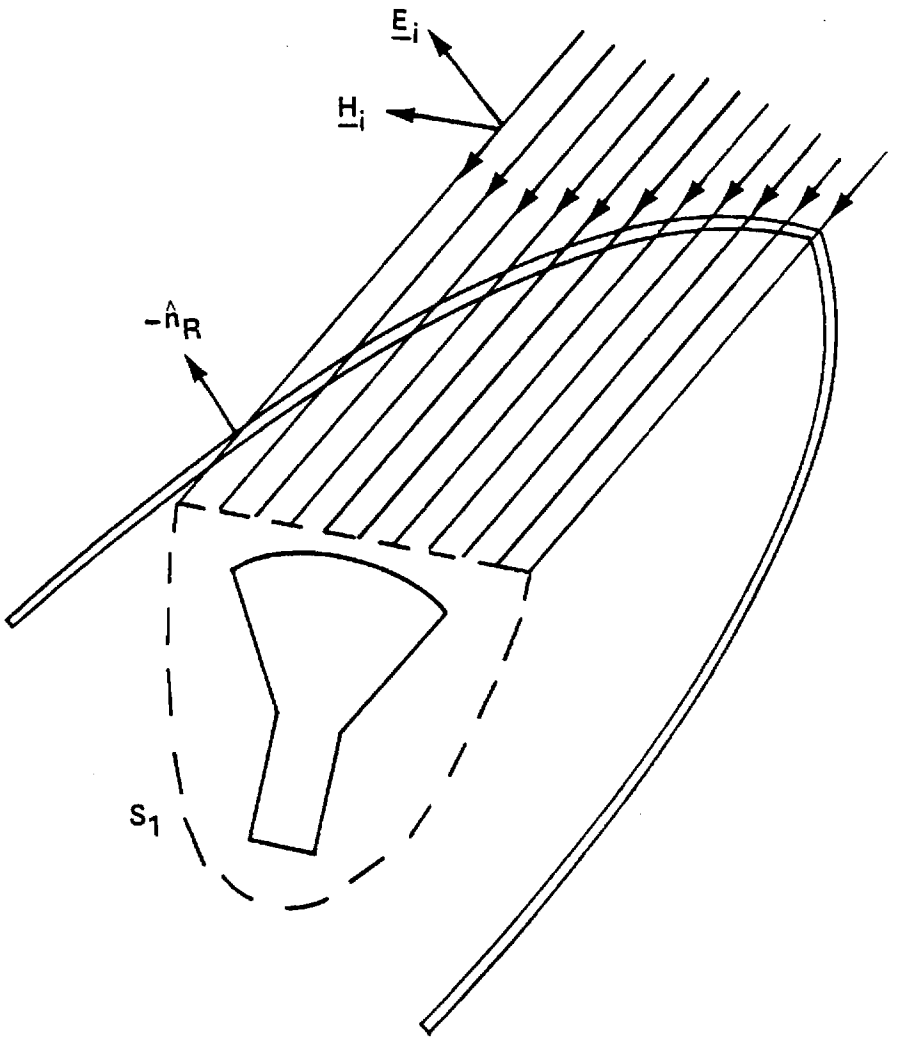

Figure 8-1. Illustration of the Fast Receiving Method of Radome Analysis

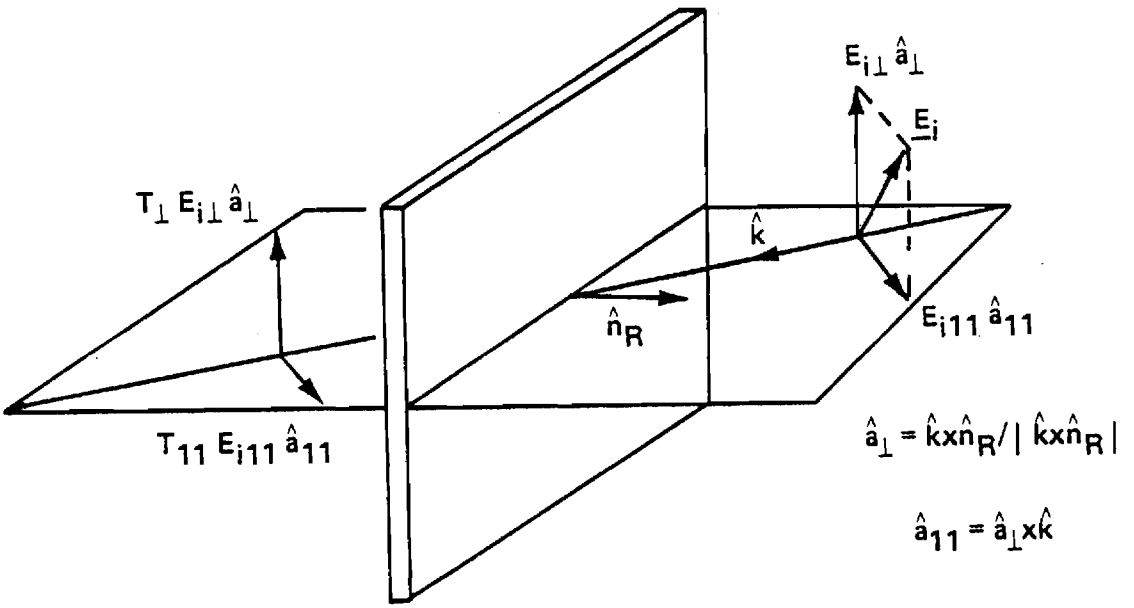

Figure 8-2. Plane Wave Propagation Through an Infinite Plane Sheet

The ray tracing is carried out in radome coordinates (x_R, y_R, z_R), and transformations of points and vectors from antenna coordinates (x_A, y_A, z_A) to radome coordinates, and vice versa, are required. (These transformations are described in detail in Subroutines ORIENT, POINT, and VECTOR.) Let $(x_A, y_A, 0)$ be the point in the aperture from which the ray (line) emanates in the direction $\hat{k}$. Convert this point and unit vector to the radome coordinate system. Find the intersection (x_{RI}, y_{RI}, z_{RI}) of this ray with the inner radome surface as described by $f(\sqrt{x_R^2 + y_R^2}\, z) = \text{constant}$ since it is a surface of revolution (Subroutines TRACE and OGIVE). Compute the unit inward normal $\hat{n}_R$ to the surface

$$\hat{n}_R = -\frac{\nabla f}{|\nabla f|} = \hat{x}_R\, n_{xR} + \hat{y}_R\, n_{yR} + \hat{z}_R\, n_{zR} \tag{11}$$

and convert it to antenna coordinates

$$\hat{n}_R = \hat{n}_A = \hat{x}_A\, n_{xA} + \hat{y}_A\, n_{yA} + \hat{z}_A\, n_{zA} \tag{12}$$

Use $\hat{n}_A$ and $\hat{k}$ to determine the plane of incidence, angle of incidence, and the transmitted plane wave $\underline{E}'_R$, $\underline{H}'_R$ (see Subroutine RXMIT) for this ray. Substitute into Equation (6) and sum the results to obtain the following expression for the received voltage

$$V_R(\hat{k}) = C'' \sum_l \sum_m \left[-(1 + k_{zA})(E'_{Rx}\ E_{Tx} + E'_{Ry}\ E_{Ty}) + (k_{xA}\, E_{Tx} + k_{yA}\, E_{Ty})E'_{Rz}\right] \cdot e^{j\frac{2\pi}{\lambda}(k_{xA}\, x_A + k_{yA}\, y_A)} \tag{13}$$

where a sign change and η^{-1} have been absorbed into C".

Equation (13) with C"=1 is used in Subroutine RECM to compute the received voltage on each of the three monopulse channels. Note that the received field $\underline{E}'_R$, $\underline{H}'_R$ at each point $(x_A, y_A, 0)$ is the same for all three channels so that three summations can be carried simultaneously to maximize computational speed. In each summation, only the data corresponding to E_{Tx}, E_{Ty} for the sum, elevation difference, and azimuth difference channels need to be changed. Note also that Equation (13) can be rewritten as

$$V_R(\hat{k}) = \sum_l \sum_m [E_{Tx}(\eta H'_{Ry} - E'_{Rx}) - E_{Ty}(\eta H'_{Rx} + E'_{Ry})]e^{j\frac{2\pi}{\lambda}(k_{xA} x_A + k_{yA} y_A)} \tag{14}$$

where $\eta H'_{Ry}$, $\eta H'_{Rx}$ are given by Equation (5).

8-5. Program Flow

Line 12: Initialize the ray counter NRAY.

Lines 13-18: Compute λ (cm), $k_o=2\pi/\lambda$, Δx_A, Δy_A, and the midpoint of the NX X NY data arrays corresponding to $x_A=0$, $y_A=0$.

Lines 21-24: Set $z_A=0=PA(3)$ and precalculate $k_o k_{xA}$ and $k_o k_{yA}$. Transform $\hat{k}_A$ to radome coordinates $\hat{k}_R=\hat{x}_R k_{xR} + \hat{y}_R k_{yR} + \hat{z}_R k_{zR}$ in preparation for the ray tracing.

Lines 26-28: Initialize the summations VR(1), VR(2), VR(3) for the received voltages on the sum, difference elevation, and difference azimuth channels, respectively.

Lines 30-33: Iterate for each aperture point $x_A=PA(1)$; precalculate x_A^2 and $k_o k_{xA} x_A$ outside the subsequent loop for y_A.

Lines 34-40: Iterate for each aperture point y_A=PA(2). Compute $x_A^2+y_A^2$=RSQ: if point is outside RSQMAX, omit from computation.

Lines 41-47: Transform $(x_A, y_A, 0)$ to radome coordinates and trace ray to radome inner surface to find unit inward normal $\hat{n}_R$. If metal tip or bulkhead is encountered by ray, omit this ray from computation of received voltages.

Lines 48-52: Transform $\hat{n}_R$ to antenna coordinates and compute the transmitted plane wave PWT=$(E'_{Rx}, E'_{Ry}, E'_{Rz})$.

Lines 53-57: Compute phase PC=$e^{j\frac{2\pi}{\lambda}(k_{xA}x_A + k_{yA}y_A)}$ and apply to E'_{Rx}, E'_{yR}, E'_{Rz}.

Lines 58-71: Form $\eta \underline{H}'_R = \underline{E}'_R \times \hat{k}$ and use Equation (14) to add the contribution of this ray to the received voltage on each of the three channels.

Lines 72-73: Increment ray counter and continue the iteration until all aperture points have been used. Upon completion, NRAY equals the number of rays used in the summation for each received voltage.

Lines 74-75: If SUPPRS is false, write NRAY.

RETURN

END

8-6. Test Case: See Chapter 2.

8-7. References

1. G. K. Huddleston, H. L. Bassett, and J. M. Newton, "Parametric Investigation of Radome Analysis Methods," 1978 IEEE APS Symposium Digest, pp. 199-201, May 1978.

2. Microwave Antenna Theory and Design, ed. by S. Silver, McGraw Hill, New York, pp. 161-162, 1949.

8-8. Program Listing: See following pages.

```
      SUBROUTINE RECM(PWI,KA,NX,NY,KXMAX,KYMAX,FGHZ,ROTATE,TRANSL,          1
     $ SUMX,SUMY,DELX,DELY,DAZX,DAZY,VR,TABLE,SUPPRS,RSQMAX)                2
C  NOTE: HXI,HYI MAGNETIC FIELDS HAVE NOT BEEN DIVIDED BY ETA0.            3
      REAL KXMAX,KYMAX,LAMBDA,KO,ROTATE(3,3),TRANSL(3)                     4
      REAL KR(3),KA(3),NIR(3),NIA(3),PR(3),PA(3),PIR(3)                    5
      LOGICAL ATOR,RTOA,METAL,TABLE,SUPPRS                                 6
      COMPLEX SUMX(NX,NY),SUMY(NX,NY),DELX(NX,NY),DELY(NX,NY)              7
      COMPLEX DAZX(NX,NY),DAZY(NX,NY),VR(3)                                8
      COMPLEX PWI(3),PWT(3),HPWT(3),PC                                     9
      DATA ATOR,RTOA/.TRUE.,.FALSE./                                      10
      DATA TUPI/6.2831853071796/,NDO/0/                                   11
    1 NRAY=0                                                              12
      LAMBDA=29.97925/FGHZ                                                13
      KO=TUPI/LAMBDA                                                      14
      DX=LAMBDA/(2*KXMAX)                                                 15
      DY=LAMBDA/(2*KYMAX)                                                 16
      MIDNX=NX/2+1                                                        17
      MIDNY=NY/2+1                                                        18
C                                                                         19
C  RSQMAX IS THE SQUARE OF THE MAXIMUM RADIUS OF THE APERTURE             20
      PA(3)=0.                                                            21
      PHKA1=KO*KA(1)                                                      22
      PHKA2=KO*KA(2)                                                      23
      CALL VECTOR(KA,KR,ATOR,ROTATE)                                      24
C                                                                         25
      VR(1)=(0.,0.)                                                       26
      VR(2)=(0.,0.)                                                       27
      VR(3)=(0.,0.)                                                       28
C  ITERATE FOR EACH APERTURE POINT                                        29
      DO 10 L=1,NX,1                                                      30
      PA(1)=(L-MIDNX)*DX                                                  31
    3 APA=PA(1)*PA(1)                                                     32
      PAKA=PA(1)*PHKA1                                                    33
      DO 10 M=1,NY,1                                                      34
      PA(2)=(M-MIDNY)*DY                                                  35
C                                                                         36
C   IF APERTURE POINT IS OUTSIDE CIRCULAR APERTURE, OMIT FROM CALCULATIO  37
C                                                                         38
```

```
      RSQ=APA+PA(2)*PA(2)                                                39
      IF(RSQ.GT.RSQMAX) GO TO 10                                         40
    4 CALL POINT(PA,PR,ATOR,ROTATE,TRANSL)                               41
C                                                                        42
C   TRACE RAY TO FIRST INTERSECTION POINT                                43
C   NOTE: ALL APERTURE POINTS MUST BE CONTAINED WITHIN RADOME.           44
C                                                                        45
      CALL TRACE(PR,KR,PIR,NIR,METAL)                                    46
      IF(METAL) GO TO 10                                                 47
      CALL VECTOR(NIP,NIA,RTOA,ROTATE)                                   48
C                                                                        49
C  TABLE OF XMN COEFS IS FORMED ON FIRST CALL TO XMIT                    50
C                                                                        51
    5 CALL RXMIT(PWI,PWT,KA,NIA,PIR,TABLE,SUPPRS,KO)                     52
      PHASE=PAKA+PA(2)*PHKA2                                             53
      PC=CEXP(CMPLX(0.0,+AMOD(PHASE,TUPI)))                              54
      PWT(1)=PWT(1)*PC                                                   55
      PWT(2)=PWT(2)*PC                                                   56
      PWT(3)=PWT(3)*PC                                                   57
C  FORM MAGNETIC FIELD                                                   58
      CALL CAXB(PWT,KA,HPWT)                                             59
C  COMPUTE CONTRIBUTION TO RECEIVED VOLTAGE ON EACH CHANNEL:             60
C     VR(I)=EYT*HPWT(1)-EXT*HPWT(2)+PWT(1)*HYT                          61
C    $ -PWT(2)*HXT+VR(I)                                                 62
      VR(1)=VR(1)+SUMX(L,M)*(HPWT(2)-PWT(1))-SUMY(L,M)*                  63
     $ (HPWT(1)+PWT(2))                                                  64
      VR(2)=VR(2)+DELX(L,M)*(HPWT(2)-PWT(1))-DELY(L,M)*                  65
     $ (HPWT(1)+PWT(2))                                                  66
      VR(3)=VR(3)+DAZX(L,M)*(HPWT(2)-PWT(1))-DAZY(L,M)*                  67
     $ (HPWT(1)+PWT(2))                                                  68
C  GEOMETRIC OPTICS APPROXIMATION IS USED ABOVE IN EXPRESSIONS           69
C  FOR REC"D VOLTAGES  I.E.,HT=ZHAT X ET IN APERTURE.                    70
C  DIVISION BY ETA0 IS NOT DONE TO SAVE COMPUTATION TIME.                71
      NRAY=NRAY+1                                                        72
   10 CONTINUE                                                           73
      NCO=1                                                              74
      IF (.NOT.SUPPRS) WRITE(6,16) NRAY                                  75
   16 FORMAT(" NUMBER OF RAYS USED IN COMPUTING APERTURE FIELD =",I10)   76
```

```
 25 RETURN
    END
```

77
78

Chapter 9

SUBROUTINE TRACE

9-1. Purpose: To direct the ray tracing to find the intersection of a ray emanating from a point inside the radome and the inner radome surface. All dimensions are in centimeters. Radome coordinates are implied.

9-2. Usage: CALL TRACE (PO, K, P, N, METAL)

COMMON/TRACC/Z2, Z1

9-3. Arguments

PO - Real input array of three elements containing the point PO(x_o, y_o, z_o) from which the ray emanates.

K - Real input array of three elements containing the direction cosines of the ray; i.e., K(1) = k_x, K(2) = k_y, K(3) = k_z.

P - Real output array of three elements containing the point of intersection P(x, y, z) of the ray and the inner radome surface.

N - Real output array containing the direction cosines of the unit inward normal vector to the radome inner surface at P(x, y, z); i.e., N(1) = n_x, N(2) = n_y, N(3) = n_z where $\hat{n} = \hat{x}n_x + \hat{y}n_y + \hat{z}n_z$.

METAL - Logical output variable which indicates any opaque surfaces encountered, such as a metal tip or bulkhead: METAL = .TRUE. indicates that P(x, y, z) lies on such an opaque surface.

Z2 - Real input variable which designates the z_R coordinate (cm) of the intersection of the ogive section of the radome, and the metal tip (if any); must be set in main program prior to the first call to TRACE.

Z1 - Real input variable which designates the z_R coordinate (cm) of the intersection of the ogive section and the bulkhead of the air frame; must be set in main program prior to the first call to TRACE.

9-4. Comments and Method

a. Subroutines required: OGIVE, TDISK, BDISK, OGIVEN, TDISKN, BDISKN

b. The inner surface of the radome is represented by three distinct surfaces as indicated in Figure 9-1: a planar bottom disk (bulkhead), a tangent ogive, and a planar top disk (base of a metal tip). The ray is traced to the ogive surface first to find a point of intersection P(x, y, z):

(1) If $z_1<z<z_2$, then the ogive section of the radome was struck, the unit normal is computed (OGIVEN), METAL is set to .FALSE. and the program returns.

(2) If $z>z_2$, it is assumed that the ray encountered the top disk before impinging on the ogive surface (which actually extends beyond the z_2 coordinate). The ray is then traced to find its intersection with the plane $z = z_2$. If the top disk is indeed struck, then METAL is set .TRUE. and $\hat{n} = -\hat{z}$ is returned.

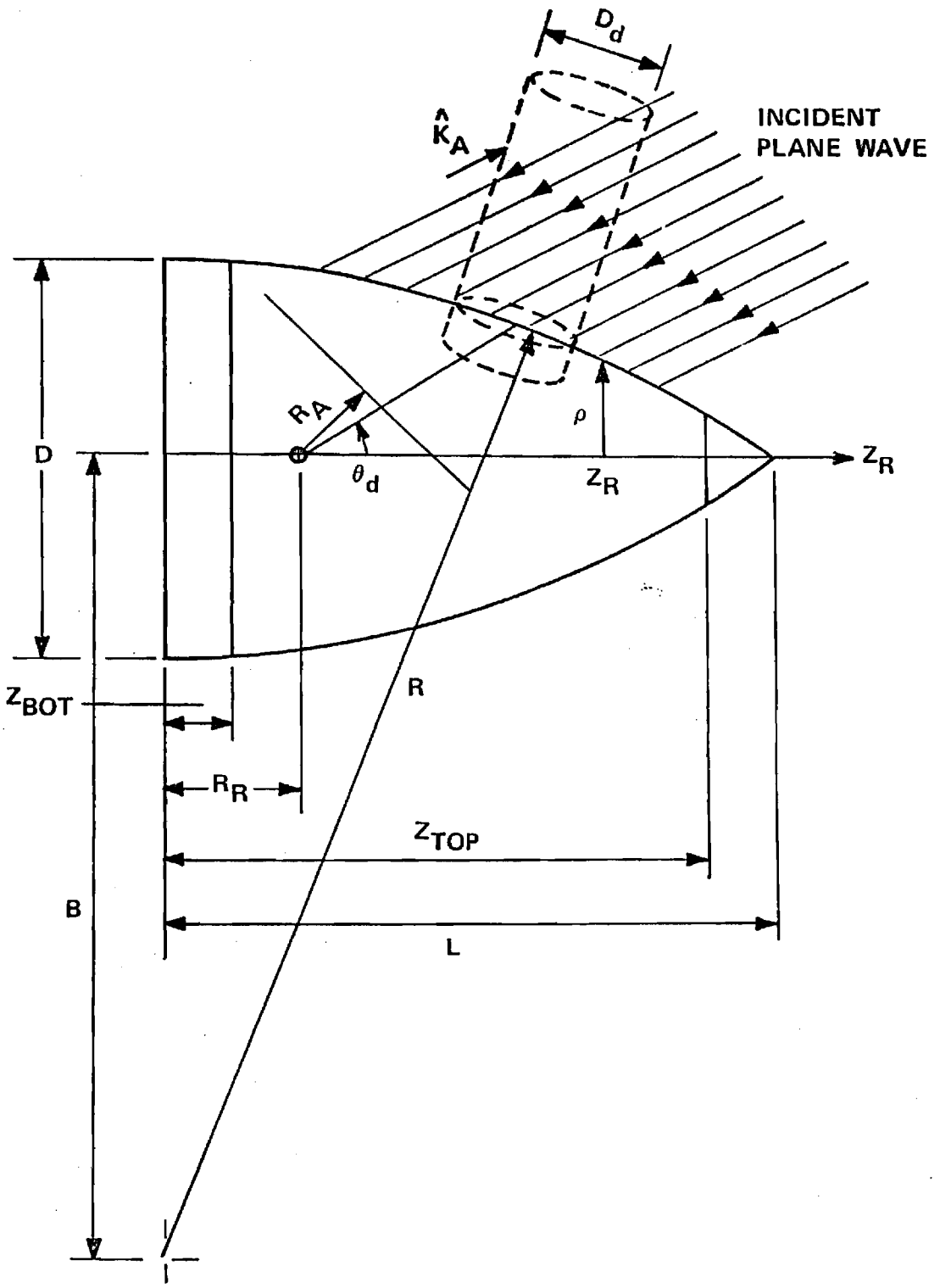

Figure 9-1. Tangent Ogive Radome Geometry.

(3) If $z<z_1$ from (1) above, it is assumed that the bottom disk was struck by the ray before it encountered the ogive surface. The ray is traced again to find its intersection with the plane $z = z_1$. If this bottom disk is indeed struck, then METAL = .TRUE. and $\hat{n} = \hat{z}$ is returned.

The steps in (2) and (3) above appear to be unnecessary; however, they are included to ensure that the ray tracing procedure works correctly and to alert the user if it does not. For example, if incorrect variable values are passed to the supporting subroutines, there is a good chance that no intersection will be found with any one of the three surfaces, in which case the following error message is outputted:

"THERE IS A HOLE IN THIS RADOME"

The message is continued with the values of (x_o, y_o, z_o) and (k_x, k_y, k_z). Incorrect values of geometry variables passed to the supporting subroutines, and attempts to trace a ray from a point exterior to the inner radome surface, will prompt the error message and alert the user of his mistake.

9-5. Program Flow: See listing below.

9-6. See Chapter 2.

9-7. References: None

9-8. Program Listing: See following pages.

```
      SUBROUTINE TRACE(PO,K,P,N,METAL)                                  1
C                                                                       2
C     SUBROUTINE TRACE TRACES A RAY FROM ITS POINT OF ORIGIN PO(3)      3
C     TO ITS POINT OF INTERSECTION WITH THE RADOME WALL, P(3)           4
C     THE RAY IS TRAVELING IN THE DIRECTION K(3)                        5
C                                                                       6
      REAL PO(3),K(3),P(3),N(3)                                         7
      LOGICAL METAL,HIT                                                 8
C                                                                       9
C   SET SURFACE INTERSECTION Z VALUES                                  10
C   Z2 IS THE INTERSECTION OF THE TOP DISK AND THE OGIVE               11
C   Z1 IS THE INTERSECTION OF THE OGIVE AND THE BOTTOM DISK            12
      COMMON/TRACC/Z2,Z1                                                13
C                                                                       14
C   DETERMINE IF RAY INTERSECTS WITH OGIVE SECTION                     15
      CALL OGIVE(PO,K,P,HIT)                                            16
      IF(.NOT.HIT) GO TO 2                                              17
      IF(P(3).LT.Z1) GO TO 2                                            18
      IF(P(3).GT.Z2) GO TO 1                                            19
      GO TO 10                                                          20
C                                                                       21
C   DETERMINE IF RAY INTERSECTS WITH TOP DISK                          22
    1 CALL TDISK(PO,K,P,HIT)                                            23
      IF(HIT) GO TO 11                                                  24
      GO TO 13                                                          25
C                                                                       26
C   DETERMINE IF RAY INTERSECTS WITH BOTTOM DISK                       27
    2 CALL BDISK(PO,K,P,HIT)                                            28
      IF(HIT) GO TO 12                                                  29
   13 WRITE(6,100)                                                      30
  100 FORMAT(/,2X,"THERE IS A HOLE IN THIS RADOME")                     31
      WRITE(6,101)PO,K                                                  32
  101 FORMAT(2X,"RAY STARTED HERE",3G10.4,"RAY TRAVELED IN THIS DIRECTIO 33
     $N",3G10.4//)                                                      34
      RETURN                                                            35
   10 CALL OGIVEN(P,N)                                                  36
      METAL=.FALSE.                                                     37
      RETURN                                                            38
```

```
11 CALL TDISKN(N)                                                    39
   METAL=.TRUE.                                                      40
   RETURN                                                            41
12 CALL BDISKN(N)                                                    42
   METAL=.TRUE.                                                      43
   RETURN                                                            44
   END                                                               45
```

Chapter 10

SUBROUTINE RXMIT

10-1. Purpose: To compute the complex rectangular vector components of the electric field $\underline{E}_T$ transmitted through the radome wall, where it is assumed that the incident field $\underline{E}_i$, $\underline{H}_i$ is locally a plane wave and that the radome wall behaves as an infinite plane dielectric sheet. The direction of propagation of the plane wave $-\hat{k}$ and the unit inward normal $\hat{n}$ at the point $P_1(x, y, z)$ are used to determine the angle of incidence and the plane of incidence of the plane wave. All dimensions are in centimeters. Radome coordinates are implied.

10-2. Usage: CALL RXMIT (PWI, PWT, K, NORM, P1, TABLE, SUPPRS, BETA)
COMMON/TRANSC/DIN(6), ER(6), TD(6), TZ, WALTOL, N, NN, D(6), ZB, TK

10-3. Arguments

PWI - Complex input array containing the vector components of the incident electric field; i.e., PWI (E_{xi}, E_{yi}, E_{zi}).

PWT - Complex output array containing the vector components of the transmitted electric field; i.e., PWT (E_{xt}, E_{yt}, E_{zt}).

K - Real input array containing the direction cosines of the direction from whence the plane wave emanates; i.e., $K(k_x, k_y, k_z) = \hat{x}\, k_x + \hat{y}\, k_y + \hat{z}\, k_z$.

NORM - Real input array containing the rectangular components of the unit inward normal $\hat{n} = \hat{x}\, n_x + \hat{y}\, n_y + \hat{z}\, n_z$; i.e., NORM ($n_x$, n_y, n_z).

P1 - Real input array containing the coordinates (x, y, z) of the point on the radome inner surface where the transmitted plane wave is assumed to emerge; i.e., P1(x, y, z).

TABLE - Logical input variable: if TRUE, a look-up table is used to compute the insertion voltage transmission coefficients $T_\perp$, $T_{||}$ corresponding to the angle of incidence θ_i; if FALSE, $T_\perp$, $T_{||}$ are each set to unity to simulate the absence of the radome. Originally, if TABLE = .FALSE., the coefficients $T_\perp$, $T_{||}$ were computed at each point P1(x, y, z) by a call to Subroutine WALL as in the case of the wall configuration being dependent on position (temperature variables, prescription tapers, etc.)

SUPPRS - Logical input variable: if FALSE, a table of transmission coefficients versus $\sin\theta_i$ is printed. Actually, $|T_\perp|^2$, $|T_{||}|^2$, $|R_\perp|^2$, $|R_{||}|^2$ and the phases of $T_\perp$, $T_{||}$, $R_\perp$, $R_{||}$ are printed.

BETA - Real input variable $\beta = 2\pi/\lambda$, where λ is the free space wavelength (cm).

DIN, ER, TD, D, - Real input arrays which specify the thickness in inches, relative dielectric constant ε_r, and loss tangent $\tan\delta$ of the N layers comprising the multilayer radome wall. Layer 1 is the first layer on

N, NN — the exit side of the wall; layer N is the first layer on the incident side. ER(NN), TD(NN) specify ε_r, tanδ of the medium in which the N-layer structure is immersed (normally, free space so that ER(NN) = 1.0, TD(NN) = 0.0). The real array D contains, after the first call to RXMIT, the thickness in centimeters of each layer.

TZ, WALTOL, ZB, TK — Real variables used previously to specify longitudinal and circumferential variations in wall thickness and in the tolerance on thickness. These variables are not active in this version of RXMIT.

10-4. Comment and Method

a. Subroutines required: WALL, AMPHS, AXB

b. The transmission of an incident plane wave through a plane dielectric sheet immersed in free space ($\varepsilon_o = 8.854 \times 10^{-12}$ farads/m, $\mu_o = 4\pi \times 10^{-7}$ henries/m) may be described in terms of the insertion voltage transmission coefficients

$$T_{\perp} = \frac{E_{t\perp}(P')}{E_{i\perp}(P')} \tag{1}$$

$$T_{||} = \frac{E_{t||}(P')}{E_{i||}(P')} \tag{2}$$

where $E_{t\perp}$, $E_{t||}$ are the transmitted fields at P' with the sheet in place, and $E_{i\perp}$, $E_{i||}$ are the incident fields at the same point in the absence of the sheet. The point P' lies on the colinear extension of the incident ray and is located on the exit side of the sheet.

Since the transmission coefficients $T_\perp$, $T_{||}$ are different, it is necessary to resolve the incident electric field $\underline{E}_i$ into perpendicular and parallel components; i.e., vector components which are perpendicular to and parallel to the plane of incidence (POI) defined by $\hat{k}$ and $\hat{n}_R$ as illustrated in Figure 10-1. The unit vector perpendicular to the POI is given by

$$k = \frac{\hat{k} \times \hat{n}_R}{|\hat{k} \times \hat{n}_R|} = \frac{\hat{k} \times \hat{n}_R}{\sin \underline{|\hat{k}, \hat{n}_R}} \tag{3}$$

A unit vector parallel to the POI is given by

$$\hat{k}_{||} = \hat{k}_\perp \times \hat{k} \tag{4}$$

The incident electric field may be written as

$$\underline{E}_i = \hat{x} E_{xi} + \hat{y} E_{yi} + \hat{z} E_{iz} = \hat{k}_\perp E_{i\perp} + \hat{k}_{||} E_{i||} \tag{5}$$

where

$$E_{i\perp} = \hat{k}_\perp \cdot \underline{E}_i = k_{x\perp} E_{xi} + k_{y\perp} E_{yi} + k_{z\perp} E_{zi} \tag{6}$$

$$E_{i||} = \hat{k}_{||} \cdot \underline{E}_i = k_{x||} E_{xi} + k_{y||} E_{yi} + k_{z||} E_{zi} \tag{7}$$

and where $k_{x\perp}$, $k_{x||}$, etc. are the vector components of $\hat{k}_\perp$, $\hat{k}_{||}$. In terms of the coordinate system (x, y, z),

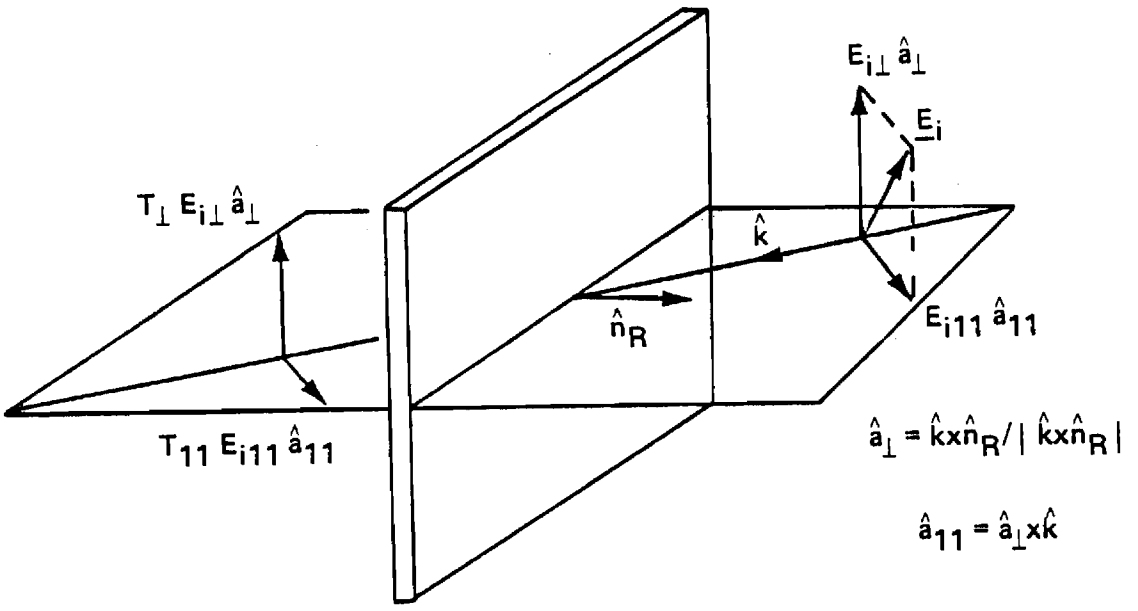

Figure 10-1. Plane Wave Propagation Through an Infinite Plane Sheet

$$\underline{E}_i = \hat{x}(E_{xi\perp} + E_{xi\parallel}) + \hat{y}(E_{yi\perp} + E_{yi\parallel}) + \hat{z}(E_{zi\perp} + E_{zi\parallel}) \tag{8}$$

where, for example

$$E_{xi\perp} = \hat{x} \cdot \hat{k}_\perp E_{i\perp} = k_{x\perp} E_{i\perp} \tag{9}$$

The transmitted plane wave is then given by

$$\underline{E}_T = \hat{k}_\perp T_\perp E_{i\perp} + \hat{k}_\parallel T_\parallel E_{i\parallel} \tag{10}$$

$$\underline{E}_T = \hat{x}(T_\perp E_{xi\perp} + T_\parallel E_{xi\parallel}) + \hat{y}(T_\perp E_{yi\perp} + T_\parallel E_{yi\parallel}) + \hat{z}(T_\perp E_{zi\perp} + T_\parallel E_{zi\parallel}) \tag{11}$$

10-5. Program Flow

Lines	Comments
Line 9:	Set NANGLE = number of entries used in the look-up tables for $T_\perp$, $T_\parallel$.
Lines 10-12:	NDO causes initialization of variables and the computation of the look-up tables on the first call to RXMIT (lines 11-59).
Lines 15-16:	Convert layer thicknesses from inches to centimeters.
Lines 17-59:	Compute look-up tables for $T_\perp$, $T_\parallel$ at NANGLE points spaced equally in $\sin\theta_i$ over the range (0, 1). If SUPPRS = .FALSE., print a table of transmission coefficients (every fifth point only). If ER(1)< 1.05, set AIR = .TRUE. and compute unity transmission coefficients for the "air" radome (for testing).

Lines 60-78: Compute $\sin\theta_i$.

Lines 79-86: Interpolate in table to compute $T_\perp$, $T_\parallel$ at $\sin\theta_i$.

Lines 87-100: Normalize the vector $\hat{k}_\perp$.

Lines 101-112: Compute $E_{xi\perp}$, $E_{yi\perp}$, $E_{zi\perp}$.

Lines 113-124: Compute $E_{xi\parallel}$, $E_{yi\parallel}$, $E_{zi\parallel}$.

Lines 125-129: Compute E_{xt}, E_{yt}, E_{zt} and return.

Lines 130-136: If $\sin\theta_i$ is out of range of the table, write error message, set $T_\perp$, $T_\parallel$ to unity, and continue.

10-6. Test Case: See Chapter 2.

10-7. References: None

10-8. Program Listing: See following pages.

```
      SUBROUTINE RXMIT(PWI,PWT,K,NORM,P1,TABLE,SUPPRS,BETA)                    1
      COMPLEX PWI(3),PWT(3),EZPER,EZPAR                                        2
      COMPLEX EXPAR,EYPAR,EXPER,EYPER,TPARI,TPERI,DOT,RPERI,RPARI              3
      REAL K(3),NORM(3),KPER(3),P1(3),AMP(4),PHS(4),KPAR(3)                    4
      LOGICAL TABLE,SUPPRS,AIR                                                 5
      COMPLEX TPER(250),TPAR(250),RPER,RPAR                                    6
      COMMON/TRANSC/DIN(6),ER(6),TO(6),TZ,WALTOL,N,NN,D(6),ZB,TK               7
      DATA PI/3.14159265/                                                      8
      DATA NANGLE/250/                                                         9
      DATA NDO/0/                                                             10
      IF (NDO.EQ.1) GO TO 5                                                   11
      NDO=1                                                                   12
      AIR=.FALSE.                                                             13
      IF (ER(1).LT.1.05) AIR=.TRUE.                                           14
      DO 90 I=1,NN                                                            15
   90 D(I)=DIN(I)*2.54                                                        16
      PIO2=PI/2.                                                              17
C                                                                             18
C   FORM WALL TRANSMISSION TABLES                                             19
C                                                                             20
      MANGLE=NANGLE-1                                                         21
      ANGLE=MANGLE                                                            22
      RAD=180./PI                                                             23
      IF (.NOT.SUPPRS) WRITE(6,115)                                           24
  115 FORMAT(/" ANGLE",7X,"TPERI**2",8X,"TPARI**2",8X,                        25
     $ "RPERI**2",8X,"RPARI**2"//)                                            26
  116 FORMAT(1X,F5.2,4(3X,F5.3,F8.1))                                         27
      DO 100 I=1,MANGLE                                                       28
      SINE=(I-1)/ANGLE                                                        29
      IF (AIR) GO TO 91                                                       30
      CALL WALL(EETA,SINE,D,ER,TO,N,NN,TPER(I),TPAR(I),RPER,RPAR)             31
      GO TO 92                                                                32
   91 TPER(I)=(1.,0.)                                                         33
      TPAR(I)=(1.,0.)                                                         34
      RPER=(0.,0.)                                                            35
      RPAR=(0.,0.)                                                            36
   92 IF (MOD(I,5).NE.0) GO TO 100                                            37
      ANG=ASIN(SINE)*RAD                                                      38
```

```
      CALL AMPHS(TPER(I),AMP(1),PHS(1))                                    39
      CALL AMPHS(TPAR(I),AMP(2),PHS(2))                                    40
      CALL AMPHS(RPER,AMP(3),PHS(3))                                       41
      CALL AMPHS(RPAR,AMP(4),PHS(4))                                       42
C CONVERT TO POWER XMN COEFFICIENTS                                        43
      DO 95 L=1,4                                                          44
   95 AMP(L)=AMP(L)**2                                                     45
      IF (.NOT.SUPPRS) WRITE(6,116) ANG,((AMP(J),PHS(J)),J=1,4)            46
  100 CONTINUE                                                             47
      XC=0.                                                                48
      IF (ER(1).LT.1.05) XC=1.0                                            49
      TPER(NANGLE)=CMPLX(XC,0.)                                            50
      TPAR(NANGLE)=CMPLX(XC,0.)                                            51
      ANG=90.                                                              52
      CALL AMPHS(TPER(NANGLE),AMP(1),PHS(1))                               53
      CALL AMPHS(TPAR(NANGLE),AMP(2),PHS(2))                               54
      CALL AMPHS(RPER,AMP(3),PHS(3))                                       55
      CALL AMPHS(RPAR,AMP(4),PHS(4))                                       56
      IF (.NOT.SUPPRS) WRITE(6,116) ANG,((AMP(J),PHS(J)),J=1,4)            57
      IF (.NOT.SUPPRS) WRITE(6,105)                                        58
  105 FORMAT(//" TABLE OF XMN COEF. IS FORMED"//)                          59
    5 CONTINUE                                                             60
C                                                                          61
C   FIND VECTOR NORMAL TO NORM AND K                                       62
C                                                                          63
      CALL AXB(K,NORM,KPER)                                                64
C                                                                          65
C   FIND MAGNITUE OF KPER (THIS IS ALSO THE SINE OF THE INCLUDED ANGLE)    66
C                                                                          67
      SINE=SQRT(KPER(1)*KPER(1)+KPER(2)*KPER(2)+KPER(3)*KPER(3))           68
      IF(SINE.GT.1.0) SINE = 1.0                                           69
      IF(TABLE) GO TO 25                                                   70
      TPERI=(1.,0.)                                                        71
      TPARI=(1.,0.)                                                        72
      RPERI=(0.,0.)                                                        73
      RPARI=(0.,0.)                                                        74
      GO TO 3                                                              75
C                                                                          76
```

```
C   USE TABLE OF TRANSMISSION COEFFICIENTS                              77
C                                                                       78
   25 RI=SINE*MANGLE+1.0                                                79
      IL=RI                                                             80
      IF((IL.GE.NANGLE).OR.(IL.LT.1)) GO TO 50                          81
      IH=IL+1                                                           82
      X=RI-IL                                                           83
      TPERI=(1.0-X)*TPER(IL)+X*TPER(IH)                                 84
      TPARI=(1.0-X)*TPAR(IL)+X*TPAR(IH)                                 85
C                                                                       86
C   TEST FOR NORMAL INCIDENCE                                           87
C                                                                       88
    3 IF(SINE.LT.1E-10) GO TO 2                                         89
C                                                                       90
C   UNITIZE PERPENDICULAR VECTOR                                        91
C                                                                       92
      SEC=1/SINE                                                        93
      KPER(1)=KPER(1)*SEC                                               94
      KPER(2)=KPER(2)*SEC                                               95
      KPER(3)=KPER(3)*SEC                                               96
      GO TO 1                                                           97
    2 KPER(1)=1.0                                                       98
      KPER(2)=0.0                                                       99
      KPER(3)=0.0                                                      100
    1 CONTINUE                                                         101
C                                                                      102
C   FIND DOT PRODUCT OF INCIDENT ELECTRIC FIELD WITH KPER              103
C                                                                      104
      DOT=PWI(1)*KPER(1)+PWI(2)*KPER(2)+PWI(3)*KPER(3)                 105
C                                                                      106
C   FIND PERPENDICULAR COMPONENTS OF ELECTRC FIELD                     107
C                                                                      108
      EXPER=DOT*KPER(1)                                                109
      EYPER=DOT*KPER(2)                                                110
      EZPER=DOT*KPER(3)                                                111
C                                                                      112
C   FIND PARALLEL COMPONENTS OF ELECTRIC FIELD                         113
C                                                                      114
```

```
C      EXPAR=PWI(1)-EXPER                                                115
C      EYPAR=PWI(2)-EYPER                                                116
C      EZPAR=PWI(3)-EZPER                                                117
       CALL AXB(KPER,K,KPAR)                                             118
C   KPAR IS A UNIT VECTOR AS REQUIRED                                    119
       DOT=PWI(1)*KPAR(1)+PWI(2)*KPAR(2)+PWI(3)*KPAR(3)                  120
       EXPAR=DOT*KPAR(1)                                                 121
       EYPAR=DOT*KPAR(2)                                                 122
       EZPAR=DOT*KPAR(3)                                                 123
C                                                                        124
C    FIND X AND Y COMPONENTS OF TRANSMITTED FIELD                        125
C                                                                        126
       PWT(1)=EXPAR*TPARI+EXPER*TPERI                                    127
       PWT(2)=EYPAR*TPARI+EYPER*TPERI                                    128
       PWT(3)=EZPAR*TPARI+EZPER*TPERI                                    129
       RETURN                                                            130
   50  WRITE(6,55) SINE                                                  131
   55  FORMAT(/10X,"SINE="F10.7," IS NOT IN THE WALL TABLE "/)           132
       TPERI=(1.,0.)                                                     133
       TPARI=(1.,0.)                                                     134
       GO TO 3                                                           135
       END                                                               136
```

Chapter 11

SUBROUTINE WALL

11-1. Purpose: To compute the transmission and reflection coefficients of a N-layer dielectric sheet having thicknesses d_n, dielectric constants ε_{rn}, and loss tangents $\tan\delta_n$ for each layer when a plane wave is incident at angle θ_i.

11-2. Usage: CALL WALL (BETA, SINE, D, ER, TD, N, NN, TPER, TPAR, RPER, RPAR)

11-3. Arguments

BETA - Real input variable = $2\pi/\lambda$, where λ is the free space wavelength.

SINE - Real input variable = $\sin\theta_i$.

D, ER, TD - Real input arrays containing the thickness (cm), dielectric constant ε_r, and loss tangent $\tan\delta$ of each layer.

N - Integer input variable equal to the number of layers.

NN - Integer input = N+1.

TPER,TPAR - Complex output variables equal to the insertion voltage transmission coefficients for the components of the incident electric field perpendicular to and parallel to the plane of incidence, respectively.

RPER,RPAR - Complex output variables equal to the reflection coefficients $R_\perp$, $R_\parallel$.

11-4. Comment and Method

a. Layer 1 is the first layer on the exit side of the panel; layer N is the first layer on the incident side. $T_{\perp}$, $T_{\parallel}$ have the same value for either side of the panel being the incident side; however, $R_{\perp}$, $R_{\parallel}$ are different (in phase) for the two cases.

b. The details of the method are presented in Reference 1 and are reproduced in Appendix E.

11-5. Program Flow: See Reference 1.

11-6. Test Case: See Chapter 2.

11-7. References

1. E. B. Joy and G. K. Huddleston, "Radome Effects on the Performance of Ground Mapping Radar," Technical Report, Contract DAAH01-72-C-0598, U. S. Army Missile Command, March 1973.

11-8. Program Listing: See following pages.

```
      SUBROUTINE WALL(BETA,SINE,D,ER,TD,N,NN,TPER,TPAR,RPER,RPAR)
C   SUBROUTINE WALL COMPUTES THE TRANSMISSION AND REFLECTION
C   COEFFICIENTS FOR AN N LAYER, PLANE DIELECTRIC PANEL FOR PLANE
C   WAVE INCIDENT AT SINE(ANGLE) FOR PERPENDICULAR AND
C   PARALLEL POLARIZATIONS.
C   PARAMETERS OF THE WALL: N= THE NUMBER OF LAYERS
C                           NN= N+1 REQUIRED TO DIMENSION ARRAYS
C                           D= THICKNESS OF EACH LAYER IN CENTIMETERS
C                           ER= RELATIVE DIELECTRIC CONSTANT OF EACH LAY
C                           TD= THE LOSS TANGENT FOR EACH LAYER
C TN1,TN2 ARE THE NORMAL VOLTAGE XMN COEFFICIENTS; TPER,TPAR ARE THE
C INSERTION VOLTAGE TRANSMISSION COEFFICIENTS. IT IS IMPORTANT TO
C NOTE THAT THE XMN COEFS ARE THE SAME FOR PLANE WAVE INCIDENT FROM
C EITHER SIDE OF THE STRATIFIED DIELECTRIC PANEL IMMERSED IN FREE SPACE:
C HOWEVER, THE REFLECTION COEFS ARE NOT. THAT IS, FOR COMPUTING RPER,
C RPAR, THE ORDERING OF ER(NN),TD(NN) IS IMPORTANT WITH LAYER 1 BEING
C THE FIRST LAYER ON THE EXIT SIDE, LAYER N BEING THE FIRST LAYER ON THE
C INCIDENT SIDE.  LAYER NN  AND  LAYER 0  ARE JUST FREE SPACE  LAYERS
C OF SEMI-INFINITE DEPTH.
C E,G,R1,R2, ARE ARRAYS USED IN THE SUBROUTINE HAVING NN DIM'L LIMITS
      COMPLEX E(6),G(6),R1(6),R2(6),GG,EE,RR1,RR2,AA1,AA2,X1,X2,
     $X3,X4,Y1,Y2,Y3,Y4,U1,U2,U3,U4,V1,V2,V3,V4,P1,P2,P3,P4,Q1,Q2,Q3,Q4
      COMPLEX TPER,TPAR,RPER,RPAR,U,V,TN1,TN2
      DIMENSION ER(NN),TD(NN),D(N)
      ER(NN)=1.0
      TD(NN)=0.
      DO 50 I=1,NN
   50 E(I)=CMPLX(ER(I),-ER(I)*TD(I))
      AB=BETA*0.707070707071
C
C   CALCULATE TOTAL THICKNESS OF WALL IN CM
C
      DTOTAL=0.0
      DO 200 I=1,N
  200 DTOTAL=DTOTAL+D(I)
C   S IS THE SINE OF THE ANGLE SQUARED
C   C IS THE COSINE OF THE ANGLE
      S=SINE*SINE
```

```
      C=SQRT(1.0-S)                                                          39
      AD=ER(1)-S                                                             40
      ET=ER(1)*TD(1)                                                         41
      SR=SQRT(AD*AD+ET*ET)                                                   42
      IF(SR-AD) 76,76,77                                                     43
   76 A=0.                                                                   44
      GO TO 78                                                               45
   77 A=AB*SQRT(SR-AD)                                                       46
   78 B=AB*SQRT(SR+AD)                                                       47
      G(1)=CMPLX(A,B)                                                        48
      GG=CMPLX(0.0,BETA*C)                                                   49
      EE=1.0                                                                 50
      SUM=0.                                                                 51
      SUM=SUM+D(1)/SQRT(AD)                                                  52
      RR1=(G(1)-GG)/(G(1)+GG)                                                53
      RR2=(EE*G(1)-E(1)*GG)/(EE*G(1)+E(1)*GG)                                54
      DO 84 I=1,N                                                            55
      II=I+1                                                                 56
      AD=ER(II)-S                                                            57
      ET=ER(II)*TD(II)                                                       58
      IF (I-N) 176,177,177                                                   59
  176 SUM=SUM+D(II)/SQRT(AD)                                                 60
  177 CONTINUE                                                               61
      SR=SQRT(AD*AD+ET*ET)                                                   62
      IF(SR-AD) 79,79,80                                                     63
   79 A=0.                                                                   64
      GO TO 81                                                               65
   80 A=AB*SQRT(SR-AD)                                                       66
   81 B=AB*SQRT(SR+AD)                                                       67
      G(II)=CMPLX(A,B)                                                       68
      R1(I)=(G(II)-G(I))/(G(II)+G(I))                                        69
   84 R2(I)=(E(I)*G(II)-E(II)*G(I))/(E(I)*G(II)+E(II)*G(I))                  70
      SUM=S*SUM                                                              71
      AA1=1.0-RR1                                                            72
      AA2=1.0-RR2                                                            73
      DO 85 I=1,N                                                            74
      AA1=AA1*(1.0-R1(I))                                                    75
   85 AA2=AA2*(1.0-R2(I))                                                    76
```

```
      AA1=1.0/ AA1                                                      77
      AA2=1.0/ AA2                                                      78
      U=-G(1)*D(1)                                                      79
      V=G(1)*D(1)                                                       80
      X1=CEXP(U)                                                        81
      X4=CEXP(V)                                                        82
      X2=-RR1*X4                                                        83
      X3=-RR1*X1                                                        84
      Y1=X1                                                             85
      Y4=X4                                                             86
      Y2=-RR2*Y4                                                        87
      Y3=-RR2*Y1                                                        88
      DO 105 I=2,NN                                                     89
      IF(I-NN) 95,90,1                                                  90
   90 U1=1.0                                                            91
      U2=-R1(N)                                                         92
      U3=-R1(N)                                                         93
      U4=1.0                                                            94
      V1=1.0                                                            95
      V2=-R2(N)                                                         96
      V3=-R2(N)                                                         97
      V4=1.0                                                            98
      GO TO 100                                                         99
   95 II=I-1                                                           100
      U=-G(I)*D(I)                                                     101
      V=G(I)*D(I)                                                      102
      U1=CEXP(U)                                                       103
      U4=CEXP(V)                                                       104
      U2=-R1(II)*U4                                                    105
      U3=-R1(II)*U1                                                    106
      V1=U1                                                            107
      V4=U4                                                            108
      V2=-R2(II)*V4                                                    109
      V3=-R2(II)*V1                                                    110
  100 P1=X1*U1+X2*U3                                                   111
      P2=X1*U2+X2*U4                                                   112
      P3=X3*U1+X4*U3                                                   113
      P4=X3*U2+X4*U4                                                   114
```

```
      Q1=Y1*V1+Y2*V3                                                    115
      Q2=Y1*V2+Y2*V4                                                    116
      Q3=Y3*V1+Y4*V3                                                    117
      Q4=Y3*V2+Y4*V4                                                    118
      X1=P1                                                             119
      X2=P2                                                             120
      X3=P3                                                             121
      X4=P4                                                             122
      Y1=Q1                                                             123
      Y2=Q2                                                             124
      Y3=Q3                                                             125
  105 Y4=Q4                                                             126
      RPER=-X3/X4                                                       127
C     TN1,TN2 ARE NORMAL VOLTAGE XMN COEFFICIENTS.                      128
      RPAR=-Y3/Y4                                                       129
      TN1=(X1+X2*RPER)*AA1                                              130
      U=CMPLX(0.0,-SUM*BETA)                                            131
      U=CEXP(U)                                                         132
C     TPER,TPAR HERE ARE VOLTAGE XMN COEFFICIENTS AT EXIT POINT OF RAY. 133
      TPER=TN1*U                                                        134
      TN2=(Y1+Y2*RPAR)*AA2                                              135
      TPAR=TN2*U                                                        136
C     MODIFY TRANSMISSION COEFFICIENTS FOR INSERTION                    137
      U=CMPLX(0.0,BETA*OTOTAL*C)                                        138
      U=CEXP(U)                                                         139
      TPER=TN1*U                                                        140
      TPAR=TN2*U                                                        141
    1 CONTINUE                                                          142
  300 RETURN                                                            143
      END                                                               144
```

Chapter 12

SUBROUTINE AXB

12-1. Purpose: To compute the real vector cross product $\underline{C} = \underline{A} \times \underline{B}$, where $\underline{A}$, $\underline{B}$, $\underline{C}$ are expressed in rectangular components.

12-2. Usage: CALL AXB(A, B, C)

12-3. Arguments

A, B - Real input arrays containing the rectangular components of $\underline{A} = \hat{x}\, A_x + \hat{y}\, A_y + \hat{z}\, A_z$ and $\underline{B}$; i.e., $A(A_x, A_y, A_z)$, $B(B_x, B_y, B_z)$.

C - Real output array containing the rectangular components of the vector $\underline{C} = \underline{A} \times \underline{B}$; i.e., $C(C_x, C_y, C_z)$.

12-4. Comment and Method

a. Both input vectors must be real.

b. The computation of $\underline{C} = \underline{A} \times \underline{B}$ is elementary.

12-5. Program Flow: See listing below.

12-6. Test Case: None

12-7. References: None

12-8. Program Listing: See following page.

```
      SUBROUTINE AXB(A,B,C)                                              1
C     COMPUTE VECTOR CROSS PRODUCT OF A CROSS B, RESULTING IN C          2
      DIMENSION A(3),B(3),C(3)                                           3
      C(1)=A(2)*B(3)-A(3)*B(2)                                           4
      C(2)=A(3)*B(1)-A(1)*B(3)                                           5
      C(3)=A(1)*B(2)-A(2)*B(1)                                           6
      RETURN                                                             7
      END                                                                8
```

Chapter 13

SUBROUTINE CAXB

13-1. Purpose: To compute the complex vector cross product $\underline{C} = \underline{A} \times \underline{B}$, where $\underline{A}$ is a complex vector and $\underline{B}$ is a real vector expressed in rectangular coordinates.

13-2. Usage: CALL CAXB (A, B, C)

13-3. Arguments

A - Complex input array containing the rectangular components of the vector $\underline{A} = \hat{x} A_x + \hat{y} A_y + \hat{z} A_z$; i.e., A ($A_x$, A_y, A_z).

B - Real input array B (B_x, B_y, B_z) representing the vector $\underline{B}$.

C - Complex output array C (C_x, C_y, C_z) representing the vector $\underline{C} = \underline{A} \times \underline{B}$.

13-4. Comment and Method: None

13-5. Program Flow: See listing below.

13-6. Test Case: None

13-7. References: None

13-8. Program Listing: See following page.

```
      SUBROUTINE CAXB(A,B,C)                                            1
C     CAXB COMPUTES VECTOR CROSS PRODUCT AXB=C, WHERE A AND C           2
C     ARE COMPLEX AND B IS REAL.                                        3
      COMPLEX A(3),C(3)                                                 4
      REAL B(3)                                                         5
      C(1)=A(2)*B(3)-A(3)*B(2)                                          6
      C(2)=A(3)*B(1)-A(1)*B(3)                                          7
      C(3)=A(1)*B(2)-A(2)*B(1)                                          8
      RETURN                                                            9
      END                                                              10
```

Chapter 14

SUBROUTINE RECBS

14-1. Purpose: To compute the angle of arrival $\hat{k}$ of a plane wave on a monopulse antenna which yields an electrical boresight indication which, due to the radome, may be different from the mechanical boresight along the z axis of the antenna. The antenna aperture lies in the xy plane. All dimensions are in centimeters. Antenna coordinates are implied.

14-2. Usage: CALL RECBS (SUMX, SUMY, DELX, DELY, DAZX, DAZY, NX, NY, LMAX, NS, IOPT, VR, DMRAD, ROTATE, TRANSL, FGHZ, KXMAX, KYMAX, TABLE, SINOS, K, AZTM, ELTM, RSQMAX, VMAX, SMAX, SUPPRS)

14-3. Arguments

SUMX, SUMY, DELX, DELY, DAZX, DAZY - Complex input arrays of NX by NY elements each containing the aperture distributions of the monopulse antenna. See Subroutine HACNF.

LMAX - Integer input variable which controls the maximum number of iterations that will be done to find the electrical boresight within the tolerance specified by DMRAD.

NS - Inactive integer variable.

IOPT - Integer input variable which selects the polarization of the incident plane wave. See Subroutine INCPW.

VR - Complex array of three elements representing the received voltage on the sum, elevation difference,

and azimuth difference channels of the antenna, respectively (output).

DMRAD - Real input variable equal to the tolerance to which the electrical boresight in milliradians is to be computed; i.e., 0.1 milliradian.

ROTATE, - Variables required by Subroutine RECM.

TRANSL, See Chapter 8.

FGHZ,

KXMAX,

KYMAX,

TABLE

SINOS - Real variable equal to the sine of the angle θ_{os} (measured from the z-axis) in the $\phi = 45°$ plane (ϕ measured from +x toward +y) at which the first target return arrives; e.g., $\theta_{os} = 3$ degrees.

K - Real output array containing the direction of arrival of the final target return; i.e., $K(k_x, k_y, k_z)$.

AZTM, - Real output variables equal to angles (mrad) in

ELTM the azimuth and elevation planes of the antenna which specify the direction of arrival of the final target return. If $\hat{k}$ is the unit vector pointing from the origin in the direction of the final return, then the orthographic projection of this vector onto the xz-plane makes an angle AZTM with the z-axis; its projection onto the yz-plane makes an angle ELTM with the z-axis.

RSQMAX - Real variable needed by Subroutine RECM. See Chapter 8.

VMAX - Unused.

SMAX - Real output variable equal to the magnitude of the received sum voltage for the final return; used to compute loss in antenna gain.

SUPPRS - Logical input variable which controls the computation and printing of additional antenna outputs around the boresight direction. If TRUE, the complex voltage outputs of the difference channels will be computed at one milliradian increments over the range ±3.0 mrad, centered on the direction of the final target return.

14-4. Comments and Method

a. Subroutines required: AMPHS, RECM, INCPW.

b. Subroutine RECBS uses a linear tracking model to determine the direction of arrival $\hat{k} = \hat{x}\, k_x + \hat{y}\, k_y + \hat{x}\, k_z$ of a plane wave which will produce null indications in the elevation and azimuth difference channels of the monopulse antenna inside the radome. Subroutine RECM is used to compute the received voltage on each channel for the specified polarization (IOPT) and direction of arrival.

The first target return is made to arrive from the direction

$$\hat{k}_1 = \hat{x} \sin\theta_{os} + \hat{y} \sin\theta_{os} + \hat{z}\sqrt{1-2\sin^2\theta_{os}} \qquad (1)$$

to produce outputs

$$U_{AZ1} = \text{Im} \left\{ \frac{V_{\Delta AZ}}{V_{\Sigma}} \right\} \tag{2a}$$

$$U_{EL1} = \text{Im} \left\{ \frac{V_{\Delta EL}}{V_{\Sigma}} \right\} \tag{2b}$$

where V_{Σ}, $V_{\Delta EL}$, $V_{\Delta AZ}$ are the complex voltage outputs of the three-channel outputs of the three-channel antenna. The second return is made to arrive from

$$\hat{k}_A = \hat{x}(-\sin\theta_{os}) + \hat{y}(-\sin\theta_{os}) + \hat{z}\sqrt{1-2\sin^2\theta_{os}} \tag{3}$$

to produce outputs U_{AZ2}, U_{EL2}.

Construct a linear model for each channel independently using the slope/intercept equation for a line; i.e.,

$$U_{AZ} = M_{AZ}\, k_x + b_{AZ} \tag{4a}$$

$$U_{EL} = M_{EL}\, k_y + b_{EL} \tag{4b}$$

where

$$M_{AZ} = (U_{AZ1} - U_{AZ2})/\,(k_{x1} - k_{x2}) \tag{5a}$$

$$M_{EL} = (U_{EL1} - U_{EL2})/(k_{y1} - k_{y2}) \tag{5b}$$

$$b_{AZ} = U_{AZ1} - M_{AZ}\, k_{x1} \tag{6a}$$

$$b_{EL} = U_{EL1} - M_{EL}\, k_{y1} \tag{6b}$$

Use this model to estimate the values of k_x, k_y that will make $U_{AZ} = U_{EL} = 0$; i.e.,

$$k_x = - b_{AZ}/M_{AZ} \tag{7a}$$

$$k_y = - b_{EL}/M_{EL} \tag{7b}$$

where the value of k_z follows from

$$k_x^2 + k_y^2 + k_z^2 = 1 \tag{8}$$

The third target return is made to arrive from this direction and the values of U_{AZ}, U_{EL} are computed via Subroutine RECM. Now, according to the last linear model, a value of U_{AZ} within the range

$$|U_{AZ}| < |M_{AZ} \sin\theta_{tol} + b_{AZ}| \tag{9}$$

would indicate that the null has been found within the tolerance θ_{tol} (=DMRAD) specified. If this tolerance is not satisfied for both channels, then the process is repeated until it is or until LMAX is exceeded. In continuing the iterations, $\hat{k}_2$ becomes $\hat{k}$, and the estimated point becomes $\hat{k}_2$.

On the last return, the direction of arrival in specified by $\hat{k}$. The angles in the azimuth and elevation planes are given in milliradians by

$$AZTM = \sin^{-1}\left(\frac{k_x}{1-k_y^2}\right) \cdot 1000 \tag{10}$$

$$ELTM = \sin^{-1}\left(\frac{k_y}{1-k_x^2}\right) \cdot 1000 \qquad (10b)$$

The monopulse error slopes, M_{AZ}, M_{EL}, are also computed in volts/degree according to

$$MESAZ = M_{AZ}/57.3 \qquad (11a)$$

$$MESEL = M_{EL}/57.3 \qquad (11b)$$

where the maximum amplitude SMAX received on the sum channel is assumed to be one volt for normalization purposes.

If SUPPRS = .FALSE., additional outputs around the boresight direction $\hat{k}$ are computed. The directions are specified by the angle θ

$$\hat{k}_1 = \hat{x}\,(\sin\theta + k_x) + \hat{y}(\sin\theta + k_y) + \hat{z}\,k_z \qquad (12)$$

where θ varies over the range ±3 mrad. At each direction, the monopulse outputs U_{AZ}, U_{EL} are printed as well as the complex monopulse tracking functions shown in the brackets of Equations (2). It is noteworthy that the phase of the tracking function will change from ~-90° to ~+90° as the angle θ in Equation (12) goes from negative to positive values. This behavior is a consequence of the phasing chosen for the aperture distributions for the difference channels in Subroutine HACNF.

14-5. Program Flow

Line Nos.	Comments
Lines 11-15:	Initialize variables. Convert DMRAD to radians and compute sine.

Lines 16-30: Compute first two target returns to construct linear tracking model.

Lines 31-38: Compute slopes M_{AZ} = SLPAZ, M_{EL} = SLPEL from first two returns.

Line 39: Iterate on linear model up to LMAX times.

Lines 43-44: If the increment in Δk is larger than sin(DMRAD/1000), then use it to compute slopes; if not, use the last computed values of slopes to avoid division by too small a number.

Lines 45-46: Compute intercepts b_{AZ}, b_{EL}.

Lines 47-48: Compute accuracy criteria based on current slopes and intercepts.

Lines 49-51: Compute direction $\hat{k}$ that the model indicated will produce nulls $U_{AZ} \approx 0$, $U_{EL} \approx 0$ in both planes.

Lines 52-56: Compute U_{EL}, U_{AZ} for this direction $\hat{k}$.

Lines 57-92: Update the linear tracking model by storing the last two points in each channel as U(1), U(2); e.g., $U_{AZ}(1) = U_{AZ}(2)$ and $U_{AZ}(2) = U_{AZ}$, $K_1(1) = K_2(1)$ and $K_2(1) = K(1)$, etc.

Line 93: At least three iterations are always used.

Lines 94-95: If U_{AZ}, U_{EL} are within error bounds, exit the loop; if not, continue to iterate.

Lines 96-97: If LMAX exceeded, inform the user.

Line 98: Compute amplitude SMAX on sum channel for final target return.

Lines 99-100: Compute slopes for final return.

Lines 101-102: Compute boresight error AZTM, ELTM.

Lines 103-104: Compute k_z for $\hat{k}_1$ and $\hat{k}_2$.

Lines 105-108: Convert slopes to volts/degree.

Lines 109-117: If SUPPRS = .FALSE, print results.

Lines 118-139: Compute and print additional outputs around the boresight direction $\hat{k}$.

Lines 140-144: Compute and print the slopes of a linear tracking model based on the points at +3 mrad and -3 mrad (hence, the division by .006 = 6 mrad).

Line 145: RETURN

Line 146: END

14-6. Test Case: See Chapter 2.

14-7. References: None.

```
      SUBROUTINE RECBS(SUMX,SUMY,DELX,DELY,DAZX,DAZY,NX,                 1
     $NY,LMAX,NS,IOPT,VR,DMRAD,ROTATE,TRANSL,FGHZ,KXMAX,KYMAX,           2
     $ TABLE,SINCS,K,AZTM,ELTM,RSQMAX,VMAX,SMAX,SUPPRS)                  3
C DMRAD IS THE DESIRED ACCURACY OF BORESIGHT DATA (INPUT IN MRAD)        4
      COMPLEX SUMX(NX,NY),SUMY(NX,NY),DELX(NX,NY),DELY(NX,NY)            5
      COMPLEX DAZX(NX,NY),DAZY(NX,NY),VR(3)                              6
      COMPLEX EINC(3)                                                    7
      REAL ROTATE(3,3),TRANSL(3),KXMAX,KYMAX                             8
      REAL K1(3),K2(3),UAZ(2),UEL(2),K(3)                                9
      LOGICAL TABLE,SUPPPS                                              10
      DRAD=DMRAD/1000.                                                  11
      SDRAD=SIN(DRAD)                                                   12
      SINOFF=0.                                                         13
      SALFA=0.                                                          14
      AMUL=1                                                            15
      DO 70 J=1,2                                                       16
      IF (J.EQ.2) AMUL=-1.                                              17
      K2(1)=SINOS*AMUL                                                  18
      K2(2)=SINOS*AMUL                                                  19
C  COMPUTE UAZ,UEL AT K2:                                               20
      K2(3)=SQRT(1.-K2(1)**2-K2(2)**2)                                  21
      CALL INCPW(K2,EINC,IOPT)                                          22
      CALL RECM(EINC,K2,NX,NY,KXMAX,KYMAX,FGHZ,ROTATE,TRANSL,           23
     $ SUMX,SUMY,DELX,DELY,DAZX,DAZY,VR,TABLE,SUPPRS,RSQMAX)            24
      UAZ(J)=AIMAG(VR(3)/VR(1))                                         25
      UEL(J)=AIMAG(VR(2)/VR(1))                                         26
   70 CONTINUE                                                          27
      K1(1)=SINOS                                                       28
      K1(2)=SINOS                                                       29
      K1(3)=SQRT(1.-K1(1)**2-K1(2)**2)                                  30
      LCTR=0                                                            31
C  ENSURE THAT INITIAL ESTIMATES MEET PROPER CONDITIONS:                32
C     IF ((UAZ(1).LT.0.).OR.(UAZ(2).GT.0.).OR.(UEL(1).LT.0.).OR.        33
C    $(UEL(2).GT.0.)) GO TO 101                                         34
      C=K1(1)-K2(1)                                                     35
      D=K1(2)-K2(2)                                                     36
      SLPAZ=(UAZ(1)-UAZ(2))/C                                           37
      SLPEL=(UEL(1)-UEL(2))/D                                           38
```

```
      DO 80 IP=1,LMAX                                                    39
      LCTR=LCTR+1                                                        40
C     K(1)=(K1(1)+K2(1))*0.5                                             41
C     K(2)=(K1(2)+K2(2))*0.5                                             42
      IF (ABS(C).GT.SQRAD) SLPAZ=(UAZ(1)-UAZ(2))/C                       43
      IF (ABS(D).GT.SQRAD) SLPEL=(UEL(1)-UEL(2))/D                       44
      BAZ=UAZ(1)-SLPAZ*K1(1)                                             45
      BEL=UEL(1)-SLPEL*K1(2)                                             46
      ACCAZ=ABS(SLPAZ*SQRAD+BAZ)                                         47
      ACCEL=ABS(SLPEL*SQRAD+BEL)                                         48
      K(1)=-BAZ/SLPAZ                                                    49
      K(2)=-BEL/SLPEL                                                    50
      K(3)=SQRT(1.-K(1)**2-K(2)**2)                                      51
      CALL INCPW(K,EINC,IOPT)                                            52
      CALL RECM(EINC,K,NX,NY,KXMAX,KYMAX,FGHZ,ROTATE,TRANSL,             53
     $ SUMX,SUMY,CELX,DELY,CAZX,DAZY,VR,TABLE,SUPPRS,RSQMAX)             54
      UA=AIMAG(VR(3)/VR(1))                                              55
      UE=AIMAG(VR(2)/VR(1))                                              56
      IF (IP.GT.1) GO TO 65                                              57
      IF (UA.GT.0.) GO TO 76                                             58
      UAZ(2)=UA                                                          59
      K2(1)=K(1)                                                         60
      JAZ=1                                                              61
      GO TO 77                                                           62
   76 UAZ(1)=UA                                                          63
      K1(1)=K(1)                                                         64
      JAZ=2                                                              65
   77 IF(UE.GT.0.) GO TO 78                                              66
      UEL(2)=UE                                                          67
      K2(2)=K(2)                                                         68
      JEL=1                                                              69
      GO TO 79                                                           70
   78 UEL(1)=UE                                                          71
      K1(2)=K(2)                                                         72
      JEL=2                                                              73
      GO TO 79                                                           74
   65 IF (JAZ.EQ.2) GO TO 66                                             75
      UAZ(1)=UA                                                          76
```

```
      K1(1)=K(1)                                                          77
      JAZ=2                                                               78
      GO TO 67                                                            79
   66 UAZ(2)=UA                                                           80
      K2(1)=K(1)                                                          81
      JAZ=1                                                               82
   67 IF (JEL.EQ.2) GO TO 68                                              83
      UEL(1)=UE                                                           84
      K1(2)=K(2)                                                          85
      JEL=2                                                               86
      GO TO 79                                                            87
   68 UEL(2)=UE                                                           88
      K2(2)=K(2)                                                          89
      JEL=1                                                               90
   79 C=K1(1)-K2(1)                                                       91
      D=K1(2)-K2(2)                                                       92
      IF (IP.LT.3) GO TO 80                                               93
      IF ((ABS(UA).LT.ACCAZ).AND.(ABS(UE).LT.ACCEL)) GO TO 85             94
   80 CONTINUE                                                            95
      WRITE(6,25)                                                         96
   25 FORMAT(/" LMAX EXCEEDED BEFORE ACCURACY CRITERION MET"//)           97
   85 SMAX=CABS(VP(1))                                                    98
      IF (ABS(C).GT.SORAD) SLPAZ=(UAZ(1)-UAZ(2))/C                        99
      IF (ABS(D).GT.SORAD) SLPEL=(UEL(1)-UEL(2))/D                       100
      AZTM=ASIN(K(1)/SQRT(1.-K(2)**2))*1000.                             101
      ELTM=ASIN(K(2)/SQRT(1.-K(1)**2))*1000.                             102
      K1(3)=SQRT(1.-K1(1)**2-K1(2)**2)                                   103
      K2(3)=SQRT(1.-K2(1)**2-K2(2)**2)                                   104
C  CONVERT SLOPES TO VOLTS/DEG, WHERE THE SIGNAL RECEIVED BY SUM         105
C  CHANNEL IS CONSIDERED TO BE ONE VOLT:                                 106
      SLPAZ=SLPAZ/57.3                                                   107
      SLPEL=SLPEL/57.3                                                   108
      IF (SUPPRS) RETURN                                                 109
      WRITE(6,90) K1,K2,AZTM,ELTM,SLPAZ,SLPEL,UAZ,UEL,SMAX,LCTR          110
   90 FORMAT(//" FINAL ANSWERS FOR MONOPULSE SYSTEM: "//" K1: ",3E12.5/  111
     $" K2: ",3E12.5//" AZTM= ",E12.5," MRAD"/" ELTM= ",E12.5," MRAD"//  112
     $ " MESAZ= ",E12.5," VOLTS/DEG"/" MESEL= ",E12.5," VOLTS/DEG"       113
     $//" UAZ: ",2E12.5/" UEL: ",2E12.5//" SMAX= ",E21.14,               114
```

```
     $"     LCTR= ",I3//)                                                    115
      WRITE(6,98)                                                           116
   98 FORMAT(//" ADDITIONAL MONOPULSE OUTPUTS AROUND BORESIGHT: "//)        117
      DO 99 IP=1,7                                                          118
      K1(1)=SIN((-3.+IP-1)/1000.)+K(1)                                      119
      K1(2)=SIN((-3.+IP-1)/1000.)+K(2)                                      120
      ANG=-3.+IP-1                                                          121
      K1(3)=SQRT(1.-K1(1)**2-K1(2)**2)                                      122
      CALL INCPW(K1,EINC,IOPT)                                              123
      CALL RECM(EINC,K1,NX,NY,KXMAX,KYMAX,FGHZ,ROTATE,TRANSL,               124
     $ SUMX,SUMY,DELX,DELY,DAZX,DAZY,VR,TABLE,SUPPRS,RSQMAX)                125
      UAZ(1)=AIMAG(VR(3)/VR(1))                                             126
      UEL(1)=AIMAG(VR(2)/VR(1))                                             127
      IF (IP.EQ.1) SLP1=UAZ(1)                                              128
      IF (IP.EQ.1) SLP2=UEL(1)                                              129
      WRITE(6,96) ANG,UAZ(1),UEL(1)                                         130
   96 FORMAT(" ANG= ",F5.1," MRAD FROM BORESIGHT     VRAZ= ",E12.5,         131
     $" VOLTS    VREL= ",E12.5," VOLTS"/)                                   132
      VR(3)=VR(3)/VR(1)                                                     133
      VR(2)=VR(2)/VR(1)                                                     134
      CALL AMPHS(VR(3),C,D)                                                 135
      CALL AMPHS(VR(2),E,F)                                                 136
      WRITE(6,94) C,D,E,F                                                   137
   94 FORMAT(" DAZ(AMP,PHS)= ",2E12.5,"    DEL(AMP,PHS)= ",2E12.5/)       138
   99 CONTINUE                                                              139
      SLP1=(UAZ(1)-SLP1)/(.006*57.3)                                        140
      SLP2=(UEL(1)-SLP2)/(.006*57.3)                                        141
      WRITE(6,97) SLP1,SLP2                                                 142
   97 FORMAT(/" AVERAGE SLPAZ= ",E12.5," VOLTS/DEG"/                        143
     $" AVERAGE SLPEL= ",E12.5," VOLTS/DEG"/"  SUM=1.0 VOLT"//)             144
  100 RETURN                                                                145
      END                                                                   146
```

Chapter 15

SUBROUTINE RECPTN

15-1. Purpose: To compute the receiving patterns of a monopulse antenna at NREC points in a specified principal plane. A plane wave of specified polarization (ICOMP) is made to be incident on the antenna at equal increments in $\sin\theta$ over the range (-KMAX, KMAX -DK) in either the elevation plane (ICUT = 1) or azimuth plane. The received voltage in each channel is computed in the presence of the radome and stored for return to the calling program.

15-2. Usage: CALL RECPTN (SUMX, SUMY, DELX, DELY, DAZX, DAZY, NX, NY, ICUT, ICOMP, KMAX, NREC, VREC, KXMAX, KYMAX, FGHZ, ROTATE, TRANSL, TABLE, SUPPRS, RSQMAX)

15-3. Arguments

SUMX, SUMY, DELX, DELY, DAZX, DAZY,- Complex input arrays of NX by NY elements containing the aperture field distributions of the monopulse antenna. See Subroutine HACNF.

ICUT - Integer input variable which specifies the principal plane in which the pattern is computed: elevation (ICUT = 1) or azimuth (ICUT = 2).

ICOMP - Integer input variable which specifies the linear polarization of the incident plane wave: elevation component $\hat{\varepsilon}$ only (ICOMP = 1) or azimuth component $\hat{\alpha}$ only (ICOMP = 2). See Figure 15-1 for further clarification.

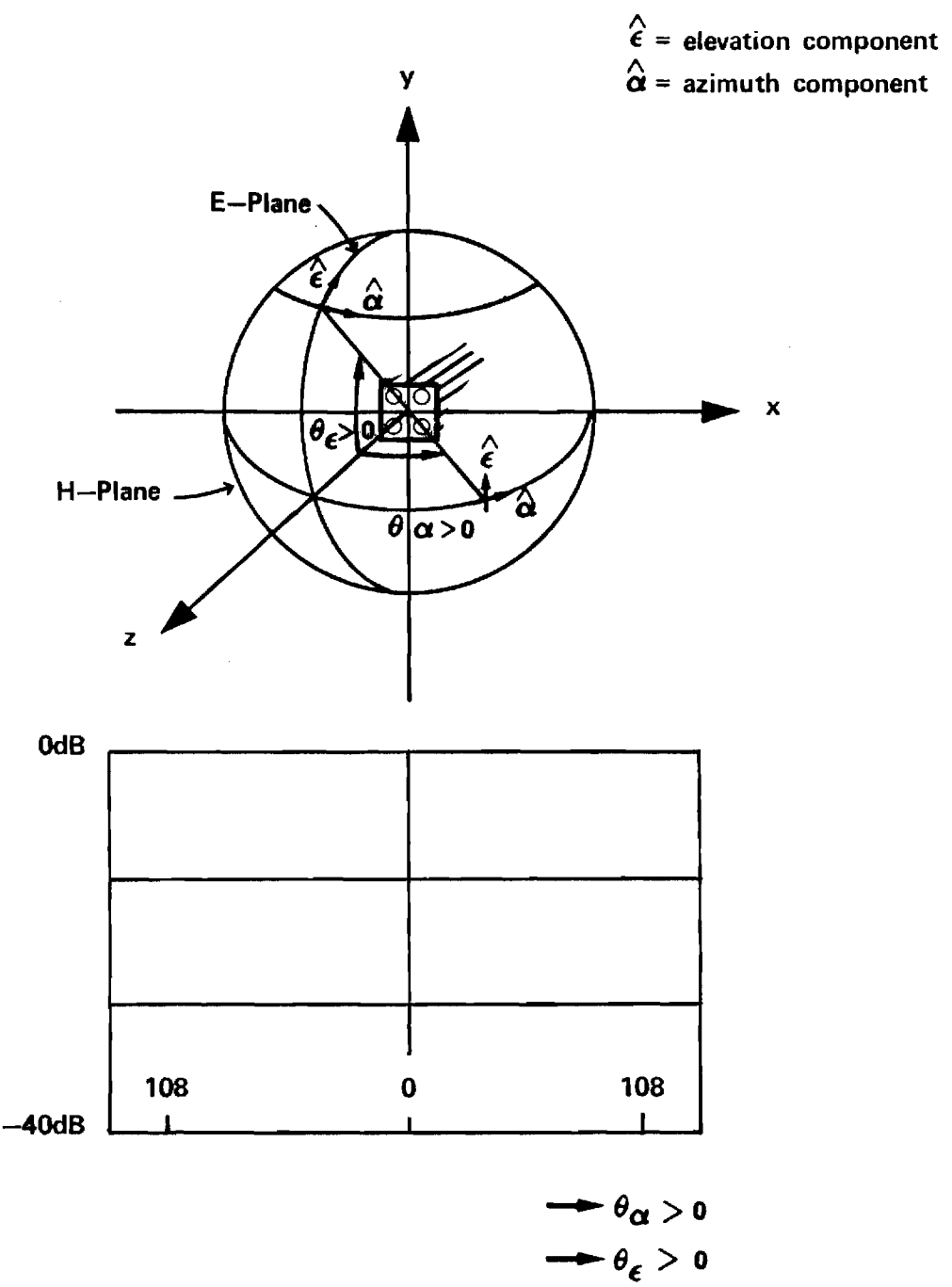

Figure 15-1 Coordinate System for Far Field Patterns

KMAX - Real input variable equal to $\sin\theta_{max}$, where the pattern is computed over the angular range $(-\theta_{max}, \theta_{max})$, but in equal increments in $\sin\theta$ so that Fourier interpolation can be applied directly in the wavenumber domain using the Fast Fourier Transform.

NREC - Integer input variable equal to the number of points at which the pattern is computed.

VREC - Complex output array of NREC by 3 elements containing the computed receiving patterns for the sum, elevation difference, and azimuth difference patterns of the monopulse antenna.

KXMAX,KYMAX,FGHZ,ROTATE TRANSL,TABLE, SUPPRS,RSQMAX - Input variables required by Subroutine RECM. See Chapter 8.

15-4. Comments and Method

Subroutines INCPW and RECM are used to compute the incident plane wave and the received voltage in each channel for each direction of arrival in the specified plane. For the elevation plane, the direction of arrival is given by

$$\hat{k} = \hat{x}\ (0) + \hat{y}\ \sin\theta + \hat{z}\sqrt{1-\sin^2\theta} \qquad (1)$$

where θ is the angle measured from the z-axis. For the azimuth plane

$$\hat{k} = \hat{x}\ \sin\theta + \hat{y}\ (0) + \hat{z}\sqrt{1-\sin^2\theta} \qquad (2)$$

The increments in angle are given by

$$\Delta k = 2\ k_{max} / N_{REC} \qquad (3)$$

Values of $k_{max}>1$ correspond to the invisible region and must be excluded from consideration.

15-5. Program Flow: Compare program listing below directly to the discussion above.

15-6. Test Case: See Chapter 2.

15-7. References: None

15-8. Program Listing: See following page.

```
      SUBROUTINE RECPTN(SUMX,SUMY,DELX,DELY,DAZX,DAZY,NX,NY,ICUT,ICOMP,
     $ KMAX,NREC,VREC,KXMAX,KYMAX,FGHZ,ROTATE,TRANSL,
     $ TABLE,SUPPRS,RSQMAX)
C SUBR RECPTN COMPUTES THE RECEIVING VOLTAGE PATTERN OF THE ANTENNA
C WHOSE TRANSMITTING NEAR FIELD ON ZA=0 PLANE IS EXT,EYT.
C RAY TRACING IS USED TO ACCOUNT FOR RADOME (SUBR RECM).
C NREC=NUMBER OF POINTS AT WHICH PATTERN IS COMPUTED
C ICUT=1 FOR EL CUT, =2 FOR AZ CUT
C ICOMP=1 FOR EL COMPONENT, =2 FOR AZ COMPONENT
C KMAX<1. SPECIFIES ANGULAR LIMITS (ANALAGOUS TO KXMAX)
      COMPLEX SUMX(NX,NY),SUMY(NX,NY),DELX(NX,NY),DELY(NX,NY)
      COMPLEX DAZX(NX,NY),DAZY(NX,NY)
      COMPLEX VREC(NREC,3),EINC(3),VR(3)
      REAL KXMAX,KYMAX,KMAX,KA(3),ROTATE(3,3),TRANSL(3)
      LOGICAL TABLE,SUPPRS
      DATA PI/3.14159265/
      ETA0=120.*PI
      IF (IABS(ICUT).GT.2) ICUT=2
      J=1
      IF (KMAX.GE.1.) KMAX=1.-2./NREC
      DK=2.*KMAX/NREC
      IF (ICUT.EQ.1) J=2
      ANGMAX=ASIN(KMAX)*180./PI
      WRITE(6,10) ICUT,ICOMP,KMAX,NREC,DK,ANGMAX
      DO 5 I=1,NREC
      KA(ICUT)=0.
      KA(J)=-KMAX+(I-1)*DK
      KA(3)=SQRT(1.-KA(J)**2)
      CALL INCPW(KA,EINC,ICOMP)
      CALL RECM(EINC,KA,NX,NY,KXMAX,KYMAX,FGHZ,ROTATE,TRANSL,
     $ SUMX,SUMY,DELX,DELY,DAZX,DAZY,VR,TABLE,SUPPRS,RSQMAX)
      VREC(I,1)=VR(1)
      VREC(I,2)=VR(2)
      VREC(I,3)=VR(3)
    5 CONTINUE
      WRITE(6,10) ICUT,ICOMP,KMAX,NREC,DK,ANGMAX
   10 FORMAT(/" RECEIVING PATTERN COMPUTED FOR: "/"   ICUT= ",I2/
     $ "  ICOMP= ",I2/"   KMAX= ",F7.3/"   NREC= ",I5/"      DK= "
```

```
$ ,E12.5/" ANGMAX= ",F6.2/" (ICUT=1 FOR EL CUT, =2 FOR AZ CUT"/          39
$ " (ICOMP=1 FOR EL COMPONENT, =2 FOR AZIMUTH) "//)                      40
 RETURN                                                                  41
 END                                                                     42
```

Chapter 16

SUBROUTINE OGIVE

16-1. Purpose: To solve for the intersection PH(x, y, z) of a line (ray) and a tangent ogive surface. The ray starts at point $PO(x_o, y_o, z_o)$ and travels in the direction $K(k_x, k_y, k_z) = \hat{k} = \hat{x}k_x + \hat{y}k_y + \hat{z}k_z$. Dimensions are in centimeters. Radome coordinates are implied.

16-2. Usage: CALL OGIVE (PO, K, PH, HIT)

COMMON/OGIVC/RP, BSQ, AP, RINV, B, RSQ1, RP2

16-3. Arguments

PO - Real input array containing the point of origin of the ray $PO(x_o, y_o, z_o)$.

K - Real input array containing the direction cosines of the ray $K(k_x, k_y, k_z)$.

PH - Real output array containing the point of intersection PH(x, y, z), if HIT = .TRUE.

HIT - Logical output variable which indicates if an intersection solution was found (TRUE).

The following variables are common with the main program and are precalculated to speed up the ray tracing computations. Refer to Figure 16-1 of the radome geometry for the definitions of R and B.

RP - Real input variable = $R^2 - B^2$.

BSQ - Real input variable = B^2.

AP - Real input variable = 0. See APIN in Section 2-4.

RINV - Real input variable = 1/R.

B - Real input variable. See Figure 16-1.

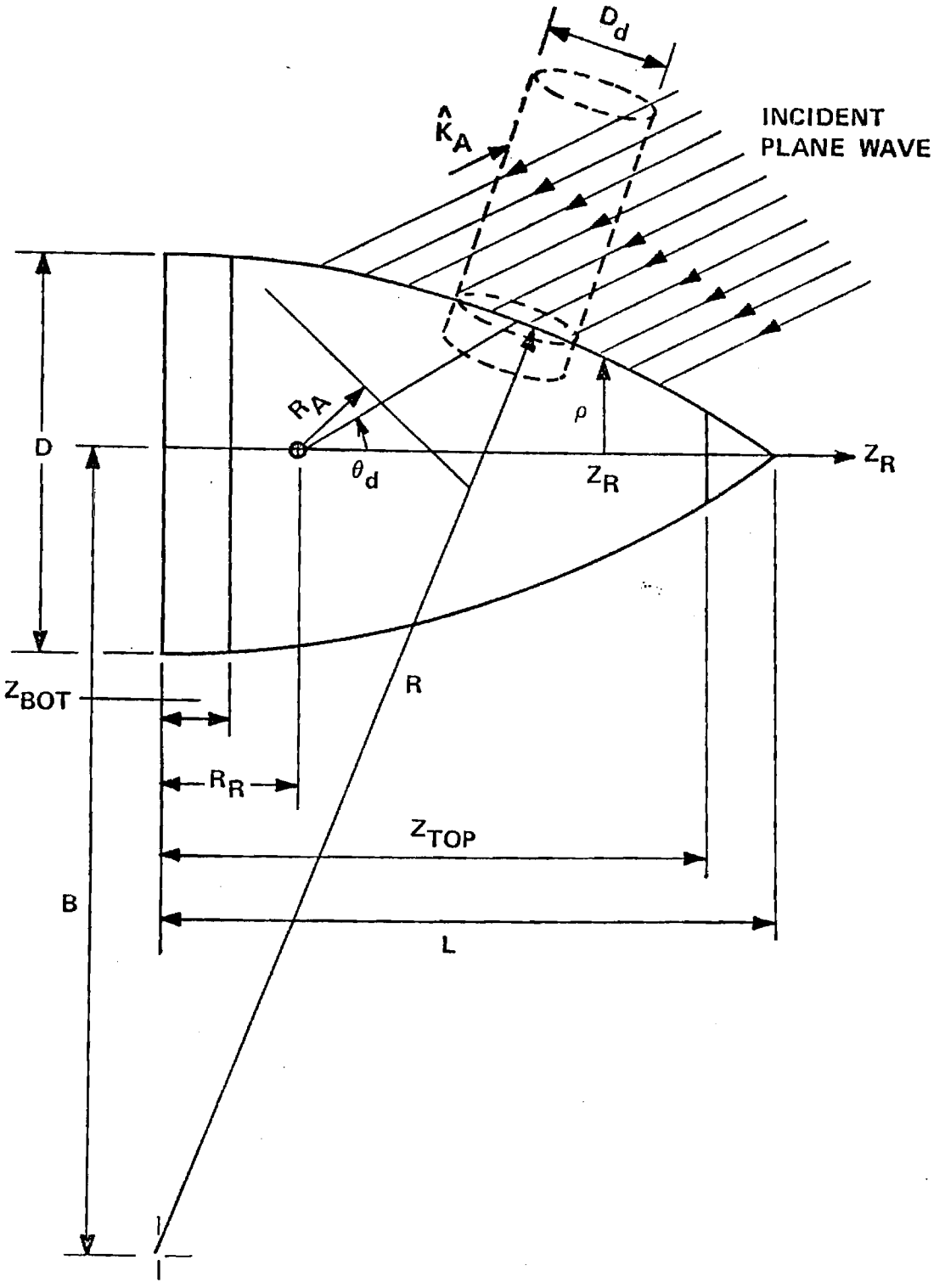

Figure 16-1. Tangent Ogive Radome Geometry.

RSQ1 - Real input variable = R^2.

RP2 - Real input variable = $R^2 + B^2$.

16-4. Comment and Method

a. The common variables must be computed in the main program prior to the first call to OGIVE.

b. Subroutines required: CBRT, SQR, XY. Real function CBRT(x) computes cube root; SQR computes square root with test for negative argument.

c. The intersection of a ray and ogive surface requires the solution of a quartic equation in the parameter z_p as follows [1]

$$z_p^4 + C_4 z_p^3 + C_3 z_p^2 + C_2 z_p + C_1 = 0 \tag{1}$$

where

$$C_4 = \frac{2(1+U)(2A+V)}{(1+U)^2} \tag{2}$$

$$C_3 = \frac{2(1+U)(-R_p+A^2+W) + (2A+V)^2 - 4B^2U}{(1+U)^2} \tag{3}$$

$$C_2 = \frac{2(2A+V)(-R_p+A^2+W) - 4B^2V}{(1+U)^2} \tag{4}$$

$$C_1 = \frac{(-R_p+A^2+W)^2 - 4B^2W}{(1+U)^2} \tag{5}$$

and where

$$U = \frac{K_1^2 + K_2^2}{K_3^2} \tag{6}$$

$$V = \frac{2(K_1P_1 + K_2P_2)}{K_3} \tag{7}$$

$$W = P_1^2 + P_2^2 \tag{8}$$

$$R_p = R^2 - B^2 \tag{9}$$

The variables R and B are defined on Figure 16-1 and by the ogive equation

$$r = \sqrt{x^2 + y^2} = \sqrt{R^2 - (z-a_p)^2} - B \tag{10}$$

where the z-axis is the axis of revolution for the ogive shape. The variable a_p provides for an offset along z of the coordinates for the ogive. Equations (1) through (9) result when the following equations for a ray (line) passing through the point $PO(x_o, y_o, z_o)$ in the direction $\hat{k} = \hat{x}k_x + \hat{y}k_y + \hat{z}k_z$ are substituted into Equation (10):

$$\frac{z - z_o}{k_z} = \frac{x - x_o}{k_x} = \frac{y - y_o}{k_y} = \text{constant} \tag{11}$$

All four roots of the quartic equation may be found from the resolvent cubic equation [2]

$$p^3 - C_3p^2 + (C_4C_2 - 4C_1)p - C_4^2C_1 + 4C_3C_1 - C_2^2 = 0 \tag{12}$$

This cubic equation has at least one real root p_o given by

$$= \left[-\frac{T}{2} + \sqrt{\frac{T^2}{4} + \frac{S^3}{27}} \right]^{1/3} + \left[-\frac{T}{2} - \sqrt{\frac{T^2}{4} + \frac{S^3}{27}} \right]^{1/3} \tag{13}$$

where

$$S = \frac{1}{3}[3(C_4C_2 - 4C_1) - C_3{}^2] \tag{14}$$

$$T = \frac{1}{27}\,[-2C_3{}^3 + 9C_3(C_4C_2 - 4C_1) + 27(-C_4{}^2C_1 + 4C_3C_1 - C_2{}^2)] \tag{15}$$

Once p_o is found, the roots of the quartic equation follow from

$$z_{p1,2} = \frac{C_3}{4} + \frac{R_1}{2} \pm \frac{D}{2} \tag{16}$$

$$z_{p3,4} = \frac{C_3}{4} - \frac{R_1}{2} \pm \frac{E}{2} \tag{17}$$

where

$$R_1 = \sqrt{\frac{C_4{}^2}{4} - C_3 + p_o} \tag{18}$$

$$D = \sqrt{\frac{3C_4{}^2}{4} - R_1{}^2 - 2C_3 + \frac{4C_4C_3 - 8C_2 - C_4{}^3}{4R_1}} \tag{19}$$

$$E = \sqrt{\frac{3C_4{}^2}{4} - R_1{}^2 - 2C_3 - \frac{4C_4C_3 - 8C_2 - C_4{}^3}{4R_1}} \tag{20}$$

The correct root z_{po} is chosen as the one with the smallest absolute value and which has the same sign as k_z. The intersection point P(x, y, z)

follows from

$$z = z_o + z_{po} \tag{21}$$

$$x = \frac{k_x}{k_z} z_{po} + x_o \tag{22}$$

$$y = \frac{k_y}{k_z} z_{po} + y_o \tag{23}$$

The rectangular components of the unit inward normal vector at P(x, y, z) are given by

$$n_x = -x \frac{B + \sqrt{x^2+y^2}}{R\sqrt{x^2+y^2}} \tag{24}$$

$$n_y = -y \frac{B + \sqrt{x^2+y^2}}{R\sqrt{x^2+y^2}} \tag{25}$$

$$n_z = -\frac{z - a_p}{R} \tag{26}$$

In the the special case of $k_z=0$, the z coordinate does not change so that

$$z = z_o \tag{27}$$

The equations of the line in the $z=z_o$ plane become

$$x = x_o + k_x t \tag{28}$$

$$y = y_o + k_y t \tag{29}$$

where the parameter t is the distance along the line from (x_o, y_o, z_o) to (x, y, z). Substituting Equations (27) - (29) into (10) yields the following quadratic equation in t

$$t^2 + 2 (k_x x_o + k_y y_o) t + (x_o^2 + y_o^2) = \left(\sqrt{R^2 - (z_o - a_p)^2} - B \right)^2 = R_s^2 \tag{30}$$

The quadratic formula yields the following solutions to the above equation

$$t_{1,2} = - (k_x x_o + k_y y_o) \pm [(k_x x_o + k_y y_o)^2 - (x_o + y_o^2) + R_s^2]^{1/2}$$

The unit normal may be computed by Equations (24) through (26).

10-5. Program Flow: See listing below and compare directly to the above equations.

10-6. Test Case: See Chapter 2.

10-7. References

1. E. B. Joy and G. K. Huddleston, "Radome Effects on the Performance of Ground Mapping Radar," Technical Report, Contract DAAH01-72-C-0598, U. S. Army Missile Command, March 1973.

2. Stegun, and Abromowitz, Handbook of Mathematical Functions, National Bureau of Standards, June 1964, p. 17.

10-8. Program Listing: See following pages.

```
      SUBROUTINE OGIVE(PO,K,PH,HIT)                                      1
      REAL SQR,A,M1,M2,U,V,W,ASQ,AINV,A0,A1,A2,A22,A44,COEF(             2
     $4)                                                                 3
C     THIS SUBROUTINE SOLVES FOR THE INTERSECTION OF A RAY AND AN OGIVE. 4
C        INPUT   PO--REAL ARRAY OF COEFFICIENTS OF INSIDE POINT          5
C                K --REALARRAY OF DIRECTION COSINES OF RAY               6
C         OUTPUT  PH--COORINATES OF THE INTERSECTION WITH THE RADOME     7
C                 HIT--=.TRUE. IF THE RAY HIT THE SURFACE                8
      REAL PO(3),PH(3),K(3)                                              9
      COMMON/OGIVC/RP,BSQ,AP,RINV,B,RSQ1,RP2                            10
      LOGICAL HIT                                                       11
      HIT=.TRUE.                                                        12
C     UNIT OF DISTANCE IS CENTIMETER                                    13
C     THE OGIVE SHAPE IS DESCRIBED BY THE EQUATION                      14
C        SQRT(X**2+Y**2)=SQRT(R**2-(Z-AP)**2)-B                         15
C     GIVEN A FINENESS RATIO ,F, AND A DIAMETER D. R AND B              16
C     MAY BE CALCULATED AS FOLLOWS.                                     17
C      R=F*D/(SIN(PI-2*ATAN(2*F))                                       18
C      B=R-D/2                                                          19
C     AP= Z COORDINATE OF THE GENERATION CENTER OF THE OGIVE            20
C         COORDINATES.                                                  21
C     THE DATA NEEDED FOR THE DATA STATEMENT IS                         22
C              RP=R**2-B**2                                             23
C              BSQ=B**2                                                 24
C              AP=AP                                                    25
C              RINV=1.0/R                                               26
C              B=B                                                      27
C              RSQ1=R**2                                                28
C              RP2=R**2+B**2                                            29
      IF(ABS(K(3)).LT.1E-7)GO TO 390                                    30
      IF(ABS(K(3)).GT.1.-1E-7) GO TO 380                                31
      A=PO(3)-AP                                                        32
      M1=1.0/K(3)                                                       33
      M2=K(2)*M1                                                        34
      M1=K(1)*M1                                                        35
      U=M1*M1+M2*M2                                                     36
      V=2.0*(M1*PO(1)+M2*PO(2))                                         37
      W=PO(1)*PO(1)+PO(2)*PO(2)                                         38
```

```
      ASQ=A*A                                                                  39
      AINV=1.0/(1.0+U*(2.0+U))                                                 40
      COEF (4)=2.0*(2.0*A+V)*(1.0+U)*AINV                                      41
      COEF(3)=(2.0*(-RP+U*(W-RP2       )+W+2.0*A*V+ASQ*(3.0+U))+V*V)*AINV      42
      COEF(2)=(4.0*A*(-RP+ASQ+W)+2.0*V*(ASQ+W-RP2         ))*AINV              43
      COEF(1)=(W*(2.0*(ASQ-RP2         )+W)+RP*(RP-2.0*ASQ)+ASQ*ASQ)*AINV      44
      A2=COEF(3)*0.3333333333                                                  45
      A1=COEF(2)*COEF(4)-4.0*COEF(1)                                           46
      A0=-COEF(2)*COEF(2)-COEF(1)*COEF(4)*COEF(4)+4.0*COEF(1)*COEF(3)          47
      A22=A2*A2                                                                48
      A44=COEF(4)*0.25                                                         49
      Q=A1*.3333333333-A22                                                     50
      R1=(-A1*COEF(3)-3.0*A0)*0.1666666667+A2*A22                              51
      RADSQ=Q**3+R1*R1                                                         52
      IF (RADSQ.LT.0.) GO TO 330                                               53
      RAD=SQR(RADSQ)                                                           54
      Y=CBRT(R1+RAD)+CBRT(R1-RAD)+A2                                           55
340   RSQ=COEF(4)*A44-COEF(3)+Y                                                56
      IF (ABS(RSQ).LT.1.0E-05) GO TO 350                                       57
      R=SQR(RSQ)                                                               58
      IF (K(3).LT.0.) GO TO 360                                                59
      Z=PO(3)-A44+(R-SQR(3.0*COEF(4)*A44-RSQ-2.0*COEF(3)+(4.0*COEF(4)*         60
     2         COEF(3)-8.0*COEF(2)-COEF(4)**3)/(4.0*R)))*0.5                   61
      CALL XY(PC,K,Z,PH)                                                       62
      RETURN                                                                   63
360   Z=PO(3)-A44-(R-SQR(3.0*COEF(4)*A44-RSQ-2.0*COEF(3)-(4.0*COEF(4)*         64
     2         COEF(3)-8.0*COEF(2)-COEF(4)**3)/(4.0*R)))*0.5                   65
      CALL XY(PC,K,Z,PH)                                                       66
      RETURN                                                                   67
330   PHI =ACOS(R1/SQR(-Q**3))                                                 68
      Y=2.0*SQR(-Q)*COS(PHI*0.3333333333)+A2                                   69
      GO TO 340                                                                70
350   IF (K(3).LT.0.0) GO TO 370                                               71
      Z=PO(3)-A44+(R-SQR(3.0*COEF(4)*A44-2.0*COEF(3)+2.0*SQR(Y*Y-              72
     2       4.0*COEF(1))))*0.5                                                73
      CALL XY(PC,K,Z,PH)                                                       74
      RETURN                                                                   75
370   Z=PO(3)-A44+(R+SQR(3.0*COEF(4)*A44-2.0*COEF(3)-2.0*SQR(Y*Y-              76
```

```
     2       4.0*COEF(1))))*0.5                                                77
             CALL XY(PO,K,Z,PH)                                                78
             RETURN                                                            79
380          Z=AP+SIGN(1.,K(3))*SQRT(RSQ1-(SQRT( (PO(1))**2+ (PO(2))**2)+      80
            $ (B))**2)                                                         81
             PH(1)=PO(1)                                                       82
             PH(2)=PO(2)                                                       83
             PH(3)=Z                                                           84
             RETURN                                                            85
390          RSQ2=SQRT(RSQ1-(PO(3)-AP)**2)-B                                   86
             RSQ2=RSQ2**2                                                      87
             RLP=-(PO(1)*K(1)+PO(2)*K(2))+SQRT((PO(1)*K(1)+PO(2)*K(2))**2-     88
            $(PO(1)**2+PO(2)**2-RSQ2))                                         89
             RLN=-(PO(1)*K(1)+PO(2)*K(2))-SQRT((PO(1)*K(1)+PO(2)*K(2))**2-     90
            $(PO(1)**2+PO(2)**2-RSQ2))                                         91
             PH(3)=PO(3)                                                       92
             IF(RLN.LT.0.) GO TO 391                                           93
             PH(1)=PO(1)+RLN*K(1)                                              94
             PH(2)=PO(2)+RLN*K(2)                                              95
             RETURN                                                            96
391          PH(1)=PO(1)+PLP*K(1)                                              97
             PH(2)=PO(2)+RLP*K(2)                                              98
             RETURN                                                            99
             END                                                              100
```

```
      FUNCTION CBRT(X)                                                  1
      SIGNX=1.0                                                         2
      IF(X.LT.0.0) SIGNX=-1.0                                           3
      CBRT=SIGNX*(SIGNX*X)**0.33333333333333                            4
      RETURN                                                            5
      END                                                               6
```

```
      FUNCTION SQR(SQ)                                          1
      IF(SQ.LE.0.)GO TO 99                                      2
      SQR=SQRT(SQ)                                              3
      RETURN                                                    4
99    SQR=0.                                                    5
      RETURN                                                    6
      END                                                       7
```

Chapter 17

SUBROUTINE OGIVEN

17-1. Purpose: To compute the unit inward normal vector $\hat{n} = \hat{x}\, n_x + \hat{y}\, n_y + \hat{z}\, n_z$ to the tangent ogive surface at the point PI(x, y, z). Dimensions are in centimeters and radome coordinates are implied.

17-2. Usage: CALL OGIVEN (PI, N)

COMMON/OGIVC/RP, BSQ, AP, RINV, B, RSQ1, RP2

(See Chapter 16 for common variables.)

17-3. Arguments

PI - Real input array containing the point PI(x, y, z) on the tangent ogive surface at which the unit normal is desired, as computed by Subroutine OGIVE.

N - Real output array containing the direction cosines (n_x, n_y, n_z) of the unit inward normal vector.

17-4. Comments and Method

The tangent ogive surface is described by

$$f(r,z) = r - \sqrt{R^2 - (z-a_p)^2} + B = 0 \qquad (1)$$

where $r = \sqrt{x^2+y^2}$ and where R and B are defined in Figure 16-1. The unit inward normal to this surface is given by

$$\hat{n} = -\frac{\nabla f}{|\nabla f|} = -\frac{1}{|\nabla f|}\left[\hat{x}\,\frac{df}{dr}\frac{dr}{dx} + \hat{y}\,\frac{df}{dr}\frac{dr}{dy} + \hat{z}\,\frac{df}{dz}\right] \qquad (2)$$

where ∇ is the gradient operator. Equation (2) can be rewritten as

$$\hat{n} = \frac{-1}{|\nabla f|}\left[\hat{x}\,\frac{x}{r} + \hat{y}\,\frac{y}{r} + \hat{z}\,\frac{df}{dz}\right] \tag{3}$$

where the differentiation with respect to r has been done and df/dr = 1 has been used. The remaining terms are given by

$$\frac{df}{dz} = \frac{(z-a_p)}{\sqrt{R^2 - (z-a_p)^2}} \tag{4}$$

$$|\nabla f| = \sqrt{1 + \frac{(z-a_p)^2}{R^2 - (z-z_p)^2}} = \frac{R}{\sqrt{R^2 - (z-a_p)^2}} \tag{5}$$

since $r^2 = x^2 + y^2$. The direction cosines can be written explicitly as

$$n_z = -\,(z-a_p)/R \tag{6}$$

$$n_x = -\left(\frac{x}{r}\right)\frac{\sqrt{R^2 - (z-a_p)^2}}{R} = -\,\frac{x}{r}\,\frac{(r+B)}{R} \tag{7}$$

$$n_y = -\left(\frac{y}{r}\right)\frac{(r+B)}{R} \tag{8}$$

where the relation $(r+B) = \sqrt{R^2 - (z-a_p)^2}$ from Equation (1) has been used.

17-5. Program Flow: Compare Equations (6) - (8) directly to the listing below.

17-6. Test Case: See Chapter 2.

17-7. Reference

1. Smail, L. L., Analytic Geometry and Calculus, Appleton-Century-Crofts, Inc., New York, 1953.

17-8. Program Listing: See following page.

```
      SUBROUTINE OGIVEN (PI,N)                                          1
C     THIS SUBROUTINE CALCULATES THE INWARD NORMAL TO THE OGIVE SURFACE  2
C    AS A PARTICULAR POINT.                                             3
C        INPUT    PI--REAL ARRAY OF COEFFICIENTS OF THE POINT           4
C        OUTPUT   N --REAL ARRAY OF DIRECTION COSINES OF NORMAL TO      5
C                    SURFACE AT POINT OF INTERSECTION                   6
      REAL N(3),NTAN,PI(3)                                              7
      COMMON/OGIVE/RP,RSQ,AP,RINV,B,RSQ1,RP2                            8
      N(3)=-(PI(3)-AP)*RINV                                             9
      R=SQRT(PI(1)*PI(1)+PI(2)*PI(2))                                  10
      NTAN=-(R+B)*RINV/R                                               11
      N(1)=PI(1)*NTAN                                                  12
      N(2)=PI(2)*NTAN                                                  13
      RETURN                                                           14
      END                                                              15
```

Chapter 18

SUBROUTINE XY

18-1. Purpose: To compute the x and y coordinates of the intersection point PI(x, y, z) of a line (ray) having direction cosines $K(k_x, k_y, k_z)$ with a surface of revolution when z is known. The line passes through the known point $P(x_o, y_o, z_o)$. All dimensions are in centimeters.

18-2. Usage: CALL XY (P, K, Z, PI)

18-3. Arguments

P - Real input array containing the known point through which the ray passes; i.e., $P(x_o, y_o, z_o)$.

K - Real input array of the direction cosines of the ray; i.e., $K(k_x, k_y, k_z)$.

Z - Real input variable equal to the known z coordinate of the intersection as found, for example, from Subroutine OGIVE.

PI - Real output array containing the desired point of intersection PI(x, y, z).

18-4. Comments and Method

The parametric equations for a line in space passing through the point $P(x_o, y_o, z_o)$ and having direction cosines (k_x, k_y, k_z) are given by

$$x = x_o + k_x t \tag{1a}$$

$$y = y_o + k_y t \tag{1b}$$

$$z = z_o + k_z t \tag{1c}$$

where t is the distance along the line from $P(x_o, y_o, z_o)$ to PI(x, y, z). When one coordinate z is known, t follows from Equation (1c), provided $k_z \neq 0$.

18-5. Program Flow: Compare the listing below directly to the equation above.

18-6. Test Case: See Chapter 2.

18-7. References: None

18-8. Program Listing: See following page.

```
      SUBROUTINE XY(P,K,Z,PI)                                          1
C                                                                      2
C   XY CALCULATES THE X AND Y COMPONENTS OF AN INTERSECTION POINT PI   3
C   FOR THE CASE WHEN THE POINT OF EMINATION P, THE DIRECTION OF       4
C   PROPAGATION K AND THE Z COORDINATE OF THE INTERSECTION POINT       5
C   ARE GIVEN                                                          6
C                                                                      7
      REAL P(3),K(3),PI(3)                                             8
      PI(3)=Z                                                          9
      T=(PI(3)-P(3))/K(3)                                             10
      PI(1)=P(1)+K(1)*T                                               11
      PI(2)=P(2)+K(2)*T                                               12
      RETURN                                                          13
      END                                                             14
```

Chapter 19

SUBROUTINES BDISK, BDISKN, TDISK, TDISKN

19-1. Purpose: To compute the intersection PI(x, y, z) of a line (ray) emanating from the point $P(x_o, y_o, z_o)$ having direction cosines $K(k_x, k_y, k_z)$ with a planar disk at $z = z_{bot}$ or at $z = z_{top}$. Subroutine BDISKN is used to compute the unit inward normal $\hat{n} = \hat{z}$. Subroutine TDISKN is used to compute the normal $\hat{n} = -\hat{z}$.

19-2. Usage:

CALL BDISK (P, K, PI, HIT)	CALL TDISK (P, K, PI, HIT)
COMMON/BDISKC/ZBOT, RBSQ	COMMON/TDISKC/ZTOP, RTSQ
CALL BDISKN (N)	CALL TDISKN (N)

19-3. Arguments

P - Real input array containing the point $P(x_o, y_o, z_o)$ from which the ray emanates.

K - Real input array of direction cosines $K(k_x, k_y, k_z)$.

PI - Real input array containing the desired point of intersection PI(x, y, z).

HIT - Logical output variable which is TRUE if an intersection is found.

ZBOT - Real input variable equal to the z coordinate of the planar disk.

RBSQ - Real input variable equal to the square of the radius of the planar disk.

N - Real output array containing the direction cosines of the unit inward normal vector; viz., N(0, 0, 1).

19-4. Comments and Method

From the parametric equations for the ray

$$x = x_o + k_x t \tag{1a}$$

$$y = y_o + k_y t \tag{1b}$$

$$z = z_o + k_z t \tag{1c}$$

and the equation of the plane $z = z_{bot}$, the parameter t is given by

$$t = (z_{bot} - z_o)/k_z \tag{2}$$

provided $k_z \neq 0$. The x and y coordinates follow from the above equations; however, if $(x^2 + y^2) > r_b^2$ (where r_b is the radius of the disk), no intersection is found. Similar statements apply for the top disk.

19-5. Program Flow: Compare the listings below directly to the equations above.

19-6. Test Case: See Chapter 2.

19-7. References: None

19-8. Program Listing: See following pages.

```
      SUBROUTINE BDISK(P,K,PI,HIT)                                      1
C                                                                       2
C   BDISK CALCULATES THE POINT OF INTERSECTION PI OF A DISK HORIZONTAL   3
C   TO THE XY PLANE WITH A RAY EMANATING FROM POINT P AND TRAVELING     4
C   IN THE K DIRECTION.                                                 5
C                                                                       6
C     THE EQUATION USED FOR THE BOT DISK IS Z=ZBOT  FOR (X**2+Y**2)<RSQ 7
C                                                                       8
      COMMON/BDISKC/ZBOT,RBSQ                                           9
      REAL P(3),K(3),PI(3)                                             10
      LOGICAL HIT                                                      11
      ZT=ZBOT-P(3)                                                     12
      IF(ZT.GE.0.0) GO TO 1                                            13
      PI(3)=ZBOT                                                       14
      T=ZT/K(3)                                                        15
      PI(1)=P(1)+K(1)*T                                                16
      PI(2)=P(2)+K(2)*T                                                17
      PITSQ=PI(1)*PI(1)+PI(2)*PI(2)                                    18
      IF(PITSQ.GT.RBSQ+0.1) GO TO 1                                    19
      HIT=.TRUE.                                                       20
      RETURN                                                           21
    1 HIT=.FALSE.                                                      22
      RETURN                                                           23
      END                                                              24
```

```
      SUBROUTINE BDISKN(N)                                              1
C                                                                       2
C   CALCULATE INWARD NORMAL OF BOTTOM DISK                              3
C                                                                       4
      REAL N(3)                                                         5
      N(1)=0.0                                                          6
      N(2)=0.0                                                          7
      N(3)=+1.0                                                         8
      RETURN                                                            9
      END                                                              10
```

```
      SUBROUTINE TDISK(P,K,PI,HIT)                                      1
C                                                                       2
C     TDISK CALCULATES THE POINT OF INTERSECTION PI OF A DISK HORIZONTAL 3
C     TO THE XY PLANE WITH A RAY EMANATING FROM POINT P AND TRAVELING   4
C     IN THE K DIRECTION.                                               5
C                                                                       6
C       THE EQUATION USED FOR THE TOP DISK IS Z=ZTOP  FOR (X**2+Y**2)<RSQ 7
C                                                                       8
      COMMON/TDISKC/ZTOP,RTSQ                                           9
      REAL P(3),K(3),PI(3)                                             10
      LOGICAL HIT                                                      11
      ZT=ZTOP-P(3)                                                     12
      IF(ZT.LE.0.0) GO TO 1                                            13
      PI(3)=ZTOP                                                       14
      T=ZT/K(3)                                                        15
      PI(1)=P(1)+K(1)*T                                                16
      PI(2)=P(2)+K(2)*T                                                17
      PITSQ=PI(1)*PI(1)+PI(2)*PI(2)                                    18
      IF(PITSQ.GT.RTSQ+0.1) GO TO 1                                    19
      HIT=.TRUE.                                                       20
      RETURN                                                           21
    1 HIT=.FALSE.                                                      22
      RETURN                                                           23
      END                                                              24
```

```
      SUBROUTINE TDISKN(N)                                              1
C                                                                       2
C   CALCULATE INWARD NORMAL OF TOP DISK                                 3
C                                                                       4
      REAL N(3)                                                         5
      N(1)=0.0                                                          6
      N(2)=0.0                                                          7
      N(3)=-1.0                                                         8
      RETURN                                                            9
      END                                                              10
```

Chapter 20

SUBROUTINE FAR

20-1. Purpose: To compute the far field pattern in wavenumber coordinates (k_x, k_y) of an antenna whose radiating characteristics are specified by the complex plane wave spectra $A_x(k_x, k_y)$, $A_y(k_x, k_y)$. The antenna is located in a plane perpendicular to the z (polar) axis.

20-2. Usage: CALL FAR (FIELD, XFIELD, YFIELD, NX, NY, FGHZ, KXMAX, KYMAX, RADIUS, IPWR, FMAX)

20-3. Arguments

FIELD - Real output array of NX by NY elements containing the far field power pattern at discrete wavenumbers $k_x = \sin\theta\cos\phi$, $k_y = \sin\theta\sin\phi$, where θ and ϕ are the usual polar and azimuthal angles.

XFIELD, YFIELD - Complex input arrays of NX by NY elements containing the plane wave spectra A_x, A_y at discrete wavenumbers k_x, k_y.

NX, NY - Integer input variables equal to the array sizes.

FGHZ - Real input variable equal to the frequency in gigahertz.

KXMAX,KYMAX- Real input variables equal to the maximum wavenumber associated with the elements of the arrays FIELD, XFIELD, and YFIELD. The element I=1, J=1 in these arrays corresponds to the wavenumber coordinate (-KXMAX, -KYMAX). For any (I,J), the wavenumber coordinates are given by

$$KX = (I - \frac{NX}{2} - 1) * KXINC$$

$$KY = (J - \frac{NY}{2} - 1) * KYINC$$

where

KXINC = 2*KXMAX/NX

KYINC = 2*KYMAX/NY

RADIUS - Real input variable equal to the radius r in centimeters of the sphere on which the far field pattern is computed. This variable effects only the term e^{-jkr}/r, and r is set to unity in the calling program for normal use.

IPWR - Integer input variable which selects the vector components to be used in computing the power pattern:

1 = Elevation component only

2 = Azimuth component only

3 = Total power

4 = Right hand circular polarization

5 = Left hand circular polarization

FMAX - Real input and output variable. On input, if FMAX $\leq$ 0, the program will normalize the array FIELD from zero to one and output the normalizing factor as FMAX. If FMAX > 0 on input, it will be used as the normalizing factor; on output it will be unchanged.

20-4. Comments and Method

Let $E_x(x, y, 0)$, $E_y(x, y, 0)$ be the tangential electric fields of a rectangular antenna aperture located in the z= plane and centered at the origin of the coordinate system. The plane wave spectra of the aperture fields are defined by

$$A_x(k_x, k_y) = \frac{1}{(2\pi)^2} \int_{-\infty}^{\infty} \int_{-\infty}^{\infty} E_x(x, y, 0)\, e^{+j(k_x x + k_y y)}\, dxdy \qquad (1)$$

$$A_y(k_x, k_y) = \frac{1}{(2\pi)^2} \int_{-\infty}^{\infty} \int_{-\infty}^{\infty} E_y(x, y, 0)\, e^{+j(k_x x + k_y y)}\, dxdy \qquad (2)$$

$$A_z(k_x, k_y) = \frac{-k_x A_x - k_y A_y}{k_z} \qquad (3)$$

where

$$k_x^2 + k_y^2 + k_z^2 = k^2 = \left(\frac{2\pi}{\lambda}\right)^2 \qquad (4)$$

The electric field E_ℓ (ℓ = x, y, or z) at any point (x, y, z > 0) is given by

$$E_\ell(x, y, z) = \int_{-\infty}^{\infty} \int_{-\infty}^{\infty} A_\ell(k_x, k_y)\, e^{-j\, \underline{k} \cdot \underline{r}}\, dk_x dk_y \qquad (5)$$

where

$$\underline{r} = \hat{x}x + \hat{y}y + \hat{z}z \qquad (6)$$

$$\underline{k} = \hat{x}k_x + \hat{y}k_y + \hat{z}k_z \qquad (7)$$

And for the special case of large r, the rectangular field components E_ℓ approach their asymptotic values [1]

$$E_{\ell ff}\ (r,\ k_{xo},\ k_{yo}) \sim j2\pi k\ \frac{e^{-jkr}}{r}\ \cos\theta\ A_\ell(k_{xo},\ k_{yo}) \tag{8}$$

where the stationary phase points are given by

$$k_{xo} = k\ \sin\theta\ \cos\phi \tag{9}$$

$$k_{yo} = k\ \sin\theta\ \sin\phi \tag{10}$$

$$k_{zo} = k\ \cos\theta \tag{11}$$

In the above equations, θ is the polar angle measured from the z axis, and ϕ is the azimuthal angle measured from +x toward +y in the conventional spherical coordinate manner.

Consider the antenna measurement coordinate system in Figure 20-1. Let the wavenumbers k_x, k_y, k_z be normalized by $k = 2\pi/\lambda$, so that for $k_x^2 + k_y^2 < 1$, they represent direction cosines of the direction specified by (θ,ϕ), or equivalently by (ε,α). In terms of these normalized wavenumbers, the unit vectors $\hat{\varepsilon},\hat{\alpha}$ may be written as

$$\hat{\varepsilon} = \hat{x}\ \frac{-k_x k_y}{\sqrt{1 - k_y^2}}\ + \hat{y}\sqrt{1-k_y^2}\ + \hat{z}\ \frac{-k_y k_z}{\sqrt{1 - k_y^2}} \tag{12}$$

$$\hat{\alpha} = \hat{x}\ \frac{k_z}{\sqrt{1 - k_y^2}}\ + \hat{y}\ (0)\ + \hat{z}\ \frac{-k_x}{\sqrt{1 - k_y^2}} \tag{13}$$

The elevation and azimuth components of the far field $\underline{E}_{ff}$ then follow via the vector dot product as

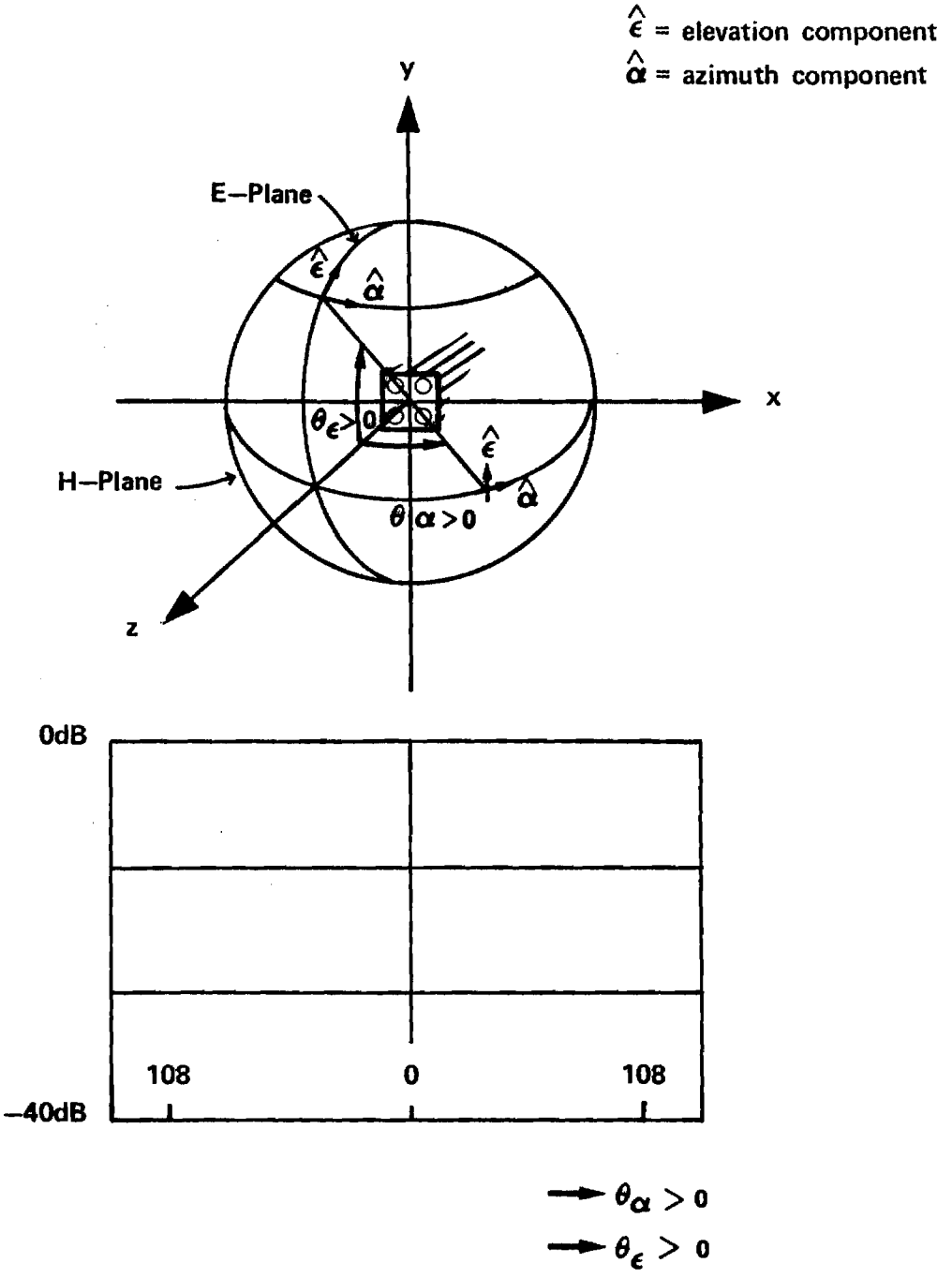

Figure 20-1**Coordinate System for Far Field Patterns**

$$E_{\varepsilon ff} = \hat{\varepsilon} \cdot \underline{E}_{ff} = j2\ k\ \frac{e^{-jkr}}{r}\ \hat{\varepsilon} \cdot [\hat{x}\ k_z A_x + \hat{y}\ A_y + \hat{z}(-k_x A_x - k_y A_y)] \quad (14)$$

$$E_{\alpha ff} = j2\pi k\ \frac{e^{-jkr}}{r}\ \hat{\alpha} \cdot \underline{E}_{ff} \quad (15)$$

(In Subroutine FAR, the factor $j2\pi k$ is not used, and the plane wave spectra A_x, A_y are provided as computed previously using the Fast Fourier Transform.)

It is convenient to recall that the receiving and transmitting patterns of an antenna are identical, and that the receiving pattern $V_R(\hat{k})$ is given in terms of the far field $\underline{E}_{ff}$ by [2]

$$V_R(\hat{k}) = C\ \hat{n}_b \cdot \underline{E}_{ff}(\hat{k}) \quad (16)$$

where $\hat{n}_b$ is a infinitesimal current source (probe) located on the far-field measurement sphere, and C is a complex constant which is set to unity for convenience. The elevation component of the receiving <u>power</u> pattern is given simply by

$$|V_R(\hat{k})|_\varepsilon^2 = |\hat{\varepsilon} \cdot \underline{E}_{ff}(\hat{k})|^2 = |E_{\varepsilon ff}(\hat{k})|^2, \quad (17)$$

and the azimuth component by

$$|V_R(\hat{k})|_\alpha^2 = |\hat{\alpha} \cdot \underline{E}_{ff}(\hat{k})|^2 = |E_{\alpha ff}(\hat{k})|^2. \quad (18)$$

The total power pattern is given by

$$|V_R(\hat{k})|_T^2 = |E_{\alpha ff}|^2 + |E_{\varepsilon ff}|^2 = |E_{xff}|^2 + |E_{yff}|^2 + |E_{zff}|^2 \quad (19)$$

and is the receiving pattern when the probe is polarization matched at every point to the test antenna.

In the case of circularly polarized fields, the probe $\hat{n}_b$ can be expressed as

$$\text{RHC:} \quad \hat{n}_b = \frac{\hat{\varepsilon} + \hat{\alpha}\, e^{-j\frac{\pi}{2}}}{\sqrt{2}} \tag{20}$$

$$\text{LHC:} \quad \hat{n}_b = \frac{\hat{\varepsilon}\, e^{-j\frac{\pi}{2}} + \hat{\alpha}}{\sqrt{2}} \tag{21}$$

The receiving patterns in the two cases are then given by

$$|V_R|^2_{\text{HC}} = |\hat{n}_b \cdot \underline{E}_{ff}|^2 \tag{22}$$

where the appropriate $\hat{n}_b$ is used.

Subroutine FAR implements the above equations and computes the power patterns for an aperture in an infinite ground plane; i.e., the use of only A_x and A_y is tantamount to the assumption that $\underline{E}_{tan}$ outside the finite aperture area is zero. For the extended case of a finite aperture in free space, the tangential magnetic field $\underline{H}_{tan}$ also contributes to the radiated field, and the far fields are given by Equations (3-46) - (3-49) of Reference 3. In fact, it is only by including the effects of $\underline{H}_{tan}$ that the transmitting and receiving formulations for the finite aperture can be shown to be equivalent [4].

The current version of Subroutine FAR listed below could be easily modified to include the additional terms. If the geometrical optics approximation for the aperture fields is made; viz.,

$$\underline{H}_{tan} = \frac{\hat{z} \times \underline{E}_{tan}}{\eta} \tag{23}$$

then the far-field expressions become

$$\begin{aligned} \underline{E}_{ff}(k_x, k_y) = {} & \hat{x}[(k_z + 1 - k_x^2) A_x - k_x k_y A_y] \\ & + \hat{y}[-k_x k_y A_x + (k_z + 1 - k_y^2) A_y] \\ & + \hat{z}[-k_x(1 + k_z) A_x - k_y(1 + k_z) A_y] \end{aligned} \tag{24}$$

These modifications would involve changes only to Lines 70 - 72 of Subroutine FAR.

20-5. Program Flow: Compare listing below directly to Equations (1) - (22) above.

20-6. Test Case: See Chapter 2.

20-7. References

1. P. C. Clemmow, The Plane Wave Spectrum Representation of Electromagnetic Fields, Pergamon Press, Oxford, 1966.
2. G. K. Huddleston, H. L. Bassett, and J. M. Newton, "Parametric Investigation of Radome Analysis Methods", 1978 IEEE/AP-S Symposium Digest, pp. 199-202, May 1978, and in Proc. of the Fourteenth Symposium on Electromagnetic Windows, pp. 21-28, June 1978.
3. G. K. Huddleston, "Optimum Probes for Near-Field Measurements on a Plane", Ph.D. Dissertation, Georgia Institute of Technology, Atlanta, Georgia, August 1978.
4. G. K. Huddleston, "Equivalence of Transmitting and Receiving Formulations in Radome Analysis", in preparation.

20-8. Program Listing: See following pages.

```
      SUBROUTINE FAR(FIELD,XFIELD,YFIELD,NX,NY,FGHZ,KXMAX,KYMAX,          1
     $  RADIUS,IPWR,FMAX)                                                 2
C                                                                         3
C         FIELD IS A TWO DIMENSIONAL REAL ARRAY (NX,NY).  ON OUTPUT       4
C             IT CONTAINS THE FAR FIELD POWER PATTERN OF A COMPLEX        5
C             VECTOR PLANE WAVE SPECTRUM.                                 6
C         XFIELD AND YFIELD ARE TWO DIMENSIONAL COMPLEX ARRAYS WHICH      7
C             CONTAIN RESPECTIVELY THE X AND Y COMPONENTS OF A            8
C             COMPLEX PLANE WAVE SPECTRUM                                 9
C         KXMAX AND KYMAX ARE RESPECTIVELY THE MAXIMUM ABSOLUTE          10
C             VALUES OF KX AND KY WAVENUMBERS FOR WHICH THE FAR FIELD     11
C             IS CALCULATED.  KXMAX AND KYMAX ARE NORMALIZED SUCH THAT    12
C             KX=1.0 AND KY=1.0 CORRESPOND TO THE VISIBLE                 13
C             REGION OF WAVENUMBER SPACE.                                 14
C         FMAX IS AN INPUT-OUTPUT VARIABLE.  IF FMAX IS LESS THAN OR      15
C             EQUAL TO ZERO ON INPUT, THE FIELD ARRAY IS NORMALIZED       16
C             FROM ZERO TO ONE AND FMAX IS THE NORMALIZING FACTOR.        17
C             IF FMAX IS GREATER THAN ZERO ON INPUT IT REMAINS            18
C             UNCHANGED AND IS USED AS THE NORMALIZING FACTOR.            19
C         IPWR DETERMINES WHICH POWER COMPONENT WILL BE USED IN THE       20
C             FAR FIELD CALCULATIONS.  IPWR=1 FOR ELEVATION COMPONENTS,   21
C             IPWR=2 FOR AZIMUTH COMPONENTS, AND IPWR=3 FOR TOTAL POWER   22
C             IPWR=4 FOR RIGHT-HAND CIRCULAR POLARIZATION COMPONENTS      23
C             IPWR=5 FOR LEFT-HAND CIRCULAR POLARIZATION COMPONENTS       24
C         RADIUS SPECIFIES THE RADIUS OF THE FAR FIELD SPHERE IN          25
C             CENTIMETERS                                                 26
C                                                                         27
      REAL FIELD(NX,NY)                                                   28
      REAL K,KX,KY,KZ,KXINC,KYINC,KXMAX,KYMAX                            29
      COMPLEX XFIELD(NX,NY),YFIELD(NX,NY),Q,C,EZ,EX,EY                    30
      COMPLEX HTHETA,HPHI,HX,HY,HZ                                        31
      IM=1+NX/2                                                           32
      JM=1+NY/2                                                           33
      SR2=SQRT(2.)                                                        34
      HTHETA=CMPLX(1.,0.)/SR2                                             35
      HPHI=CMPLX(0.,1.)/SR2                                               36
      IF (IPWR.EQ.5) HPHI=-HPHI                                           37
      IF(IPWR.GE.1.AND.IPWR.LE.5) GO TO 101                               38
```

```
      WRITE(6,100)                                                          39
  100 FORMAT(1H1,3X,"VALUE ASSIGNED TO THE ARGUMENT IPWR IN SUBROUTINE      40
     -FAR IS NOT ALLOWED.  IPWR=3 ASSUMED.")                                41
      IPWR=3                                                                42
  101 CONTINUE                                                              43
      PI=3.14159265358898                                                   44
      K=2*PI*FGHZ/29.97925                                                  45
      Q=(0.0,1.0)                                                           46
      NX2=NX/2                                                              47
      NY2=NY/2                                                              48
      KXINC=0.0                                                             49
      KYINC=0.0                                                             50
      IF(NX2.EQ.0) GO TO 1                                                  51
      KXINC=KXMAX/NX2                                                       52
    1 IF(NY2.EQ.0) GO TO 2                                                  53
      KYINC=KYMAX/NY2                                                       54
    2 CONTINUE                                                              55
C                                                                           56
C           CALCULATE THE POWER PATTERN ON A SPHERE.                        57
C                                                                           58
      R=RADIUS                                                              59
      RE=AMOD(K*R,2.0*PI)                                                   60
      C=Q*K*CEXP(-Q*RE)/R                                                   61
      DO 6 I=1,NX,1                                                         62
      DO 6 J=1,NY,1                                                         63
      KX=(I-NX2-1.0)*KXINC                                                  64
      KY=(J-NY2-1.0)*KYINC                                                  65
      KZ=1.0-KX**2-KY**2                                                    66
      IF(KZ.LE.0.0) GO TO 5                                                 67
      KZ=SQRT(KZ)                                                           68
      D=SQRT(1.-KY**2)                                                      69
      EZ=-C*(KX*XFIELD(I,J) +KY*YFIELD(I,J))                                70
      EX=C*KZ*XFIELD(I,J)                                                   71
      EY=C*KZ*YFIELD(I,J)                                                   72
      XFIELD(I,J)=EX                                                        73
      YFIELD(I,J)=EY                                                        74
      IF(IPWR.EQ.1) FIELD(I,J)=CABS(-EX*KY*KX/D+EY*D-EZ*KZ*KY/D)**2         75
      IF(IPWR.EQ.2) FIELD(I,J)=CABS(-EY*KZ/D-EZ*KX/D)**2                    76
```

```
      IF(IPWR.EQ.3) FIELD(I,J)=CABS(EX)**2+CABS(EY)**2+CABS(EZ)**2
      IF(IPWR.GE.1.AND.IPWR.LE.3) GO TO 6
      IF (I.EQ.IM.AND.J.EQ.JM) GO TO 7
      RAD=SQRT(KX**2+KY**2)
      HX=(HTHETA*KX*KZ-HPHI*KY)/RAD
      HY=(HTHETA*KY*KZ+HPHI*KX)/RAD
      HZ=-HTHETA*RAD
      GO TO 10
    7 HX=HTHETA
      HY=HPHI
      HZ=CMPLX(0.,0.)
   10 FIELD(I,J)=CABS(EX*HX+EY*HY+EZ*HZ)**2
      GO TO 6
    5 FIELD(I,J)=0.0
    6 CONTINUE
C
C
C          NORMALIZE THE POWER PATTERN.
C
      IF(FMAX.GT.0.0)  GO TO 9
      DO 8  I=1,NX
      DO 8  J=1,NY
      R=FIELD(I,J)
      IF(R.GT.FMAX) FMAX=R
    8 CONTINUE
    9 CONTINUE
      DO 11 I=1,NX
      DO 11 J=1,NY
      FIELD(I,J)=FIELD(I,J)/FMAX
   11 CONTINUE
      RETURN
      END
```

Chapter 21

SUBROUTINE AMPHS

21-1. Purpose: To convert a complex number c = x + jy from rectangular to polar form $c = |c|e^{j\phi}$.

21-2. Usage: CALL AMPHS (C, AMP, PHS)

21-3. Arguments

C - Complex input variable containing the rectangular components of the complex number to be converted; i.e., C = CMPLX(X,Y).

AMP - Real output variable equal to $\sqrt{x^2+y^2}$.

PHS - Real output variable equal to the phase angle ϕ in degrees.

21-4. Comment

The intrinsic Fortran function ATAN2 is used to compute PHS.

21-5. Program Flow: See listing below.

21-6. Test Case: None

21-7. References: None

21-8. Program Listing: See following page.

```
      SUBROUTINE AMPHS(C,AMP,PHS)                                    1
      COMPLEX C                                                      2
      DATA PI/3.1+159265/                                            3
      AMP=CABS(C)                                                    4
      X=REAL(C)                                                      5
      Y=AIMAG(C)                                                     6
      IF (ABS(X).LT.1E-18) GO TO 2                                   7
      PHS=ATAN2(Y,X)*180./PI                                         8
      RETURN                                                         9
    2 PHS=90.                                                       10
      IF (Y.LT.0.) PHS=-90.                                         11
      IF (AMP.LT.1E-18) PHS=-180.                                   12
      RETURN                                                        13
      END                                                           14
```

Chapter 22

SUBROUTINE DBPV

22-1. Purpose: To convert a real array of linear values, normalized to lie between zero and unity, to decibels.

22-2. Usage: CALL DBPV (FIELD, NX, NY, IPV)

22-3. Arguments

FIELD - Real input/output array of NX by NY elements: on input, it contains the values to be converted; on output, it contains the corresponding decibel values on the range (-40, 0). All input values less than 10^{-2} are set to -40 dB on output.

NX, NY - Integer input variables which specify the size of the array FIELD.

IPV - Integer input variable which specifies whether the input values in FIELD represent power (IPV=1) or voltage (IPV=2). If IPV=1, F(I, J) = 10 $\log_{10}$ F(I, J) is returned; if IPV=2, F(I, J) = 20 $\log_{10}$ F(I, J) is returned.

22-4. Comments

It is intended that the input array FIELD be normalized prior to the call to Subroutine DBPV.

22-5. Program Flow: See listing below.

22-6. Test Case: None

22-7. References: None

22-8. Program Listing: See following page.

```
      SUBROUTINE DBPV(FIELD,NX,NY,IPV)                                  1
C  MODIFIED BY GKH 4/78 TO PERMIT POWER (IPV=1) OR VOLTAGE (IPV=2) DB.   2
C                                                                        3
C  SUBROUTINE DB CONVERTS AN INPUT ARRAY (FIELD(NX,NY)) OF               4
C  VOLTAGE OR POWER VALUES TO DECIBLES AND RETURNS DB VALUES IN THE      5
C  SAME ARRAY.                                                           6
C  ALL VALUES OF POWER LESS THAN 40 DB DOWN ARE SET EQUAL TO  -40DB      7
C                                                                        8
      DIMENSION FIELD(NX,NY)                                             9
      DO 10  I=1,NX                                                     10
      DO 10  J=1,NY                                                     11
      IF (IPV.EQ.2) FIELD(I,J)=FIELD(I,J)**2                            12
      IF(FIELD(I,J).LE.1E-4) FIELD(I,J)=1E-4                            13
      FIELD(I,J)=10.0*ALOG10(FIELD(I,J))                                14
   10 CONTINUE                                                          15
      RETURN                                                            16
      END                                                               17
```

Chapter 23

SUBROUTINE NORMH

23-1. Purpose: To normalize a two-dimensional real array of field values so that all values in the array lie between zero and unity.

23-2. Usage: CALL NORMH (FIELD, IMAX, JMAX, LDB)

23-3. Arguments

FIELD - Real array of IMAX by JMAX elements. On input, it contains the field values expressed as non-negative real linear amplitude or as amplitude in decibels. On output, the linear amplitudes are replaced by their scaled values FIELD(I,J)/FMAX, where FMAX is the maximum amplitude value in the array; the logarithmic amplitude values are replaced by (FIELD(I,J)+40.)/40., where -40 decibels is assumed to be the lower bound on the original data.

IMAX,JMAX - The number of elements in FIELD.

LDB - A logical variable set TRUE if the values in FIELD are in decibels.

23-4. Comments and Method

A function f(x,y) of two variables having minimum value f_{min} and maximum value f_{max} may be normalized to $0 \le f_n(x,y) \le 1$ according to

$$f_n(x,y) = \frac{f(x,y) - f_{min}}{f_{max} - f_{min}} \qquad (1)$$

provided that the denominator is not zero. In this procedure, the $f_n=0$ corresponds to $f=f_{min}$, and $f_n=1$ corresponds to $f=f_{max}$.

When f(x,y) represents a linear (vice logarithmic) variable, it is desirable to force f_{min} to be zero if the minimum value of f is actually greater than zero. In this special case, f_n becomes

$$f_n(x,y) = \frac{f(x,y)}{f_{max}} \qquad (2)$$

Equation (2) is also used to treat the special case of $f_{max} - f_{min} \approx 0$; however if $|f_{max}|<1$, f_{max} is set equal to $\pm 1.$, where the sign used is that of f_{max}. This refinement has the effect of producing a constant function whose value lies between zero and unity; without it, f_n would be simply set to unity or division by zero may result.

When f(x,y) represents a logarithmic variable, such as the amplitude in decibels of an electromagnetic field, all of the foregoing discussion applies; however, a minimum value f_{min} must be imposed. If $f_{min}<-40$, f_{min} is set equal to -80 (decibels); otherwise, a -40 decibel level is assumed. A value of f_{max} equal to zero decibel is also assumed.

23-5. Program Flow

Lines 9-16: Find minimum MN and maximum MX values of data in FIELD; form their difference DR=MX-MN.

Line 17: If array values are in decibels, go to 50.

Line 18: If all values in the array are the same, go to 25 and scale the data to lie between zero and unity (Lines 28-37).

Lines 19-27: If all linear amplitude values in FIELD are not identical, scale the data according to FIELD(I,J) = (FIELD(I,J) - Min. Value)/(Maximum Value - Minimum Value).

Line 38: If values in FIELD are in decibels, and the minimum value is less than -41dB, then assume a -80dB lower bound, go to 60 (Lines 47-52), and scale the data according to (FIELD(I,J) + 80.)/80.

Lines 39-46: Scale the data according to a -40dB lower bound; i.e., (FIELD(I,J) + 40.)/40.

Lines 53-54: Write MN and MX.

23-6. Test Case: See Chapter 2.

23-7. References: None.

23-8. Program Listing: See following pages.

```
      SUBROUTINE NORMH(FIELD,IMAX,JMAX,LDB)                              1
C  MODIFIED BY GKH 4/78 TO CAUSE PROPER NORMALIZATION OF BOTH             2
C  LINEAR AND DB ARRAYS.                                                  3
C                                                                         4
C           NORMALIZE FIELD SO THAT ALL VALUES ARE BETWEEN ZERO AND ONE.  5
C                                                                         6
      REAL MN,MX,FIELD(IMAX,JMAX)                                        7
      LOGICAL LDB                                                        8
      MX=FIELD(1,1)                                                      9
      MN=MX                                                             10
      DO 20  I=1,IMAX                                                   11
      DO 20  J=1,JMAX                                                   12
      MN=AMIN1(MN,FIELD(I,J))                                           13
      MX=AMAX1(MX,FIELD(I,J))                                           14
   20 CONTINUE                                                          15
      DR=MX-MN                                                          16
      IF (LDB) GO TO 50                                                 17
      IF (DR.LT.1E-18) GO TO 25                                         18
      TMN=MN                                                            19
      IF (MN.GT.0.) TMN=0.                                              20
      TDR=DR                                                            21
      IF (MN.GT.0.) TDR=MX                                              22
      DO 21  I=1,IMAX                                                   23
      DO 21  J=1,JMAX                                                   24
      FIELD(I,J)=(FIELD(I,J)-TMN)/TDR                                   25
   21 CONTINUE                                                          26
      GO TO 35                                                          27
C  CASE WHERE ALL VALUES ARE THE SAME:                                    28
   25 TMX=MX                                                            29
      IF (ABS(MX).LT.1.0) TMX=SIGN(1.,MX)                               30
      DO 30 I=1,IMAX                                                    31
      DO 30 J=1,JMAX                                                    32
      FIELD(I,J)=FIELD(I,J)/TMX                                         33
C  FIELD IS FILLED WITH SAME VALUES SCALED BETWEEN ZERO AND UNITY.        34
      IF (FIELD(I,J).LT.0.) FIELD(I,J)=0.                               35
   30 CONTINUE                                                          36
      GO TO 35                                                          37
   50 IF (MN.LT.-41.) GO TO 60                                          38
```

```
C  ASSUME 0 TO -40. SCALE:                                                    39
      DO 55 I=1,IMAX                                                         40
      DO 55 J=1,JMAX                                                         41
      FIELD(I,J)=(FIELD(I,J)+40.)/40.                                        42
      IF (FIELD(I,J).LT.0.) FIELD(I,J)=0.                                    43
      IF (FIELD(I,J).GT.1.) FIELD(I,J)=1.                                    44
   55 CONTINUE                                                               45
      GO TO 35                                                               46
   60 DO 65 I=1,IMAX                                                         47
      DO 65 J=1,JMAX                                                         48
      FIELD(I,J)=(FIELD(I,J)+80.)/80.                                        49
      IF (FIELD(I,J).LT.0.) FIELD(I,J)=0.                                    50
      IF (FIELD(I,J).GT.1.) FIELD(I,J)=1.                                    51
   65 CONTINUE                                                               52
   35 WRITE(6,40) MN,MX                                                      53
   40 FORMAT(//"  SUBROUTINE NORM:  MIN= ",E10.3,"  MAX= ",E10.3//)          54
      RETURN                                                                 55
      END                                                                    56
```

Chapter 24

SUBROUTINE CNPLTH AND FUNCTION PSI

24-1. Purpose: To plot (Calcomp) single dimensional far field patterns at constant wavenumber k_{fix}.

24-2. Usage: CALL CNPLTH (FIELD, N, KMAX, KCNTR, KFIX)

$$PSI = ATAN2 \quad (K/\sqrt{1. - K^2 - K_{fix}^2})$$

24-3. Arguments

FIELD - Real input array of N elements containing the field values in decibels but normalized so that -40 dB corresponds to 0 and 0 dB corresponds to unity on the normalized scale.

N - Integer input variable which specifies the number of elements in FIELD.

KMAX - Real input variable equal to the half width of the wavenumber range corresponding to the array elements 1 through N of the array FIELD; i.e., the increment in wavenumber corresponding to the distance between the Ith and (I+1)st element is 2 KMAX/N.

KCNTR - Real input variable equal to the wavenumber coordinate of the (N/2 + 1)st element of the array FIELD. FIELD(1) has wavenumber coordinate KCNTR - KMAX.

KFIX - Real input variable equal to the fixed value of the other wavenumber coordinate. For example, if k_x varies, then k_y = KFIX.

24-4. Comment and Method

Let $F(k_x, k_y)$ represent the far-field power pattern of an antenna where k_x and k_y are normalized wavenumbers as defined in Chapter 20. A pattern cut at constant wavenumber is a conical cut about the real axis; e.g., a k_x = constant cut is a conical cut about the x axis of the coordinate system.

For principal plane cuts, $k_x = 0$ yields an E-plane pattern as defined in Figure 2-3; $k_y = 0$ yields an H-plane pattern. For principal plane cuts, KCNTR = 0 and KFIX = 0.

The plotting commands are set up to produce a 4" X 8" rectangular pattern plot on a standard pattern scale. The plot is positioned on the paper to give margins of 2" on the left, 1" on the right, and 2.25" from the bottom and, hence, is suitable for direct use as a figure in a technical report.

24-5. Program Flow: See listing below.

24-6. Test Case: See Chapter 2 and pattern plots in Appendices B and D.

24-7. References: None

24-8. Program Listing: See following pages.

```
      SUBROUTINE CNPLTH(FIELD,N,KMAX,KCNTR,KFIX)                        1
C   MODIFIED BY GKH 4/28/78 TO GIVE 4 X 8 SA PLOTS WITH MARGINS         2
C   OF 2" FROM LEFT, 2.25 FROM BTM, AND 1" ON RIGHT.                    3
C                                                                       4
C     THIS SUBROUTINE PLOTS SINGLE DIMENSIONAL FAR FILED PATTERNS       5
C      THE PLOTS ARE CONSTANT WAVENUMBER PLOTS WHICH CORRESPOND         6
C      TO CONICAL FAR FIELD PATTERNS                                    7
C      FIELD(N) IS A ONE DIMENSIONAL FAR FIELD POWER PATTERN            8
C      NORMALIZED FROM ZERO(CORRESPONDING TO -40 DB) TO ONE             9
C      (CORRESPONDING TO 0 DB)                                         10
C      KMAX IS THE HALF WIDTH OF THE WAVENUMBER REGION OF FIELD        11
C      KCNTR IS THE CENTER WAVENUMBER COORDINATE OF THE INPUT FIELD    12
C      FIELD(1) HAS A WAVENUMBER COORDINATE KCNTR-KMAX                 13
C      FIELD(N/2+1) HAS WAVENUMBER COORDINATE KCNTR                    14
C      KFIX IS THE FIXED VALUE OF THE OTHER WAVENUMBER COORDINATE      15
C                                                                      16
      REAL FIELD(N),K,KMAX,KCNTR,KFIX                                  17
      PSIMIN=PSI(KCNTR-KMAX,KFIX)                                      18
      PSIMAX=PSI(KCNTR+KMAX-2*KMAX/N,KFIX)                             19
      PSIMID=PSI(KCNTR,KFIX)                                           20
      DELPSI=2*AMAX1(PSIMID-PSIMIN,PSIMAX-PSIMID)                      21
      ISCALE=360                                                       22
      IF(DELPSI.LE.60) ISCALE=60                                       23
      IF(DELPSI.LE.10) ISCALE=10                                       24
C   INITIALIZE FACTOR TO UNITY AND DRAW LEFT MARGIN FOR GUIDE LATER.   25
      CALL FACTOR(1.)                                                  26
      CALL PLOT(0.,0.0,-3)                                             27
      CALL PLOT(0.,8.5,2)                                              28
      CALL PLOT(0.,0.,3)                                               29
C   SET LOGICAL ORIGIN OF SA PLOT:                                     30
      CALL PLOT(2.,2.25,-3)                                            31
C   PLOT AT .4 SCALE FACTOR OF FULL SIZE SA PLOT (10 X 20):            32
      CALL FACTOR(.4)                                                  33
C                                                                      34
C     DRAW RECTANGULAR PERIMETER BOX                                   35
      CALL PLOT(0.0,0.75,3)                                            36
      CALL PLOT(0.0,10.625,2)                                          37
      CALL PLOT(20.0,10.625,2)                                         38
```

```
      CALL PLOT(20.0,.75,2)                                              39
      CALL PLOT(0.0,.75,2)                                               40
C                                                                        41
C     PLOT HORIZONTAL DECIBEL SCALES                                     42
      Y=0.75+2.46875                                                     43
      DO 1 I=2,4,1                                                       44
      DB=40.000001-(I-1)*10.0                                            45
      CALL PLOT(0.0,Y,3)                                                 46
      CALL PLOT(5.0,Y,2)                                                 47
      CALL NUMBER(5.0633,Y-0.07,0.14,DB,0.0,-1)                          48
      CALL PLOT(5.3333,Y,3)                                              49
      CALL PLOT(15.3333,Y,2)                                             50
      CALL NUMBER(15.3833,Y-0.07,0.14,DB,0.0,-1)                         51
      CALL PLOT(15.6666,Y,3)                                             52
      CALL PLOT(20.0,Y,2)                                                53
    1 Y=Y+2.46875                                                        54
C                                                                        55
C     PLOT HORIZONTAL ANGLE TICK MARKS                                   56
      X=0.6666667                                                        57
      DO 2 I=1,29,1                                                      58
      CALL PLOT(X,0.75,3)                                                59
      CALL PLOT(X,0.85,2)                                                60
    2 X=X+0.66666667                                                     61
C                                                                        62
C     PLOT HORIZONTAL ANGLE SCALE                                        63
      DO 3 I=1,9,1                                                       64
      ANG=IABS(5-I)*ISCALE/10.0+0.0001                                   65
      DX=0.18                                                            66
      IF(ANG.LT.100.0)DX=0.11                                            67
      IF(ANG.LT.10.0)DX=0.04                                             68
      X=I*2.0-DX                                                         69
      Y=0.90                                                             70
      CALL NUMBER(X,Y,0.14,ANG,0.0,-1)                                   71
    3 CONTINUE                                                           72
C                                                                        73
C     DIGRESS TO PLOT INTERIOR VERTICLE DECIBLE SCALES AND LABLES        74
      DX=-1.0                                                            75
      X= 5.3333                                                          76
```

```
      DO 6 I=1,2,1                                                          77
      Y=0.75                                                                78
      CALL PLOT(X,Y,3)                                                      79
      CALL PLOT(X,10.625,2)                                                 80
      CALL SYMBOL(X-DX*0.14+0.07,3.85,0.14, 27HRELATIVE POWER ONE WAY (D    81
     $B),90.0,27)                                                           82
      DO 5 J=1,4,1                                                          83
      DO 4 L=1,4,1                                                          84
      DB=10-2*L+0.0001                                                      85
      Y=Y+9.875/20.0                                                        86
      CALL PLOT(X,Y,3)                                                      87
      CALL PLOT(X+DX*0.07,Y,2)                                              88
      CALL NUMBER(X+DX*0.16666-0.04,Y-0.07,0.14,DB,0.0,-1)                  89
    4 CONTINUE                                                              90
    5 Y=Y+9.875/20.0                                                        91
      X=14.6667                                                             92
    6 DX=-DX                                                                93
C                                                                           94
C   PLOT CONE ANGLE AND CENTER OF ROTATION ANGLE                            95
      CONE=ACOS(KFIX)*180/3.14159265358 98                                  96
      CALL SYMBOL(6.5,0.54,0.14,13HCONE ANGLE = ,0.0,13)                    97
      CALL NUMBER(999.,999.,0.14,CONE,0.0,1)                                98
      CALL SYMBOL(999.,999.,0.14,29H     CENTER ROTATION ANGLE = ,0.0,      99
     $29)                                                                  100
      CALL NUMBER (999.,999.,0.14,PSIMID,0.0,1)                            101
C                                                                          102
C     PLOT PATTERN                                                         103
      IPEN=3                                                               104
      DO 10 I=1,N,1                                                        105
      K=KCNTR+(I-N/2.-1)*KMAX*2/N                                          106
      A=PSI(K,KFIX)-PSIMID                                                 107
      X=10.0+20.0*A/ISCALE                                                 108
      Y=FIELD(I)                                                           109
      IF(Y.LT.0.0) Y=0.0                                                   110
      IF(Y.GT.1.0) Y=1.0                                                   111
      Y=Y*9.875+0.75                                                       112
      IF(X.LT.0.0)X=0.0                                                    113
      IF(X.GT.20.0) X=20.0                                                 114
```

```
      CALL PLOT(X,Y,IPEN)                                              115
      IPEN=2                                                           116
   10 CONTINUE                                                         117
C  RESTORE FACTOR AND CONCLUDE PLOT AT BTM RT CORNER OF PAGE:          118
      CALL FACTOR(1.0)                                                 119
      CALL PLOT(9.,-2.25,-3)                                           120
      RETURN                                                           121
      END                                                              122
```

```
      FUNCTION PSI(K,KFIX)                                              1
      REAL K,KFIX,KZ                                                    2
      KZ=1.-K**2-KFIX**2                                                3
      IF (KZ.LE.0.) KZ=0.                                               4
      KZ=SQRT(KZ)                                                       5
      PSI=ATAN2(K,KZ)*180./3.141592653                                  6
      RETURN                                                            7
      END                                                               8
```

Chapter 25

SUBROUTINES PLT3DH AND PLTT

25-1. Purpose: To plot (Calcomp) the two-dimensional array FIELD (I, J).

25-2. Usage: CALL PLT3DH (XSIZE, YSIZE, HEIGHT, FIELD, IMAX, JMAX, NMZ, LDB)

25-3. Arguments

XSIZE, YSIZE, HEIGHT	-	Real input variables in inches defined on Figure 1.
FIELD, IMAX, JMAX	-	Real input array of IMAX by JMAX elements containing the values to be plotted. These values must be normalized to the range (0, 1) before plotting.
NMZ	-	Logical input variable. If NMZ = .TRUE., the array FIELD will be normalized with respect to its own maximum value; if NMZ = .FALSE., no normalization will be done.
LDB	-	Logical input variable required by Subroutine NORMH (Chapter 23).

25-4. Comments

In Figure 25-1, the axes and labels shown are not produced by the subroutine; these axes are presented to demonstrate the perspective of the plot and to identify its dimensions. Report size plots will be produced suitable for one 8 1/2" X 11" page when FACTOR = 1.0 and

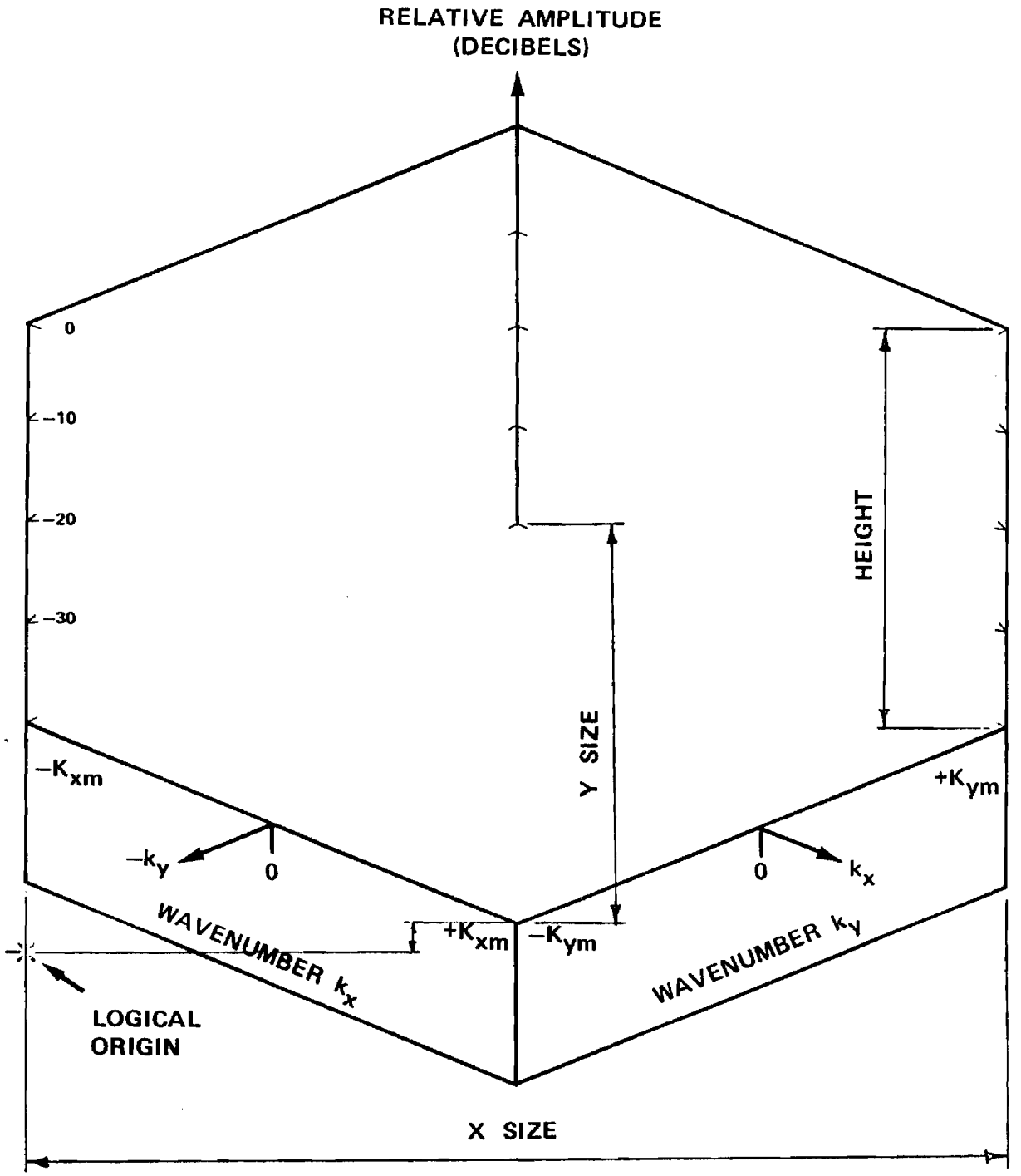

Figure 25—1. Dimensions of Three—Dimensional Plot.

XSIZE = 6.0"

YSIZE = 2.5"

HEIGHT = 2.5"

Margins in this case will be 1.5" on the left, 1" on the right, and 4.25" from the bottom of the plot paper. Margin lines are provided on the plot paper to outline the 8 1/2" X 11" page. Also, the plot itself can be carefully cut from the plot paper and cemented onto a set of axes as has evidently been done in Appendices B and D.

25-5. Program Flow: See listing below.

25-6. Test Case: See Chapter 2 and Appendices B and D.

25-7. References: None.

25-8. Program Listing: See following pages.

```
      SUBROUTINE PLT3DH(XSIZE,YSIZE,HEIGHT,FIELD,IMAX,JMAX,NMZ,LDB)
C  LDB IS REQUIRED BY SUBR NORMH TO SPECIFY IF ARRAY FIELD
C  IS IN DB (TRUE) OR NOT (LDB=.FALSE.).
C  MODIFIED BY GKH 4/28/78 TO GIVE REPORT SIZE PLOTS WHEN
C  XSIZE=6.0, YSIZE=2.5, HEIGHT=2.5.  I.E., LEFT MARGIN OF
C  1.5", RIGHT OF 1" AND 4.25" FROM BTM MARGIN.
C
C          XSIZE IS THE MAXIMUM LENGTH OF THE PLOT IN INCHES.
C          YSIZE IS THE MAXIMUM WIDTH OF A ZERO PLOT IN INCHES.
C          THE SUM OF 1/2 INCH + YSIZE + HEIGHT MUST BE LESS THAN
C              OR EQUAL TO THE PAPER WIDTH.
C          FIELD(IMAX,JMAX) IS THE TWO-DIMENSIONAL REAL ARRAY TO
C              BE PLOTTED. IF FIELD IS NOT NORMALIZED ON INPUT, NMZ
C              MUST BE .TRUE.  .
C          NMZ(NORMALIZE) IS A LOGICAL INPUT VARIABLE.  IF ITS VALUE
C              IS .TRUE. THE VALUES IN FIELD WILL BE REPLACED WITH
C              THEIR NORMALIZED(ZERO TO ONE) COMPONENTS.
C
      REAL FIELD(IMAX,JMAX),HID(128)
      LOGICAL NMZ,LDB
      REAL LASTX,LASTY,LASTH,LASTHM
      IF(NMZ)  CALL NORMH(FIELD,IMAX,JMAX,LDB)
      XPAGE=0.0
      YPAGE=0.0
      LASTHM=0.0
      NIJ=IMAX+JMAX
      RI=IMAX-1.0
      RJ=JMAX-1.0
C  INITIALIZE FACTOR TO UNITY, DRAW LEFT MARGIN,AND SET LOGICAL ORIGIN:
      CALL FACTOR(1.0)
      CALL PLOT(0.,0.0,-3)
      CALL PLOT(0.,11.,2)
      CALL PLOT(0.,0.,3)
      CALL PLOT(1.5,3.75,-3)
      DO 1 I=1,NIJ
    1 HID(I)=-0.5
      DO 7 J=1,JMAX
      AJ=J-1.0
```

```
      DO 7 I=1,IMAX                                                          39
      AI=I-1.0                                                               40
      LASTX=XPAGE                                                            41
      XPAGE=(AJ+AI)*XSIZE/(RI+RJ)                                            42
      LASTY=YPAGE                                                            43
      YPAGE=(AJ*RI/RJ-AI*RJ/RI+RJ)*YSIZE/(RJ+RI)+HEIGHT*FIELD(I,J)           44
      LASTH=LASTHM                                                           45
      LASTHM=HID(I+J)                                                        46
      IF(YPAGE-HID(I+J)) 5,5,2                                               47
    2 IF(I.NE.1) GO TO 3                                                     48
      CALL PLTT(XPAGE,YPAGE,3)                                               49
      IPEN=2                                                                 50
      GO TO 4                                                                51
    3 CALL PLTT(XPAGE,YPAGE,IPEN)                                            52
      IPEN=2                                                                 53
    4 HID(I+J)=YPAGE                                                         54
      GO TO 7                                                                55
    5 IF(I.EQ.1) IPEN=3                                                      56
      IF(IPEN.EQ.3) GO TO 6                                                  57
      X1N=LASTX*HID(I+J)-LASTH*XPAGE-LASTX*YPAGE+XPAGE*LASTY                 58
      X1D=HID(I+J)-LASTH-YPAGE+LASTY                                         59
      X1=X1N/X1D                                                             60
      Y1=(X1*(HID(I+J)-LASTH)+LASTH*XPAGE-LASTX*HID(I+J))/(XPAGE-LASTX)      61
      CALL PLTT(X1,Y1,2)                                                     62
      IPEN=3                                                                 63
    6 CALL PLTT(XPAGE,YPAGE,IPEN)                                            64
    7 CONTINUE                                                               65
      DO 8 I=1,NIJ                                                           66
    8 HID(I)=-0.5                                                            67
      DO 16 II=1,IMAX,1                                                      68
      I=IMAX-II+1                                                            69
      AI=I-1                                                                 70
      DO 16 J=1,JMAX                                                         71
      AJ=J-1                                                                 72
      LASTX=XPAGE                                                            73
      XPAGE=(AJ+AI)*XSIZE/(RI+RJ)                                            74
      LASTY=YPAGE                                                            75
      YPAGE=(AJ*RI/RJ-AI*RJ/RI+RJ)*YSIZE/(RJ+RI)+HEIGHT*FIELD(I,J)           76
```

```
      LASTH=LASTHM                                                          77
      LASTHM=HID(I+J)                                                       78
      IF(YPAGE-HID(I+J)) 13,14,9                                            79
    9 IF(J.NE.1) GO TO 10                                                   80
      CALL PLTT(XPAGE,YPAGE,3)                                              81
      IPEN=2                                                                82
      GO TO 12                                                              83
   10 IF(IPEN.EQ.2) GO TO 11                                                84
      X1N=LASTX*YPAGE-LASTY*XPAGE-LASTX*HID(I+J)+XPAGE*HID(I+J-1)           85
      X1D=YPAGE-LASTY-HID(I+J)+HID(I+J-1)                                   86
      X1=X1N/X1D                                                            87
      Y1=(X1*(YPAGE-LASTY)+LASTY*XPAGE-LASTX*YPAGE)/(XPAGE-LASTX)           88
      CALL PLTT(X1,Y1,3)                                                    89
      IPEN=2                                                                90
   11 CALL PLTT(XPAGE,YPAGE,IPEN)                                           91
   12 HID(I+J)=YPAGE                                                        92
      GO TO 16                                                              93
   13 IPEN=3                                                                94
      GO TO 15                                                              95
   14 IF(J.EQ.1) IPEN=3                                                     96
   15 CALL PLTT(XPAGE,YPAGE,IPEN)                                           97
   16 CONTINUE                                                              98
C  CONCLUDE PLOT AT RT BTM CORNER OF REPORT PAGE:                           99
      CALL PLOT(XSIZE+1.,-3.75,-3)                                         100
      RETURN                                                               101
      END                                                                  102
```

```
      SUBROUTINE PLTT(X,Y,IPEN)                                          1
C                                                                        2
C          SUBROUTINE PLTT ELIMINATES MOVING PEN FOR HIDDEN LINES.       3
C                                                                        4
      XLAST=XN                                                           5
      YLAST=YN                                                           6
      ILAST=IN                                                           7
      XN=X                                                               8
      YN=Y                                                               9
      IN=IPEN                                                           10
      IF(IPEN.EQ.2.AND.ILAST.EQ.2) CALL PLOT(X,Y,IPEN)                  11
      IF(IPEN.EQ.2.AND.ILAST.EQ.3) CALL PLOT(XLAST,YLAST,ILAST)         12
      IF(IPEN.EQ.2.AND.ILAST.EQ.3) CALL PLOT(X,Y,IPEN)                  13
      IF(IPEN.NE.2.AND.IPEN.NE.3) CALL PLOT(X,Y,IPEN)                   14
      RETURN                                                            15
      END                                                               16
```

Chapter 26

SUBROUTINE FFTA

26-1. Purpose: To compute the Discrete Fourier Transform (DFT) or its inverse of a sequence of complex numbers consisting of 2^N elements, where N is an integer. The Cooley-Tukey algorithm is used to perform computations in place to speed up the computations and to return the transformed values in the input array.

26-2. Usage: CALL FFTA (FIELD, NEXP, IBMISN)

26-3. Arguments

FIELD - Complex array of 2** NEXP elements: on input it contains the sample data to be transformed; on output it contains the transformed data. See below for ordering of data.

NEXP - Integer exponent; e.g., for 64 elements in FIELD, NEXP=6.

IBMISN - Integer parameter which controls operation:
IBMISN = 3 performs the inverse DFT
IBMISN ≠ 3 performs the DFT as defined in 4 below.

26-4. Comments and Method

a. Subroutine FFTA is machine-dependent in that the bit reversed number, IFLIP, must be generated using Fortran instructions which are peculiar to a particular machine. Also, the word length must be taken into account. Lines 38-42 of the attached program listing are used to effect the desired operation for the CDC Cyber 70 (60-bit word, numbered

0 through 59 from right to left with Bit 0 being the least significant):

```
      IFLIP=0
      DO 4 II=1, IEXP, 1
      J=60 - II
      IFLIP=2*IFLIP + AND (SHIFT(I,1+J), 1B)
    4 CONTINUE
```

The SHIFT(I,1+J) operation shifts the bits of the integer I to the left by 1+J bit positions. The AND operation strips off the right most bit of the shifted result. E.G., when II=1, the right most bit of I (Bit 0) is extracted from I by the AND(SHIFT) operation. The current value of IFLIP is then shifted one bit to the left by the 2*IFLIP operation. The two results are then added together. A total of NEXP bits are extracted, starting with Bit 0, followed by Bits 1, 2,...(NEXP-1).

The net result of these operations is to take the NEXP-bit binary representation of the array element number I, reverse the order of the bits, and right justify the result. Array elements in FIELD numbered I and IFLIP are then interchanged if I>IFLIP. The first and last elements of FIELD always remain in place. The array elements are rearranged in this manner so that they will be ordered after transforming [1].

b. To explain the ordering of the data in the complex array FIELD, it is convenient to consider the specific example of using FFTA to compute the Fourier transform G(f) of a time function g(t) as defined by

$$G(f) = \int_{-T_{max}}^{T_{max}} g(t)\ e^{-j2\pi ft}\ dt \qquad (1)$$

and as approximated by

$$G(f) \approx \Sigma\, g(t_i)\, e^{-j2\, ft_i}\, \Delta t \qquad (2)$$

where t_i are the equally spaced points along the t axis when g is sampled over the interval $-T_{max} \leq t \leq T_{max}$.

There are $N=2^{NEXP}$ samples in the input array FIELD(I) corresponding to I=1,N. The first sample (I=1) corresponds to $g(-T_{max})$. The last sample (I=N) corresponds to $g(T_{max}-\Delta t)$. The I=(N/2+1)th sample corresponds to g(0); i.e., the value of g at t=0. The DFT assumes periodicity of the sampled data so that the value at $t=T_{max}$ is identical to that at $t=-T_{max}$. The sample spacing is

$$\Delta t = 2\, T_{max}/N \qquad (3)$$

and corresponds to a folding frequency f_{max} of

$$f_{max} = 1/2\Delta t \qquad (4)$$

On output, the array FIELD contains the frequency components G(f) at N equally spaced frequencies Δf over the band $-f_{max} \leq f \leq f_{max}$, where I=1 corresponds to $f=-f_{max}$, I=(N/2+1) to f=0, and I=N to $f=f_{max}-\Delta f$, where

$$\Delta f = 2\, f_{max}/N \qquad (5)$$

and where

$$T_{max} = \frac{1}{2\Delta f} \tag{6}$$

Also, by the inversion integral [2],

$$g(t) = \int_{-f_{max}}^{f_{max}} G(f)\ e^{+j2\pi ft}\ df \approx \Delta f \sum_p G(f_p)\ e^{j2\pi f_p t} \tag{7}$$

This version of Subroutine FFTA is written so that division by N is done when the Fourier transform (kernel = $e^{-j2\pi ft}$) is computed. When the expression in Equation (3) for Δt is used in (2), there results

$$G(f_p) = 2\ T_{max}\ \frac{1}{N} \sum_i g(t_i)\ e^{-j2\pi f_p t_i} \tag{8}$$

Transposing $2\ T_{max}$ and using Equation (6) yields

$$\Delta f\ G(f_p) = \frac{1}{N} \sum_i g(t_i)\ e^{-j2\pi f_p t_i} \tag{9}$$

where the righthand side is the definition of the Discrete Fourier Transform as computed by FFTA. Inversely,

$$g(t_i) = \sum_p \Delta f\ G(f_p)\ e^{+j2\pi f_p t_i} \tag{10}$$

which is the Inverse DFT as computed by FFTA.

Conversely, if the original data in the input array FIELD are samples of a frequency spectrum G(f), a similar analysis shows that FFTA computes $\Delta t\ g(t_i)$ as the inverse transform (IBMISN=3); i.e., the time function is modified in amplitude by Δt. Of course, when the forward transform (IBMISN≠3) is performed on this result, the original sampled data $G(f_i)$ are obtained in FIELD on output.

From the above considerations, the following conclusions can be drawn concerning the use of FFTA to compute the Fourier transform G(f) of a windowed time function g(t):

$$G(f_p) = 2\ T_{max} \cdot \text{FFTA}\{g(t_i)\} \tag{11}$$

$$g(t_i) = \frac{1}{2\ T_{max}} \cdot \text{IFFTA}\{G(f_p)\} = \text{IFFTA}\{\Delta f\ G(f_p)\} \tag{12}$$

As an example, let g(t) be the rectangular pulse function which has constant amplitude V_o for $|t| \le t_o$ and which is windowed in the larger time interval $|t| \le T_{max}$. The Fourier transform G(f) is given by [3]

$$G(f) = 2\ t_o V_o \frac{\sin 2\pi f t_o}{2\pi f t_o} \tag{13}$$

Let g(t) be sampled at $N=2^{NEXP}$ points over the interval $|t| \le T_{max}$, and let these sampled points be placed in the array FIELD. Then the spectrum G(f) will be closely approximated at discrete frequencies f_p by

$$G(f_p) \approx 2\ T_{max} * FIELD(I)$$

where

$$f_p = -f_{max} + (I-1) * \Delta f$$

and where FIELD is the output of FFTA according to CALL FFTA (FIELD, N, 0).

Proper consideration should be given to the sampling of the time function so that the DFT produces a good estimate of the actual integral transform. For example, if $t_o=T_{max}$, and all samples are constant, then the DFT will produce a single nonzero frequency component at f=0 (corresponding to the (N/2+1)th element of FIELD); i.e., a delta function. Such a result follows from the facts that the Fourier transform of a constant $g(t)=V_o$ is $G(f)=V_o\delta(f)$ and that the DFT assumes a periodicity of the sequence of samples provided to it.

Consider the other extreme. Let the pulse g(t) be represented by only one sample at t=0 in the window $|t| \leq T_{max}$. The Fourier transform of $g(t)=V_o\delta(t)$ is $G(f)=V_o$, a constant.

It is clear from the above considerations that the time function must be properly windowed and properly sampled to produce a good estimate of its transform via the DFT. Simply stated, the time function should be sampled at a rate Δt which is twice the highest frequency contained in the function as interpreted by the DFT.

26-5. Program Flow

Lines 22-24: Compute $N=2^{NEXP}$ and set the sign ISN of the exponent in the Fourier kernel.

Lines 26-29: Compute IEXP=NEXP from N. This is a redundant computation made when the original FFT subroutine was modified to conform to the call to a library version on another computer system.

Lines 30-35: Rearrange the order of the input data so that samples for $t \geq 0$ are placed in the lower half of the array, and those for $t<0$ are placed in the upper half. For a frequency function, the data are rearranged so that the first N/2 points give the components for non-negative frequencies (I=1 corresponds to f=0), and the last N/2 points contain the data for the negative frequencies.

Lines 36-49: Rearrange the data in FIELD so that it will be ordered <u>after</u> transforming as described for Lines 30-35 above.

Lines 50-73: Perform the summation using the Cooley-Tukey algorithm [1].

Lines 74-79: If forward transform is being done, divide all values in FIELD by N.

Lines 80-85: Rearrange the output data in FIELD so that it conforms to that used on input; i.e., $f_i=f_{max} + (I-1)\Delta f$ or $t_i=-T_{max} + (I-1)\Delta t$ as appropriate.

26-6. Test Case

A rectangular pulse function with amplitude $V_o=100$ was chosen for g(t) with $t_o=.10$ second $T_{max}=1.60$ seconds, and $N=2048=2^{11}$. The resulting

sample increment Δt and folding frequency f_{max} were 0.116 second 320.0 Hertz, respectively. The comparison of the central nine points of the computed and true frequency spectra were as follows (CDC Cyber 70):

		True G(f)		Computed G(f)	
I	f (Hz)	Amp.	Phase(°)	Amp.	Phase(°)
1021	-1.250	18.006	0.00	18.006	0.35
1022	-0.938	18.863	0.00	18.863	0.26
1023	-0.625	19.490	0.00	19.490	0.18
1024	-0.313	19.872	0.00	19.872	0.09
1025	0.000	20.000	0.00	20.000	0.00
1026	0.313	19.872	0.00	19.872	-0.09
1027	0.625	19.490	0.00	19.490	-0.26
1028	0.938	18.863	0.00	18.863	-.035

26-7. References

1. Cochran, W. T., et al, "What is the Fast Fourier Transform?", Proc, IEEE, 55, pp. 1664-1674.
2. Papoulis, A., The Fourier Integral and Its Application, McGraw-Hill, New York, Ch. 2, 1962.
3. Stein and Jones, Modern Communication Principles, McGraw-Hill, New York, pp. 10-11, 1967.

26-8. Program Listing: See following pages. The second listing, Subroutine FFT, is for use on the IBM 3033 at JHU/APL. It employs the subroutine FFTA available on that system library. Use of this subroutine requires the calls in Subroutines JOYFFT and MAGFFT to be changed from CALL FFTA to CALL FFT.

```
      SUBROUTINE FFTA(FIELD,NEXP,IBMISN)                                 1
C   MODIFIED TO SIMULATE FFTA ON IBM 3033 AT APL/JHU                     2
C   DIVISION BY N IS DONE WHEN ISN=-1 (GKH 10 20 76)                     3
C   CDC CONVERSION DONE 1 JUNE 1976                                      4
C                                                                        5
C   ************************************************************       6
C   *                                                          *       7
C   *   THIS SUBROUTINE CALCULATES THE FAST FOURIER TRANSFORM OR *       8
C   *   THE INVERSE FAST FOURIER TRANSFORM OF AN INPUT COMPLEX   *       9
C   *   ARRAY FIELD AND RETURNS THE RESULT IN THE SAME ARRAY     *      10
C   *                                                          *      11
C   *   N MUST BE AN INTEGER POWER OF TWO                        *      12
C   *                                                          *      13
C   *   ISN IS AN INTEGER WHICH MAY BE EITHER ONE OR MINUS ONE   *      14
C   *   IF ISN IS -1 THE FAST FOURIER TRANSFORM IS CALCULATED    *      15
C   *   IF ISN IS +1 THE INVERSE FOURIER TRANSFORM IS CALCULATED *      16
C   *                                                          *      17
C   ************************************************************       18
C                                                                       19
      COMPLEX FIELD(512)                                                20
      COMPLEX  T,F                                                      21
      N=2**NEXP                                                         22
      ISN=-1                                                            23
      IF (IBMISN.EQ.3) ISN=+1                                           24
      PI2=6.2831853071796                                               25
      IEXP=0                                                            26
    1 IEXP=IEXP + 1                                                     27
      M=2**IEXP                                                         28
      IF(N-M) 10,2,1                                                    29
    2 N2=N/2                                                            30
      DO 3 I=1,N2,1                                                     31
      K=I+N2                                                            32
      T=FIELD(I)                                                        33
      FIELD(I)=FIELD(K)                                                 34
    3 FIELD(K)=T                                                        35
      N1=N-2                                                            36
      DO 5 I=1,N1,1                                                     37
      IFLIP=0                                                           38
```

```
      DO 4 II=1,IEXP,1                                                  39
      J=60-II                                                           40
      IFLIP=2*IFLIP+AND(SHIFT(I,1+J),1B)                                41
    4 CONTINUE                                                          42
      IF(I.LE.IFLIP) GO TO 5                                            43
      I1=I+1                                                            44
      I2=IFLIP+1                                                        45
      T=FIELD(I2)                                                       46
      FIELD(I2)=FIELD(I1)                                               47
      FIELD(I1)=T                                                       48
    5 CONTINUE                                                          49
      DO 6 I=1,IEXP,1                                                   50
      NEL=2**I                                                          51
      NEL2=NEL/2                                                        52
      NSET=N/NEL                                                        53
      SI=SIN(PI2/NEL)                                                   54
      CI=COS(PI2/NEL)                                                   55
      DO 86 J=1,NSET,1                                                  56
      INCR=(J-1)*NEL                                                    57
      SO=0.0                                                            58
      CO=1.0                                                            59
      DO 96 II=1,NEL2,1                                                 60
      J1=II+INCR                                                        61
      J2=J1+NEL2                                                        62
      T=FIELD(J1)                                                       63
      F=FIELD(J2)*CMPLX(CO,ISN*SO)                                      64
      FIELD(J1)=T+F                                                     65
      FIELD(J2)=T-F                                                     66
      SN=SO*CI+CO*SI                                                    67
      CS=CO*CI-SO*SI                                                    68
      CO=CS                                                             69
      SO=SN                                                             70
   96 CONTINUE                                                          71
   86 CONTINUE                                                          72
    6 CONTINUE                                                          73
      IF(ISN.GT.0) GO TO 8                                              74
C  DIVISION BY N IS DONE FOR FORWARD TRANSFORM (GKH 10-20-76)           75
      DO 7 I=1,N,1                                                      76
```

```
      FIELD(I)=FIELD(I)/N                                              77
    7 CONTINUE                                                         78
    8 CONTINUE                                                         79
      DO 9 I=1,N2,1                                                    80
      K=I+N2                                                           81
      T=FIELD(I)                                                       82
      FIELD(I)=FIELD(K)                                                83
      FIELD(K)=T                                                       84
    9 CONTINUE                                                         85
   10 CONTINUE                                                         86
      RETURN                                                           87
      END                                                              88
```

```
      SUBROUTINE FFT(FIELD,NEXP,IBMISN)                                 1
C  MODIFIED TO UTILIZE FFTA ON IBM 3033 AT APL/JHU BY GKH FEB 80.        2
C   ***************************************************************   3
C   *                                                             *     4
C   *   THIS SUBROUTINE CALCULATES THE FAST FOURIER TRANSFORM OR  *     5
C   *   THE INVERSE FAST FOURIER TRANSFORM OF AN INPUT COMPLEX    *     6
C   *   ARRAY FIELD AND RETURNS THE RESULT IN THE SAME ARRAY      *     7
C   *  IBMISN (INTEGER) CONTROLS THE DIRECTION OF THE TRANSFORM:        8
C   *        =1 FOR FORWARD (NEGATIVE EXPONENTIAL) TRANSFORM            9
C   *        =3 FOR INVERSE TRANSFORM                                  10
C   *  SEE JHU/APL SCIENTIFIC SUBR LIBRARY ROUTINE NO. 6.04.051 FOR    11
C   *  OTHER VALUES OF IBMISN IN SUBR FFTA USED HEREIN.                12
C   *  ORDERING OF DATA:                                               13
C   *    ON INPUT AND OUTPUT, I=1 CORRESPONDS TO MOST NEGATIVE         14
C   *    ABSCISSA, I=N/2+1 TO ORIGIN, I=N TO MOST POSITIVE ABSCISSA.   15
C   ***************************************************************   16
C                                                                       17
      COMPLEX FIELD(1)                                                  18
      COMPLEX  T,F                                                      19
      N=2**NEXP                                                         20
      DATA PI2/6.2831853071796/                                         21
    2 N2=N/2                                                            22
C  ORDER THE DATA FOR FFTA  I.E., NONNEGATIVE ABSCISSAE CORRESPOND      23
C  TO I=1 TO N/2, NEGATIVE ABSCISSAE TO I=N/2+1 TO N.                   24
      DO 3 I=1,N2,1                                                     25
      K=I+N2                                                            26
      T=FIELD(I)                                                        27
      FIELD(I)=FIELD(K)                                                 28
    3 FIELD(K)=T                                                        29
      MFFTA=NEXP+1                                                      30
      CALL FFTA(FIELD,MFFTA,IBMISN)                                     31
C  REORDER THE DATA FOR OUTPUT.                                         32
      DO 9 I=1,N2,1                                                     33
      K=I+N2                                                            34
      T=FIELD(I)                                                        35
      FIELD(I)=FIELD(K)                                                 36
      FIELD(K)=T                                                        37
    9 CONTINUE                                                          38
```

```
      RETURN                                                            39
      END                                                               40
```

Chapter 27

SUBROUTINE MAGFFT

27-1. Purpose: To increase the resolution of a complex array of data points using Fourier interpolation and the Fast Fourier Transform. The number of points in each array must be an integer power of two.

27-2. Usage: CALL MAGFFT (A, NA, B, NB)

27-3. Arguments

A,NA - Complex input array of NA = 2^M < NB data points.

B,NB - Complex output array of NB = 2^N data points.

27-4. Comment and Method

a. Subroutines required: FFTA, PWRTWO

b. By Shannon's sampling theorem, a band-limited function is represented by its samples, and it can be reconstructed at any point from them. The computation of the value of the function at a point other than a sample point is called Fourier interpolation. Such interpolation can be used to increase the resolution of a function.

The Fast Fourier Transform (FFT) can be used to facilitate Fourier interpolation. Briefly, the original function $A(k_x)$, known at NA points on the range $(-K_M, +K_M)$, is transformed to yield $E(x) = F\{A(k_x)\}$ at NA sample points. These NA values of E(x) are then placed in the center of an array containing NB = 2^N > NA = 2^M points to form the function E'(x). This function is then inverse transformed to produce $A(k_x)$ at NB points over the same range $(-K_M, +K_M)$. (Actually, the range is $(-K_M, +K_M - \Delta k)$ since the FFT considers the sampled function to be periodic outside the known range so that the (NB + 1)st point would be the same as the first point in the array.)

27-5. Program Flow: See listing below.

27-6. Test Case: See Chapter 2.

27-7. References: See Chapter 26.

27-8. Program Listing: See following page.

```
      SUBROUTINE MAGFFT(A,NA,B,NB)                                      1
      COMPLEX A(NA),B(NB)                                               2
      IF (NB.LE.NA) GO TO 1                                             3
      GO TO 2                                                           4
    1 WRITE(6,3)                                                        5
    3 FORMAT(/" NB IS LESS THAN OR EQUAL TO NA IN MAGFFT "/)            6
      RETURN                                                            7
    2 CONTINUE                                                          8
      NAC=NA/2+1                                                        9
      NBC=NB/2+1                                                       10
      N=NBC-NAC                                                        11
      DO 5 I=1,NB                                                      12
      B(I)=(0.,0.)                                                     13
    5 CONTINUE                                                         14
      CALL PWRTWO(NA,INA)                                              15
      CALL FFTA(A,INA,3)                                               16
      DO 10 I=1,NA                                                     17
      J=N+I                                                            18
      B(J)=A(I)                                                        19
   10 CONTINUE                                                         20
      CALL PWRTWO(NB,INB)                                              21
      CALL FFTA(B,INB,1)                                               22
      RETURN                                                           23
      END                                                              24
```

Chapter 28

SUBROUTINE JOYFFT

28-1. Purpose: To compute the two-dimensional Fast Fourier Transform of a complex array of NXI by NYI points and to provide magnification of a specified portion of the transformed data.

28-2. Usage: CALL JOYFFT (INPUT, NXI, NYI, MX, MY, NXC, NYC, OUTPUT, NXO, NYO, XYFFT, NXY, ISN)

28-3. Arguments

INPUT, NXI, NYI - Complex input array of NXI by NYI points.

MX, MY - Integer input variables, equal to an integer power of two, which specify the magnification in the I and J directions, respectively.

NXC, NYC - Integer input variables which specify the center coordinate I = NXC, J = NYC of the sector to be magnified.

OUTPUT, NXO, NYO - Complex output array of NXO by NYO points containing the transformed points of the magnified sector.

XYFFT, NXY - Complex working array of NXY points.

ISN - Integer input variable which specifies the direction of the FFT: ISN = 3 for inverse FFT; ISN = 1 for FFT. See Chapter 26.

28-4. Comment

a. Subroutines required: FFTA, PWRTWO.

b. All integer input variables must be integer powers of 2 and must satisfy the following restrictions:

(1) NXO*NYO $\leq$ NXI*NYI

(2) NXO $\leq$ NXI or NYO $\leq$ NYI

(3) MX*NXI $\leq$ NXY and MY*NYI $\leq$ NXY

28-5. Program Flow: See listing below.

28-6. Test Case: See Chapter 2.

28-7. References: None

28-8. Program Listing: See following pages.

```
      SUBROUTINE JOYFFT(INPUT,NXI,NYI,MX,MY,NXC,NYC,OUTPUT,NXO,NYO,      1
     $XYFFT,NXY,ISN)                                                     2
      COMPLEX INPUT(NXI,NYI),OUTPUT(NXO,NYO),XYFFT(NXY)                  3
C                                                                        4
C     ***************************************************************** 5
C     *                                                                 6
C     *   SUBROUTINE JOYFFT CALCULATES THE TWO DIMENSIONAL COMPLEX FAST 7
C     *   FOURIER TRANSFORM FOR ISN=+1 OR THE INVERSE FAST FOURIER      8
C     *   TRANSFORM FOR ISN=+3 ,OUTPUT(NXC,NYO), OR A TWO DIMENSIONAL   9
C     *   COMPLEX ARRAY, INPUT(NXI,NYI)                                10
C     *   JOYFFT ALSO PERMITS CALCULATION OF A MAGNIFIED SECTOR OF THE  11
C     *   FFT AS FOLLOWS.  MX IS THE MAGNIFICATION FACTOR FOR THE X     12
C     *   DIMENSION AND MY IS THE MAGNIFICATION FACTOR FOR THE Y        13
C     *   DIMENSION.  THE CENER COORDINATE OF THE MAGNIFIED SECTOR,     14
C     *   (NXC,NYC) IS SPECIFIED WITH REFERENCE TO THE UNMAGNIFED FFT   15
C     *                                                                 16
C     *   THE XYFFT(NXY) ARRAY IS A COMPLEX TEMPORARY STORAGE ARRAY USED 17
C     *   TO PERFORM THE MAGNIFIED X AND Y SINGLE DIMENSION FFTS        18
C     *                                                                 19
C     *   FOLLOWING ARE RESTRICTIONS ON THE INPUT AND OUTPUT PARAMETERS 20
C     *   "<" BELOW MEANS LESS THAN OR EQUAL TO                         21
C     *      NXO*NYO<NXI*NYI                                            22
C     *      NXO<NXI OR NYO<NYI                                         23
C     *      MX*NXI<NXY AND MY*NYI<NXY                                  24
C     *     NYI=2**(ANY NON-NEGATIVE INTEGER)                           25
C     *     NXI=2**(ANY NON-NEGATIVE INTEGER)                           26
C     *     NXO=2**(ANY NON-NEGATIVE INTEGER)                           27
C     *     NYO=2**(ANY NON-NEGATIVE INTEGER)                           28
C     *      MX=2**(ANY NON-NEGATIVE INTEGER)                           29
C     *      MY=2**(ANY NON-NEGATIVE INTEGER)                           30
C     *                                                                 31
C     *   MAGNIFICATION IS NOT PERMITTED FOR INPUT DIMENSIONS OF ONE    32
C     *                                                                 33
C     *   THE OUTPUT SECTOR MUST BE CONTAINED IN THE MAGNIFIED FFT      34
C     *         NXC/2<MX*MIN(NXC-1,NXI+1-NXC)                          35
C     *         AND                                                     36
C     *         NYO/2<MY*MIN(NYC-1,NYI+1-NYC)                          37
C     *                                                                 38
```

```
C    *    THE INPUT AND OUTPUT ARRAY MAY BE EQUIVALENCED USING THE
C    *    FOLLOWING EQUIVALENCE STATEMENT IN THE MAIN PROGRAM
C    *    EQUIVALENCE(INPUT(1,1),OUTPUT(1,1))
C    ************************************************************
C
C    NXO*NYO<NXI*NYI
       IF(NXI*NYI.GE.NXO*NYO) GO TO 2
C      WRITE(6,1)
C    1 FORMAT(5X,"THE SIZE OF THE OUTPUT ARRAY EXCEEDS THE SIZE OF THE IN
C     $PUT ARRAY")
C
C    NXI,NYI,NXO,NYO,MX,MY EACH MUST EQUAL TWO RAISED TO SOME NON
C    NEGATIVE INTEGER POWER
     2 CALL PWRTWO(NXI,INXI)
       CALL PWRTWO(NYI,INYI)
       CALL PWRTWO(NXO,INXO)
       CALL PWRTWO(NYO,INYO)
       CALL PWRTWO(MX,IMX)
       CALL PWRTWO(MY,IMY)
C
       IF(NXO.LE.NXI.OR.NYO.LE.NYI) GO TO 220
       WRITE(6,210)
   210 FORMAT(5X,"THE SIZE OF THE FIRST FFT EXCEEDS THE SIZE OF THE INPU
      $T ARRAY")
       RETURN
C
C    MX*NXI<NXY AND MY*NYI<NXY
   220 NX=NXI*MX
       IF(NXY.GE.NX) GO TO 4
       WRITE(6,3) NXY
     3 FORMAT(I15,"  THIS DIMENSION IS INSUFFICIENT TO CARRY OUT THE MAGN
      $IFICATION IN X")
       RETURN
     4 NY=NYI*MY
       IF(NXY.GE.NY) GO TO 6
       WRITE(6,5) NXY
     5 FORMAT(I15,"  THIS DIMENSION IS INSUFFICIENT TO CARRY OUT THE MAGN
      $IFICATION IN Y")
```

```
      RETURN                                                            77
C                                                                       78
    6 IF(NXO/2.LE.MX*MIN0(NXC-1,NXI+1-NXC)) GO TO 8                     79
      WRITE(6,7)                                                        80
    7 FORMAT(5X,"THE OUTPUT SECTOR DESIRED IS NOT CONTAINED WITHIN THE C 81
     $ALCULATED FFT")                                                   82
      RETURN                                                            83
C                                                                       84
    8 IF(NYO/2.LE.MY*MIN0(NYC-1,NYI+1-NYC)) GO TO 9                     85
      WRITE(6,7)                                                        86
      RETURN                                                            87
C                                                                       88
C   DETERMINE THE ORDER IN WHICH X AND Y FFTS WILL BE CALCULATED        89
    9 IF(NYO.GT.NXO) GO TO 21                                           90
C                                                                       91
C   PERFORM SINGLE DIMENSION FFTS FOR Y THEN X                          92
C                                                                       93
C LOAD Y VALUES IN XYFFT ARRAY                                          94
      NYS=NYI-NYO                                                       95
      IF(NYI.EQ.1) GO TO 15                                             96
      NZ=(NY-NYI)/2                                                     97
      NXYS=(NYC-1)*MY-NYO/2                                             98
      DO 14 I=1,NXI,1                                                   99
      IF(NZ.EQ.0) GO TO 11                                             100
      DO 10 J=1,NZ,1                                                   101
      XYFFT(J)=(0.0,0.0)                                               102
      XYFFT(J+NZ+NYI)=(0.0,0.0)                                        103
   10 CONTINUE                                                         104
   11 DO 12 J=1,NYI,1                                                  105
      XYFFT(J+NZ)=INPUT(I,J)                                           106
   12 CONTINUE                                                         107
C                                                                      108
C   PERFORM SINGLE DIMENSION FFT FOR Y                                 109
      CALL PWRTWC(NY,INY)                                              110
      CALL FFTA(XYFFT,INY,ISN)                                         111
C                                                                      112
C   EXTRACT OUTPUT SECTOR OF INTEREST AND STORE IN INPUT ARRAY         113
      DO 13 J=1,NYO,1                                                  114
```

```
      INPUT(I,J+NYS)=XYFFT(J+NXYS)                                          115
   13 CONTINUE                                                              116
   14 CONTINUE                                                              117
C                                                                           118
C    PERFORM NYO MAGNIFIED FFTS IN X AND STORE SELECTED  SECTORS OF FFTS    119
C    IN OUTPUT ARRAY                                                        120
   15 NZ=(NX-NXI)/2                                                         121
      NXYS=(NXC-1)*MX-NXO/2                                                 122
      DO 20 J=1,NYO,1                                                       123
C                                                                           124
C    LOAD X VALUES IN XYFFT ARRAY                                           125
      IF(NZ.EQ.0) GO TO 17                                                  126
      DO 16 I=1,NZ,1                                                        127
      XYFFT(I)=(0.0,0.0)                                                    128
      XYFFT(I+NZ+NXI)=(0.0,0.0)                                             129
   16 CONTINUE                                                              130
   17 DO 18 I=1,NXI,1                                                       131
      XYFFT(I+NZ)=INPUT(I,J+NYS)                                            132
   18 CONTINUE                                                              133
C                                                                           134
C    PERFORM SINGLE DIMENSION FFTS IN X                                     135
      CALL PWRTWO(NX,INX)                                                   136
      CALL FFTA(XYFFT,INX,ISN)                                              137
C                                                                           138
C    EXTRACT OUTPUT SECTOR OF INTEREST AND STORE IN OUTPUT ARRAY            139
      DO 19 I=1,NXO,1                                                       140
      OUTPUT(I,J)=XYFFT(I+NXYS)                                             141
   19 CONTINUE                                                              142
   20 CONTINUE                                                              143
      RETURN                                                                144
C                                                                           145
C    PERFORM SINGLE DIMENSION FFTS FOR X THEN Y                             146
   21 NXS= NXI-NXC                                                          147
      IF(NXI.EQ.1) GO TO 27                                                 148
      NZ=(NX-NXI)/2                                                         149
      NXYS=(NXC-1)*MX-NXO/2                                                 150
C                                                                           151
C    LOAD X VALUES IN XYFFT ARRAY                                           152
```

```
      DO 26 J=1,NYI,1                                                    153
      IF(NZ.EQ.0) GO TO 23                                               154
      DO 22 I=1,NZ,1                                                     155
      XYFFT(I)=(0.0,0.0)                                                 156
      XYFFT(I+NZ+NXI)=(0.0,0.0)                                          157
   22 CONTINUE                                                           158
   23 DO 24 I=1,NXI,1                                                    159
      XYFFT(I+NZ)=INPUT(I,J)                                             160
   24 CONTINUE                                                           161
C                                                                        162
C     PERFORM SINGLE DIMENSION FFT IN X                                  163
      CALL PWRTWO(NX,INX)                                                164
      CALL FFTA(XYFFT,INX,ISN)                                           165
C                                                                        166
C     EXTRACT OUTPUT SECTOR OF INTEREST AND STORE IN INPUT ARRAY         167
      DO 25 I=1,NXO,1                                                    168
      INPUT(I+NXS,J)=XYFFT(I+NXYS)                                       169
   25 CONTINUE                                                           170
   26 CONTINUE                                                           171
C                                                                        172
C     PERFORM NXC MAGNIFIED FFTS IN  Y AND STORE SELECTED SECTOR OF FFT  173
C    IN OUTPUT ARRAY                                                     174
   27 NZ=(NY-NYI)/2                                                      175
      NXYS=(NYC-1)*MY-NYO/2                                              176
      DO 32 I=1,NXO,1                                                    177
C                                                                        178
C     LOAD Y VALUES IN XYFFT ARRAY                                       179
      IF (NZ.EQ.0) GO TO 29                                              180
      DO 28 J=1,NZ,1                                                     181
      XYFFT(J)= (0.0,0.0)                                                182
      XYFFT(J+NZ+NYI)=(0.0,0.0)                                          183
   28 CONTINUE                                                           184
   29 DO 30 J=1,NYI,1                                                    185
      XYFFT(J+NZ)=INPUT(I+NXS,J)                                         186
   30 CONTINUE                                                           187
C                                                                        188
C     PERFORM SINGLE DIMENSION FFT IN Y                                  189
      CALL PWRTWO(NY,INY)                                                190
```

```
      CALL FFTA(XYFFT,INY,ISN)                                          191
C                                                                       192
C     EXTRACT OUTPUT SECTOR OF INTEREST AND STORE IN OUTPUT ARRAY       193
      DO 31 J=1,NYO,1                                                   194
      OUTPUT(I,J)=XYFFT(J+NXYS)                                         195
   31 CONTINUE                                                          196
   32 CONTINUE                                                          197
      RETURN                                                            198
      END                                                               199
```

```
      SUBROUTINE PWRTWO(N,I)                                                  1
      I=0                                                                     2
1     M=2**I                                                                  3
      IF (N-M) 3,5,2                                                          4
2     I=I+1                                                                   5
      GO TO 1                                                                 6
3     WRITE(6,4) N                                                            7
4     FORMAT(I15," THIS INTEGER DOES NOT EQUAL TWO RAISED TO A NON NEGA       8
     $TIVE INTEGER")                                                          9
5     RETURN                                                                 10
      END                                                                    11
```

APPENDIX A

Test Case 1 for RTFRACP

```
 TEST DATA TO TEST IBMRACP WITHOUT PLOTS (CASE I,F0,RHC,N=5)                1
F,F,F,F,T,00                                                               2
1,2,5,16.267,3.05,15.657,48.8020001,11.80285,2.                            3
5,.3,1,5.592,1522.,3,1,5,1                                                 4
.01525,6.00,.009                                                           5
.17180,2.40,.005                                                           6
.01525,6.00,.009                                                           7
.17180,2.40,.005                                                           8
.01525,6.00,.009                                                           9
3.00                                                                      10
0.                                                                        11
90.                                                                       12
0.                                                                        13
14.                                                                       14
16.                                                                       15
18.                                                                       16
20.                                                                       17
```

```
 TEST DATA TO TEST IBMRACP WITHOUT PLOTS (CASE I,F0,RHC,N=5)
 GRAF3D= F GRAFSA= F GRAFTR= F GRAFRV= F  TABLE= F

 NFINE=    1 NPHI=  2  NTHETA=  5  OSANG=  2.00

 NX,NY,NXE,NYE,NXY,MX,MY:  16  16 256   1 512  16   1
 KXMAX=KYMAX=  .65094  XY SPACING=  .76812 WAVELENGTHS
  KXM=  .65094  KYM=  .04068
 TANGENT OGIVE PARAMETERS:  ROS(IN)=150.46975 BOS(IN)=142.33625
                            FINOS=3.000 FINIS= 3.07245
1      RESULTS OF RADOME ANALYSIS
 TEST DATA TO TEST IBMRACP WITHOUT PLOTS (CASE I,F0,RHC,N=5)
 FINENESS RATIO=  3.00  DIAMETER=16.26700 IN.  LENGTH=48.80200 IN.
 FREQUENCY= 11.803 GHZ
 RA= 7.74700 IN.  RR=39.76878 IN.  ANTENNA D= 11.1840 WAVELENGTHS
 IPOL= 3  ICASE= 1  IOPT= 1

 LAYER  THICKNESS(IN.)   ER       TAND

    1       .01525     6.000    .0090
    2       .17180     2.400    .0050
    3       .01525     6.000    .0090
    4       .17180     2.400    .0050
    5       .01525     6.000    .0090


  PHI   THETA   BSEEL    BSEAZ    SLPEL      SLPAZ      GAIN
 (DEG)  (DEG)  (MRAD)   (MRAD) (DEG/DEG)  (DEG/DEG)   (DB)

   0.0    0.0    -.00      .00   0.0000     0.0000    -2.1
   0.0   14.0    4.45    -4.82    .0182     -.0197    -1.2
   0.0   16.0    4.39    -4.23   -.0018      .0168    -1.2
   0.0   18.0    4.27    -3.71   -.0033      .0148    -1.2
   0.0   20.0    4.15    -3.27   -.0036      .0128    -1.2
  90.0    0.0     .00      .00   -.0036      .0128    -2.1
  90.0   14.0    2.97     6.61    .0122      .0270    -1.3
  90.0   16.0    2.02     6.38   -.0273     -.0067    -1.2
```

90.0	18.0	1.44	6.06	-.0167	-.0091	-1.1
90.0	20.0	1.07	5.73	-.0106	-.0094	-1.0

RECEIVED SUM VOLTAGE WITHOUT RADOME= .35400E+03

APPENDIX B

Test Case 2 for RTFRACP

```
 TEST DATA TO TEST IBMRACP WITH PLOTS (CASE I,FO,RHC,N=5)                  1
F,T,T,T,F,00                                                              2
1,1,1,16.267,3.05,15.657,48.8020001,11.80285,2.                           3
5,.3,1,5.592,1522.,3,1,5,1                                                4
.01525,6.00,.009                                                          5
.17180,2.40,.005                                                          6
.01525,6.00,.009                                                          7
.17180,2.40,.005                                                          8
.01525,6.00,.009                                                          9
3.00                                                                     10
0.                                                                       11
14.                                                                      12
16.                                                                      13
18.                                                                      14
20.                                                                      15
```

TEST DATA TO TEST IBMRACP WITH PLOTS (CASE I,F0,RHC,N=5)
GRAF3D= F GRAFSA= T GRAFTR= T GRAFRV= T TABLE= F

NFINE= 1 NPHI= 1 NTHETA= 1 OSANG= 2.00

NX,NY,NXE,NYE,NXY,MX,MY: 16 16 256 1 512 16 1

ANGLE	TPERI**2		TPARI**2		RPERI**2		RPARI**2	
.92	.819	-99.2	.819	-99.2	.156	-149.9	.156	30.1
2.07	.819	-99.2	.820	-99.2	.157	-149.8	.156	30.2
3.22	.819	-99.3	.820	-99.2	.157	-149.8	.156	30.3
4.38	.819	-99.4	.821	-99.3	.157	-149.7	.155	30.4
5.53	.818	-99.5	.821	-99.4	.158	-149.6	.154	30.6
6.69	.818	-99.6	.822	-99.5	.158	-149.4	.153	30.7
7.85	.817	-99.8	.824	-99.6	.159	-149.2	.152	31.0
9.01	.816	-100.0	.825	-99.7	.160	-149.0	.151	31.2
10.18	.815	-100.3	.826	-99.9	.160	-148.8	.149	31.6
11.35	.814	-100.5	.828	-100.1	.161	-148.6	.147	31.9
12.53	.813	-100.9	.830	-100.3	.163	-148.3	.145	32.3
13.71	.812	-101.2	.832	-100.5	.164	-148.0	.143	32.7
14.89	.810	-101.6	.834	-100.8	.165	-147.6	.141	33.2
16.09	.809	-102.0	.837	-101.0	.166	-147.3	.138	33.7
17.29	.807	-102.4	.840	-101.3	.168	-146.9	.135	34.2
18.50	.806	-102.9	.843	-101.6	.170	-146.5	.132	34.8
19.72	.804	-103.4	.846	-102.0	.171	-146.0	.129	35.4
20.94	.802	-104.0	.849	-102.3	.173	-145.6	.126	36.1
22.16	.800	-104.6	.853	-102.7	.175	-145.1	.122	36.8
23.43	.798	-105.3	.857	-103.1	.177	-144.6	.118	37.6
24.69	.795	-106.0	.861	-103.5	.179	-144.0	.114	38.4
25.96	.793	-106.7	.865	-104.0	.181	-143.5	.109	39.2
27.25	.791	-107.5	.870	-104.5	.184	-142.9	.105	40.1
28.55	.788	-108.4	.874	-105.0	.186	-142.3	.100	41.1
29.87	.785	-109.3	.879	-105.6	.189	-141.7	.095	42.1
31.20	.783	-110.3	.885	-106.2	.191	-141.0	.089	43.1
32.56	.780	-111.4	.890	-106.8	.194	-140.3	.084	44.2
33.93	.777	-112.5	.895	-107.5	.197	-139.7	.078	45.4

```
35.33     .773   -113.7     .901   -108.2     .200   -138.9     .072     46.6          39
36.75     .770   -115.0     .907   -108.9     .203   -138.2     .067     47.9          40
38.20     .767   -116.4     .913   -109.7     .206   -137.5     .061     49.2          41
39.68     .763   -117.9     .918   -110.6     .209   -136.7     .055     50.6          42
41.20     .759   -119.5     .924   -111.5     .213   -136.0     .049     52.0          43
42.74     .755   -121.2     .930   -112.5     .216   -135.2     .043     53.5          44
44.33     .751   -123.1     .936   -113.6     .220   -134.4     .037     55.0          45
45.96     .747   -125.1     .941   -114.8     .224   -133.7     .031     56.6          46
47.64     .742   -127.3     .946   -116.1     .228   -132.9     .026     58.3          47
49.38     .737   -129.7     .951   -117.5     .233   -132.2     .021     60.1          48
51.18     .731   -132.3     .956   -119.1     .237   -131.4     .016     61.9          49
53.05     .725   -135.1     .960   -120.8     .243   -130.8     .012     63.8          50
55.01     .718   -138.3     .963   -122.8     .249   -130.1     .009     65.8          51
57.07     .710   -141.9     .966   -125.0     .256   -129.6     .006     67.9          52
59.25     .700   -145.9     .969   -127.5     .265   -129.2     .003     70.3          53
61.58     .688   -150.4     .970   -130.4     .275   -128.9     .002     73.4          54
64.11     .672   -155.8     .971   -133.8     .290   -128.9     .001     78.5          55
66.88     .649   -162.2     .971   -137.8     .310   -129.3     .000    101.1          56
70.01     .616   -170.3     .970   -142.7     .341   -130.5     .000   -128.0          57
73.71     .558    178.8     .967   -149.1     .395   -133.0     .001   -116.9          58
78.50     .436    161.4     .959   -158.3     .514   -139.4     .001   -117.0          59
90.00   0.000   -180.0     0.000   -180.0     .894   -156.6     .072   -124.4          60
                                                                                       61
                                                                                       62
TABLE OF XMN COEF. IS FORMED                                                           63
                                                                                       64
                                                                                       65
KXMAX=KYMAX=   .65094   XY SPACING=   .76812 WAVELENGTHS                               66
 KXM=   .65094   KYM=   .04068                                                        67
                                                                                       68
                                                                                       69
 SUBROUTINE NORM:  MIN=   0.          MAX=    .100E+01                                 70
                                                                                       71
                                                                                       72
                                                                                       73
                                                                                       74
 SUBROUTINE NORM:  MIN=   0.          MAX=    .100E+01                                 75
                                                                                       76
```

```
 IPOWER OF PATTERN= 1

  SUBROUTINE NORM:  MIN=  0.          MAX=    .100E+01

  SUBROUTINE NORM:  MIN=  0.          MAX=    .100E+01

  SUBROUTINE NORM:  MIN=  0.          MAX=    .100E+01

  SUBROUTINE NORM:  MIN=  0.          MAX=    .100E+01

 TANGENT OGIVE PARAMETERS:  ROS(IN)=150.46975 BOS(IN)=142.33625
                            FINOS=3.000 FINIS= 3.07245
1      RESULTS OF RADOME ANALYSIS
 TEST DATA TO TEST IBMRACF WITH PLOTS (CASE I,F0,RHC,N=5)
 FINENESS RATIO=  3.00  DIAMETER=16.26700 IN.  LENGTH=48.80200 IN.
 FREQUENCY= 11.803 GHZ
 RA= 7.74700 IN.  RR=39.76878 IN.  ANTENNA D= 11.1840 WAVELENGTHS
 IPOL= 3  ICASE= 1  ICPT= 1

 LAYER  THICKNESS(IN.)   ER      TAND

    1       .01525     6.000    .0090
    2       .17180     2.400    .0050
    3       .01525     6.000    .0090
    4       .17180     2.400    .0050
    5       .01525     6.000    .0090
```

```
 PHI   THETA   BSEEL    BSEAZ    SLPEL      SLPAZ      GAIN
(DEG) (DEG)   (MRAD)   (MRAD) (DEG/DEG)  (DEG/DEG)   (DB)



RECEIVING PATTERN COMPUTED FOR:
  ICUT=   1
 ICOMP=   1
  KMAX=     .651
  NREC=      32
    DK=    .40684E-01
ANGMAX=   40.61
(ICUT=1 FOR EL CUT, =2 FOR AZ CUT
(ICOMP=1 FOR EL COMPONENT, =2 FOR AZIMUTH)



RECEIVING PATTERN COMPUTED FOR:
  ICUT=   1
 ICOMP=   1
  KMAX=     .651
  NREC=      32
    DK=    .40684E-01
ANGMAX=   40.61
(ICUT=1 FOR EL CUT, =2 FOR AZ CUT
(ICOMP=1 FOR EL COMPONENT, =2 FOR AZIMUTH)



MIN AND MAX VALUES OF REC'G PATTERN:



 SUBROUTINE NORM:  MIN=    .450E-03   MAX=    .146E+04
```

REC"G PATTERN, EL CUT, EL COMP (DB):

-39.5	-39.621	2.8
-38.0	-37.725	28.1
-36.5	-35.089	43.8
-35.1	-34.174	48.7
-33.7	-37.001	48.1
-32.3	-40.000	6.7
-30.9	-36.564	-129.0
-29.6	-31.693	-134.5
-28.2	-31.087	-140.6
-26.9	-33.941	-150.6
-25.6	-40.000	172.7
-24.3	-39.726	64.3
-23.1	-36.316	45.1
-21.8	-40.000	34.8
-20.5	-40.000	-143.9
-19.3	-30.439	-150.9
-18.1	-27.703	-155.2
-16.9	-29.545	-158.3
-15.6	-40.000	-163.7
-14.4	-28.379	19.6
-13.2	-22.832	19.5
-12.0	-22.511	21.4
-10.8	-29.557	34.4
-9.7	-25.875	-177.6
-8.5	-17.361	-167.1
-7.3	-15.087	-162.4
-6.1	-17.991	-155.1
-5.0	-26.575	-16.2
-3.8	-10.558	14.1
-2.6	-4.613	19.0
-1.5	-1.520	22.3
-.3	-.154	25.5
.9	-.175	28.9
2.0	-1.523	32.9
3.2	-4.353	38.6

4.4	-9.173	48.2	191
5.5	-17.241	74.3	192
6.7	-21.965	161.0	193
7.9	-19.100	-159.4	194
9.1	-20.684	-141.1	195
10.3	-27.131	-111.0	196
11.4	-29.660	-13.7	197
12.6	-24.951	22.6	198
13.8	-25.182	38.5	199
15.0	-29.936	59.3	200
16.2	-36.905	144.5	201
17.5	-30.525	-158.1	202
18.7	-29.242	-142.8	203
19.9	-32.625	-130.5	204
21.2	-40.000	-84.0	205
22.4	-37.897	30.3	206
23.7	-35.771	47.6	207
25.0	-40.000	75.8	208
26.3	-39.654	-161.4	209
27.6	-32.550	-140.9	210
28.9	-30.924	-134.2	211
30.2	-33.116	-129.7	212
31.6	-40.000	-118.6	213
33.0	-40.000	38.0	214
34.4	-34.909	46.0	215
35.8	-34.916	46.6	216
37.2	-38.169	37.5	217
38.7	-40.000	8.0	218
40.2	-40.000	-9.5	219

220

MIN AND MAX VALUES OF REC"G PATTERN:

221
222
223
224

SUBROUTINE NORM: MIN= .161E-03 MAX= .736E+03

225
226
227
228

REC"G PATTERN, EL CUT, EL COMP (DB):

			229
			230
-39.5	-40.000	-17.5	231
-38.0	-35.637	-10.4	232
-36.5	-36.309	-1.6	233
-35.1	-40.000	28.2	234
-33.7	-40.000	95.4	235
-32.3	-38.291	103.4	236
-30.9	-40.000	50.5	237
-29.6	-31.965	-16.0	238
-28.2	-25.426	-31.2	239
-26.9	-22.047	-37.8	240
-25.6	-20.687	-42.1	241
-24.3	-20.852	-44.7	242
-23.1	-22.151	-44.8	243
-21.8	-23.656	-41.1	244
-20.5	-23.525	-37.4	245
-19.3	-21.046	-40.4	246
-18.1	-17.659	-46.9	247
-16.9	-14.780	-52.2	248
-15.6	-13.038	-55.1	249
-14.4	-12.690	-55.0	250
-13.2	-13.901	-50.9	251
-12.0	-16.570	-39.9	252
-10.8	-19.217	-23.4	253
-9.7	-19.064	-26.9	254
-8.5	-14.123	-50.7	255
-7.3	-8.073	-61.9	256
-6.1	-3.685	-64.7	257
-5.0	-1.040	-64.2	258
-3.8	-.005	-61.9	259
-2.6	-.660	-57.8	260
-1.5	-3.545	-49.6	261
-.3	-10.383	-20.5	262
.9	-9.741	76.4	263
2.0	-3.403	102.3	264
3.2	-.784	111.1	265
4.4	-.199	116.8	266

```
      5.5        -1.076     121.8                                        267
      6.7        -3.200     126.7                                        268
      7.9        -6.451     131.6                                        269
      9.1       -10.550     135.1                                        270
     10.3       -14.470     133.3                                        271
     11.4       -15.973     124.7                                        272
     12.6       -14.762     119.7                                        273
     13.8       -13.182     121.0                                        274
     15.0       -12.485     124.8                                        275
     16.2       -12.967     129.2                                        276
     17.5       -14.648     133.6                                        277
     18.7       -17.376     137.2                                        278
     19.9       -20.548     138.5                                        279
     21.2       -22.648     135.9                                        280
     22.4       -22.415     132.6                                        281
     23.7       -20.995     132.7                                        282
     25.0       -20.057     135.1                                        283
     26.3       -20.405     138.6                                        284
     27.6       -22.482     142.9                                        285
     28.9       -26.958     149.2                                        286
     30.2       -35.698     166.2                                        287
     31.6       -40.000     -99.7                                        288
     33.0       -40.000     -77.8                                        289
     34.4       -40.000    -152.0                                        290
     35.8       -37.149     160.7                                        291
     37.2       -34.461     155.7                                        292
     38.7       -36.684     157.7                                        293
     40.2       -40.000     168.2                                        294
                                                                         295
RECEIVING PATTERN COMPUTED FOR:                                          296
  ICUT=  2                                                               297
 ICOMP=  1                                                               298
  KMAX=    .651                                                          299
  NREC=    32                                                            300
    DK=   .40684E-01                                                     301
ANGMAX=  40.61                                                           302
(ICUT=1 FOR EL CUT, =2 FOR AZ CUT                                        303
(ICOMP=1 FOR EL COMPONENT, =2 FOR AZIMUTH)                               304
```

```
RECEIVING PATTERN COMPUTED FOR:
  ICUT=  2
 ICOMP=  1
  KMAX=    .651
  NREC=    32
    DK=   .40684E-01
ANGMAX=  40.61
(ICUT=1 FOR EL CUT, =2 FOR AZ CUT
(ICOMP=1 FOR EL COMPONENT, =2 FOR AZIMUTH)


MIN AND MAX VALUES OF REC"G PATTERN:


 SUBROUTINE NORM:  MIN=   .571E-03  MAX=   .146E+04


REC"G PATTERN, AZ CUT,EL COMP (DB):

   -39.5      -40.000      31.5
   -38.0      -36.745      49.9
   -36.5      -33.491      59.4
   -35.1      -33.713      62.9
   -33.7      -39.057      64.0
   -32.3      -40.000    -127.1
   -30.9      -34.787    -122.0
   -29.6      -31.082    -121.7
   -28.2      -31.410    -122.9
   -26.9      -36.733    -131.5
   -25.6      -40.000     120.7
   -24.3      -37.454      77.6
   -23.1      -39.335      75.8
```

-21.8	-40.000	-160.1	343
-20.5	-32.176	-132.3	344
-19.3	-28.247	-128.6	345
-18.1	-28.970	-126.6	346
-16.9	-30.666	-122.6	347
-15.6	-32.046	47.8	348
-14.4	-24.938	47.3	349
-13.2	-23.864	46.3	350
-12.0	-29.007	48.4	351
-10.8	-31.981	-147.4	352
-9.7	-20.749	-140.9	353
-8.5	-17.851	-140.1	354
-7.3	-20.216	-138.3	355
-6.1	-31.144	4.8	356
-5.0	-12.630	28.5	357
-3.8	-6.112	28.9	358
-2.6	-2.513	28.3	359
-1.5	-.605	27.3	360
-.3	0.000	26.5	361
.9	-.617	25.9	362
2.0	-2.576	26.0	363
3.2	-6.224	27.7	364
4.4	-12.452	35.5	365
5.5	-22.048	87.6	366
6.7	-18.055	158.2	367
7.9	-15.815	171.5	368
9.1	-17.121	179.9	369
10.3	-21.503	-165.5	370
11.4	-28.414	-125.7	371
12.6	-30.506	-58.8	372
13.8	-30.374	-17.0	373
15.0	-31.544	23.4	374
16.2	-33.250	72.8	375
17.5	-33.509	135.4	376
18.7	-32.031	-178.3	377
19.9	-33.585	-148.9	378
21.2	-39.613	-119.4	379
22.4	-40.000	-88.6	380

```
     23.7        -40.000    -148.2                                          381
     25.0        -40.000    -146.2                                          382
     26.3        -40.000    -147.3                                          383
     27.6        -36.203    -153.3                                          384
     28.9        -31.588    -152.3                                          385
     30.2        -31.347    -149.9                                          386
     31.6        -37.585    -150.3                                          387
     33.0        -40.000      45.5                                          388
     34.4        -35.293      36.6                                          389
     35.8        -33.897      33.4                                          390
     37.2        -34.787      32.0                                          391
     38.7        -37.285      30.8                                          392
     40.2        -40.000      25.7                                          393
                                                                            394
 MIN AND MAX VALUES OF REC"G PATTERN:                                       395
                                                                            396
                                                                            397
                                                                            398
  SUBROUTINE NORM:  MIN=    .125E-02   MAX=    .699E+03                     399
                                                                            400
                                                                            401
                                                                            402
 REC"G PATTERN, AZ CUT,EL COMP (DB):                                        403
                                                                            404
    -39.5       -39.781    -10.5                                           405
    -38.0       -36.284     -5.7                                           406
    -36.5       -39.216      2.5                                           407
    -35.1       -40.000     72.5                                           408
    -33.7       -39.142    129.5                                           409
    -32.3       -39.306    137.4                                           410
    -30.9       -40.000    -13.7                                           411
    -29.6       -29.812    -26.8                                           412
    -28.2       -23.835    -28.1                                           413
    -26.9       -21.102    -30.5                                           414
    -25.6       -20.375    -33.3                                           415
    -24.3       -21.155    -35.9                                           416
    -23.1       -22.714    -39.1                                           417
    -21.8       -23.300    -43.2                                           418
```

-20.5	-21.372	-44.7	419
-19.3	-18.037	-43.3	420
-18.1	-14.997	-42.5	421
-16.9	-13.069	-42.9	422
-15.6	-12.335	-44.1	423
-14.4	-13.077	-45.6	424
-13.2	-15.083	-47.8	425
-12.0	-17.250	-51.6	426
-10.8	-16.774	-55.0	427
-9.7	-12.809	-55.3	428
-8.5	-8.035	-55.0	429
-7.3	-4.123	-55.5	430
-6.1	-1.473	-56.4	431
-5.0	-.147	-57.4	432
-3.8	-.227	-58.3	433
-2.6	-2.054	-58.8	434
-1.5	-7.006	-57.4	435
-.3	-26.585	22.1	436
.9	-7.098	108.3	437
2.0	-2.131	110.2	438
3.2	-.356	110.4	439
4.4	-.283	110.5	440
5.5	-1.439	111.3	441
6.7	-3.632	114.1	442
7.9	-6.678	121.3	443
9.1	-9.961	134.4	444
10.3	-12.522	146.9	445
11.4	-14.364	145.5	446
12.6	-15.044	128.4	447
13.8	-14.188	113.0	448
15.0	-13.406	108.0	449
16.2	-13.404	108.8	450
17.5	-14.140	111.6	451
18.7	-15.562	116.0	452
19.9	-17.667	121.9	453
21.2	-20.314	124.7	454
22.4	-22.486	115.0	455
23.7	-22.146	101.8	456

```
     25.0        -20.919     103.5                                          457
     26.3        -20.650     113.3                                          458
     27.6        -21.995     120.8                                          459
     28.9        -25.783     121.1                                          460
     30.2        -33.923     113.7                                          461
     31.6        -40.000     -64.9                                          462
     33.0        -37.120     -77.1                                          463
     34.4        -40.000     -82.0                                          464
     35.8        -40.000     145.0                                          465
     37.2        -37.488     140.8                                          466
     38.7        -38.234     153.6                                          467
     40.2        -40.000     171.1                                          468
NUMBER OF RAYS USED IN COMPUTING APERTURE FIELD =        177                469
NUMBER OF RAYS USED IN COMPUTING APERTURE FIELD =        177                470
NUMBER OF RAYS USED IN COMPUTING APERTURE FIELD =        177                471
NUMBER OF RAYS USED IN COMPUTING APERTURE FIELD =        177                472
NUMBER OF RAYS USED IN COMPUTING APERTURE FIELD =        177                473
                                                                            474
                                                                            475
FINAL ANSWERS FOR MONOPULSE SYSTEM:                                         476
                                                                            477
K1:  -.49509E-02  .44512E-02  .99998E+00                                    478
K2:  -.48156E-02  .46031E-02  .99998E+00                                    479
                                                                            480
AZTM=  -.48156E+01 MRAD                                                     481
ELTM=   .44513E+01 MRAD                                                     482
                                                                            483
MESAZ=   .27700E+00 VOLTS/DEG                                               484
MESEL=   .28484E+00 VOLTS/DEG                                               485
                                                                            486
UAZ:  -.21485E-02  .16656E-04                                               487
UEL:   .48346E-05  .24790E-02                                               488
                                                                            489
SMAX=   .30726299056550E+03     LCTR=   3                                   490
                                                                            491
                                                                            492
                                                                            493
                                                                            494
```

```
ADDITIONAL MONOPULSE OUTPUTS AROUND BORESIGHT:                                  495
                                                                                496
                                                                                497
NUMBER OF RAYS USED IN COMPUTING APERTURE FIELD =       177                     498
ANG=  -3.0 MRAD FROM BORESIGHT    VRAZ=  -.45076E-01 VOLTS    VREL=  -.47809E-01 VOLTS
                                                                                500
DAZ(AMP,PHS)=   .55030E-01 -.54996E+02   DEL(AMP,PHS)=   .15714E+00 -.17713E+02
                                                                                502
NUMBER OF RAYS USED IN COMPUTING APERTURE FIELD =       177                     503
ANG=  -2.0 MRAD FROM BORESIGHT    VRAZ=  -.30037E-01 VOLTS    VREL=  -.31850E-01 VOLTS
                                                                                505
DAZ(AMP,PHS)=   .43727E-01 -.43387E+02   DEL(AMP,PHS)=   .15338E+00 -.11985E+02
                                                                                507
NUMBER OF RAYS USED IN COMPUTING APERTURE FIELD =       177                     508
ANG=  -1.0 MRAD FROM BORESIGHT    VRAZ=  -.15009E-01 VOLTS    VREL=  -.15916E-01 VOLTS
                                                                                510
DAZ(AMP,PHS)=   .35359E-01 -.25118E+02   DEL(AMP,PHS)=   .15128E+00 -.60391E+01
                                                                                512
NUMBER OF RAYS USED IN COMPUTING APERTURE FIELD =       177                     513
ANG=   0.0 MRAD FROM BORESIGHT    VRAZ=   .16656E-04 VOLTS    VREL=   .48346E-05 VOLTS
                                                                                515
DAZ(AMP,PHS)=   .32280E-01  .29564E-01   DEL(AMP,PHS)=   .15091E+00  .18355E-02
                                                                                517
NUMBER OF RAYS USED IN COMPUTING APERTURE FIELD =       177                     518
ANG=   1.0 MRAD FROM BORESIGHT    VRAZ=   .15049E-01 VOLTS    VREL=   .15921E-01 VOLTS
                                                                                520
DAZ(AMP,PHS)=   .35880E-01  .24798E+02   DEL(AMP,PHS)=   .15227E+00  .60018E+01
                                                                                522
NUMBER OF RAYS USED IN COMPUTING APERTURE FIELD =       177                     523
ANG=   2.0 MRAD FROM BORESIGHT    VRAZ=   .30097E-01 VOLTS    VREL=   .31843E-01 VOLTS
                                                                                525
DAZ(AMP,PHS)=   .44582E-01  .42461E+02   DEL(AMP,PHS)=   .15531E+00  .11831E+02
                                                                                527
NUMBER OF RAYS USED IN COMPUTING APERTURE FIELD =       177                     528
ANG=   3.0 MRAD FROM BORESIGHT    VRAZ=   .45169E-01 VOLTS    VREL=   .47779E-01 VOLTS
                                                                                530
DAZ(AMP,PHS)=   .56180E-01  .53653E+02   DEL(AMP,PHS)=   .15996E+00  .17379E+02
                                                                                532
```

```
AVERAGE SLPAZ=    .26249E+00 VOLTS/DEG
AVERAGE SLPEL=    .27803E+00 VOLTS/DEG
 SUM=1.0 VOLT


  0.0  14.0     4.45    -4.82    0.0000     0.0000    -1.2


RECEIVED SUM VOLTAGE WITHOUT RADOME=   .35400E+03
```

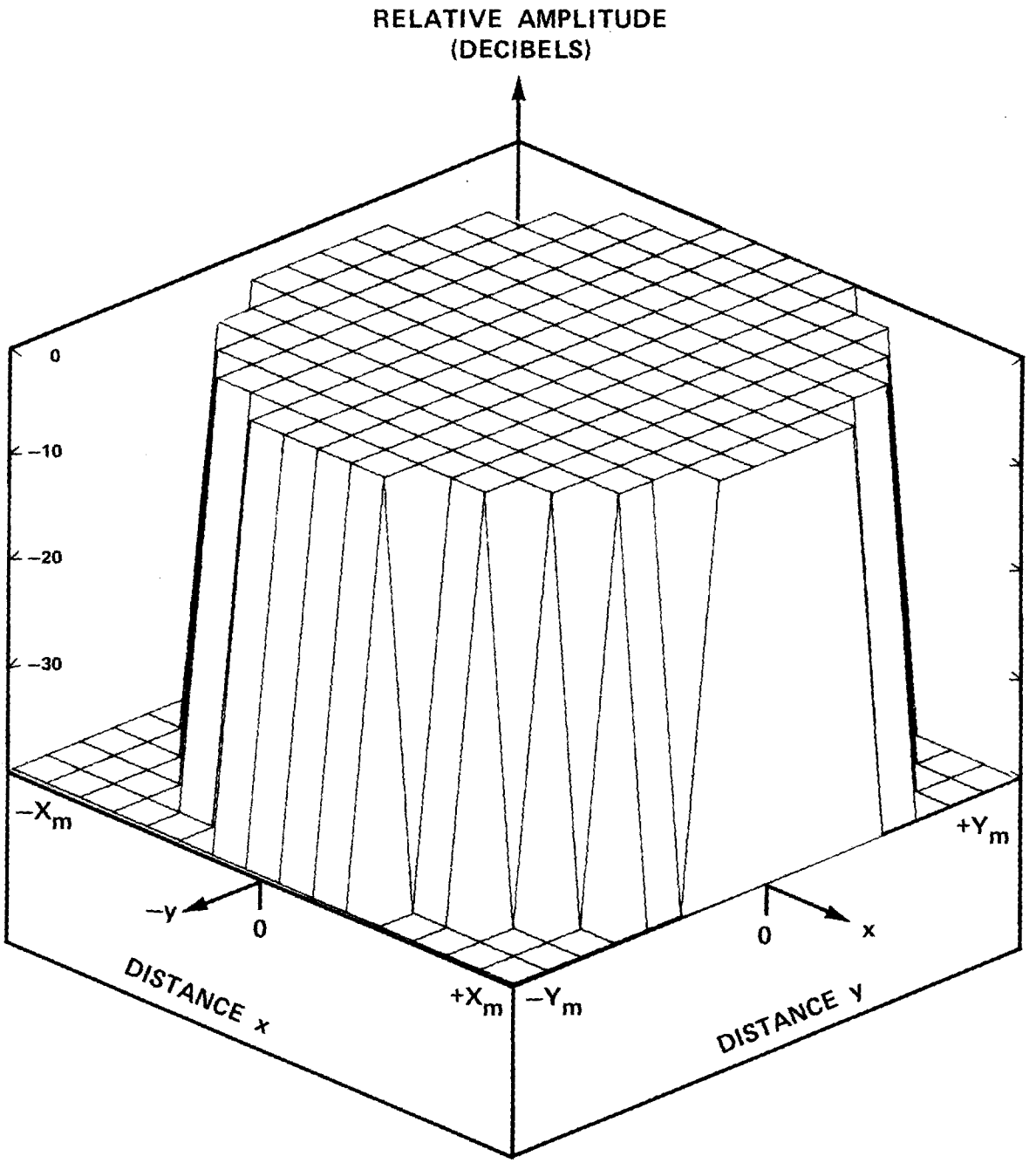

Figure B-1. $|E_{x\Sigma}|$ or $|E_{y\Sigma}|$ of the RHC (ICASE=1) Antenna.

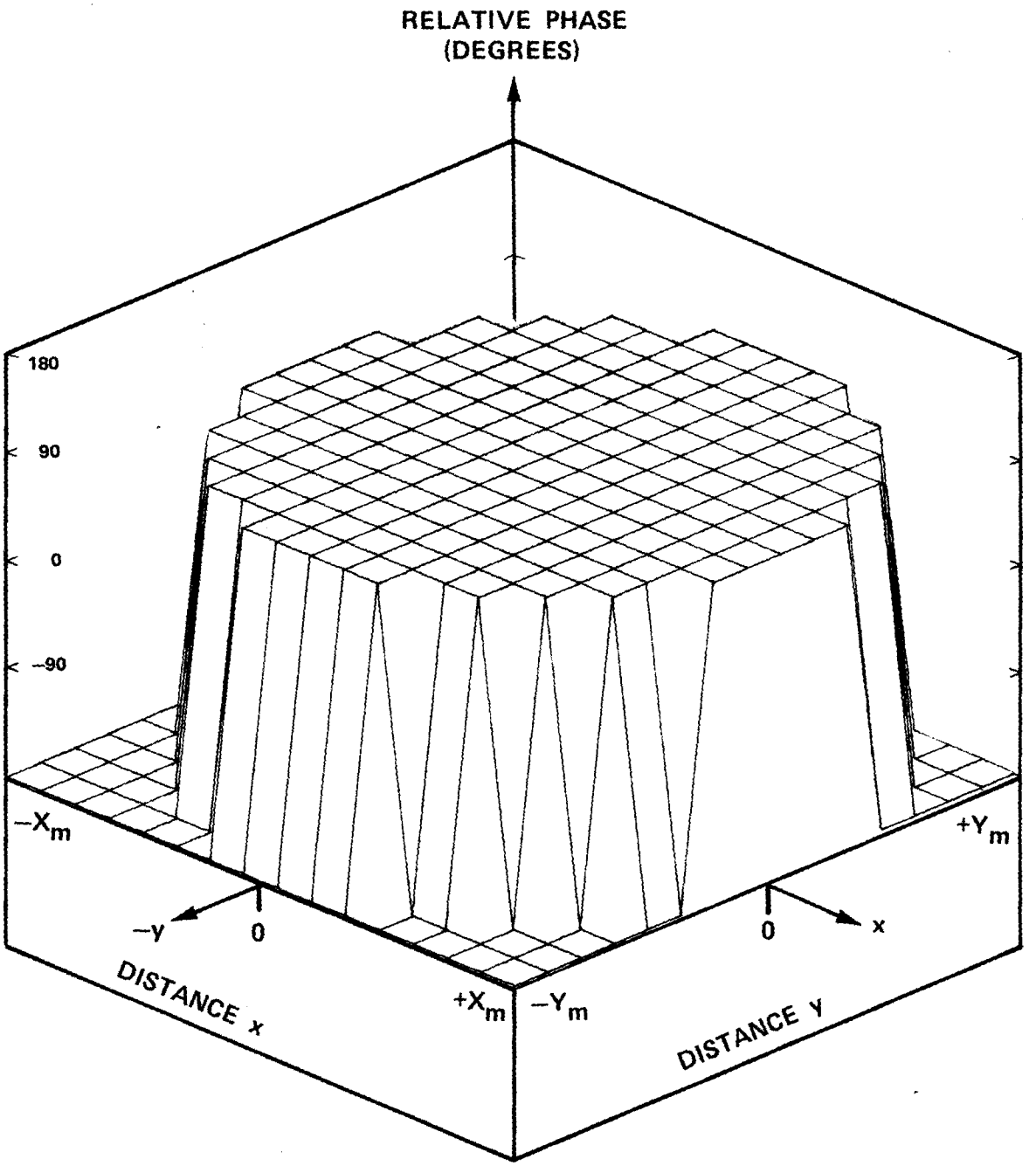

Figure B-2. Phase of $E_{x\Sigma}$ for RHC (ICASE=1) Antenna.

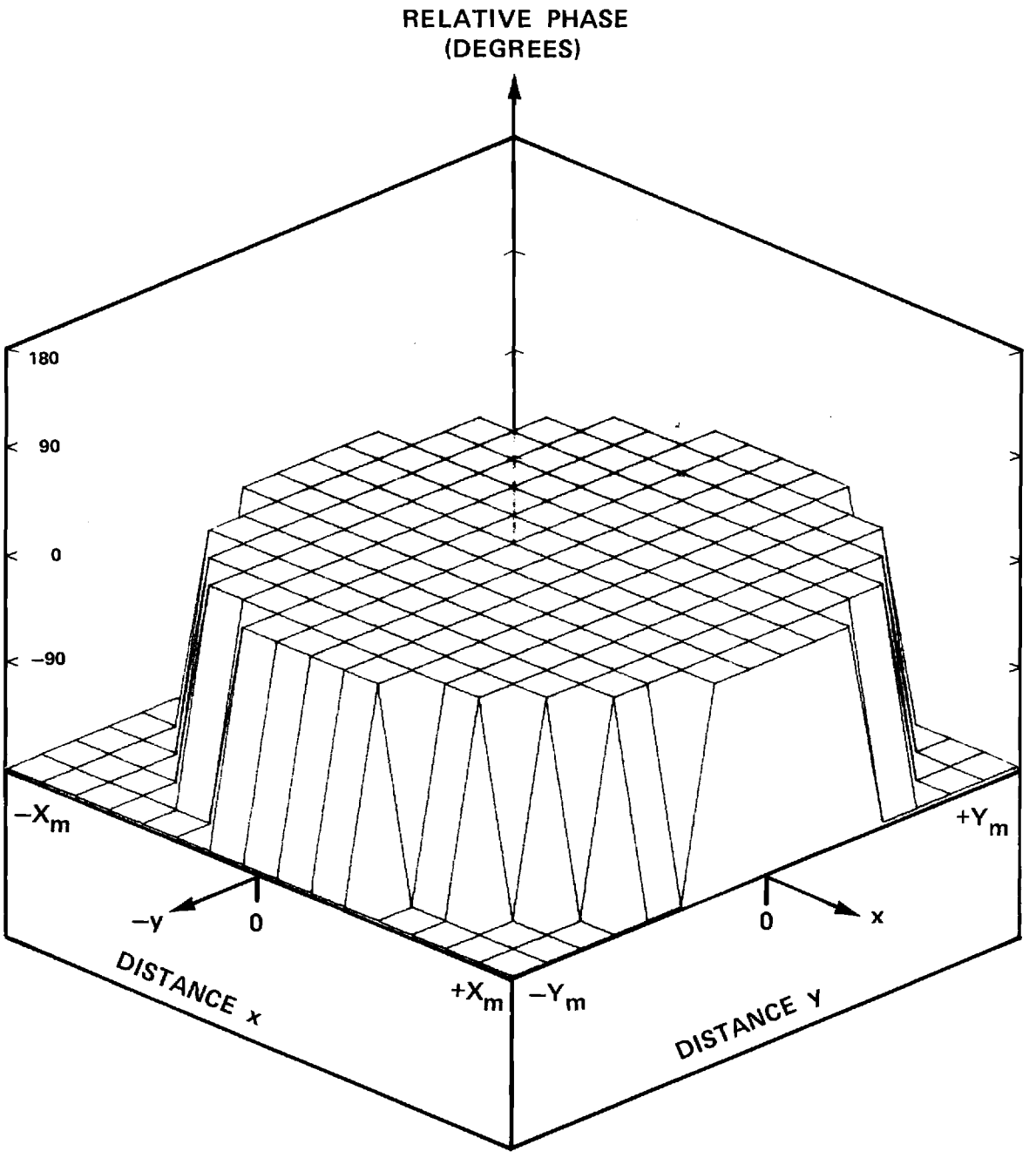

Figure B-3. Phase of $E_{y\Sigma}$ for RHC Antenna.

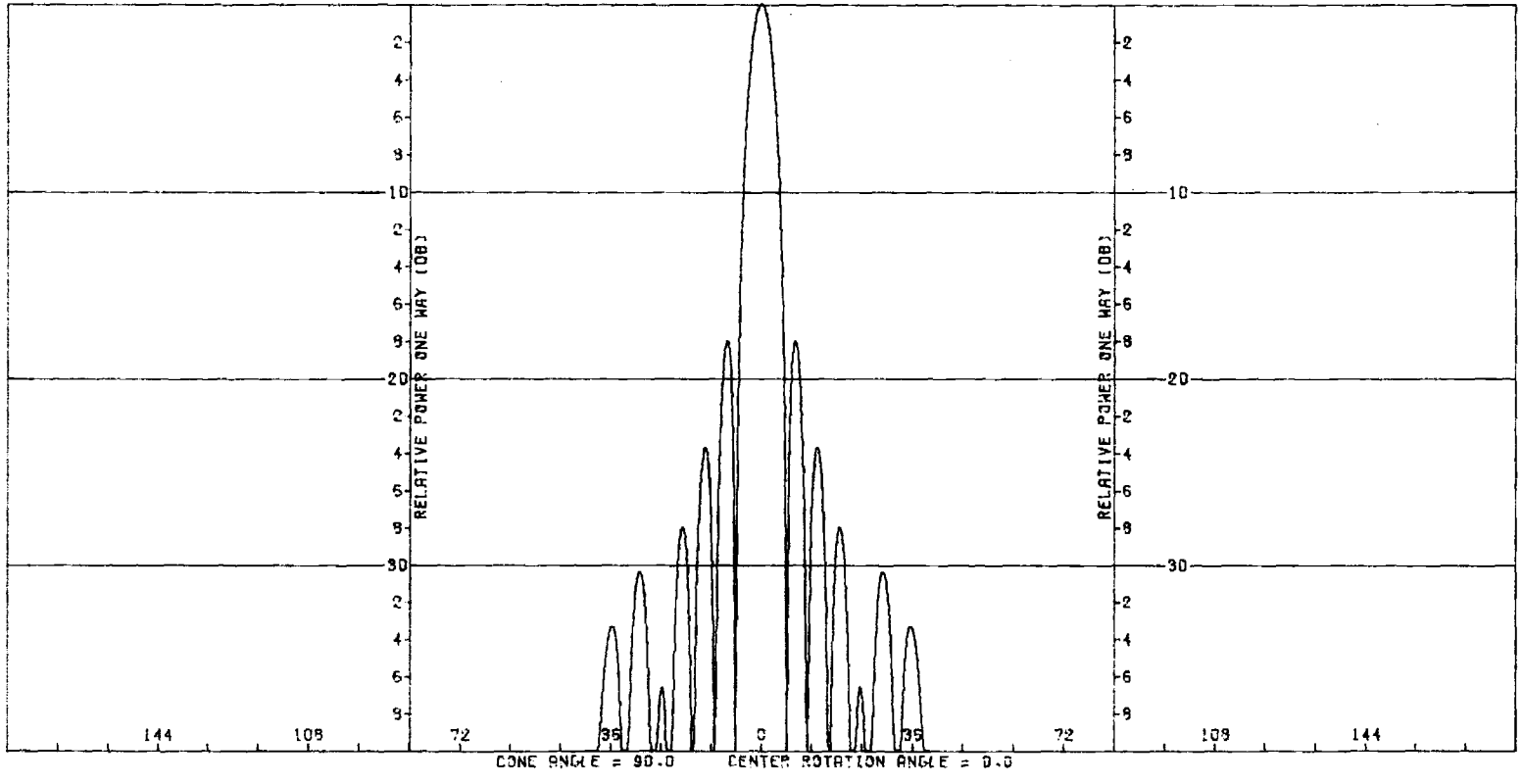

Figure B-4. Transmitting E-Plane Σ Pattern of RHC Antenna Without Radome.

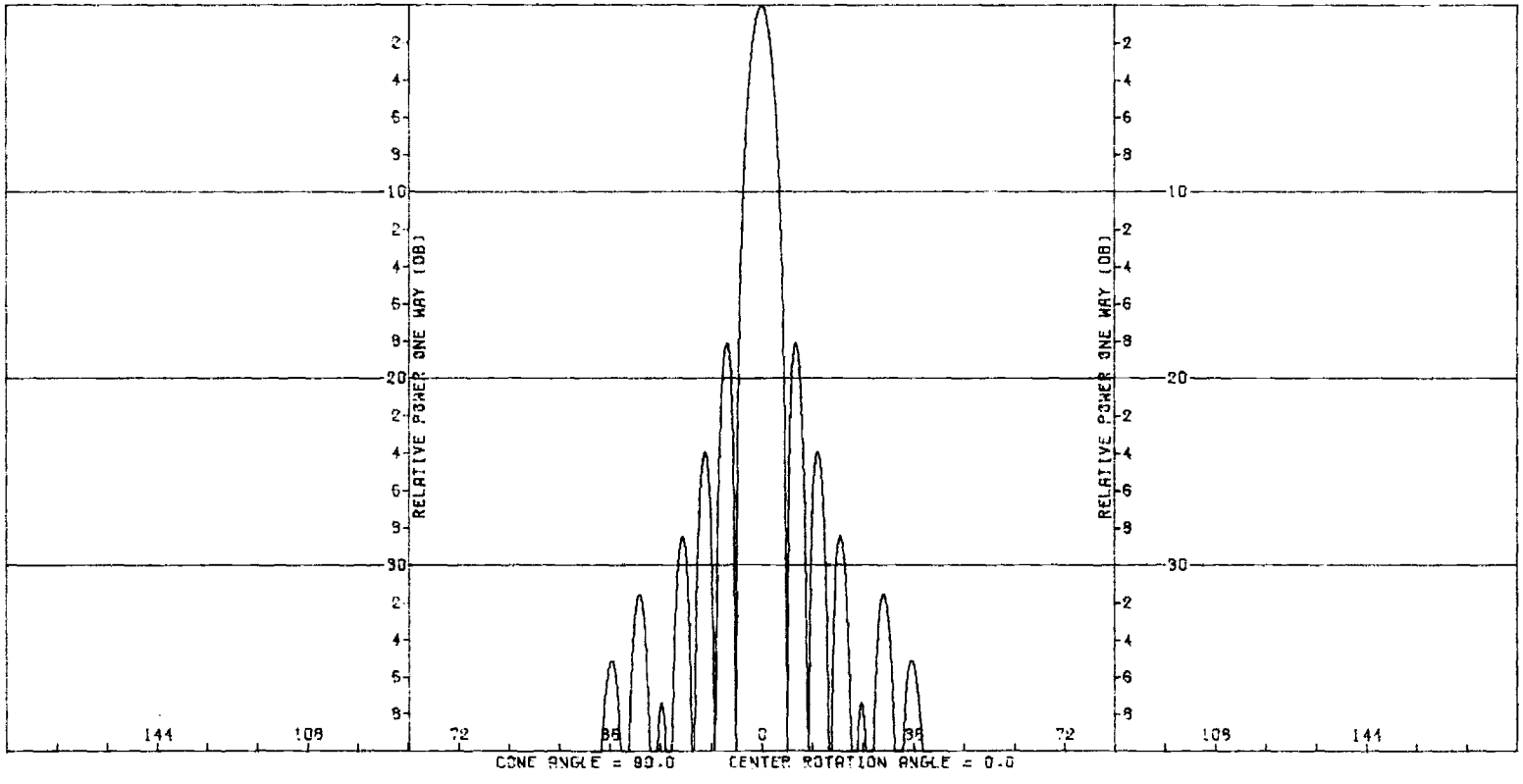

Figure B-5. Transmitting H-Plane Σ Pattern of RHC Antenna Without Radome.

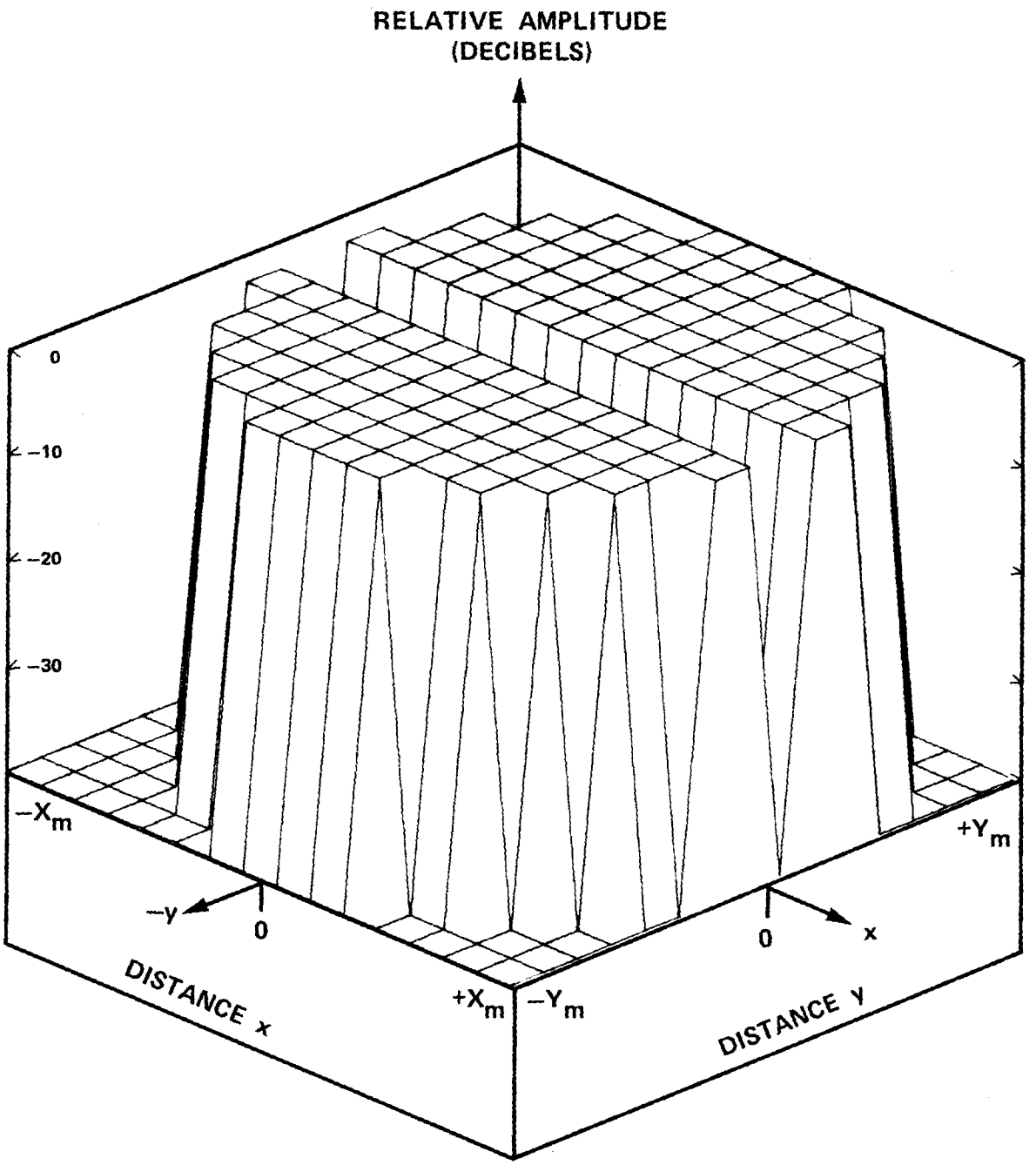

Figure B-6. $|E_x|_{\Delta EL}$ or $|E_y|_{\Delta EL}$ of RHC Antenna.

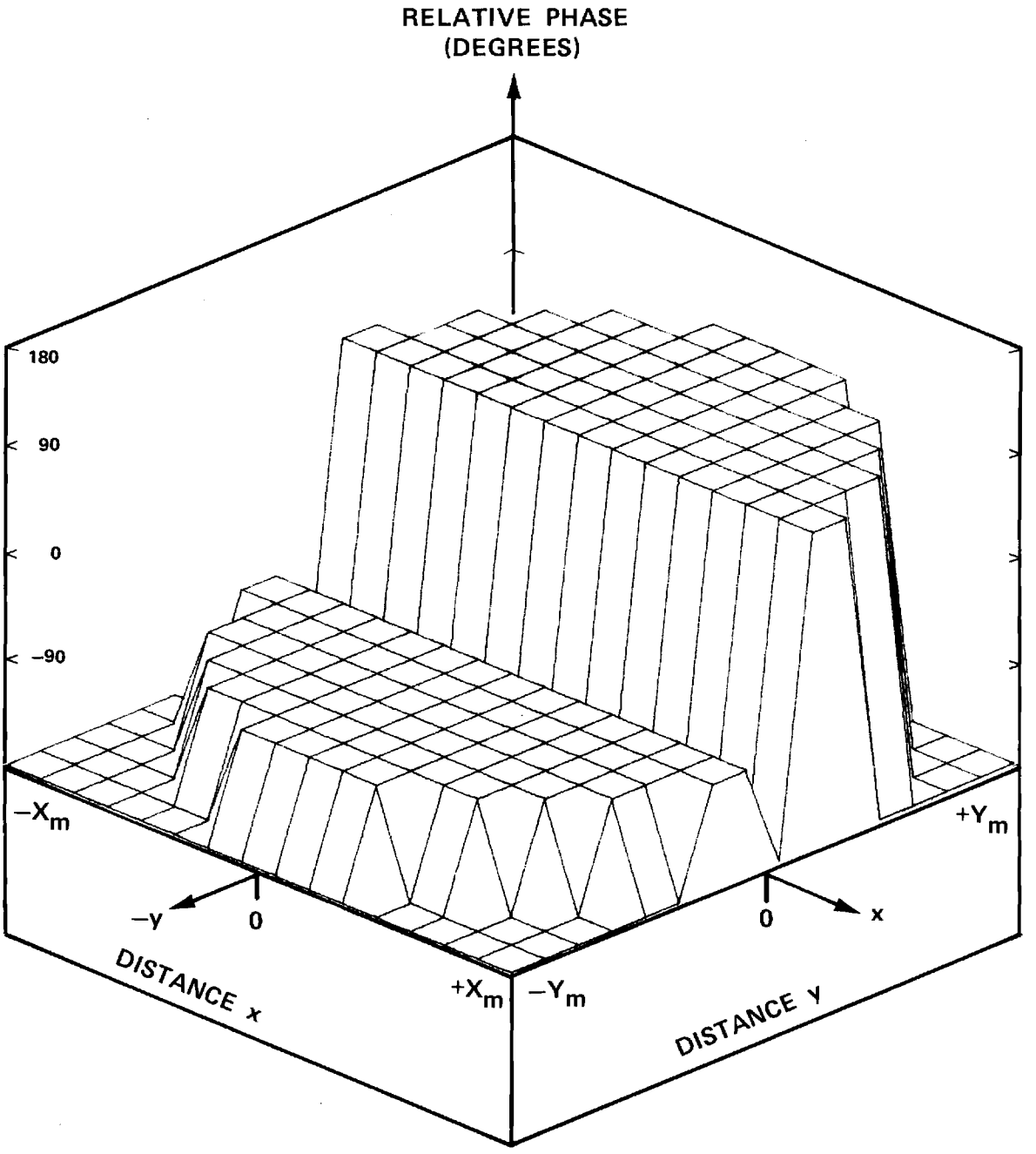

Figure B-7. Phase of $E_{x\Delta EL}$ of RHC Antenna.

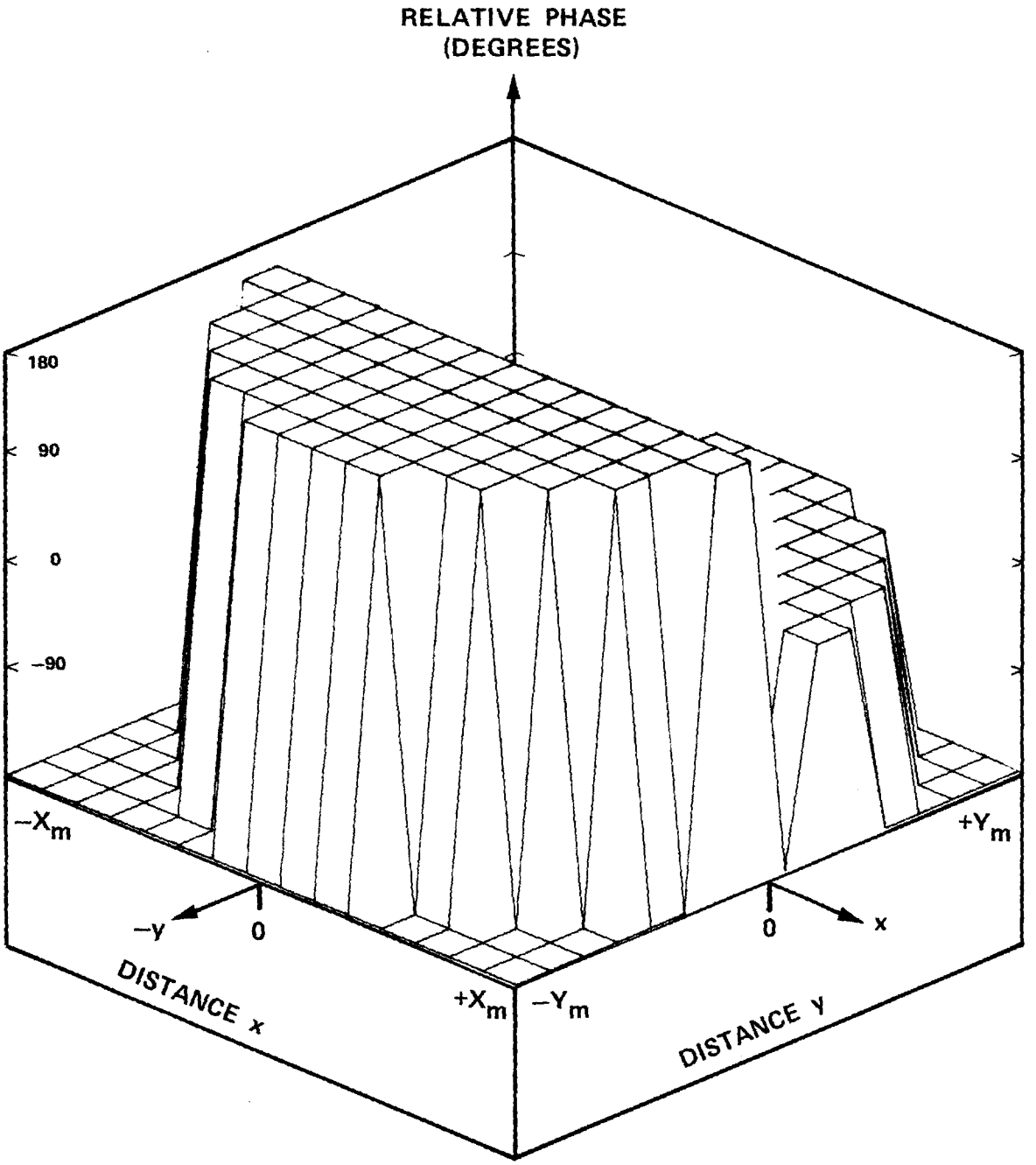

Figure B-8. Phase of $E_{y\Delta EL}$ of RHC Antenna.

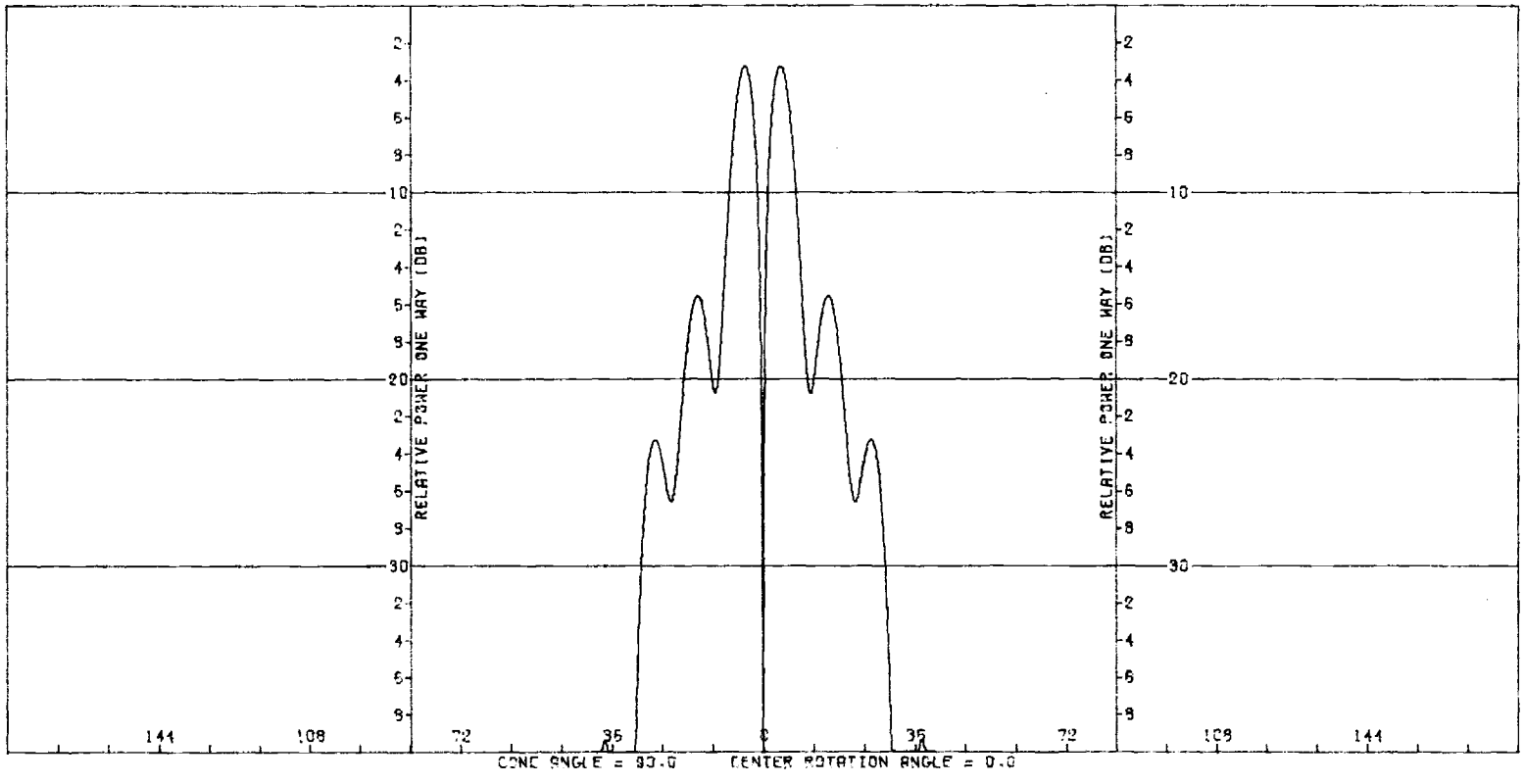

Figure B-9. Transmitting E-Plane Δ_{EL} Pattern of RHC Antenna Without Radome.

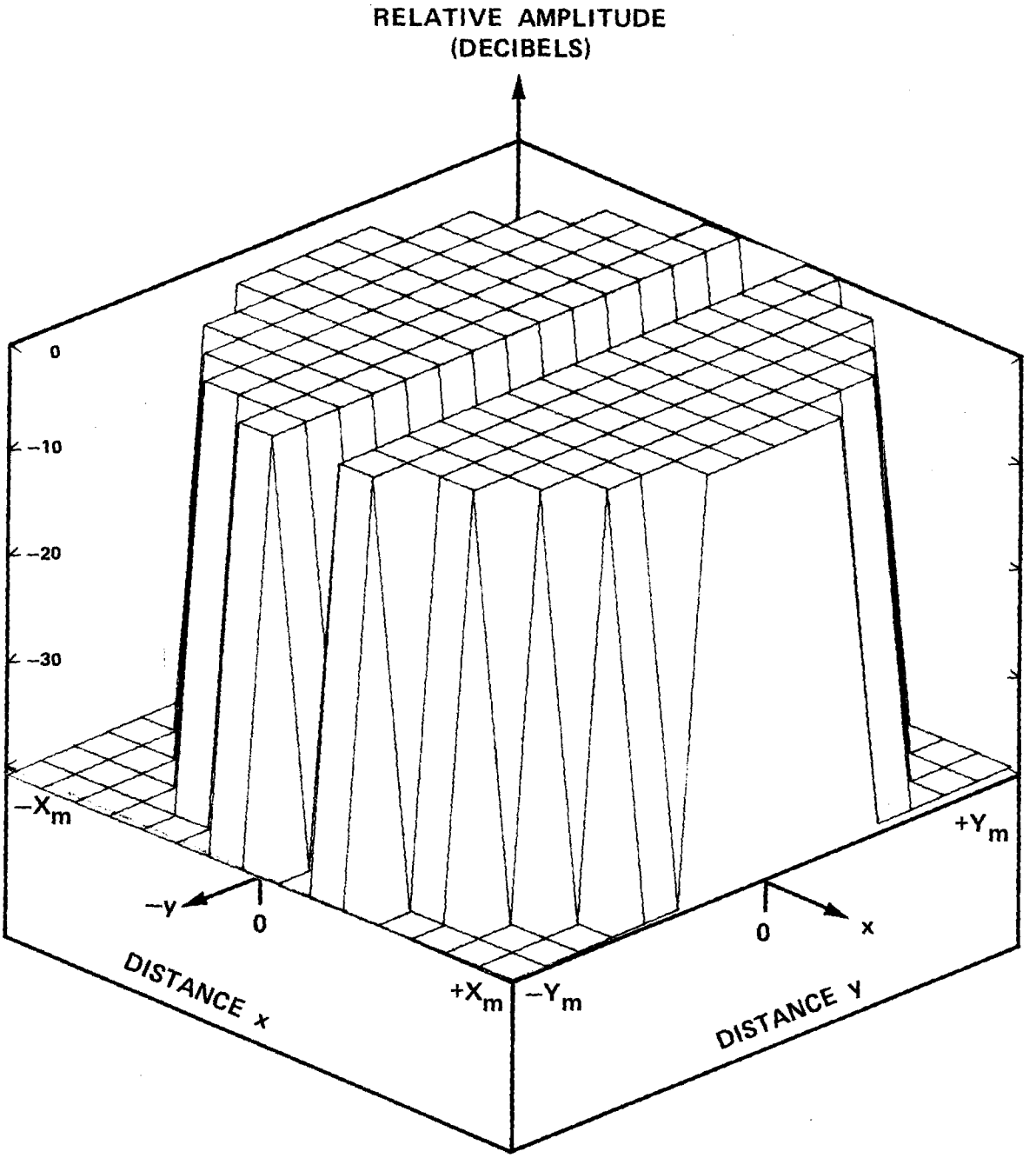

Figure B-10. $|E_x|_{\Delta AZ}$ or $|E_y|_{\Delta AZ}$ of RHC Antenna.

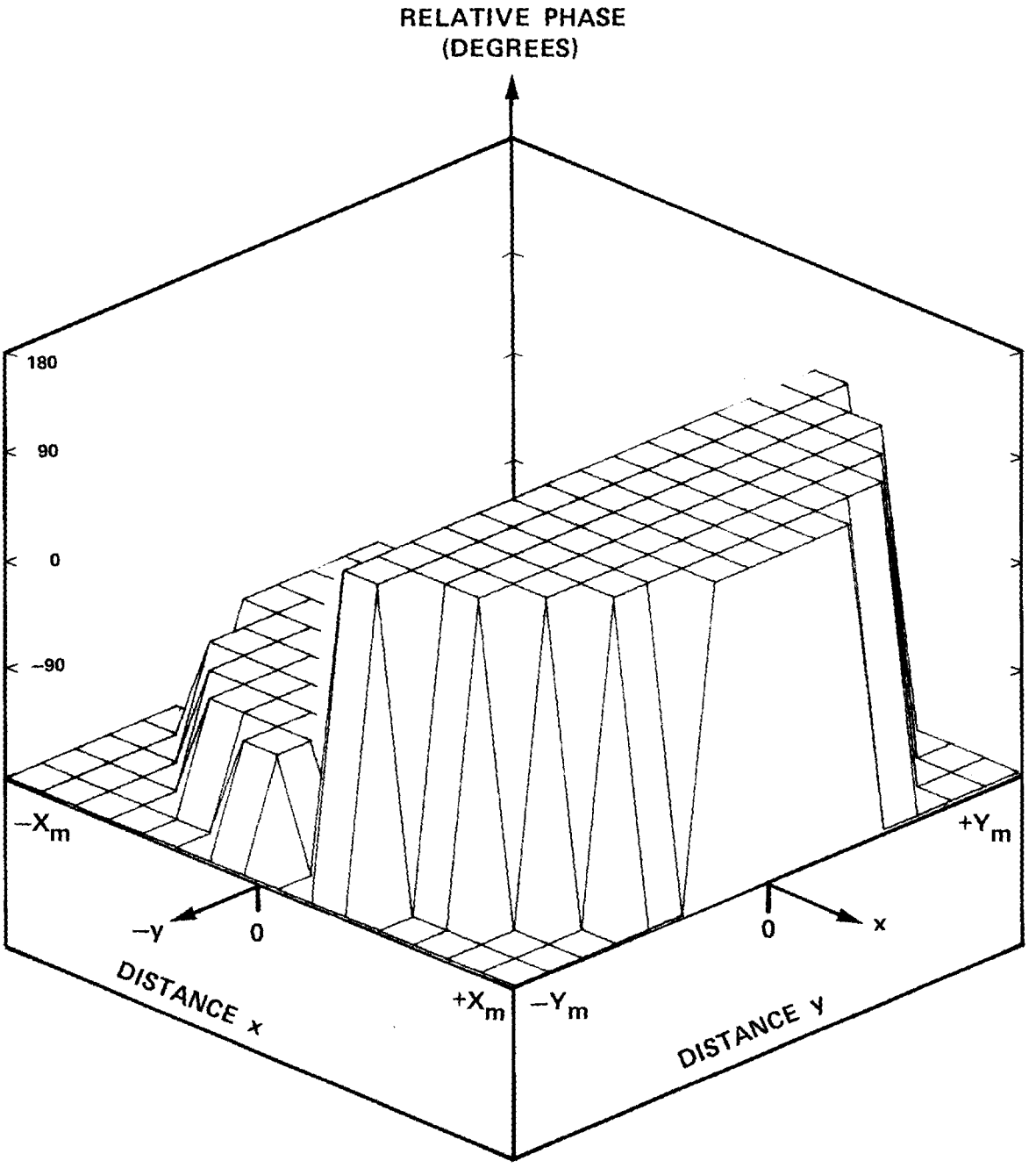

Figure B-11. Phase of $E_{x\Delta AZ}$ of RHC Antenna.

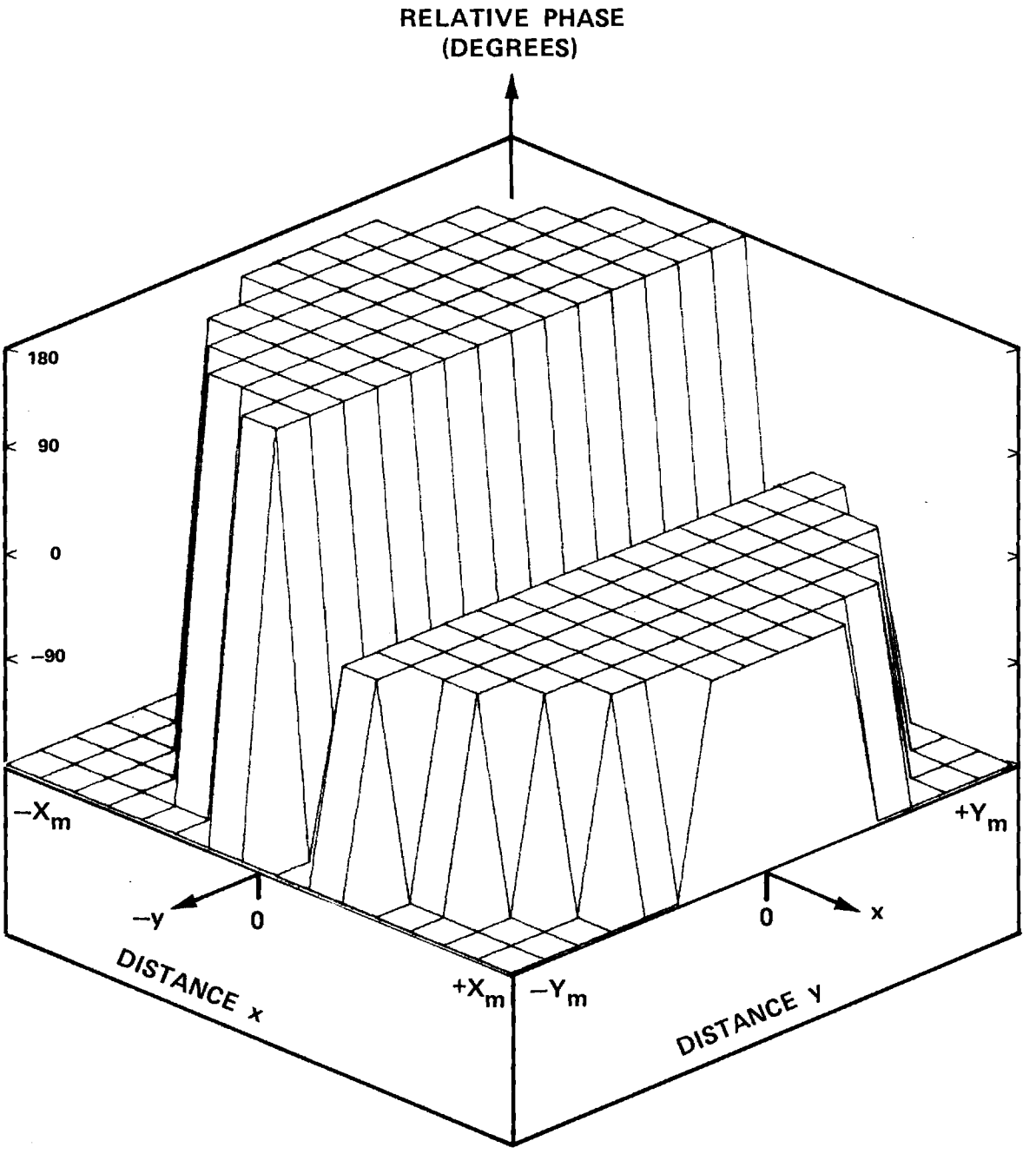

Figure B-12. Phase of $E_{y\Delta AZ}$ of RHC Antenna.

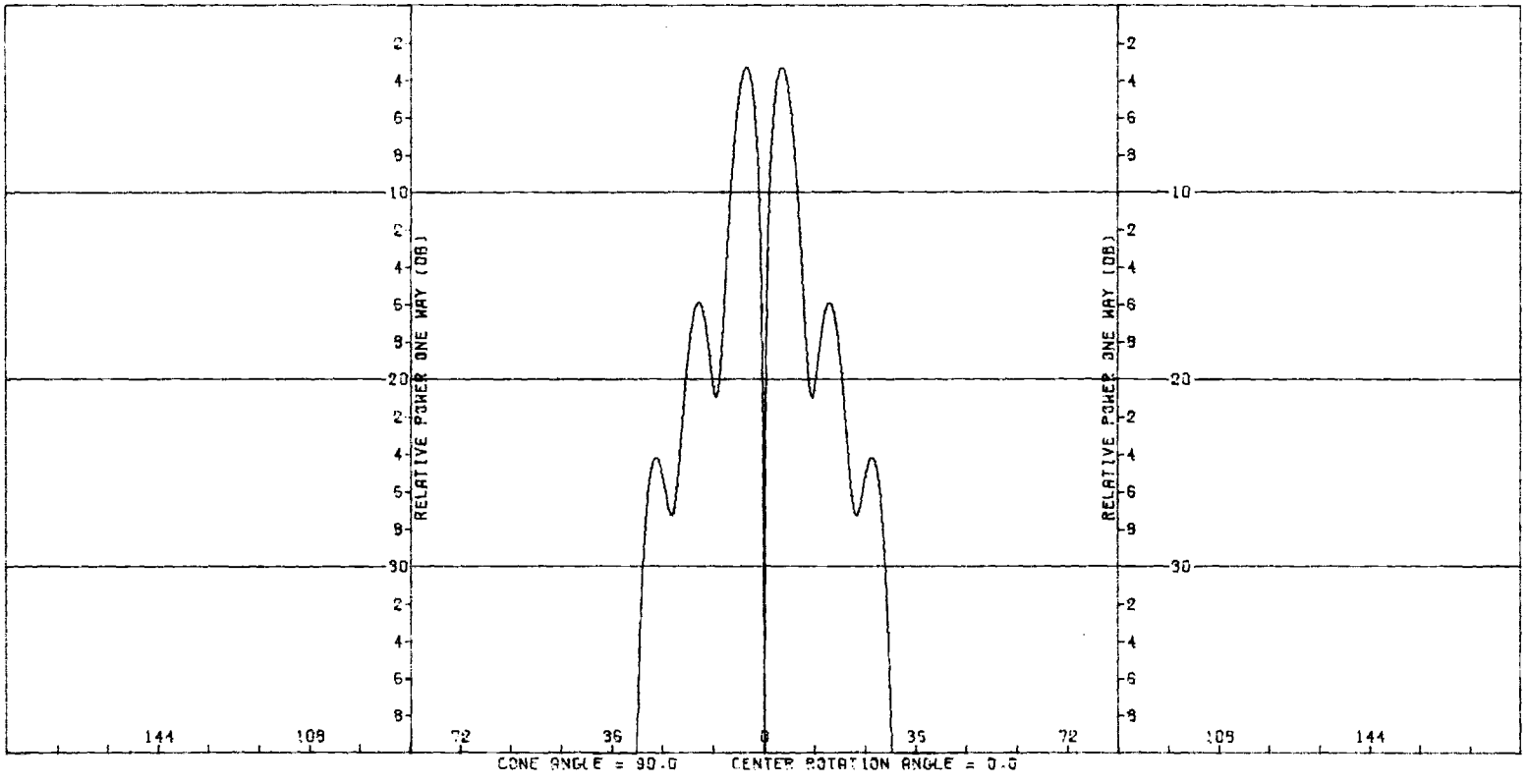

Figure B-13. Transmitting H-Plane Δ_{AZ} Pattern of RHC Antenna Without Radome.

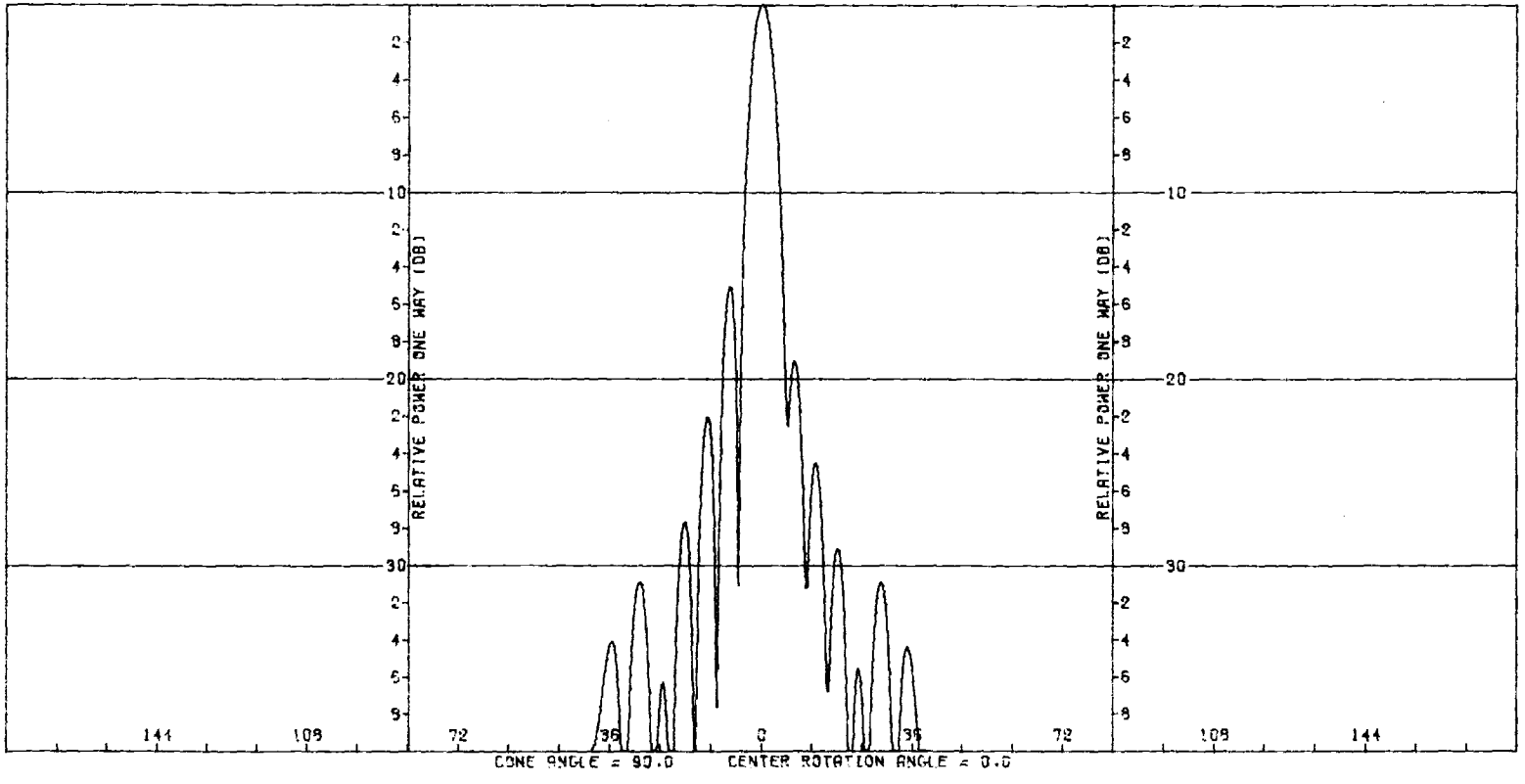

Figure B-14. Receiving E-Plane Σ Pattern of RHC Antenna With Radome at (0°,14°).

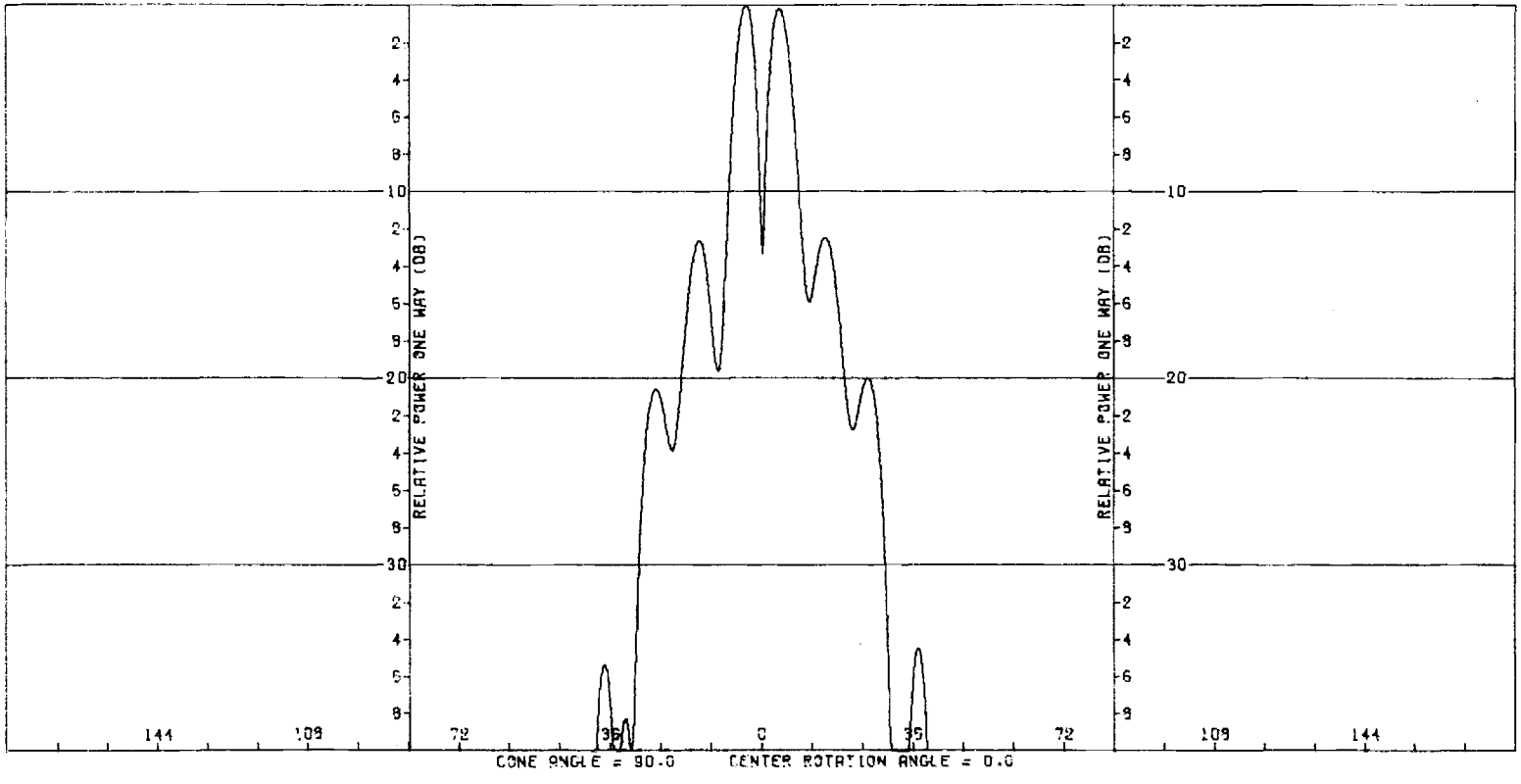

Figure B-15. Receiving E-Plane Δ_{EL} Pattern of RHC Antenna With Radome at (0°,14°).

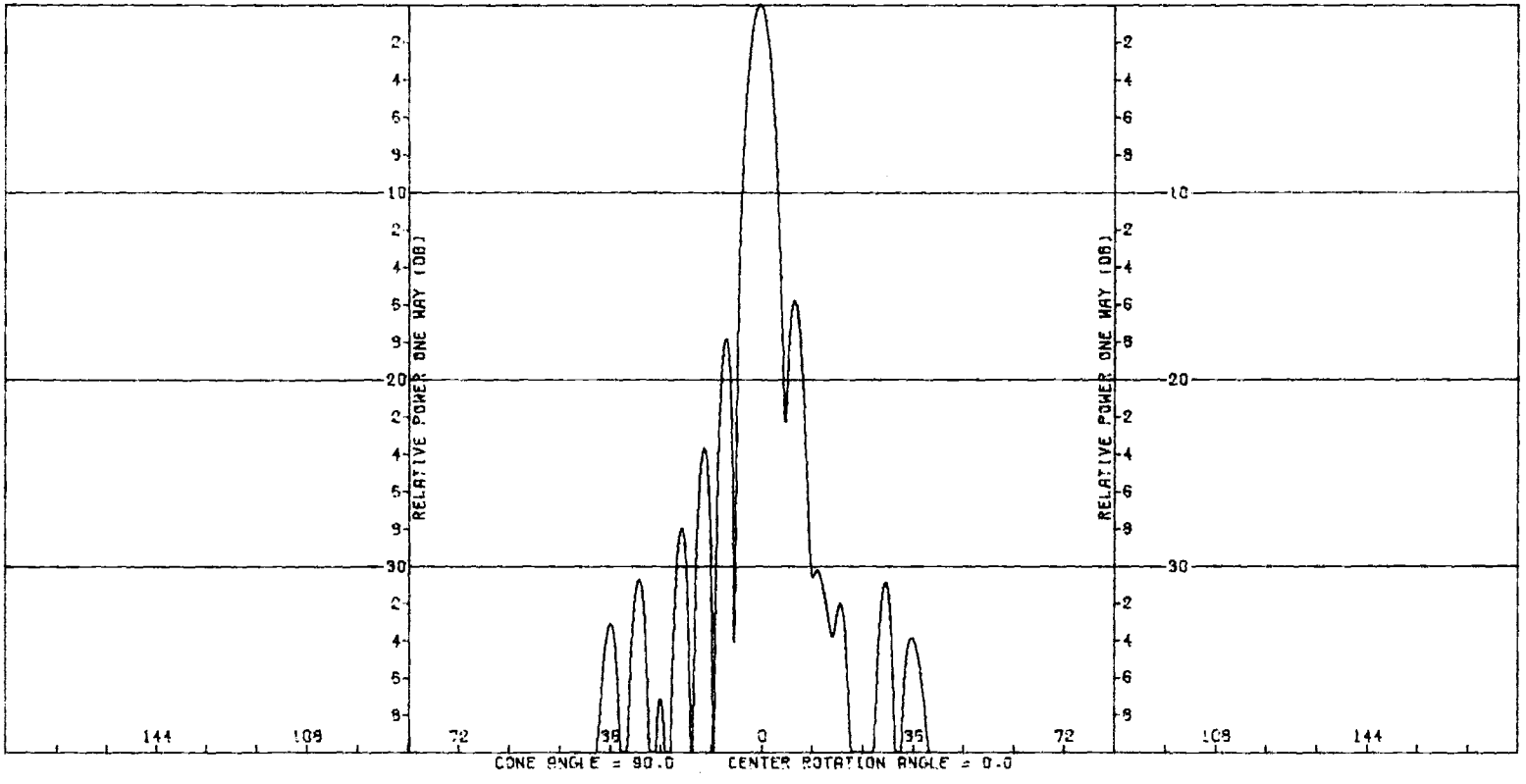

Figure B-16. Receiving H-Plane Σ Pattern of RHC Antenna With Radome at (0°,14°).

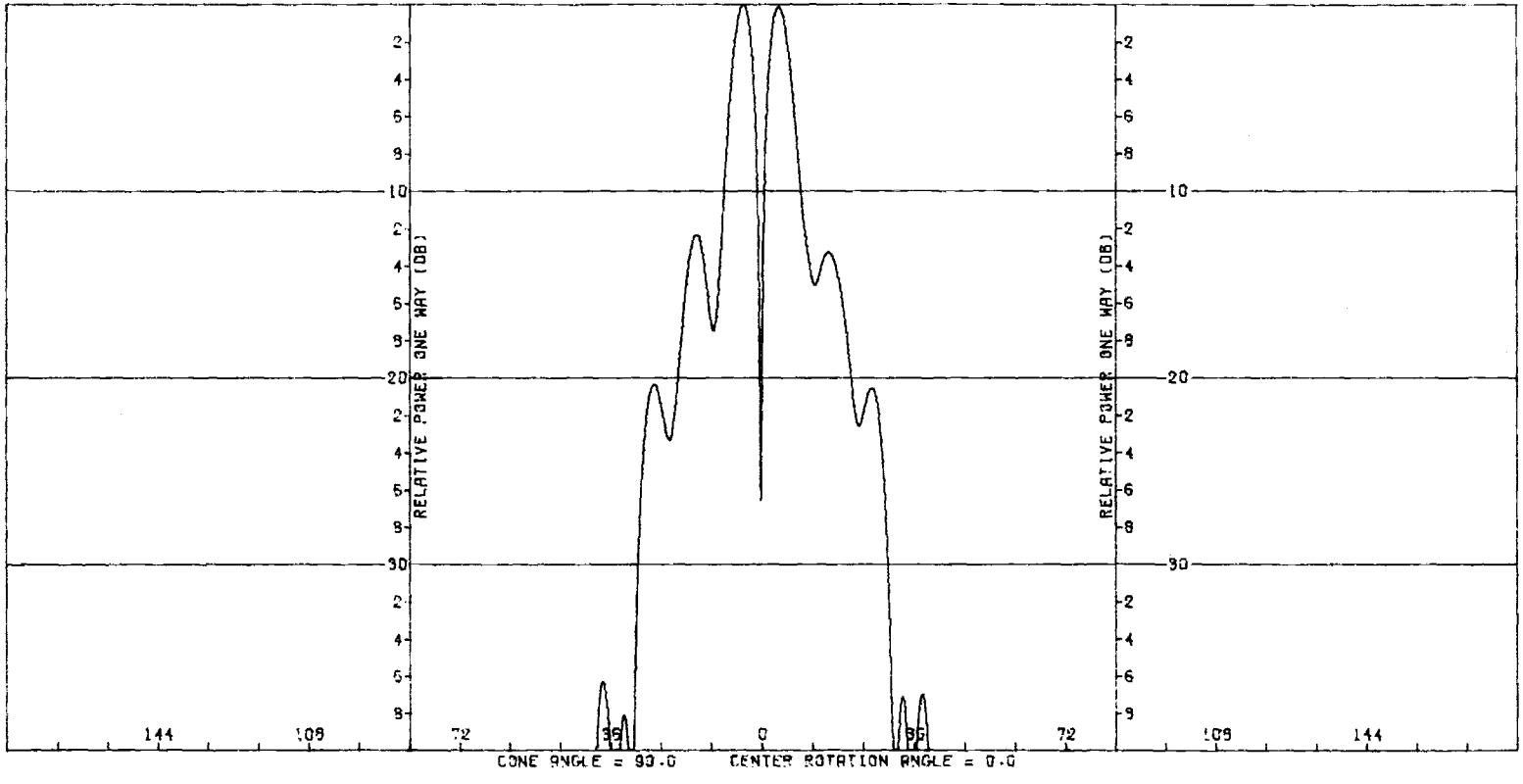

Figure B-17. Receiving H-Plane Δ_{AZ} Pattern of RHC Antenna With Radome at (0°,14°).

APPENDIX C

Test Case 3 for RTFRACP

```
 TEST DATA TO TEST IBMRACP WITHOUT PLOTS (CASE 3,FD,LINEAR,N=5)
F,F,F,F,T,DD
1,2,5,16.267,3.05,15.657,48.8020001,11.80285,2.
5,.3,1,2.5996,1522.,1,3,5,1
.01525,6.00,.009
.17180,2.40,.005
.01525,6.00,.009
.17180,2.40,.005
.01525,6.00,.009
3.00
0.
90.
0.
14.
16.
18.
20.
```

```
 TEST DATA TO TEST IBMRACP WITHOUT PLOTS (CASE 3,FO,LINEAR,N=5)
 GRAF3D= F GRAFSA= F GRAFTR= F GRAFRV= F  TABLE= F

 NFINE=    1 NPHI=  2  NTHETA=  5  OSANG=  2.00

 NX,NY,NXE,NYE,NXY,MX,MY:  16  16 256   1 512  16   1
 KXMAX=KYMAX= 1.38696  XY SPACING=  .36050 WAVELENGTHS
  KXM= 1.38696  KYM=  .08669
 TANGENT OGIVE PARAMETERS:  ROS(IN)=150.46975 BOS(IN)=142.33625
                            FINOS=3.000 FINIS= 3.07245
1      RESULTS OF RADOME ANALYSIS
 TEST DATA TO TEST IBMRACP WITHOUT PLOTS (CASE 3,FO,LINEAR,N=5)
 FINENESS RATIO=  3.00  DIAMETER=16.26700 IN.  LENGTH=48.80200 IN.
 FREQUENCY= 11.803 GHZ
 RA= 7.74700 IN.  RR=39.76878 IN.  ANTENNA D=  5.1992 WAVELENGTHS
 IPOL= 1  ICASE= 3  IOPT= 1

 LAYER  THICKNESS(IN.)    ER       TAND

    1        .01525      6.000    .0090
    2        .17180      2.400    .0050
    3        .01525      6.000    .0090
    4        .17180      2.400    .0050
    5        .01525      6.000    .0090


  PHI   THETA   BSEEL    BSEAZ    SLPEL      SLPAZ      GAIN
 (DEG)  (DEG)  (MRAD)   (MRAD)  (DEG/DEG)  (DEG/DEG)   (DB)


   0.0    0.0      .00     -.00   0.0000     0.0000    -1.6
   0.0   14.0      .00    -5.37    .0000     -.0220    -1.6
   0.0   16.0      .00    -4.77   -.0000      .0170    -1.6
   0.0   18.0      .00    -4.27   -.0000      .0143    -1.5
   0.0   20.0      .00    -3.84   -.0000      .0123    -1.5
  90.0    0.0      .00     -.00   -.0000      .0123    -1.5
  90.0   14.0    -2.27     -.00   -.0093     -.0000     -.3
  90.0   16.0    -2.18     -.00    .0026      .0000     -.3
```

90.0	18.0	-2.05	-.00	.0037	.0000	-.2
90.0	20.0	-1.90	-.00	.0043	.0000	-.2

RECEIVED SUM VOLTAGE WITHOUT RADOME= .14615E+03

APPENDIX D

Test Case 4 for RTFRACP

```
 TEST DATA TO TEST IBMRACP WITH PLOTS (CASE 3,F0,LINEAR,N=5)                1
F,T,T,T,F,00                                                                2
1,1,1,16.267,3.05,15.657,48.8020001,11.80285,2.                             3
5,.3,1,2.5996,1522.,1,3,5,1                                                 4
.01525,6.00,.009                                                            5
.17180,2.40,.005                                                            6
.01525,6.00,.009                                                            7
.17180,2.40,.005                                                            8
.01525,6.00,.009                                                            9
3.00                                                                       10
0.                                                                         11
14.                                                                        12
16.                                                                        13
18.                                                                        14
20.                                                                        15
```

TEST DATA TO TEST IBMRACP WITH PLOTS (CASE 3,F0,LINEAR,N=5)
GRAF3D= F GRAFSA= T GRAFTR= T GRAFRV= T TABLE= F

NFINE= 1 NPHI= 1 NTHETA= 1 OSANG= 2.00

NX,NY,NXE,NYE,NXY,MX,MY: 16 16 256 1 512 16 1

ANGLE	TPERI**2		TPARI**2		RPERI**2		RPARI**2	
.92	.819	-99.2	.819	-99.2	.156	-149.9	.156	30.1
2.07	.819	-99.2	.820	-99.2	.157	-149.8	.156	30.2
3.22	.819	-99.3	.820	-99.2	.157	-149.8	.156	30.3
4.38	.819	-99.4	.821	-99.3	.157	-149.7	.155	30.4
5.53	.818	-99.5	.821	-99.4	.158	-149.6	.154	30.6
6.69	.818	-99.6	.822	-99.5	.158	-149.4	.153	30.7
7.85	.817	-99.8	.824	-99.6	.159	-149.2	.152	31.0
9.01	.816	-100.0	.825	-99.7	.160	-149.0	.151	31.2
10.18	.815	-100.3	.826	-99.9	.160	-148.8	.149	31.6
11.35	.814	-100.5	.828	-100.1	.161	-148.6	.147	31.9
12.53	.813	-100.9	.830	-100.3	.163	-148.3	.145	32.3
13.71	.812	-101.2	.832	-100.5	.164	-148.0	.143	32.7
14.89	.810	-101.6	.834	-100.8	.165	-147.6	.141	33.2
16.09	.809	-102.0	.837	-101.0	.166	-147.3	.138	33.7
17.29	.807	-102.4	.840	-101.3	.168	-146.9	.135	34.2
18.50	.806	-102.9	.843	-101.6	.170	-146.5	.132	34.8
19.72	.804	-103.4	.846	-102.0	.171	-146.0	.129	35.4
20.94	.802	-104.0	.849	-102.3	.173	-145.6	.126	36.1
22.18	.800	-104.6	.853	-102.7	.175	-145.1	.122	36.8
23.43	.798	-105.3	.857	-103.1	.177	-144.6	.118	37.6
24.69	.795	-106.0	.861	-103.5	.179	-144.0	.114	38.4
25.96	.793	-106.7	.865	-104.0	.181	-143.5	.109	39.2
27.25	.791	-107.5	.870	-104.5	.184	-142.9	.105	40.1
28.55	.788	-108.4	.874	-105.0	.186	-142.3	.100	41.1
29.87	.785	-109.3	.879	-105.6	.189	-141.7	.095	42.1
31.20	.783	-110.3	.885	-106.2	.191	-141.0	.089	43.1
32.56	.780	-111.4	.890	-106.8	.194	-140.3	.084	44.2
33.93	.777	-112.5	.895	-107.5	.197	-139.7	.078	45.4

35.33	.773	-113.7	.901	-108.2	.200	-138.9	.072	46.6	39
36.75	.770	-115.0	.907	-108.9	.203	-138.2	.067	47.9	40
38.20	.767	-116.4	.913	-109.7	.206	-137.5	.061	49.2	41
39.68	.763	-117.9	.918	-110.6	.209	-136.7	.055	50.6	42
41.20	.759	-119.5	.924	-111.5	.213	-136.0	.049	52.0	43
42.74	.755	-121.2	.930	-112.5	.216	-135.2	.043	53.5	44
44.33	.751	-123.1	.936	-113.6	.220	-134.4	.037	55.0	45
45.96	.747	-125.1	.941	-114.8	.224	-133.7	.031	56.6	46
47.64	.742	-127.3	.946	-116.1	.228	-132.9	.026	58.3	47
49.38	.737	-129.7	.951	-117.5	.233	-132.2	.021	60.1	48
51.18	.731	-132.3	.956	-119.1	.237	-131.4	.016	61.9	49
53.05	.725	-135.1	.960	-120.8	.243	-130.8	.012	63.8	50
55.01	.718	-138.3	.963	-122.8	.249	-130.1	.009	65.8	51
57.07	.710	-141.9	.966	-125.0	.256	-129.6	.006	67.9	52
59.25	.700	-145.9	.969	-127.5	.265	-129.2	.003	70.3	53
61.58	.688	-150.4	.970	-130.4	.275	-128.9	.002	73.4	54
64.11	.672	-155.8	.971	-133.8	.290	-128.9	.001	78.5	55
66.88	.649	-162.2	.971	-137.8	.310	-129.3	.000	101.1	56
70.01	.616	-170.3	.970	-142.7	.341	-130.5	.000	-128.0	57
73.71	.558	178.8	.967	-149.1	.395	-133.0	.001	-116.9	58
78.50	.436	161.4	.959	-158.3	.514	-139.4	.001	-117.0	59
90.00	0.000	-180.0	0.000	-180.0	.894	-156.6	.072	-124.4	60

61
62
TABLE OF XMN COEF. IS FORMED 63
64
65
KXMAX=KYMAX= 1.38696 XY SPACING= .36050 WAVELENGTHS 66
KXM= 1.38696 KYM= .08669 67
68
69
SUBROUTINE NORM: MIN= 0. MAX= 0. 70
71
72
73
74
SUBROUTINE NORM: MIN= 0. MAX= .103E+01 75
76

```
 IPOWER OF PATTERN= 1

  SUBROUTINE NORM:  MIN=  0.          MAX=  0.


  SUBROUTINE NORM:  MIN=  0.          MAX=   .103E+01


  SUBROUTINE NORM:  MIN=  0.          MAX=  0.


  SUBROUTINE NORM:  MIN=  0.          MAX=   .103E+01

 TANGENT OGIVE PARAMETERS:  ROS(IN)=150.46975 BOS(IN)=142.33625
                          FINOS=3.000 FINIS= 3.07245
1       RESULTS OF RADOME ANALYSIS
 TEST DATA TO TEST IBMRACP WITH PLOTS (CASE 3,F0,LINEAR,N=5)
 FINENESS RATIO=  3.00  DIAMETER=16.26700 IN.  LENGTH=48.80200 IN.
 FREQUENCY= 11.803 GHZ
 PA= 7.74700 IN.  RR=39.76878 IN.  ANTENNA D=  5.1992 WAVELENGTHS
 IPOL= 1  ICASE= 3  IOPT= 1

 LAYER  THICKNESS(IN.)    ER       TAND

    1        .01525      6.000    .0090
    2        .17180      2.400    .0050
    3        .01525      6.000    .0090
    4        .17180      2.400    .0050
    5        .01525      6.000    .0090
```

```
 PHI   THETA   BSEEL    BSEAZ    SLPEL      SLPAZ      GAIN
(DEG) (DEG)   (MRAD)   (MRAD) (DEG/DEG) (DEG/DEG)   (DB)



RECEIVING PATTERN COMPUTED FOR:
  ICUT=  1
 ICOMP=  1
  KMAX=     .996
  NREC=     32
    DK=    .62250E-01
ANGMAX=  84.87
(ICUT=1 FOR EL CUT, =2 FOR AZ CUT
(ICOMP=1 FOR EL COMPONENT, =2 FOR AZIMUTH)



RECEIVING PATTERN COMPUTED FOR:
  ICUT=  1
 ICOMP=  1
  KMAX=     .996
  NREC=     32
    DK=    .62250E-01
ANGMAX=  84.87
(ICUT=1 FOR EL CUT, =2 FOR AZ CUT
(ICOMP=1 FOR EL COMPONENT, =2 FOR AZIMUTH)



MIN AND MAX VALUES OF REC"G PATTERN:



 SUBROUTINE NORM:  MIN=    .101E-04  MAX=    .228E+03
```

REC"G PATTERN, EL CUT, EL COMP (DB):

-76.6	-40.000	78.7
-70.3	-40.000	77.8
-65.6	-40.000	77.2
-61.6	-40.000	66.3
-58.0	-40.000	-99.0
-54.8	-40.000	-103.2
-51.8	-40.000	-106.0
-49.0	-40.000	-107.6
-46.4	-40.000	-108.7
-43.8	-40.000	-166.1
-41.4	-40.000	71.6
-39.1	-37.260	68.2
-36.8	-35.283	65.4
-34.6	-35.754	63.1
-32.5	-40.000	60.2
-30.4	-40.000	-100.3
-28.3	-35.580	-118.9
-26.3	-30.221	-123.2
-24.4	-28.026	-127.5
-22.4	-28.432	-133.1
-20.5	-33.677	-149.2
-18.6	-33.095	78.1
-16.7	-21.696	56.4
-14.9	-15.563	49.6
-13.0	-11.306	44.8
-11.2	-8.095	40.7
-9.4	-5.591	37.0
-7.6	-3.625	33.5
-5.8	-2.113	30.6
-4.0	-1.014	28.3
-2.2	-.314	26.7
-.4	-.013	26.0
1.3	-.112	26.3
3.1	-.614	27.4
4.9	-1.514	29.3

```
     6.7       -2.816      32.0                                          191
     8.5       -4.546      35.2                                          192
    10.3       -6.766      38.8                                          193
    12.1       -9.599      42.7                                          194
    14.0      -13.273      47.1                                          195
    15.8      -18.294      52.5                                          196
    17.7      -26.211      62.5                                          197
    19.5      -40.000     157.6                                          198
    21.5      -30.057    -138.2                                          199
    23.4      -27.878    -129.7                                          200
    25.3      -28.820    -125.2                                          201
    27.3      -32.344    -121.5                                          202
    29.4      -40.000    -116.2                                          203
    31.4      -40.000      53.5                                          204
    33.5      -37.178      61.7                                          205
    35.7      -35.213      64.8                                          206
    37.9      -35.968      67.0                                          207
    40.2      -39.335      68.9                                          208
    42.6      -40.000      72.9                                          209
    45.1      -40.000    -113.2                                          210
    47.7      -40.000    -108.6                                          211
    50.4      -40.000    -106.0                                          212
    53.3      -40.000    -104.3                                          213
    56.4      -40.000    -102.9                                          214
    59.7      -40.000     -95.8                                          215
    63.5      -40.000      72.8                                          216
    67.8      -40.000      77.0                                          217
    73.2      -40.000      79.7                                          218
    81.2      -40.000      80.6                                          219
                                                                         220
MIN AND MAX VALUES OF REC"G PATTERN:                                     221
                                                                         222
                                                                         223
                                                                         224
 SUBROUTINE NORM:  MIN=    .644E-26   MAX=    .102E+03                   225
                                                                         226
                                                                         227
                                                                         228
```

REC"G PATTERN, EL CUT, EL COMP (DB):

-76.6	-21.003	-9.8
-70.3	-21.534	-11.2
-65.6	-22.362	-14.4
-61.6	-20.830	-14.3
-58.0	-18.981	-13.5
-54.8	-18.031	-15.3
-51.8	-17.095	-17.7
-49.0	-15.637	-18.3
-46.4	-14.298	-18.5
-43.8	-13.500	-20.3
-41.4	-12.975	-22.6
-39.1	-12.458	-23.7
-36.8	-12.052	-24.4
-34.6	-11.815	-26.3
-32.5	-11.494	-28.5
-30.4	-10.840	-29.7
-28.3	-9.849	-30.6
-26.3	-8.590	-32.5
-24.4	-7.110	-34.7
-22.4	-5.534	-36.5
-20.5	-4.020	-38.4
-18.6	-2.668	-41.0
-16.7	-1.542	-44.0
-14.9	-.699	-46.8
-13.0	-.179	-49.7
-11.2	0.000	-52.9
-9.4	-.222	-56.1
-7.6	-.967	-58.9
-5.8	-2.418	-61.3
-4.0	-4.918	-63.4
-2.2	-9.523	-64.9
-.4	-23.261	-65.7
1.3	-13.798	114.6
3.1	-6.822	115.8
4.9	-3.504	117.6
6.7	-1.592	119.8

```
     8.5          -.514     122.5                                    257
    10.3          -.052     125.5                                    258
    12.1          -.053     128.7                                    259
    14.0          -.402     131.8                                    260
    15.8         -1.068     134.7                                    261
    17.7         -2.066     137.5                                    262
    19.5         -3.344     140.2                                    263
    21.5         -4.774     142.6                                    264
    23.4         -6.279     144.5                                    265
    25.3         -7.848     146.5                                    266
    27.3         -9.329     148.4                                    267
    29.4        -10.422     149.8                                    268
    31.4        -11.094     151.0                                    269
    33.5        -11.627     152.6                                    270
    35.7        -12.087     154.5                                    271
    37.9        -12.308     155.9                                    272
    40.2        -12.496     157.0                                    273
    42.6        -13.120     158.6                                    274
    45.1        -14.167     160.4                                    275
    47.7        -15.081     161.6                                    276
    50.4        -15.851     162.2                                    277
    53.3        -17.315     163.6                                    278
    56.4        -19.516     165.5                                    279
    59.7        -20.441     166.1                                    280
    63.5        -19.637     166.2                                    281
    67.8        -20.764     167.4                                    282
    73.2        -30.741     170.9                                    283
    81.2        -26.071     -11.3                                    284
                                                                     285
RECEIVING PATTERN COMPUTED FOR:                                      286
  ICUT=  2                                                           287
 ICOMP=  1                                                           288
  KMAX=    .996                                                      289
  NREC=    32                                                        290
    OK=   .62250E-01                                                 291
ANGMAX=  84.87                                                       292
(ICUT=1 FOR EL CUT, =2 FOR AZ CUT                                    293
(ICOMP=1 FOR EL COMPONENT, =2 FOR AZIMUTH)                           294
```

```
RECEIVING PATTERN COMPUTED FOR:
  ICUT=  2
 ICOMP=  1
  KMAX=    .996
  NREC=    32
    DK=   .62250E-01
ANGMAX=  84.87
(ICUT=1 FOR EL CUT, =2 FOR AZ CUT
(ICOMP=1 FOR EL COMPONENT, =2 FOR AZIMUTH)


MIN AND MAX VALUES OF REC"G PATTERN:


 SUBROUTINE NORM:  MIN=   .303E-03  MAX=   .229E+03


REC"G PATTERN, AZ CUT,EL COMP (DB):

   -76.6      -40.000    127.4
   -70.3      -40.000     94.2
   -65.6      -40.000     56.9
   -61.6      -40.000     23.4
   -58.0      -40.000   -116.4
   -54.8      -39.928   -105.7
   -51.8      -40.000    -87.3
   -49.0      -40.000    -97.8
   -46.4      -40.000   -113.9
   -43.8      -40.000   -135.2
   -41.4      -39.043     67.2
   -39.1      -35.989     70.6
   -36.8      -36.603     73.5
```

-34.6	-35.967	70.0	343
-32.5	-36.664	67.1	344
-30.4	-40.000	78.0	345
-28.3	-34.943	-116.5	346
-26.3	-30.795	-118.5	347
-24.4	-30.255	-122.5	348
-22.4	-30.934	-123.4	349
-20.5	-38.339	-114.9	350
-18.6	-29.339	50.2	351
-16.7	-19.348	51.3	352
-14.9	-14.037	48.1	353
-13.0	-10.218	44.8	354
-11.2	-7.115	42.8	355
-9.4	-4.693	40.8	356
-7.6	-2.928	37.9	357
-5.8	-1.640	34.7	358
-4.0	-.704	32.2	359
-2.2	-.145	29.9	360
-.4	-.002	26.9	361
1.3	-.234	23.4	362
3.1	-.815	20.9	363
4.9	-1.797	19.5	364
6.7	-3.237	17.0	365
8.5	-5.219	13.3	366
10.3	-8.013	13.9	367
12.1	-11.552	27.5	368
14.0	-14.019	48.4	369
15.8	-16.014	48.5	370
17.7	-18.720	25.1	371
19.5	-23.462	-.4	372
21.5	-39.094	-110.6	373
23.4	-26.638	-170.7	374
25.3	-28.957	-161.4	375
27.3	-36.279	-119.9	376
29.4	-40.000	-119.0	377
31.4	-40.000	134.8	378
33.5	-38.563	48.8	379
35.7	-32.843	25.7	380

```
     37.9       -34.848      36.1                                    381
     40.2       -40.000      78.6                                    382
     42.6       -40.000      82.8                                    383
     45.1       -40.000     -33.7                                    384
     47.7       -40.000    -110.6                                    385
     50.4       -37.358    -138.4                                    386
     53.3       -39.200    -126.8                                    387
     56.4       -40.000     -78.0                                    388
     59.7       -40.000     -73.0                                    389
     63.5       -40.000     163.6                                    390
     67.8       -40.000      89.6                                    391
     73.2       -40.000      51.7                                    392
     81.2       -40.000      64.1                                    393
                                                                     394
MIN AND MAX VALUES OF REC"G PATTERN:                                 395
                                                                     396
                                                                     397
                                                                     398
 SUBROUTINE NORM:  MIN=    .684E-02  MAX=    .987E+02                 399
                                                                     400
                                                                     401
                                                                     402
REC"G PATTERN, AZ CUT,EL COMP (DB):                                  403
                                                                     404
   -76.6       -20.835      -9.9                                    405
   -70.3       -21.287      -9.5                                    406
   -65.6       -22.002     -11.6                                    407
   -61.6       -20.511     -11.0                                    408
   -58.0       -18.741      -9.7                                    409
   -54.8       -17.779     -11.2                                    410
   -51.8       -16.811     -13.7                                    411
   -49.0       -15.418     -14.0                                    412
   -46.4       -14.172     -13.9                                    413
   -43.8       -13.400     -15.6                                    414
   -41.4       -12.873     -18.0                                    415
   -39.1       -12.419     -19.0                                    416
   -36.8       -12.098     -19.6                                    417
   -34.6       -11.870     -21.6                                    418
```

-32.5	-11.512	-24.1	419
-30.4	-10.874	-25.5	420
-28.3	-9.907	-26.8	421
-26.3	-8.589	-28.9	422
-24.4	-7.027	-31.3	423
-22.4	-5.426	-33.1	424
-20.5	-3.906	-35.0	425
-18.6	-2.520	-37.3	426
-16.7	-1.369	-39.7	427
-14.9	-.555	-42.0	428
-13.0	-.104	-44.3	429
-11.2	-.014	-46.8	430
-9.4	-.369	-49.4	431
-7.6	-1.328	-52.0	432
-5.8	-3.071	-54.7	433
-4.0	-5.955	-57.2	434
-2.2	-11.276	-58.9	435
-.4	-33.185	-42.0	436
1.3	-12.689	112.4	437
3.1	-6.709	109.9	438
4.9	-3.650	107.0	439
6.7	-1.879	104.9	440
8.5	-.957	103.9	441
10.3	-.579	103.4	442
12.1	-.443	103.7	443
14.0	-.460	105.7	444
15.8	-.818	109.4	445
17.7	-1.724	112.5	446
19.5	-3.141	112.9	447
21.5	-4.750	111.1	448
23.4	-6.359	110.9	449
25.3	-8.050	114.5	450
27.3	-9.664	119.0	451
29.4	-10.813	121.2	452
31.4	-11.471	122.7	453
33.5	-12.034	126.3	454
35.7	-12.523	130.6	455
37.9	-12.673	133.1	456

```
    40.2        -12.745     135.1
    42.6        -13.325     138.6
    45.1        -14.361     142.6
    47.7        -15.188     145.1
    50.4        -15.839     146.9
    53.3        -17.275     150.2
    56.4        -19.510     154.5
    59.7        -20.371     156.7
    63.5        -19.466     158.0
    67.8        -20.596     161.3
    73.2        -30.702     168.1
    81.2        -25.865     -14.0
NUMBER OF RAYS USED IN COMPUTING APERTURE FIELD =       169
NUMBER OF RAYS USED IN COMPUTING APERTURE FIELD =       169
NUMBER OF RAYS USED IN COMPUTING APERTURE FIELD =       169
NUMBER OF RAYS USED IN COMPUTING APERTURE FIELD =       169
NUMBER OF RAYS USED IN COMPUTING APERTURE FIELD =       169


FINAL ANSWERS FOR MONOPULSE SYSTEM:

K1:  -.53886E-02 -.35755E-04  .99999E+00
K2:  -.53667E-02  .14448E-07  .99999E+00

AZTM=  -.53667E+01 MRAD
ELTM=   .14449E-04 MRAD

MESAZ=   .93465E-01 VOLTS/DEG
MESEL=   .10196E+00 VOLTS/DEG

UAZ:  -.11735E-03  .45944E-07
UEL:  -.20898E-03  .84448E-07

SMAX=   .12096280585064E+03     LCTR=   3
```

```
ADDITIONAL MONOPULSE OUTPUTS AROUND BORESIGHT:                                  495
                                                                                496
                                                                                497
NUMBER OF RAYS USED IN COMPUTING APERTURE FIELD =       169                     498
ANG=  -3.0 MRAD FROM BORESIGHT    VRAZ=  -.16052E-01 VOLTS    VREL=  -.17502E-0
                                                                                500
DAZ(AMP,PHS)=   .16703E-01 -.73959E+02   DEL(AMP,PHS)=   .17507E-01 -.91343E+02
                                                                                502
NUMBER OF RAYS USED IN COMPUTING APERTURE FIELD =       169                     503
ANG=  -2.0 MRAD FROM BORESIGHT    VRAZ=  -.10706E-01 VOLTS    VREL=  -.11675E-0
                                                                                505
DAZ(AMP,PHS)=   .11671E-01 -.66530E+02   DEL(AMP,PHS)=   .11678E-01 -.91340E+02
                                                                                507
NUMBER OF RAYS USED IN COMPUTING APERTURE FIELD =       169                     508
ANG=  -1.0 MRAD FROM BORESIGHT    VRAZ=  -.53557E-02 VOLTS    VREL=  -.58410E-0
                                                                                510
DAZ(AMP,PHS)=   .71136E-02 -.48840E+02   DEL(AMP,PHS)=   .58426E-02 -.91340E+02
                                                                                512
NUMBER OF RAYS USED IN COMPUTING APERTURE FIELD =       169                     513
ANG=   0.0 MRAD FROM BORESIGHT    VRAZ=   .45944E-07 VOLTS    VREL=   .84448E-0
                                                                                515
DAZ(AMP,PHS)=   .47179E-02  .55796E-03   DEL(AMP,PHS)=   .84471E-07  .88662E+02
                                                                                517
NUMBER OF RAYS USED IN COMPUTING APERTURE FIELD =       169                     518
ANG=   1.0 MRAD FROM BORESIGHT    VRAZ=   .53599E-02 VOLTS    VREL=   .58486E-0
                                                                                520
DAZ(AMP,PHS)=   .71646E-02  .48426E+02   DEL(AMP,PHS)=   .58502E-02  .88664E+02
                                                                                522
NUMBER OF RAYS USED IN COMPUTING APERTURE FIELD =       169                     523
ANG=   2.0 MRAD FROM BORESIGHT    VRAZ=   .10724E-01 VOLTS    VREL=   .11705E-0
                                                                                525
DAZ(AMP,PHS)=   .11746E-01  .65927E+02   DEL(AMP,PHS)=   .11708E-01  .88665E+02
                                                                                527
NUMBER OF RAYS USED IN COMPUTING APERTURE FIELD =       169                     528
ANG=   3.0 MRAD FROM BORESIGHT    VRAZ=   .16093E-01 VOLTS    VREL=   .17570E-0
                                                                                530
DAZ(AMP,PHS)=   .16802E-01  .73301E+02   DEL(AMP,PHS)=   .17575E-01  .88667E+02
                                                                                532
```

```
AVERAGE SLPAZ=    .93500E-01 VOLTS/DEG
AVERAGE SLPEL=    .10201E+00 VOLTS/DEG
 SUM=1.0 VOLT


  0.0   14.0      .00    -5.37    0.0000     0.0000    -1.6


RECEIVED SUM VOLTAGE WITHOUT RADOME=  .14615E+03
```

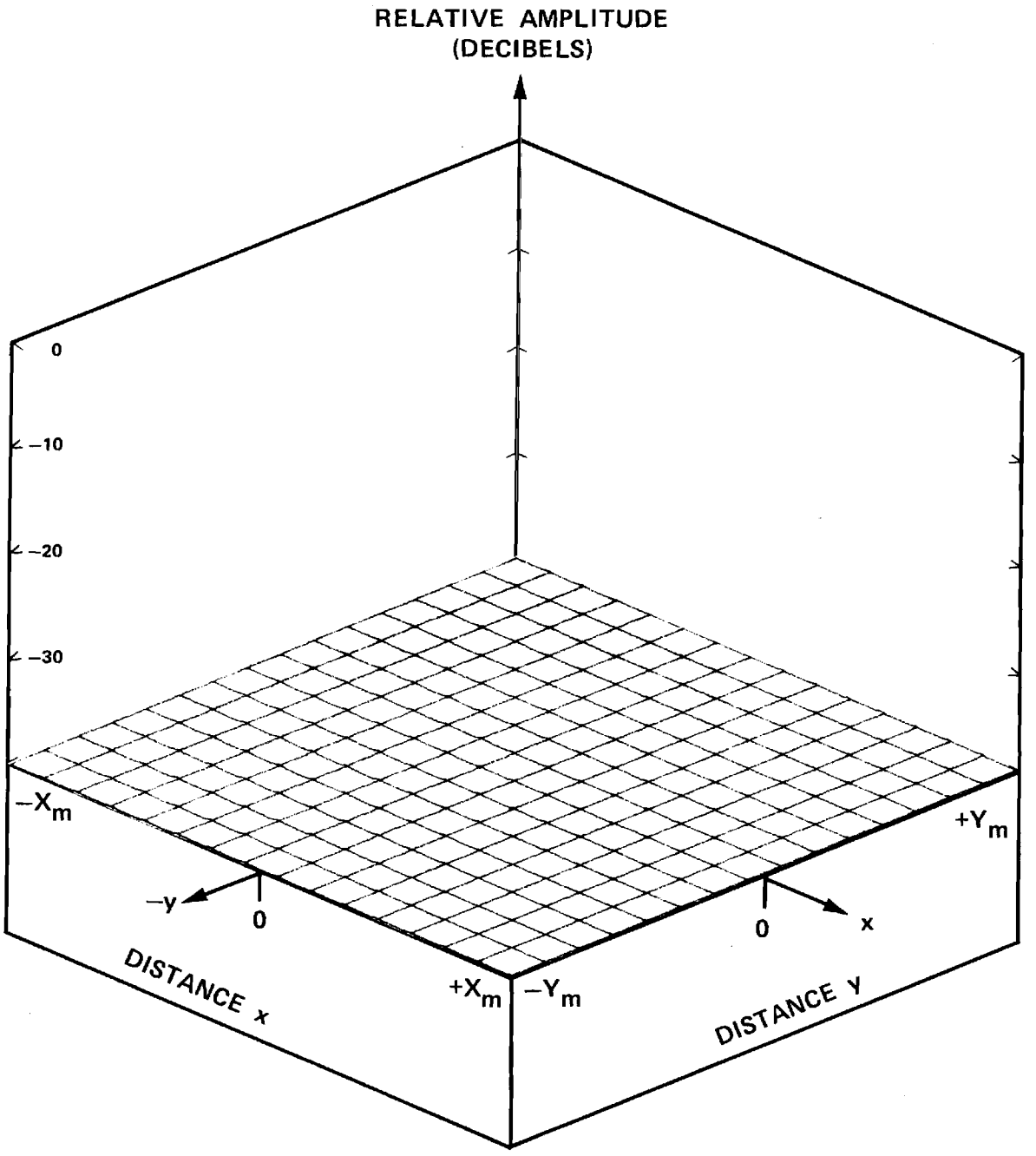

Figure D-1. $|E_x|$ of Flat Plate Antenna (ICASE=3) for Sum, Elevation Difference, and Azimuth Difference Channels.

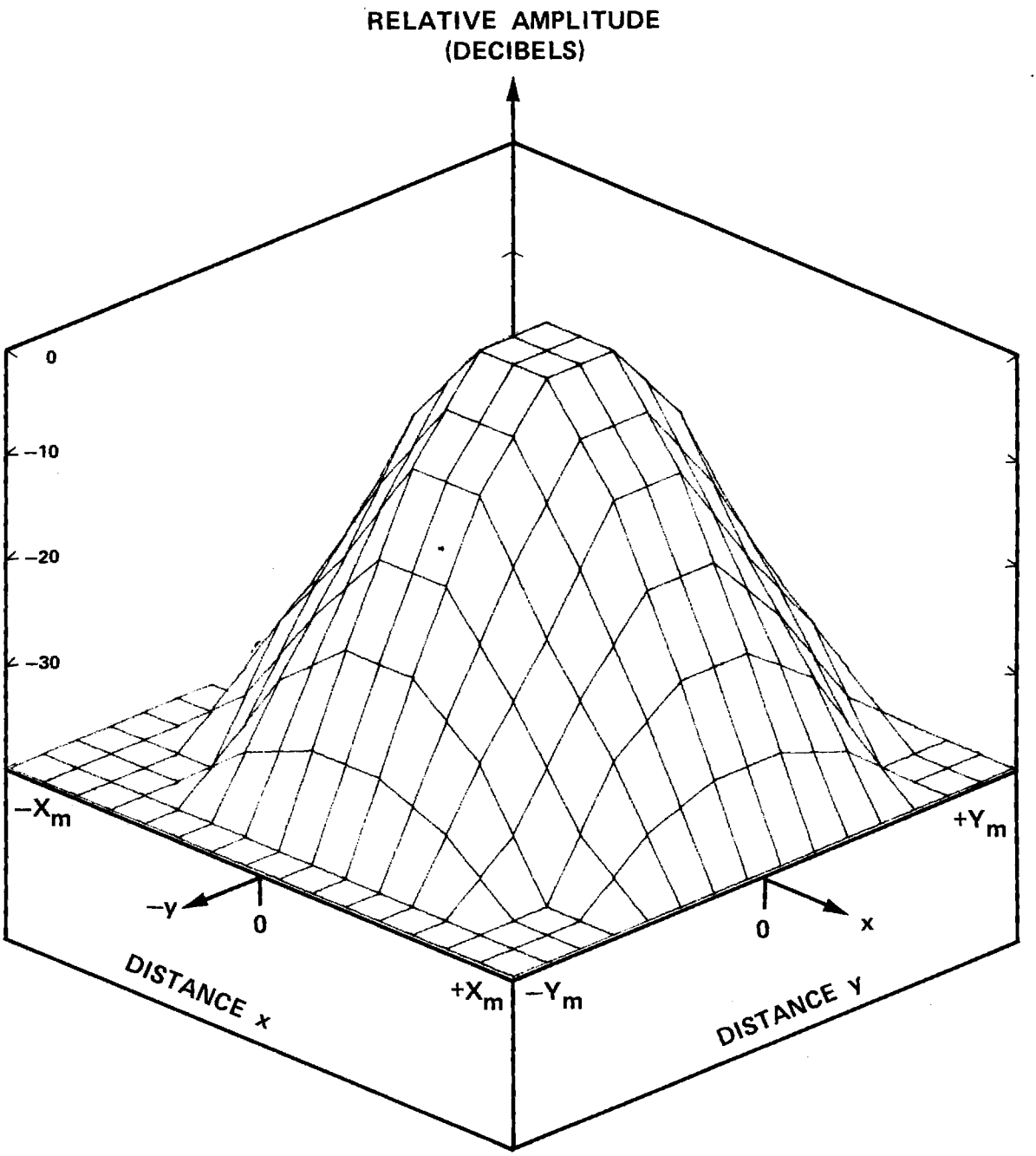

Figure D-2. $|E_Y|_\Sigma$ of Flat Plate Antenna.

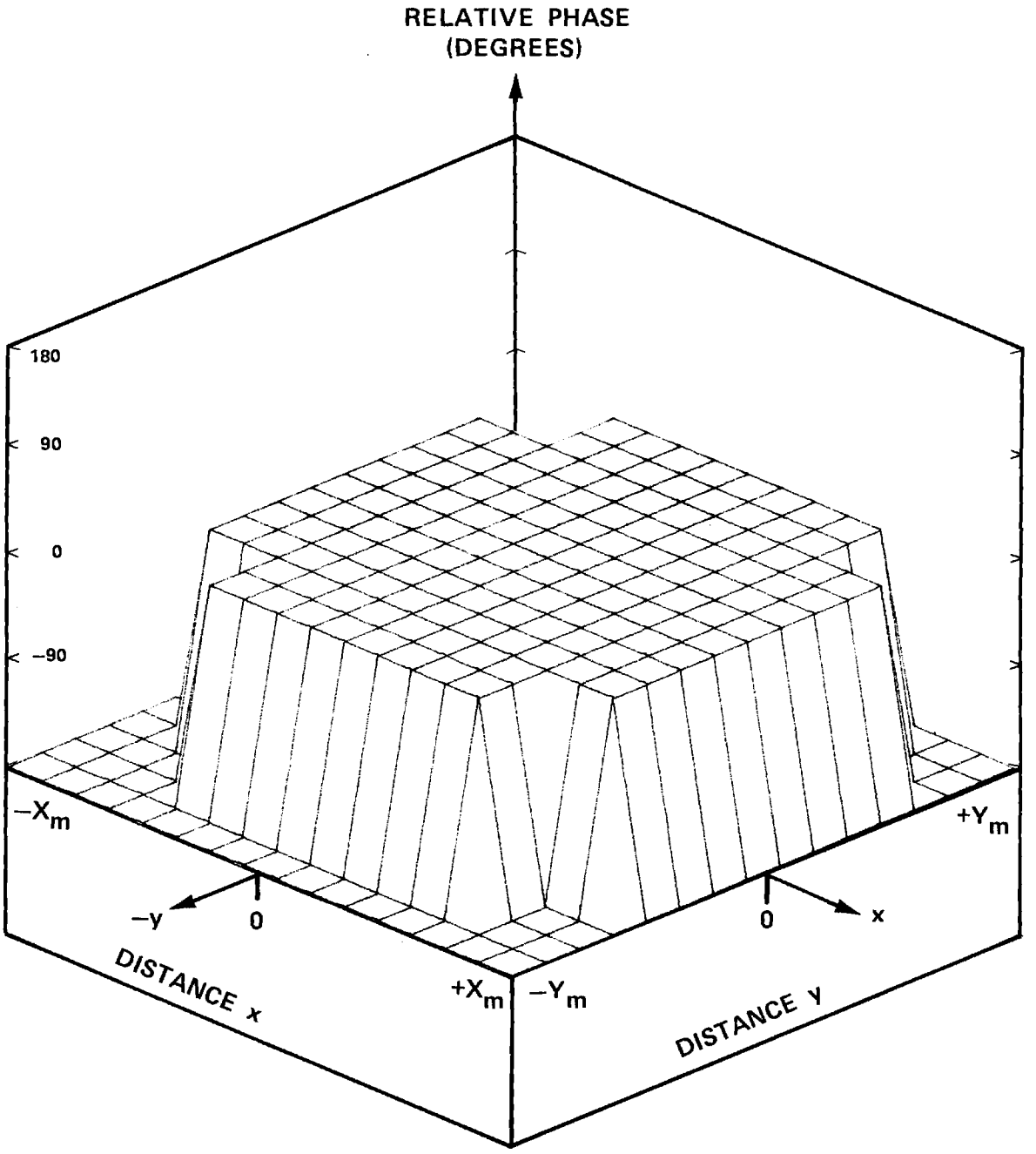

Figure D-3. Phase of $E_{Y\Sigma}$ of Flat Plate Antenna.

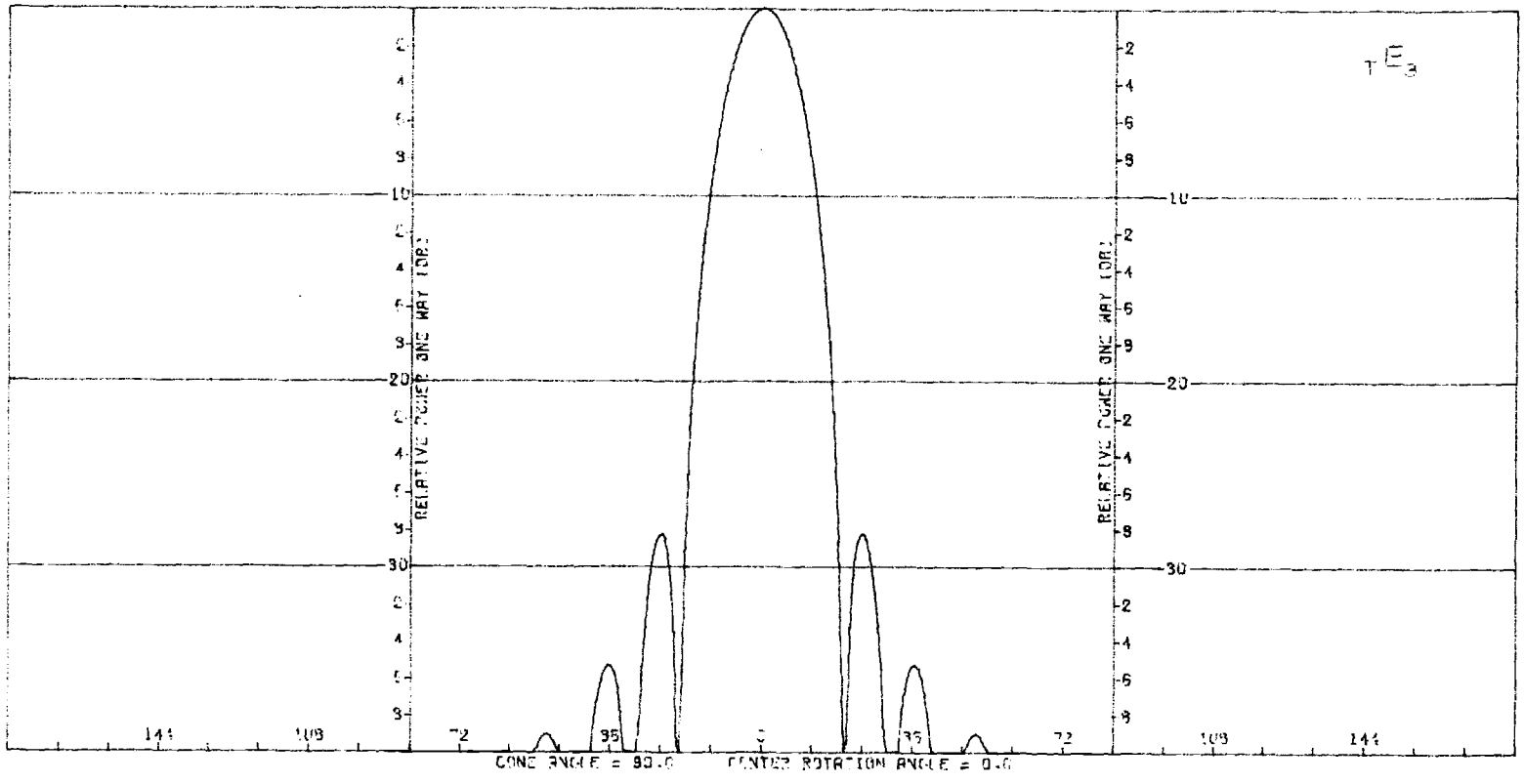

Figure D-4. Transmitting E-Plane Sum Pattern of Flat Plate Antenna.

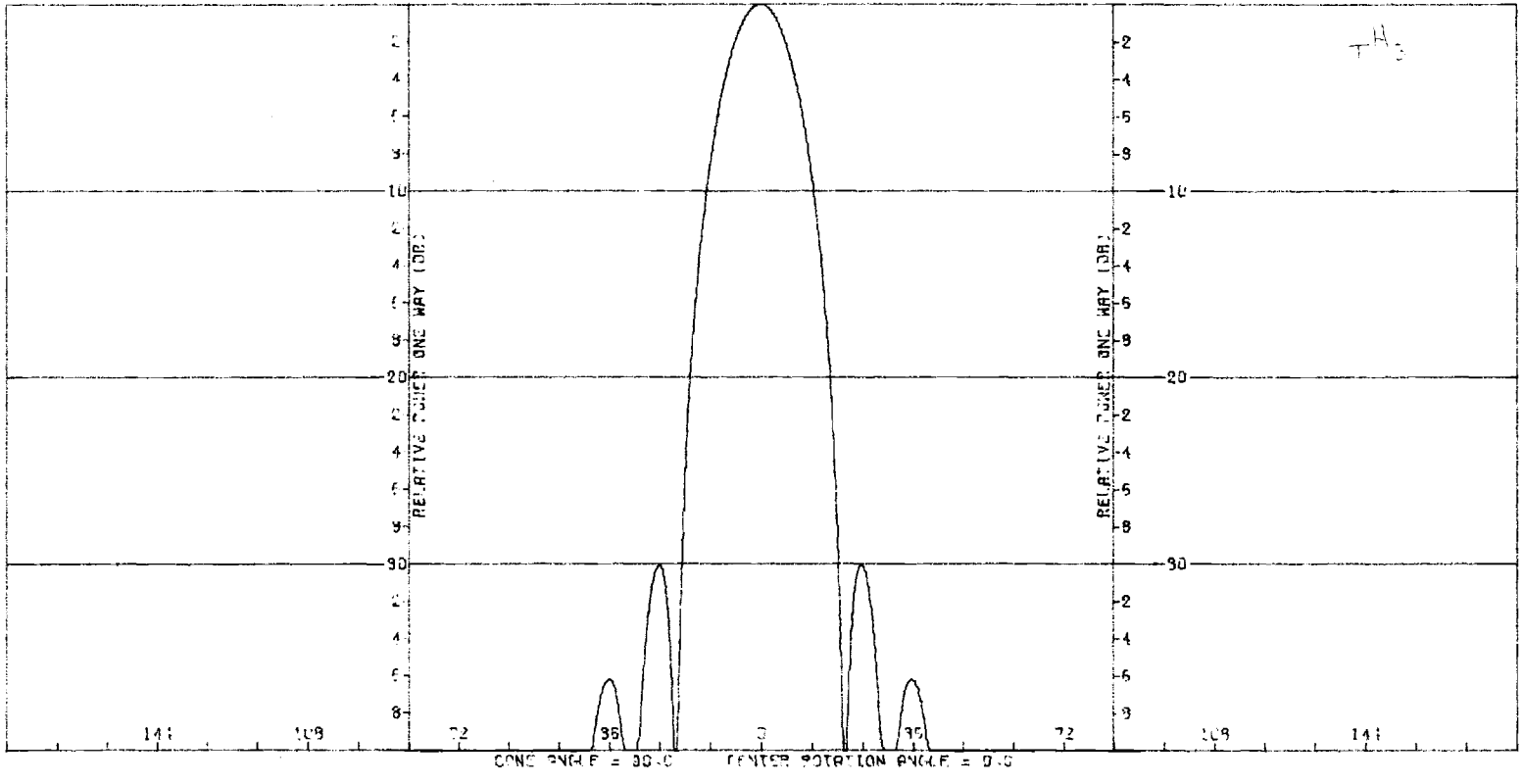

Figure D-5. Transmitting H-Plane Sum Pattern of Flat Plate Antenna.

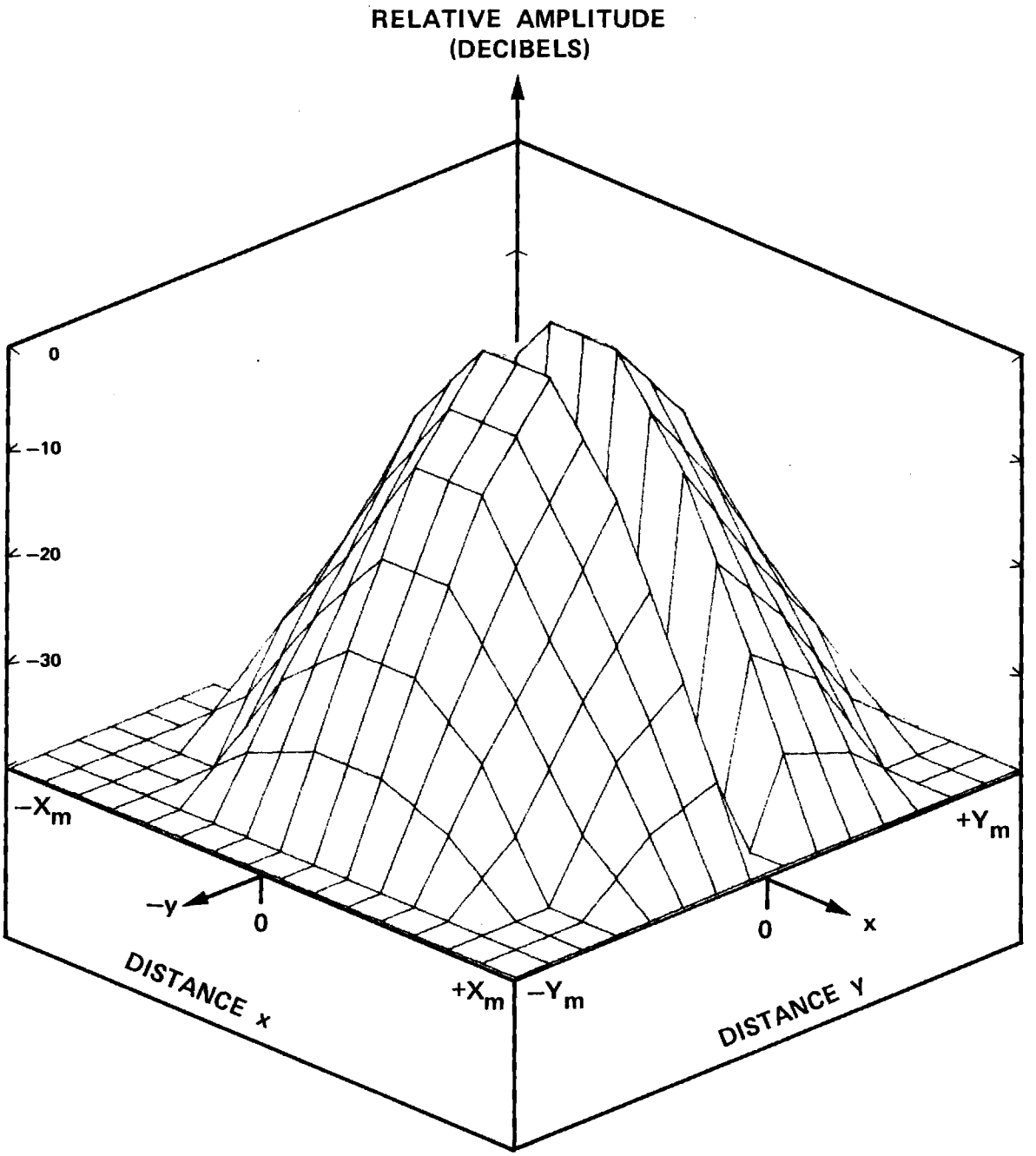

Figure D-6. $|E_{Y\Delta EL}|$ of Flat Plate Antenna.

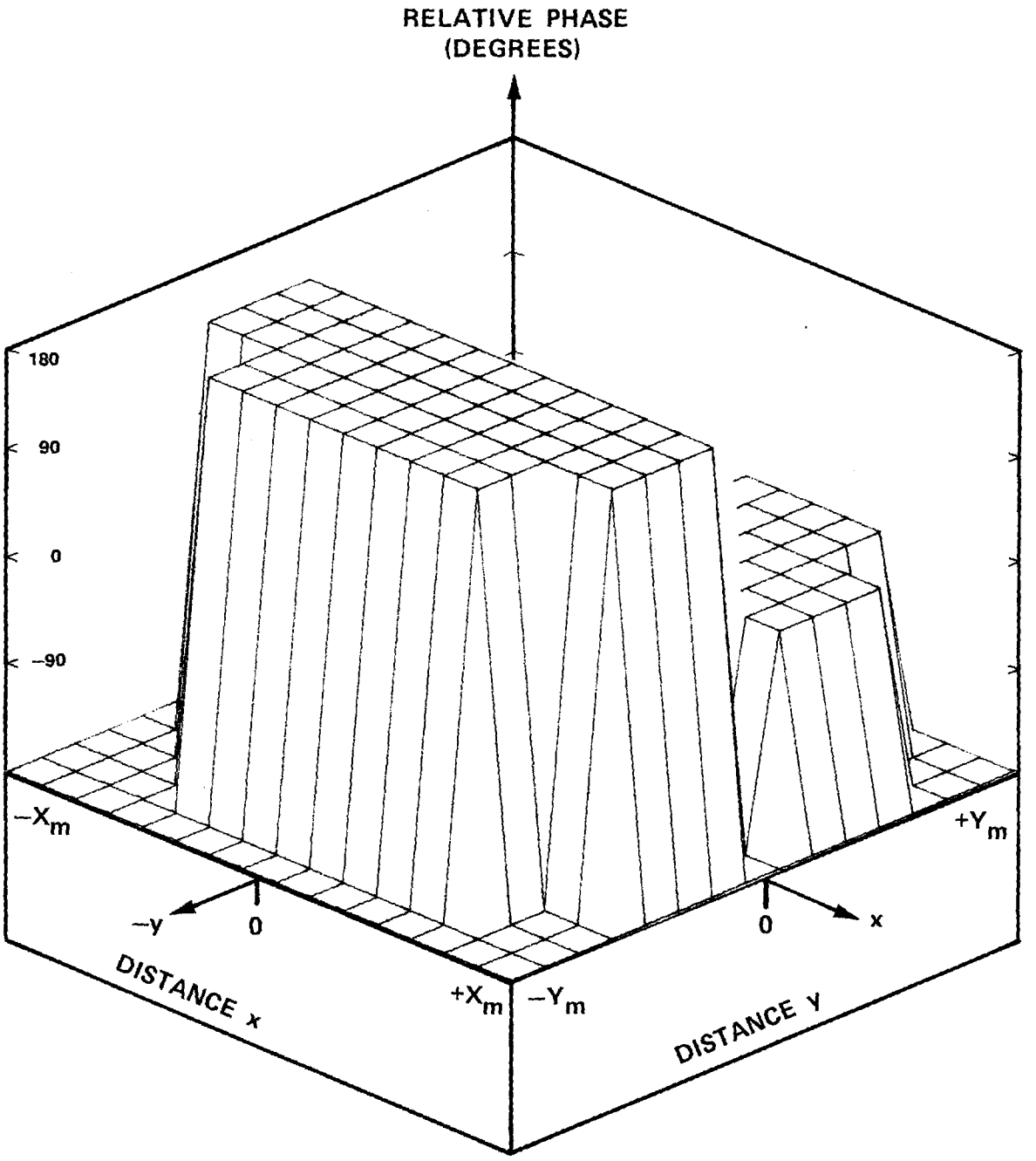

Figure D-7. Phase of $E_{Y\Delta EL}$ of Flat Plate Antenna.

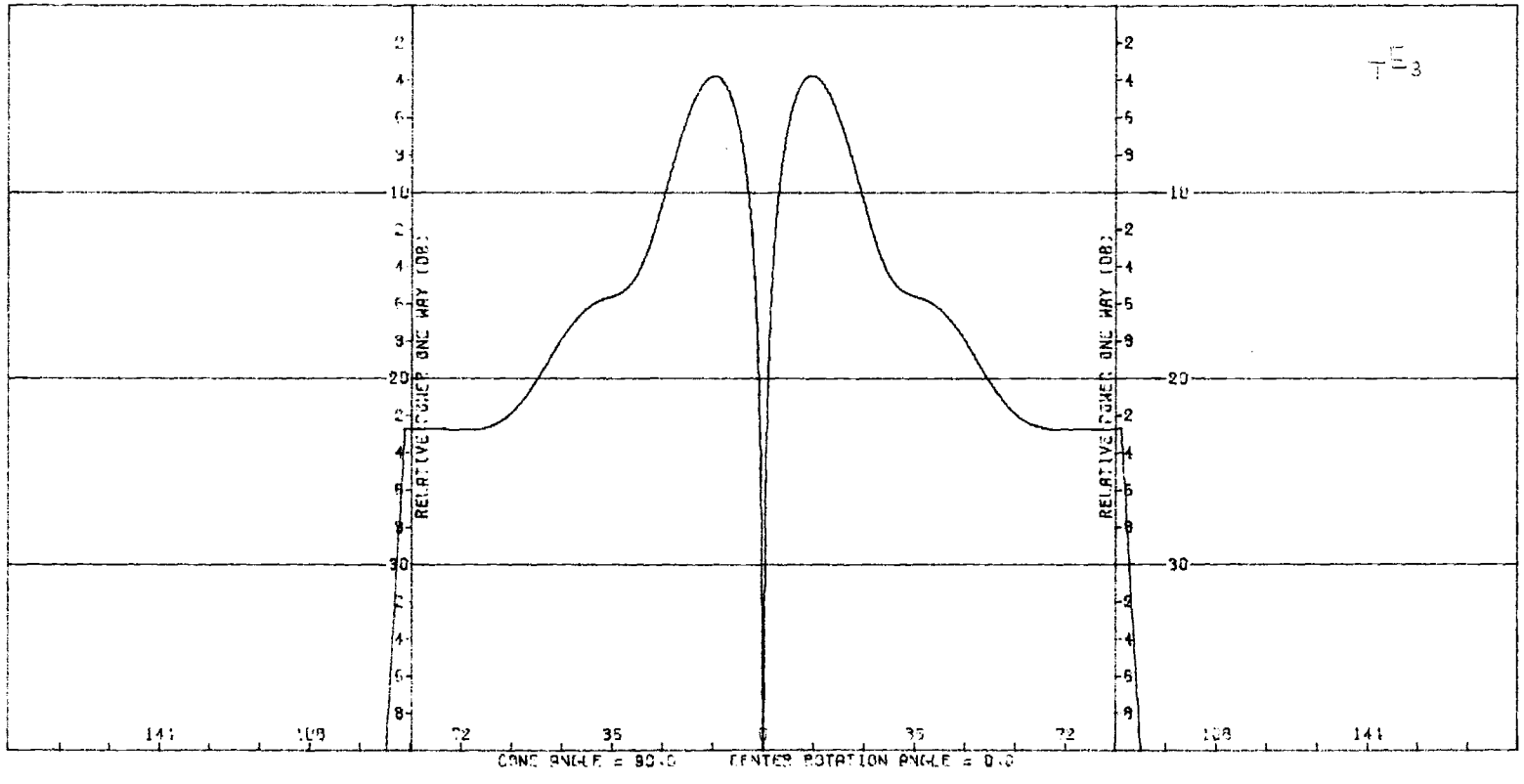

Figure D-8. Transmitting E-Plane Δ_{EL} Pattern of Flat Plate Antenna.

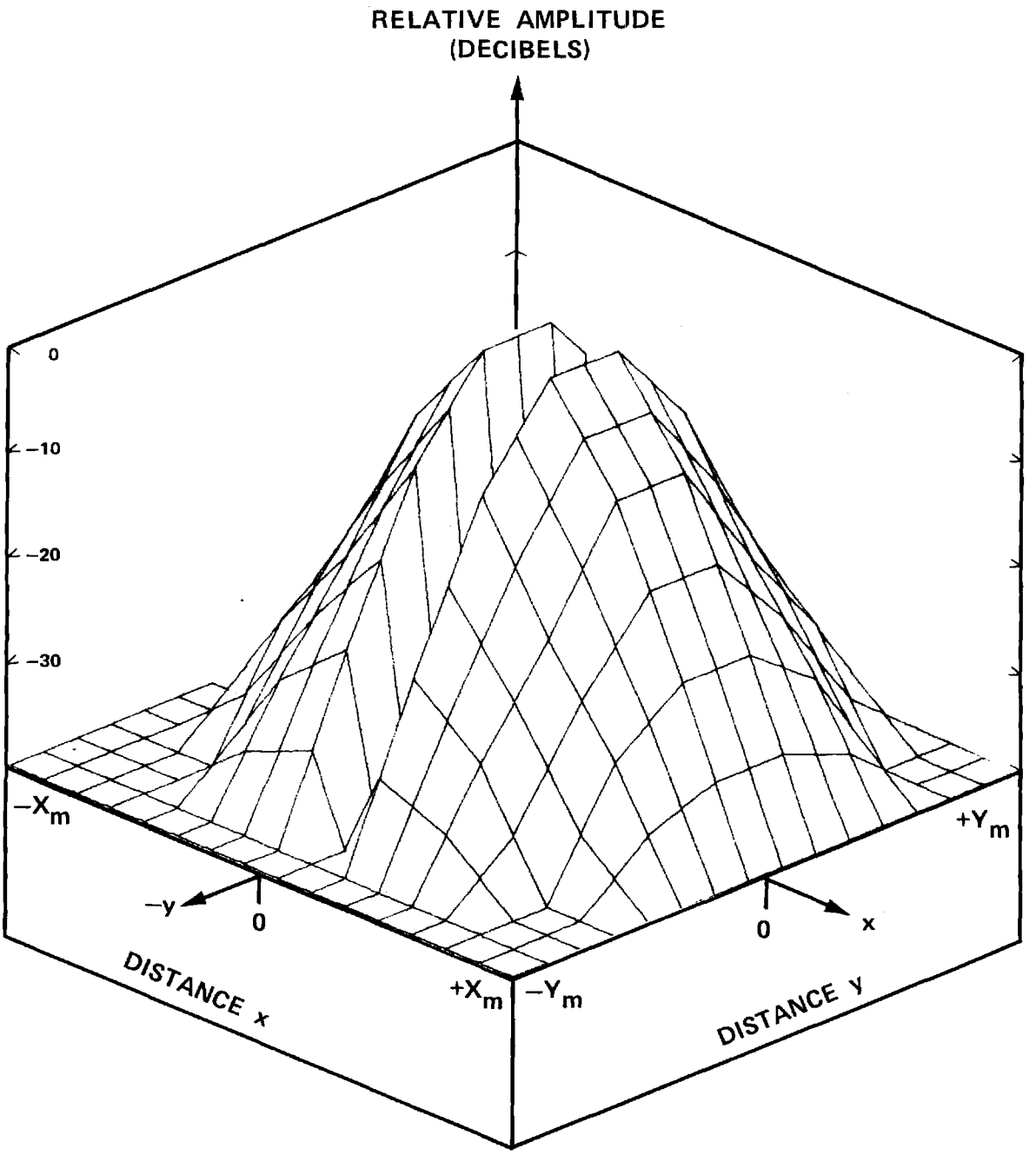

Figure D-9. $|E_{Y\Delta AZ}|$ of Flat Plate Antenna.

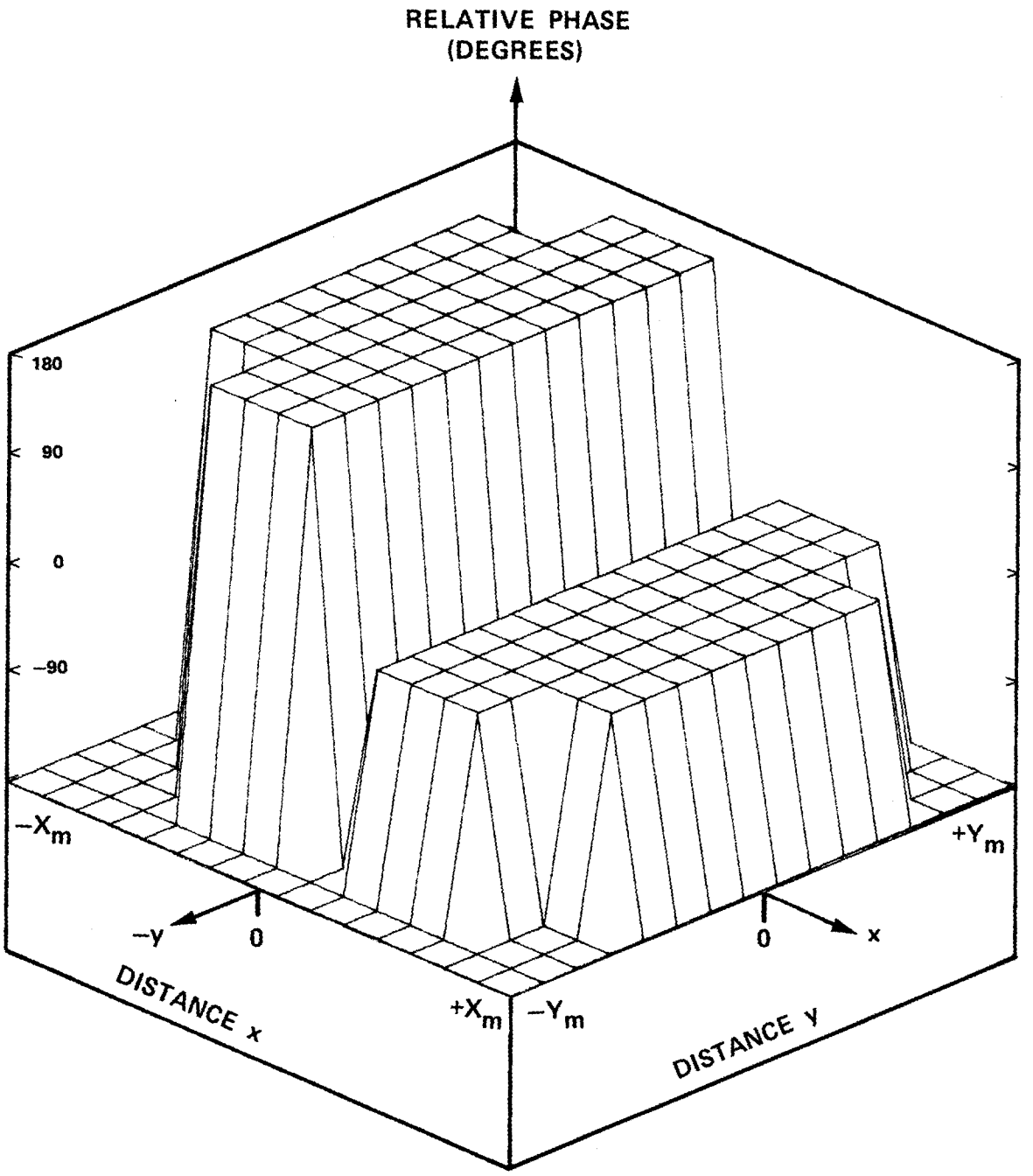

Figure D-10. Phase of $E_{Y\Delta AZ}$ of Flat Plate Antenna.

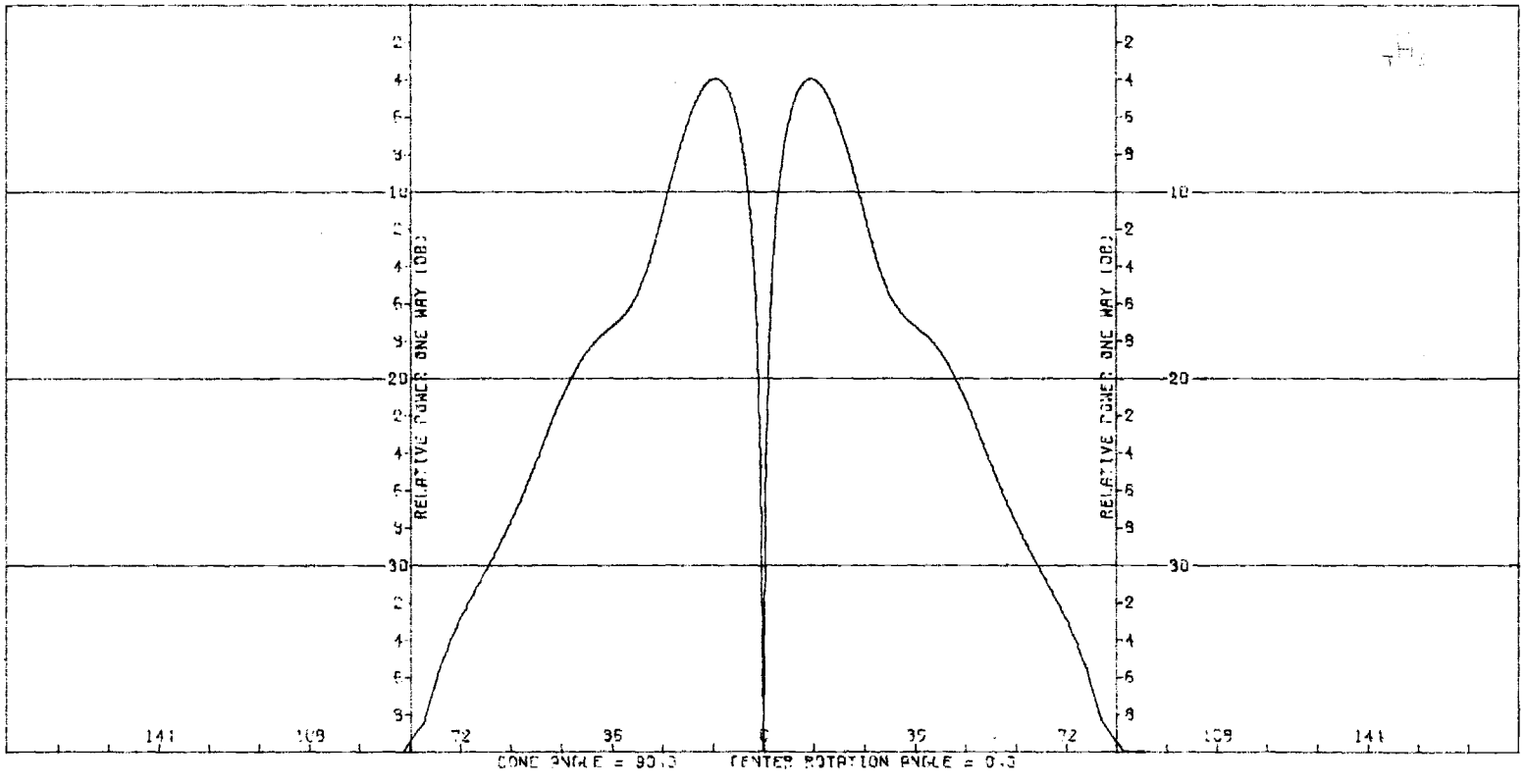

Figure D-11. Transmitting H-Plane Δ_{AZ} Pattern of Flat Plate Antenna.

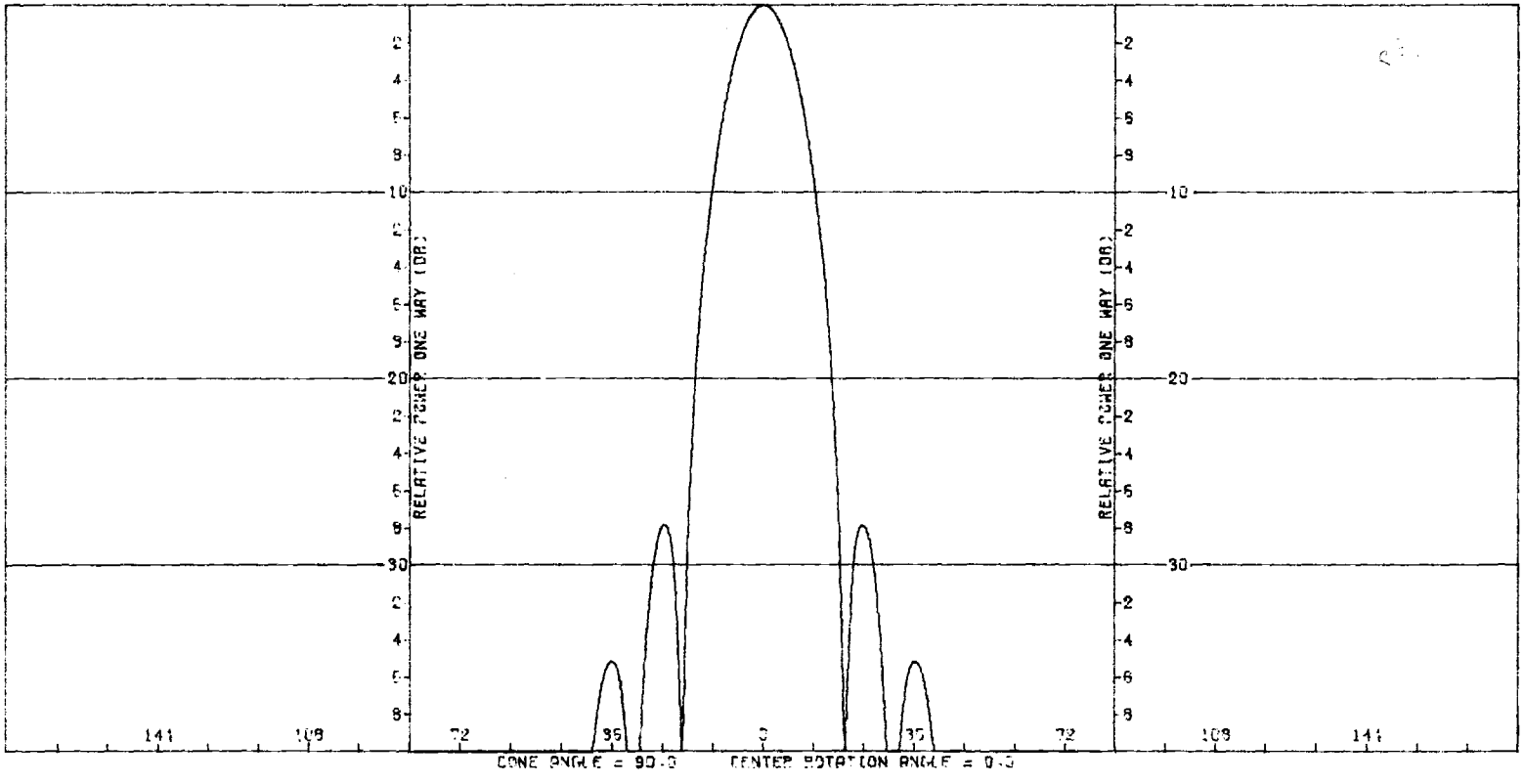

Figure D-12. Receiving E-Plane Sum Pattern of Flat Plate Antenna With Radome.

PARAMETRIC INVESTIGATION OF RADOME ANALYSIS METHODS:

COMPUTER–AIDED RADOME ANALYSIS USING THE HUYGENS–FRESNEL PRINCIPLE AND LORENTZ RECIPROCITY

By

G. K. Huddleston, H. L. Bassett, & J. M. Newton

Prepared for

AIR FORCE OFFICE OF SCIENTIFIC RESEARCH (AFSC)
BOLLING AIR FORCE BASE, D. C. 20332

FINAL TECHNICAL REPORT, VOLUME III OF IV
GRANT AFOSR–77–3469
30 September 1977 – 31 December 1980

February 1981

GEORGIA INSTITUTE OF TECHNOLOGY
SCHOOL OF ELECTRICAL ENGINEERING &
Engineering Experiment Station
Atlanta, Georgia 30332

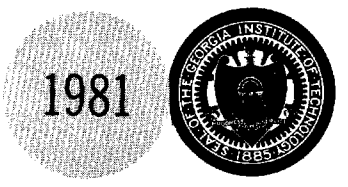

UNCLASSIFIED

SECURITY CLASSIFICATION OF THIS PAGE *(When Data Entered)*

REPORT DOCUMENTATION PAGE		READ INSTRUCTIONS BEFORE COMPLETING FORM
1. REPORT NUMBER	2. GOVT ACCESSION NO.	3. RECIPIENT'S CATALOG NUMBER
4. TITLE *(and Subtitle)* PARAMETRIC INVESTIGATION OF RADOME ANALYSIS METHODS: COMPUTER-AIDED RADOME ANALYSIS USING THE HUYGENS-FRESNEL PRINCIPLE AND LORENTZ RECIPROCITY		5. TYPE OF REPORT & PERIOD COVERED Final Technical Report, Vol. 3 of 4 30 September 1977-31 Dec. 1980 6. PERFORMING ORG. REPORT NUMBER
7. AUTHOR(s) G. K. Huddleston, H. L. Bassett, & J. M. Newton		8. CONTRACT OR GRANT NUMBER(s) AFOSR-77-3469
9. PERFORMING ORGANIZATION NAME AND ADDRESS Georgia Institute of Technology School of Electrical Engineering & Engineering Experiment Station Atlanta, Georgia 30332		10. PROGRAM ELEMENT, PROJECT, TASK AREA & WORK UNIT NUMBERS 61102F 2301/A6
11. CONTROLLING OFFICE NAME AND ADDRESS Air Force Office of Scientific Research Physics Directorate (Code NP-77-148) Bolling Air Force Base, D. C. 20332		12. REPORT DATE February 1981 13. NUMBER OF PAGES 133
14. MONITORING AGENCY NAME & ADDRESS*(if different from Controlling Office)*		15. SECURITY CLASS. *(of this report)* UNCLASSIFIED 15a. DECLASSIFICATION/DOWNGRADING SCHEDULE

16. DISTRIBUTION STATEMENT *(of this Report)*

Approved for public release; distribution unlimited.

17. DISTRIBUTION STATEMENT *(of the abstract entered in Block 20, if different from Report)*

18. SUPPLEMENTARY NOTES

19. KEY WORDS *(Continue on reverse side if necessary and identify by block number)*

Radome Analysis
Huygens-Principle
Lorentz Reciprocity
Surface Integration

20. ABSTRACT *(Continue on reverse side if necessary and identify by block number)*

A Fortran computer program is described for computing the effects of a tangent ogive radome on the receiving patterns and boresight directions of a monopulse antenna. A receiving formulation with the inside surface of the radome being the surface of integration is used. Aperture integration is used to compute the near fields of the antenna. The main program and seven subroutines are well documented.

DD FORM 1 JAN 73 1473 EDITION OF 1 NOV 65 IS OBSOLETE

UNCLASSIFIED

PARAMETRIC INVESTIGATION OF

RADOME ANALYSIS METHODS:

COMPUTED-AIDED RADOME ANALYSIS USING

THE HUYGENS-FRESNEL PRINCIPLE AND

LORENTZ RECIPROCITY

by

G. K. Huddleston, H. L. Bassett, & J. M. Newton
School of Electrical Engineering &
Engineering Experiment Station
Georgia Institute of Technology

Final Technical Report, Volume III of IV

for

Air Force Office of Scientific Research (AFSC)
Physics Directorate (Code NP-77-148)
Bolling Air Force Base, D. C. 20332

under

Grant AFOSR-77-3469
30 September 1977 - 31 December 1980

February 1981

TABLE OF CONTENTS

LIST OF ILLUSTRATIONS

LIST OF TABLES

Chapter 1

INTRODUCTION AND SUMMARY

1-1. Introduction

This Volume III of this final technical report of four volumes documents a surface integration radome analysis computer program written in Fortran IV for use on the Cyber 70/74 computing system at Georgia Institute of Technology and the IBM 3033 computing system at Johns Hopkins University Applied Physics Laboratory. The program was developed at Georgia Institute of Technology over the past three years under grant AFOSR-77-3469 and documented herein under the cognizance of R. C. Mallaleiu (APL Contract 60153).

The analysis package described was used during the research to analyze the antennas and radomes as described in Volumes I and IV. Its documentation was done in conjunction with an on-going radome technology program at JHU/APL. It is intended to serve as part of a technology base for the radome technical community.

This report is organized by chapters, where each chapter describes the main program or one subprogram not already described in Reference 1 (Ray Tracing Formulation). The main program (Chapter 2) described herein differs only slightly from that in Reference 1. Only six new subroutines are required for the surface integration formulation as described in Chapters 3-8. References cited in each chapter are listed therein. Each chapter is terminated with the program listing.

This software us currently being used in a parametric investigation of radome analysis methods, and additional information concerning its speed and accuracy is presented in Volume I [2].

1-2. Description of the Analysis

The basis of analysis is illustrated in Figure 1-1. The inner surface of the radome S_1 is chosen as one surface of integration in the Lorentz reciprocity integral (upper left in figure). A surface S_2 enclosing the antenna and extending into its interior, as illustrated, comprises the second surface. Together, $S_1 + S_2$ enclose the source-free Volume V indicated; hence, the Lorentz surface integral is identically zero and the integral over S_1 equals the negative of the integral over S_2.

Consider the surface S_2 more closely. The surface integral over S_2 is zero except over that part of S_2 which is placed across the waveguiding structure that connects the Source "a" to the radiating (flared) part of the antenna. Call this surface S_2'. If there can be defined a single dominant mode in the waveguide when Source "a" is activated, then voltage and current V_a, I_a can be defined at this terminal plane [4]. When Source "b" is activated, voltage and current V_b, I_b at S_2' can also be defined; in fact, V_b is the "received voltage". The received current I_b is related to V_b by a linear impedance relationship

$$V_b = I_b Z_a \tag{1}$$

where Z_a is the impedance seen at S_2' looking toward Source "a" (sinusoidal steady state assumed; time variations of the form $e^{j\omega t}$ understood and suppressed). Also, I_a and V_a are related by

$$V_a = I_a Z_1 \tag{2}$$

$$\oint_{S_1+S_2} (\underline{E}_a \times \underline{H}_b - \underline{E}_b \times \underline{H}_a).\hat{n}da = 0$$

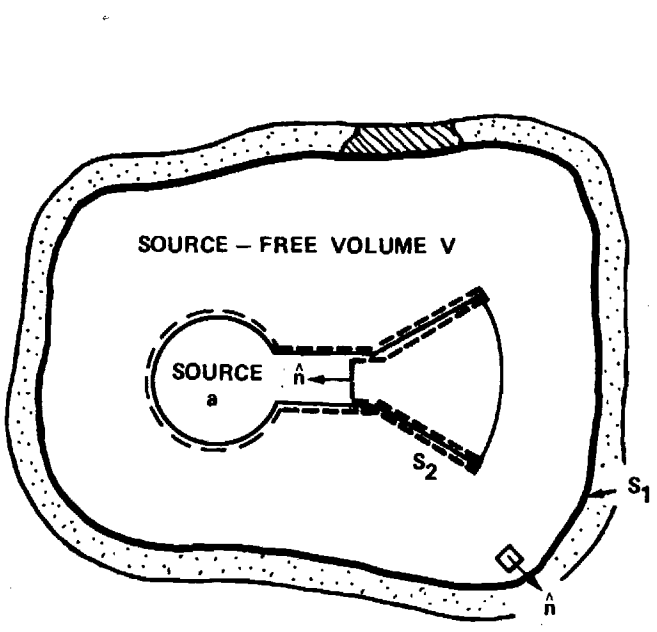

$$\int_{S_1} (\underline{E}_a \times \underline{H}_b - \underline{E}_b \times \underline{H}_a) .\hat{n}da$$

$$= -\int_{S_2} (\underline{E}_a \times \underline{H}_b - \underline{E}_b \times \underline{H}_a).\hat{n}da$$

$$= V_a I_b + V_b I_a$$

$$\underline{E}(x,y,z) = 1/4\pi \int_S [-j\omega\mu\psi(\hat{n} \times \underline{H}) + (\hat{n} \times \underline{E}) \times \nabla\psi + (\hat{n} \cdot \underline{E})\nabla\psi] \, dS$$

$$\underline{H}(x,y,z) = 1/4\pi \int_S [j\omega\epsilon(\hat{n} \times \underline{E})\,\psi + (\hat{n} \times \underline{H}) \times \nabla\psi + (\hat{n} \cdot \underline{H})\,\nabla\psi] \, dS$$

FIGURE 1–1. THEORETICAL BASIS OF RADOME ANALYSIS.

where Z_1 is the impedance seen at S_2' looking to the right in Figure 1-1. Combining these results yields the desired expression for the received voltage V_b; viz.,

$$V_b = V_{REC} = \frac{Z_1 Z_a}{V_a (Z_1 + Z_a)} \int_{S_1} (\underline{E}_a \times \underline{H}_b - \underline{E}_b \times \underline{H}_a) \cdot \hat{n} \, da \quad . \qquad (3)$$

Note that the unit normal is directed positively outward from volume V as dictated by Gauss' theorem.

When Source "b" in Figure 1-1 is removed a great distance from the antenna/radome structure, the fields of "b" approach those of an electromagnetic plane wave (target return). The practical analysis approach then takes the form shown in Figure 1-2. The inner radome surface is divided into a number of contiguous elemental areas ΔA, each of which is represented by a sample point P' at its center. The fields $\underline{E}_T$ $\underline{H}_T$ at P' are assumed to be those present there in the absence of the radome and are found by aperture integration, the theoretical basis of which is the Huygens-Fresnel principle [5] as stated by the lower integrals in Figure 1-1. The fields $\underline{E}_R$, $\underline{H}_R$ at P' are found by applying the normal voltage transmission coefficients [6] to the plane wave incident on the outside at point P. The received voltage is found by summing all the contributions as indicated in Equation (3).

The method of analysis indicated by Equation (3) is exact; however, certain approximations are necessarily introduced in its implementation. The fields $\underline{E}_T$, $\underline{H}_T$ should correctly include reflections from the inner radome surface. The use of the flat panel transmission coefficients to transform the incident plane wave at P to P' is an approximate method based on the theory of geometrical optics (zero wavelength) and whose

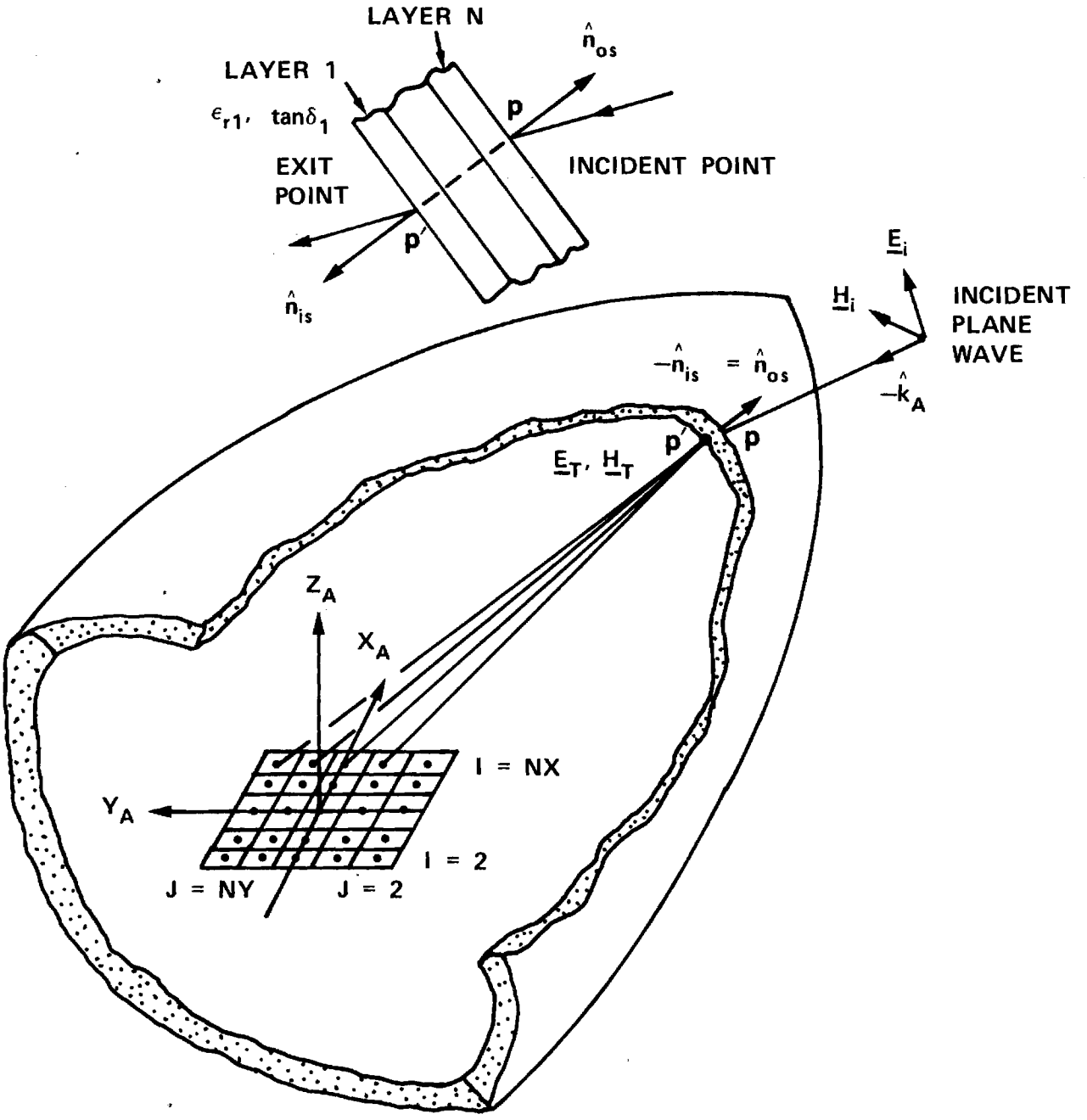

FIGURE 1–2. ILLUSTRATION OF RADOME ANALYSIS METHOD USING INSIDE RADOME SURFACE AS SURFACE OF INTEGRATION IN RECIPROCITY INTEGRAL.

accuracy depends upon the radius of curvature of the radome wall. The accuracy of the method also depends on the size of the samples used to represent the radiating aperture as well as the radome surface. The computational speed of the analysis most certainly depends on the number of these samples.

1-3. References

1. G. K. Huddleston, H. L. Bassett, & J. M. Newton, "Parametric Investigation of Radome Analysis Methods: Computer-aided Radome Analysis Using Geometrical Optics and Lorentz Reciprocity", Final Technical Report, Volume II of IV, Grant AFOSR-77-3469, February 1981.

2. G. K. Huddleston, H. L. Bassett, J. M. Newton, "Parametric Investigation of Radome Analysis Methods: Salient Results", Final Technical Report, Volume I of IV, Grant AFOSR-77-3469, February 1981.

3. R. E. Collin and F. J. Zucker, Antenna Theory, Part 1, Section 4.2, McGraw-Hill, New York, 1969.

4. S. Silver, Microwave Antenna Theory and Design, Ch. 2, Mc-Graw-Hill, New York, 1949.

5. Ibid, Ch. 3.

6. J. H. Richmond, "Calculation of Transmission and Surface Wave Data for Plane Multilayers and Inhomogeneous Plane Layers", Air Force Contract AF 33(615)-1081, The Antenna Laboratory, Ohio State University, Columbus, Ohio, October 1963.

Chapter 2

PROGRAM SIIRACP

2-1. Purpose: SIIRACP is a Fortran computer program used to analyze the effects of a tangent ogive radome on the performance of a monopulse aperture antenna. It consists of a main program and 28 subroutines, 22 of which are identical to those used in Program RTFRACP [1]. It uses complex arithmetic and requires 66600 octal words of core memory for execution on the CDC Cyber 70 system (60-bit words) at Georgia Institute of Technology. Execution time to compute boresight error on the Cyber 70 is approximately 255 seconds per look direction when the small antenna aperture is represented by 7 x 7 = 49 sample data points and the radome is represented by 826 sample points; i.e., approximately 1.26 millisecond per aperture sample point per radome sample point.

The computer-aided radome analysis uses a receiving formulation based on the Lorentz reciprocity theorem as described earlier [1,2]. The voltage produced at the terminals of a linear antenna by an incident plane wave is given by

$$V_R(\hat{k}) = \iint_S (\underline{E}_T \times \underline{H}_R - \underline{E}_R \times \underline{H}_T) \cdot \hat{n}\, da \qquad (1)$$

where $\underline{E}_T$, $\underline{H}_T$ are the fields produced on the surface S enclosing the antenna when the antenna is transmitting; $\underline{E}_R$, $\underline{H}_R$ are the incident fields produced on S by the incident plane wave or perturbations thereof; $\hat{k}$ is a unit vector which points from the antenna toward the direction from which the plane

wave arrives; and $\hat{n}$ is a unit vector normal to the surface S and pointing into the source-free region.* The fields $\underline{E}_T$, $\underline{H}_T$ are taken to be those produced by the planar aperture on surface S when the antenna is transmitting in the absence of the radome. The geometrical optics approximation

$$\underline{H}_T + \frac{\hat{n} \times \underline{E}_T}{\eta} \tag{2}$$

is used to generate the magnetic field in the aperture from the aperture illumination specified by $\underline{E}_T$.

The surface S is taken to be the inner surface of the radome. At each sample point P'on this surface, the plane wave fields $\underline{E}_R$, $\underline{H}_R$ incident from the outside are weighted with the flat panel normal voltage transmission coefficients as determined by the radome wall configuration, the angle of incidence, and the plane of incidence. The fields $\underline{E}_T$, $\underline{H}_T$ at P'are found by aperture integration. The individual contributions are summed up as indicated in Equation (1) and was illustrated in Figure 1-2.

The parameters of the tangent ogive radome are indicated in Figure 2-1. The outside base diameter D_{os} and fineness ratio F_{os} determine the outside length according to

$$F_{os} = L_{os}/D_{os} \tag{3}$$

A similar relation holds for the inside dimensions; viz.,

$$F_{is} = L_{is}/D_{is} \tag{4}$$

*By choosing $\hat{n}$ this way, the minus sign in Figure (1-1) is removed.

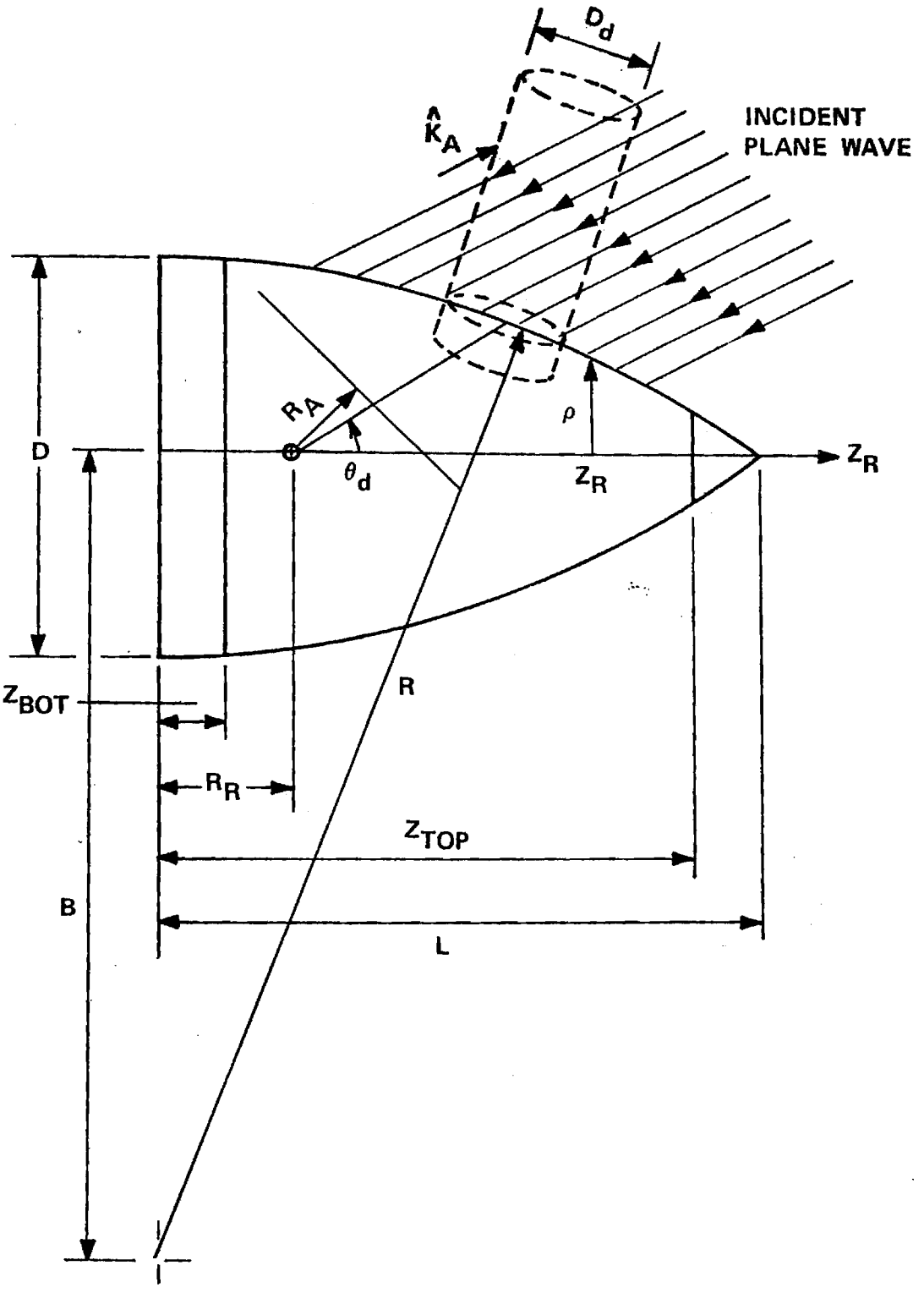

Figure 2-1. Tangent Ogive Radome Geometry.

The radius of curvature of the outside wall R_{os} is given by

$$R_{os} = F_{os} D_{os} / \sin (\pi - 2 \text{Tan}^{-1}(2F_{os})) \quad (5)$$

and the dimension B is given by

$$B = R_{os} - D_{os}/2 \quad (6)$$

The placements of a bulkhead (bottom disk) and metal tip (top disk) can be specified by Z_{BOT} and Z_{TOP}, respectively. The thickness, dielectric constant, and loss tangent of the wall may also be specified for up to N=5 layers. The radome is assumed to be a body of revolution with uniform wall dimensions independent of location. The dashed cylindrical shape of a diameter D_d in Figure 2-1 was used earlier to simulate a laser-induced defect and is not pertinent here.

The subroutine which generates the antenna aperture fields represents three types of antennas: circular or square aperture with tapered (cos x) illumination and any one of four polarizations (vertical, horizontal, RHC, LHC); flat plate antenna with tapered illumination and vertical polarization. For either antenna, the fields are computed for one of three selected channels: sum, azimuth difference, elevation difference. Inputs include the number of samples N_X, N_Y and the aperture diameter D_{AP}/λ in wavelengths.

The antenna/radome orientation is specified according to the parameters defined in Figure 2-2. The angle ϕ_p selects the plane of scan of the radome tip with respect to the antenna coordinate system: $\phi_p = 0°$ selects the azimuth plane; $\phi_p = 90°$ selects the elevation plane. The angle θ_L scans the tip in the selected plane.

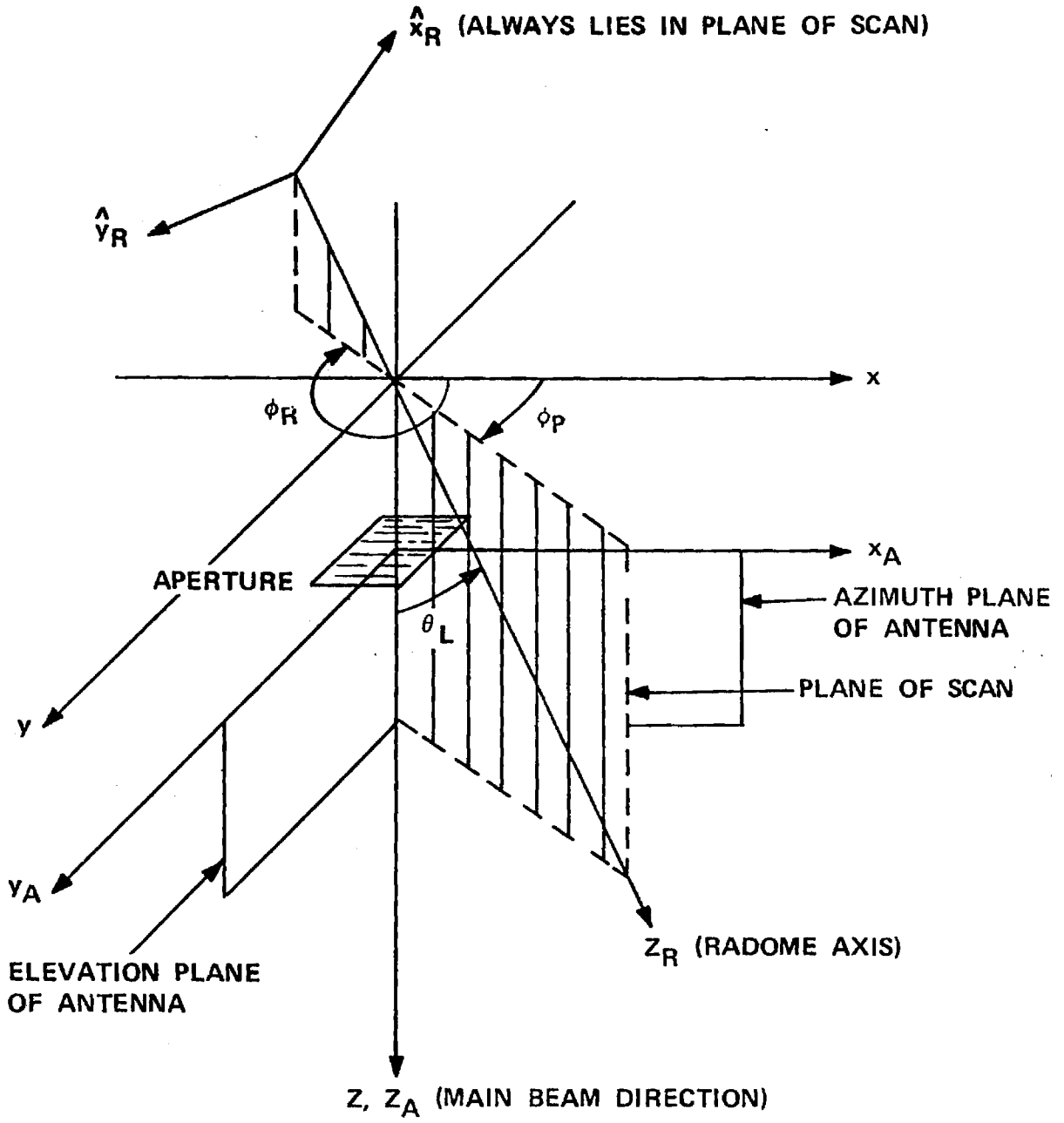

Figure 2-2. Coordinate Systems Used in Radome Analysis.

The program computes boresight errors in the azimuth and elevation planes of the antenna. The radome orientation is specified by ϕ_p and ϕ_L. The first target return (plane wave) is made to arrive from the direction

$$\hat{k}_1 = \hat{x}_A \sin \theta_{os} + \hat{y}_A \sin \theta_{os} + \hat{z}_A \sqrt{1 - 2 \sin^2 \theta} \tag{7}$$

where θ_{os} is the initial specified offset angle; e.g., 2°. The voltage received by each channel is computed and stored. The second return is made to arrive from

$$\hat{k}_2 = \hat{x}_A(-\sin \theta_{os}) + \hat{y}_A(-\sin \theta_{os}) + \hat{z}_A \sqrt{1 - 2 \sin^2 \theta_{os}} \tag{8}$$

and the voltages are again computed. The data from these two points are used to construct a linear tracking model in the two planes, and a direction of arrival $\hat{k}$ is predicted which will yield null indications in both planes. The process is repeated until a desired error tolerance is satisfied or a maximum number of iterations is exceeded. Upon completion, the output $\hat{k}$ indicates the direction from which the plane arrives which yields an electrical boresight indication. If α and β represent the boresight error angles in the azimuth and elevation planes, respectively, then they are related to the direction $\hat{k} = \hat{x}_A k_x + \hat{y}_A k_y + \hat{z}_A k_z$ by

$$\sin \alpha = \frac{k_x}{\sqrt{1 - k_y^2}} \tag{9}$$

$$\sin \beta = \frac{k_y}{\sqrt{1 - k_x^2}} \tag{10}$$

where

$$k_z = \sqrt{1 - k_x^2 - k_y^2} \quad . \tag{11}$$

Options are also provided whereby principal plane patterns as shown in Figure 2-3 and additional outputs around boresight can be computed and printed. These options are useful when preparing software for a new type of antenna and to ensure correct operation whenever curious results are obtained.

2-2. Usage:

	Line No.
DATA APIN/0./	47
DATA ZBOTIN/0.00/	49
DATA RADIUS/1E0/	52
DATA THETAA, PHIA, AGAM3A/0.0,90.0,0.0/	53
DATA NX, NY, NYE, NXY/4,4,1,512/	56
DATA MY/1/,NREC/61	57
READ (5,6) TITLE	63
READ (5,*) GRAF3D, GRAFSA, GRAFTR, GRAFRV, SUPPRS, IPENCD, SQUARE	65
READ (5,*) NFINE, NPHI, NTHE, DIAOS, RAIN, RRIN, ZTOPIN, FREQ, OSANG	67
READ (5,*) LMAX, DMRAD, IOPT, RAPMAX, VAIRM, IPOL, ICASE, N, IPWR, KMAX, NXE	76
READ (5,*) DSTHIN, DSPHIN, NTHMIN, NPHIMIN	79
READ (5,*) DIN(I), ER(I), TD(I) (I=1,N)	115
READ (5,*) FINR(I) (I=1,NFINE)	124
READ (5,*) PHI(I) (I=1, NPHI)	127
READ (5,*) THETA(I) (I=1,NTHE)	129

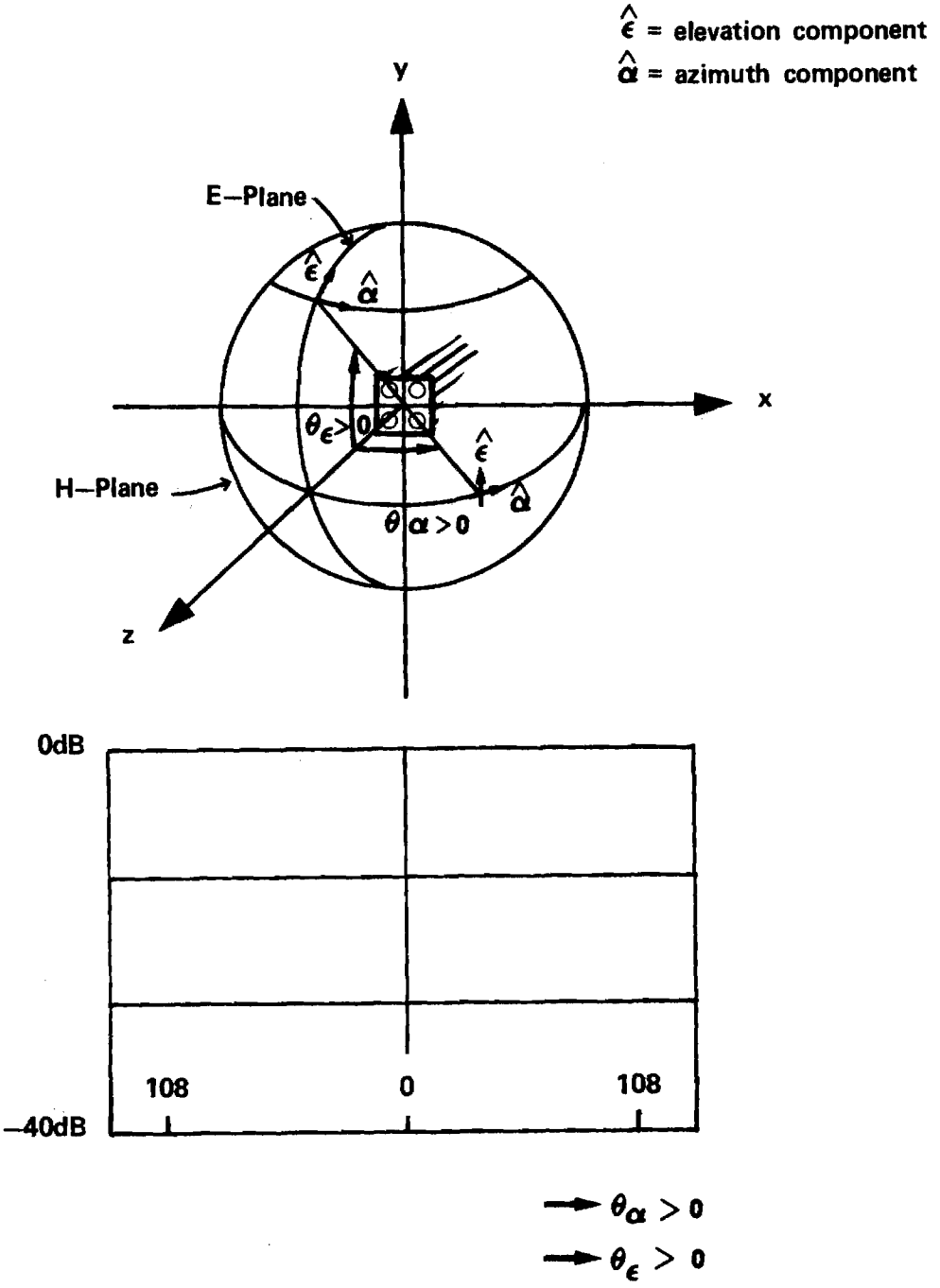

Figure 2.3 Coordinate System for Far Field Patterns

2-3. Arguments

a. Inputs. Units of arguments on input are distances in inches, angles in degrees, and frequency in gigahertz, unless otherwise noted. Units of arguments passed to subroutines are centimeters, radians, and gigahertz. An asterisk is used to denote those DATA arguments that do not normally need to be changed by the user.

APIN* - Height of a cylindrical base section of the tangent ogive radome. It is no longer included in the ray tracing algorithms and should not be changed from its zero value.

ZBOTIN - Distance from base of tangent ogive radome to missile bulkhead (Figure 2-1).

RADIUS* - The radius R used in the far field factor e^{-jkR}/R by Subroutine FAR. Do not change.

THETAA* - Angle θ_a between z-axis and the position vector $\underline{r}_a$ to the antenna origin. This angle was used in earlier work to locate the antenna origin in the reference system using spherical coordinates (r_a, θ_a, ϕ_a). Do not change.

PHIA* - Angle ϕ_a between the projection of z_A axis onto the xy-plane and the x-axis. Do not change.

AGAM3A* - Angle between z_A-axis and z-axis in Figure 2-2. Do not change.

NX,NY - Integer powers of two equal to the number of sample points in the antenna aperture; e.g., 16, 32, 64, etc. Changing NX and NY necessitates compatible changes in Lines 16-18.

NYE (NXE) - Integer powers of two which specify the expanded number of sample points desired when computing the transmitting patterns of the antenna by inverse Fourier transforming the aperture fields. Subroutine JOYFFT provides this capability of increased resolution in one or both dimensions. Changes in NXE, NYE necessitate compatible changes in Lines 16, 20, 22 and 23. Note that NXE*NYE$\leq$NX*NY and either NXE$\leq$NX or NYE$\leq$NY.

NXY - Integer power of two used by Subroutine JOYFFT for dimension of complex working array XYFFT. Note that MX*NX$\leq$NXY and MY*NY$\leq$NSY. See below for MX and MY.

NREC - Integer variable equal to the number of points at which to compute the receiving pattern in either principal plane. The received voltage is computed at points θ_i equally spaced in $\sin\theta$, where θ is the angle measured from the z_A-axis as indicated in Figure 2-3, where $\sin\theta_i$ = -KMAX + (I-1)*2*KMAX/NREC, and where KMAX = $\sin\theta_{max} < 1.0$.

NS - Not used. It was originally used by Subroutine RECBS. Do not remove.

MX,MY - Integer powers of two equal to the magnification factors desired in the k_x (H-plane) and k_y (E-plane) directions, respectively, of the transmitting antenna patterns. Note that the restrictions MX*NY$\leq$NXY and MY*NY$\leq$NXY must be observed. The data cited

above indicates increased resolutions in the NX direction of MX=16 and no magnification (MY=1) in the NY direction. Consequently, note that NXE=MX*NX=256.

TITLE - A Hollerith string of up to 72 characters which describes briefly the analysis being done. A format of 18A4 is specified and should work for machines with word length greater than or equal to 32 bits. The dimension of TITLE (Line 31) should be at least 18.

GRAF3D - A logical variable used to control the plotting of the incident fields on the antenna aperture. This feature has been removed from the program, and GRAF3D should always be FALSE.

GRAFSA - A logical variable which (if TRUE) controls the plotting of the transmitting power patterns of the antenna as follows: E-plane sum, E-plane difference equation (Δ_{EL}), H-plane sum, and H-plane difference azimuth (Δ_{AZ}). The radome is absent.

GRAFTR - A logical variable which controls the plotting of the amplitude and phase of the antenna aperture fields in the following order:

$E_{X\Sigma}$, $E_{Y\Sigma}$, $E_{X\Delta EL}$, $E_{Y\Delta EL}$, $E_{X\Delta AZ}$, $E_{Y\Delta AZ}$.

GRAFRV - A logical variable which controls the plotting of the receiving patterns of the antenna with radome in the same order as specified under GRAFSA above.

SUPPRS - A logical variable which controls the printing of numerous results. When TRUE, the printing of these numerous results are suppressed. This feature is convenient to aid in debugging new portions of software prior to making production runs.

IPENCD - An integer variable which selects pen and paper for the Calcomp. This variable may be system dependent. For the Cyber 70, IPENCD=00 yields ballpoint pen and 11" wide plain paper; IPENCD=40 yields a heavier ink pen and the same paper.

SQUARE - Logical input variable which selects a square aperture (TRUE) in Subroutine TRECNF.

NFINE - Integer variable equal to the number of fineness ratios to be considered for the tangent ogive radome; e.g., NFINE=1.

NPHI - Integer variable equal to the number of scan planes; e.g., NPHI=2.

NTHE - Integer variable equal to the number of angles in each scan plane at which to compute boresight errors, etc. Note: The program is set up to iterate on fineness ratio, scan plane, and scan angle as outer loop, middle loop, and inner loop, respectively. Therefore, for each of NFINE fineness ratios, the analysis will be done for NTHE scan angles in NPHI different scan planes.

DIAOS - Real variable equal to the outside base diameter (in.) of the radome. See Figure 2-1.

RAIN - Real variable equal to the distance (in.) from the gimbal point to the antenna aperture.

RRIN - Real variable equal to the distance (in.) from the gimbal point to the base of the radome.

ZTOPIN - Real variable equal to the distance (in.) from the base of the radome to the face of a metal tip on the radome.

FREQ - Real variable equal to the frequency of operation in gigahertz.

OSANG - Real variable equal to the offset angle in degrees at which the first target return is to arrive on the antenna; e.g., OSANG=3.0.

LMAX - Integer variable equal to the maximum number of iterations allowed by Subroutine RECBS in computing boresight error; e.g., LMAX=5.

DMRAD - Real variable equal to the tolerance in milliradians allowed on computing boresight error; e.g., DMRAD=0.1.

IOPT - Integer variable which selects the polarization of the incident plane wave as follows:

1. Linear, elevation component
2. Linear, azimuth component
3. Right hand circular
4. Left hand circular

RAPMAX - Real variable equal to the maximum radius (in.) of the antenna aperture.

VAIRM - Real variable equal to the maximum amplitude of sum channel received voltage without radome. Any

real value can be entered for this variable since a subsequent program modification (Lines 345-362) causes VAIRM to be computed automatically.

IPOL - Integer variable which selects the polarization of the antenna when ICASE=1 according to the same code as used above for IOPT.

ICASE - Integer variable which selects the type of antenna aperture for the analysis: ICASE=1 or 2 selects a circular or square aperture with tapered illumination; ICASE=3 selects a flat plate antenna with programmed illumination. See Subroutine TRECNF in Chapter 4.

N - Integer variable equal to the number of layers (up to 5) in the radome wall. For cases where more than 5 layers are required, the dimensional arrays on Line 37 must be changed to NN=N+1.

IPWR - Integer variable which selects the component for which to compute the transmitting power patterns as follows:

1. Elevation Components
2. Azimuth Component
3. Total power

KMAX - Real variable equal to the sine of the maximum angle at which receiving patterns are to be computed.

NXE - Integer variable used by JOYFFT as explained above.

DSTHIN, DSPHIN - Real variables equal to the distance between adjacent sample points on the radome surface in the

longitudinal (θ) and circumferential (ϕ) directions, respectively. See Chapter 3.

NTHMIN, NPHIMIN - Integer variables equal to the minimum acceptable number of radome sample points in the two directions.

DIN,ER,TD - Subscripted real variables equal to the thickness (in.), dielectric constant (ϵ_r), and loss tangent (tan δ) of each layer of the radome wall. I=1 corresponds to the first layer and is the layer on exit side of the wall. Layer N is the first layer encountered by the incident plane wave. See Subroutine WALL.

FINR - Subscripted real variable equal to NFINE fineness ratios.

PHI - Subscripted real variable equal to NPHI angles (degrees) which specify the scan planes.

THETA - Subscripted real variable equal to NTHE angles (degrees) which specify the scan angles in the scan plane.

b. Outputs. The parameters of analysis which are computed and outputted by the program depend on whether SUPPRS is true. In what follows, it is assumed that SUPPRS=FALSE so that all possible outputs are obtained. Since many of the original input parameters are printed directly, only those parameters not already explained above will be included below. Additional clarification may be found in Section 2-6.

TABLE - Logical variable which, if TRUE, causes a look-up table to be used in computing transmission coefficients. When SUPPRS=FALSE, an abbreviated table

of transmission coefficients of the radome wall is printed by Subroutine WALL with variables as explained immediately below.

ANGLE - Real variable equal to the angle of incidence (degrees) of the plane wave on a plane sheet of infinite extent having the layered configuration specified for the radome wall. The entries in the table are computed at 250 equal increments in sin θ_i, but only every fifth result is printed.

TPERI,TPARI - Complex variables equal to the normal voltage transmission coefficients of the sheet for the two cases of $\underline{E}_i$ perpendicular to the plane of incidence ($T_\perp$) and $\underline{E}_i$ parallel to the plane of incidence ($T_{||}$). In the printed table, the power transmission coefficients $|T_\perp|^2$ are $|T_{||}|^2$ are printed; adjacent to each, the phases of $T_\perp$ and $T_{||}$ are also printed.

RPERI,RPARI - Complex variables equal to the reflection coefficients $R_\perp$, $R_{||}$ of the plane dielectric sheet. Actually, $|R_\perp|^2$ and $|R_{||}|^2$ are printed, accompanied by the phases of $R_\perp$ and $R_{||}$.

KXMAX - Real variable equal to the folding wavenumber associated with sampling the aperture fields according to KXMAX = 1./(2($\Delta x/\lambda$), where x is the distance between samples.

DXWL - Real variable equal to $\Delta x/\lambda$.

KXM,KYM - Real variables equal to the folding wavenumbers of the principal plane patterns after magnification

for increased resolution. KXM=KYMAX*NXE/(MX*NX) and applies to the H-plane.

KYM=KYMAX*NYE/(MY*NY) and applies to the E-plane. Usually, the expanded dimension NXE and magnigication factor MX are selected so that KXM=KXMAX. Also, NYE and MY are usually selected so that KYM<<KYMAX.

MIN,MAX - Real variables equal to the minimum and maximum values of the amplitude of the complex arrays containing the aperture fields are processed by Subroutine NORMH in preparation for 3D plotting by Subroutine PLT3DH.

ROS - Real variable equal to the radius of curvature of the outside shape of the tangent ogive radome.

BOS - Real variable equal to the distance B in inches defined in Figure 2-1.

FINOS - Real variable equal to the fineness ratio of the radome as based on the outside dimensions.

FINIS - Real variable equal to the fineness ratio of the radome as based on the inside dimensions.

The following variables are printed when the receiving patterns are computed and printed:

ICUT - Integer variable which defines the E-plane (ICUT=1) or H-plane (ICUT=2) pattern. See Figure 2-3.

ICOMP - Integer variable which defines the field component of the plane wave incident on the receiving antenna: ICOMP=1 for elevation component; ICOMP=2 for azimuth component.

KMAX - Real variable equal to the sine of the maximum angle off broadside for which the received voltage is computed.

NREC - Integer variable (power of 2) equal to the number of points at which the receiving pattern is computed. The pattern is computed at NREC points spaced equally in $k_{xy}=\sin\theta$ according to $\Delta k_{xy} = 2$ KMAX/NREC.

DK - Real variable equal to 2*KMAX/NREC.

ANGMAX - Real variable equal to $\sin^{-1}$(KMAX).

The receiving pattern is computed at NREC points and magnified using Subroutine MAGFFT to 256 points equally spaced in sin θ over the range (-KMAX, KMAX-DK). Three parameters are printed: angle in degrees, amplitude in decibels, and phase in degrees. Only every fourth point in the 256 points is printed. The receiving patterns are printed in the following order:

E-Plane: Σ_{EL}, Δ_{EL}

H-Plane: Σ_{AZ}, Δ_{AZ}

Subroutine RECBS computes the boresight error of the antenna as produced by the radome. When SUPPRS=FALSE, the following parameters are printed:

K1, K2 - Real subscripted variables containing the direction cosines (k_{xi},k_{yi},k_{zi}) of the last and next to last true directions to the target. One of these variables is equal to K, the subscripted variable containing the direction cosines of the last target return.

AZTM,ELTM - Real variables equal to the boresight error in the H-plane and E-plane associated with the last target return (k_x,k_y,k_z). Expressed in milliradians, these errors are computed according to

$$AZTM = Sin^{-1}(k_x/\sqrt{1-k_y^2})*1000.$$

$$ELTM = Sin^{-1}(k_y/\sqrt{1-k_x^2})*1000.$$

Let $\hat{k} = \hat{x}_A k_x + \hat{y}_A k_y + \hat{z}_A k_z$. Then AZTM is the angle between the z_A-axis and the projection of $\hat{k}$ onto the $x_A z_A$ (azimuth) plane. ELTM is the angle between the z_A-axis and the projection of $\hat{k}$ onto the $y_A z_A$ (elevation) plane.

MESAZ,MESEL - Real variables equal to the monopulse error slopes in the azimuth and elevation channels expressed in units of volts per degree, where the maximum signal received by the sum channel is considered to be one volt.

UAZ,UEL - Real subscripted variables equal to the received tracking functions $I_{mag}\{\Delta/\Sigma\}$ corresponding to the target returns K1 and K2 above; e.g., UAZ(1) = $I_{mag}\{\Delta_{AZ}/\Sigma_{AZ}\}$ for K1.

SMAX - Real variable equal to the maximum amplitude of the received sum channel voltage.

LCTR - Integer variable equal to the number of iterations (target returns) used by Subroutine RECBS to compute boresight error.

Subroutine RECBS also computes and prints six additional monopulse outputs around the apparent boresight direction $\hat{k}_o$. The directions $\hat{k}$ chosen lie in the plane $k_x=k_y$ and are spaced one milliradian apart over the range ±3 mrad and centered on the direction $\hat{k}_o$. The variables printed are as follows:

ANG - Real variable equal to the angle in milliradians between $\hat{k}_o$ and $\hat{k}$.

VRAZ,VREL - Real variables equal to $I_{mag}\{\Delta/\Sigma\}$ for the target return from direction $\hat{k}$ for the azimuth and elevation channels, respectively.

DAZ,DEL - Amplitude and phase (degrees) of the complex voltages received on the Δ_{AZ} and Δ_{EL} channels, respectively, for target return $\hat{k}$.

SLPAZ,SLPEL - Average values of the monopulse error slopes (volts/degree) in the azimuth and elevation channels, respectively, obtained by a linear approximation of the tracking functions based on their values at ANG = ±3 mrad. For example,

SLPAZ = [VRAZ(3 mrad) - VRAZ(-3 mrad)]/(.006*57.3)

The main program always prints the boresight error in azimuth (BSEAZ) and elevation (BSEEL), and the values printed are identical to AZTM and

ELTM defined above. Main also computes the gain of the antenna in decibels with the radome in place according to

GAIN = 20. * ALOG1Ø(SMAX/VAIRM)

For other than an "air radome", GAIN is negative and indicates a loss in antenna maximum gain due to radome reflections and ohmic (tan δ) losses. The amplitude of received sum voltage, VAIRM, is always printed as the last item prior to termination of the program.

2-4. Comments and Method

a. Method. The method of analysis has been presented in Section 2.1. Additional details of analysis are presented in the descriptions of each subroutine, especially Subroutine RECM.

b. Supporting Subroutines. Twenty eight supporting subroutines are required by SIIRACP, 22 of which are identical to those used by RTFRACP. The purpose of each one is briefly described below. Those subroutines peculiar to SIIRACP and explained in Chapters 3-8 are denoted by asterisks below.

*(1) TRECNF--Computes complex vector aperture electric fields of antenna for all three monopulse channels at NX x NY sample points.

(2) ORIENT--Computes matrices ROTATE and TRANSLate used for coordinate transformations by Subroutines POINT and VECTOR.

(3) POINT--Transforms a point $P(x_A, y_A, z_A)$ in antenna system to the same point $P(x_R, y_R, z_R)$ in radome coordinate system, and vice versa.

(4) VECTOR--Transforms a vector from radome to antenna coordinate system, and vice versa.

(5) INCPW--Computes the rectangular electric field components of a plane wave incident from the direction $\hat{k}_A$ in antenna coordinates. The power density of the plane wave is unity.

*(6) RECM--Computes the voltage received by each channel of the antenna for a plane wave EINC(E_x, E_y, E_z) incident on the radome from the direction KA(k_x, k_y, k_z).

(7) OGIVEN--Computes the unit inward normal to the tangent ogive radome surface at a specified point.

(8) RXMIT--Computes the transmitted electric fields of the plane wave traveling in direction $-\hat{k}$ and incident on a flat dielectric wall with unit inner normal $\hat{n}$. The unit vectors $\hat{k}$, $\hat{n}$ are used to resolve the incident plane wave into vector components perpendicular and parallel to the plane of incidence, and to determine the angle of incidence.

*(9) WALL-Computes the normal voltage transmission coefficients of flat panel model of the radome wall as function of the sine of the incidence angle.

(10) AXB--Computes real vector cross product $\underline{C} = \underline{A} \times \underline{B}$.

(11) CAXB--Computes the complex vector cross product $\underline{C} = \underline{A} \times \underline{B}$, where $\underline{A}$ is complex and $\underline{B}$ is real.

(12) RECBS--Computes boresight errors of antenna enclosed by the radome for the specified orientation, fineness ratio, etc.

(13) RECPTN--Computes receiving patterns of all three channels.

*(14) APINT--Computes the fields of specified planar aperture fields using equivalent currents.

*(15) DIPOLES--Computes the fields of electric and magnetic dipoles located on a planar surface as required by Subroutine APINT.

*(16) CAXCB--Computes the complex vector product $\underline{C} = \underline{A} \times \underline{B}$, where $\underline{A}$ and $\underline{B}$ are complex.

(17) FAR--Computes the amplitude of the power pattern from the complex plane wave spectra $A_x(k_x,k_y)$, $A_y(k_x,k_y)$ of an antenna.

(18) AMPHS--Converts a complex number from rectangular to polar form. This subroutine utilizes the intrinsic function ATAN2. The amplitude produced is linear (not decibels), and the phase is in degrees on the range (-180, 180).

(19) DBPV--Converts a real, two-dimensional array from linear to logarithmic values in decibels on the range 0 to -40 dB.

(20) NORMH--Normalizes a two-dimensional real array to values between 0 and 1.

(21) CNPLTH--Plots single dimensional far field patterns on axes patterned after standard pattern recorder paper. CNPLTH calls Subroutine PSI in addition to the usual Calcomp subroutines.

(22) PSI--Used by Subroutine CNPLTH to compute the azimuthal angle ψ.

(23) PLT3DH--Yields three-dimensional plots of the data in the two-dimensional real array FIELD. PLT3DH calls Subroutines PLTT, NORMH as well as the usual Calcomp subroutines.

(24) PLTT-Used by Subroutine PLT3DH to eliminate moving the pen for hidden lines.

(25) FFTA--Computes the Fast Fourier Transform of a one-dimensional complex array having 2**IEXP elements. Proper operation is machine dependent.

(26) MAGFFT--Provides increased resolution of a sampled function using FFT and Discrete Fourier Transform techniques.

(27) JOYFFT--Provides increased resolution of selected portions of a two-dimensional Fourier transform. JOYFFT calls Subroutines FFTA and PWRTWO.

(28) PWRTWO--Used by Subroutine JOYFFT to ensure that a given integer is a power of 2.

2-5. Program Flow

For the following, refer to the program listing in Section 2-8 and the line numbers shown on the right-hand margin of that listing.

Line Nos.	Explanation
15	All variables beginning with the letter K in the main program are real.
16-31	Declare variables and array dimensions. Note equivalence statements in Lines 23-25. The dimension of IBUF in Line 28 may be computer system dependent. Note in Line 31 that only twenty fineness ratios, scan planes, and scan angles can be accommodated.
32-38	Label common is used as a convenient means to transmit variables to subroutines not directly called by MAIN. The labels are generated from the names of the subroutines which receive the variables, and each label is terminated with the letter C to denote common; e.g., RECIC denotes variables common to MAIN and Subroutine RECM.

40-42	Declare namelists for printing data. These namelists are no longer used except for occasional debugging purposes.
43-57	Set data in DATA statements as described above in Section 2-3.
61-62	Set SMAX and VMAX to unity to prevent division by zero.
63-64	Read and write TITLE according to 18A4 format.
65-67	Read input data using free-field format.
68	Compute sine of the offset angle θ_{OS}.
69	Set TABLE=FALSE so that normalizing factor VAIRM can be computed via a call to Subroutines RECM and RXMIT. In the latter, TABLE=FALSE causes $T_{\perp}$, $T_{\parallel}$ to be set unity as in the case of no radome.
71-75	Write input data.
76-80	Read input data and set VAIRM needlessly.
81-111	Comments explaining input variables.
112	Set NN=N+1= Number of wall layers plus one.
113	Initialize DINCH= total thickness of radome wall in inches.
114	Read wall data and compute total thickness.
117	Compute DIAIN= inside base diameter of the radome in inches.
118-119	Compute indices of the center element of near-field arrays corresponding to x_A=y_A=0.
120-121	Write array dimensional data.
122-129	Read fineness ratios, scan planes, and scan angles.

130-133 Compute wavelength in inches and centimeters. Compute $\beta=2\pi/\lambda_{cm}$.

134 Compute DAPWL= diameter of antenna aperture in wavelengths.

135-148 Convert variables in inches to centimeters for input to subroutines. Some variables are multiply defined to avoid conflicts in labeled common; e.g., ZBOT and Z1. Note that DIACM is the inside diameter of the radome in centimeters.

149-153 Convert angles from degrees to radians using RAD=π/180.

154-160 Compute near fields of three channel monopulse antenna using Subroutine TRECNF.

161-168 Set KYMAX=KXMAX, compute magnified folding wavenumbers KXM, KYM, and print results.

169-187 Initialize Calcomp plotter, if required. The commented initialization (Lines 175-185) applies to the IBM 3033 system at JHU/APL.

Note: Lines 188-268 are used to plot the near fields of the antenna and/or the transmitting principal plane power patterns.

189-190 Initialize the maximum values FMXEL, FMXDAZ of the E- and H-plane patterns so that when used initially as inputs to Subroutine FAR, the resulting pattern will be normalized with respect to its own maximum and FMXEL and FMXDAZ will be set equal to these respective maxima. On subsequent calls to FAR, the resulting patterns will be normalized with respect to FMXEL and FMXDAZ. Hence,

the relative gain of the difference and sum patterns will be correctly displayed in the graphs.

191 Iterate for each of three monopulse antenna channels.

192-201 Equate complex arrays EXT, EYT to the selected near field and compute the amplitude NF of EXT.

202 Assume transmitting near fields are to be plotted (GRAFTR=T).

204 Call Subroutine PLT3DH to plot the amplitude of EXT. The inputs XSIZE=6., YSIZE=2.5, HEIGHT=2.5 yield a 3D plot that will fit on a 8½" x 11" report page. The inputs NF, NX, NY specify the real array to be plotted and its dimensions. The input NMZ=.TRUE. directs the subroutine to normalize NF so that its values be between 0 and 1. The input LDB=.FALSE indicates that the array NF contains linear values rather than logarithmic values (decibels).

205-212 Compute and plot phase of EXT on a scale of -180 degrees to +180 degrees. Note that Line 210 ensures that the real array NF contains these phase values scaled to the required 0 to 1 range.

213-226 Repeat amplitude and phase 3D plots for EYT.

227 Assume GRAFSA=T so that principal plane patterns are plotted.

230 If IP=3, go to Line 254 and plot H-plane patterns; otherwise, plot E-plane patterns.

233 Call Subroutine JOYFFT to calculate the inverse Fourier transform of the x_A-component of near field EXT to

produce the plane wave spectrum XEEL from which the radiation field can be computed. In the process of computing the transform, provide increased resolution from NX x NY points to NYE x NXE points through point (NXC,NYC) in the array EXT. In the k_x direction, the plane wave spectrum is magnified by MY; it is magnified by MX in the k_y direction. The array FFTXY is a working array.

234 Repeat for EYT to produce the plane wave spectrum YEEL for the y_A-component of field.

235 Call Subroutine FAR to calculate the E-plane elevation (IPWR=3) power pattern FFSEL of the near field at equal samples in $\sin\theta$ over the range (-KXM, KXM $-\Delta K$). If FMXEL$\leq$0 (and it is for IP=1), normalize FFSEL with respect to its own maximum.

237 Call Subroutine DBPV and convert the power pattern to decibels on a scale of 0 to -40 dB.

238-241 Scale the values in FFSEL to the range of 0 to 1 for plotting.

242 Call Subroutine CNPLTH and plot the power pattern. If KXM<1, the pattern is plotted over the angular range corresponding to $\sin^{-1}$(KXM); if KXM$\geq$1, the angular range is (-90°, 90°). Subroutine CNPLTH actually plots conical cuts corresponding to k_x= constant or k_y= constant as specified by inputs KXC, KYC. In the call here, KXY=KYC=0 so that a principal pattern is produced.

243-247 Write a figure title for the plot and establish a new origin for the next plot.

248 If IP=2, the E-plane patterns are finished.

249-253 Since JOYFFT changes the input arrays EXT,EYT it is necessary to recompute them so that increased resolution can be obtained in the plane wave spectra in the H-plane.

254-269 Repeat computation and plotting for H-plane power patterns.

271 Iterate the radome analysis for NFINE fineness ratios.

272 Set FINE = outside fineness ratio.

273-277 Calculate and write R_{OS}, B, F_{OS}, F_{IS} as defined in Figure 2-1 for the radome geometry.

278 Compute RDML = distance from the base of the radome to the theoretical tip on the inside of the radome.

279-283 If ZTOPIN<RDML, the radome has a metal tip, and a message is written to that effect.

284-309 Compute parameters needed by Subroutine OGIVE to describe the radome shape. R and B are in centimeters and apply to the inside dimensions. AP, the height of the cylinder in centimeters, is not used. RTSQ= square of the radius of the top disk. RBSQ= square of the radius of the bottom disk (bulkhead). The other variables, BSQ, RINV, RSQ1, RP, and RP2, are precalculated here to speed later computations in OGIVE.

310	Compute conversion factor DPMR for converting milli-radians to degrees.
311-314	Initialize the "last" values of boresight error in azimuth (AZL) and elevation (ELL) and the "last" value THL of scan angle. These variables are used later to compute boresight error slope in degrees per degree from the present and last values of bore-sight error.
315-316	Write title for analysis results.
317-319	Write parameters of radome wall.
320-322	Write heading for table of boresight error and gain data.
323-334	Write this same data to logical unit 7 for subsequent storage as a disk file, if desired.
335	Iterate the radome analysis for NPHI scan planes.
336-338	Compute ϕ_r in radians as required by Subroutine ORIENT.
339	Iterate the analysis for NTHE scan angles in each scan plane.
340-342	Compute θ_r in radians as required by Subroutine ORIENT.
343	Call Subroutine ORIENT and compute the rotation matrix ROTATE and translation matrix TRANSL required for coor-dinate transformations using Subroutines POINT and VECTOR.
344	On the first iteration, TABLE is false so that the maximum amplitude of the received voltage on the sum channel is computed without the radome.

345-347	Set the direction cosines of the incident plane wave so that it arrives from the $\hat{z}_A$ direction.
348	Call Subroutine INCPW and compute the rectangular components PWI of the incident plane wave having polarization specified by IOPT.
349-354	Set TSUP=T and TABLE=F so that an air radome wall be used and so that printing by Subroutine RXMIT and RECM will be suppressed.
355-356	Call Subroutine RECM and compute the complex voltages VR received on the sum, difference elevation, and difference azimuth channels, respectively, corresponding to VR(I), I=1,3.
360	Compute VAIRM=|VR(1)|.
362	Set TABLE=T so that on subsequent iterations VAIRM will not be recomputed, and so that the table of transmission coefficients will be utilized when RXMIT is called.
363	If SUPPRS=F, compute and print the E-plane and H-plane receiving power patterns of the antenna with the radome in place.
366	Iterate in J for E-plane (ICUT=1) and H-plane (ICUT=2) patterns.
368	Set the desired far field component.
369	Set the temporary logical variable TSUP=T so that printing will be suppressed.

370-371	Call Subroutine RECPTN and compute the complex received voltages on each of three channels at NREC points over the range (-KMAX, KMAX - DK).
372-375	Increase the resolution and print results for all three channels. Do not print results that are known to be identically zero.
376-377	Transfer the received voltage into a one-dimensional array VREC.
378	If NREC>NXE, there is no need to increase the resolution.
379	Call Subroutine MAGFFT to increase the resolution of VREC from NREC points to NXE points. The result is contained in complex array XYFFT on output.
380-384	Compute linear power pattern.
385	Select NXX= larger of NXE and NREC.
386	Write heading for printed results from Subroutine NORMH.
388	Call Subroutine NORMH to normalize the NXX values in real array MVREC to be between zero and one. The input argument LDB=.FALSE. since the values are not in decibels.
389	Call Subroutine DBPV to convert the power pattern in MVREC to decibels.
390-391	Write correct heading for E-plane or H-plane.
392	Compute the increment in $\sin\theta$ at which power pattern has been computed and resolved.
393-404	Scale the power pattern to have values between 0 and 1. If SUPPRS=F, compute the angle θ=ANG and the phase

of the pattern, and print the results for every fourth angle.

405 If GRAFRV=T, plot the receiving power patterns.

406-416 Call Subroutine CNPLTH and plot the receiving patterns in turn. Write an appropriate figure title following each pattern plot. Re-origin the plotter pen for subsequent plots. The result of Lines 330-383 is four principal plane patterns: E-plane sum, E-plane Δ_{EL}, H-plane sum, H-plane Δ_{AZ}.

417-419 Call Subroutine RECBS and compute the boresight errors AZT, ELT in the azimuth and elevation planes of the antenna as caused by the radome. On output, the real array KA contains the direction cosines of the last target return and, hence, gives the true direction to the target at the time that the tracking functions in the azimuth and elevation planes indicated the electrical boresight direction.

420 If this is the first iteration in scan angle, do not attempt to compute boresight error slope.

421-422 Compute boresight error slope (degrees/degree) in azimuth and elevation channels.

423-425 Set the "last" values of boresight errors and scan angle to the current values in preparation for next iteration.

426-428 Compute loss in maximum gain of the antenna sum channel due to the radome.

429-430	Write results to logical units 6 and 7.
434-435	Write maximum amplitude of received sum voltage VAIRM without radome.
436	Terminate plotting software.
	STOP
	END

2-6. Test Case

A test case has been delivered to JHU/APL under separate cover. Typical input data are shown in Table 2-1.

2-7. References

1. G. K. Huddleston and E. B. Joy, "Development of Fabrication and Processing Techniques for Laser Hardened Missile Radomes: Radome Electrical Design Analysis", Martin Marietta Purchase Agreement 573712, April 1977.
2. G. K. Huddleston, H. L. Bassett, and J. M. Newton, "Parametric Investigation of Radome Analysis Methods", IEEE AP-S Symposium Digest, pp. 199-202, May 1978; also, Proc. Fourteenth Symposium on Electromagnetic Windows, pp. 21-28, June 1978.
3. E. B. Joy and G. K. Huddleston, "Radome Effects on the Performance of Ground Mapping Radar," U.S. Army Missile Command, DAAH-01-72-C-0598, March 1973.

2-8. Program Listing: See following pages.

```
 TEST SIIRACP FEB 80                                                    1
F,F,F,F,F,00,T                                                          2
1.,1.,1.,1.1241,.01,.01,1.70,35.,3.                                     3
5.,.5,1.,.159,1.0,1.,1.,1.,.5,4                                         4
.11241.,.11241,8,8                                                      5
.001,1.00,0.000                                                         6
1.505                                                                   7
0.                                                                      8
0.                                                                      9
```

Table 2-1. Input Data for SIIRACP.

```
C  THIS RADOME ANALYSIS COMPUTER PROGRAM, SIIRACP, WAS PREPARED FOR          1
C  JOHNS HOPKINS APL BY G.K. HUDDLESTON, JANUARY 1980, UNDER THE             2
C  COGNIZANCE OF ROBERT C. MALLALIEU.                                        3
C  SUBR TRECNF COMPUTES NEAR FIELDS SUITABLE FOR THIS SURFACE                4
C  INTEGRATION (INNER RADOME SURFACE) ANALYSIS APPROACH.                     5
C  COMPUTED RESULTS ARE ALSO WRITTEN TO TAPE7 FOR LATER USE.                 6
C                                                                            7
C-----------------------------------------------------------------------     8
C                                                                            9
C       IMPLEMENTATION AT APL/JHU  2/11/80  FOR IBM 3033                    10
C                                                                           11
C-----------------------------------------------------------------------    12
C  *** LIBRARIES LSIIRAC AND MISCFFT ARE REQUIRED FOR EXECUTION ***         13
      PROGRAM SIIRACP(INPUT,OUTPUT,TAPE5=INPUT,TAPE6=OUTPUT,TAPE7)          14
      IMPLICIT REAL(K)                                                      15
      REAL NF(4,4),MVREC(256),KA(3)                                         16
      COMPLEX SUMX(4,4),SUMY(4,4),DELX(4,4),DELY(4,4)                       17
      COMPLEX DAZX(4,4),DAZY(4,4),EXT(4,4),EYT(4,4)                         18
      COMPLEX VR(16),VREC3(6,3),VREC(32)                                    19
      REAL FFS(256,1),FFSEL(1,256)                                          20
      COMPLEX XE(256,1),YE(256,1),XYFFT(512),PWI(3)                         21
      COMPLEX XEEL(1,256),YEEL(1,256)                                       22
      EQUIVALENCE(XE(1,1),XEEL(1,1))                                        23
      EQUIVALENCE(YE(1,1),YEEL(1,1))                                        24
      EQUIVALENCE(FFS(1,1),MVREC(1),FFSEL(1,1))                             25
C                                                                           26
      LOGICAL GRAF3D,GRAFSA,GRAFTR,GRAFRV,TABLE,SUPPRS,TSUP,SQUARE          27
      INTEGER IBUF(512)                                                     28
C                                                                           29
      REAL ROTATE(3,3),TRANSL(3),TITLE(18)                                  30
      REAL FINR(20),PHI(20),THETA(20)                                       31
      COMMON/RECIC/DSTH,DSPHI,NTHMIN,NPHIMIN,AREA,NPOINTS,ROS,RIS,          32
     $ZBOTCM,ZTOPCM,BCM,RR                                                  33
      COMMON/TDISKC/ZTOP,RTSQ                                               34
      COMMON/TRACC/Z2,Z1                                                    35
      COMMON/BDISKC/ZBOT,RBSQ                                               36
      COMMON/TRANSC/DIN(6),ER(6),TD(6),TZ,WALTOL,N,NN,D(6),ZB,TK            37
      COMMON/OGIVC/RP,BSQ,AP,RINV,B,RSQ1,RP2                                38
```

```
C                                                                       39
      NAMELIST/GEOM/RR,RA,APIN,ZBOTIN,NX,NY,NXE,NYE,NXY,MX,MY,NXC,NYC  40
      NAMELIST/KDATA/KXMAX,KYMAX,KXM,KYM                                41
      NAMELIST/NEW/LMAX,DMRAD,IOPT,RAPMAX,VAIRM                         42
C  BOUNDARY VALUES NEEDED BY SUBR TRACE (INCHES, CONVERT TO CM BELOW)   43
C Z1=ZR COORDINATE OF BOTTOM DISK                                       44
C Z2=ZR COORDINATE OF TOP DISK (Z1,Z2 IN CM)                            45
C  APIN IS HEIGHT OF CYLINDER IN INCHES, CONVERT TO CM BELOW            46
      DATA APIN/0./                                                     47
C  ZBOTIN IS ZR COORD OF BOTTOM DISK (BULKHEAD) IN RADOME COORD IN INCHE 48
      DATA ZBOTIN/0.00/                                                 49
C  KXMAX,KYMAX ARE OUTPUTS OF NEAR FIELD SUBR                           50
C  INITIALIZE CONSTANTS                                                 51
      DATA RADIUS/1E0/                                                  52
      DATA THETAA,PHIA,AGAM3A/0.0,90.0,0.0/                             53
      DATA PI/3.1415926535898/                                          54
C************                                                           55
      DATA NX,NY,NYE,NXY/4,4,1,512/                                     56
      DATA MY/1/,NREC/6/                                                57
C************                                                           58
C                                                                       59
C  READ IN DESCRIPTION OF RADOME WALL                                   60
      SMAX=1.0                                                          61
      VMAX=1.0                                                          62
      READ(5,6)TITLE                                                    63
      WRITE(6,6) TITLE                                                  64
      READ(5,*) GRAF3D,GRAFSA,GRAFTR,GRAFRV,SUPPRS,IPENCD,SQUARE        65
  260 FORMAT(4L6)                                                       66
      READ(5,*) NFINE,NPHI,NTHE,DIAOS,RAIN,RRIN,ZTOPIN,FREQ,OSANG      67
      SINOS=SIN(OSANG*PI/180.)                                          68
      TABLE=.FALSE.                                                     69
C  TABLE IS SET FALSE SO THAT NORMALIZING FACTOR CAN BE COMPUTED.       70
      WRITE(6,265) GRAF3D,GRAFSA,GRAFTR,GRAFRV,TABLE                    71
  265 FORMAT(" GRAF3D=",L2," GRAFSA=",L2," GRAFTR=",L2," GRAFRV=",L2,   72
     $ "  TABLE=",L2)                                                   73
      WRITE(6,270) NFINE,NPHI,NTHE,OSANG                                74
  270 FORMAT(/" NFINE=",I5," NPHI=",I3,"  NTHETA=",I3,"  OSANG= ",F5.2/) 75
      READ(5,*) LMAX,DMRAD,IOPT,RAPMAX,VAIRM,IPOL,ICASE,N,IPWR,KMAX,NXE 76
```

```
      MX=NXE/NX                                                          77
      IF (MX.LT.1) MX=1                                                  78
      READ(5,*) DSTHIN,DSPHIN,NTHMIN,NPHIMIN                             79
      IF (VAIRM.LE.0.) VAIRM=1.0                                         80
C DIAOS=OUTSIDE DIAMETER OF BASE OF TANGENT OGIVE RADOME                 81
C VAIR=MAXIMUM REC"D VOLTAGE W/O RADOME AT KX=0.,KY=0.                   82
C NFINE=NO. OF FINENESS RATIOS                                           83
C  NPHI=NUMBER OF SCAN PLANES                                            84
C  NTHE=NUMBER OF ANGLES IN EACH SCAN PLANE                              85
C DIAIN=INSIDE BASE DIAMETER OF RADOME IN INCHES                         86
C ZTOPIN=ZR COORD (IN) OF TOP DISK (METAL TIP)                           87
C FREQ=FREQUENCY IN GHZ                                                  88
C GRAF3D=.TRUE. GIVES 3D PLOTS OF INCIDENT FIELDS ON APERTURE (DELETED)  89
C GRAFRV=.TRUE. GIVES SA PLOTS OF RECEIVING PATTERNS (AZ & EL)           90
C GRAFSA=.TRUE. GIVES SA PLOTS OF TRANSMITTING PATTERN WITHOUT RADOME    91
C SUPPRS=.TRUE. SUPPRESSES THE PRINTING OF NUMEROUS RESULTS              92
C RAPMAX=MAX RADIUS OF ANTENNA APERTURE IN INCHES.                       93
C  IOPT SELECTS POLARIZATION OF INCIDENT PLANE WAVE:                     94
C      =1 ELEV (VERTICAL)                                                95
C      =2 AZIMUUTH (HORIZONTAL)                                          96
C      =3 RHC                                                            97
C      =4 LHC                                                            98
C  IPOL SELECTS POLARIZATION OF ANTENNA WHEN ICASE=1:                    99
C      = SAME CODE AS FOR IOPT                                          100
C  ICASE=1 OR 2 FOR CIRC APERTURE, UNIFORM ILLUMINATION                 101
C       =3 FOR FLAT PLATE WITH SPECIFIED ILLUM, VERT POL (CASE III)     102
C  N=NUMBER OF LAYERS IN RADOME WALL                                    103
C  OSANG=ANGLE IN DEG IN 45 PLANE OFF BORESIGHT OF FIRST TARGET RETURN  104
C       USED BY SUBR RECBS IN GETTING INITIAL DATA.                     105
C  IPWR=1 FOR POWER IN ELEV COMP OF FAR FIELD PATTERN                   106
C      =2 FOR AZIMUTH COMP,=3 FOR TOTAL POWER.                          107
C  DSTHIN=SAMPLE DISTANCE (IN.) ON RADOME SURFACE IN THETA DIRECTION    108
C  DSPHIN=  -DITTO-                                    PHI DIRECTION    109
C  NTHMIN=MINIMUM NUMBER OF SAMPLES IN THETA DIRECTION                  110
C NPHIMIN=  -DITTO-                        PHI DIRECTION                111
      NN=N+1                                                           112
      DINCH=0.                                                         113
      DO 5 I=1,N                                                       114
```

```
      READ(5,*) DIN(I),ER(I),TD(I)                                      115
    5 DINCH=DIN(I)+DINCH                                                116
      DIAIN=DIAOS-DINCH*2.                                              117
      NXC=NX/2+1                                                        118
      NYC=NY/2+1                                                        119
      WRITE(6,4) NX,NY,NXE,NYE,NXY,MX,MY                                120
    4 FORMAT(" NX,NY,NXE,NYE,NXY,MX,MY:",7I4)                           121
C READ FINENESS RATIOS FOR THIS RUN--BASED ON OUTSIDE DIMENSIONS         122
      DO 13 I=1,NFINE                                                   123
   13 READ(5,*) FINR(I)                                                 124
C READ ORIENTATIONS FOR THIS RUN (DEGREES)                              125
      DO 14 I=1,NPHI                                                    126
   14 READ(5,*) PHI(I)                                                  127
      DO 15 I=1,NTHE                                                    128
   15 READ(5,*) THETA(I)                                                129
C  COMPUTE WAVELENGTH:                                                  130
      WLIN=29.97925/(FREQ*2.54)                                         131
      WLCM=WLIN*2.54                                                    132
      BETA=2.*PI/WLCM                                                   133
      DAPWL=2.*RAPMAX/WLIN                                              134
C  CONVERT TO CENTIMETER AND RADIANS                                    135
      ZBOT=ZBOTIN*2.54                                                  136
      Z1=ZBOT                                                           137
      RSQMAX=(2.54*RAPMAX)**2                                           138
      DIACM=DIAIN*2.54                                                  139
      ZTOP=ZTOPIN*2.54                                                  140
      ZB=ZTOP                                                           141
      Z2=ZTOP                                                           142
      ZTOPCM=ZTOP                                                       143
      ZBOTCM=ZBOT                                                       144
      RA=RAIN*2.54                                                      145
      RR=RRIN*2.54                                                      146
      DSTH=DSTHIN*2.54                                                  147
      DSPHI=DSPHIN*2.54                                                 148
      RAD=PI/180.0                                                      149
    6 FORMAT(18A4)                                                      150
      THETAA=THETAA*RAD                                                 151
      PHIA=PHIA*RAD                                                     152
```

```
      AGAM3A=AGAM3A*RAD                                                 153
C  COMPUTE FIELDS OF ANTENNA WHEN XMITTING:                            154
      CALL TRECNF(SUMX,NX,NY,1,IPOL,1,DAPWL,DXWL,KXMAX,ICASE,SQUARE)    155
      CALL TRECNF(SUMY,NX,NY,1,IPOL,2,DAPWL,DXWL,KXMAX,ICASE,SQUARE)    156
      CALL TRECNF(DELX,NX,NY,2,IPOL,1,DAPWL,DXWL,KXMAX,ICASE,SQUARE)    157
      CALL TRECNF(DELY,NX,NY,2,IPOL,2,DAPWL,DXWL,KXMAX,ICASE,SQUARE)    158
      CALL TRECNF(DAZX,NX,NY,3,IPOL,1,DAPWL,DXWL,KXMAX,ICASE,SQUARE)    159
      CALL TRECNF(DAZY,NX,NY,3,IPOL,2,DAPWL,DXWL,KXMAX,ICASE,SQUARE)    160
      KYMAX=KXMAX                                                       161
      KXM=KXMAX*NXE/MX/NX                                               162
      KYM=KYMAX*NYE/MY/NY                                               163
      DYWL=DXWL                                                         164
      WRITE(6,3) KXMAX,DXWL,KXM,KYM,DSTHIN,DSPHIN,NTHMIN,NPHIMIN       165
    3 FORMAT(" KXMAX=KYMAX=",F8.5,"   DXWL=DYWL=",E12.5," WAVELENGTHS"/ 166
     $" KXM=",F8.5,"  KYM=",F8.5//" DSTHIN=",E12.5,"  DSPHIN=",        167
     $E12.5,"  NTHMIN=",I3,"  NPHIMIN=",I3//)                          168
C                                                                       169
C  INITIALIZE PLOTTER SOFTWARE                                          170
      IF (GRAF3D.OR.GRAFSA.OR.GRAFTR.OR.GRAFRV) GO TO 200               171
      GO TO 205                                                         172
  200 CONTINUE                                                          173
C                                                                       174
C-------------------- CALCOMP INITIALIZATION --------------------------175
C                                                                       176
C     CALL TITL36("RADOME ANALYSIS COMPUTER PROGRAM",                   177
C    *            "          G.K. HUDDLESTON       ",                  178
C    *            " GEORGIA INSTITUTE OF TECHNOLOGY"  )                179
C     CALL INIT36( MDAY )                                               180
CC                                                                      181
C     CALL PLOT(0.,-3.,-3)                                              182
      CALL PLOTS(IBUF,512,3,IPENCD)                                     183
C                                                                       184
C-----------------------------------------------------------------------185
C                                                                       186
      IF (GRAFTR.OR.GRAFSA) GO TO 201                                   187
      GO TO 205                                                         188
  201 FMXEL=0.                                                          189
      FMXDAZ=0.                                                         190
```

```
      DO 30 IP=1,3                                                    191
      DO 35 I=1,NX                                                    192
      DO 35 J=1,NY                                                    193
      IF (IP.EQ.1) EXT(I,J)=SUMX(I,J)                                 194
      IF (IP.EQ.1) EYT(I,J)=SUMY(I,J)                                 195
      IF (IP.EQ.2) EXT(I,J)=DELX(I,J)                                 196
      IF (IP.EQ.2)EYT(I,J)=DELY(I,J)                                  197
      IF (IP.EQ.3) EXT(I,J)=DAZX(I,J)                                 198
      IF (IP.EQ.3) EYT(I,J)=DAZY(I,J)                                 199
      NF(I,J)=CABS(EXT(I,J))                                          200
   35 CONTINUE                                                        201
      IF (.NOT.GRAFTR) GO TO 215                                      202
C PLOT 3D NEAR FIELDS X-COMPONENTS                                    203
      CALL PLT3DH(6.,2.5,2.5,NF,NX,NY,.TRUE.,.FALSE.)                 204
C  PLOT PHASE ALSO                                                    205
      DO 40 I=1,NX                                                    206
      DO 40 J=1,NY                                                    207
      NF(I,J)=0.                                                      208
      CALL AMPHS(EXT(I,J),RLF,AIF)                                    209
      NF(I,J)=(AIF+180.)/360.                                         210
   40 CONTINUE                                                        211
      CALL PLT3DH(6.,2.5,2.5,NF,NX,NY,.FALSE.,.FALSE.)                212
C PLOT 3D NEAR FIELDS Y-COMPONENTS                                    213
      DO 45 I=1,NX                                                    214
      DO 45 J=1,NY                                                    215
      NF(I,J)=CABS(EYT(I,J))                                          216
   45 CONTINUE                                                        217
      CALL PLT3DH(6.,2.5,2.5,NF,NX,NY,.TRUE.,.FALSE.)                 218
C  PLOT PHASE ALSO                                                    219
      DO 50 I=1,NX                                                    220
      DO 50 J=1,NY                                                    221
      NF(I,J)=0.                                                      222
      CALL AMPHS(EYT(I,J),RLF,AIF)                                    223
      NF(I,J)=(AIF+180.)/360.                                         224
   50 CONTINUE                                                        225
      CALL PLT3DH(6.,2.5,2.5,NF,NX,NY,.FALSE.,.FALSE.)                226
      IF (GRAFSA) GO TO 215                                           227
      GO TO 30                                                        228
```

```
  215 CONTINUE                                                          229
      IF (IP.EQ.3) GO TO 220                                            230
C CALC EL CUT OF SUM                                                    231
C  NOTE THAT  JOYFFT CHANGES EXT,EYT.                                  232
      CALL JOYFFT(EXT,NX,NY,MY,MX,NXC,NYC,XEEL,NYE,NXE,XYFFT,NXY,3)     233
      CALL JOYFFT(EYT,NX,NY,MY,MX,NXC,NYC,YEEL,NYE,NXE,XYFFT,NXY,3)     234
      CALL FAR(FFSEL,XEEL,YEEL,NYE,NXE,FREQ,KYM,KXM,RADIUS,IPWR,FMXEL)  235
C SA PLOTS OF ELEVATION RESULTS                                         236
      CALL DBPV(FFSEL,NYE,NXE,1)                                        237
      DO 216 I=1,NYE                                                    238
      DO 216 J=1,NXE                                                    239
      FFSEL(I,J)=1.0+FFSEL(I,J)/40.                                     240
  216 CONTINUE                                                          241
      CALL CNPLTH(FFSEL,NXE,KXM,0.,0.)                                  242
      CALL SYMBOL(.5,6.5,.140000,39HFIGURE     TRANSMITTING ELEVATION PO 243
     $WER,0.,39)                                                        244
      RPWR=FLOAT(IPWR)                                                  245
      CALL NUMBER(999.,999.,.14,RPWR,0.,0)                              246
      CALL PLOT(8.5,0.,-3)                                              247
      IF (IP.EQ.2) GO TO 30                                             248
C  RECOMPUTE SUMX,SUMY FOR JOYFFT:                                      249
      CALL TRECNF(EXT,NX,NY,1,IPOL,1,DAPWL,DXWL,KXMAX,ICASE,SQUARE)     250
      WRITE(6,219) IPWR                                                 251
  219 FORMAT(" IPOWER OF PATTERN=",I2)                                  252
      CALL TRECNF(EYT,NX,NY,1,IPOL,2,DAPWL,DXWL,KXMAX,ICASE,SQUARE)     253
  220 CALL JOYFFT(EXT,NX,NY,MX,MY,NXC,NYC,YE,NXE,NYE,XYFFT,NXY,3)       254
      CALL JOYFFT(EYT,NX,NY,MX,MY,NXC,NYC,YE,NXE,NYE,XYFFT,NXY,3)       255
      CALL FAR(FFS,XE,YE,NXE,NYE,FREQ,KXM,KYM,RADIUS,IPWR,FMXDAZ)       256
C SA PLOTS OF AZIMUTH RESULTS                                           257
      CALL DBPV(FFS,NXE,NYE,1)                                          258
      DO 10 I=1,NXE,1                                                   259
      DO 10 J=1,NYE                                                     260
      FFS(I,J)=1.0+FFS(I,J)/40.0                                        261
   10 CONTINUE                                                          262
      CALL CNPLTH(FFS,NXE,KXM,0.,0.)                                    263
  226 CALL SYMBOL(.5,6.5,.14000,37HFIGURE     TRANSMITTING AZIMUTH POWER 264
     $,0.,37)                                                           265
      CALL NUMBER(999.,999.,.14,RPWR,0.,0)                              266
```

```
      CALL PLOT(8.5,0.,-3)                                              267
   30 CONTINUE                                                          268
  205 CONTINUE                                                          269
C                                                                       270
      DO 100 NG=1,NFINE                                                 271
      FINE=FINR(NG)                                                     272
C CALCULATE INSIDE FINENESS RATIO                                       273
      RIN=FINE*DIAOS/(SIN(PI-2.*ATAN(2.*FINE)))                         274
      ROS=RIN*2.54                                                      275
      BIN=RIN-DIAOS/2.                                                  276
      FINE=SQRT((RIN-DINCH)**2-BIN**2)/DIAIN                            277
      RDML=FINE*DIAIN+APIN                                              278
      IF (ZTOPIN.LT.RDML) WRITE(6,25) ZTOPIN                            279
   20 FORMAT(" TANGENT OGIVE PARAMETERS: "," ROS(IN)="                  280
     $ ,F9.5," BOS(IN)=",F9.5,/26X," FINOS=",F5.3,                      281
     $ " FINIS=",F8.5,"  RINV=",E12.5)                                  282
   25 FORMAT(/" THIS RADOME HAS A TOP DISK AT ZTOPIN= ",E12.5/)         283
C  COMPUTE PARAMETERS NEEDED BY SUBR OGIVE                             284
      R=FINE*DIACM/(SIN(PI-2.*ATAN(2.*FINE)))                           285
      RIS=R                                                             286
      TLIS=DIAIN*FINE                                                   287
      IF (ZTOPIN.GT.TLIS) ZTOPIN=TLIS                                   288
      ZTOP=ZTOPIN*2.54                                                  289
      ZB=ZTOP                                                           290
      Z2=ZTOP                                                           291
      ZTOPCM=ZTOP                                                       292
      IF (ZTOPCM.GT.RIS) ZTOPCM=RIS                                     293
      B=R-DIACM/2.                                                      294
      BCM=B                                                             295
      AP=APIN*2.54                                                      296
      RTSQ=R**2-(ZTOP-AP)**2                                            297
      IF (RTSQ.LT.0.) RTSQ=0.                                           298
      RTSQ=(SQRT(RTSQ)-B)**2                                            299
      RBSQ=R**2-(ZBOT-AP)**2                                            300
      IF (RBSQ.LT.0.) RBSQ=0.                                           301
      RBSQ=(SQRT(RBSQ)-B)**2                                            302
      BSQ=B**2                                                          303
      RINV=1./R                                                         304
```

```
      RSQ1=R**2                                                          305
      RP=RSQ1-BSQ                                                        306
      RP2=RSQ1+BSQ                                                       307
      WRITE(6,20) RIN,BIN,FINR(NG),FINE,RINV                             308
C                                                                        309
      DPMR=180./(PI*1000.)                                               310
      AZL=0.                                                             311
      ELL=0.                                                             312
      THL=0.                                                             313
      TLOS=DIAOS*FINR(NG)                                                314
      WRITE(6,2) TITLE,FINR(NG),DIAOS,TLOS,FREQ,RAIN,RRIN,DAPWL,IPOL,    315
     $ICASE,IOPT                                                         316
      DO 8 I=1,N                                                         317
    8 WRITE(6,7) I,DIN(I),ER(I),TD(I)                                    318
    7 FORMAT(2X,I3,F13.5,F10.3,F9.4)                                     319
      WRITE(6,9)                                                         320
    9 FORMAT(//"  PHI   THETA  BSEEL    BSEAZ    SLPEL      SLPAZ      GAIN"/  321
     $       " (DEG) (DEG)  (MRAD)  (MRAD) (DEG/DEG) (DEG/DEG)  (DB)"//)  322
      WRITE(7,2) TITLE,FINR(NG),DIAOS,ZTOPIN,FREQ,RAIN,RRIN,DAPWL,IPOL,  323
     $ICASE,IOPT                                                         324
      DO 18 I=1,N                                                        325
   18 WRITE(7,7) I,DIN(I),ER(I),TD(I)                                    326
      WRITE(7,9)                                                         327
    2 FORMAT(1H1,5X," RESULTS OF RADOME ANALYSIS USING INSIDE SURFACE IN  328
     1TEGRATION"/18A4/" FINENESS RATIO=",F8.5,2X,                        329
     2"DIAMETER=",F8.5," IN.  LENGTH=",F8.5," IN."/" FREQUENCY=",        330
     3F8.5," GHZ "/                                                      331
     4" RA=",F8.5," IN.  RR=",F8.5," IN.  ANTENNA D=",F8.4,              332
     5" WAVELENGTHS"/" IPOL=",I2,"  ICASE=",I2,"  IOPT=",I2//            333
     6" LAYER  THICKNESS(IN.)   ER      TAND"/)                          334
      DO 100 IPHI=1,NPHI                                                 335
      PHIP=PHI(IPHI)                                                     336
      PHIR=PHIP+180.                                                     337
      PHIR=PHIR*RAD                                                      338
      DO 100 ITHE=1,NTHE                                                 339
      THETAL=THETA(ITHE)                                                 340
      THETAR=180.-THETAL                                                 341
      THETAR=THETAR*RAD                                                  342
```

```
      CALL ORIENT(RA,THETAA,PHIA,RR,THETAR,PHIR,AGAM3A,ROTATE,TRANSL)        343
      IF (TABLE) GO TO 23                                                   344
C  COMPUTE NORMALIZING FACTOR:                                              345
      KA(1)=0.                                                              346
      KA(2)=0.                                                              347
      KA(3)=1.                                                              348
      CALL INCPW(KA,PWI,IOPT)                                               349
      TSUP=SUPPRS                                                           350
      TABLE=.FALSE.                                                         351
      ZTEMP=ZTOPCM                                                          352
      ZTOPCM=DIACM*FINE                                                     353
      IF (ZTOPCM.GT.RIS) ZTOPCM=RIS                                         354
      CALL RECM(PWI,KA,NX,NY,KXMAX,KYMAX,FREQ,ROTATE,TRANSL,                355
     $SUMX,SUMY,DELX,DELY,DAZX,DAZY,VR,TABLE,TSUP,RSQMAX)                   356
C  SET ZTOPCM BACK TO THE INPUTTED VALUE.                                   357
      IF (ZTOPCM.LT.ZTEMP) ZTEMP=ZTOPCM                                     358
      ZTOPCM=ZTEMP                                                          359
      VAIRM=CABS(VR(1))                                                     360
      WRITE(6,105) VAIRM                                                    361
      TABLE=.TRUE.                                                          362
   23 IF (.NOT.SUPPRS) GO TO 24                                             363
      GO TO 350                                                             364
   24 CONTINUE                                                              365
      DO 320 J=1,2                                                          366
      ICUT=J                                                                367
      ICOMP=IOPT                                                            368
      TSUP=.TRUE.                                                           369
      CALL RECPTN(SUMX,SUMY,DELX,DELY,DAZX,DAZY,NX,NY,ICUT,ICOMP,KMAX,      370
     $NREC,VREC3,KXMAX,KYMAX,FREQ,ROTATE,TRANSL,TABLE,TSUP,RSQMAX)          371
      DO 325 MM=1,3                                                         372
      ICHAN=MM                                                              373
      IF ((ICUT.EQ.1).AND.(ICHAN.EQ.3)) GO TO 325                           374
      IF ((ICUT.EQ.2).AND.(ICHAN.EQ.2)) GO TO 325                           375
      DO 26 I=1,NREC                                                        376
   26 VREC(I)=VREC3(I,ICHAN)                                                377
      IF (NREC.GE.NXE) GO TO 31                                             378
      CALL MAGFFT(VREC,NREC,XYFFT,NXE)                                      379
      DO 305 I=1,NXE                                                        380
```

```
  305 MVREC(I)=CABS(XYFFT(I))**2                                          381
      GO TO 33                                                            382
   31 DO 32 I=1,NREC                                                      383
   32 MVREC(I)=CABS(VREC(I))**2                                           384
   33 NXX=MAXO(NXE,NREC)                                                  385
      WRITE(6,306)                                                        386
  306 FORMAT(/" MIN AND MAX VALUES OF REC""G PATTERN: "/)                 387
      CALL NORMH(MVREC,NXX,1,.FALSE.)                                     388
      CALL DBPV(MVREC,NXX,1,1)                                            389
      IF (J.EQ.1) WRITE(6,308)                                            390
      IF (J.EQ.2) WRITE(6,309)                                            391
      DK=2.*KMAX/NXX                                                      392
      IMOD=4                                                              393
      IF (NREC.GE.NXE) IMOD=1                                             394
      DO 307 I=1,NXX,1                                                    395
      IF (SUPPRS) GO TO307                                                396
      ANG=ASIN(-KMAX+(I-1)*DK)*180./PI                                    397
      CALL AMPHS(XYFFT(I),AMP,PHS)                                        398
      IF (NREC.GE.NXE) CALL AMPHS(VREC(I),AMP,PHS)                        399
      IF (MOD(I,IMOD).EQ.0) WRITE(6,310) ANG,MVREC(I),PHS                 400
  307 MVREC(I)=1.0+MVREC(I)/40.                                           401
  308 FORMAT(/" REC""G PATTERN, EL CUT, EL COMP (DB): "/)                 402
  309 FORMAT(/" REC""G PATTERN, AZ CUT,EL COMP (DB): "/)                  403
  310 FORMAT(F9.1,5X,F8.3,3X,F6.1)                                        404
      IF (.NOT.GRAFRV) GO TO 325                                          405
      CALL CNPLTH(MVREC,NXX,KMAX,0.,0.)                                   406
      IF (J.EQ.1) CALL SYMBOL(.5,6.5,.140,43HFIGURE       RECVG POWER PA  407
     $TTERN-ELEV PLANE,0.,43)                                             408
      IF (J.EQ.2) CALL SYMBOL(.5,6.5,.140,41HFIGURE       RECVG POWER PA  409
     $TTERN-AZ PLANE,0.,41)                                               410
      CALL PLOT(8.5,0.,-3)                                                411
  325 CONTINUE                                                            412
  320 CONTINUE                                                            413
  350 CONTINUE                                                            414
C COMPUTE BORESIGHT ERROR                                                 415
  275 CONTINUE                                                            416
      CALL RECBS(SUMX,SUMY,DELX,DELY,DAZX,DAZY,NX,NY,                     417
     $ LMAX,NS,IOPT,VR,DMRAD,ROTATE,TRANSL,FREQ,KXMAX,KYMAX,              418
```

```
     $ TABLE,SINOS,KA,AZT,ELT,RSQMAX,VMAX,SMAX,SUPPRS)                    419
      IF (ITHE.EQ.1) GO TO 300                                            420
      SLPAZ=(AZT-AZL)*DPMR/(THETAL-THL)                                   421
      SLPEL=(ELT-ELL)*DPMR/(THETAL-THL)                                   422
  300 AZL=AZT                                                             423
      ELL=ELT                                                             424
      THL=THETAL                                                          425
      GAINM=SMAX/VAIRM                                                    426
      IF (GAINM.LT.1E-2) GAINM=1E-2                                       427
      GAINM=20.*ALOG10(GAINM)                                             428
      WRITE(6,11) PHIP,THETAL,ELT,AZT,SLPEL,SLPAZ,GAINM                   429
      WRITE(7,11) PHIP,THETAL,ELT,AZT,SLPEL,SLPAZ,GAINM                   430
   11 FORMAT(1X,F5.1,F6.1,F8.2,F8.2,F9.4,F10.4,F7.1)                      431
C  GRAF3D OPTION HAS BEEN REMOVED.                                        432
  100 CONTINUE                                                            433
      WRITE(6,105) VAIRM                                                  434
  105 FORMAT(//" RECEIVED SUM VOLTAGE WITHOUT RADOME=",E12.5//)           435
      IF (GRAF3D.OR.GRAFSA.OR.GRAFTR.OR.GRAFRV) CALL PLOT(0.,0.,999)      436
      STOP                                                                437
      END                                                                 438
```

```
      BLOCK DATA                                                        1
C                                                                       2
      COMMON/TRANSC/DIN(6),ER(6),TD(6),TZ,WALTOL,N,NN,D(6),ZB,TK        3
C                                                                       4
      DATA WALTOL,TK,TZ/0.,0.,0./                                       5
C                                                                       6
      END                                                               7
```

Chapter 3

SUBROUTINE RECM

3-1. Purpose: To compute the complex voltages produced at the terminals of the three channels of a radome enclosed monopulse antenna by a plane wave of specified polarization and direction of arrival.

3-2. Usage: CALL RECM (EINC, KA, NX, NY, KXMAX, FREQ, ROTATE, TRANSL, SUMX, SUMY, DELX, DELY, DAZX, DAZY, VREC, TABLE, SUPPRS, RSQMAX)

COMMON/RECIC/DSTH, DSPHI, NTHMIN, NPHIMIN, AREA, NPOINTS, ROS, RIS, ZBOTCM, ZTOPCM, BCM, RR

3-3. Arguments

EINC - A complex array of three elements containing E_x, E_y, E_z of the incident plane wave. See Subroutine INCPW.

KA - A real array of three elements containing the direction cosines k_{xA}, k_{yA}, k_{zA} of the unit vector $\hat{k}_A$ which points from the antenna origin in the direction from whence the plane wave emanates.

NX,NY - The even integer number of sample points in x_A and y_A directions used to represent the antenna aperture fields.

KXMAX,KYMAX - Real variables which represent the normalized folding wavenumbers corresponding to the sample distances Δx_A, Δy_A according to $\Delta x_A=\lambda/(2*KXMAX)$, $\Delta y_A=\lambda/(2*KYMAX)$, where λ is the free space wavelength.

FREQ - Frequency in gigahertz of the monochromatic plane wave.

ROTATE,TRANSL- Real matrices of direction cosines and translation distances used to carry out coordinate transformations of points and vectors from antenna to radome coordinate systems, and vice versa. See Subroutine ORIENT.

SUMX,SUMY - Two dimensional (NX X NY) complex arrays of the x and y vector components of the antenna aperture fields for the sum channel of a three-channel monopulse antenna. The element at I=NX/2+1, J=NY/2+1, corresponds to that at x_A=0, y_A=0 in the aperture. The general correspondence is given by

$$x_A = - x_{max} + (I-1)*\Delta x_A = (I-MIDNX)*\Delta x_A$$

$$y_A = - y_{max} + (J-1)*\Delta y_A = (J-MIDNY)*\Delta y_A$$

where $x_{max} = \Delta x_A * NX/2$ and $y_{max} = \Delta y_A * NY/2$.

Also see Subroutine TRECNF.

DELX,DELY - Antenna aperture fields for the difference elevation channel.

DAZX,DAZY - Antenna aperture fields for the difference azimuth channel.

VREC - Complex array of three elements which on output contains the complex terminal voltage of the antenna

for the sum, elevation difference, and azimuth difference channels, respectively.

TABLE - Logical variable required by Subroutine RXMIT: if TRUE, a look-up table is used to calculate the transmission coefficients of the radome wall; if FALSE, these coefficients are calculated exactly for each angle of incidence specified.

SUPPRS - Logical variable used to control the printing of results from Subroutine RXMIT: if FALSE, a table of power transmission and reflection coefficients for equal increments in the sine of the incidence angle is printed. The phases of the complex voltage transmission and reflection coefficients of the radome wall are also printed.

RSQMAX - Real variable denoting the maximum radius of the antenna aperture such that any point $(x_A^2+y_A^2)>$RSQMAX is omitted from the summation procedure used to compute the received voltages VREC.

DSTH,DSPHI - Real input variables which specify the sample distance in the θ and ϕ directions on the radome surface; e.g., $\lambda/3$.

NTHMIN, NPHIMIN - Integer input variables which specify the minimum acceptable number of samples N_θ, N_ϕ in the two directions; e.g., $N_{\phi MIN}=4$.

AREA - Real output variable equal to the surface area of the radome included in the surface integration.

NPOINTS - Integer output variable equal to the number of sample points on the radome surface.

ROS,RIS - Real input variables equal to the generating radii of the inside and outside surfaces of the tangent ogive radome shape (Figure 3-1).

ZBOTCM, ZTOPCM - Real input variables which specify the Z_R coordinates of the bulkhead and opaque tip (if any), respectively (Figure 3-1).

BCM,RR - Real input variables defined in Figure 3-1.

3-4. Comments and Method

a. Subroutines Required: APINT, VECTOR, POINT, RXMIT, CAXB, OGIVEN, CAXCB.

b. Method: The voltage V_R induced at the terminals of a linear antenna by a "received" electromagnetic plane wave $\underline{E}_R$, $\underline{H}_R$ is given by the Lorentz reciprocity theorem as [1]

$$V_R(\hat{k}_A) = C \oint_S (\underline{E}_T \times \underline{H}_R - \underline{E}_R \times \underline{H}_T) \cdot \hat{n} da \qquad (1)$$

where $\hat{k}_A$ is the unit vector which points in the direction from whence the plane wave emanates and where $\underline{E}_T$, $\underline{H}_T$ are the electromagnetic fields of the antenna as produced on the closed surface S which surrounds the antenna when it is transmitting. The unit vector $\hat{n}$ is the normal to S pointing into the region not containing any sources, and C is a complex constant.

When the inside surface of the radome is chosen as (closed) surface of integration, the source-free volume is that inside the radome, excluding the space occupied by the antenna; hence, $\hat{n}$ is equal to the unit inward

normal n_{is} to the inside radome surface. The surface can be divided into elemental areas ΔA_{lm}, and the received voltage can be approximated by

$$V_R(\hat{k}_A) = C \sum_l \sum_m (\underline{E}_T \times \underline{H}_R - \underline{E}_R \times \underline{H}_T) \cdot \hat{n}_{is} \Delta A_{lm} \tag{2}$$

where the fields are evaluated at the same points P'_{lm} on the radome surface. The elemental areas ΔA_{lm} differ, in general, from point to point, and must be included under the summation.

It is assumed that the fields $\underline{E}_T$, $\underline{H}_T$ on S with the radome in place are the same as those that would exist in the absence of the radome. They are computed at points P' from their specified aperture values $\underline{E}_{ap}$, $\underline{H}_{ap}$ via the Huygens-Fresnel principle as explained in Chapters 5 and 6. The received fields $\underline{E}_R$, $\underline{H}_R$ at P' are computed by applying the flat panel normal transmission coefficients $T_{n\perp}$, $T_{n\parallel}$ to the incident plane wave $\underline{E}_i$, $\underline{H}_i = \underline{E}_i \times \hat{k}_A/\eta$ at the point P on the outside surface of the radome that is colinear with the inside point P' with respect to the unit normal $\hat{n}_{is}$. (See Figure 1-2).

The tangent ogive radome surface is divided into elemental (trapezoidal) areas by sections made in the longitudinal (θ) and circumferential (ϕ) directions. In both cases, desired sampling intervals ΔS_θ, ΔS_ϕ (e.g., $\lambda/3$) are specified as input data. For the θ direction of Figure 3-1, the number of samples N_θ is given by

$$N_\theta = \text{MAX} \left\{ \frac{R(\theta_{TOP} - \theta_{BOT})}{\Delta S_\theta} , N_{\theta MIN} \right\} \tag{3}$$

where R is the generating radius of the ogive surface

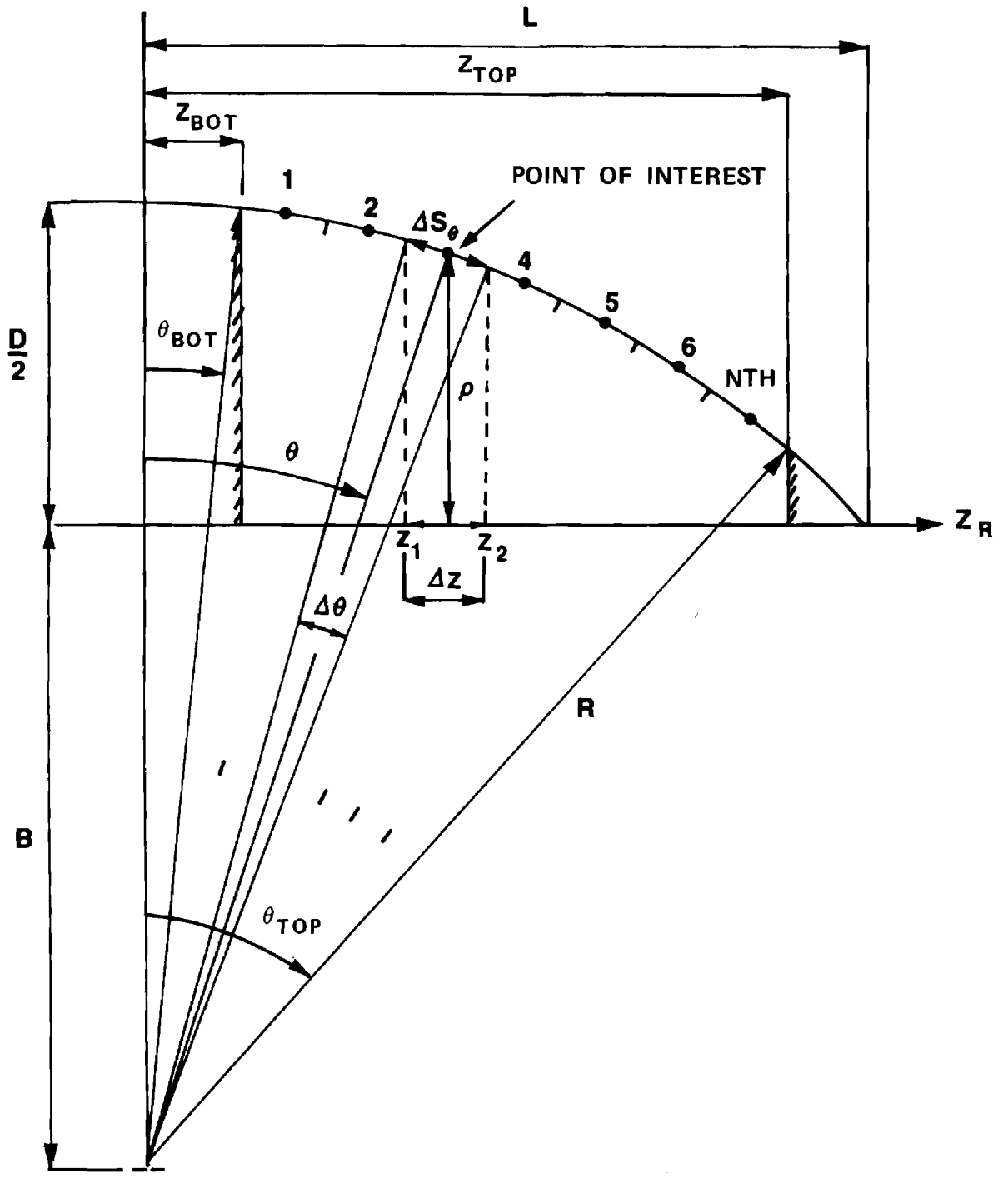

FIGURE 3–1. RADOME GEOMETRY FOR DEFINING ELEMENTAL SURFACE AREA IN θ DIRECTION.

$$R = L/\ \sin(\pi - 2\ \mathrm{Tan}^{-1}(2L/D)) \tag{4}$$

and where the other variables are defined in Figure 3-1. (A minimum acceptable number of samples $N_{\theta MIN}$ is also specified). The angular limits are given by

$$\theta_{BOT} = \sin^{-1}\ (Z_{BOT}/R) \tag{5}$$

$$\theta_{TOP} = \sin^{-1}\ (Z_{TOP}/R) \tag{6}$$

Since N_θ is an integer, the sample interval ΔS_θ must be recomputed as

$$\Delta S'_\theta = R(\theta_{TOP} - \theta_{BOT})/N_\theta\ = R\Delta\theta \tag{7}$$

For iteration in I, a sample point at the center of an elemental area on the radome surface is specified by

$$\theta\ = \theta_{BOT} + \Delta\theta/2 + (I-1)*\Delta\theta\ , \tag{8}$$

and the corresponding Z_R coordinate is given by

$$Z_R = R\ \sin\ \theta \tag{9}$$

The elemental areas are formed in the circumferential (ϕ) direction as indicated in Figure 3-2. Using ΔS_ϕ as input data, the number of samples N_ϕ in the ϕ direction is given by

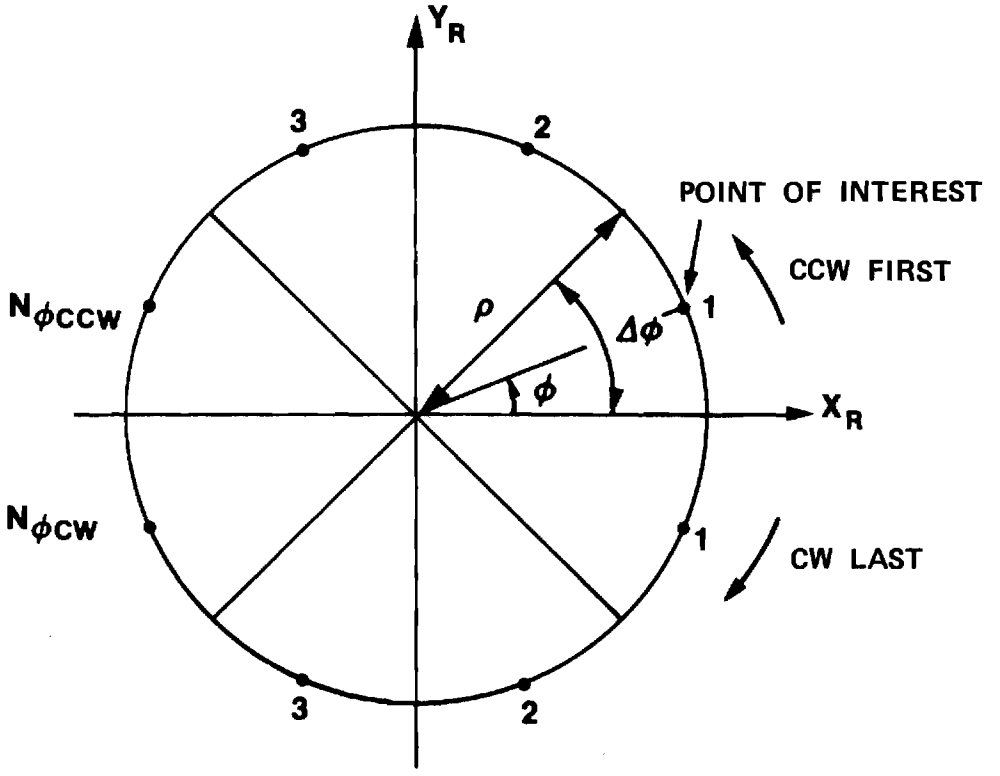

(a) DEFINITIONS IN ϕ–DIRECTION

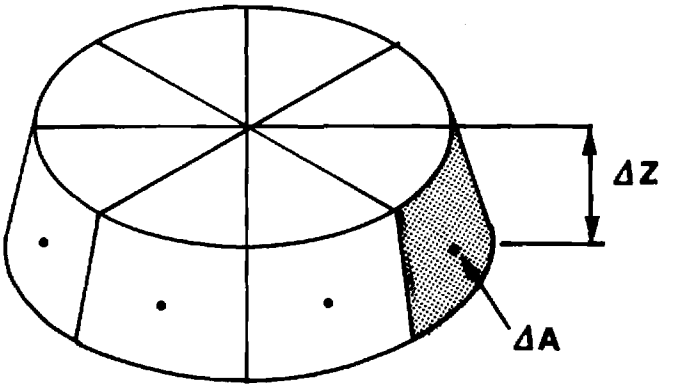

(b) TYPICAL ELEMENTAL VOLUME

FIGURE 3–2 DEFINITION OF ELEMENTAL SURFACE AREA IN ϕ DIRECTION.

$$N_\phi = \text{MAX}\left\{\frac{2\pi\rho}{\Delta S_\phi},\ N_{\phi MIN}\right\} \tag{10}$$

where ρ is defined in Figure 3-1 and is given by

$$\rho = \sqrt{R^2 - Z_R^2} - B \tag{11}$$

Since N_ϕ is an integer, the sampling distance in ϕ must be recomputed as

$$\Delta S'_\phi = 2\pi\rho/N_\phi \tag{12}$$

The sample point at the center of an elemental area is specified in ϕ by (for iteration J)

$$\phi = \phi_o + (J-1)\Delta\phi \tag{13}$$

where $\Delta\phi=2\pi/N_\phi$ and where ϕ_o is a specified initial point in ϕ. The area ΔA of a surface element specified by (θ,ϕ) is given by

$$\Delta A = R(\Delta Z - B\Delta\theta) \tag{14}$$

where

$$\Delta Z = Z_2 - Z_1 = R[\sin(\theta + \frac{\Delta\theta}{2}) - \sin(\theta - \frac{\Delta\theta}{2})] \tag{15}$$

It is deemed advantageous to set ϕ_o above in Equation (13) to some midpoint of the illuminated surface of the radome. This is done by transforming the unit vector $\hat{k}_A$ to radome coordinates; i.e.,

$$\hat{k}_A = x_A k_{xA} + \hat{y}_A k_{yA} + \hat{z}_A k_{zA} = \hat{x}_R k_{xR} + \hat{y}_R k_{yR} + \hat{z}_R k_{zR} \tag{16}$$

The angle ϕ_o follows as

$$\phi_o = \cos^{-1} \left(\frac{k_{xR}}{\sqrt{k_{xR}^2 + k_{yR}^2}} \right) \tag{17}$$

The computations in ϕ proceed first in the counterclockwise (CCW) direction and then in the clockwise (CW) direction as indicated in Figure 3-2(a). For the CCW direction, the coordinates of the sample point are given by (J=1, $N_\phi/2+1$)

$$x_R = \rho \cos (\phi_o + (J-1)\Delta\phi) \tag{18}$$

$$y_R = \rho \sin (\phi_o + (J-1)\Delta\phi) \tag{19}$$

For the CW direction, there results

$$x_R = \rho \cos (\phi_o - J\Delta\phi) \tag{20}$$

$$y_R = \rho \sin (\phi_o - J\Delta\phi) \tag{21}$$

where J is incremented from unity to $N_\phi/2$. (The z_R coordinate is given by Equation (9).)

For each elemental area specified, two tests may be performed to determine if the contribution of the fields on that surface element should be included in the received voltage. The first test consists of ensuring that the sample point (x_R, y_R, z_R) lies forward of the aperture plane of the antenna; i.e., that $z_A \geq 0$. The second test (which may be disabled as deemed appropriate) determines if the surface element is directly illuminated by the incident plane wave. The test is performed by computing the angle of incidence θ according to

$$\cos \theta = n_{is} \cdot \hat{k}_A \tag{22}$$

If $\cos \theta < 0$, the point is illuminated and should certainly be included in the summation indicated in Equation (2); if $\cos \theta \geq 0$, the point lies in the shadow region, and, under certain circumstances, may be omitted from the computation to save time. The effect of this omission is not completely understood in all cases.

3-5. Program Flow (Refer to Program Listing below)

Line Number(s)	Comments
1-39	Declare variables, initialize constants.
40-52	Initialize Subroutines DIPOLES and APINT; compute and write fields $\underline{E}_T$, $\underline{H}_T$ at point $(0, 0, 2D^2/\lambda)$ for reference.
53-55	Initialize Subroutine RXMIT.
56-67	Compute θ_{TOP}, θ_{BOT}, N_θ, $\Delta S'_\theta$, $\Delta\theta$.
68-76	Compute ϕ_o and initialize summation of V_{REC}.
77-85	Iterate in θ on radome surface.

86-90	Compute Z_{ROS}, Z_{RIS}, ρ_{OS}, ρ_{IS} and ensure that surface element does not lie forward of metal tip or aft of bulkhead.
91-97	Compute N_{ϕ} and $\Delta S'_{\phi}$.
98-104	Compute $N_{\phi CCW}$, $N_{\phi CW}$, and $\Delta\phi$.
105-106	Compute ΔZ and ΔA.
107-119	Iterate in ϕ: CCW first, CW second.
120-125	Compute inside coordinates x_{RIS}, y_{RIS}.
126-135	Compute unit inward normal $\hat{n}_{IS}$ and apply illumination test (disabled).
136-141	Convert coordinates of sample point on surface to antenna coordinates to ensure $z_A \geq 0$.
142-152	Compute phase of incident plane wave at outside point (x_{ROS}, y_{ROS}, z_{ROS}) with respect to the antenna origin. Adjust phase of the specified incident plane wave and store temporarily as $\underline{H}_{RP}$.
153-156	Compute antenna coordinates of inside point in wavelengths.
157-163	Compute transmitted plane wave $\underline{E}'_R$, $\underline{H}'_R$ at inside point.
164-171	Use aperture integration to compute the transmitted fields $\underline{E}_{Ti}$, $\underline{H}_{Ti}$ of the antenna at the inside point for each channel of the monopulse antenna.
172-176	Disabled statements pertaining to surface integration using the outside radome surface.
177-179	Form the vector cross products $\underline{S}_1 = \underline{E}_T \times \underline{H}'_R$, $\underline{S}_2 = \underline{E}'_R \times \underline{H}_T$.

180-182	Add contribution to received voltage V_{Ri}.
183-184	Incement AREA.
185-186	Increment NCUS = number of points omitted.
187-189	Increment NPOINTS.
190-197	If SUPPRS=.FALSE., compute and write total surface area, received voltages, number of points used, and number of points omitted.

3-6. Test Case: None

3-7. References

1. G. K. Huddleston, H. L. Bassett, and J. M. Newton, "Parametric Investigation of Radome Analysis Methods", 1978 IEEE AP-S Symposium Digest, pp. 199-201, May 1978.

3-8. Program Listing (See following pages)

```
      SUBROUTINE RECM(EINC,KA,NX,NY,KXMAX,KYMAX,FREQ,ROTATE,TRANSL,          1
     $ SUMX,SUMY,DELX,DELY,DAZX,DAZY,VREC,TABLE,SUPPRS,RSQMAX)               2
C  SUBR RECM COMPUTES THE RECEIVED VOLTAGE OF AN ANTENNA INSIDE A TANGENT
C  OGIVE RADOME AS PRODUCED BY A PLANE WAVE INCIDENT FROM THE DIRECTION     4
C  SPECIFIED BY KA.  THE INSIDE SURFACE OF THE RADOME IS USED AS THE SURFACE
C  OF INTEGRATION IN THE RECIPROCITY INTEGRAL, AND THE NORMAL TRANSMISSION
C  COEFFICIENT IS USED TO TRANSFER THE INCIDENT PLANE WAVE FROM THE POINT
C  P ON THE OUTSIDE SURFACE TO THE POINT P' ON THE INSIDE SURFACE, WHERE    8
C  P AND P' ARE COLINEAR WITH THE NORMAL TO EITHER SURFACE.                 9
C  THE CALL TO THIS SUBR IS IDENTICAL TO THE CALL TO SUBR RECM             10
C  USED IN THE RAY TRACING FORMULATION  HOWEVER, ADDITIONAL VARIABLES      11
C  ARE NEEDED BY THIS SUBR AND ARE PASSED FROM MAIN PROGRAM VIA LABEL      12
C  COMMON/RECIC/ AS SHOWN BELOW.                                           13
      COMPLEX ET(3),HT(3),ERP(3),HRP(3)                                    14
      COMPLEX S1(3),S2(3),U,C,EINC(3),VREC(3)                              15
      COMPLEX SUMX(NX,NY),SUMY(NX,NY),DELX(NX,NY),DELY(NX,NY),             16
     $ DAZX(NX,NY),DAZY(NX,NY)                                             17
      REAL KXMAX,KYMAX,ROTATE(3,3),TRANSL(3),LAMBDA,NISA(3)                18
      REAL PIR(3),NIS(3),KR(3),KA(3),PT(3),PISR(3),PO(3),PTWL(3)           19
      LOGICAL TABLE,ATOR,RTOA,SUPPRS,INIT                                  20
      COMMON/RECIC/DSTH,DSPHI,NTHMIN,NPHIMIN,AREA,NPOINTS,ROS,RIS,         21
     $ZBOTCM,ZTOPCM,BCM,RR                                                 22
      NAMELIST/ATDR/DSTH,BETA,DKX,DKY,DKXY,THTOP,THBOT,STH,NTH             23
      DATA ATOR/.TRUE./,RTOA/.FALSE./                                      24
      DATA PI/3.14159265/                                                  25
      DATA ZERO/1E-6/                                                      26
      DATA TUPI/6.28318530/                                                27
      DATA ETA/376.9911185/,NDO/0/                                         28
      DATA NISA/0.,0.,-1./,PT/0.,0.,0./                                    29
      AREA=0.                                                              30
      B=BCM                                                                31
      NPOINTS=0                                                            32
      NCUS=0                                                               33
      DKX=2.*KXMAX/NX                                                      34
      DKY=2.*KYMAX/NY                                                      35
      NXMID=NX/2+1                                                         36
      NYMID=NY/2+1                                                         37
      DXWL=.5/KXMAX                                                        38
```

```
      DYWL=.5/KYMAX                                                          39
      IF (NDO.GT.0) GO TO 4                                                  40
C  INITIALIZE CONSTANTS IN SUBR DIPOLES:                                     41
      LAMBDA=29.97925/FREQ                                                   42
      BETA=2.*PI/LAMBDA                                                      43
      INIT=.TRUE.                                                            44
      PTWL(1)=0.                                                             45
      PTWL(2)=0.                                                             46
      PTWL(3)=2.*4.*RSQMAX/LAMBDA                                            47
      CALL APINT(PTWL,SUMX,SUMY,NX,NY,NXMID,NYMID,DXWL,DYWL,ET,HT,INIT)      48
      WRITE(6,3) PTWL(3),ET,HT                                               49
    3 FORMAT(" SUBR DIPOLES INITIALIZED BY SUBR RECI"/                       50
     $"  AT Z=2*D**2/WL= ",E12.5,"  ET= ",6E12.5/                            51
     $30X,"  HT= ",6E12.5/)                                                  52
      RTD=180./PI                                                            53
      CALL RXMIT(HRP,ERP,KA,NISA,PT,TABLE,SUPPRS,BETA)                       54
    4 CONTINUE                                                               55
      DKXY=DKX*DKY                                                           56
      THTOP=ASIN(ZTOPCM/RIS)                                                 57
      THBOT=ASIN(ZBOTCM/RIS)                                                 58
      STH=RIS*(THTOP-THBOT)                                                  59
      NTHP=STH/DSTH                                                          60
      IF(NTHP.GE.NTHMIN) GO TO 10                                            61
      NTH=NTHMIN                                                             62
      GO TO 15                                                               63
10    NTH=NTHP                                                               64
15    DSTHP=STH/NTH                                                          65
      DTH=(THTOP-THBOT)/NTH                                                  66
      IF (.NOT.SUPPRS) WRITE(6,ATDR)                                         67
C  DETERMINE ANGLE PHI0 OF CENTER OF ILLUMINATED AREA ON RADOME:             68
      CALL VECTOR(KA,KR,ATOR,ROTATE)                                         69
      RAD=KR(1)**2+KR(2)**2                                                  70
      IF (RAD.GT.ZERO) GO TO 16                                              71
      PHI0=0.                                                                72
      GO TO 31                                                               73
   16 PHI0=ACOS(KR(1)/SQRT(RAD))                                             74
   31 DO 32 I=1,3                                                            75
   32 VREC(I)=(0.,0.)                                                        76
```

```
C     SELECT CIRCLE ON SURFACE OF RADOME AT CONSTANT THETA                    77
C     AND ITERATE IN I                                                        78
      TH=THBOT-DTH/2.                                                         79
      IF ((NDO.EQ.0).AND.(.NOT.SUPPRS)) WRITE(6,33)                           80
   33 FORMAT(3X,"THDEG",4X,"PHIDEG",12X,"PT",23X,"NIR"/)                      81
      DO 20 I=1,NTH                                                           82
      TH=TH+DTH                                                               83
      THD=TH*RTD                                                              84
      SINTH=SIN(TH)                                                           85
      PIR(3)=ROS*SINTH                                                        86
      RHOOS=SQRT(ROS**2-PIR(3)**2)-B                                          87
      PISR(3)=RIS*SINTH                                                       88
      IF ((PISR(3).GT.ZTOPCM).OR.(PISR(3).LT.ZBOTCM)) GO TO 20                89
      RHOIS=SQRT(RIS**2-PISR(3)**2)-B                                         90
      NPHIP=TUPI*RHOIS/DSPHI                                                  91
      IF(NPHIP.GE.NPHIMIN) GO TO 40                                           92
      NPHI=NPHIMIN                                                            93
      GO TO 50                                                                94
40    NPHI=NPHIP                                                              95
C     DIVIDE THE INNER SURFACE INTO NPHI EQUAL PARTS                          96
50    DSPHIP=TUPI*RHOIS/NPHI                                                  97
      NPHI2=NPHI/2                                                            98
      NPHICW=NPHI2                                                            99
      NPHICCW=NPHI2                                                          100
      IF(2.*NPHICCW.LT.NPHI) GO TO 55                                        101
      GO TO 60                                                               102
55    NPHICCW=NPHICW+1                                                       103
60    DPHI=TUPI/NPHI                                                         104
      DZ=RIS*(SIN(TH+DTH/2.)-SIN(TH-DTH/2.))                                 105
      DA=RIS*(DZ-B*DTH)*DPHI                                                 106
110   DO 61 J1=1,2                                                           107
      JMAX=NPHICCW                                                           108
      IF(J1.EQ.2) JMAX=NPHICW                                                109
C   SELECT A POINT ON INNER SURFACE OF RADOME AT CONSTANT PHI                110
C   AND ITERATE IN J, FIRST CCW, THEN CLOCKWISE.                             111
      PHI=PHI0-DPHI                                                          112
      IF (J1.EQ.2) PHI=PHI0                                                  113
120   DO 62 J=1,JMAX                                                         114
```

```
      IF (J1.EQ.2) GO TO 41                                              115
      PHI=PHI+DPHI                                                       116
      GO TO 42                                                           117
   41 PHI=PHI-DPHI                                                       118
   42 CONTINUE                                                           119
      PHID=PHI*RTD                                                       120
      CPHI=COS(PHI)                                                      121
      SPHI=SIN(PHI)                                                      122
      PISR(1)=RHOIS*CPHI                                                 123
      PISR(2)=RHOIS*SPHI                                                 124
C    THE POINT OF INTEREST ON INSIDE SURFACE HAS RADOME COORD PISR(XR,YR,ZR).
C    CALL OGIVEN TO FIND INNER UNIT NORMAL NIS TO RADOME SURFACE         126
      CALL OGIVEN(PISR,NIS)                                              127
      IF ((NDO.EQ.0).AND.(.NOT.SUPPRS)) WRITE(6,56) THD,PHID,PISR,NIS    128
   56 FORMAT(2(2X,F7.2),6E10.3)                                          129
C    TEST NOW IF THIS POINT IS ILLUMINATED BY PLANE WAVE                 130
C      CUS=NIS(1)*KR(1)+NIS(2)*KR(2)+NIS(3)*KR(3)                       131
C      IF CUS IS GREATER THAN ZERO,AREA IS NOT ILLUMINATED              132
C      IF(CUS.GT.0.) GO TO 59                                           133
C      IF(CUS.LT.0.) GO TO 65                                           134
C      GO TO 59                                                         135
C   CONVERT INSIDE POINT PISR(XR,YR,ZR) TO ANTENNA COORD PT(XA,YA,ZA):  136
   65 CALL POINT(PISR,PT,RTOA,ROTATE,TRANSL)                           137
C    TEST TO INSURE THAT POINT XR,YR,ZR IS ILLUMINATED                   138
C    BY THE ANTENNA INSIDE THE RADOME                                    139
C       IF ZA>0.,POINT IS ILLUMINATED                                    140
      IF (PT(3).LT.0.) GO TO 59                                          141
C    COMPUTE PHASE OF INCIDENT PLANE WAVE AT OUTSIDE POINT:              142
      PIR(1)=RHOOS*CPHI                                                  143
      PIR(2)=RHOOS*SPHI                                                  144
      CALL POINT(PIR,PO,RTOA,ROTATE,TRANSL)                              145
      PHS=AMOD(BETA*(KA(1)*PO(1)+KA(2)*PO(2)+KA(3)*PO(3)),TUPI)          146
      U=CMPLX(0.,PHS)                                                    147
      C=CEXP(U)                                                          148
C   ADJUST PHASE OF INCIDENT ELECTRIC FIELD AT OUTSIDE POINT AND STORE AS HRP:
      HRP(1)=EINC(1)*C                                                   150
      HRP(2)=EINC(2)*C                                                   151
      HRP(3)=EINC(3)*C                                                   152
```

```
C  COMPUTE ANTENNA FIELDS AT INSIDE POINT PISR:                          153
      PTWL(1)=PT(1)/LAMBDA                                              154
      PTWL(2)=PT(2)/LAMBDA                                              155
      PTWL(3)=PT(3)/LAMBDA                                              156
C  TRANSMIT INCIDENT PLANE WAVE THRU WALL USING NORMAL XMN COEFS:        157
      CALL VECTOR(NIS,NISA,RTOA,ROTATE)                                 158
      IF ((NDO.EQ.0).AND.(.NOT.SUPPRS)) WRITE(6,57) THD,PHID,PT,NISA    159
   57 FORMAT(2(2X,F7.2),6E10.3/)                                        160
      CALL RXMIT(HRP,ERP,KA,NISA,PT,TABLE,SUPPRS,BETA)                  161
C COMPUTE CORRESPONDING MAGNETIC FIELD*ETA:                             162
      CALL CAXB(ERP,KA,HRP)                                             163
      DO 58 ICH=1,3                                                     164
      IF (ICH.EQ.1)                                                     165
     $CALL APINT(PTWL,SUMX,SUMY,NX,NY,NXMID,NYMID,DXWL,DYWL,ET,HT,INIT) 166
      IF (ICH.EQ.2)                                                     167
     $CALL APINT(PTWL,DELX,DELY,NX,NY,NXMID,NYMID,DXWL,DYWL,ET,HT,INIT) 168
      IF (ICH.EQ.3)                                                     169
     $CALL APINT(PTWL,DAZX,DAZY,NX,NY,NXMID,NYMID,DXWL,DYWL,ET,HT,INIT) 170
C  SUBR APINT COMPUTES HT*ETA.                                          171
C ****************************                                        172
C  THE NEXT TWO STATEMENTS ARE FOR OUTSIDE SURFACE CASE.                173
C     CALL POYNTIN(E,H,S)                                               174
C     CALL RXMIT(ETR,HTR,STR,NIS,PISP,TABLE,BETA,ETRP,HTRP)             175
C ****************************                                        176
C   FORM CONTRIBUTION TO RECEIVED VOLTAGE                               177
      CALL CAXCB(ET,HRP,S1)                                             178
      CALL CAXCB(ERP,HT,S2)                                             179
      VREC(ICH)=VREC(ICH)-((S1(1)-S2(1))*NIS(1)+(S1(2)-S2(2))*NIS(2)+   180
     $ (S1(3)-S2(3))*NIS(3))*DA                                         181
   58 CONTINUE                                                          182
      AREA=AREA+DA                                                      183
      GO TO 62                                                          184
59    NCUS=NCUS+1                                                       185
62    CONTINUE                                                          186
      NPOINTS=NPOINTS+JMAX                                              187
61    CONTINUE                                                          188
20    CONTINUE                                                          189
      NDO=1                                                             190
```

```
      IF (SUPPRS) RETURN                                                  191
      PERCNT=100.*(1.-FLOAT(NCUS)/FLOAT(NPOINTS))                         192
      WRITE(6,25) AREA,VREC,NPOINTS,PERCNT,NCUS                           193
   25 FORMAT(//" SUBR RECI: AREA=",E12.5/" VREC=",6E12.5/" NPOINTS=",     194
     &I5,"   PERCENT=",F5.1,"   NCUS=",I6//)                             195
      RETURN                                                              196
      END                                                                 197
```

Chapter 4

SUBROUTINE TRECNF

4-1. Purpose: To compute near-field aperture distributions for four types of three-channel monopulse antennas: (1) circular aperture with tapered amplitude and uniform phase distributions; (2) flat plate antenna with a programmed amplitude distribution and uniform phase; (3) square aperture with cos x amplitude and uniform phase; (4) single element. Four polarizations can be selected for the circular and square apertures. The flat plate antenna is vertically ($\hat{y}_A$) polarized only.

4-2. Usage: CALL TRECNF (E, NX, NY, ICHAN, IPOL, IXY, DAPWL, DXWL, KXMAX, ICASE, SQUARE)

4-3. Arguments

E - Complex array of NX by NY elements which, on output, contains the values of the specified (IXY) rectangular component (x_A or y_A) of the electric field distribution over the specified (ICASE) antenna aperture having the specified (IPOL) polarization for the specified (ICHAN) channel of a three-channel monopulse antenna.

NX,NY - Even integer number of points in a rectangular array at which the aperture distribution is computed in the x_A and y_A directions, respectively. The point I=NX/2 + 1, J=NY/2 + 1 corresponds to x_A=0, y_A=0. For the single element case, NX=NY=2.

ICHAN - Integer control variable with values 1, 2, or 3 which selects the sum, elevation difference, or azimuth difference channel, respectively.

IPOL - Integer control variable which selects the antenna polarization as follows:

1 - Vertical ($\hat{y}_A$) polarization

2 - Horizontal ($\hat{x}_A$) "

3 - Right-hand circular "

4 - Left-hand circular "

IXY - Integer control variable having values 1 or 2 to select the x_A or y_A component of aperture electric field.

DAPWL - Diameter, in wavelengths, of the antenna aperture.

DXWL - Spacing, in wavelengths, between samples in aperture in x_A and y_A directions (output).

KXMAX - Maximum value of normalized wavenumber corresponding to KXMAX = 1./(2.*DXWL) (output).

ICASE - Integer control variable having values 1 or 2 to specify a circular aperture antenna with uniform amplitude and phase. If ICASE=3, a flat plate antenna having a programmed amplitude distribution (see Table 4-2) with vertical polarization is selected.

SQUARE - Logical input variable; if TRUE, square aperture is used.

4-4. Comments and Method

a. The integers NX,NY must each be equal to each other and even; e.g., NX=NY=16. In addition, when ICASE=3 (flat plate antenna), NX and NY must equal 16. If NX=NY=2, the fields of a single element at $x_A=y_A=0$ are specified. If NX=NY=32, only the central 15 x 15 elements are non-zero.

b. The actual shape of the circular aperture, as approximated by a rectangular array of sample points, is shown in Figure 4-1 for the case of NX=NY=16. Row 1 and Column 1 of the array contain null elements. The elements inside and on the boundary of the aperture may contain non-zero values as shown in Table 4-1 for the various cases when ICHAN=1 (sum channel). Note that specification of D_{AP} in Figure 4-1 determines the sample spacings according to

$$\Delta x_A = \Delta y_A = \frac{D_{Ap}\cos\alpha}{(N_x-2)} = \frac{D_{Ap}\cos\alpha}{(N_y-2)} \qquad (1)$$

where $\alpha = \mathrm{Tan}^{-1}(2/7)$.

The aperture distributions for three monopulse channels are formed by phasing the elements in the four quadrants of the aperture appropriately. The sum channel distribution is formed by assigning equal phases to all elements. The azimuth difference channel is formed by multiplying all elements in Quadrants II and III of the sum distribution by minus one and by zeroing all elements along $x_A=0$. For the elevation difference channel, Quadrants III and IV are negated, and all elements along the line $y_A=0$ are made zero for symmetry reasons.

The phasing chosen models a tracking antenna and provides outputs in two orthogonal channels from which the direction of arrival of a target return can be mathematically determined. Let $\hat{k}$ be a unit vector which

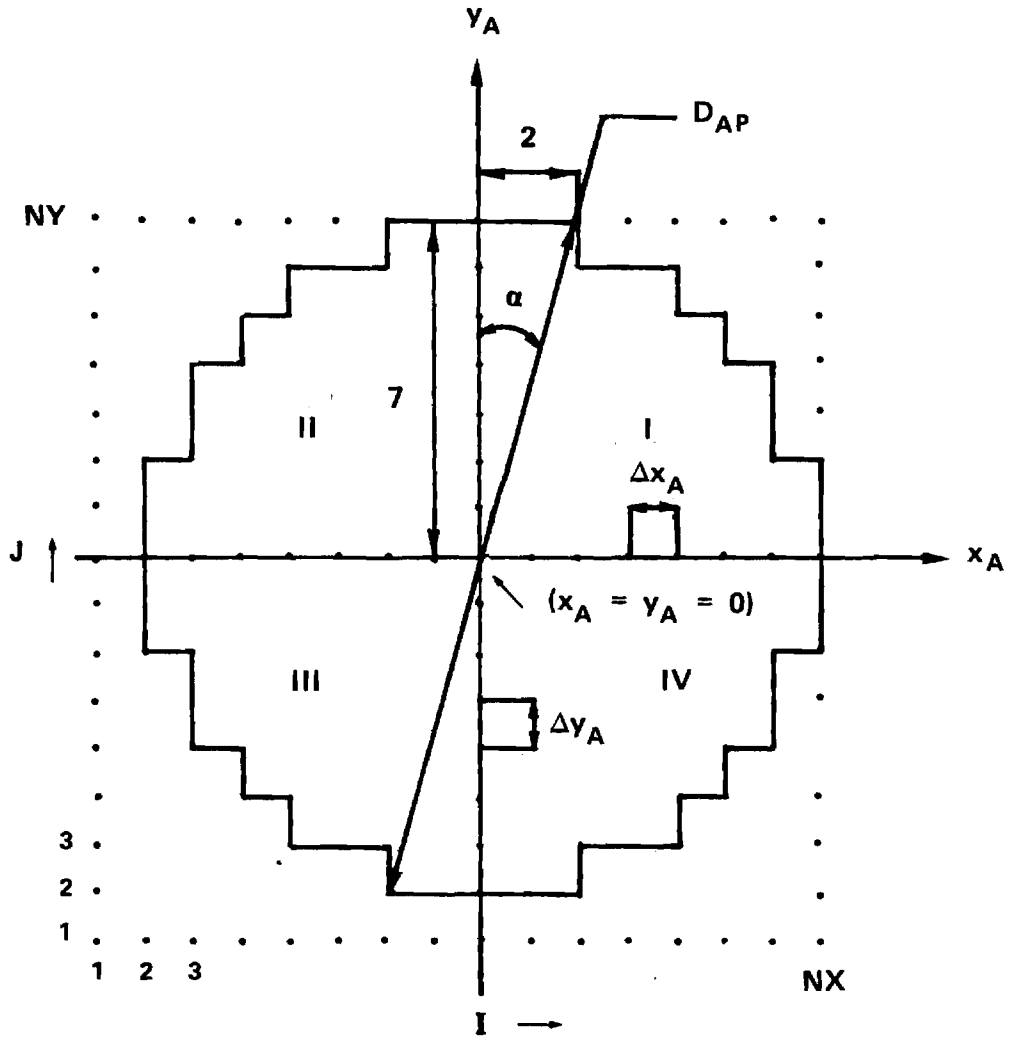

FIGURE 4–1. APPROXIMATION OF CIRCULAR APERTURE BY RECTANGULAR GRID OF SAMPLE POINTS.

points from the antenna origin toward the direction from whence the plane wave (target return) emanates; i.e.,

$$\hat{k} = \hat{x}_A k_x + \hat{y}_A k_y + \hat{z}_A k_z \tag{2}$$

Define the tracking functions for this plane wave as

$$f_i(k_x,k_y) = \frac{\Delta_i(k_x,k_y)}{\Sigma(k_x,k_y)} \tag{3}$$

where Δ_i represents the output of the elevation (ε) or azimuth (α) difference channel and Σ represents the sum channel output. Then for small $k_x>0$, the phase of f_α is + $\pi/2$; for small $k_x<0$, the phase of f_α is $-\pi/2$. Similarly, for small $k_y>0$, arg $(f_\varepsilon) = \pi/2$; for small $k_y<0$, arg $(f_\varepsilon) = -\pi/2$. Hence, the change in phase by π in either channel represents the boresight direction of the antenna, and tracking is done using the imaginary parts of the tracking functions rather than their real parts.

c. The shape and sampling grid used to model the flat plate antenna are shown in Figure 4-2. In Subroutine TRECNF, the integers NX and NY must both equal 16, and only linear polarization ($\hat{y}_A$) is applicable to the flat plate antenna (ICASE=3). The phasing of the four quadrants is done as described above to model the three monopulse channels so that tracking can be simulated. Note that specification of D_{Ap} determines the sample spacing according to

$$\Delta x_A = \Delta y_A = \frac{D_{Ap}\cos\alpha}{\left(\frac{N_x}{2} - 2\right)} \tag{4}$$

where $\alpha = \text{Tan}^{-1}$ (4/6).

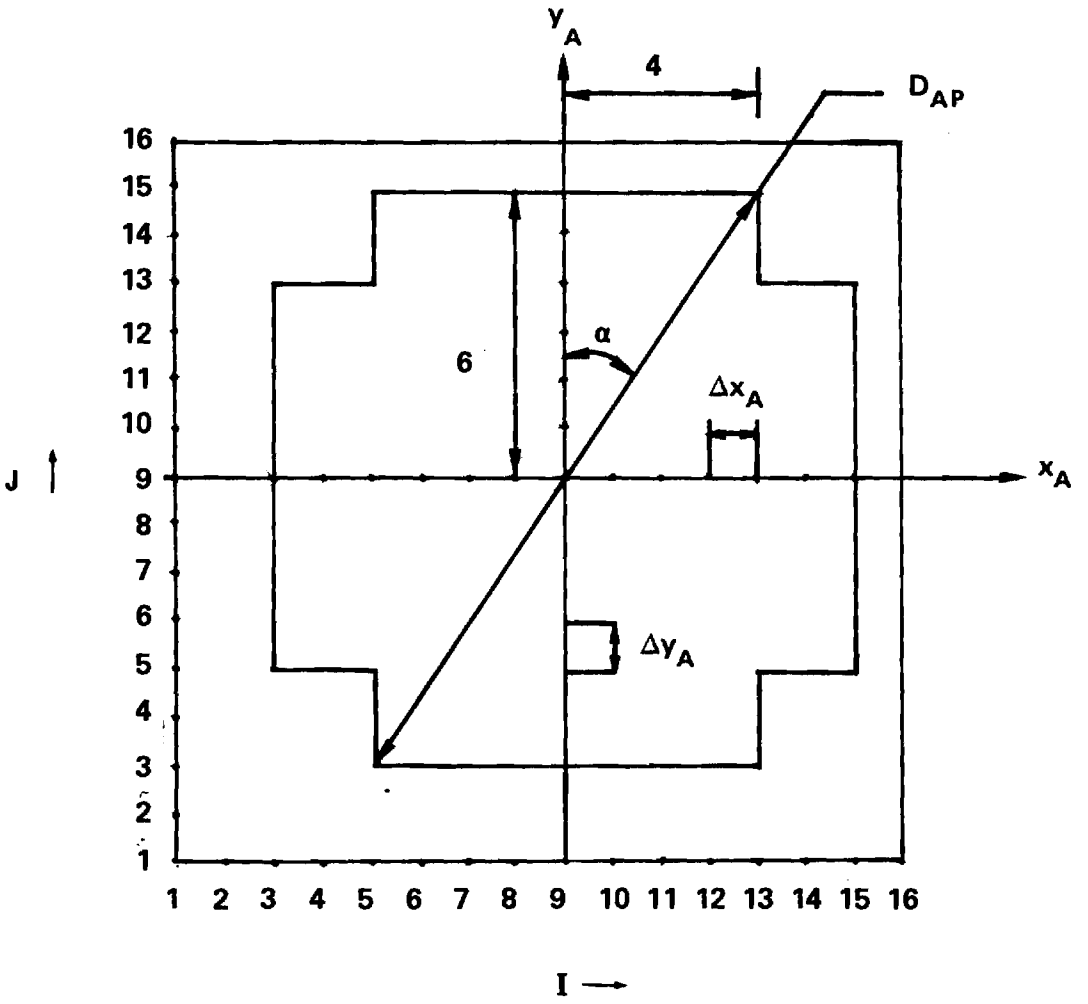

FIGURE 4–2. GEOMETRY OF FLAT PLATE ANTENNA.

Table 4-1. Values of Non-Zero Elements in Circular Aperture (ICHAN=1, ICASE=1 or 2)

IPOL	IXY	Value	Polarization Type
1	1	(0 + j0)	Vertical
1	2	(1 + j0)	"
2	1	(1 + j0)	Horizontal
2	2	(0 + j0)	"
3	1	(0 + j1)	RHC
3	2	(1 + j0)	"
4	1	(0 - j1)	LHC
4	2	(1 + j0)	"

The phase of each sample point in Figure 4-2 for the sum channel is made equal, but the amplitudes are tapered in the x_A and y_A directions as shown in Table 4-2. The amplitude distribution is separable and symmetrical so that

$$E_{yA}(x_A,y_A) = g(x_A)h(y_A) = E_{yA}(-x_A,y_A) = E_{yA}(x_A,-y_A) \qquad (5)$$

It is noted that samples 10, 12, 14, and 16 are actually specified in the program, and samples 9, 11, 13, and 15 are obtained from them by averaging.

d. The square aperture is formed by setting to zero Row 1 and Column 1 of the array of Figure 4-1 for symmetry reasons. The values of field at the other points in the aperture are computed to yield a cos x amplitude taper in the x_A direction and a uniform amplitude in y_A; i.e.,

$$E(x,y) = \cos \frac{\pi x}{2\, x_{max}} \qquad (5)$$

where x_{max} corresponds to the sample at I=NX.

3-5. Program Flow

Line Nos.	Comments
19	Assign complex values to CFAC to use in generating vertical, horizontal, RHC, and LHC polarization according to IPOL.
20-22	Compute the angle α and the upper bound R_{max} of the radius of the circular aperture.
23-24	Ensure that IPOL has correct values of 1, 2, 3, or 4.

Table 4-2. Symmetrical Amplitude Distribution for Flat Plate Antenna

Sample No.	x_A	Amplitude	y_A	Amplitude
9	0	1.0280	0	1.0280
10	Δx	1.0280	Δy	1.0280
11	$2\Delta x$	.9120	$2\Delta y$	.9170
12	$3\Delta x$	.7959	$3\Delta y$	.8060
13	$4\Delta x$	.6077	$4\Delta y$	.6155
14	$5\Delta x$	.4194	$5\Delta y$	.4250
15	$6\Delta x$	.2097	$6\Delta y$	.2125
16	$7\Delta x$	0.0	$7\Delta y$	0.0

25	If NX≠NY and SQUARE=FALSE, write error message and stop the program.
26-29	Compute indices of midpoint ±7.
30-31	Ensure that IXY=1 or 2.
32	If NX and NY are not even, stop the program.
33	Test value of ICASE: if ICASE=3 generate fields of flat plate antenna (Lines 64-105); otherwise, generate fields of circular or square aperture (Lines 34-60).
34-56	Assign complex field value to each sample point $(x_A, y_A, 0)$ in the circular aperture according to the values shown in Table 4-1. If $\sqrt{x_A^2 + y_A^2} > R_{max}$, make the field value zero. Multiply the non-zero elements by CFAC(IPOL) to generate the correct polarization. For the square aperture, zero Column 1 and Row 1, and insert cos x taper (Line 37).
57-60	Compute sample spacing $\Delta x_A/\lambda$ and go to statement 60.
61-63	Error message and STOP.
64-65	Flat plate antenna-- if NX≠16, write error message and STOP (Lines 131-133).
66-67	Compute sample spacing $\Delta x_A/\lambda$.
68	Ensure NX=NY
69-72	Zero all elements in the aperture. If IXY=1 (x_A-component), to to statement 60.

73-80	Assign tapered amplitude values to eight "even" elements in Quadrant III.
81-89	Compute amplitude values for the "odd" elements in Quadrant III.
90-93	Compute amplitude values for elements 3-9 along y_A=0 line and along x_A=0 line.
94-97	Generate symmetrical amplitude values in Quadrant IV.
98-105	Generate symmetrical amplitude values in Quadrants I and II.
106	Compute k_{xmax} and d_x/λ.
107-111	Test to determine if the sum channel data generated should be phased to produce the aperture distribution for a specified difference channel (ICHAN).
112-120	Form aperture distribution for difference elevation channel by zeroing all elements along y_A=0 and negating all elements for y_A<0. RETURN.
121-129	Form aperture distribution for difference azimuth channel by zeroing all elements along x_A=0 and negating all elements x_A<0. RETURN.
130-134	Error message for ICASE=3 and NX≠16.
	END

4-6. Test Case: None.

4-7. References

1. D. R. Rhodes, Introduction to Monopulse, McGraw Hill, New York, 1959.

4-8. Program Listing: See following pages.

```
      SUBROUTINE TRECNF(E,NX,NY,ICHAN,IPOL,IXY,DAPWL,DXWL,KXMAX,ICASE,
     &SQUARE)
C *** MODIFIED JAN 80 FOR SQUARE APERTURE AND FOR SINGLE ELEMENT***
C SUBR TRECNF COMPUTES ELECTRIC FIELDCOMPONENTS OVER A CIRCULAR APERTURE
C OF RADIUS RMAX=(NX/2-1)/COS(ATAN(2/7)) AND RETURNS SAME IN E(NX,NY).
C NX MUST EQUAL NY AND MUST BE EVEN.
C  ICHAN=1 FOR SUM CHANNEL   IPOL=1 FOR VERT-Y POL.    IXY=1 FOR X-COMP.
C       =2 FOR ELEV DIFF          =2 FOR HORIZ-X POL       =2 FOR Y-COMP.
C       =3 FOR AZ DIFF            =3 FOR RHC POL
C       =                         =4 FOR LHC POL
C DAPWL=DIAMETER OF APERTURE IN WAVELENGTHS (INPUT)
C  DXWL=SAMPLE SPACING IN APERTURE (OUTPUT)
C KXMAX=MAXIMUM WAVENUMBER (OUTPUT)
C  ICASE=1 OR 2 FOR UNIFORM, CIRCULAR APERTURE (ADA M.'S CASE I AND II)
C       =3 FOR FLAT-PLATE ANTENNA, VERTICAL POL (CASE III).
      COMPLEX E(NX,NY),CFAC(4)
      REAL KXMAX
      LOGICAL SQUARE
      DATA CFAC/(1.,0.),(1.,0.),(0.,+1.),(0.,-1.)/
      ANG=ATAN(2./7.)
      IF (ICASE.EQ.3) ANG=ATAN(4./6.)
      RMAX=(NX/2-1)/COS(ANG)+.001
      IF (IPOL.GT.4) IPOL=4
      IF (IPOL.LT.1) IPOL=1
      IF ((.NOT.SQUARE).AND.(NX.NE.NY)) GO TO 15
      NXMM7=NX/2+1-7
      NXMP7=NX/2+1+7
      NYMM7=NY/2+1-7
      NYMP7=NY/2+1+7
C  FOR NX,NY=32, ONLY THE CENTRAL 15 X 15 ELEMENTS ARE NONZERO.
      IF ((IXY.LT.1).OR.(IXY.GT.2)) IXY=2
      IF (MOD(NX,2).NE.0) GO TO 15
      IF (ICASE.EQ.3) GO TO 25
      TUXMX=FLOAT(NX)
      DO 10 I=1,NX
      X=FLOAT(-(NX/2)+I-1)
      COSX=COS(3.14159265*X/TUXMX)
      DO 10 J=1,NY
```

```
      IF ((I.EQ.1).OR.(J.EQ.1)) GO TO 9                                  39
      IF (NX.EQ.16) GO TO 1                                              40
      IF ((I.LT.NXMM7).OR.(I.GT.NXMP7).OR.(J.LT.NYMM7).OR.(J.GT.NYMP7))  41
     $GO TO 9                                                            42
    1 IF(SQUARE) GO TO 8                                                 43
      Y=FLOAT(-(NY/2)+J-1)                                               44
      R=SQRT(X**2+Y**2)                                                  45
      IF (R.GT.RMAX) GO TO 9                                             46
 8    IF ((IPOL.EQ.1).AND.(IXY.EQ.1)) GO TO 9                            47
      IF ((IPOL.EQ.2).AND.(IXY.EQ.2)) GO TO 9                            48
C  IF RHC, EY=(1,0), EX=(0,1)  I.E., EX LEADS EY BY 90 DEG.              49
C  IF LHC,EY=(1,0), EX=(0,-1)  I.E., EX LAGS EY BY 90 DEG.               50
      E(I,J)=CMPLX(COSX,0.)                                              51
      IF ((IPOL.LT.3).OR.(IXY.EQ.2)) GO TO 10                            52
      E(I,J)=E(I,J)*CFAC(IPOL)                                           53
      GO TO 10                                                           54
    9 E(I,J)=(0.,0.)                                                     55
   10 CONTINUE                                                           56
      IF (NX.EQ.2) GO TO 56                                              57
      DXWL=(DAPWL/2.)*COS(ANG)/(NX/2-1)                                  58
      IF(SQUARE) DXWL=(DAPWL/SQRT(2.))/(NX-2)                            59
      GO TO 60                                                           60
   15 WRITE(6,20)                                                        61
   20 FORMAT(//" NX.NE.NY OR NX NOT EVENIN SUBR TRECNF"//)               62
      STOP                                                               63
C THE FOLLOWING IS FOR ADA M.'S CASE III (ICASE=2):                      64
   25 IF (NX.NE.16) GO TO 90                                             65
      DXWL=(DAPWL/2.)*COS(ANG)/(NX/2-2)                                  66
      IF(SQUARE) DXWL=(DAPWL/SQRT(2.))/(NX-2)                            67
      NY=NX                                                              68
      DO 26 I=1,NX                                                       69
      DO 26 J=1,NY                                                       70
   26 E(I,J)=(0.,0.)                                                     71
      IF (IXY.EQ.1) GO TO 60                                             72
      E(6,4)=(.2824,0.)                                                  73
      E(8,4)=(.4250,0.)                                                  74
      E(4,6)=(.2888,0.)                                                  75
      E(6,6)=(.5218,0.)                                                  76
```

```
      E(8,6)=(.8060,0.)                                                  77
      E(4,8)=(.4194,0.)                                                  78
      E(6,8)=(.7959,0.)                                                  79
      E(8,8)=(1.028,0.)                                                  80
      DO 30 J=4,8,2                                                      81
      DO 30 I=3,8,1                                                      82
      IF ((MOD(J,2).EQ.0).AND.(MOD(I,2).EQ.0)) GOTO 30                   83
      E(I,J)=(E(I-1,J)+E(I+1,J))/2.                                      84
   30 CONTINUE                                                           85
      DO 35 I=3,8,1                                                      86
      DO 35 J=3,8,2                                                      87
      E(I,J)=(E(I,J-1)+E(I,J+1))/2.                                      88
   35 CONTINUE                                                           89
      DO 40 I=3,9                                                        90
   40 E(I,J)=E(I,8)                                                      91
      DO 45 J=3,9                                                        92
   45 E(9,J)=E(8,J)                                                      93
      DO 50 J=3,9                                                        94
      DO 50 I=1,6                                                        95
      E(9+I,J)=E(9-I,J)                                                  96
   50 CONTINUE                                                           97
      DO 55 I=3,15                                                       98
      DO 55 J=1,6                                                        99
      E(I,9+J)=E(I,9-J)                                                 100
   55 CONTINUE                                                          101
      GO TO 60                                                          102
   56 DXWL=DAPWL/SQRT(2.)                                               103
      KXMAX=.5/DXWL                                                     104
      RETURN                                                            105
   60 KXMAX=1./(2.*DXWL)                                                106
      IF (ICHAN.EQ.1) RETURN                                            107
      IF ((IXY.EQ.1).AND.(ICASE.EQ.3)) RETURN                           108
      IF ((IXY.EQ.1).AND.(IPOL.EQ.1)) RETURN                            109
      IF ((IXY.EQ.2).AND.(IPOL.EQ.2)) RETURN                            110
      IF (ICHAN.EQ.3) GO TO 75                                          111
C  LOAD ELEVATION DIFFERENCE CHANNEL:                                   112
      J=NY/2+1                                                          113
      DO 65 I=1,NX                                                      114
```

```
   65 E(I,J)=(0.,0.)                                                        115
      JMAX=NY/2                                                             116
      DO 70 J=1,JMAX                                                        117
      DO 70 I=1,NX                                                          118
   70 E(I,J)=-E(I,J)                                                        119
      RETURN                                                                120
C  LOAD AZIMUTH DIFFERENCE CHANNEL:                                        121
   75 I=NX/2+1                                                              122
      DO 80 J=1,NY                                                          123
   80 E(I,J)=(0.,0.)                                                        124
      IMAX=NX/2                                                             125
      DO 85 I=1,IMAX                                                        126
      DO 85 J=1,NY                                                          127
   85 E(I,J)=-E(I,J)                                                        128
      RETURN                                                                129
C   DAPWL=5.047 FOR ADA M.'S CASE III                                       130
   90 WRITE(6,95)                                                           131
   95 FORMAT(//"***ERROR EXIT! NX NOT EQUAL TO 16 IN SUBR TRECNF***"//)     132
      STOP                                                                  133
      END                                                                   134
```

Chapter 5

SUBROUTINE APINT

5-1. Purpose: To compute the electromagnetic fields $\underline{E}$, $\underline{H}$ of a rectangular aperture in the z=0 plane at a point P(x,y,z>0), where the amplitude and phase of the aperture electric fields E_{xap}, E_{yap} are specified at N_x by N_y discrete points spaced d_x/λ and d_y/λ apart. The aperture magnetic fields H_{xap}, H_{yap} are derived from $\underline{E}_{ap}$ via the geometrical optics approximation.

5-2. Usage: CALL APINT (PFWL, EX, EY, NX, NY, MIDX, MIDY,
DXWL, DYWL, E, H, INIT)

5-3. Arguments

PFWL - Real input array of three elements which specifies the Cartesian coordinates in wavelengths of the point P(x/λ, y/λ, z/λ) at where the fields are to be computed; i.e., PFWL(1) = x/λ, etc.

EX,EY - Complex input arrays of NX by NY elements each which specify the aperture electric field.

NX,NY - Integer input variables equal to the number of sample points in the aperture in the x and y directions, respectively. NX and NY must be even.

MIDX, MIDY - Integer input variables equal to the indices in the arrays EX, EY corresponding to x=y=0; i.e., MIDX= NX/2+1, MIDY=NY/2+1.

DXWL, DYWL - Real input variables equal to the sample spacings in wavelengths in the x and y directions, respectively.

E,H - Complex output arrays of three elements each equal to the rectangular vector components of the electric and magnetic fields at P; i.e., E(1)=E_x, etc.

INIT - Logical input variable which controls initialization of Subroutine DIPOLES.

5-4. Comments and Method

The fields at P(x,y,z) due to the sampled aperture fields are computed by superposing the individual fields of equivalent electric and magnetic dipoles located at each sample point as explained in Section 6-4.

5-5. Program Flow

1-12	Declare variables, initialize constants.
13-14	Compute initial source point, minus d_x/λ. Set z-coordinate of source points to zero.
15-18	Initialize summations of the fields E,H.
19-23	Compute first source point $P_x(x,y,0)$.
24-27	Compute electric J^e_x, J^e_y and magnetic J^m_x, J^m_y currents according to $\underline{J}^e = \hat{z} \times \underline{H}_{ap}$ and $\underline{J}^m = \underline{E}_{ap} \times \hat{z}$.
28	Call Subroutine DIPOLES to compute the fields of the electric and magnetic dipoles $\underline{J}^e$, $\underline{J}^m$ located at the specified source point.
29-32	Add contribution of each rectangular component to the field at P(x,y,z).
33	Repeat for all source points.

5-6. Test Case: See Chapter 6.

5-7. References: See Chapter 6.

5-8. Program Listing: See following page.

```
      SUBROUTINE APINT(PFWL,EX,EY,NX,NY,MIDX,MIDY,DXWL,DYWL,E,H,INIT)          1
C  SUBR APINT COMPUTES FRESNEL FIELDS OF RECTANGULAR APERTURE WITH             2
C  APERTURE FIELDS GIVEN BY EX,EY( H FIELDS ARE DERIVED USING G.O. APPROX.)
C  FIELDS E,H ARE COMPUTED AT THE POINT PFWL.                                   4
      COMPLEX E(3),H(3),EX(NX,NY),EY(NX,NY),JE(2),JM(2),ES(3),HS(3)            5
C  JE,JM ARE ELECTRIC AND MAGNETIC SURFACE CURRENT DENSITIES FOUND FROM        6
C  EAPXZHAT AND ZHAT X HAP.                                                     7
      LOGICAL INIT                                                             8
      REAL PSWL(3),PFWL(3)                                                     9
      DATA ETA/376.9911185/                                                   10
C  NX,NY MUST BE EVEN SO THAT OMITTING ROW 1 AND COL 1 YIELDS SYM APERTURE
C  INIT=.TRUE. TO INITIALIZE CONSTANTS IN SUBR DIPOLES                         12
      PSWL(1)=(1-MIDX)*DXWL                                                   13
      PSWL(3)=0.                                                              14
      DO 1 L=1,3                                                              15
      E(L)=(0.,0.)                                                            16
      H(L)=(0.,0.)                                                            17
    1 CONTINUE                                                                18
      DO 10 I=2,NX                                                            19
      PSWL(1)=PSWL(1)+DXWL                                                    20
      PSWL(2)=(1-MIDY)*DYWL                                                   21
      DO 10 J=2,NY                                                            22
      PSWL(2)=PSWL(2)+DYWL                                                    23
      JE(1)=-EX(I,J)/ETA                                                      24
      JM(1)=EY(I,J)                                                           25
      JE(2)=-EY(I,J)/ETA                                                      26
      JM(2)=-EX(I,J)                                                          27
      CALL DIPOLES(JE,JM,PSWL,PFWL,DXWL,DYWL,ES,HS,INIT)                      28
      DO 5 L=1,3                                                              29
      E(L)=E(L)+ES(L)                                                         30
      H(L)=H(L)+HS(L)                                                         31
    5 CONTINUE                                                                32
   10 CONTINUE                                                                33
      RETURN                                                                  34
      END                                                                     35
```

Chapter 6

SUBROUTINE DIPOLES

6-1. Purpose: To compute the electromagnetic fields $\underline{E} = \hat{x}\, E_x + \hat{y}\, E_y + \hat{z}\, E_z$ and $\underline{H} = \hat{x}\, H_x + \hat{y}\, H_y + \hat{z}\, H_z$ at point $P_f(x/\lambda, y/\lambda, z/\lambda)$ as produced by electric $\underline{J}^e = \hat{z} \times \underline{H}$ and magnetic $\underline{J}^m = \underline{E} \times \hat{z}$ surface currents flowing on the planar rectangular surface of dimensions $\Delta x/\lambda$, $\Delta y/\lambda$ located at source point $P_s(x'/\lambda, y'/\lambda, z'/\lambda)$ and oriented in the $z=z'$ plane. All dimensions are in wavelengths.

6-2. Usage: CALL DIPOLES (JE, JM, PSWL, PFWL, DXWL, DYWL, E, H, INIT)

6-3. Arguments

JE, JM - Complex input arrays of two elements each containing the x and y components of the electric and magnetic surface current densities at the center of the planar element as found from $\underline{E} \times \hat{z}$ and $\hat{z} \times \underline{H}$, respectively, where $\hat{z}$ is the unit normal to the element and $\underline{E}$, $\underline{H}$ are the fields at the center of the element.

PSWL, PFWL - Real input arrays of three elements each which contain the coordinates $P_s(x'/\lambda, y'/\lambda, z'/\lambda)$, $P_f(x/\lambda, y/\lambda, z/\lambda)$ of the center of the source element and the point at which the field is to be computed, respectively.

DXWL, DYWL - Real input variables equal to the dimensions $\Delta x/\lambda$, $\Delta y/\lambda$ of the rectangular source element.

E, H - Complex output arrays of three elements each containing the fields $\underline{E}$, $\eta\ \underline{H}$ at the point P_f. Note that $\eta\ \underline{H}$ is computed rather than $\underline{H}$ above (to save time).

INIT - Logical input variable which controls initialization of various constants for repetitive calls to the subroutine: if TRUE, the constants are computed; if FALSE, the constants are not computed, and their last computed values are used.

6-4. Comments and Method

a. Comment. The source and field points cannot be any closer together than $r = .01\lambda$. This restriction is necessary to prevent division by zero due to the r^{-1} variation of the dipole fields as explained below. Actually, field points should be removed to the order of $r = \sqrt{(\Delta x/\lambda)^2 + (\Delta y/\lambda)^2}$ for validity of the discretized approximation to the physical model.

b. Method. The subroutine computation is motivated by the problem of computing the fields of a rectangular antenna aperture located in the $z=z'$ plane as illustrated in Figure 1. Let the electric and magnetic fields $\underline{E}_{ap}$, $\underline{H}_{ap}$ be specified at discrete points $(x_m, y_n, 0)$. Then, at each point, the equivalent surface current densities $\underline{J}^e$ and $\underline{J}^m$ are given by [1]

$$\underline{J}^e = \hat{z} \times \underline{H}_{ap} = \hat{x}\,(-H_{yap}) + \hat{y}\,H_{xap} = \hat{x}\,J_x^e + \hat{y}\,J_y^e \qquad (1)$$

$$\underline{J}^m = \underline{E}_{ap} \times \hat{z} = \hat{x}\,E_{yap} + \hat{y}\,(-E_{xap}) = \hat{x}\,J_x^m + \hat{y}\,J_y^m \qquad (2)$$

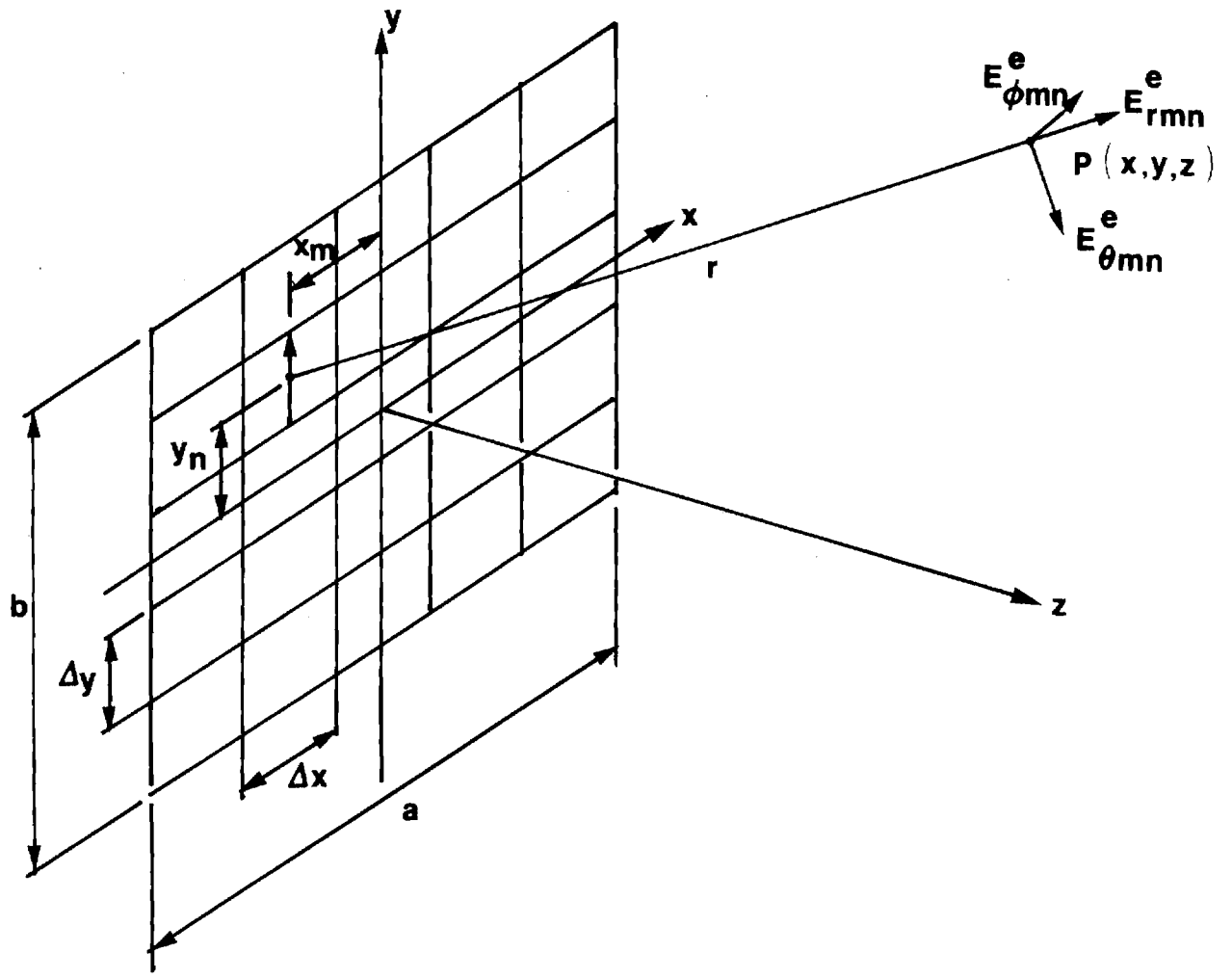

Figure 6–1. Geometry of Rectangular Aperture Antenna Approximated by Elementary Dipoles.

The surface current densities so defined can be discretized for each element $\Delta x \Delta y$ as follows. Consider the current density J_y^e. The total current entering the lower boundary and leaving the upper boundary of the element is $J_y^e \Delta x$ and can be regarded as an elementary dipole concentrated at the center of the element. The dipole moment is

$$p_o = q\ell = \frac{J_y^e \, \Delta x}{j\omega} \, \Delta y \tag{3}$$

where q is the charge and ℓ is the separation [2], and where the following relation for the sinusoidal steady state has been used:

$$q = \int I \, dt = \frac{I}{j\omega} \tag{4}$$

Similar relations hold for the other component of $\underline{J}^e$ and, by duality, for $\underline{J}^m$ as will be summarized below.

The next step in the development is to obtain expressions for the dipole fields of $\underline{J}^e$ and $\underline{J}^m$. To facilitate this step, first consider the fields radiated by electric and magnetic dipoles oriented along the z_o axis as shown in Table 1 [2]. Note that these expressions require r_o in wavelengths, and that Δx and Δy refer to the element size in the original aperture.

Matters are simplified if the spherical coordinate components of Table 1 are transformed to their corresponding rectangular components according to [3]

Table 6–1. Elementary Dipole Fields of Z–Directed Currents.

Electric	⟷ Duality ⟷	Magnetic
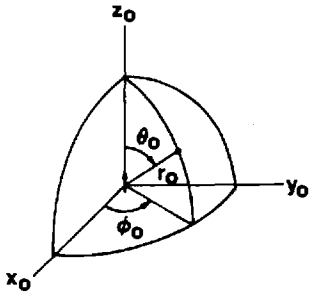	$\underline{E}^e$	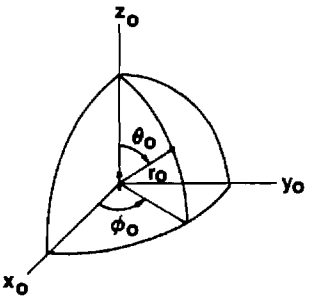
	$\underline{H}^e$	
	ϵ	
	μ	
	η	
$E^e_{ro} = J^e_{zo}\, e_o \left[\frac{1}{r_o^3} + \frac{j2\pi}{r_o^2}\right] \cos\theta_o\, e^{-j2\pi r_o}$		$H^m_{ro} = J^m_{zo}\, h_o \left[\frac{1}{r_o^3} + \frac{j2\pi}{r_o^2}\right] \cos\theta_o\, e^{-j2\pi r_o}$
$E^e_{\theta o} = J^e_{zo}\, \frac{e_o}{2} \left[\frac{1}{r_o^3} + \frac{j2\pi}{r_o^2} - \frac{(2\pi)^2}{r_o}\right] \sin\theta_o\, e^{-j2\pi r_o}$		$H^m_{\theta o} = J^m_{zo}\, \frac{h_o}{2} \left[\frac{1}{r_o^3} + \frac{j2\pi}{r_o^2} - \frac{(2\pi)^2}{r_o}\right] \sin\theta_o\, e^{-j2\pi r_o}$
$H^e_{\phi o} = J^e_{zo}\, e_o\, \frac{j\pi}{\eta} \left[\frac{1}{r_o^2} + \frac{j2\pi}{r_o}\right] \sin\theta_o\, e^{-j2\pi r_o}$		$E^m_{\phi o} = -J^m_{zo}\, h_o\, j\pi\eta \left[\frac{1}{r_o^2} + \frac{j2\pi}{r_o}\right] \sin\theta_o\, e^{-j2\pi r_o}$
$e_o = \frac{\left(\frac{\Delta x}{\lambda}\right)\left(\frac{\Delta y}{\lambda}\right)\eta}{j(2\pi)^2}$		$h_o = \frac{\left(\frac{\Delta x}{\lambda}\right)\left(\frac{\Delta y}{\lambda}\right)}{j(2\pi)^2\eta}$
r_o in wavelengths		r_o in wavelengths

$$A_{xo} = (\bar{A}_{ro} \cos\theta_o) \sin\theta_o \cos\phi_o + (\bar{A}_{\theta o} \sin\theta_o) \cos\theta_o \cos\phi_o \quad (5a)$$

$$A_{yo} = (\bar{A}_{ro} \cos\theta_o) \sin\theta_o \sin\phi_o + (\bar{A}_{\theta o} \sin\theta_o) \cos\theta_o \sin\phi_o \quad (5b)$$

$$A_{zo} = (\bar{A}_{ro} \cos\theta_o) \cos\theta_o - (\bar{A}_{\theta o} \sin\theta_o) \sin\theta_o \quad (5c)$$

$$C_{xo} = -(\bar{C}_{\phi o} \sin\theta_o) \sin\phi_o \quad (5d)$$

$$C_{yo} = (\bar{C}_{\phi o} \sin\theta_o) \cos\phi_o \quad (5e)$$

$$C_{zo} = 0 \quad (5f)$$

In the above, the trigonometric function in parentheses comes from the field expressions in Table 1; hence, the "minus" superscript indicates the field expression from Table 1 without the orientation factor $\cos\theta_o$ or $\sin\theta_o$, weighting e_o or h_o, and without the current J^m_{zo} or J^e_{zo}.

Define direction cosines k_{xo}, k_{yo}, k_{zo} related to θ_o, ϕ_o according to

$$k_{xo} = \sin\theta_o \cos\phi_o \quad (6a)$$

$$k_{yo} = \sin\theta_o \sin\phi_o \quad (6b)$$

$$k_{zo} = \cos\theta_o \quad (6c)$$

Then Equations (5) can be rewritten succinctly as

$$A_{xo} = (\bar{A}_{ro} + \bar{A}_{\theta o})\, k_{xo}\, k_{zo} \tag{7a}$$

$$A_{yo} = (\bar{A}_{ro} + \bar{A}_{\theta o})\, k_{yo}\, k_{zo} \tag{7b}$$

$$A_{zo} = (\bar{A}_{ro} + \bar{A}_{\theta o})\, k_{zo}^{2} - \bar{A}_{\theta o} \tag{7c}$$

$$C_{xo} = -\bar{C}_{\phi o}\, k_{yo} \tag{7d}$$

$$C_{yo} = \bar{C}_{\phi o}\, k_{xo} \tag{7e}$$

$$C_{zo} = 0 \tag{7f}$$

Similar expressions for cases of x-directed and y-directed dipoles may be derived from those given above merely redefining the axes in Table 1. When this is done, the generalized expressions shown in Table 2 result for all three cases.

When both electric and magnetic currents are present (x-directed and y-directed components) the expressions for $\underline{E}$ and $\underline{H}$ are obtained by adding the contributions due to each current as given in Table 2. Note that $\bar{A}_r$, $\bar{A}_\theta$, and $\bar{A}_r$ are identical for both types and directions of currents so that the expressions for the field components may be written, for example, as follows:

$$E_x = e_o \left\{ J_x^e [(\bar{A}_r + \bar{A}_\theta)\, k_x^2 - \bar{A}_\theta] + J_y^e\, k_x k_y\, (\bar{A}_r + \bar{A}_\theta) \right\}$$

$$- h_o\, j\pi\eta\, J_y^m\, k_z\, \bar{C}_\phi \tag{8a}$$

Table 6-2. Rectangular Field Components of Elementary Dipoles

Field Component	Dipole Orientation x-directed	y-directed	z-directed
A_x	$\bar{A}_{r\theta} k_x^2 - \bar{A}_\theta$	$\bar{A}_{r\theta} k_x k_y$	$\bar{A}_{r\theta} k_x k_z$
A_y	$\bar{A}_{r\theta} k_x k_y$	$\bar{A}_{r\theta} k_y^2 - \bar{A}_\theta$	$\bar{A}_{r\theta} k_y k_z$
A_z	$\bar{A}_{r\theta} k_x k_z$	$\bar{A}_{r\theta} k_y k_z$	$\bar{A}_{r\theta} k_z^2 - \bar{A}_\theta$
C_x	0	$\bar{C}_\phi k_z$	$-\bar{C}_\phi k_y$
C_y	$-\bar{C}_\phi k_z$	0	$\bar{C}_\phi k_x$
C_z	$\bar{C}_\phi k_y$	$-\bar{C}_\phi k_x$	0

where:

$$\bar{A}_{r\theta} = (\bar{A}_r + \bar{A}_\theta)$$

$$\bar{A}_r = \left(\frac{1}{r_o^3} + \frac{j2\pi}{r_o^2}\right) e^{-j2\pi r_o}$$

$$\bar{A}_\theta = \frac{1}{2}\left(\frac{1}{r_o^3} + \frac{j2\pi}{r_o^2} - \frac{(2\pi)^2}{r_o}\right) e^{-j2\pi r_o}$$

$$\bar{C}_\phi = \left(\frac{1}{r_o^2} + \frac{j2\pi}{r_o}\right) e^{-j2\pi r_o}$$

$$\eta H_x = \eta h_o \left\{ J_x^m [(A_r^- + A_\theta^-)\, k_x^2 - A_\theta^-] + J_y^m k_x k_y\, (A_r^- + A_\theta^-) \right\}$$

$$+ e_o\, j\pi\, J_y^e\, k_z\, C_\phi^- \qquad (8b)$$

Similar expressions may be obtained for the other rectangular components of $\underline{E}$ and $\underline{H}$ as given in Table 6-3 and by Lines 56-57 and 62-65 of the program listing.

6-6. Program Flow

Lines	Comment
15	If INIT=.TRUE., compute constants in Lines 18-29.
18-29	Compute $(2\pi)^2$, j, e_o, h_o, $j2\pi$, $j\pi$, $h_{oe}=-h_o\eta$, $e_{oh}=e_o/\eta$. Lines 26-27 have been added to cause $\eta\underline{H}$ to be computed instead of $\underline{H}$ to save time in Subroutine RECM (See Chapter 3).
30-33	Compute r in wavelengths; i.e., the distance from the source point to the field point.
34	If $r<.01\lambda$, write error message and stop (Lines 67-69).
35-37	Compute direction cosines k_x, k_y, k_z.
38-40	Compute exponential phase factor $e^{-j2\pi r}$.
41-45	Compute A_{ro}^-, $A_{\theta o}^-$, $C_{\phi o}^-$, $(A_{ro}^- + A_{\theta o}^-)$, and $C_\theta = (A_{ro}^- + A_{\theta o}^-)\, k_x^2 - A_{\theta o}^-$
46-49	These commented lines contain only 1/r terms and can be used to replace lines 41-45.
50-51	Precalculate $(A_{ro}^- + A_{\theta o}^-)\, k_x\, k_y$ and $C_{\phi o}^-\, k_z$ to facilitate computation of E_x and H_x.

Table 6-3. Fields of Elementary x-Directed and y-Directed Dipoles

$$\underline{E} = \underline{E}^e + \underline{E}^m$$

$$\underline{H} = \underline{H}^e + \underline{H}^m$$

$$E_x = e_o[J_x^e(\bar{A}_{r\theta}\, k_x^2 - \bar{A}_\theta) + J_y^e(k_x k_y\, \bar{A}_{r\theta})] - h_o\, j\pi\eta\, J_y^m\, k_z\, \bar{c}_\phi$$

$$E_y = e_o[J_x^e(k_x k_y\, \bar{A}_{r\theta}) + J_y^e(\bar{A}_{r\theta}\, k_y^2 - \bar{A}_\theta)] + h_o\, j\pi\eta\, J_x^m\, k_z\, \bar{c}_\phi$$

$$E_z = e_o[J_x^e(k_x k_z\, \bar{A}_{r\theta}) + J_y^e(k_y k_z\, \bar{A}_{r\theta})] + h_o\, j\pi\eta\, \bar{c}_\phi(-J_x^m\, k_y + J_y^m\, k_x)$$

$$H_x = e_o\, \frac{j\pi}{\eta}\, J_y^e\, k_z\, \bar{c}_\phi + h_o[J_x^m(\bar{A}_{r\theta}\, k_x^2 - \bar{A}_\theta) + J_y^m\, k_x k_y\, \bar{A}_{r\theta}]$$

$$H_y = -e_o\, \frac{j\pi}{\eta}\, J_x^e\, k_z\, \bar{c}_\phi + h_o[J_x^m(k_x k_y\, \bar{A}_{r\theta}) + J_y^m(\bar{A}_{r\theta}\, k_y^2 - \bar{A}_\theta)]$$

$$H_z = e_o\, \frac{j\pi}{\eta}\, \bar{c}_\phi(k_y\, J_x^e - k_x\, J_y^e) + h_o[J_x^m(k_x k_z\, \bar{A}_{r\theta}) + J_y^m(k_y k_z\, \bar{A}_{r\theta})]$$

Where: $e_o = \dfrac{(\frac{\Delta A}{\lambda^2})\eta}{j(2\pi)^2}$ $\qquad$ $h_o = \dfrac{(\frac{\Delta A}{\lambda^2})}{j(2\pi)^2\eta}$

52-53 Compute E_x and H_x due to the x-directed and y-directed electric and magnetic currents: J_x^e = JE(1), J_y^e = JE(2), J_x^m = JM(1), J_y^m = JM(2).

54 Precalculate $(\bar{A}_{ro} + \bar{A}_{\theta o})\, k_y^2 - \bar{A}_{\theta o}$.

55 See lines 46-49 above.

56-57 Compute E_y and H_y.

58-61 Precalculate common variables for E_z, H_z.

62-65 Compute E_z and H_z.

RETURN

67-69 Error message and halt.

END

6-6. Test Case

Selected test cases shown in Figure 2-15 of Reference 1 were executed. The square, 4" x 4", uniform aperture (λ= 1.18") was sampled at M=15, N=15 points in the x and y directions, respectively. Cases were done for $\underline{E}_{ap} = \hat{y}(1)$, $\underline{H}_{ap} = 0$, and for $\underline{E}_{ap} = \hat{y}(1)$, $\underline{H}_{ap} = -\hat{x}(1/\eta)$. In the latter case, the amplitudes obtained were twice as large (as expected). Although exact comparison to the graphical results in Figure 2-15 was not possible, agreement was obtained so far as could be determined. Some benchmarks as computed by Subroutine DIPOLES are shown in Tables 4 through 6.

6-7. References

1. C. H. Walter, Traveling Wave Antennas, McGraw-Hill, New York, 1965, Ch. 2.

2. S. Silver, Microwave Antenna Theory and Design, McGraw-Hill, New York, 1949, Ch. 3.

3. D. T. Paris and F. K. Hurd, Basic Electromagnetic Theory, McGraw-Hill, New York, 1969, Ch. 1.

6-8. Program Listing. See following pages.

```
      SUBROUTINE DIPOLES(JE,JM,PSWL,PFWL,DXWL,DYWL,E,H,INIT)                1
C *** MODIFIED 1-23-80 TO INCLUDE ONLY 1/R TERMS **** NULLIFIED 1-24-80**
C  SUBR DIPOLES COMPUTES THE RECTANGULAR COMPONENTS OF THE FIELDS E,H OF     3
C  ELECTRIC AND MAGNETIC DIPOLES LOCATED AT PSWL(X',Y',Z')                   4
C  AND ORIENTED IN THE X' AND Y' DIRECTIONS.  THE FIELDS ARE COMPUTED AT     5
C  THE POINT PFWL(X,Y,Z).  ALL DIMENSIONS ARE IN WAVELENGTHS.  MKS SYSTEM
C  IS USED.  FREE SPACE (ETA=377 OHMS) IS ASSUMED.                           7
      COMPLEX JE(2),JM(2),E(3),H(3),JAY,HO,EO,CPHS,JPI,JAY2PI               8
      COMPLEX ARO,ATO,CPO,ARTO,CT,ARTOK,CPOK,EOH,HOE                        9
      REAL PSWL(3),PFWL(3),KX,KY,KZ                                        10
      LOGICAL INIT                                                         11
C  DXWL,DYWL=X' AND Y' DIMENSIONS OF THE RECTANGULAR ELEMENT OVER WHICH     12
C            CURRENT DENSITIES JE AND JM FLOW TO MAKE THE DIPOLES.          13
      DATA TUPI/6.283185301/,ETA/376.9911185/                              14
      IF (INIT) GO TO 1                                                    15
      GO TO 2                                                              16
C  COMPUTE EO,HO (SEE DERIVATION DATED 7-23-79):                           17
    1 TUPI2=TUPI**2                                                        18
      JAY=(0.,1.)                                                          19
      EO=DXWL*DYWL*ETA/(JAY*TUPI2)                                         20
      HO=DXWL*DYWL/(JAY*TUPI2*ETA)                                         21
      JAY2PI=JAY*TUPI                                                      22
      JPI=JAY*TUPI/2.                                                      23
      HOE=-HO*ETA                                                          24
      EOH=EO/ETA                                                           25
      HO=HO*ETA                                                            26
      EOH=EOH*ETA                                                          27
C  THE ABOVE TWO LINES CAUSE ETA*H TO BE COMPUTED FOR USE IN RECI.          28
      INIT=.FALSE.                                                         29
    2 X=PFWL(1)-PSWL(1)                                                    30
      Y=PFWL(2)-PSWL(2)                                                    31
      Z=PFWL(3)-PSWL(3)                                                    32
      R=SQRT(X*X+Y*Y+Z*Z)                                                  33
      IF (R.LT..01) GO TO 90                                               34
      KX=X/R                                                               35
      KY=Y/R                                                               36
      KZ=Z/R                                                               37
      PHS=AMOD(TUPI*R,TUPI)                                                38
```

```
      CPHS=CMPLX(0.,-PHS)                                                39
      CPHS=CEXP(CPHS)                                                    40
      AR0=CPHS*(1./R**3+JAY2PI/R**2)                                     41
      AT0=.5*(AR0-CPHS*TUPI2/R)                                          42
      CP0=JPI*AR0*R                                                      43
      ART0=AR0+AT0                                                       44
      CT=AR0*KX**2-AT0*(1.-KX**2)                                        45
C     AT0=-.5*CPHS*TUPI2/R                                               46
C     CP0=JPI*CPHS*JAY2PI/R                                              47
C     ART0=AT0                                                           48
C     CT=-AT0*(1.-KX*KX)                                                 49
      ART0K=ART0*KX*KY                                                   50
      CP0K=CP0*KZ                                                        51
      E(1)=E0*(JE(1)*CT+JE(2)*ART0K)+JM(2)*H0E*CP0K                      52
      H(1)=H0*(JM(1)*CT+JM(2)*ART0K)+E0H*JE(2)*CP0K                      53
      CT=AR0*KY**2-AT0*(1.-KY**2)                                        54
C     CT=-AT0*(1.-KY*KY)                                                 55
      E(2)=E0*(JE(1)*ART0K+JE(2)*CT)-JM(1)*H0E*CP0K                      56
      H(2)=H0*(JM(1)*ART0K+JM(2)*CT)-JE(1)*E0H*CP0K                      57
      ART0K=ART0*KY*KZ                                                   58
      ART0=ART0*KX*KZ                                                    59
      CP0K=CP0*KY                                                        60
      CP0=CP0*KX                                                         61
      E(3)=E0*(JE(1)*ART0+JE(2)*ART0K)+H0E*(JM(1)*CP0K                   62
     $-JM(2)*CP0)                                                        63
      H(3)=H0*(JM(1)*ART0+JM(2)*ART0K)+E0H*(JE(1)*CP0K                   64
     $-JE(2)*CP0)                                                        65
      RETURN                                                             66
   90 WRITE(6,91)                                                        67
   91 FORMAT(" **** R.LT..01 WAVELENGTH IN SUBR DIPOLES--STOP****")      68
      STOP                                                               69
      END                                                                70
```

Table 6-4. Fields Computed by Subroutine DIPOLES Along z-Axis for 4" x 4" Uniform Aperture (λ=1.18").

```
1 TEST PROGRAM FOR USING ELEMENTARY SOURCES FOR COMPUTING FRESNEL FIELDS
 (REF:  WALTER(1965), PP.55-57)
 AIN= 4.00  BIN= 4.00  M,N=  15  15 LAMBDA= 1.180
 FIELD IS -10.0 DB AT Z= 24.00 INCHES
 APERTURE FIELDS:  TAP= (0.0000,0.0000)  (1.0000,0.0000)   HAP= (0.0000,0.0000)
 ERR,HRR=  .87422E+00  .23166E-02   IAX IS= 3  PFWL:   0.00   0.00   4.00
```

N	XYZIN	XYZWL	EX / HX AMPDB	EX / HX PHSDEG	EY / HY AMPDB	EY / HY PHSDEG	EZ / HZ AMPDB	EZ / HZ PHSDEG
1	4.00	3.39	-40.0	-180.0	-.1	-139.2	-40.0	177.4
			-.1	40.9	-40.0	-180.0	-40.0	-4.4
2	4.30	3.64	-40.0	-180.0	-.0	135.3	-40.0	92.5
			.0	-44.6	-40.0	-180.0	-40.0	-86.1
3	4.59	3.89	-40.0	-180.0	-.0	49.5	-40.0	10.1
			-.0	-130.4	-40.0	-180.0	-40.0	-168.7
4	4.89	4.14	-40.0	-180.0	-.1	-36.7	-40.0	-72.5
			-.1	143.4	-40.0	-180.0	-40.0	105.2
5	5.18	4.39	-40.0	-180.0	-.2	-123.1	-40.0	-157.1
			-.2	56.9	-40.0	-180.0	-40.0	19.5
6	5.48	4.64	-40.0	-180.0	-.3	150.1	-40.0	118.2
			-.3	-29.8	-40.0	-180.0	-40.0	-69.4
7	5.77	4.89	-40.0	-180.0	-.4	63.1	-40.0	30.8
			-.4	-110.8	-40.0	-180.0	-40.0	-154.4
8	6.07	5.14	-40.0	-180.0	-.6	-24.1	-40.0	-50.7
			-.6	156.0	-40.0	-180.0	-40.0	129.2
9	6.36	5.39	-40.0	-180.0	-.8	-111.5	-40.0	-138.0
			-.8	68.5	-40.0	-180.0	-40.0	38.1
10	6.66	5.64	-40.0	-180.0	-1.0	160.9	-40.0	136.4
			-1.0	-19.1	-40.0	-180.0	-40.0	-50.0
11	6.95	5.89	-40.0	-180.0	-1.2	73.1	-40.0	48.9
			-1.2	-106.9	-40.0	-180.0	-40.0	-139.9
12	7.25	6.14	-40.0	-180.0	-1.4	-14.8	-40.0	-39.3
			-1.4	165.2	-40.0	-180.0	-40.0	133.6
13	7.54	6.39	-40.0	-180.0	-1.6	-102.9	-40.0	-131.3

			(	-1.6	77.1	-40.0	-180.0	-40.0	53.6)
14	7.84	6.64		-40.0	-180.0	-1.6	168.9	-40.0	147.1
			(	-1.8	-11.1	-40.0	-180.0	-40.0	-32.2)
15	8.13	6.89		-40.0	-180.0	-2.0	80.6	-40.0	58.0
			(	-2.0	-99.4	-40.0	-180.0	-40.0	-121.4)
16	8.43	7.14		-40.0	-180.0	-2.2	-7.8	-40.0	-25.3
			(	-2.2	172.2	-40.0	-180.0	-40.0	149.3)
17	8.72	7.39		-40.0	-180.0	-2.4	-96.3	-40.0	-113.5
			(	-2.4	83.7	-40.0	-180.0	-40.0	59.3)
18	9.02	7.64		-40.0	-180.0	-2.6	175.1	-40.0	159.8
			(	-2.6	-4.9	-40.0	-180.0	-40.0	-26.4)
19	9.31	7.89		-40.0	-180.0	-2.8	86.4	-40.0	70.0
			(	-2.8	-93.6	-40.0	-180.0	-40.0	-108.5)
20	9.61	8.14		-40.0	-180.0	-3.0	-2.4	-40.0	-16.4
			(	-3.0	177.7	-40.0	-180.0	-40.0	161.1)
21	9.90	8.39		-40.0	-180.0	-3.2	-91.2	-40.0	-105.2
			(	-3.2	88.9	-40.0	-180.0	-40.0	71.3)
22	10.20	8.64		-40.0	-180.0	-3.4	179.9	-40.0	164.6
			(	-3.4	-.0	-40.0	-180.0	-40.0	-18.9)
23	10.49	8.89		-40.0	-180.0	-3.6	91.0	-40.0	71.1
			(	-3.6	-89.0	-40.0	-180.0	-40.0	-106.5)
24	10.79	9.14		-40.0	-180.0	-3.8	2.0	-40.0	-17.4
			(	-3.8	-178.0	-40.0	-180.0	-40.0	166.8)
25	11.08	9.39		-40.0	-180.0	-4.0	-87.0	-40.0	-104.3
			(	-4.0	93.0	-40.0	-180.0	-40.0	76.7)
26	11.38	9.64		-40.0	-180.0	-4.1	-176.1	-40.0	168.8
			(	-4.1	3.9	-40.0	-180.0	-40.0	-13.8)
27	11.67	9.89		-40.0	-180.0	-4.3	94.8	-40.0	76.7
			(	-4.3	-85.2	-40.0	-180.0	-40.0	-104.2)
28	11.97	10.14		-40.0	-180.0	-4.5	5.6	-40.0	-8.1
			(	-4.5	-174.4	-40.0	-180.0	-40.0	168.6)
29	12.26	10.39		-40.0	-180.0	-4.7	-83.6	-40.0	-97.5
			(	-4.7	96.4	-40.0	-180.0	-40.0	80.5)
30	12.56	10.64		-40.0	-180.0	-4.9	-172.9	-40.0	172.5
			(	-4.9	7.1	-40.0	-180.0	-40.0	-7.5)
31	12.85	10.89		-40.0	-180.0	-5.0	97.8	-40.0	84.9
			(	-5.0	-82.1	-40.0	-180.0	-40.0	-96.9)
32	13.15	11.14		-40.0	-180.0	-5.2	8.5	-40.0	-5.4

		(	-5.2	-171.5	-40.0	-180.0	-40.0	174.2)
33	13.44	11.39	-40.0	-180.0	-5.4	-60.8	-40.0	-91.0
		(	-5.4	99.2	-40.0	-180.0	-40.0	84.9)
34	13.74	11.64	-40.0	-180.0	-5.5	-170.2	-40.0	177.5
		(	-5.5	9.6	-40.0	-180.0	-40.0	-3.3)
35	14.03	11.89	-40.0	-180.0	-5.7	100.4	-40.0	89.5
		(	-5.7	-79.5	-40.0	-180.0	-40.0	-90.0)
36	14.33	12.14	-40.0	-180.0	-5.9	11.0	-40.0	-.6
		(	-5.9	-169.0	-40.0	-180.0	-40.0	176.0)
37	14.62	12.39	-40.0	-180.0	-6.0	-78.4	-40.0	-89.0
		(	-6.0	101.6	-40.0	-180.0	-40.0	90.0)
38	14.92	12.64	-40.0	-180.0	-6.2	-167.9	-40.0	-179.1
		(	-6.2	12.1	-40.0	-180.0	-40.0	-.2)
39	15.21	12.89	-40.0	-180.0	-6.3	102.7	-40.0	91.2
		(	-6.3	-77.3	-40.0	-180.0	-40.0	-90.0)
40	15.51	13.14	-40.0	-180.0	-6.5	13.2	-40.0	4.6
		(	-6.5	-166.8	-40.0	-180.0	-40.0	-179.1)
41	15.80	13.39	-40.0	-180.0	-6.6	-76.4	-40.0	-85.1
		(	-6.6	103.6	-40.0	-180.0	-40.0	90.0)
42	16.10	13.64	-40.0	-180.0	-6.8	-165.9	-40.0	-176.0
		(	-6.8	14.1	-40.0	-180.0	-40.0	2.1)
43	16.39	13.89	-40.0	-180.0	-6.9	104.6	-40.0	93.6
		(	-6.9	-75.4	-40.0	-180.0	-40.0	-90.0)
44	16.69	14.14	-40.0	-180.0	-7.0	15.0	-40.0	5.1
		(	-7.0	-165.0	-40.0	-180.0	-40.0	-175.9)
45	16.98	14.39	-40.0	-180.0	-7.2	-74.6	-40.0	-85.2
		(	-7.2	105.4	-40.0	-180.0	-40.0	90.0)
46	17.28	14.64	-40.0	-180.0	-7.3	-164.2	-40.0	-175.9
		(	-7.3	15.8	-40.0	-180.0	-40.0	6.1)
47	17.57	14.89	-40.0	-180.0	-7.5	106.2	-40.0	97.7
		(	-7.5	-73.8	-40.0	-180.0	-40.0	-83.4)
48	17.87	15.14	-40.0	-180.0	-7.6	16.6	-40.0	8.8
		(	-7.6	-163.4	-40.0	-180.0	-40.0	-172.6)
49	18.16	15.39	-40.0	-180.0	-7.7	-73.0	-40.0	-83.3
		(	-7.7	107.0	-40.0	-180.0	-40.0	97.1)
50	18.46	15.64	-40.0	-180.0	-7.8	-162.7	-40.0	-173.7
		(	-7.8	17.3	-40.0	-180.0	-40.0	7.6)
51	18.75	15.89	-40.0	-180.0	-8.0	107.7	-40.0	95.7

		(	-8.0	-72.3	-40.0	-180.0	-40.0	-82.0)
52	19.05	16.14	-40.0	-180.0	-8.1	18.0	-40.0	8.2
		(	-8.1	-162.0	-40.0	-180.0	-40.0	-171.5)
53	19.34	16.39	-40.0	-180.0	-8.2	-71.7	-40.0	-82.9
		(	-8.2	108.3	-40.0	-180.0	-40.0	98.8)
54	19.64	16.64	-40.0	-180.0	-8.3	-161.4	-40.0	-172.2
		(	-8.3	18.6	-40.0	-180.0	-40.0	9.1)
55	19.93	16.89	-40.0	-180.0	-8.5	108.9	-40.0	99.2
		(	-8.5	-71.3	-40.0	-180.0	-40.0	-80.6)
56	20.23	17.14	-40.0	-180.0	-8.6	19.2	-40.0	11.9
		(	-8.6	-160.8	-40.0	-180.0	-40.0	-170.3)
57	20.52	17.39	-40.0	-180.0	-8.7	-70.5	-40.0	-80.6
		(	-8.7	109.5	-40.0	-180.0	-40.0	100.7)
58	20.82	17.64	-40.0	-180.0	-8.8	-160.2	-40.0	-168.4
		(	-8.8	19.8	-40.0	-180.0	-40.0	11.1)
59	21.11	17.89	-40.0	-180.0	-8.9	110.1	-40.0	103.8
		(	-8.9	-69.9	-40.0	-180.0	-40.0	-78.6)
60	21.41	18.14	-40.0	-180.0	-9.1	20.4	-40.0	17.4
		(	-9.1	-159.6	-40.0	-180.0	-40.0	-168.5)
61	21.70	18.39	-40.0	-180.0	-9.2	-69.4	-40.0	-74.7
		(	-9.2	110.6	-40.0	-180.0	-40.0	102.0)
62	22.00	18.64	-40.0	-180.0	-9.3	-159.1	-40.0	-164.2
		(	-9.3	20.9	-40.0	-180.0	-40.0	12.5)
63	22.29	18.89	-40.0	-180.0	-9.4	111.1	-40.0	108.5
		(	-9.4	-68.9	-40.0	-180.0	-40.0	-77.1)
64	22.59	19.14	-40.0	-180.0	-9.5	21.4	-40.0	15.4
		(	-9.5	-158.6	-40.0	-180.0	-40.0	-166.2)
65	22.88	19.39	-40.0	-180.0	-9.6	-68.4	-40.0	-72.6
		(	-9.6	111.6	-40.0	-180.0	-40.0	104.3)
66	23.18	19.64	-40.0	-180.0	-9.7	-158.2	-40.0	-164.6
		(	-9.7	21.8	-40.0	-180.0	-40.0	16.4)
67	23.47	19.89	-40.0	-180.0	-9.8	112.0	-40.0	104.9
		(	-9.8	-68.0	-40.0	-180.0	-40.0	-72.9)
68	23.77	20.14	-40.0	-180.0	-9.9	22.3	-40.0	14.9
		(	-9.9	-157.7	-40.0	-180.0	-40.0	-162.5)

Table 6-5. Fields Computed by Subroutine DIPOLES Along x-Axis at z=8 inches.

```
1 TEST PROGRAM FOR USING ELEMENTARY SOURCES FOR COMPUTING FRESNEL FIELDS
 (REF:  WALTER(1965), PP.55-57)
 AIN= 4.00  BIN= 4.00  M,N=  15  15 LAMBDA= 1.180
 FIELD IS -10.0 DB AT Z= 24.00 INCHES
 APERTURE FIELDS:  SAP= (0.0000,0.0000)  (1.0000,0.0000)   HAP= (0.0000,0.0000)
 ERR,HRR=  .87422E+00  .23188E-02   IAXIS= 1  PFWL0:   0.00   0.00   8.00
```

N	XYZIN	XYZWL	EX (HX) AMPDB	EX (HX) PHSDEG	EY (HY) AMPDB	EY (HY) PHSDEG	EZ (HZ) AMPDB	EZ (HZ) PHSDEG
1	0.00	0.00	-40.0	-180.0	-1.9	119.5	-40.0	96.3
			-1.9	-60.4	-40.0	-180.0	-40.0	-83.6
2	.30	.25	-40.0	-180.0	-2.1	118.5	-40.0	96.4
			-2.1	-61.4	-40.0	-180.0	-30.8	65.7
3	.59	.50	-40.0	-180.0	-2.7	115.5	-40.0	91.9
			-2.7	-64.2	-40.0	-180.0	-25.4	61.6
4	.89	.75	-40.0	-180.0	-3.7	110.9	-40.0	87.9
			-3.7	-68.6	-40.0	-180.0	-23.0	54.7
5	1.18	1.00	-40.0	-180.0	-5.2	104.9	-40.0	86.2
			-5.1	-74.2	-40.0	-180.0	-22.2	45.1
6	1.48	1.25	-40.0	-180.0	-7.0	98.5	-40.0	77.5
			-6.9	-80.2	-40.0	-180.0	-22.6	33.2
7	1.77	1.50	-40.0	-180.0	-9.2	93.0	-40.0	67.2
			-9.0	-85.4	-40.0	-180.0	-24.3	19.3
8	2.07	1.75	-40.0	-180.0	-11.5	90.2	-40.0	71.7
			-11.2	-88.6	-40.0	-180.0	-27.7	5.0
9	2.36	2.00	-40.0	-180.0	-13.2	90.0	-40.0	76.9
			-12.8	-89.9	-40.0	-180.0	-34.6	-.6
10	2.66	2.25	-40.0	-180.0	-13.8	68.1	-40.0	60.3
			-13.5	-93.1	-40.0	-180.0	-38.7	80.6
11	2.95	2.50	-40.0	-180.0	-13.6	79.9	-40.0	56.7
			-13.6	-102.7	-40.0	-180.0	-30.1	86.2
12	3.25	2.75	-40.0	-180.0	-13.4	61.8	-40.0	39.5
			-13.6	-119.3	-40.0	-180.0	-26.3	63.4
13	3.54	3.00	-40.0	-180.0	-13.5	38.5	-40.0	5.5

			(	-13.9	-141.7	-40.0	-180.0	-24.4	34.6)
14	3.84	3.25		-40.0	-180.0	-14.0	10.8	-40.0	7.1
			(	-14.5	-168.5	-40.0	-180.0	-23.5	2.3)
15	4.13	3.50		-40.0	-180.0	-14.8	-20.3	-40.0	-31.6
			(	-15.5	161.5	-40.0	-180.0	-23.5	-32.6)
16	4.43	3.75		-40.0	-180.0	-16.1	-53.9	-40.0	-67.6
			(	-16.8	129.0	-40.0	-180.0	-24.1	-69.6)
17	4.72	4.00		-40.0	-180.0	-17.8	-89.1	-40.0	-109.1
			(	-18.4	95.1	-40.0	-180.0	-25.3	-108.2)
18	5.02	4.25		-40.0	-180.0	-19.9	-124.9	-40.0	-136.0
			(	-20.4	60.6	-40.0	-180.0	-27.2	-147.7)
19	5.31	4.50		-40.0	-180.0	-22.3	-159.5	-40.0	-159.9
			(	-22.6	26.8	-40.0	-180.0	-29.9	173.4)
20	5.61	4.75		-40.0	-180.0	-24.9	169.5	-40.0	165.1
			(	-24.8	-4.7	-40.0	-180.0	-33.7	139.6)
21	5.90	5.00		-40.0	-180.0	-26.9	144.1	-40.0	139.6
			(	-26.5	-33.7	-40.0	-180.0	-38.0	123.9)
22	6.20	5.25		-40.0	-180.0	-27.3	119.3	-40.0	64.5
			(	-27.2	-63.3	-40.0	-180.0	-37.5	124.2)
23	6.49	5.50		-40.0	-180.0	-26.5	87.0	-40.0	56.1
			(	-27.1	-97.9	-40.0	-180.0	-34.1	97.5)
24	6.79	5.75		-40.0	-180.0	-25.5	45.7	-40.0	15.1
			(	-26.7	-139.0	-40.0	-180.0	-31.4	53.8)
25	7.08	6.00		-40.0	-180.0	-24.6	-1.9	-40.0	-8.7
			(	-26.3	174.4	-40.0	-180.0	-29.7	3.3)
26	7.38	6.25		-40.0	-180.0	-24.1	-53.8	-40.0	-70.2
			(	-26.0	123.7	-40.0	-180.0	-28.6	-50.9)
27	7.67	6.50		-40.0	-180.0	-23.8	-108.7	-40.0	-128.1
			(	-26.0	69.9	-40.0	-180.0	-27.9	-107.6)
28	7.97	6.75		-40.0	-180.0	-23.7	-166.1	-40.0	-167.4
			(	-26.1	13.6	-40.0	-180.0	-27.5	-166.2)
29	8.26	7.00		-40.0	-180.0	-23.8	134.6	-40.0	148.5
			(	-26.4	-44.7	-40.0	-180.0	-27.3	133.5)
30	8.56	7.25		-40.0	-180.0	-24.1	73.7	-40.0	63.8
			(	-26.8	-104.8	-40.0	-180.0	-27.3	71.8)
31	8.85	7.50		-40.0	-180.0	-24.4	11.3	-40.0	-6.3
			(	-27.4	-166.3	-40.0	-180.0	-27.5	8.8)
32	9.15	7.75		-40.0	-180.0	-24.9	-52.4	-40.0	-76.2

			(	-28.0	130.8	-40.0	-165.0	-27.8	-55.4)
33	9.44	8.00		-40.0	-160.0	-25.5	-117.2	-40.0	-134.1
			(	-28.7	66.7	-40.0	-180.0	-28.2	-120.7)
34	9.74	8.25		-40.0	-180.0	-26.1	176.9	-40.0	172.9
			(	-29.5	1.5	-40.0	-180.0	-28.7	173.0)

77
78
79
80
81

Table 6-6. Fields Computed by Subroutine DIPOLES Along x-Axis at z=24 inches.

```
1 TEST PROGRAM FOR USING ELEMENTARY SOURCES FOR COMPUTING FRESNEL FIELDS
 (REF:  WALTER(1965), PP.55-57)
 AIN= 4.00  BIN= 4.00  M,N=  15  15 LAMBDA= 1.180
 FIELD IS -10.0 DB AT Z= 24.00 INCHES
 APERTURE FIELDS:  EAP= (0.0000,0.0000)  (1.0000,0.0000)   HAP= (0.0000,0.0000)
 ERO,HRO=  .87422E+01  .23188E-02   IAX IS= 1  PFWL0:   0.00   0.00  24.00
```

N	XYZIN	XYZWL	EX (HX) AMPDB	EX (HX) PHSDEG	EY HY AMPDB	EY HY PHSDEG	EZ HZ AMPDB	EZ HZ PHSDEG
1	0.00	0.00	-40.0	-180.0	-10.0	-49.3	-40.0	-56.7
			-10.0	130.7	-40.0	-180.0	-40.0	124.4
2	.30	.25	-40.0	-180.0	-10.0	-49.8	-40.0	-60.2
			-10.0	130.2	-40.0	-180.0	-40.0	-67.5
3	.59	.50	-40.0	-180.0	-10.1	-51.4	-40.0	-59.6
			-10.1	128.6	-40.0	-180.0	-40.0	-69.2
4	.89	.75	-40.0	-180.0	-10.2	-54.0	-40.0	-66.6
			-10.2	126.0	-40.0	-180.0	-38.9	-71.9
5	1.18	1.00	-40.0	-180.0	-10.4	-57.7	-40.0	-65.8
			-10.4	122.4	-40.0	-180.0	-36.6	-75.7
6	1.48	1.25	-40.0	-180.0	-10.6	-62.4	-40.0	-71.8
			-10.7	117.7	-40.0	-180.0	-34.9	-80.5
7	1.77	1.50	-40.0	-180.0	-10.9	-68.2	-40.0	-73.8
			-11.0	111.9	-40.0	-180.0	-33.6	-86.5
8	2.07	1.75	-40.0	-180.0	-11.3	-75.0	-40.0	-80.8
			-11.3	105.2	-40.0	-180.0	-32.6	-93.5
9	2.36	2.00	-40.0	-180.0	-11.7	-82.8	-40.0	-90.0
			-11.7	97.4	-40.0	-180.0	-31.9	-101.6
10	2.66	2.25	-40.0	-180.0	-12.1	-91.6	-40.0	-99.4
			-12.2	88.6	-40.0	-180.0	-31.3	-110.8
11	2.95	2.50	-40.0	-180.0	-12.7	-101.4	-40.0	-109.9
			-12.7	78.9	-40.0	-180.0	-31.0	-121.0
12	3.25	2.75	-40.0	-180.0	-13.2	-112.2	-40.0	-123.0
			-13.3	68.1	-40.0	-180.0	-30.7	-132.2
13	3.54	3.00	-40.0	-180.0	-13.9	-124.0	-40.0	-133.5

			(	-14.3	56.4	-40.0	-180.0	-33.7	-144.6)
14	3.84	3.25		-40.0	-180.0	-14.6	-136.7	-40.0	-145.6
			(	-14.7	43.8	-40.0	-180.0	-30.7	-157.9)
15	4.13	3.50		-40.0	-180.0	-15.5	-150.2	-40.0	-158.0
			(	-15.6	30.4	-40.0	-180.0	-31.3	-172.3)
16	4.43	3.75		-40.0	-180.0	-16.4	-164.7	-40.0	-171.0
			(	-16.5	16.1	-40.0	-180.0	-31.3	172.3)
17	4.72	4.00		-40.0	-180.0	-17.4	-179.9	-40.0	165.3
			(	-17.5	1.0	-40.0	-180.0	-31.8	155.9)
18	5.02	4.25		-40.0	-180.0	-18.5	164.3	-40.0	167.9
			(	-18.6	-14.7	-40.0	-180.0	-32.5	138.6)
19	5.31	4.50		-40.0	-180.0	-19.7	147.8	-40.0	139.4
			(	-19.9	-31.0	-40.0	-180.0	-33.3	120.3)
20	5.61	4.75		-40.0	-180.0	-21.1	131.1	-40.0	134.8
			(	-21.3	-47.5	-40.0	-180.0	-34.4	101.1)
21	5.90	5.00		-40.0	-180.0	-22.7	114.2	-40.0	101.9
			(	-22.8	-64.1	-40.0	-180.0	-35.8	81.0)
22	6.20	5.25		-40.0	-180.0	-24.4	97.9	-40.0	97.9
			(	-24.5	-80.2	-40.0	-180.0	-37.5	60.3)
23	6.49	5.50		-40.0	-180.0	-26.4	82.9	-40.0	81.7
			(	-26.4	-94.9	-40.0	-180.0	-39.8	39.2)
24	6.79	5.75		-40.0	-180.0	-28.4	70.6	-40.0	80.5
			(	-28.3	-107.2	-40.0	-180.0	-40.0	18.5)
25	7.08	6.00		-40.0	-180.0	-30.3	62.5	-40.0	57.1
			(	-30.1	-115.9	-40.0	-180.0	-40.0	1.4)
26	7.38	6.25		-40.0	-180.0	-31.4	58.4	-40.0	57.5
			(	-31.1	-121.5	-40.0	-180.0	-40.0	18.2)
27	7.67	6.50		-40.0	-180.0	-31.2	53.4	-40.0	90.0
			(	-31.0	-127.9	-40.0	-180.0	-40.0	86.2)
28	7.97	6.75		-40.0	-180.0	-30.2	42.8	-40.0	17.7
			(	-30.2	-139.2	-40.0	-180.0	-40.0	72.6)
29	8.26	7.00		-40.0	-180.0	-28.9	26.0	-40.0	1.7
			(	-29.1	-156.0	-40.0	-180.0	-40.0	48.4)
30	8.56	7.25		-40.0	-180.0	-27.6	4.5	-40.0	5.1
			(	-28.1	-177.3	-40.0	-180.0	-39.2	21.0)
31	8.85	7.50		-40.0	-180.0	-26.6	-20.2	-40.0	-33.3
			(	-27.2	158.3	-40.0	-180.0	-37.4	-8.1)
32	9.15	7.75		-40.0	-180.0	-26.1	-47.4	-40.0	-60.1

			(	-26.5	131.3	-40.0	-180.0	-36.0	-38.5)	77
33	9.44	8.00		-40.0	-180.0	-25.5	-76.5	-40.0	-68.6	78
			(	-26.0	102.5	-40.0	-180.0	-35.0	-70.0)	79
34	9.74	8.25		-40.0	-180.0	-25.0	-107.1	-40.0	-118.6	80
			(	-25.6	72.1	-40.0	-180.0	-34.2	-102.5)	81
35	10.03	8.50		-40.0	-180.0	-24.7	-139.1	-40.0	-139.0	82
			(	-25.3	40.4	-40.0	-180.0	-33.5	-136.1)	83
36	10.33	8.75		-40.0	-180.0	-24.5	-172.2	-40.0	-169.9	84
			(	-25.2	7.4	-40.0	-180.0	-33.0	-170.5)	85
37	10.62	9.00		-40.0	-180.0	-24.4	153.5	-40.0	150.8	86
			(	-25.1	-26.6	-40.0	-180.0	-32.7	154.2)	87
38	10.92	9.25		-40.0	-180.0	-24.4	118.3	-40.0	106.3	88
			(	-25.2	-61.7	-40.0	-180.0	-32.4	118.0)	89
39	11.21	9.50		-40.0	-180.0	-24.5	82.0	-40.0	82.3	90
			(	-25.3	-97.8	-40.0	-180.0	-32.2	81.0)	91
40	11.51	9.75		-40.0	-180.0	-24.6	44.9	-40.0	46.7	92
			(	-25.4	-134.8	-40.0	-180.0	-32.2	43.1)	93
41	11.80	10.00		-40.0	-180.0	-24.8	6.9	-40.0	-17.0	94
			(	-25.7	-172.6	-40.0	-180.0	-32.2	4.4)	95
42	12.10	10.25		-40.0	-180.0	-25.1	-32.0	-40.0	-40.3	96
			(	-26.0	148.7	-40.0	-180.0	-32.3	-35.1)	97
43	12.39	10.50		-40.0	-180.0	-25.4	-71.7	-40.0	-93.6	98
			(	-26.4	109.2	-40.0	-180.0	-32.4	-75.3)	99
44	12.69	10.75		-40.0	-180.0	-25.9	-112.2	-40.0	-121.7	100
			(	-26.9	68.9	-40.0	-180.0	-32.7	-116.3)	101
45	12.98	11.00		-40.0	-180.0	-26.3	-153.4	-40.0	-171.9	102
			(	-27.4	27.8	-40.0	-180.0	-33.0	-159.1)	103
46	13.28	11.25		-40.0	-180.0	-26.9	164.6	-40.0	153.1	104
			(	-28.0	-13.9	-40.0	-180.0	-33.4	159.4)	105
47	13.57	11.50		-40.0	-180.0	-27.5	121.9	-40.0	96.3	106
			(	-28.6	-56.4	-40.0	-180.0	-33.9	116.2)	107
48	13.87	11.75		-40.0	-180.0	-28.2	78.6	-40.0	48.4	108
			(	-29.3	-99.5	-40.0	-180.0	-34.4	72.4)	109
49	14.16	12.00		-40.0	-180.0	-28.9	34.6	-40.0	7.6	110
			(	-30.1	-143.2	-40.0	-180.0	-35.0	27.8)	111
50	14.46	12.25		-40.0	-180.0	-29.8	-9.9	-40.0	-31.7	112
			(	-31.0	172.8	-40.0	-180.0	-35.8	-17.4)	113
51	14.75	12.50		-40.0	-180.0	-30.7	-55.9	-40.0	-68.1	114

(-32.0 127.9 -40.[illegible] -180.[illegible] -36.6 -63.1)

Table 6-7. Fields Computed by Subroutine DIPOLES Along x-Axis at z=48 inches.

```
1 TEST PROGRAM FOR USING ELEMENTARY SOURCES FOR COMPUTING FRESNEL FIELDS
 (REF: WALTER(1965), PP.55-57)
 AIN= 4.00  BIN= 4.00 M,N=  15  15 LAMBDA= 1.180
 FIELD IS -10.0 DB AT Z= 24.00 INCHES
 APERTURE FIELDS: EAP= (0.0000,0.0000)  (1.0000,0.0000)   HAP= (0.0000,0.0000)
 ERO,HRO=  .87422E+00  .23188E-02   IAXIS= 1  PFWLO:   0.00   0.00  48.00
```

N	XYZIN	XYZWL	EX (HX	AMPDB	PHSDEG	EY HY	AMPDB	PHSDEG	EZ HZ)	AMPDB	PHSDEG
1	0.00	0.00		-40.0	-180.0		-15.9	-162.7		-40.0	-166.1
			(	-15.9	17.3		-40.0	-180.0		-40.0	15.6)
2	.30	.25		-40.0	-180.0		-15.9	-163.0		-40.0	-166.5
			(	-15.9	17.0		-40.0	-180.0		-40.0	-171.9)
3	.59	.50		-40.0	-180.0		-15.9	-163.8		-40.0	-167.5
			(	-15.9	16.2		-40.0	-180.0		-40.0	-172.7)
4	.89	.75		-40.0	-180.0		-15.9	-165.2		-40.0	-170.0
			(	-15.9	14.8		-40.0	-180.0		-40.0	-174.1)
5	1.18	1.00		-40.0	-180.0		-16.0	-167.1		-40.0	-171.7
			(	-16.0	12.9		-40.0	-180.0		-40.0	-176.0)
6	1.48	1.25		-40.0	-180.0		-16.0	-169.5		-40.0	-172.8
			(	-16.0	10.5		-40.0	-180.0		-40.0	-178.5)
7	1.77	1.50		-40.0	-180.0		-16.1	-172.6		-40.0	-175.1
			(	-16.1	7.5		-40.0	-180.0		-40.0	178.5)
8	2.07	1.75		-40.0	-180.0		-16.2	-176.1		-40.0	178.5
			(	-16.2	3.9		-40.0	-180.0		-40.0	174.9)
9	2.36	2.00		-40.0	-180.0		-16.3	179.8		-40.0	175.9
			(	-16.3	-.2		-40.0	-180.0		-40.0	170.8)
10	2.66	2.25		-40.0	-180.0		-16.4	175.2		-40.0	171.3
			(	-16.4	-4.8		-40.0	-180.0		-40.0	166.1)
11	2.95	2.50		-40.0	-180.0		-16.5	170.6		-40.0	166.1
			(	-16.5	-10.6		-40.0	-180.0		-40.0	160.9)
12	3.25	2.75		-40.0	-180.0		-16.7	164.3		-40.0	159.8
			(	-16.7	-15.7		-40.0	-180.0		-40.0	155.1)
13	3.54	3.00		-40.0	-180.0		-16.8	158.0		-40.0	156.7

			(	-16.8	-21.9	-40.0	-180.0	-39.5	148.8)
14	3.84	3.25		-40.0	-180.0	-17.0	151.2	-40.0	148.6
			(	-17.0	-28.7	-40.0	-180.0	-39.0	142.0)
15	4.13	3.50		-40.0	-180.0	-17.2	143.9	-40.0	139.6
			(	-17.2	-36.1	-40.0	-180.0	-38.5	134.6)
16	4.43	3.75		-40.0	-180.0	-17.4	136.0	-40.0	130.9
			(	-17.4	-43.9	-40.0	-180.0	-38.1	126.6)
17	4.72	4.00		-40.0	-180.0	-17.6	127.6	-40.0	120.4
			(	-17.6	-52.3	-40.0	-180.0	-37.6	118.1)
18	5.02	4.25		-40.0	-180.0	-17.8	118.6	-40.0	112.4
			(	-17.9	-61.3	-40.0	-180.0	-37.5	109.1)
19	5.31	4.50		-40.0	-180.0	-18.1	109.1	-40.0	105.2
			(	-18.1	-70.8	-40.0	-180.0	-37.2	99.5)
20	5.61	4.75		-40.0	-180.0	-18.3	99.1	-40.0	97.2
			(	-18.4	-80.8	-40.0	-180.0	-37.0	89.4)
21	5.90	5.00		-40.0	-180.0	-18.6	88.6	-40.0	86.5
			(	-18.6	-91.3	-40.0	-180.0	-36.9	78.8)
22	6.20	5.25		-40.0	-180.0	-18.9	77.5	-40.0	76.7
			(	-18.9	-102.3	-40.0	-180.0	-36.7	67.6)
23	6.49	5.50		-40.0	-180.0	-19.2	65.9	-40.0	63.3
			(	-19.3	-113.9	-40.0	-180.0	-36.7	55.9)
24	6.79	5.75		-40.0	-180.0	-19.5	53.8	-40.0	51.6
			(	-19.6	-126.0	-40.0	-180.0	-36.6	43.6)
25	7.08	6.00		-40.0	-180.0	-19.9	41.1	-40.0	37.7
			(	-19.9	-138.7	-40.0	-180.0	-36.6	30.8)
26	7.38	6.25		-40.0	-180.0	-20.2	28.0	-40.0	22.5
			(	-20.3	-151.8	-40.0	-180.0	-36.6	17.5)
27	7.67	6.50		-40.0	-180.0	-20.6	14.3	-40.0	9.4
			(	-20.7	-165.4	-40.0	-180.0	-36.7	3.6)
28	7.97	6.75		-40.0	-180.0	-21.0	.1	-40.0	1.1
			(	-21.1	-179.6	-40.0	-180.0	-36.8	-10.7)
29	8.26	7.00		-40.0	-180.0	-21.5	-14.6	-40.0	-20.0
			(	-21.6	165.7	-40.0	-180.0	-36.9	-25.7)
30	8.56	7.25		-40.0	-180.0	-21.9	-29.8	-40.0	-31.4
			(	-22.0	150.6	-40.0	-180.0	-37.0	-41.1)
31	8.85	7.50		-40.0	-180.0	-22.4	-45.5	-40.0	-42.8
			(	-22.5	134.9	-40.0	-180.0	-37.2	-57.0)
32	9.15	7.75		-40.0	-180.0	-22.9	-61.6	-40.0	-60.4

			(	-23.0	118.8	-40.0	-180.0	-37.5	-73.5)	77
33	9.44	8.00		-40.0	-180.0	-23.4	-78.3	-40.0	-79.6	78
			(	-23.6	102.2	-40.0	-180.0	-37.8	-90.5)	79
34	9.74	8.25		-40.0	-180.0	-24.0	-95.4	-40.0	-98.8	80
			(	-24.2	85.1	-40.0	-180.0	-38.1	-108.0)	81
35	10.03	8.50		-40.0	-180.0	-24.6	-113.0	-40.0	-118.0	82
			(	-24.8	67.5	-40.0	-180.0	-38.5	-126.0)	83
36	10.33	8.75		-40.0	-180.0	-25.3	-131.1	-40.0	-130.3	84
			(	-25.4	49.6	-40.0	-180.0	-38.9	-144.5)	85
37	10.62	9.00		-40.0	-180.0	-25.9	-149.5	-40.0	-157.9	86
			(	-26.1	31.1	-40.0	-180.0	-39.3	-163.5)	87
38	10.92	9.25		-40.0	-180.0	-26.7	-168.4	-40.0	-173.3	88
			(	-26.9	12.3	-40.0	-180.0	-39.8	176.9)	89
39	11.21	9.50		-40.0	-180.0	-27.5	172.3	-40.0	158.1	90
			(	-27.7	-6.9	-40.0	-180.0	-40.0	156.9)	91
40	11.51	9.75		-40.0	-180.0	-28.3	152.6	-40.0	145.7	92
			(	-28.5	-26.5	-40.0	-180.0	-40.0	136.4)	93
41	11.80	10.00		-40.0	-180.0	-29.2	132.7	-40.0	123.4	94
			(	-29.4	-46.4	-40.0	-180.0	-40.0	115.5)	95
42	12.10	10.25		-40.0	-180.0	-30.2	112.4	-40.0	119.5	96
			(	-30.4	-66.5	-40.0	-180.0	-40.0	94.0)	97
43	12.39	10.50		-40.0	-180.0	-31.3	92.0	-40.0	90.0	98
			(	-31.5	-86.7	-40.0	-180.0	-40.0	72.1)	99
44	12.69	10.75		-40.0	-180.0	-32.4	71.6	-40.0	63.8	100
			(	-32.6	-107.0	-40.0	-180.0	-40.0	49.8)	101
45	12.98	11.00		-40.0	-180.0	-33.7	51.2	-40.0	37.3	102
			(	-33.9	-127.2	-40.0	-180.0	-40.0	27.1)	103
46	13.28	11.25		-40.0	-180.0	-35.2	31.3	-40.0	9.5	104
			(	-35.4	-146.9	-40.0	-180.0	-40.0	4.1)	105
47	13.57	11.50		-40.0	-180.0	-36.6	12.3	-40.0	4.1	106
			(	-36.9	-165.7	-40.0	-180.0	-40.0	-19.1)	107
48	13.87	11.75		-40.0	-180.0	-38.6	-5.1	-40.0	-8.2	108
			(	-38.6	177.1	-40.0	-180.0	-40.0	-42.2)	109
49	14.16	12.00		-40.0	-180.0	-40.0	-19.5	-40.0	-3.5	110
			(	-40.0	162.7	-40.0	-180.0	-40.0	-64.5)	111
50	14.46	12.25		-40.0	-180.0	-40.0	-29.5	-40.0	-180.0	112
			(	-40.0	152.2	-40.0	-180.0	-40.0	-93.1)	113
51	14.75	12.50		-40.0	-180.0	-40.0	-34.7	-40.0	-90.0	114

		(	-40.1	142.6	-40.0	-180.0	-40.0	-72.8)	115
52	15.05	12.75	-40.0	-180.0	-40.0	-39.3	-40.0	-47.8	116
		(	-40.0	139.5	-40.0	-180.0	-40.0	-.2)	117
53	15.34	13.00	-40.0	-180.0	-40.0	-48.6	-40.0	-37.9	118
		(	-40.0	129.4	-40.0	-180.0	-40.0	-11.8)	119
54	15.64	13.25	-40.0	-180.0	-40.0	-63.7	-40.0	-180.0	120
		(	-40.0	114.1	-40.0	-180.0	-40.0	-34.8)	121
55	15.93	13.50	-40.0	-180.0	-39.0	-83.3	-40.0	-90.0	122
		(	-39.3	94.7	-40.0	-180.0	-40.0	-60.7)	123
56	16.23	13.75	-40.0	-180.0	-37.8	-106.0	-40.0	-90.0	124
		(	-38.1	72.2	-40.0	-180.0	-40.0	-87.9)	125
57	16.52	14.00	-40.0	-180.0	-36.7	-130.7	-40.0	-156.3	126
		(	-37.0	47.7	-40.0	-180.0	-40.0	-116.1)	127
58	16.82	14.25	-40.0	-180.0	-35.7	-157.0	-40.0	-159.9	128
		(	-36.1	21.6	-40.0	-180.0	-40.0	-145.0)	129
59	17.11	14.50	-40.0	-180.0	-34.9	175.6	-40.0	-170.7	130
		(	-35.4	-5.7	-40.0	-180.0	-40.0	-174.4)	131
60	17.41	14.75	-40.0	-180.0	-34.2	147.1	-40.0	143.5	132
		(	-34.7	-33.9	-40.0	-180.0	-40.0	155.5)	133
61	17.70	15.00	-40.0	-180.0	-33.6	117.9	-40.0	110.0	134
		(	-34.1	-63.1	-40.0	-180.0	-40.0	125.0)	135
62	18.00	15.25	-40.0	-180.0	-33.1	87.9	-40.0	90.0	136
		(	-33.6	-92.9	-40.0	-180.0	-40.0	93.9)	137
63	18.29	15.50	-40.0	-180.0	-32.6	57.3	-40.0	61.3	138
		(	-33.2	-123.5	-40.0	-180.0	-40.0	62.4)	139
64	18.59	15.75	-40.0	-180.0	-32.3	26.0	-40.0	14.3	140
		(	-32.8	-154.6	-40.0	-180.0	-40.0	30.4)	141
65	18.88	16.00	-40.0	-180.0	-31.9	-5.6	-40.0	-2.2	142
		(	-32.5	173.6	-40.0	-180.0	-40.0	-2.1)	143
66	19.18	16.25	-40.0	-180.0	-31.6	-34.2	-40.0	-37.5	144
		(	-32.2	141.3	-40.0	-180.0	-40.0	-35.1)	145
67	19.47	16.50	-40.0	-180.0	-31.4	-71.1	-40.0	-73.0	146
		(	-32.0	108.5	-40.0	-180.0	-40.0	-68.5)	147
68	19.77	16.75	-40.0	-180.0	-31.2	-104.5	-40.0	-90.0	148
		(	-31.8	75.2	-40.0	-180.0	-39.7	-102.3)	149

Chapter 7

SUBROUTINE WALL

7-1. Purpose: To compute the normal transmission ($T_{\perp}$,$T_{||}$) and reflection coefficients of a N-layer dielectric sheet having thicknesses d_n, dielectric constants ε_{rn}, and loss tangents $\tan\delta_n$ for each layer when a plane wave is incident at angle θ_i.

7-2. Usage: CALL WALL (BETA, SINE, D, ER, TD, N, NN, TN1, TN2, RPER, RPAR)

7-3. Arguments

BETA - Real input variable = $2\pi/\lambda$, where λ is the free space wavelength.

SINE - Real input variable = $\sin\theta_i$.

D, ER, TD - Real input arrays containing the thickness (cm), dielectric constant ε_r, and loss tangent $\tan\delta$ of each layer.

N - Integer input variable equal to the number of layers.

NN - Integer input = N+1.

TN1,TN2 - Complex output variables equal to the normal voltage transmission coefficients for the components of the incident electric field perpendicular to and parallel to the plane of incidence, respectively.

RPER,RPAR - Complex output variables equal to the reflection coefficients $R_{\perp}$, $R_{||}$.

7-4. Comment and Method

a. Layer 1 is the first layer on the exit side of the panel; layer N is the first layer on the incident side. $T_{\perp}$, $T_{||}$ have the same value for either side of the panel being the incident side; however, $R_{\perp}$, $R_{||}$ are different (in phase) for the two cases.

b. The details of the method are presented in Appendix E of Reference 1.

7-5. Program Flow: See Reference 1.

7-6. Test Case: None.

7-7. References

1. G. K. Huddleston, "Radome Analysis Computer Program: Ray Tracing Formulation", Technical Report for JHU/APL, Contract No. 601053, November 1979.

7-8. Program Listing: See following pages.

```
      SUBROUTINE WALL(BETA,SINE,D,ER,TD,N,NN,TN1,TN2,RPER,RPAR)
C    SUBROUTINE WALL COMPUTES THE TRANSMISSION AND REFLECTION
C    COEFFICIENTS FOR AN N LAYER, PLANE DIELECTRIC PANEL FOR PLANE
C    WAVE INCIDENT AT SINE(ANGLE) FOR PERPENDICULAR AND
C    PARALLEL POLARIZATIONS.
C    PARAMETERS OF THE WALL: N= THE NUMBER OF LAYERS
C                            NN= N+1 REQUIRED TO DIMENSION ARRAYS
C                            D= THICKNESS OF EACH LAYER IN CENTIMETERS
C                            ER= RELATIVE DIELECTRIC CONSTANT OF EACH LAY
C                            TD= THE LOSS TANGENT FOR EACH LAYER
C TN1,TN2 ARE THE NORMAL VOLTAGE XMN COEFFICIENTS; TPER,TPAR ARE THE
C INSERTION VOLTAGE TRANSMISSION COEFFICIENTS. IT IS IMPORTANT TO
C NOTE THAT THE XMN COEFS ARE THE SAME FOR PLANE WAVE INCIDENT FROM
C EITHER SIDE OF THE STRATIFIED DIELECTRIC PANEL IMMERSED IN FREE SPACE;
C HOWEVER, THE REFLECTION COEFS ARE NOT. THAT IS, FOR COMPUTING RPER,
C RPAR, THE ORDERING OF ER(NN),TD(NN) IS IMPORTANT WITH LAYER 1 BEING
C THE FIRST LAYER ON THE EXIT SIDE, LAYER N BEING THE FIRST LAYER ON THE
C INCIDENT SIDE.  LAYER NN  AND  LAYER 0  ARE JUST FREE SPACE  LAYERS
C OF SEMI-INFINITE DEPTH.
C E,G,R1,R2, ARE ARRAYS USED IN THE SUBROUTINE HAVING NN DIM"L LIMITS
      COMPLEX E(6),G(6),R1(6),R2(6),GG,EE,RR1,RR2,AA1,AA2,X1,X2,
     $X3,X4,Y1,Y2,Y3,Y4,U1,U2,U3,U4,V1,V2,V3,V4,P1,P2,P3,P4,Q1,Q2,Q3,Q4
      COMPLEX TPER,TPAR,RPER,RPAR,U,V,TN1,TN2
      DIMENSION ER(NN),TD(NN),D(N)
      ER(NN)=1.0
      TD(NN)=0.
      DO 50 I=1,NN
   50 E(I)=CMPLX(ER(I),-ER(I)*TD(I))
      AB=BETA*0.70707070707071
C
C   CALCULATE TOTAL THICKNESS OF WALL IN CM
C
      DTOTAL=0.0
      DO 200 I=1,N
  200 DTOTAL=DTOTAL+D(I)
C    S IS THE SINE OF THE ANGLE SQUARED
C    C IS THE COSINE OF THE ANGLE
      S=SINE*SINE
```

```
      C=SQRT(1.0-S)                                                    39
      AD=ER(1)-S                                                       40
      ET=ER(1)*TD(1)                                                   41
      SR=SQRT(AD*AD+ET*ET)                                             42
      IF(SR-AD) 76,76,77                                               43
   76 A=0.                                                             44
      GO TO 78                                                         45
   77 A=AB*SQRT(SR-AD)                                                 46
   78 B=AB*SQRT(SR+AD)                                                 47
      G(1)=CMPLX(A,B)                                                  48
      GG=CMPLX(0.0,BETA*C)                                             49
      EE=1.0                                                           50
      SUM=0.                                                           51
      SUM=SUM+D(1)/SQRT(AD)                                            52
      RR1=(G(1)-GG)/(G(1)+GG)                                          53
      RR2=(EE*G(1)-E(1)*GG)/(EE*G(1)+E(1)*GG)                          54
      DO 84 I=1,N                                                      55
      II=I+1                                                           56
      AD=ER(II)-S                                                      57
      ET=ER(II)*TD(II)                                                 58
      IF (I-N) 176,177,177                                             59
  176 SUM=SUM+D(II)/SQRT(AD)                                           60
  177 CONTINUE                                                         61
      SR=SQRT(AD*AD+ET*ET)                                             62
      IF(SR-AD) 79,79,80                                               63
   79 A=0.                                                             64
      GO TO 81                                                         65
   80 A=AB*SQRT(SR-AD)                                                 66
   81 B=AB*SQRT(SR+AD)                                                 67
      G(II)=CMPLX(A,B)                                                 68
      R1(I)=(G(II)-G(I))/(G(II)+G(I))                                  69
   84 R2(I)=(E(I)*G(II)-E(II)*G(I))/(E(I)*G(II)+E(II)*G(I))            70
      SUM=S*SUM                                                        71
      AA1=1.0-RR1                                                      72
      AA2=1.0-RR2                                                      73
      DO 85 I=1,N                                                      74
      AA1=AA1*(1.0-R1(I))                                              75
   85 AA2=AA2*(1.0-R2(I))                                              76
```

```
      AA1=1.0/ AA1                                                    77
      AA2=1.0/ AA2                                                    78
      U=-G(1)*D(1)                                                    79
      V=G(1)*D(1)                                                     80
      X1=CEXP(U)                                                      81
      X4=CEXP(V)                                                      82
      X2=-RR1*X4                                                      83
      X3=-RR1*X1                                                      84
      Y1=X1                                                           85
      Y4=X4                                                           86
      Y2=-RR2*Y4                                                      87
      Y3=-RR2*Y1                                                      88
      DO 105 I=2,NN                                                   89
      IF(I-NN) 95,90,1                                                90
   90 U1=1.0                                                          91
      U2=-R1(N)                                                       92
      U3=-R1(N)                                                       93
      U4=1.0                                                          94
      V1=1.0                                                          95
      V2=-R2(N)                                                       96
      V3=-R2(N)                                                       97
      V4=1.0                                                          98
      GO TO 100                                                       99
   95 II=I-1                                                         100
      U=-G(I)*D(I)                                                   101
      V=G(I)*D(I)                                                    102
      U1=CEXP(U)                                                     103
      U4=CEXP(V)                                                     104
      U2=-R1(II)*U4                                                  105
      U3=-R1(II)*U1                                                  106
      V1=U1                                                          107
      V4=U4                                                          108
      V2=-R2(II)*V4                                                  109
      V3=-R2(II)*V1                                                  110
  100 P1=X1*U1+X2*U3                                                 111
      P2=X1*U2+X2*U4                                                 112
      P3=X3*U1+X4*U3                                                 113
      P4=X3*U2+X4*U4                                                 114
```

```
      Q1=Y1*V1+Y2*V3                                                    115
      Q2=Y1*V2+Y2*V4                                                    116
      Q3=Y3*V1+Y4*V3                                                    117
      Q4=Y3*V2+Y4*V4                                                    118
      X1=P1                                                             119
      X2=P2                                                             120
      X3=P3                                                             121
      X4=P4                                                             122
      Y1=Q1                                                             123
      Y2=Q2                                                             124
      Y3=Q3                                                             125
  105 Y4=Q4                                                             126
      RPER=-X3/X4                                                       127
C     TN1,TN2 ARE NORMAL VOLTAGE XMN COEFFICIENTS.                      128
      RPAR=-Y3/Y4                                                       129
      TN1=(X1+X2*RPER)*AA1                                              130
      U=CMPLX(0.0,-SUM*BETA)                                            131
      U=CEXP(U)                                                         132
C     TPER,TPAR HERE ARE VOLTAGE XMN COEFFICIENTS AT EXIT POINT OF RAY. 133
      TPER=TN1*U                                                        134
      TN2=(Y1+Y2*RPAR)*AA2                                              135
      TPAR=TN2*U                                                        136
C    MODIFY TRANSMISSION COEFFICIENTS FOR INSERTION                     137
      U=CMPLX(0.0,BETA*DTOTAL*C)                                        138
      U=CEXP(U)                                                         139
      TPER=TN1*U                                                        140
      TPAR=TN2*U                                                        141
    1 CONTINUE                                                          142
  300 RETURN                                                            143
      END                                                               144
```

Chapter 8

SUBROUTINE CAXCB

8-1. Purpose: To compute the complex vector cross product $\underline{C} = \underline{A} \times \underline{B}$, where $\underline{A}$ and $\underline{B}$ are a complex vectors expressed in rectangular coordinates.

8-2. Usage: CALL CAXCB (A, B, C)

8-3. Arguments

A - Complex input array containing the rectangular components of the vector $\underline{A} = \hat{x} A_x + \hat{y} A_y + \hat{z} A_z$; i.e., A ($A_x$, A_y, A_z).

B - Complex input array B (B_x, B_y, B_z) representing the vector $\underline{B}$.

C - Complex output array C (C_x, C_y, C_z) representing the vector $\underline{C} = \underline{A} \times \underline{B}$.

8-4. Comment and Method: None

8-5. Program Flow: See listing below.

8-6. Test Case: None.

8-7. References: None.

8-8. Program Listing: See following page.

```
      SUBROUTINE CAXCB(A,B,C)                                          1
      COMPLEX A(3),B(3),C(3)                                           2
C     SUBR CAXCB COMPUTES THE VECTOR CROSS PRODUCT C=AXB OF            3
C     TWO COMPLEX VECTORS A AND B                                      4
      C(1)=A(2)*B(3)-A(3)*B(2)                                         5
      C(2)=A(3)*B(1)-A(1)*B(3)                                         6
      C(3)=A(1)*B(2)-A(2)*B(1)                                         7
      RETURN                                                           8
      END                                                              9
```

PARAMETRIC INVESTIGATION OF RADOME ANALYSIS METHODS:

EXPERIMENTAL RESULTS

By

H. L. Bassett, J. M. Newton, W. Adams, J. S. Ussailis,
M. J. Hadsell, & G. K. Huddleston

Prepared for

AIR FORCE OFFICE OF SCIENTIFIC RESEARCH (AFSC)
BOLLING AIR FORCE BASE, D. C. 20332

FINAL TECHNICAL REPORT, VOLUME IV OF IV
GRANT AFOSR–77–3469
30 September 1977 – 31 December 1980

February 1981

GEORGIA INSTITUTE OF TECHNOLOGY
Engineering Experiment Station &
SCHOOL OF ELECTRICAL ENGINEERING
ATLANTA, GEORGIA 30332

REPORT DOCUMENTATION PAGE

READ INSTRUCTIONS BEFORE COMPLETING FORM

1. REPORT NUMBER	2. GOVT ACCESSION NO. / 3. RECIPIENT'S CATALOG NUMBER
4. TITLE (and Subtitle): PARAMETRIC INVESTIGATION OF RADOME ANALYSIS METHODS: EXPERIMENTAL RESULTS	5. TYPE OF REPORT & PERIOD COVERED: Final Technical Report, Vol. 4 of 4/September 1977-Dec. 1980
	6. PERFORMING ORG. REPORT NUMBER
7. AUTHOR(s): H. L. Bassett, J. M. Newton, W. Adams, J. S. Ussailis, M. J. Hadsell, and G. K. Huddleston	8. CONTRACT OR GRANT NUMBER(s): AFOSR-77-3469
9. PERFORMING ORGANIZATION NAME AND ADDRESS: Georgia Institute of Technology, Engineering Experiment Station & School of EE, Atlanta, Georgia 30332	10. PROGRAM ELEMENT, PROJECT, TASK AREA & WORK UNIT NUMBERS: 61102F 2301/A6
11. CONTROLLING OFFICE NAME AND ADDRESS: Air Force Office of Scientific Research (AFSC), Physics Directorate (Code NP-77-148), Bolling AFB, D.C. 20332	12. REPORT DATE: February 1981 13. NUMBER OF PAGES: 189
14. MONITORING AGENCY NAME & ADDRESS(if different from Controlling Office)	15. SECURITY CLASS. (of this report): UNCLASSIFIED 15a. DECLASSIFICATION/DOWNGRADING SCHEDULE

16. DISTRIBUTION STATEMENT (of this Report)

Approved for public release; distribution unlimited.

17. DISTRIBUTION STATEMENT (of the abstract entered in Block 20, if different from Report)

18. SUPPLEMENTARY NOTES

19. KEY WORDS (Continue on reverse side if necessary and identify by block number)

Radome Measurements
Antenna Measurements
Millimeter Wave Radome
Radome Analysis

20. ABSTRACT (Continue on reverse side if necessary and identify by block number)

This Volume 4 of four volumes presents 140 measured far-field patterns and boresight error data for eight combinations of three monopulse antennas and five tangent ogive Rexolite radomes at 35 GHz. The antennas and radomes, all of different sizes, were selected to provide a range of parameters as found in the applications. The measured data serve as true data in the parametric investigation of radome analysis methods to determine the accuracies and ranges of validity of selected methods of analysis.

PARAMETRIC INVESTIGATION OF RADOME ANALYSIS METHODS:

EXPERIMENTAL RESULTS

by

H. L. Bassett, J. M. Newton*, W. Adams*,
J. S. Ussaillis, & M. J. Hadsell
Engineering Experiment Station
Electromagnetics Laboratory* and
Radar and Instrumentation Laboratory
Georgia Institute of Technology

&

G. K. Huddleston
School of Electrical Engineering
Georgia Institute of Technology
Atlanta, Georgia 30332

Final Technical Report, Volume IV of IV

for

Air Force Office of Scientific Research (AFSC)
Physics Directorate (Code NP-77-148)
Bolling Air Force Base, D. C. 20332

under

Grant AFOSR-77-3469
30 September 1977 - 31 December 1980

February 1981

TABLE OF CONTENTS

LIST OF ILLUSTRATIONS

LIST OF TABLES

PARAMETRIC INVESTIGATION OF RADOME ANALYSIS METHODS: EXPERIMENTAL RESULTS

I. Introduction

This technical report documents the pattern and boresight error measurements made on eight combinations of three monopulse antennas and five tangent ogive radomes at 35 GHz in support of the parametric investigation of radome analysis methods carried out under grant AFOSR-77-3469. The measurements program was carried out by personnel in the Electromagnetics Laboratory and the Radar and Instrumentation Laboratory of the Engineering Experiment Station at Georgia Institute of Technology during the period October 1977 through December 1980.

This report is Volume IV of four volumes which comprise the final technical report for this research grant. Volume I presents an overview of this research and salient results. Volume II documents the analytical method and Fortran computer code used to analyze the various antenna/radome combinations using a fast receiving formulation based on Lorentz reciprocity and geometrical optics. Volume III documents the analytical method and additional Fortran software required for radome analysis based on the Huygens-Fresnel principle (surface integration).

The overall objective of this research is to develop a general theory of radome analysis and to determine the accuracies of three computer-aided radome analysis methods under controlled conditions of antenna size and placement, wavelength and radome size and shape. The measured data presented here is used as true data in the assessments of the accuracies of those methods. It is expected that this measured data will be

used in the future by other investigators for the same purposes. It is for this reason, and the fact that no similar data base currently exists, that these measured data are so tediously documented.

Three antennas, representing small, medium, and large in terms of radiating aperture size, were combined with five tangent ogive radomes to provide a range of antenna/radome parameters that is likely to be encountered in the applications and for which the accuracies of likely computer codes are to be determined. The parameters of the radomes include both size (small, medium, large) and fineness ratio; i.e., ratio of radome length to diameter. The tangent ogive shape was chosen because of its ease of fabrication, analytical tractability, and widespread use in the applications. The eight combinations of antennas and radomes measured are summarized by the entries in Table 1.

The physical characteristics of the antennas and radomes used are presented below. The measurement procedures and coordinate systems are also described. The measured pattern data and boresight error data are presented in Appendices A through K. Principal plane patterns and diagonal plane patterns of the sum, elevation difference, and azimuth difference channels of the three antennas alone are presented in Appendices A, B, and C. Measured principal plane patterns of the antennas with radomes are presented in Appendices D through K for the eight combinations used. Each of these eight appendices is concluded with measured boresight error data.

II. Antennas

The antennas are four-element monopulse arrays as shown in Figures 1 and 2. Their dimensions in wavelengths (λ) at 35 GHz and in inches are given in Table 2. Each element is a conical horn with a circular to

Table 1. Ratios of Radome Inside Diameter to Antenna Aperture Diameter for Antenna/Radome Combinations Measured.

	Antenna		
Radome	Small	Medium	Large
Small (F=1.0)	2.33	--	--
Medium (F=1.0)	3.98	2.33	--
Medium (F=1.5)	--	2.33	--
Medium (F=2.0)	--	2.33	--
Large (F=1.0)	7.28	4.27	2.33

Table 2. Monopulse Array Dimensions.

Dimension	Small Array		Medium Array		Large Array	
(See Figure 1)	λ	inches	λ	inches	λ	inches
A	0.919	0.310	1.839	0.620	3.633	1.225
B	2.589	0.875	4.567	1.540	9.015	3.040
C	2.108	.160	1.054	.320	2.604	0.878
D	1.275	0.430	5.456	1.840	6.153	2.075

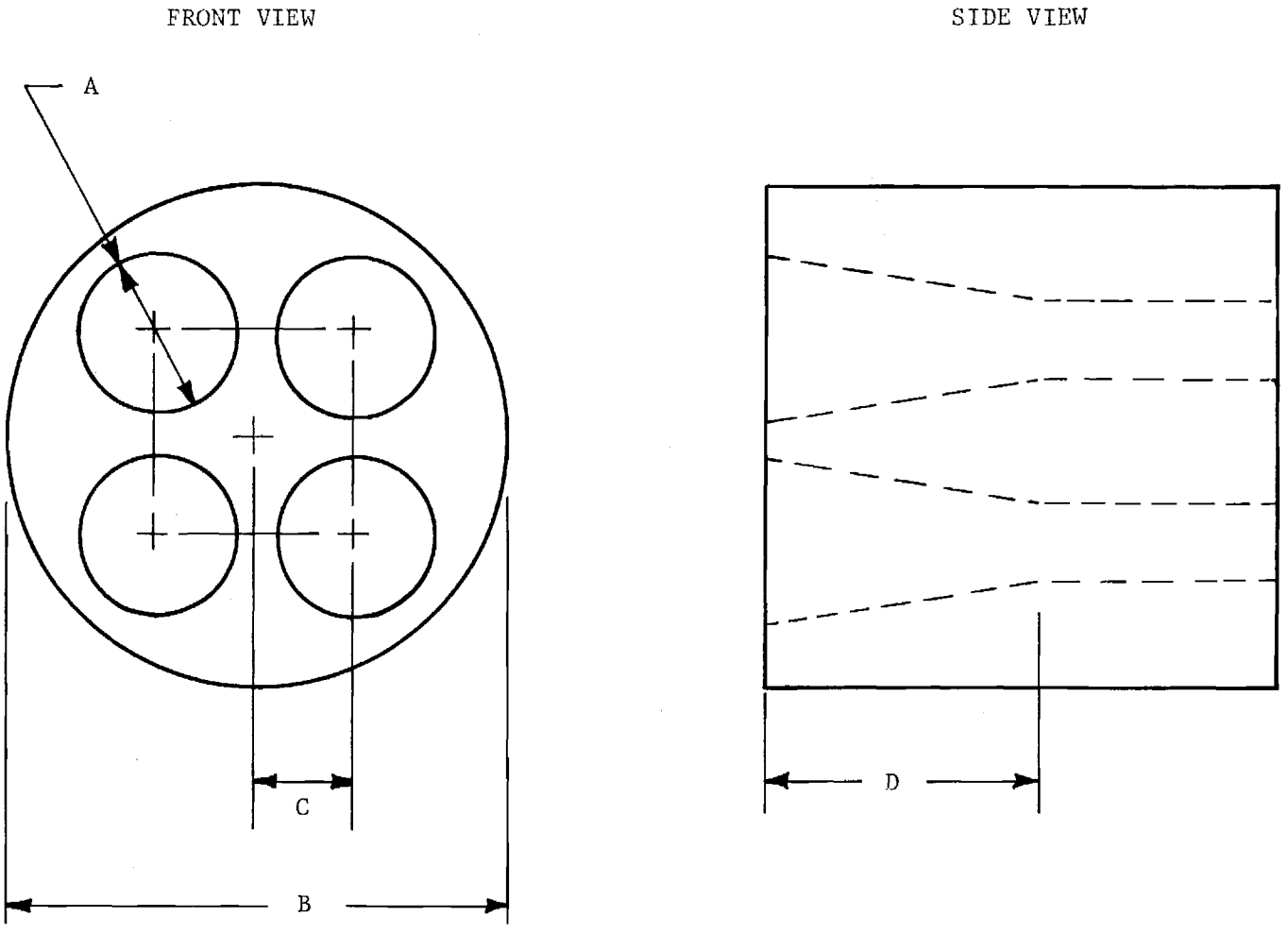

Figure 1. Schematic Drawing of Four-Horn Monopulse Antenna Array

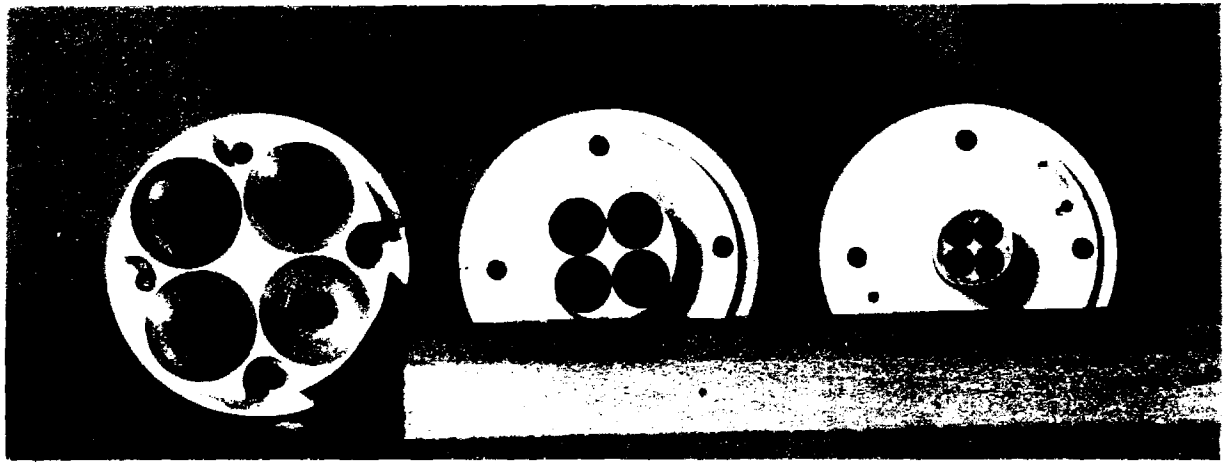

Figure 2. Photograph of Front View of Large, Medium and Small Antennas

rectangular waveguide transition at the throat. All four elements are machined into a single piece of aluminum for stability and to facilitate pattern measurements with and without the various radomes. The three arrays produce measured sum pattern beam widths of 28° (small array), 15° (medium), and 8° (large) as shown in Appendices A through C.

Signals received by the horn elements are fed into a monopulse comparator via four rectangular waveguide sections. The signal paths to this point are not of exactly equal length; hence, low-loss dielectric screws were introduced into the waveguide sections to adjust the phase delay in each signal path to a single constant. That constant was determined by the relative phase of the longest signal path at the comparator input port. An example of a waveguide section tuned in this way is shown in Figure 3.

The monopulse comparator is a single unit of several waveguide couplers. Signals received at the four input ports are combined to produce a sum, azimuth difference, and elevation difference channels. Input and output port views of the comparator are shown in Figure 4.

The complete antenna assembly for the small horn is presented in Figure 5. The elevation difference channel is shown connected to a harmonic mixer. The remaining channels are terminated in matching impedances.

III. Radomes and Mounting Hardware

Five radomes of tangent ogive shape were fabricated for use with the three antennas. Three radomes have fineness ratios of 1:1 and three different base diameters designated as small, medium and large. The remaining two radomes have medium base diameters with fineness ratios of 1.5:1 and 2.0:1. Figure 6 and Table 3 present the radome dimensions in freespace wavelengths (λ) and in inches (").

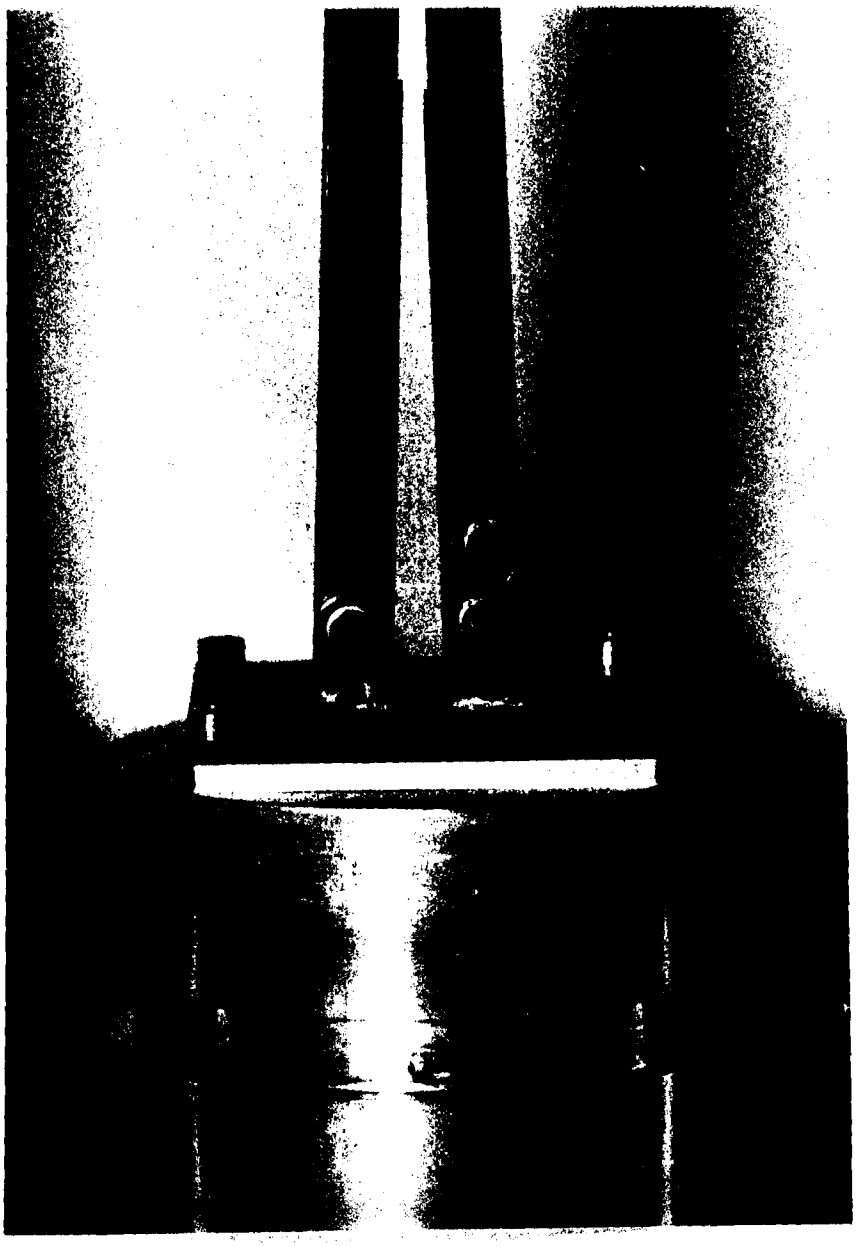

Figure 3. Photograph of Medium Antenna Showing Tuning Screws in Waveguide Feeds.

Input Port

Output Port

Figure 4. Photograph of Input and Output Ports of Monopulse Comparator.

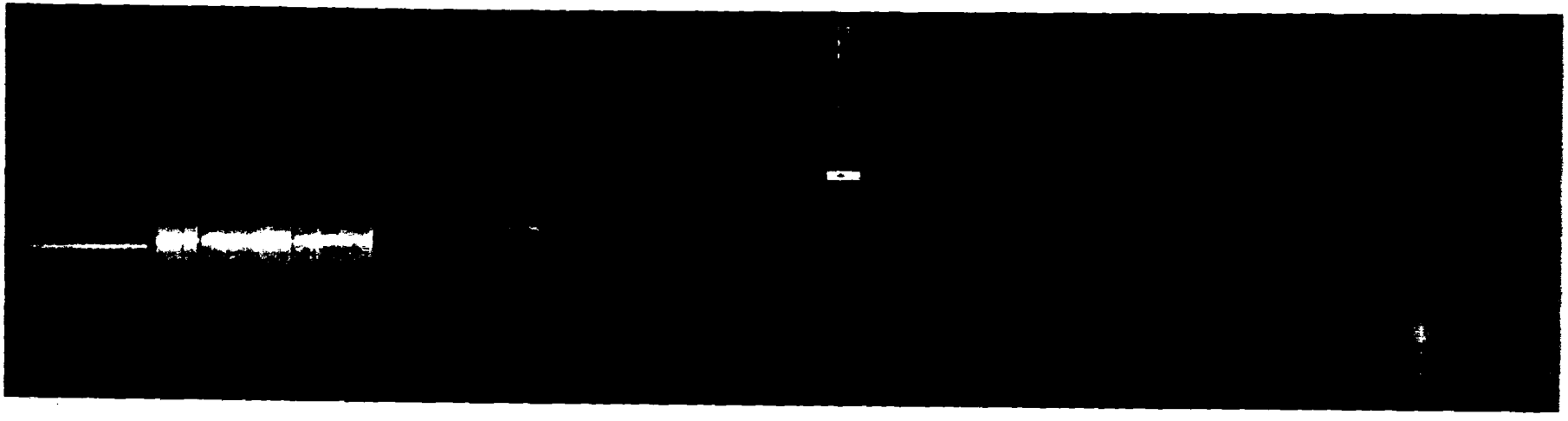

Figure 5. Photograph of Complete Antenna Assembly Using Small Array

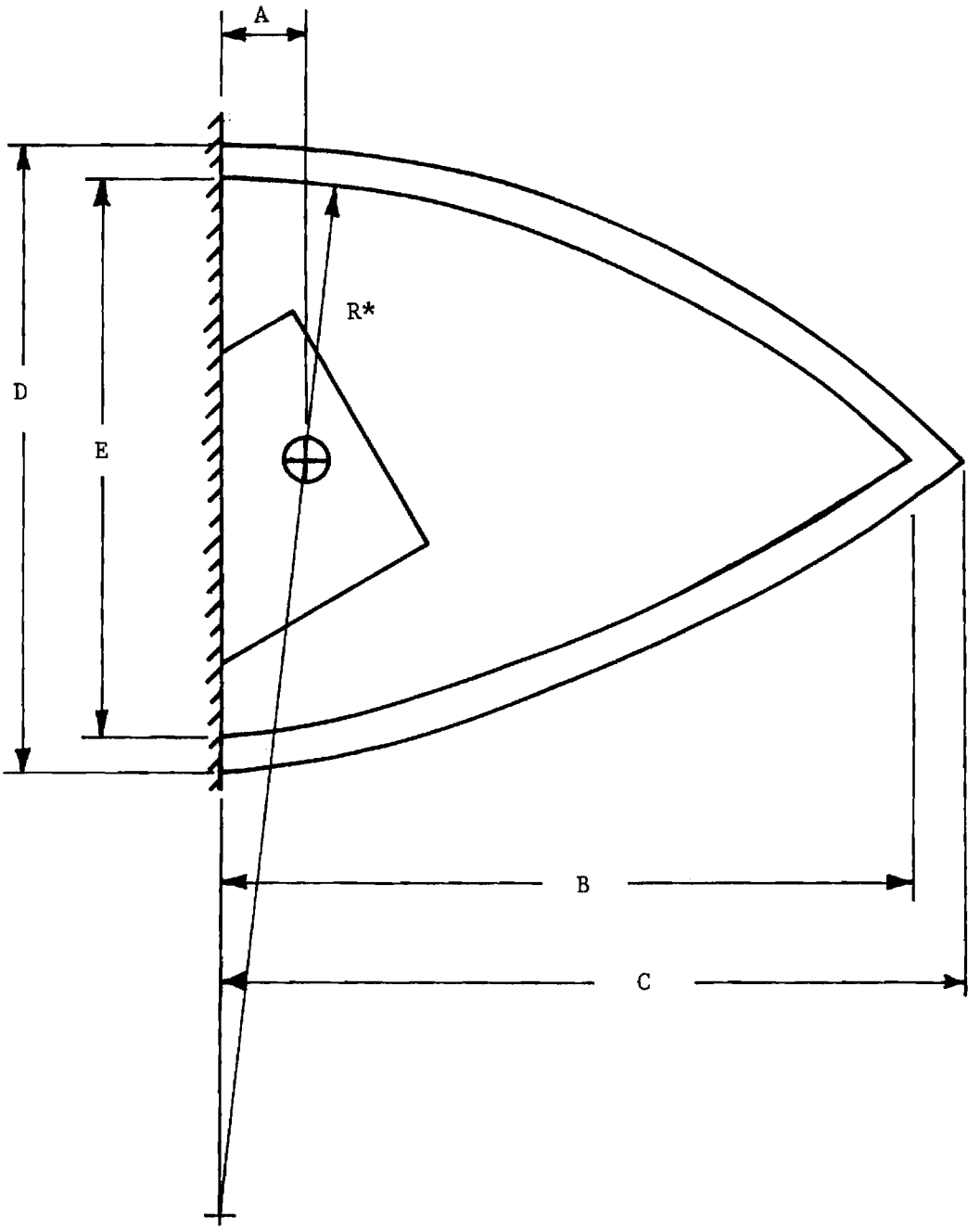

Figure 6. Illustration of Dimensions of Tangent Ogive Radomes

Table 3. Radome Dimensions in Inches.

	Small F=1.0	Medium F=1.0	Medium F=1.5	Medium F=2.0	Large F=1.0
A	0.1875	0.250	0.250	0.250	0.375
B	2.110	3.440	5.250	6.940	6.318
C	2.370	3.825	5.663	7.540	6.875
D	2.550	4.015	3.993	4.000	6.910
E	2.050	3.510	3.497	3.500	6.410

The radomes were machined from cylinders of Rexolite® ($\varepsilon_r = 2.54$). The wall thickness for all radomes was chosen to be on the order of one wavelength in Rexolite at 35 GHz. This thickness provided adequate strength and rigidity in the larger radomes and consistent effects for all sizes.

The radomes were mounted to specially machined baseplates as shown in Figure 7. The baseplates were then affixed to selected extension tubes for mounting the radome over the selected antenna. A cylindrical hole was machined in each extension tube to fix the angle between the radome axis and the antenna axis to precisely 15°, and to accurately position the antenna inside the radome.

Additional mounting hardware was fabricated to allow the radome with base plate assembly to be rotated about the axis of the antenna as shown in Figure 8. This hardware allowed for accurate positioning of the tip of the radome with respect to the principal planes of the antenna to facilitate boresight error measurements. Provision was also made to rotate the antenna/radome combination by any specified angle so that great circle pattern cuts could be made using a single azimuth positioner rotating about a vertical axis.

IV. Pattern Measurements

The far field range facilitates the measurement of microwave antennas with far field regions forty feet or less distant. For this program, a mounting pedestal was built to allow orientation of the antenna under test. The receiving (test) pedestal is supported by a Scientific Atlanta horizontal positioner unit, which can be positioned down range by rolling on four wheels along a level horizontal track. The transmitting pedestal allows adjustment of the height and polarization of the

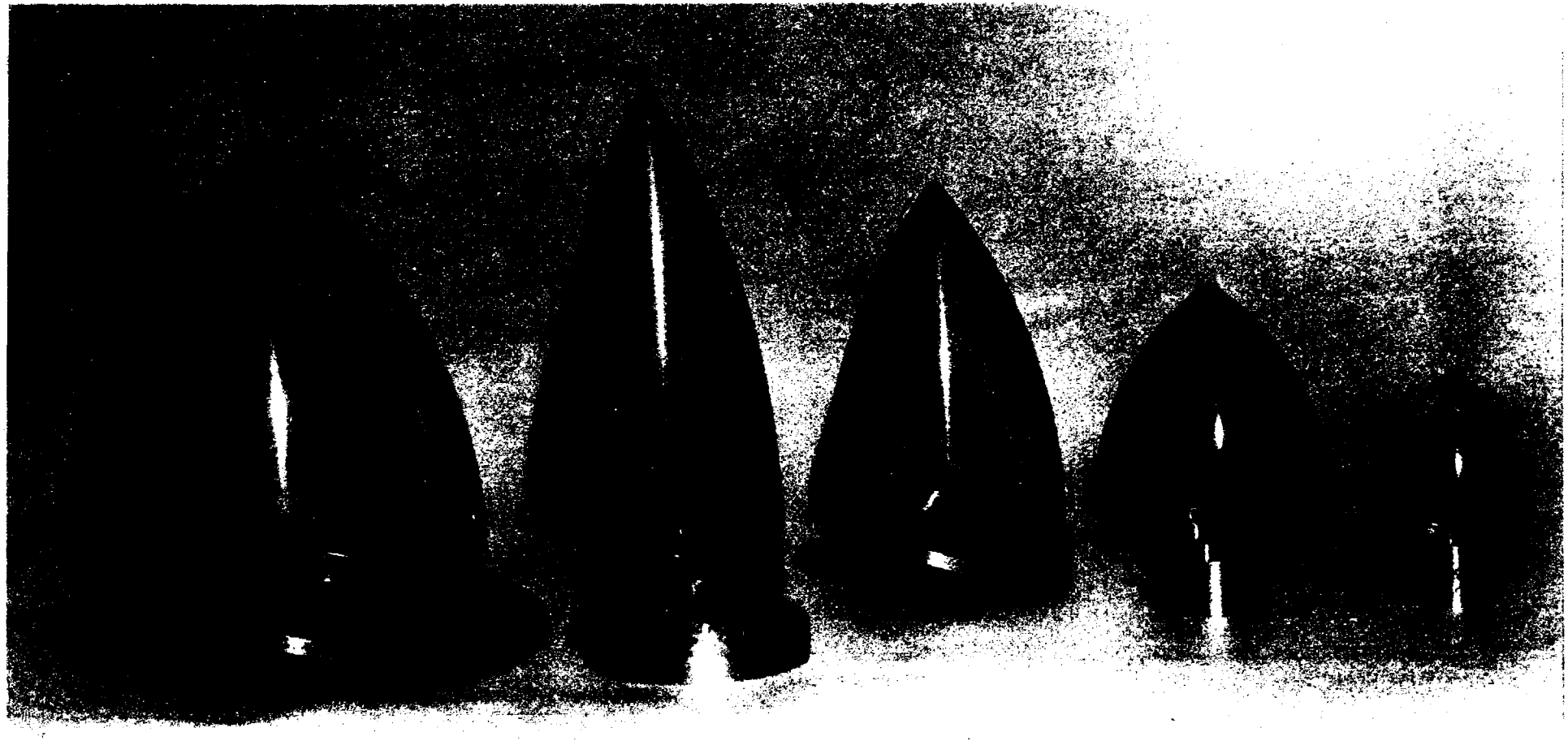

Figure 7. Photograph of the Five Radomes, Three Baseplates, Three Adapter Inserts, and Two Extension Rings Used in the Experimental Work.

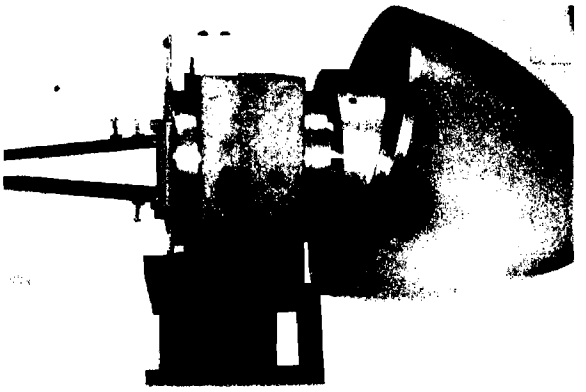

Radome Locked in Vertical Position

Rotation of Antenna with Radome Locked in Vertical Position

Rotation of Radome/Antenna Assembly to Desired Polarization

Figure 8. Radome Positioning Proceedure: Large Array and Large F=1 Radome Shown

transmitting antenna (in this case, a 35 GHz horn). Signals received by the antenna under test are heterodyned by the phase/amplitude receiver (SA 1753) as the antenna under test (AUT) is rotated about the vertical axis. From the received signal amplitudes, a 1 kHz AM signal is produced as the imput to the pattern recorder (SA 1522-40). The recorder produces a 10" x 20" rectangular plot of relative power one way versus the angular position of the antenna. The angular movement of the recorder is directly linked to the test antenna positioner through a synchro-transmitter-receiver feedback loop. No phase measurements were attempted because of instabilities in the Klystron source and because of the mechanical stability difficulties inherent at 35 GHz on an outdoor range.

To understand the pattern measurement procedure, consider the initial position of the four-horn array (AUT) on the receiving pedestal to be such that it is vertically polarized with respect to the horizontal surface of the earth. The horizontal plane containing the axis of symmetry of the antenna (z-axis) is the H-plane and corresponds to the $\phi=0°$ and $\phi=180°$ planes of the spherical coordinate system shown in Figure 9(a). H-plane measurements were made by rotating the azimuth positioner in the clockwise direction (Observer #1 looking down on it), starting from a position such that the antenna would be to the left of Observer #2 standing upright behind the receiving pedestal and looking toward the transmitting antenna at the other end of the range. When the transmitting antenna is aligned rotationally about its axis to be vertically polarized, the so called parallel polarization component V_{ϕ}^{H} in Figure 9(a) is recorded. By rotating only the transmitting antenna by 90° clockwise (Observer #2) to yield horizontal polarization, the cross polarization component V_{ϕ}^{H} in Figure 9(a) was measured.

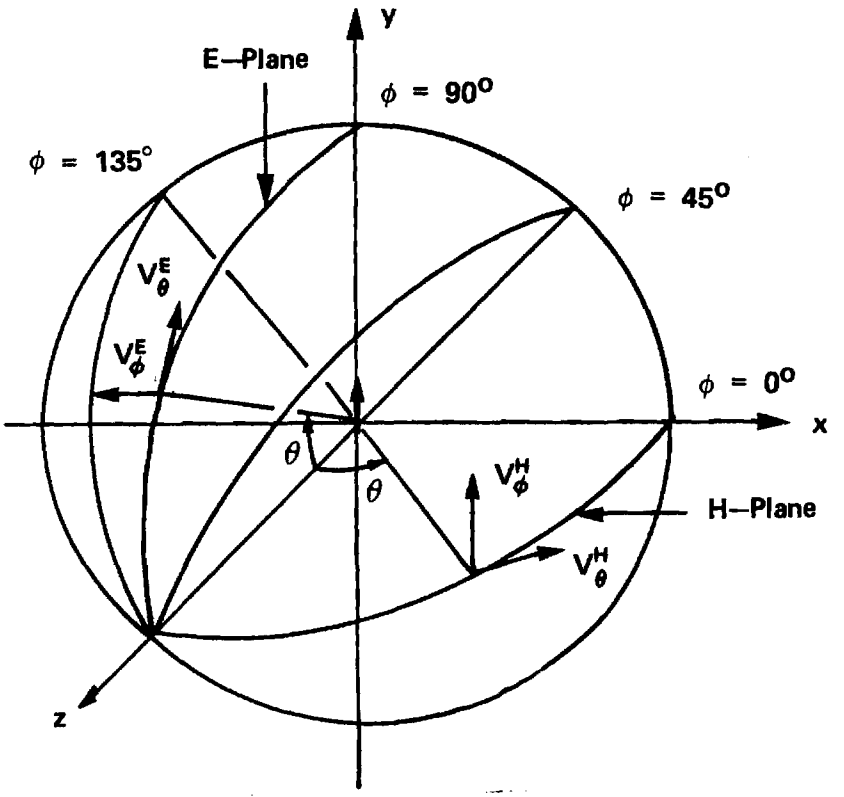

(a) Antenna Coordinate System

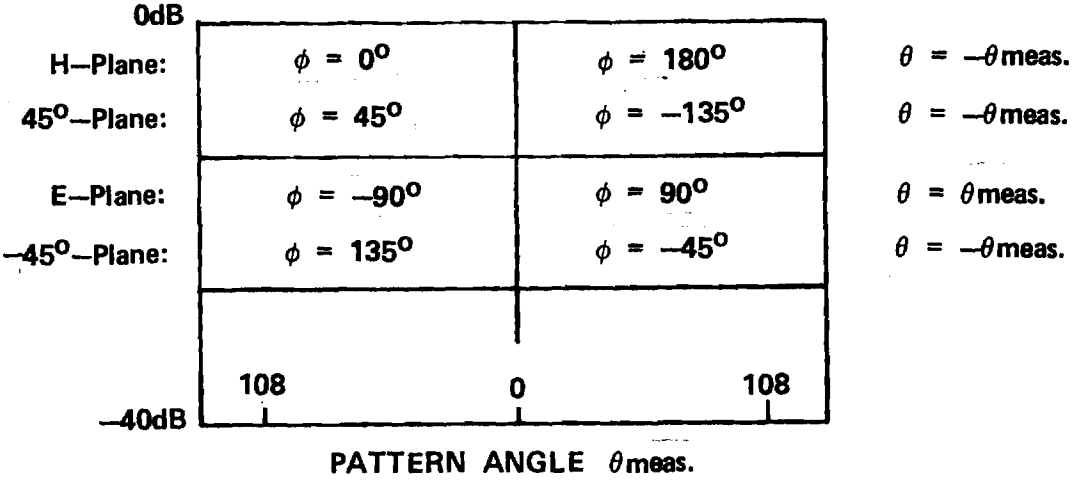

(b) Relationships to Recorded Pattern Measurements.

FIGURE 9. Coordinate System Used for Antenna Pattern Measurements.

The recorded pattern angle θ_{meas} for the H-plane patterns measured during this program is exactly the negative of the polar angle θ defined in Figure 9(a). This statement is true for all pattern measurements, except the E-plane patterns, and the relationships between the patterns presented in Appendices A through K and the antenna coordinate system are summarized in Figure 9(b). These relationships are of critical importance to ensure that accurate comparisons to computed patterns are made, especially when the radome is present.

The E-plane of the AUT is the vertical plane which contains the antenna axis of symmetry; i.e., the yz-plane of the antenna coordinate system shown in Figure 9(a). Pattern measurements in the E-plane were made by first rotating both the AUT and transmitting antenna 90° clockwise (Observer #2 behind AUT). Pattern recordings of the parallel component V_{θ}^{E} of Figure 9(a) were then made as described above for the H-plane. By rotating the transmitting antenna 90° (Observer #2), the cross component V_{ϕ}^{E} of Figure 9(a) was measured. The relationships between the recorded patterns and the antenna coordinate system are summarized in Figure 9(b).

Diagonal plane pattern measurements were made on the antennas alone for modeling purposes. The planes are defined by ϕ=45° and ϕ=-45° in the antenna coordinate system of Figure 9(a). The relationships to the recorded patterns are shown in Figure 9(b).

The receiver used had only a single channel, and pattern measurements on each channel (Σ, Δ_{EL}, Δ_{AZ}) of each antenna were done one channel at a time. The harmonic mixer was installed on the desired port of the monopulse comparator. The other ports were terminated in matched waveguide loads. The mixer and loads were interchanged until all the channels were measured.

All pattern measurements with the radomes in place were done in the same manner as with the antennas alone. The radome under test was always mounted so that its axis of symmetry made an angle of 15° with the axis of symmetry of the antenna; furthermore, the radome was rotated by angle α so that the tip was located in the $\phi = -45°$ plane of the antenna coordinate system of Figure 9(a). This position was selected to produce measurable boresight errors and pattern asymmetries in both principal planes. Boresight error measurements were later made as a function of this angle α as explained in the next section.

Measured pattern data for the antennas alone are presented in Appendices A, B, and C. Patterns with the radomes are presented in Appendices D through K. Note that for these latter patterns, the pattern of the antenna alone is shown as a dashed line for reference purposes. Although some effort was made to show the relative gain and boresight data correctly on these patterns, the boresight error graphs presented at the end of each appendix and the measured relative gain data presented below should be consulted as the final, correct data.

V. Boresight Error Measurements

When a radome is placed over the monopulse antenna, an error in the boresight of the antenna on the order of a few tens of milliradians may result. Electrical boresight is indicated when the antenna is positioned in the central nulls of the two orthogonal monopulse channels (Δ_{EL}, Δ_{AZ}). This position of the antenna without radome is the true boresight of the antenna.

Boresight error caused by the radome is defined here as being the actual angular position of the target (transmitting antenna) in the coordinate system of Figure 9(a) when electrical boresight is indicated in

the difference channels. For example, a positive boresight error in azimuth (elevation) would place the target in the ϕ=0 plane (ϕ=90° plane) of Figure 9(a). Equal, positive boresight errors in both azimuth and elevation sould place the target in the ϕ=45° plane. Negative boresight errors may also occur.

Boresight error measurements were made during this investigation using a precision milling machine rotary table as a turntable mount for the receiving monopulse antenna and radome. Error measurements were made in the elevation and azimuth channels separately. Boresight errors in azimuth were measured by first positioning the monopulse array and transmitting antenna on the far-field range to yield vertical polarization. The turntable was carefully rotated until electrical boresight in the Δ_{AZ} channel was indicated. The radome was then placed over the antenna and positioned in the angle α. The turntable was carefully adjusted to indicated electrical boresight in the Δ_{AZ} channel. The boresight error was then read directly from the vernier scale of the turntable. Boresight errors in the elevation channel (Δ_{EL}) were done similarly by rotating both antennas 90° clockwise (Observer #1) about their common axis of symmetry and repeating the above procedure.

The indication of electrical boresight was obtained using a Hewlett-Packard 415 VSWR meter, crystal detector, and 1-kHz amplitude modulation on the 35 GHz signal being transmitted. The detector was installed on the difference channel port of interest and connected to the VSWR meter. The difference channel null position was determined by measuring equal amplitudes on either side of the null as the turntable was rotated about the null position, and then taking the average of the two angular readings on the turntable vernier scale. This method was adopted

after it was discovered that such measurements using the azimuth positioner, heterodyne receiver, and pattern recorder yielded erratic results due to positioner inaccuracies.

As mentioned above, the radome mounting hardware was machined so that the radome axis of symmetry (z_R-axis) made an angle of 15° with the monopulse array axis of symmetry (z-axis). Also, the radome with baseplate could be rotated about the z-axis of the antenna such that the radome tip could be positioned to lie in any $\phi=\alpha$ plane of Figure 9(b). Boresight error measurements were made as a function of this angle α. For example, when $\alpha=0$, the radome tip lies in the $\phi=0$ plane of the antenna, causing boresight error in azimuth but none in elevation due to symmetry. When $\alpha=90°$, no boresight error in the Δ_{AZ} channel would be expected (due to symmetry), but errors in Δ_{EL} would be expected. For any other value of α, errors would be expected in both channels.

The measured boresight errors for the eight antenna/radome combinations shown in Table 1 are presented as the last figure of each of Appendices D through K. Each figure presents boresight error graphs in azimuth and in elevation. For each graph the abscissa is the angle α, and the ordinate is boresight error in degrees. Measurements were made in 15° increments in α over the complete range of zero to 360°. Ideally, the boresight errors are antisymmetric in α with a "period" of 180 degrees; hence, the measured data over two periods provide an indication of repeatability and consistency.

A radome also causes a loss in on-axis gain of the sum channel of the monopulse antenna. The gain loss was measured simply by monitoring the sum channel signal before and after the radome was installed. The monopulse antenna and transmitting antenna were aligned for maximum

received signal in the sum channel. Gain loss was measured at the four angular positions α of the radome as presented in Table 4.

Table 4. Measured Loss in Gain (decibels) For Eight Antenna/Radome Combinations

		Gain Loss (dB)		
Antenna	Radome	$\alpha=0°$	$\alpha=-45°$	$\alpha=-90°$
Small	Small (F=1.0)	0.4	0.7	0.6
"	Medium (F=1.0)	1.3	1.7	1.5
"	Large (F=1.0)	1.4	1.8	1.4
Medium	Medium (F=1.0)	1.4	1.4	0.8
"	Medium (F=1.5)	1.0	1.0	1.0
"	Medium (F=2.0)	0.2	0.5	0.6
"	Large (F=1.0)	1.8	1.4	1.4
Large	Large (F=1.0)	1.7	1.6	1.3

APPENDIX A

Antenna Patterns of Small Array Without Radome

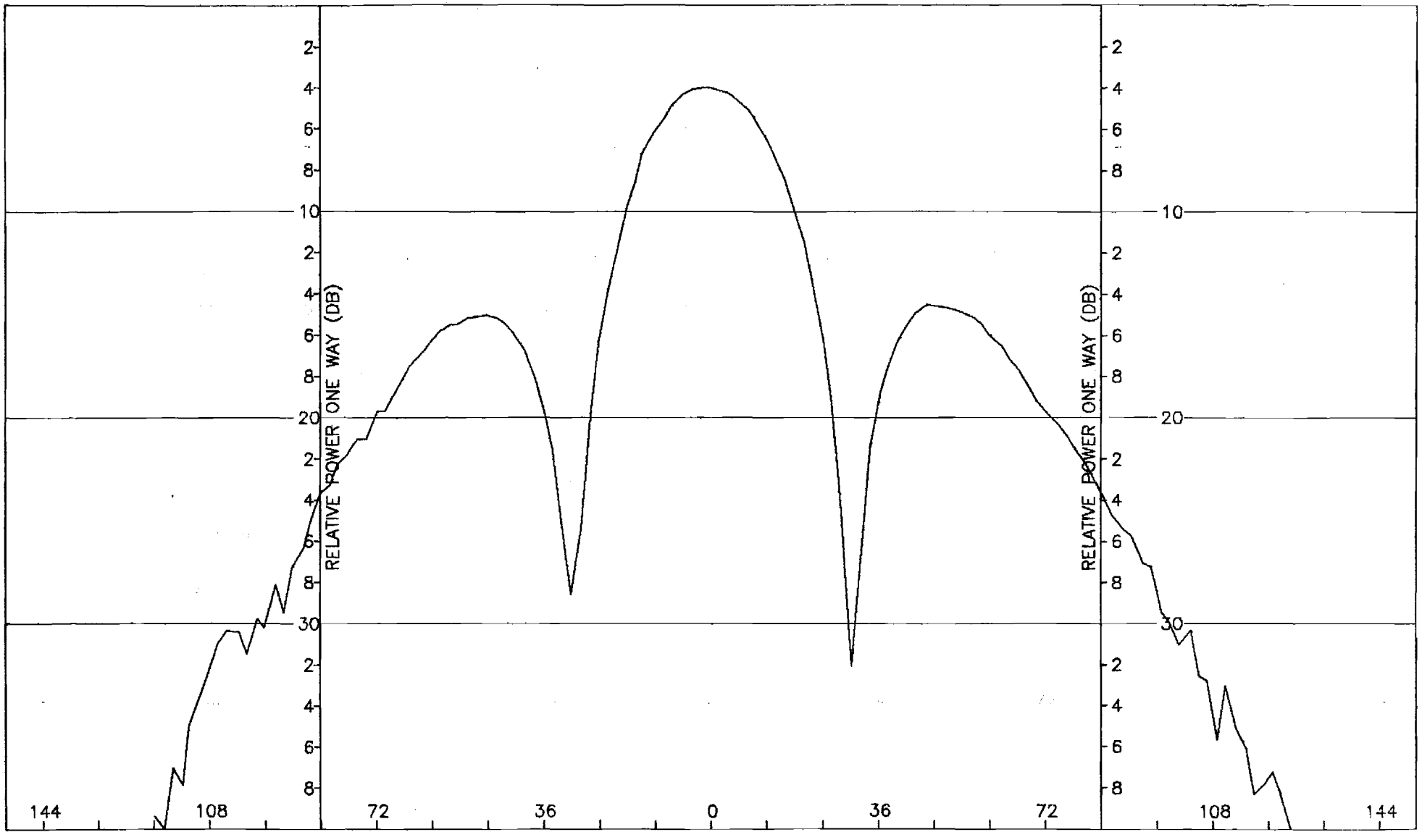

Figure A-1. Pattern of Small Array: H-Plane, Sum, ϕ-Component, No Radome.

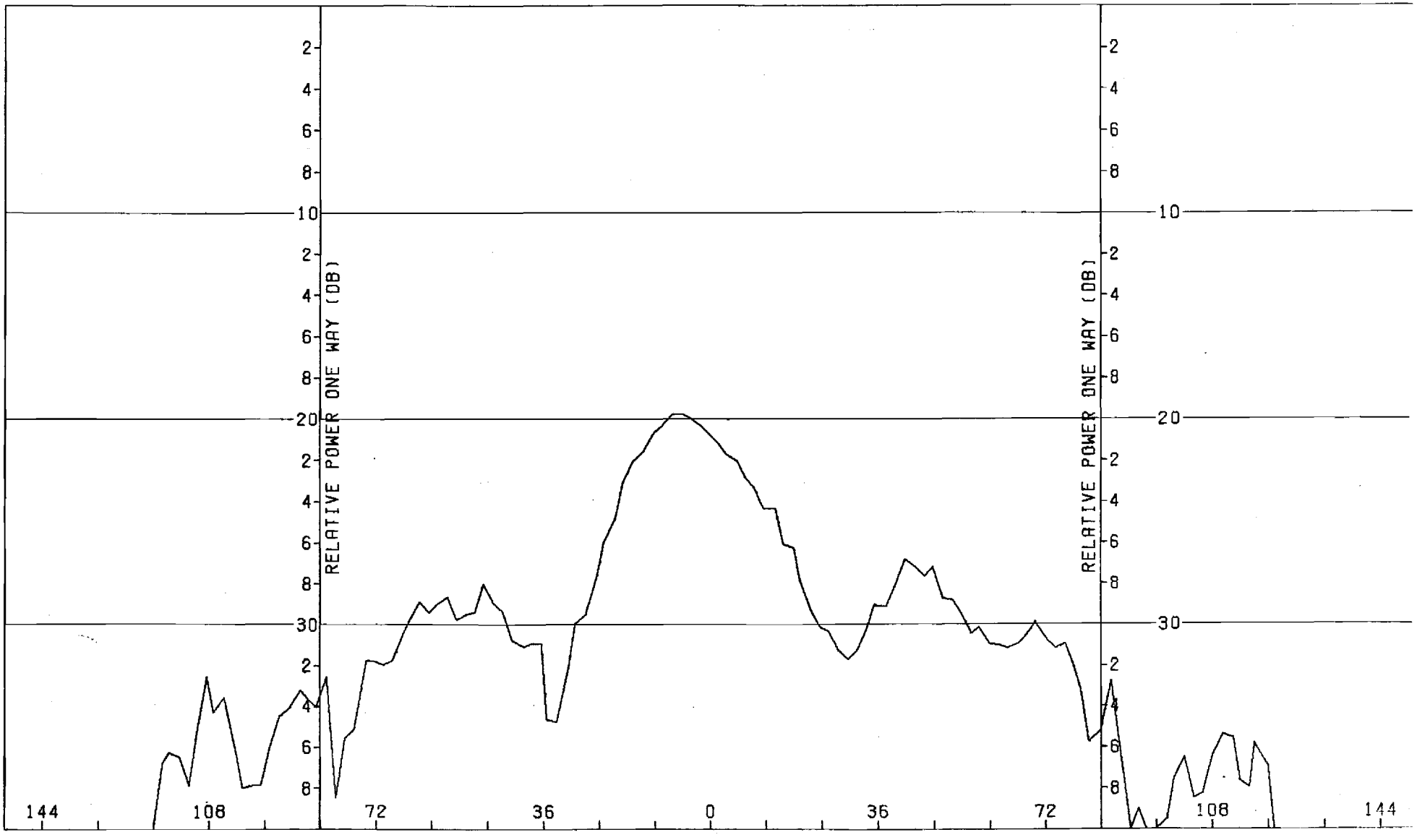

Figure A-2. Pattern of Small Array: H-Plane, Sum, θ-Component, No Radome.

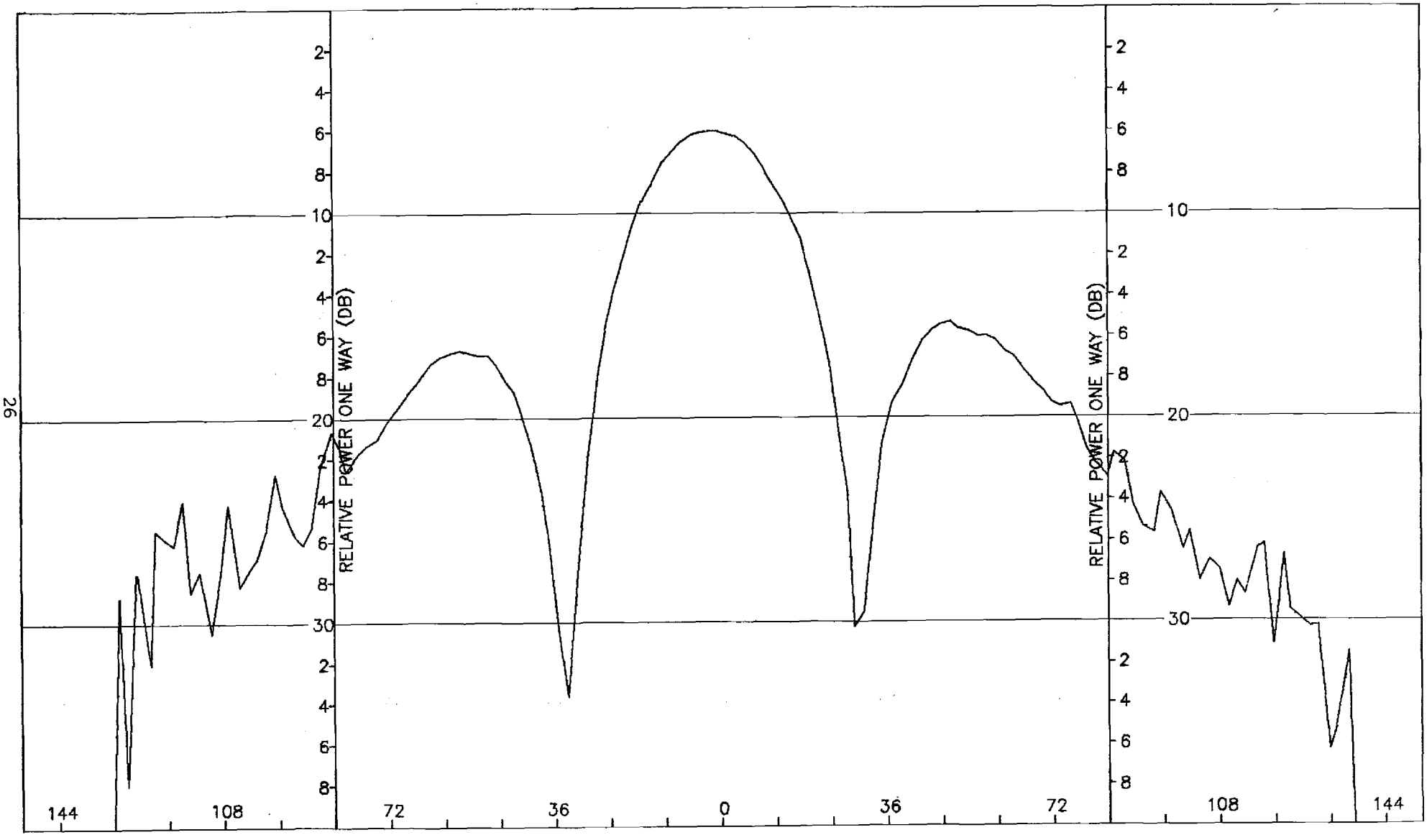

Figure A-3. Pattern of Small Array: E-Plane, Sum, θ-Component, No Radome.

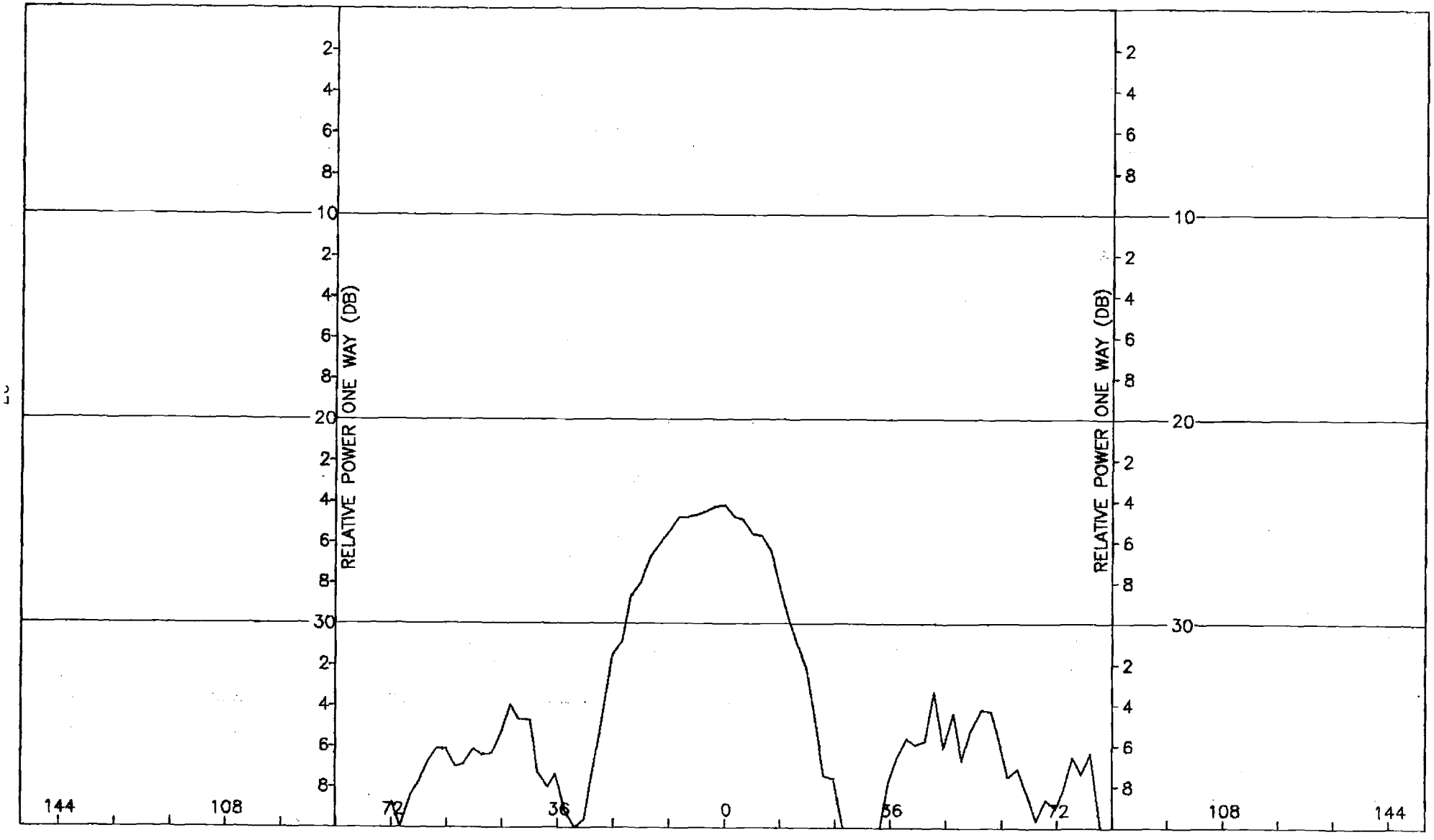

Figure A-4. Pattern of Small Array: E-Plane, Sum, ϕ-Component, No Radome.

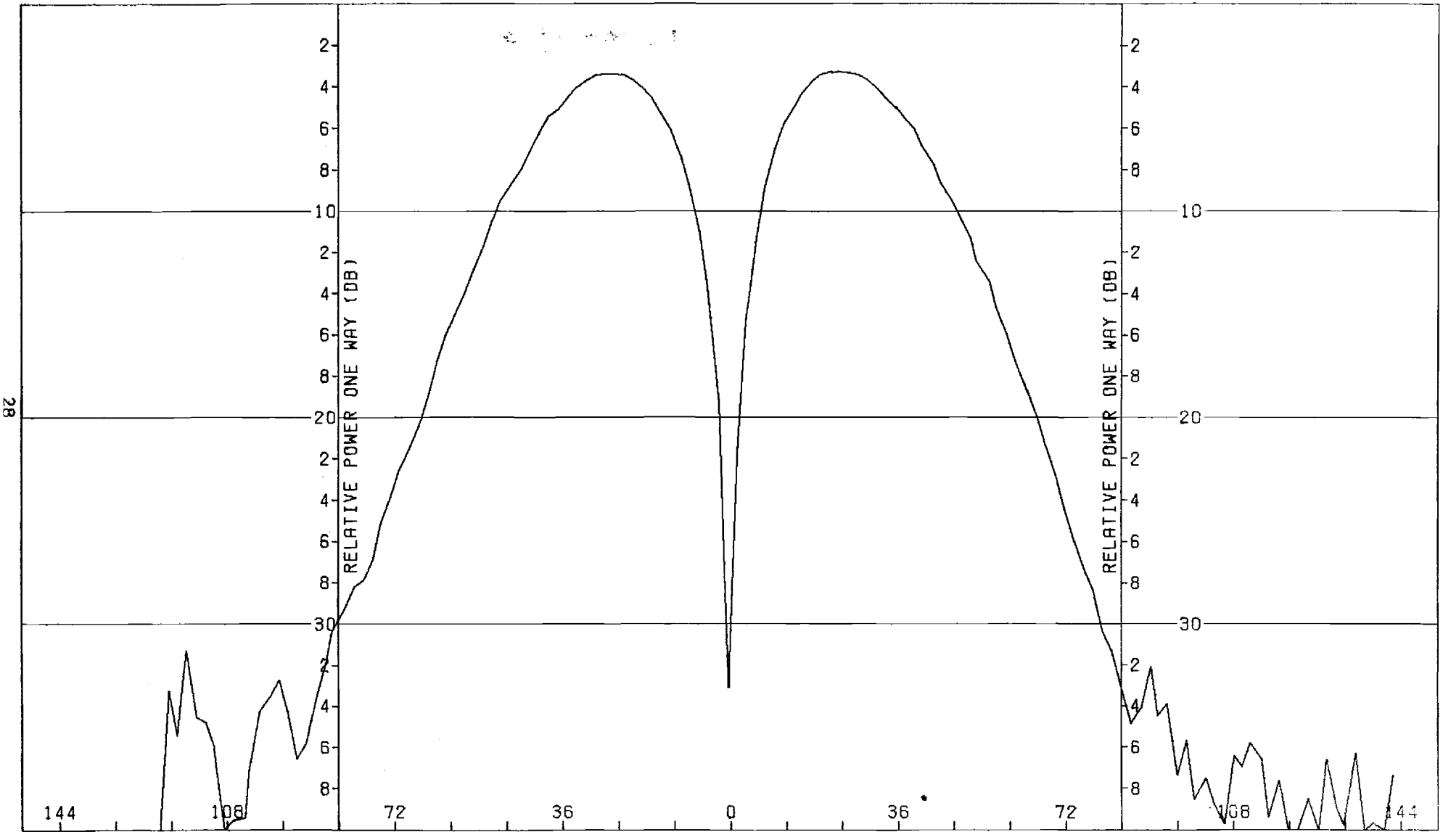

Figure A-5. Pattern of Small Array: H-Plane, Azimuth Difference, ϕ-Component, No Radome.

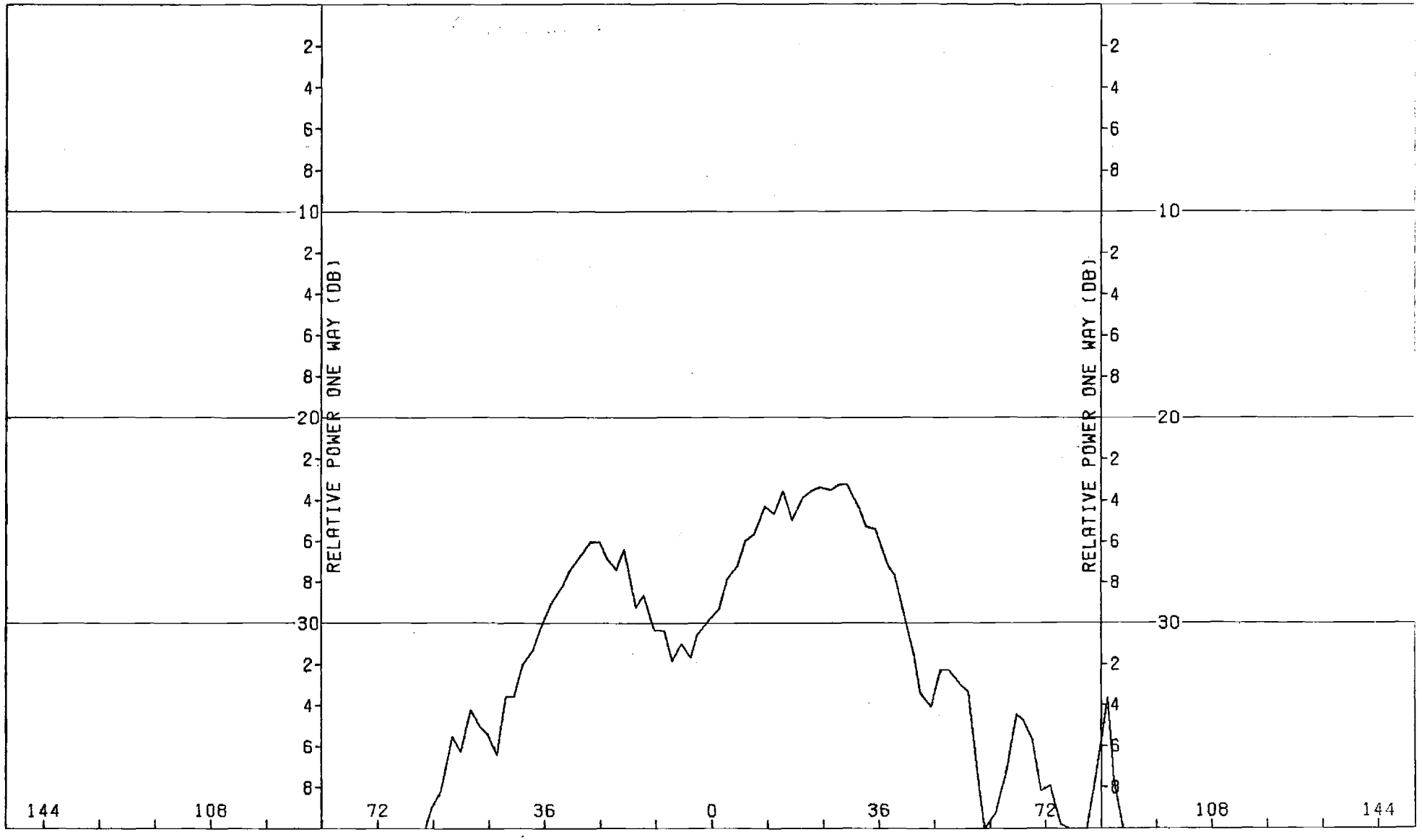

Figure A-6. Pattern of Small Array: H-Plane, Azimuth Difference, θ-Component, No Radome.

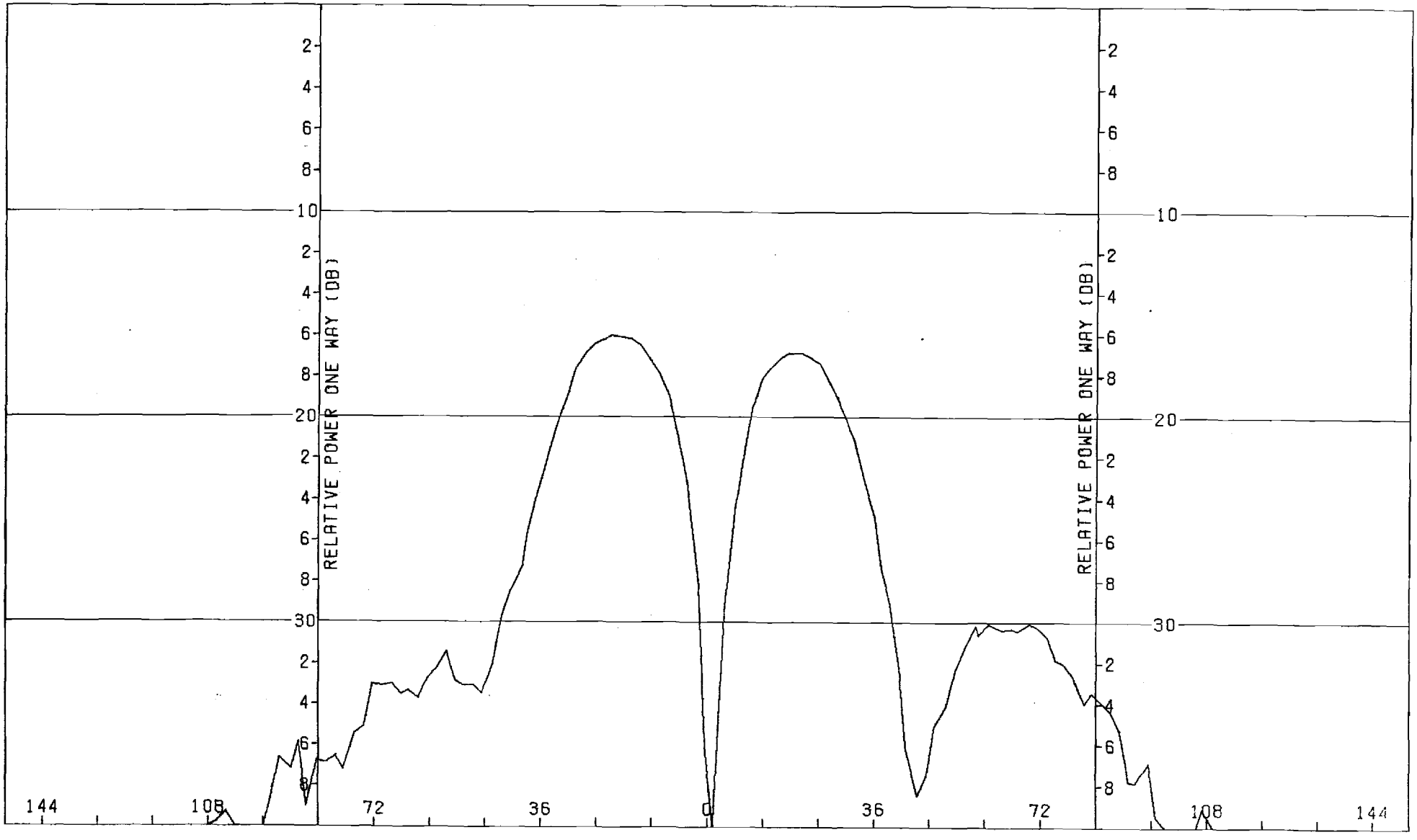

Figure A-7. Pattern of Small Array: E-Plane, Azimuth Difference, θ-Component, No Radome.

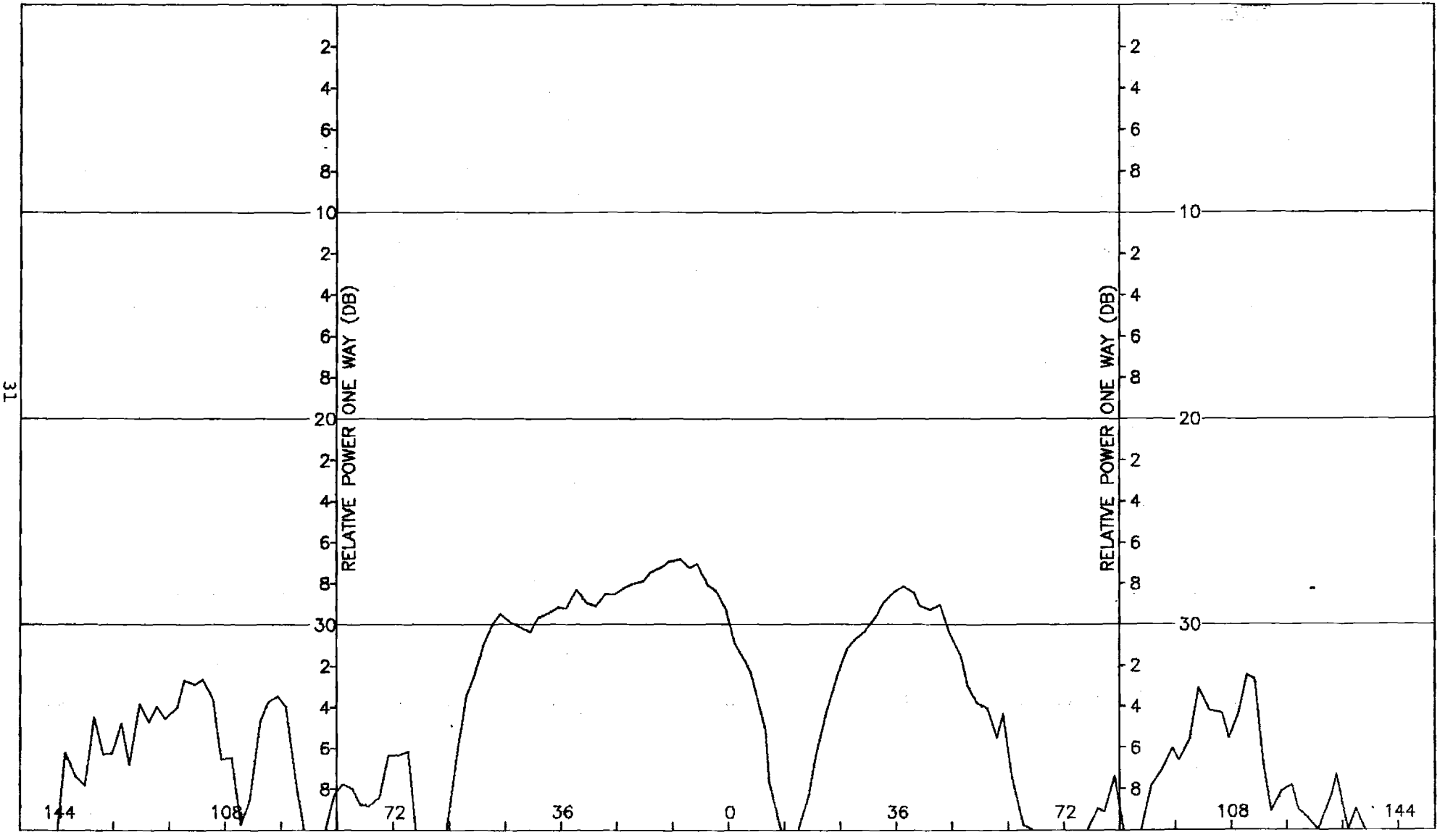

Figure A-8. Pattern of Small Array: E-Plane, Azimuth Difference, ϕ-Component, No Radome.

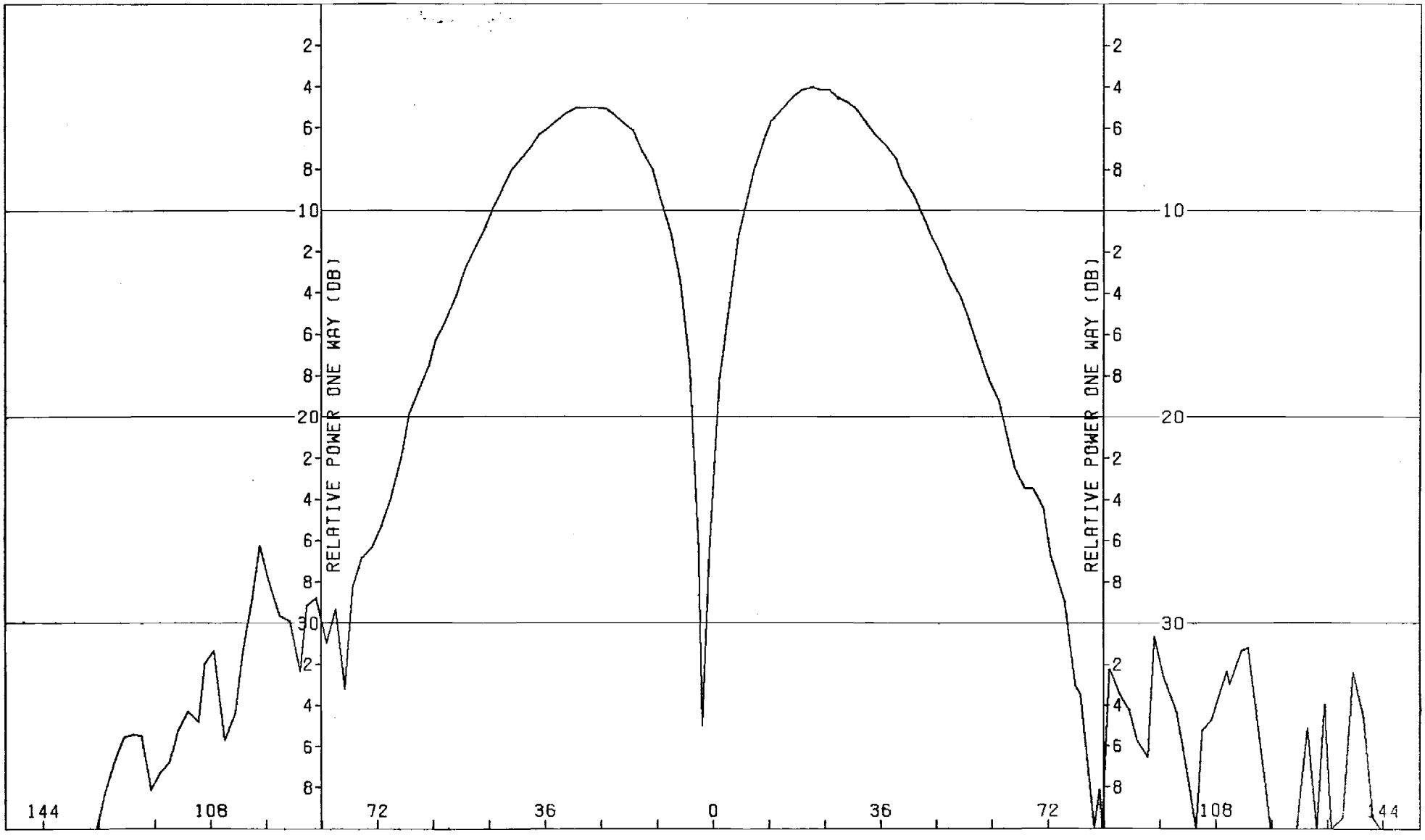

Figure A-9. Pattern of Small Array: E-Plane, Elevation Difference, θ-Component, No Radome.

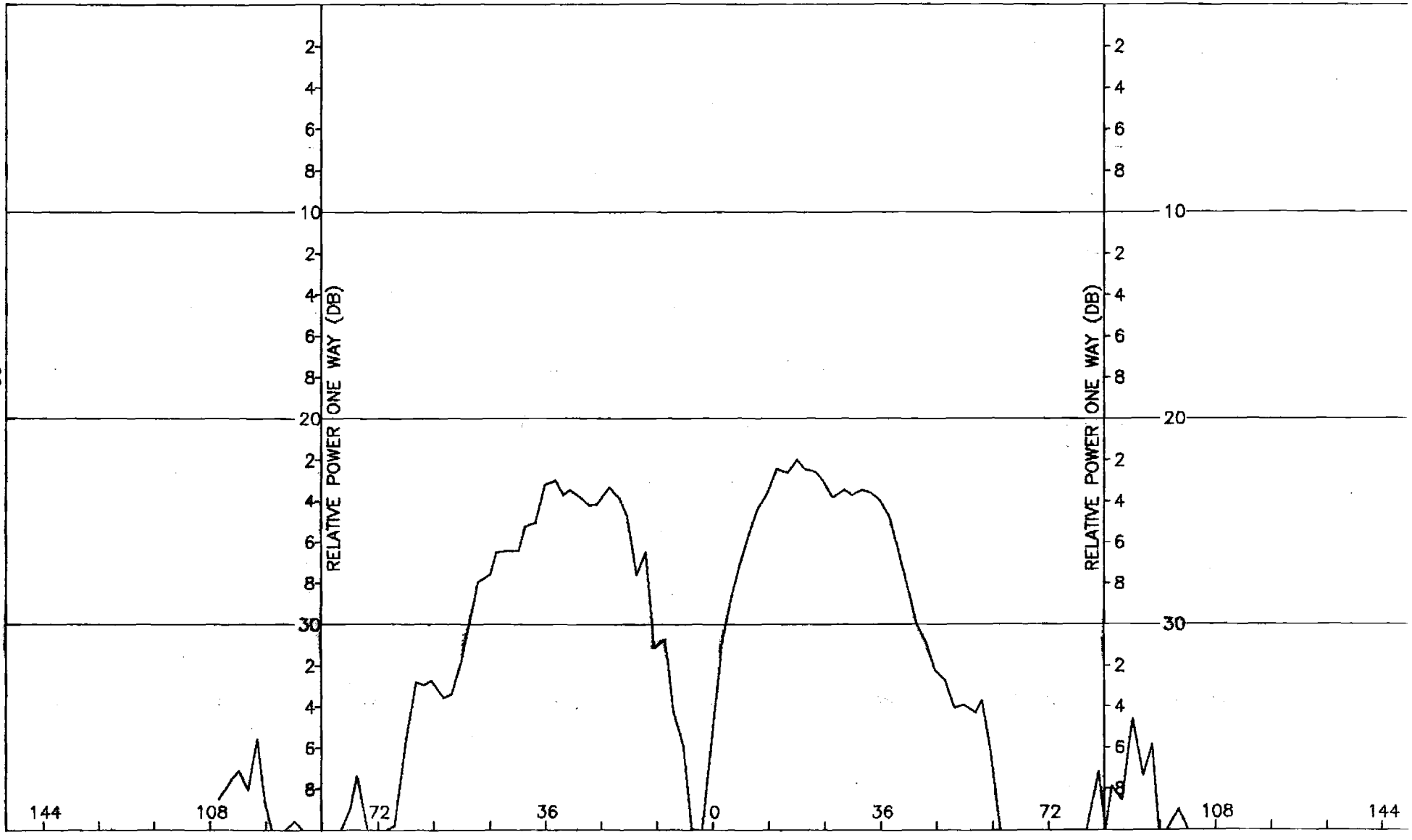

Figure A-10. Pattern of Small Array: E-Plane, Elevation Difference, ϕ-Component, No Radome.

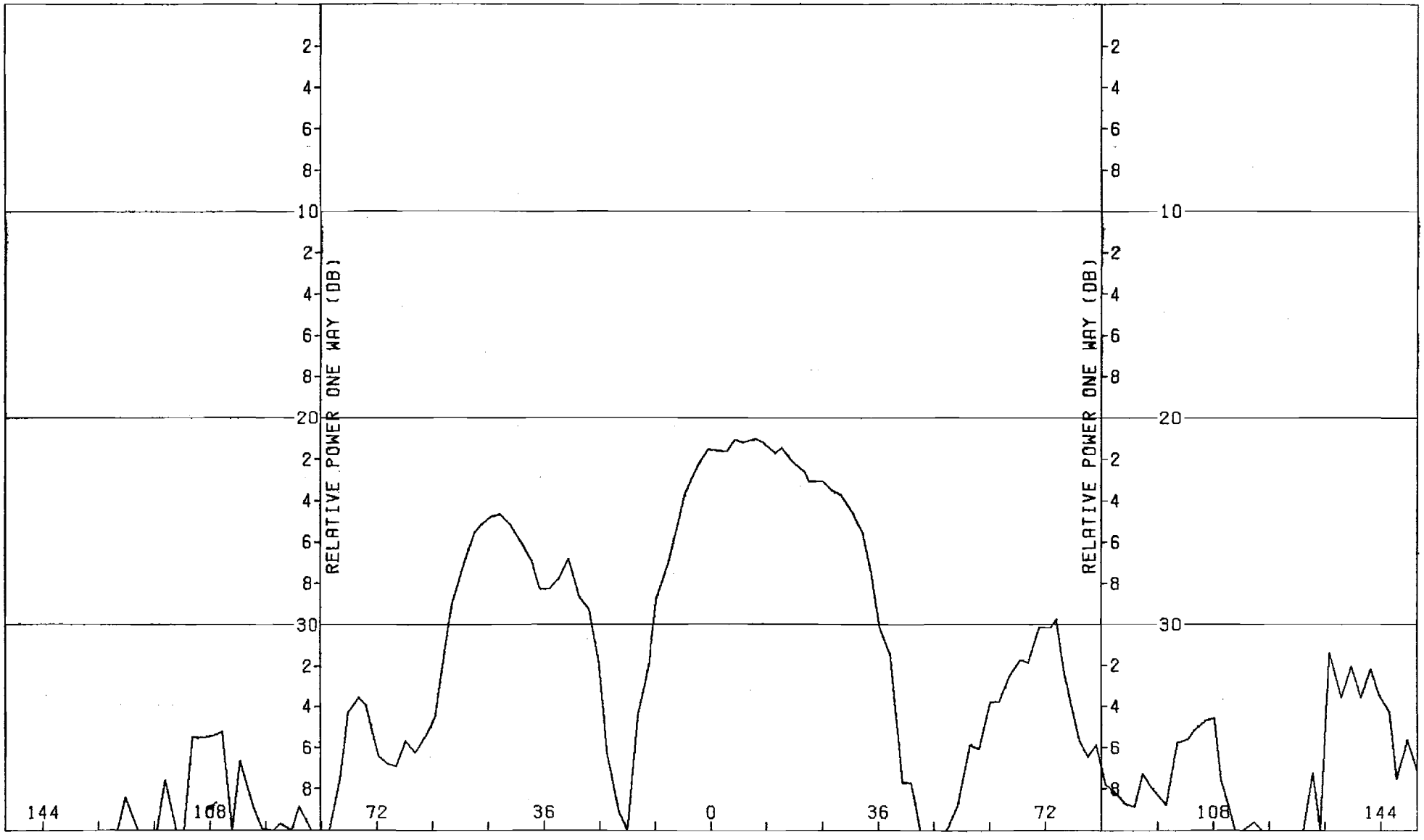

Figure A-11. Pattern of Small Array: H-Plane, Elevation Difference, ϕ-Component, No Radome.

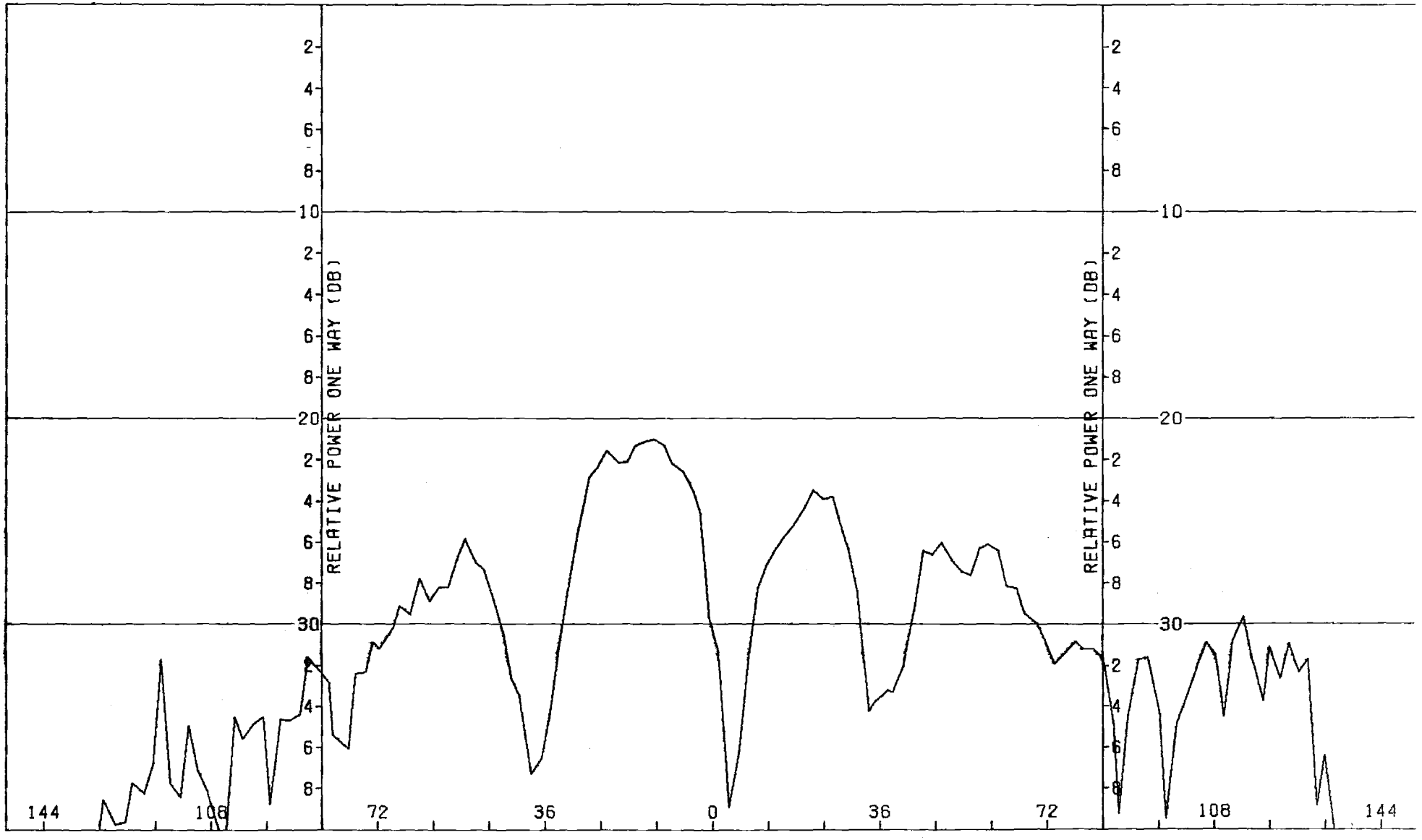

Figure A-12. Pattern of Small Array, H-Plane, Elevation Difference, θ-Component, No Radome.

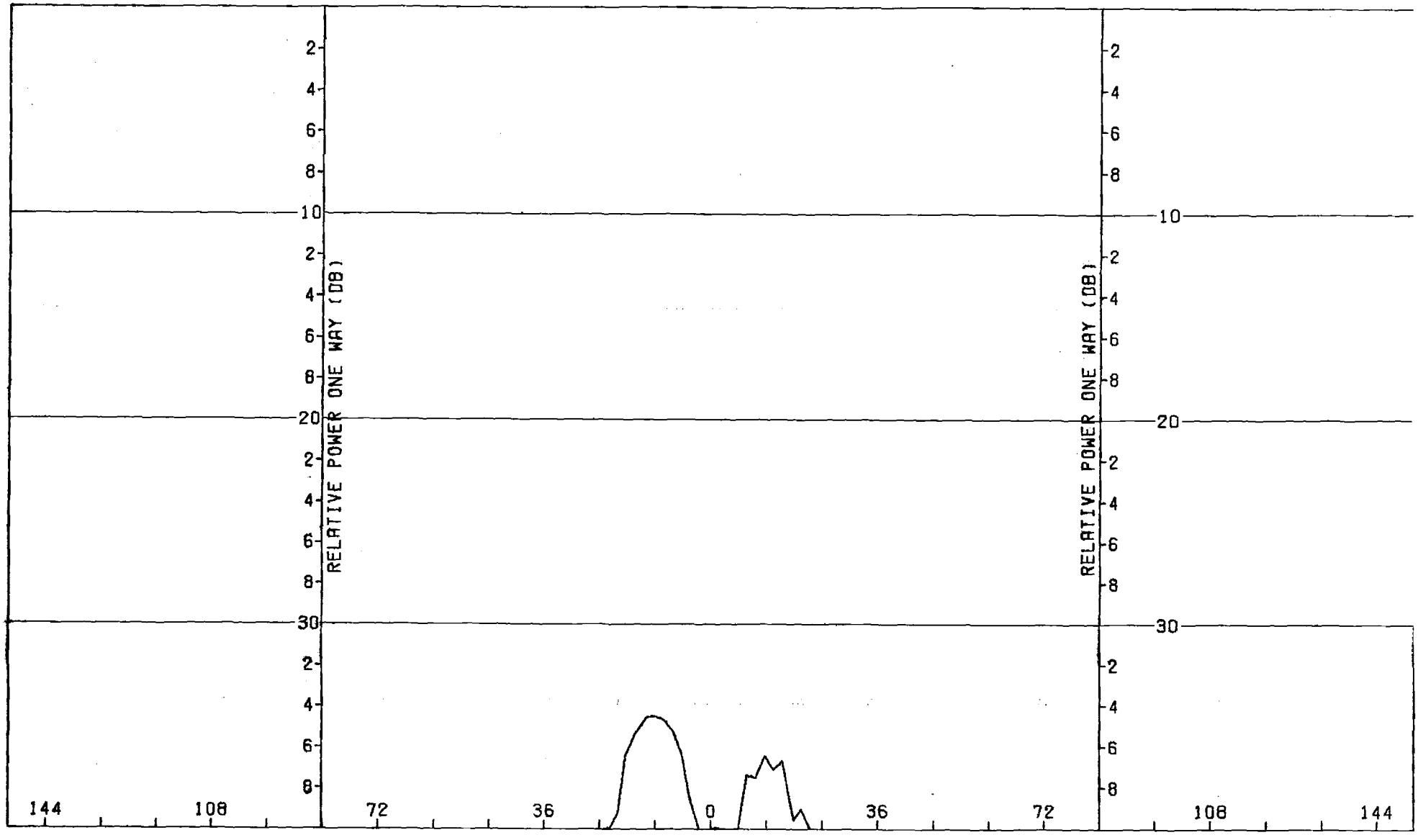

Figure B-6. Pattern of Medium Array: H-Plane, Azimuth Difference, ϕ-Component, No Radome

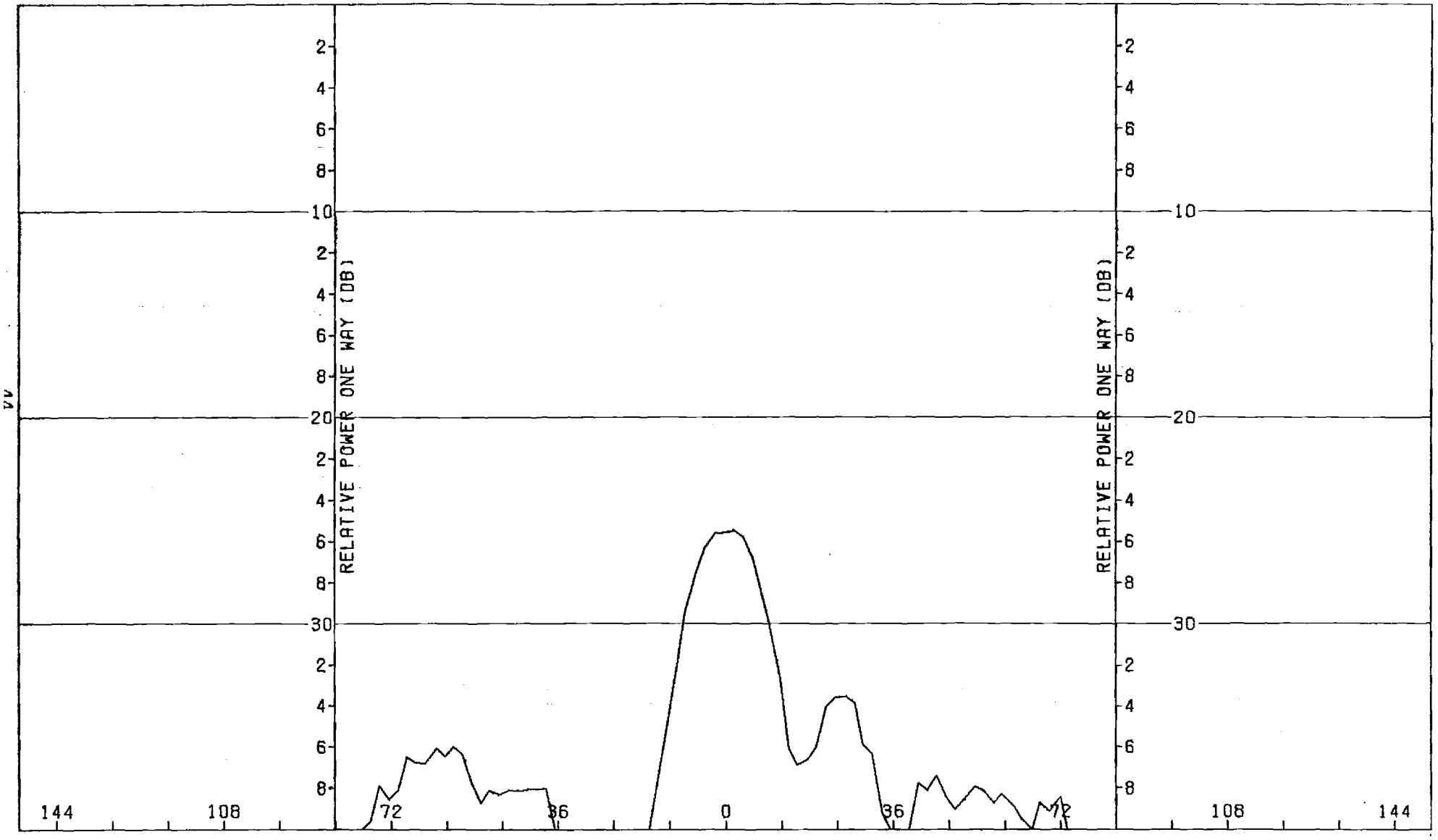

Figure B-7. Pattern of Medium Array: E-Plane, Azimuth Difference, θ-Component, No Radome

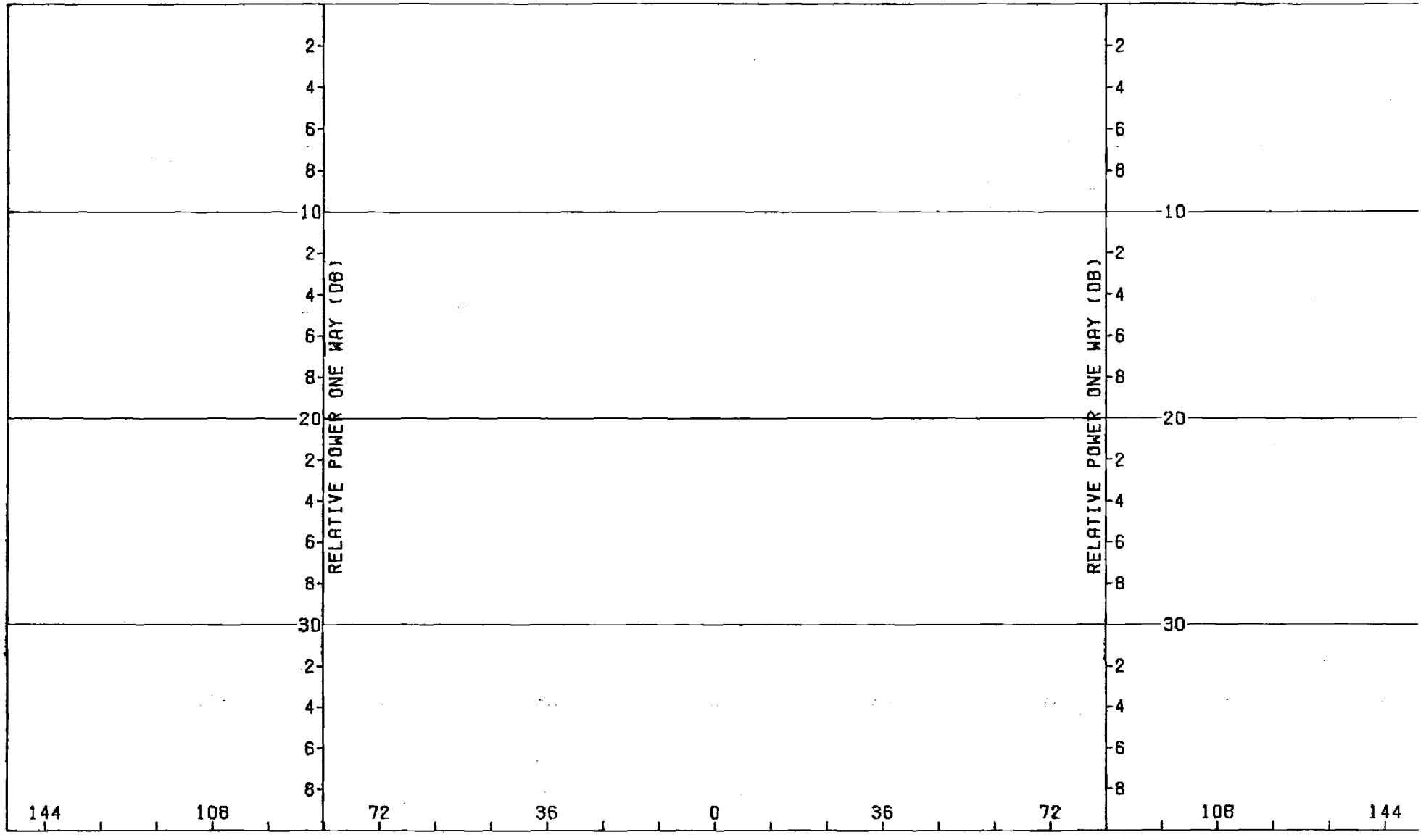

Figure B-8. Pattern of Medium Array: E-Plane, Azimuth Difference, ϕ-Component, No Radome

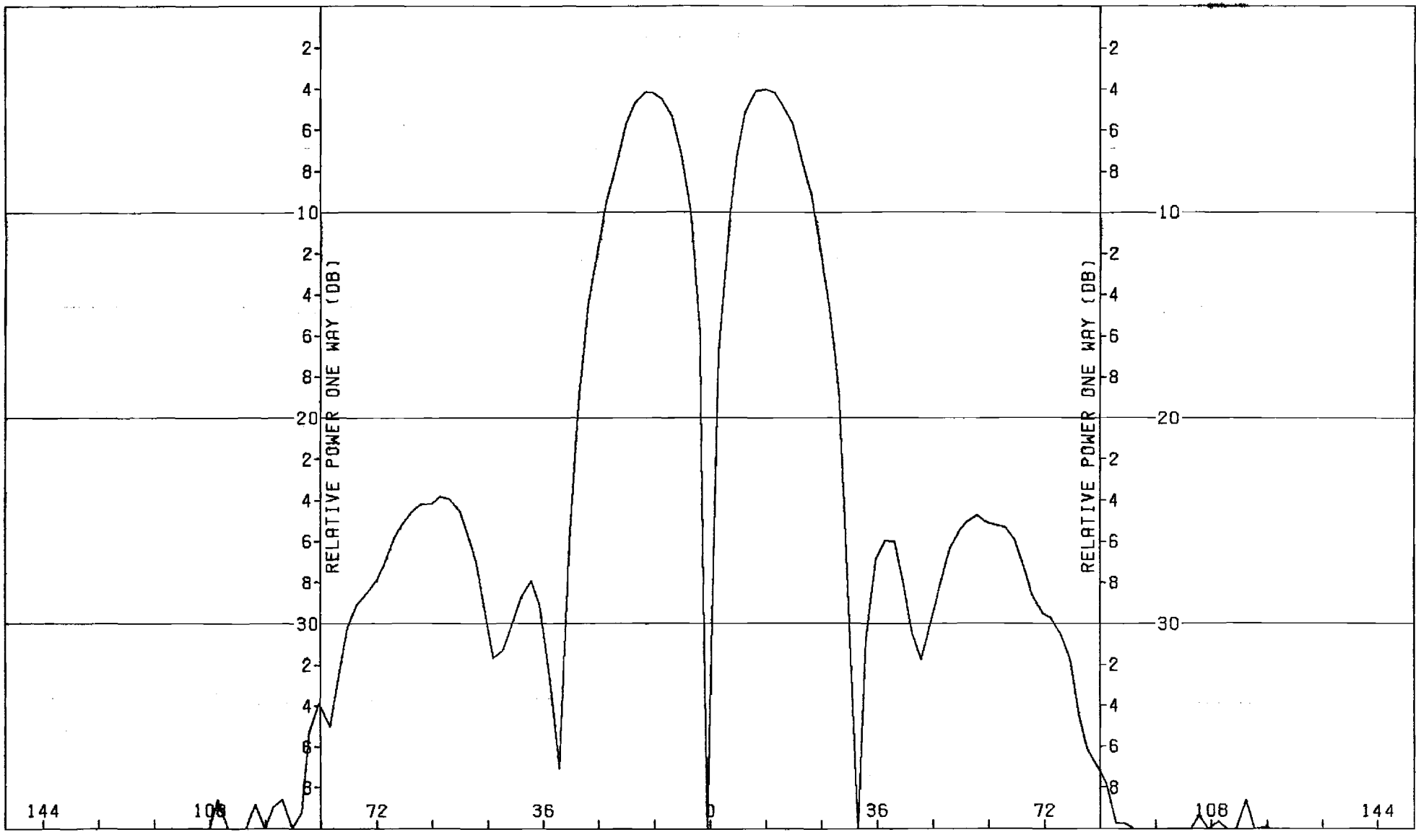

Figure B-9. Pattern of Small Array: E-Plane, Elevation Difference, θ-Component, No Radome

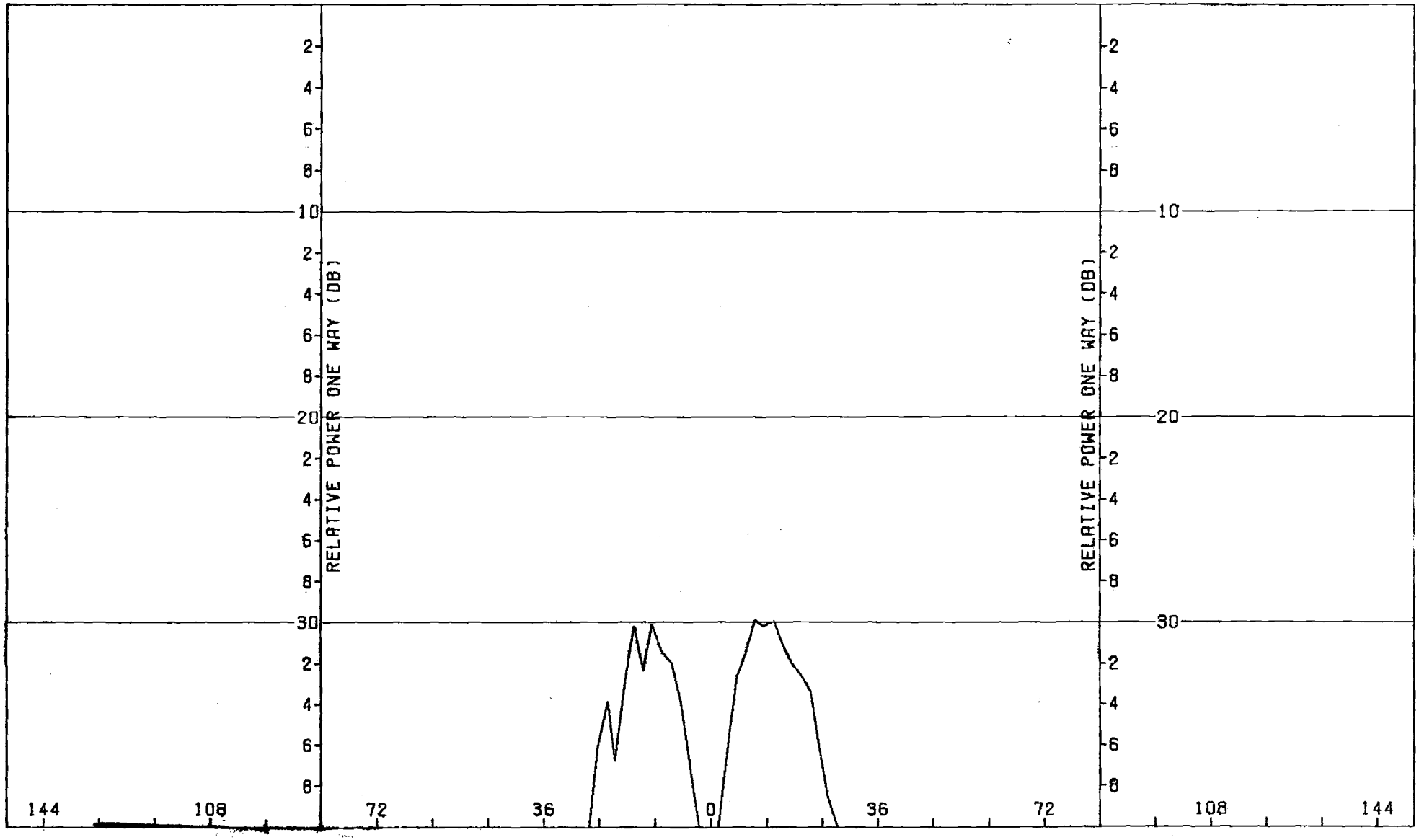

Figure B-10. Pattern of Medium Array: Elevation Difference, ϕ-Component, No Radome

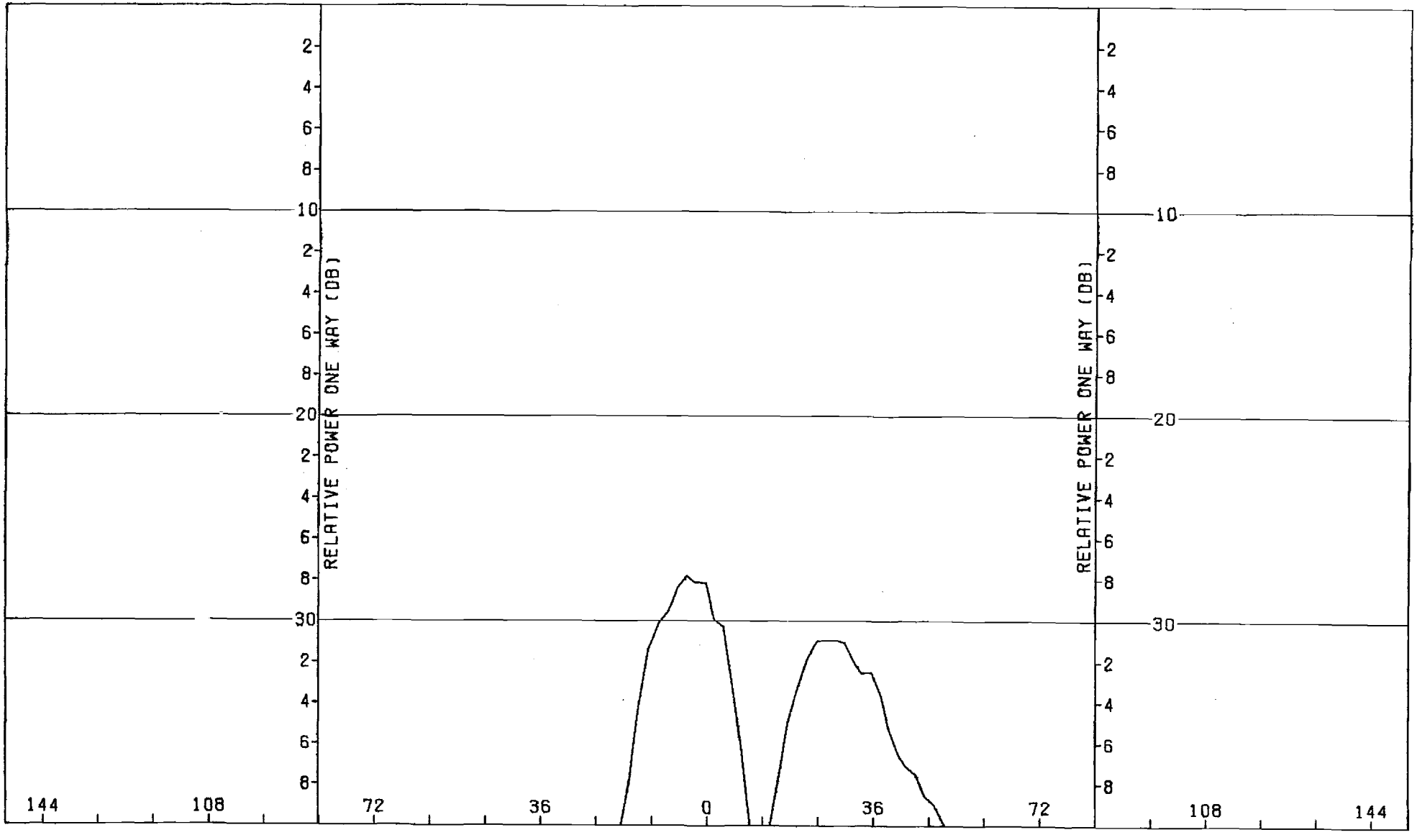

Figure B-11. Pattern of Medium Array: H-Plane, Elevation Difference, ϕ-Component, No Radome

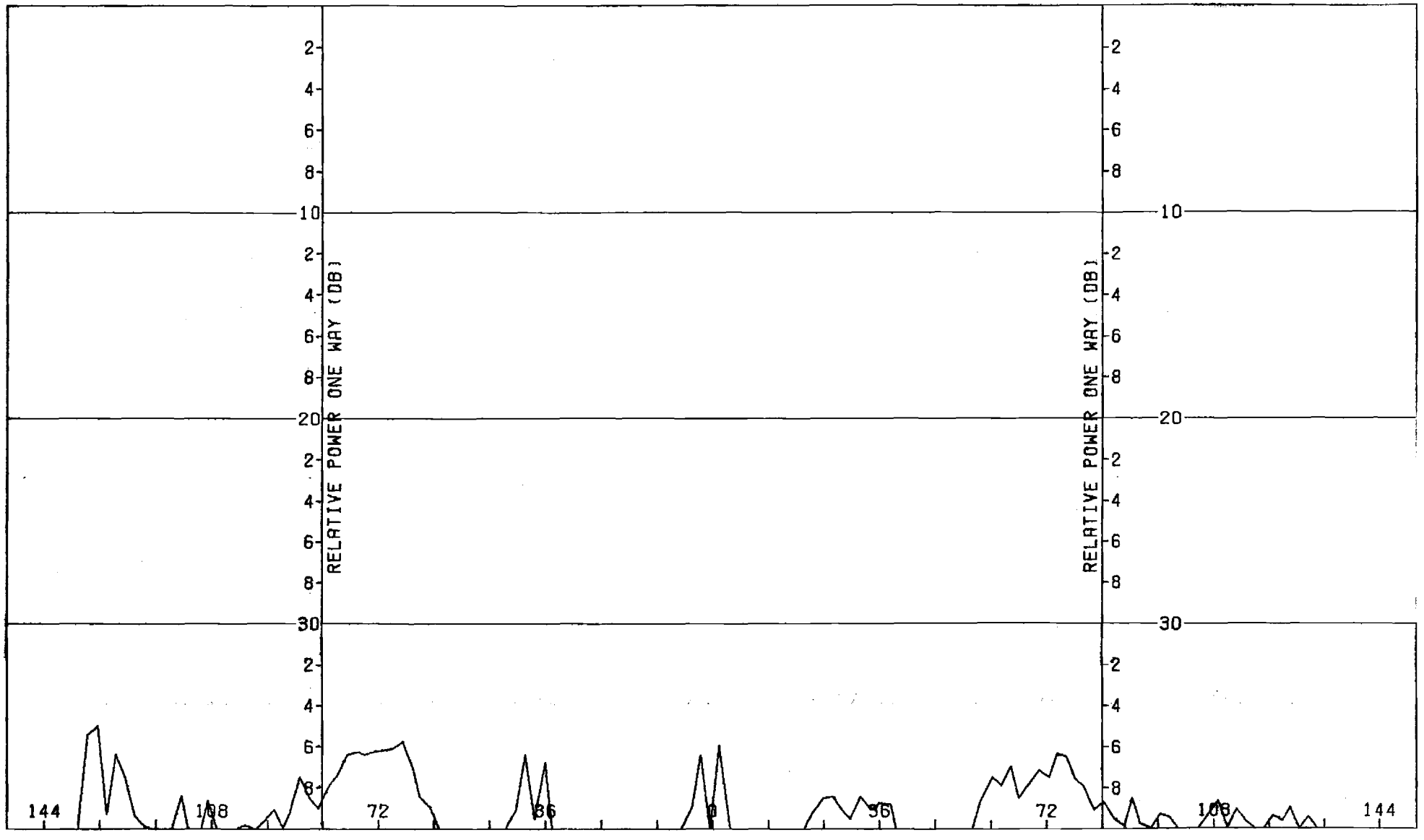

Figure B-12. Pattern of Medium Array: H-Plane, Elevation Difference, θ-Component, No Radome

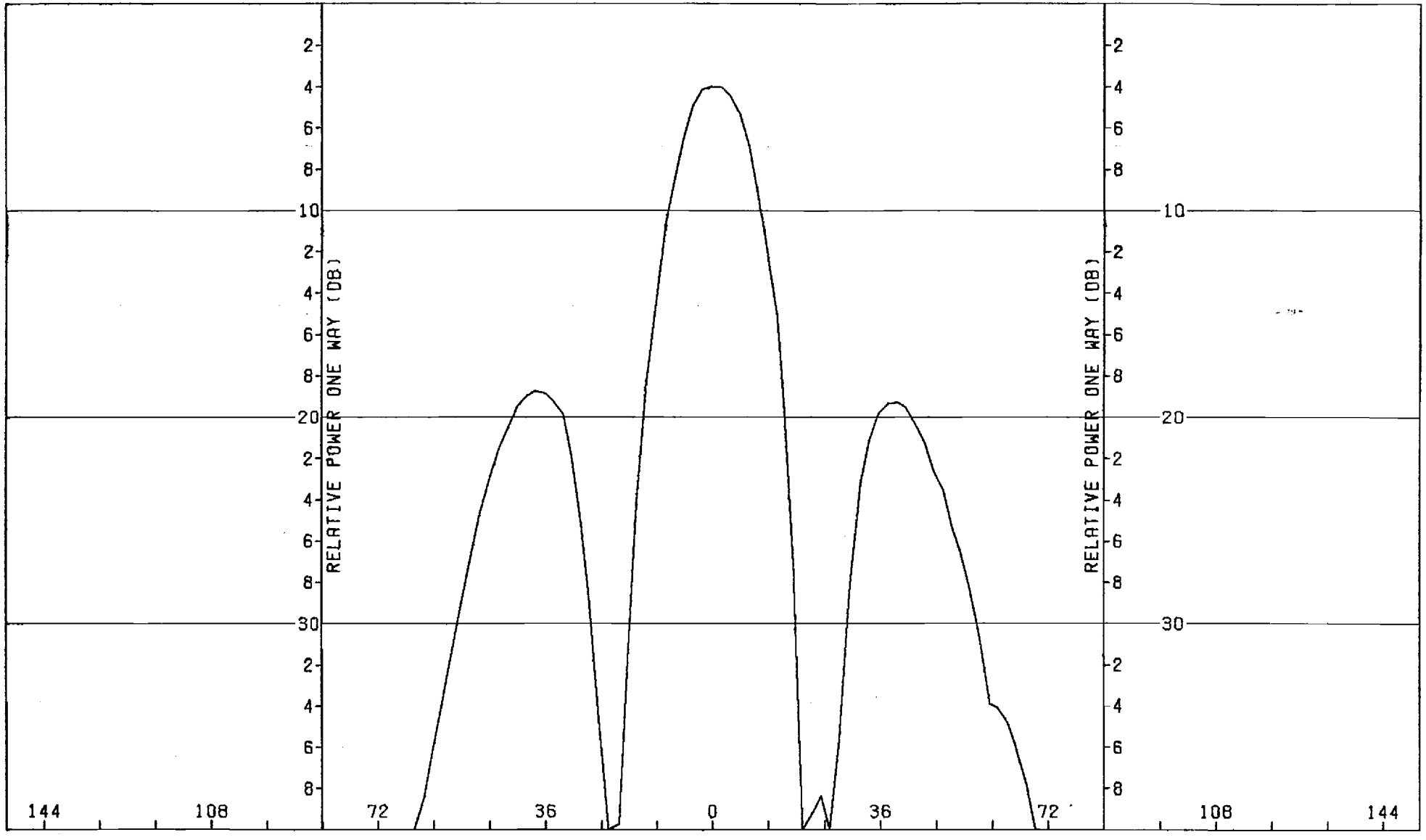

Figure B-13. Pattern of Medium Array: ϕ=45° Plane, Sum, θ-Component, No Radome

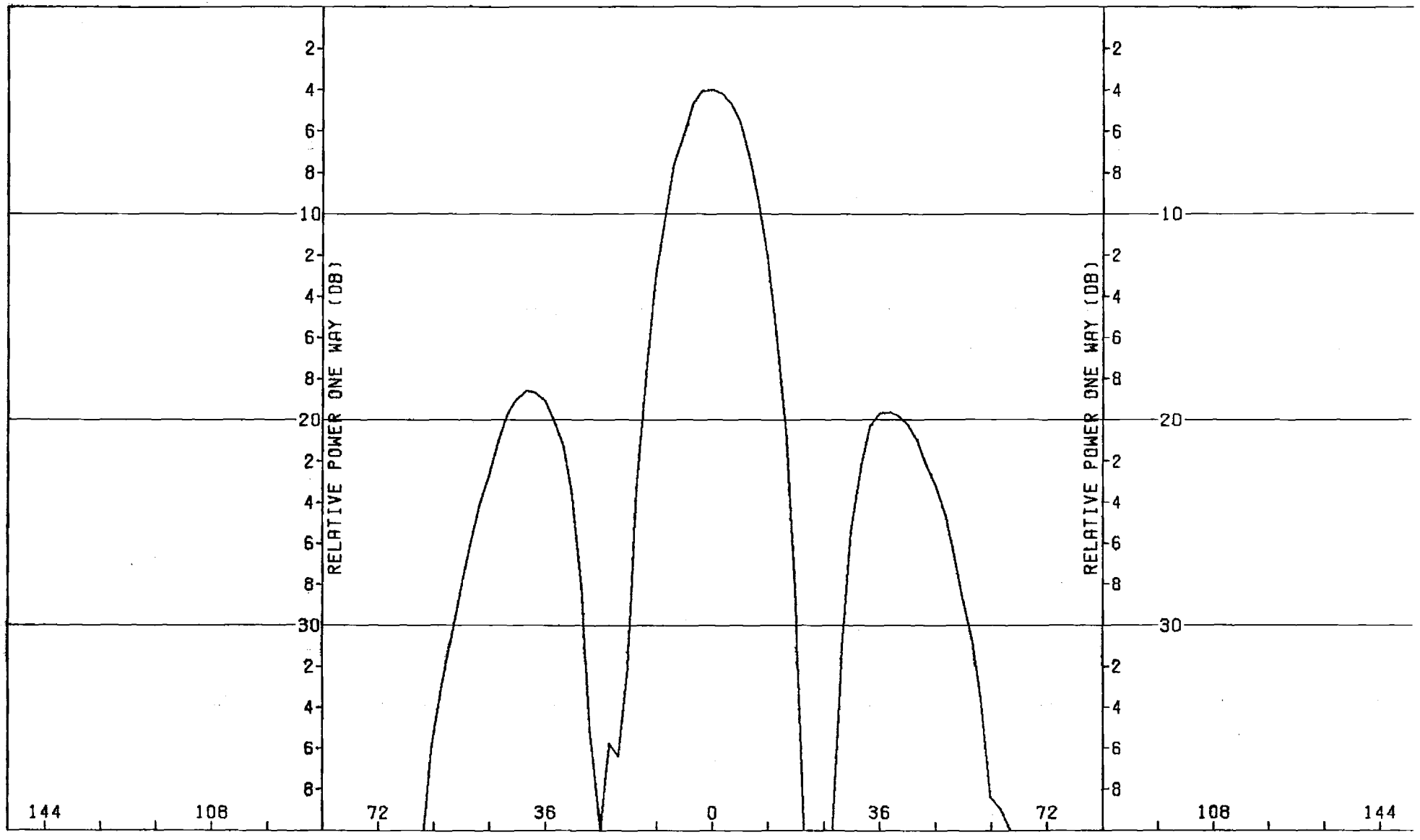

Figure B-14. Pattern of Medium Array: ϕ=45° Plane, Sum, ϕ-Component, No Radome

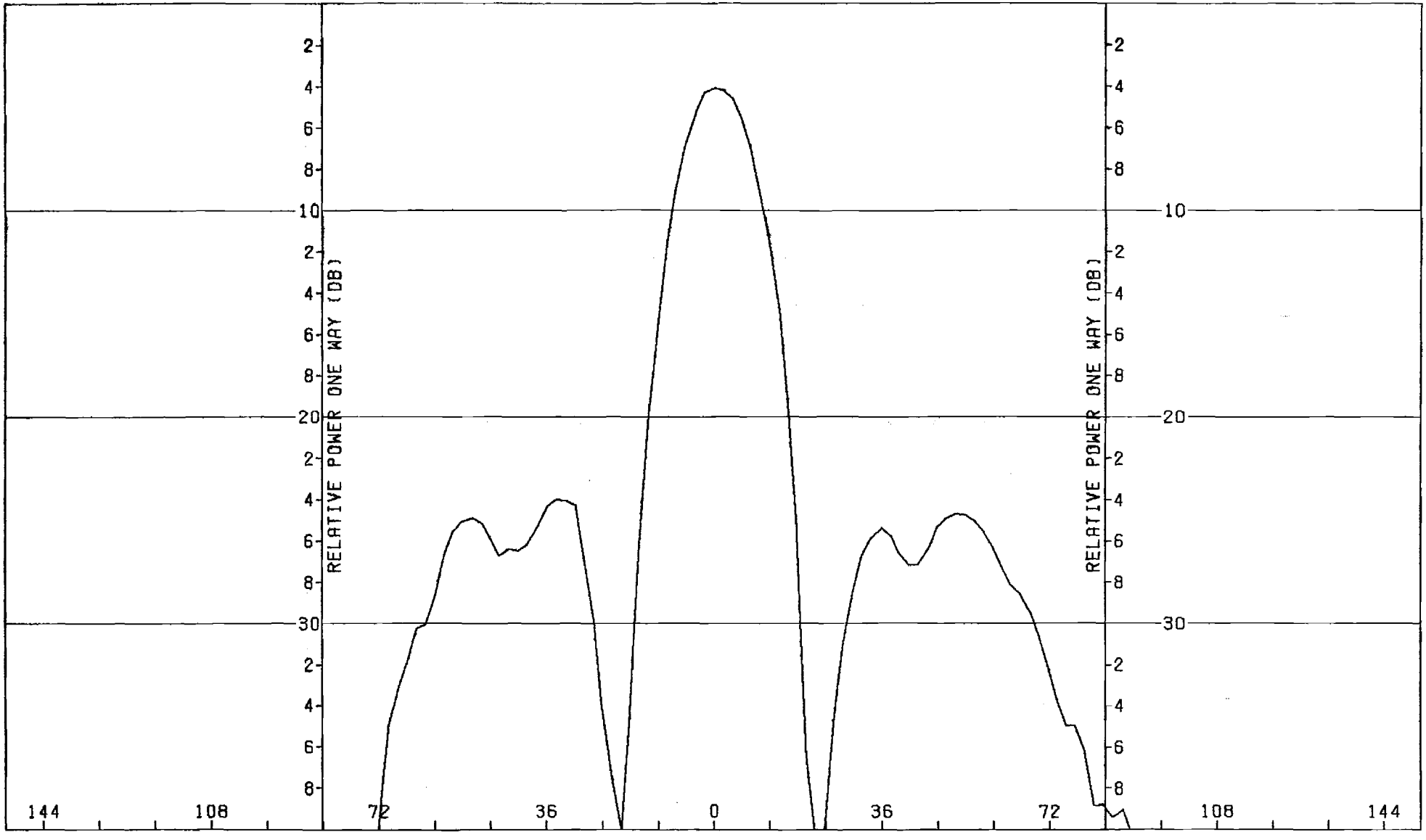

Figure B-15. Pattern of Medium Array: ϕ=-45° Plane, Sum, θ-Component, No Radome

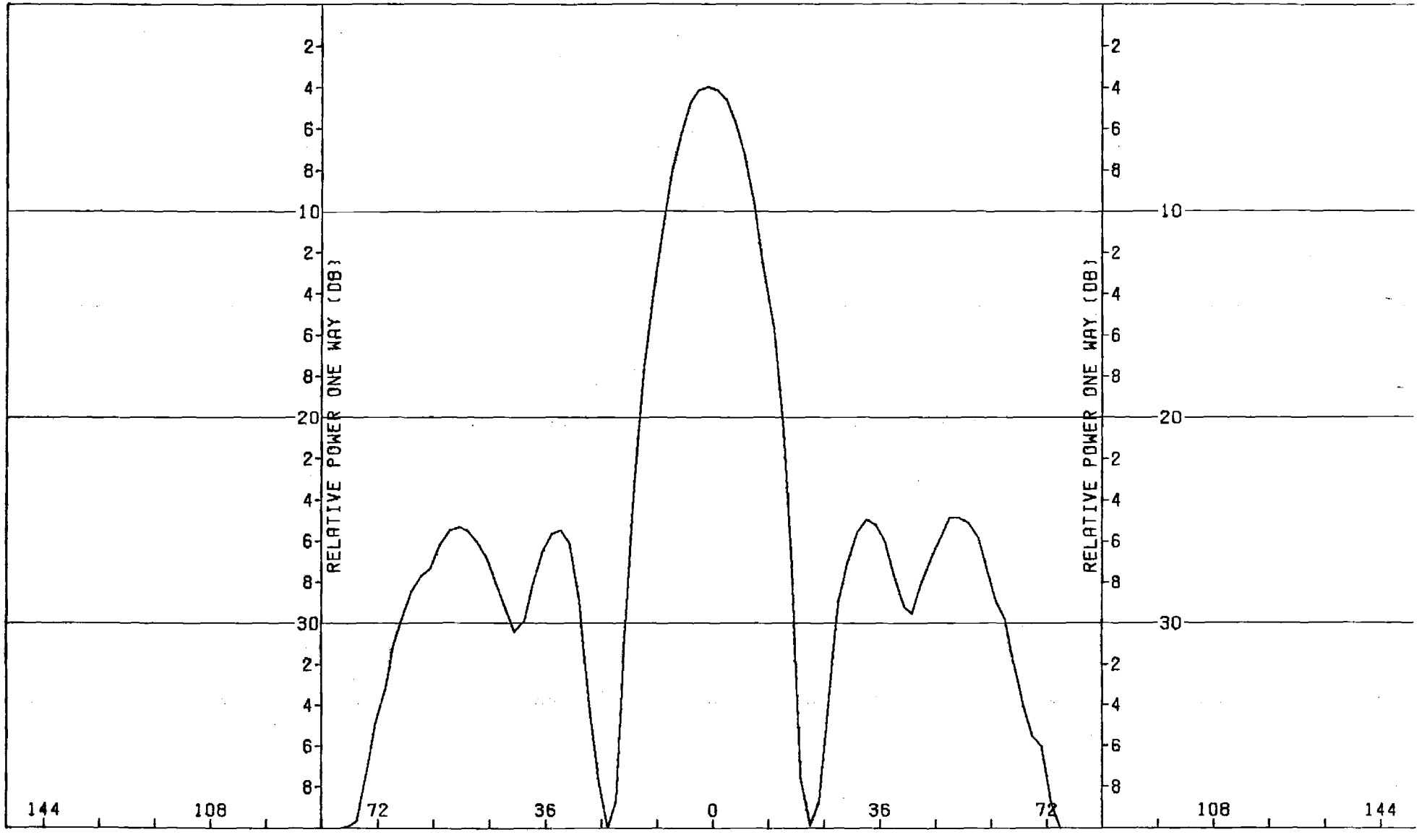

Figure B-16. Pattern of Medium Array: ϕ=-45° Plane, Sum, ϕ-Component, No Radome

APPENDIX C

Antenna Patterns of Large Array Without Radome

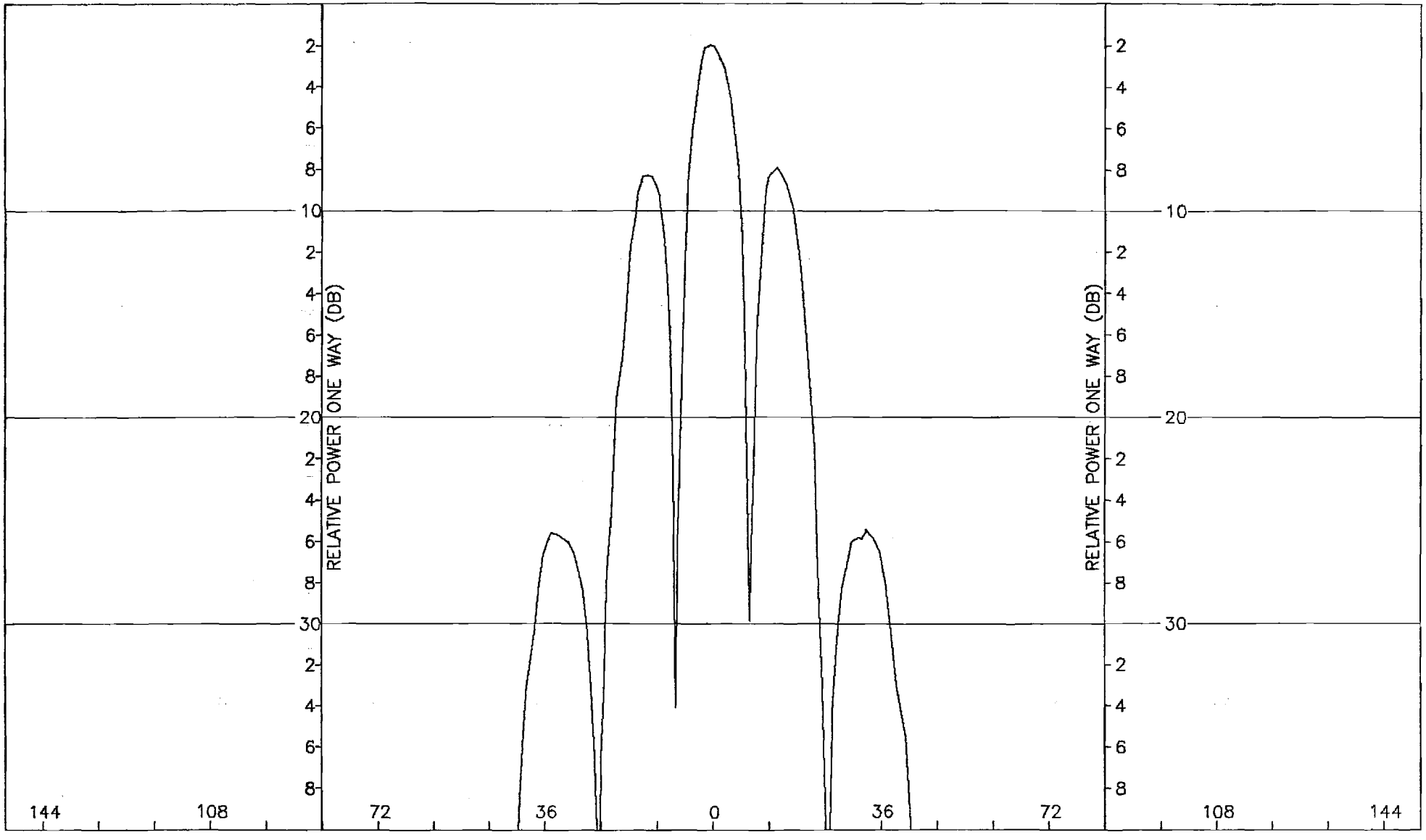

Figure C-1. Pattern of Large Array: H-Plane Sum, ϕ-Component, No Radome

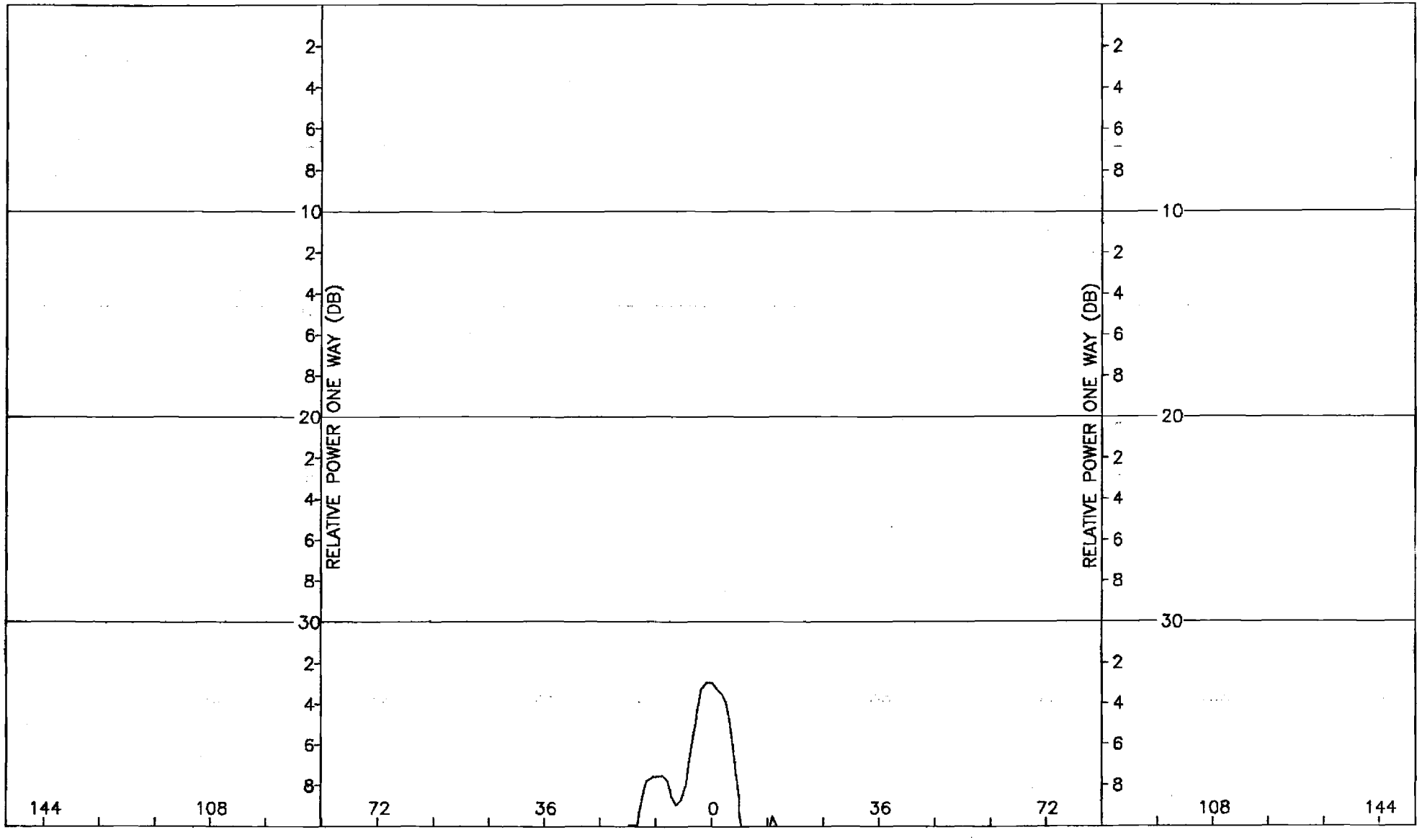

Figure C-2. Pattern of Large Array: H-Plane Sum, θ-Component, No Radome

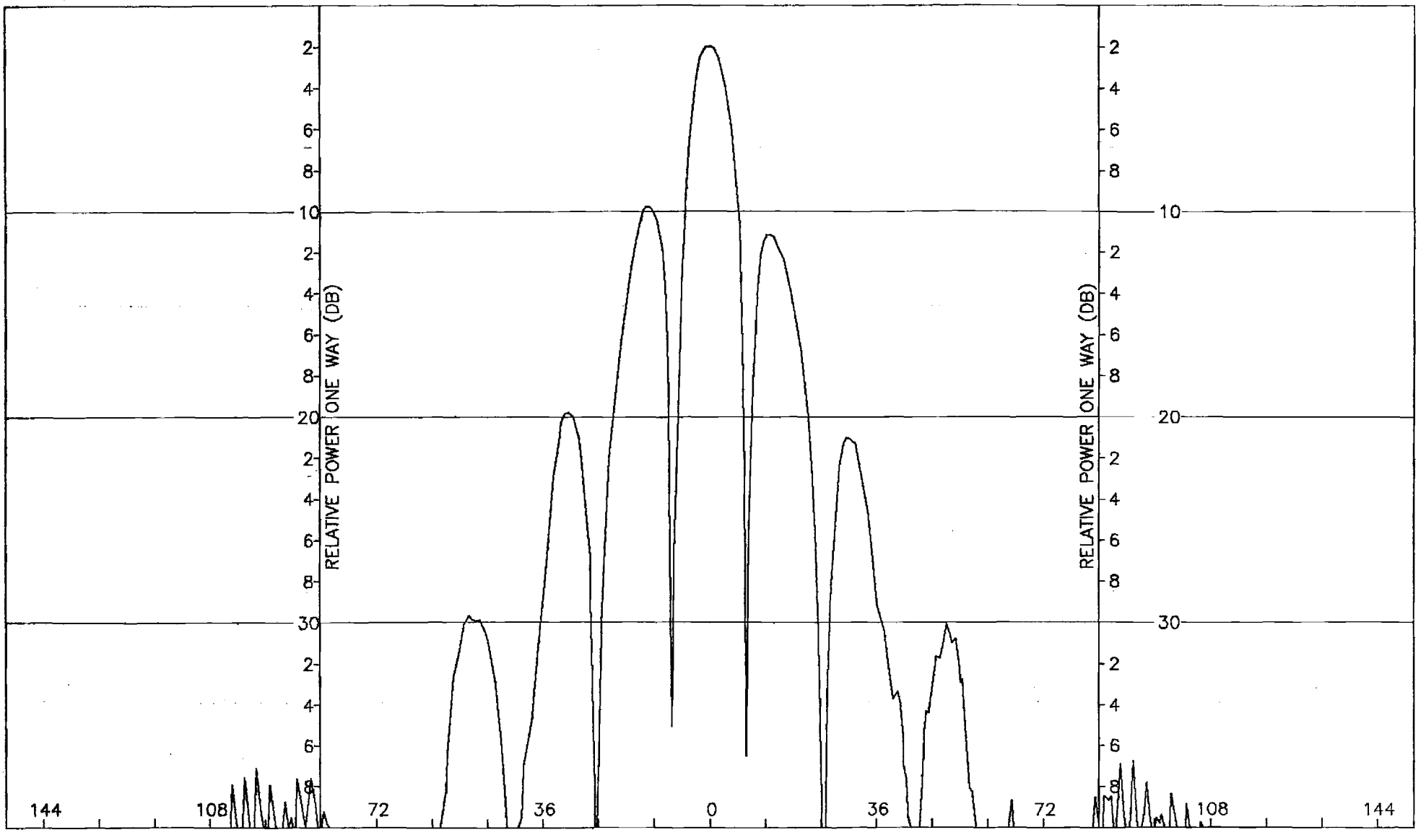

Figure C-3. Pattern of Large Array: E-Plane, Sum, θ-Component, No Radome

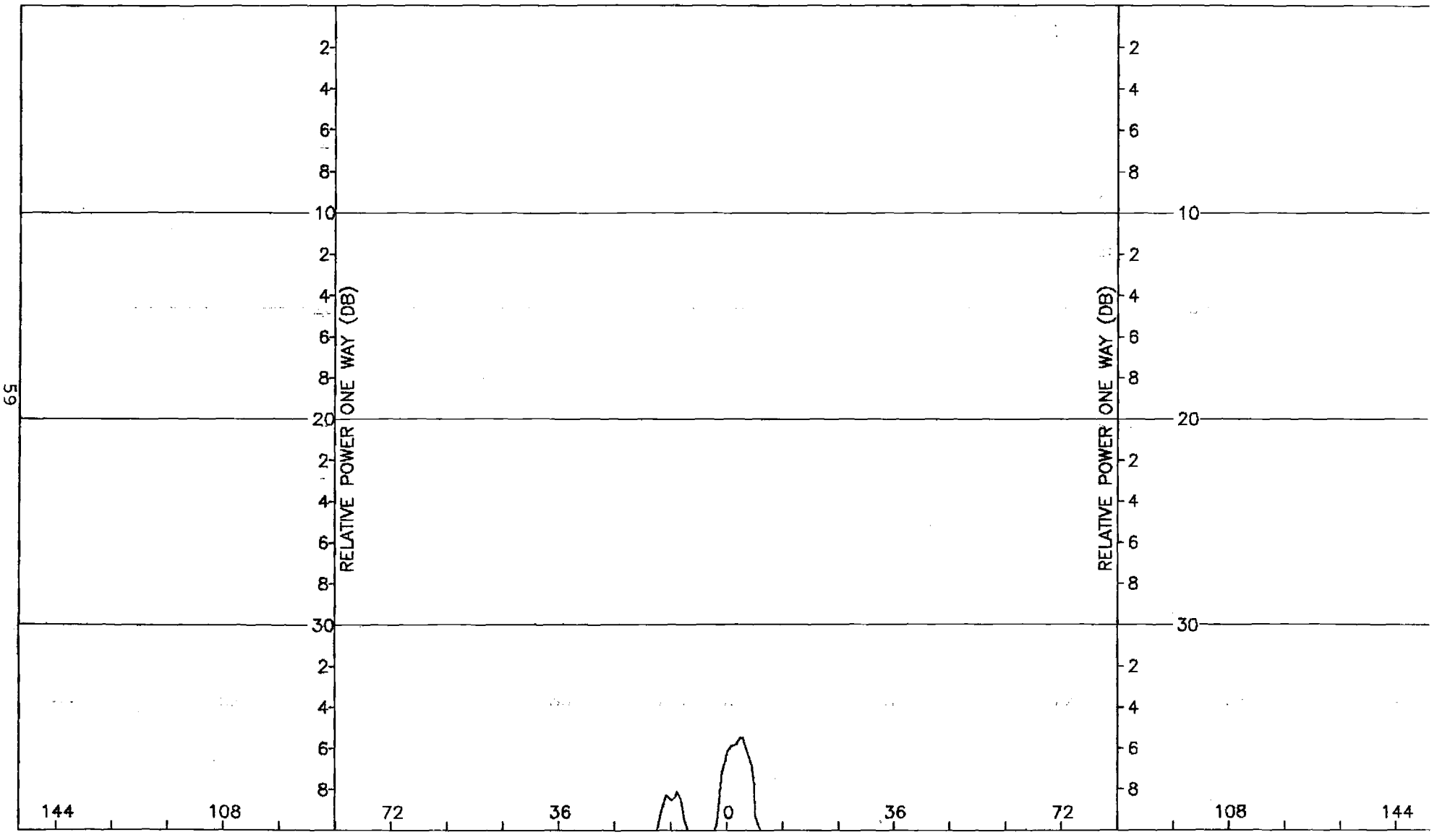

Figure C-4. Pattern of Large Array: E-Plane, Sum, θ-Component, No Radome

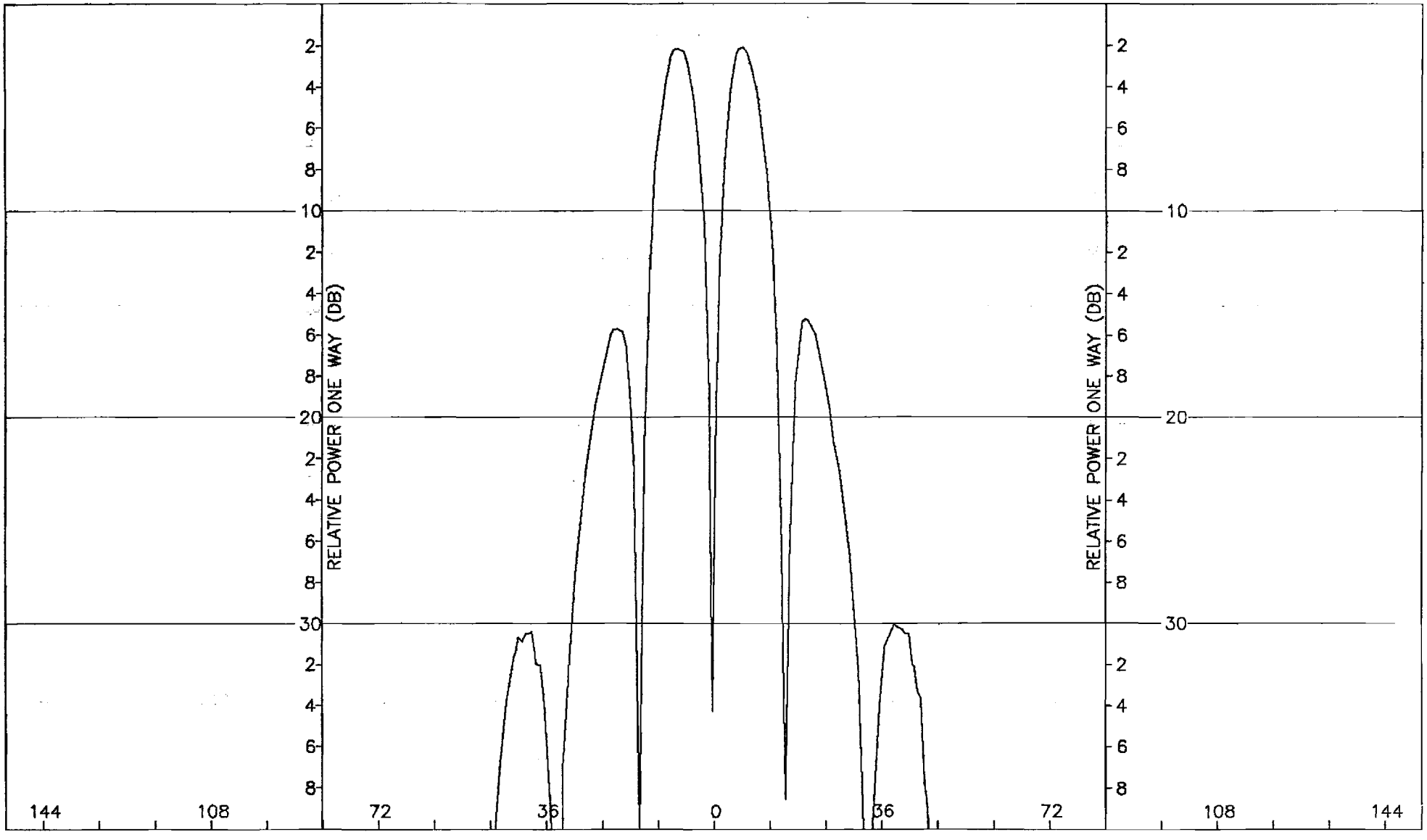

Figure C-5. Pattern of Large Array: H-Plane, Azimuth Differene, ϕ-Component, No Radome

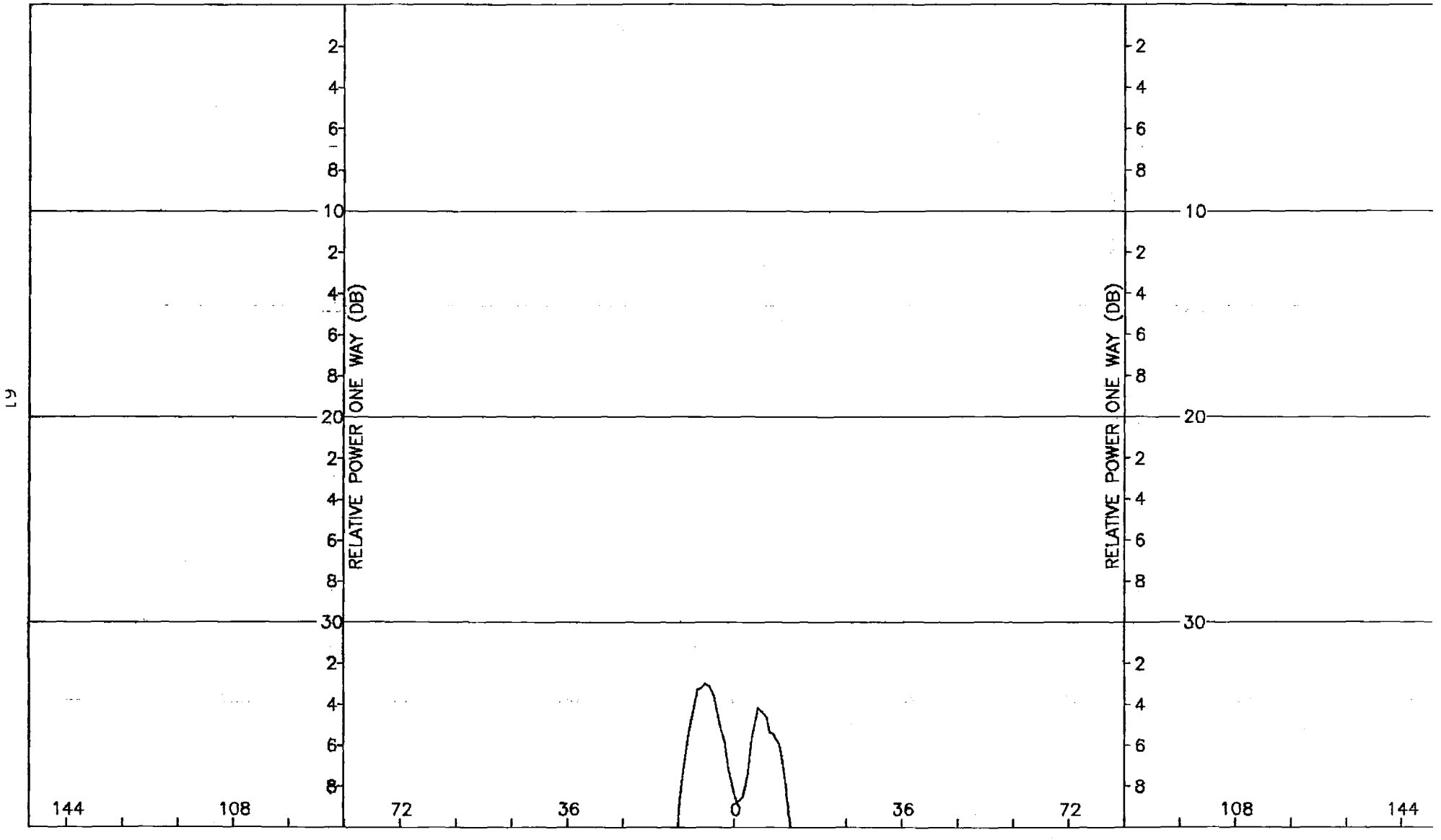

Figure C-6. Pattern of Large Array: H-Plane, Azimuth Difference, ϕ-Component, No Radome

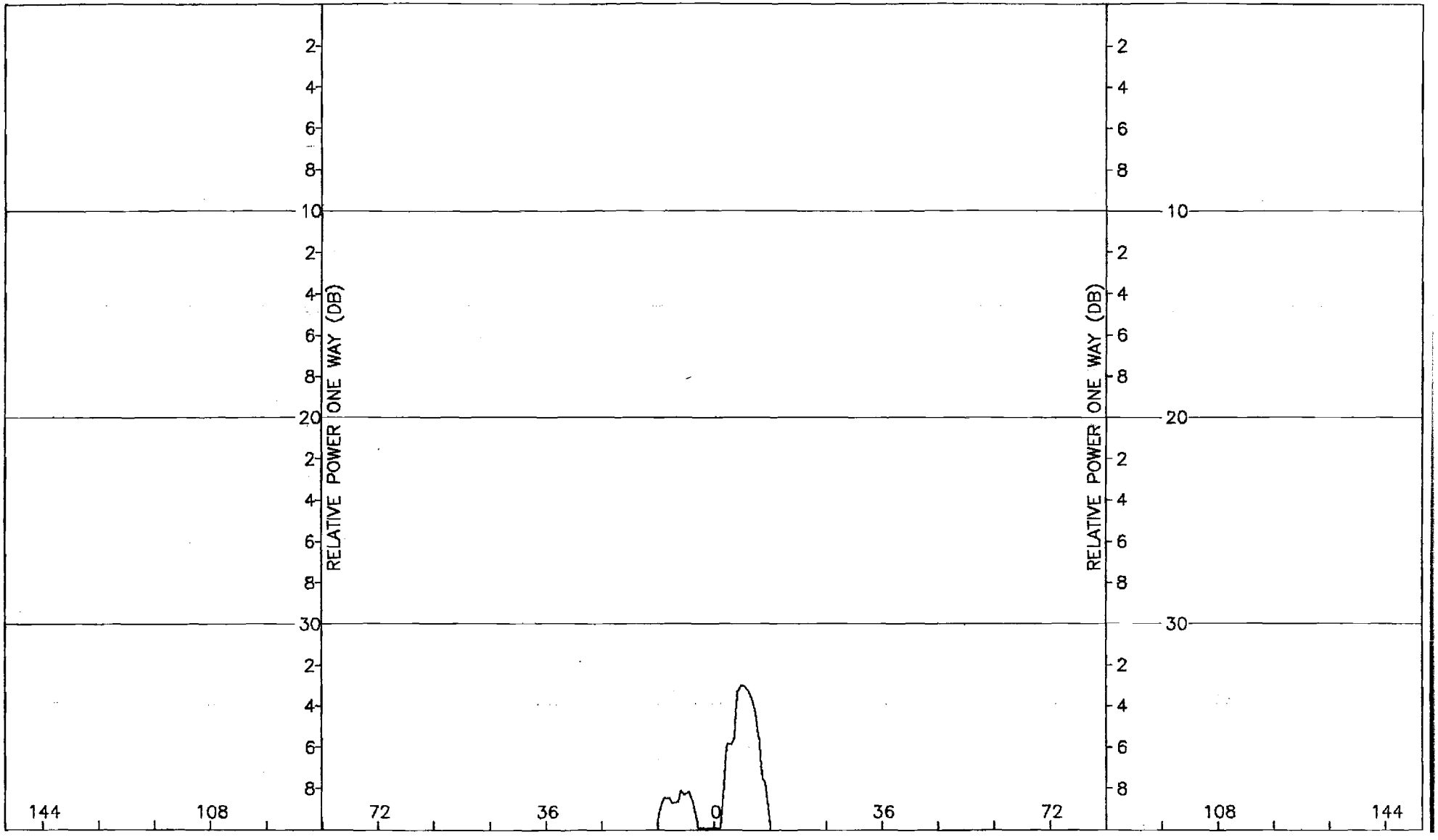

Figure C-7. Pattern of Large Array: E-Plane, Azimuth Difference, θ-Component, No Radome

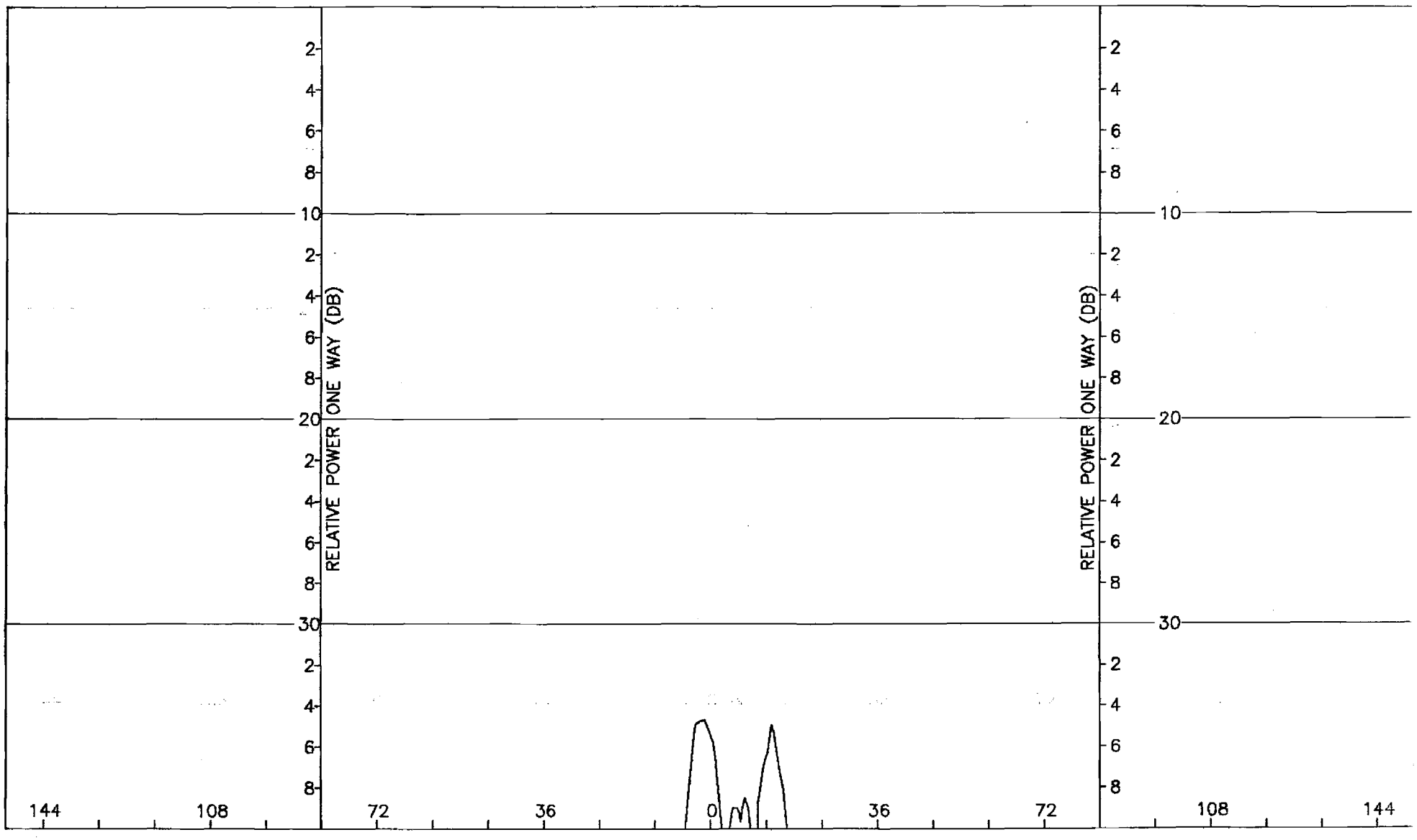

Figure C-8. Pattern of Large Array: E-Plane, Azimuth Difference, ϕ-Component, No Radome

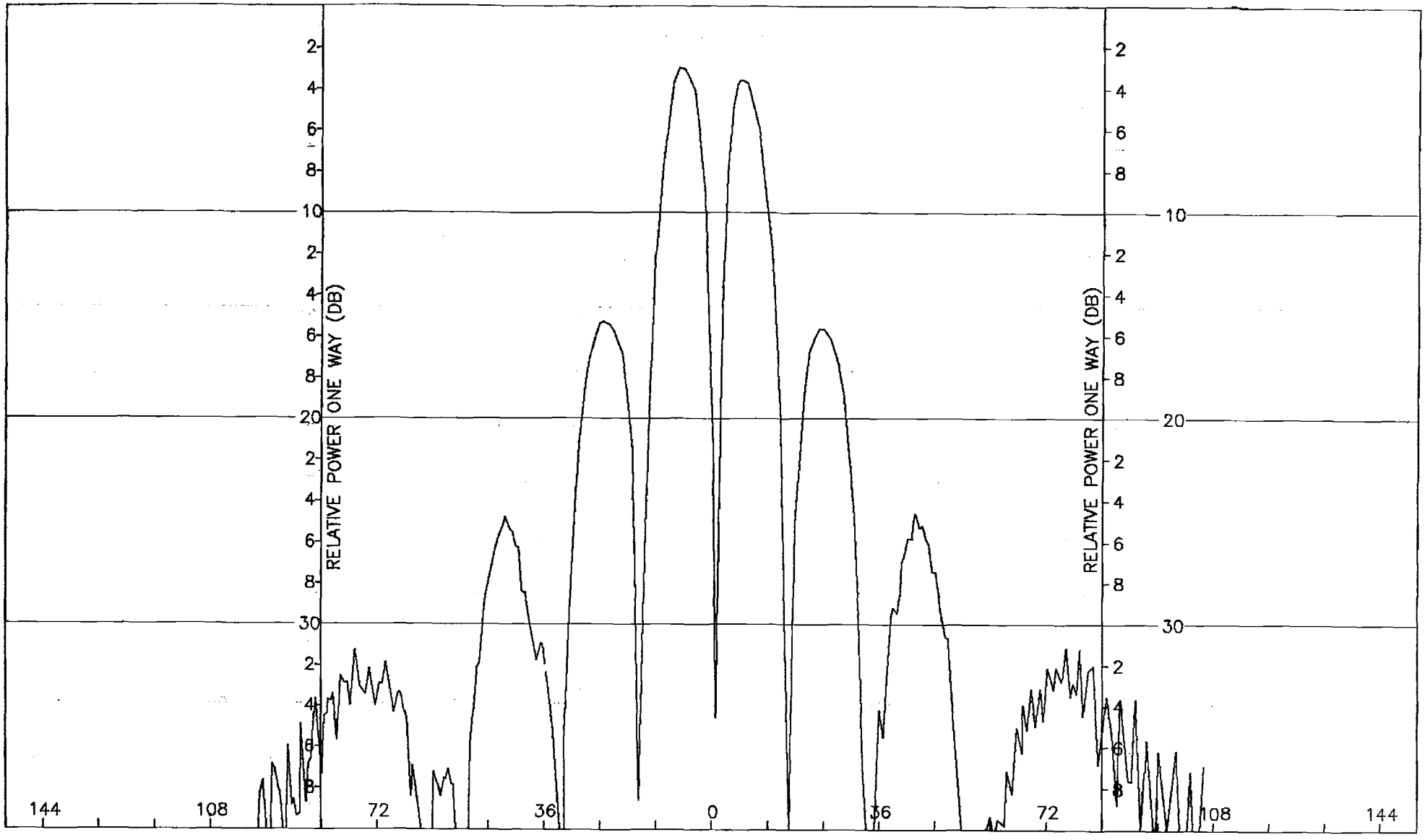

Figure C-9. Pattern of Large Array: E-Plane, Elevation Difference, θ-Component, No Radome

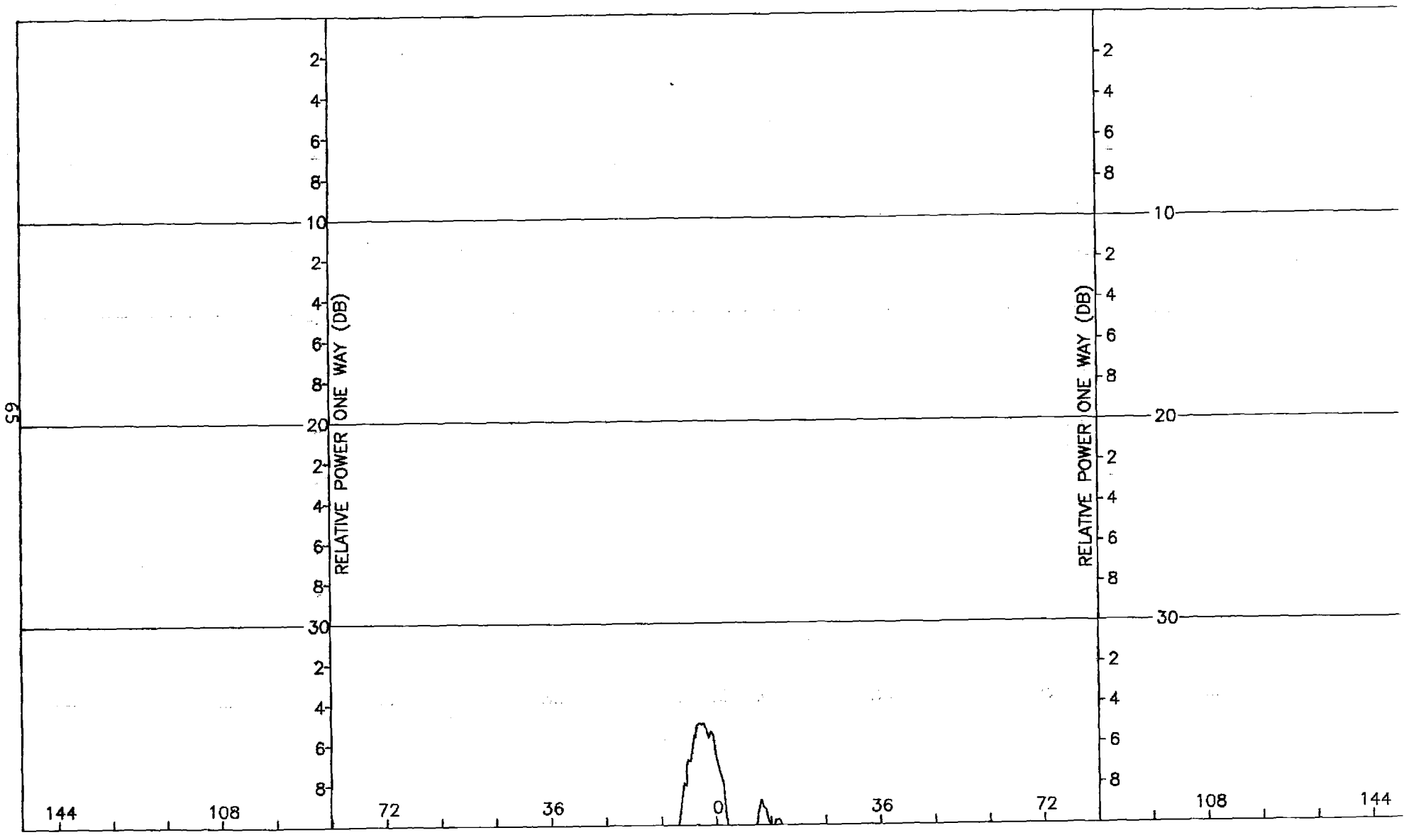

Figure C-10. Pattern of Large Array: E-Plane, Elevation Difference, ϕ-Component, No Radome

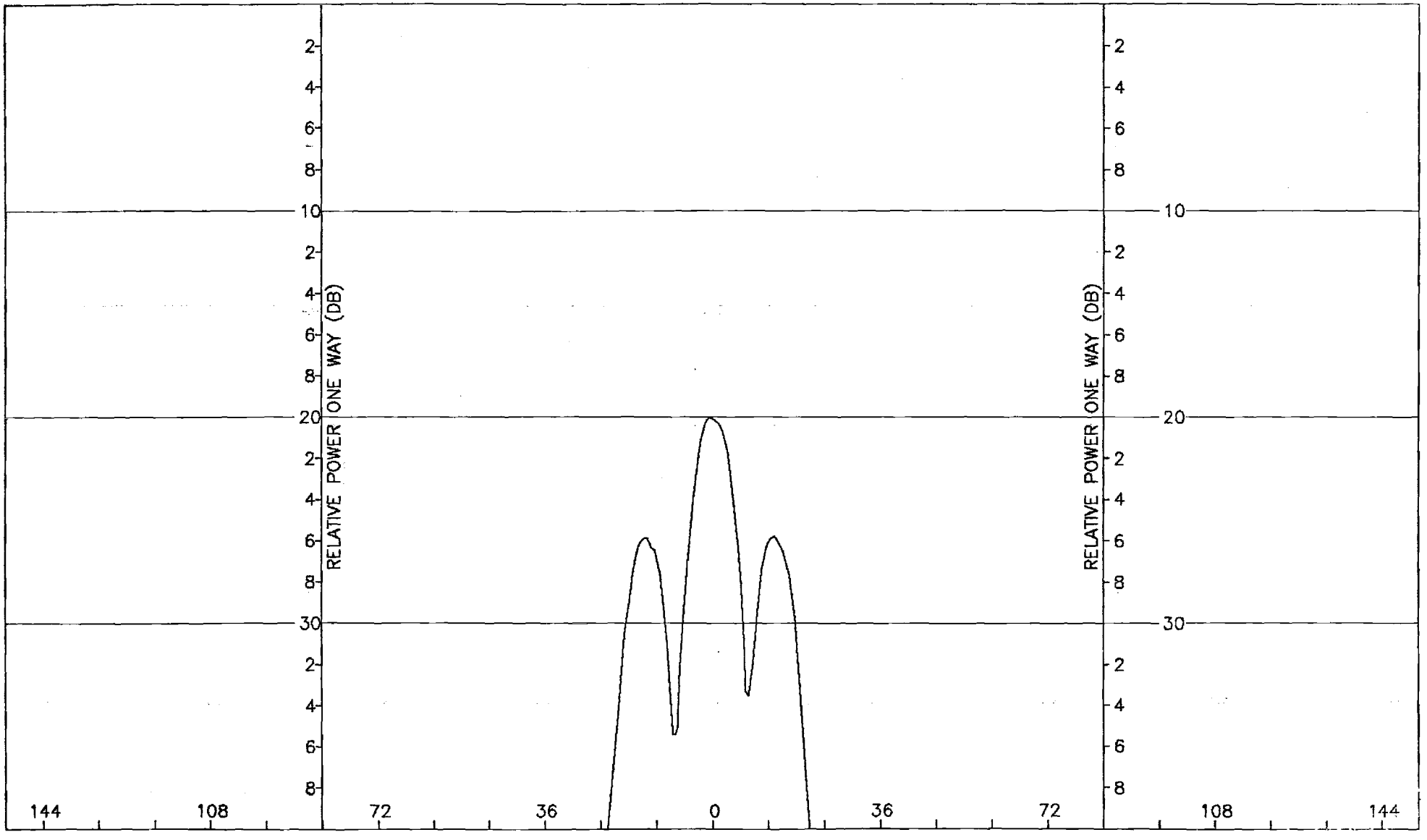

Figure C-11. Pattern of Large Array: H-Plane, Elevation Difference, ϕ-Component, No Radome

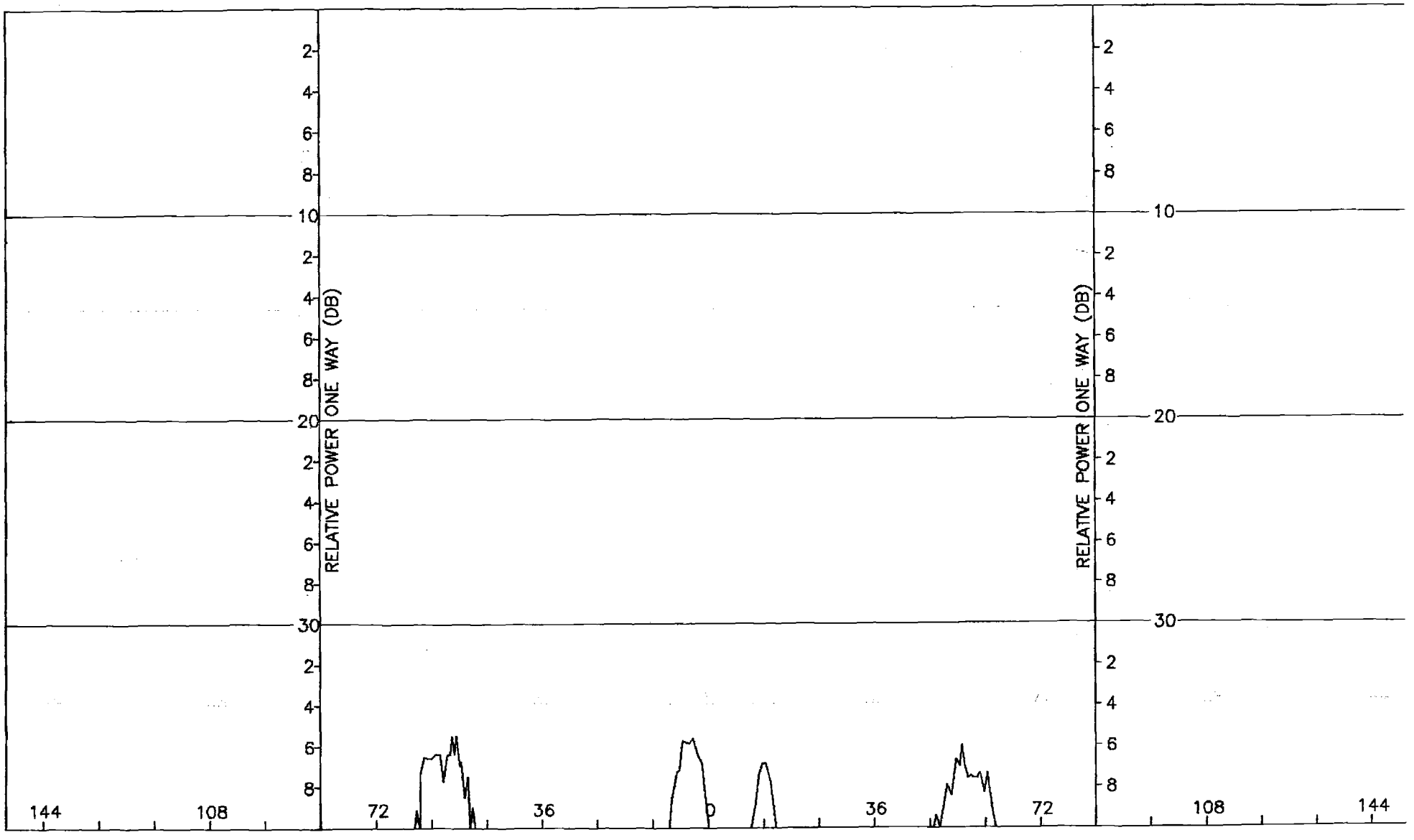

Figure C-12. Pattern of Large Array: H-Plane, Elevation Difference, θ-Component, No Radome

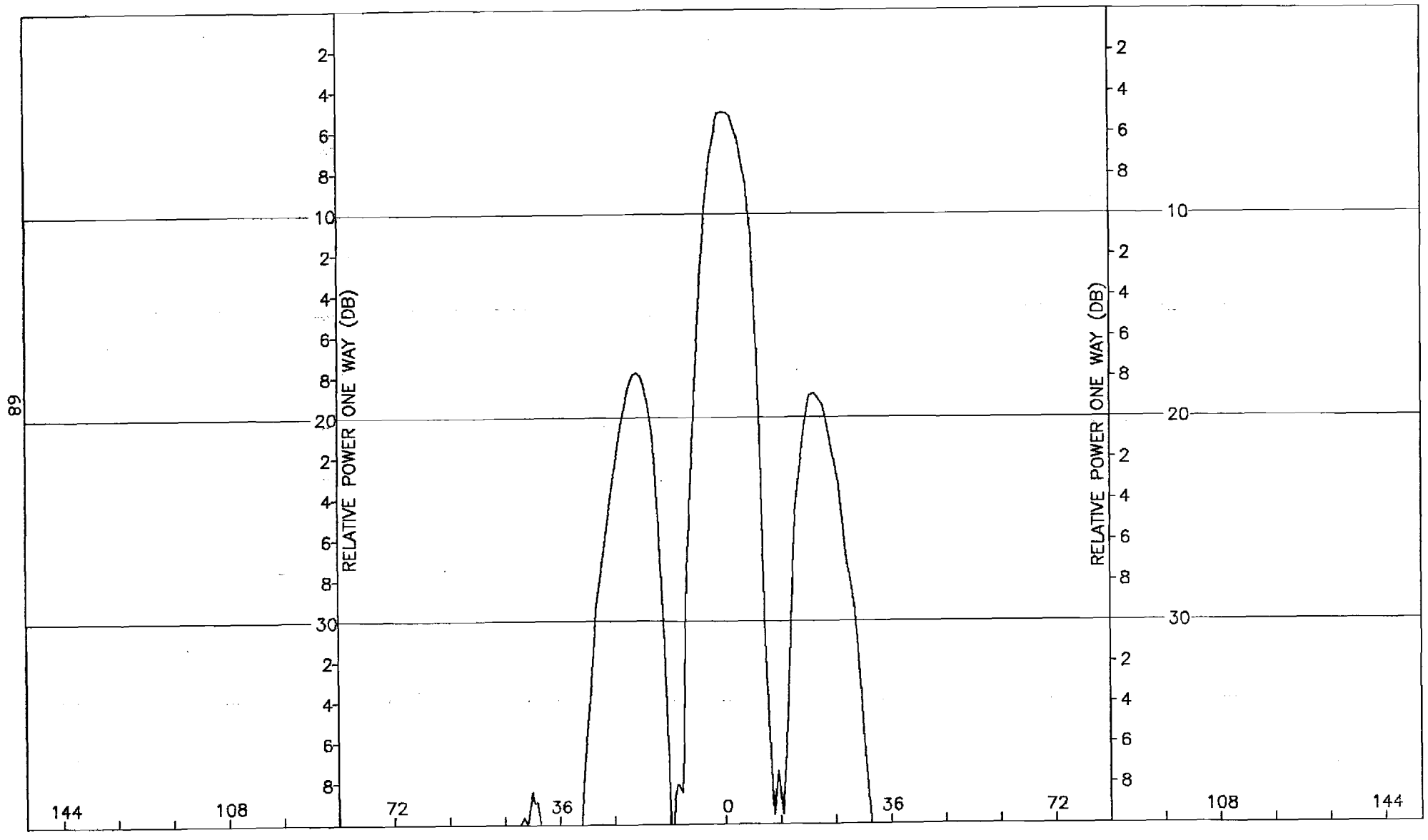

Figure C-13. Pattern of Large Array: ϕ=45° Plane, Sum, θ-Component, No Radome

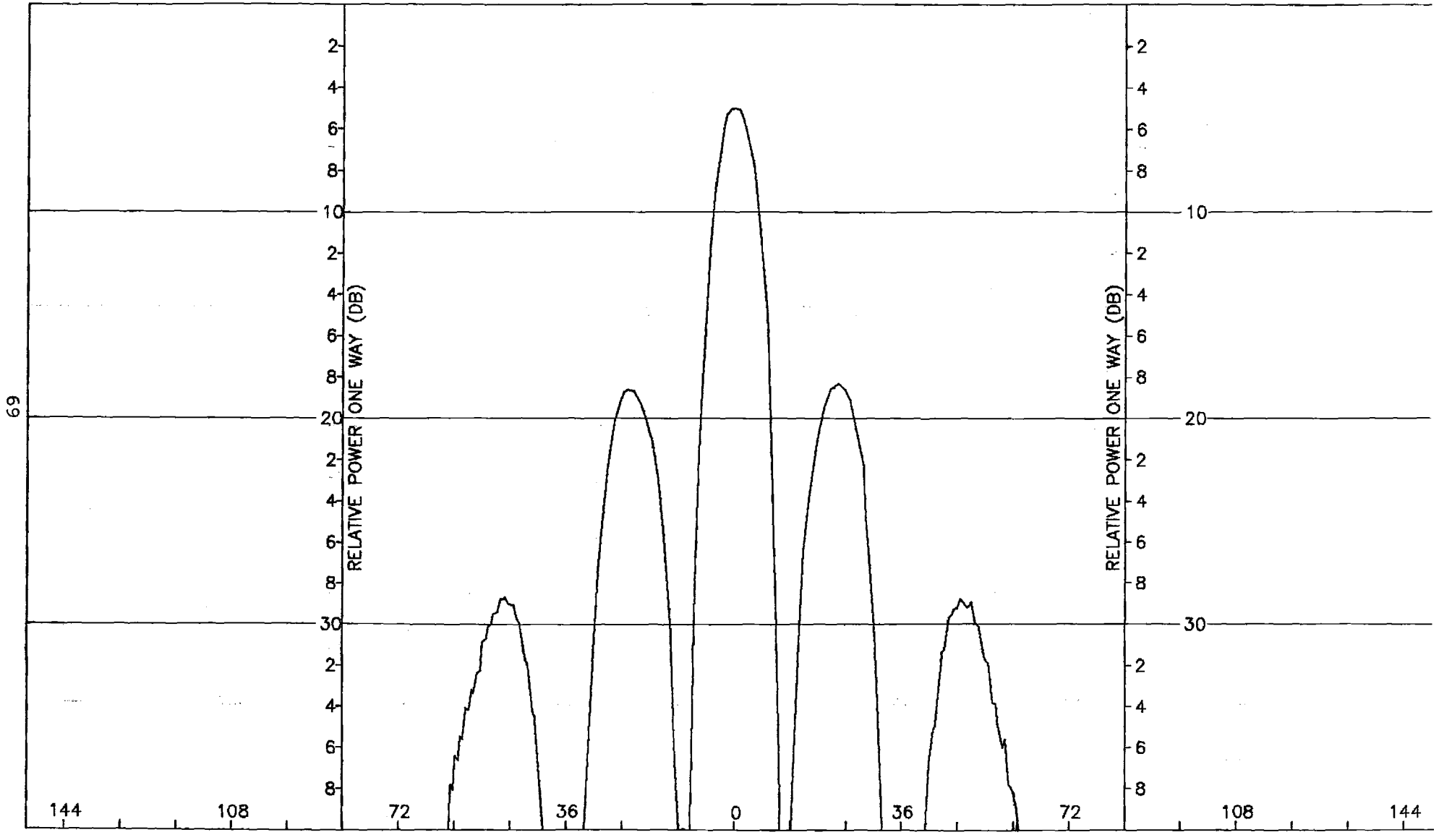

Figure C-14. Pattern of Large Array: ϕ=45° Plane, Sum, ϕ-Component, No Radome

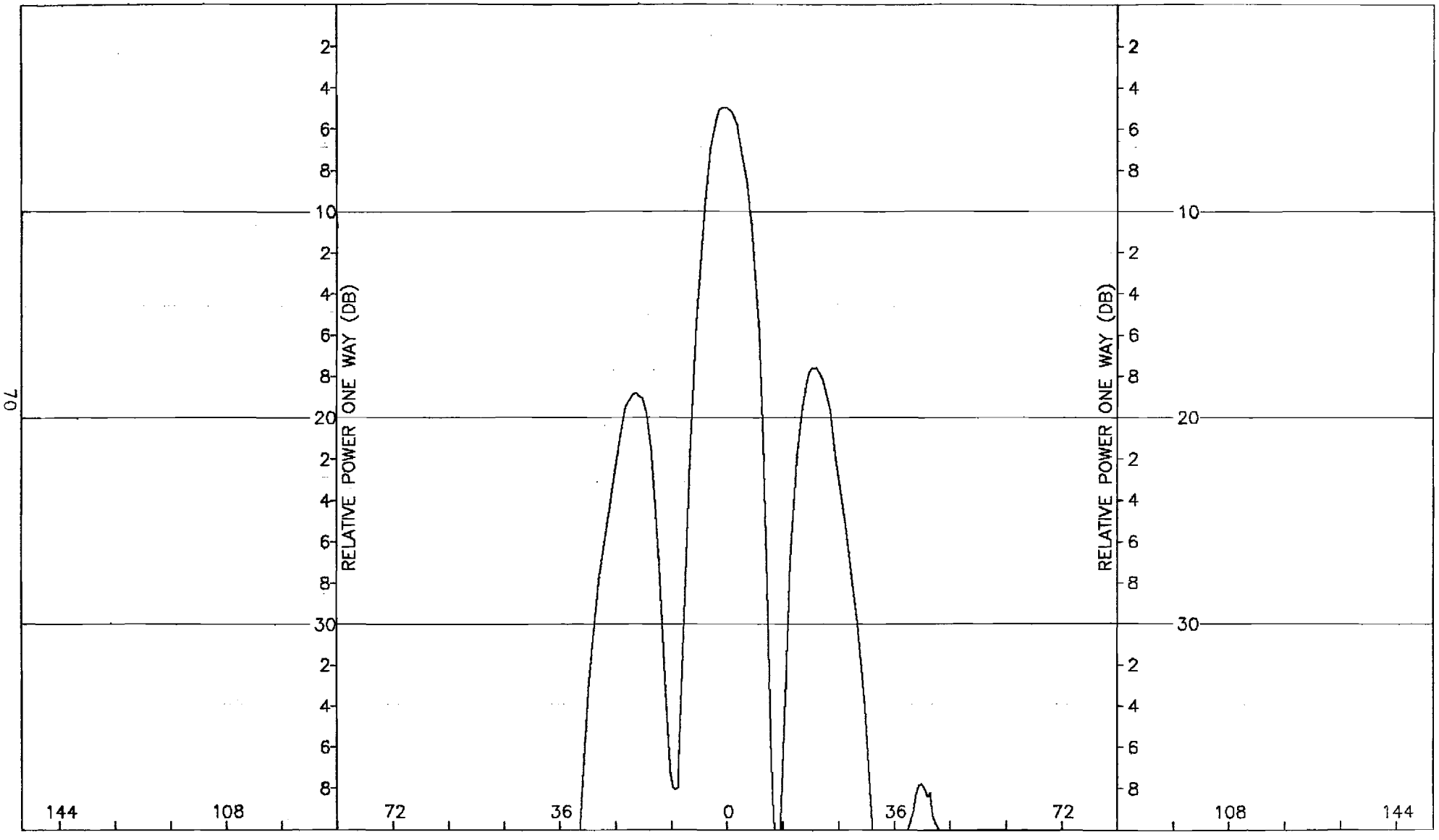

Figure C-15. Pattern of Large Array: ϕ=-45° Plane, Sum, θ-Component, No Radome

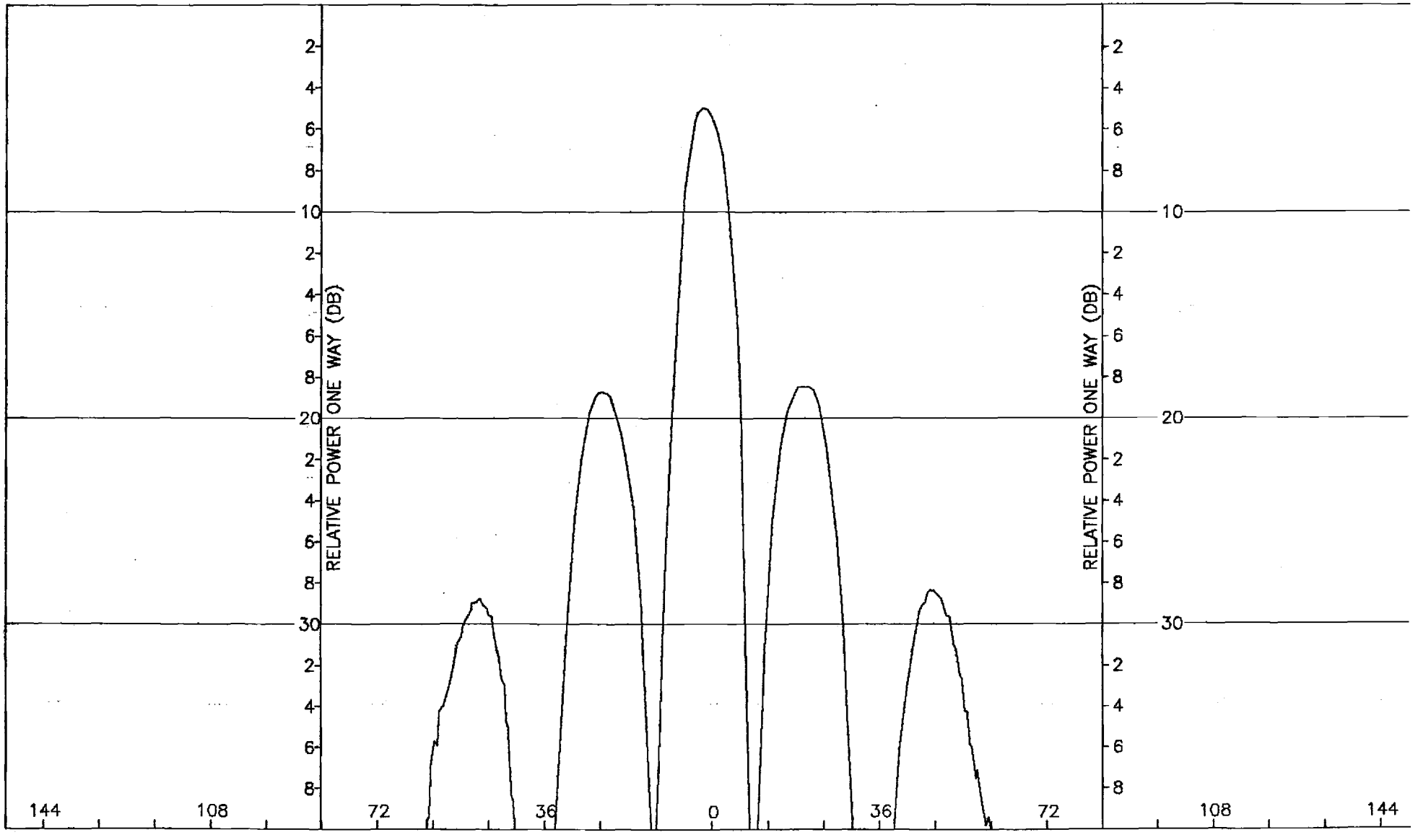

Figure C-16. Pattern of Large Array: ϕ=-45° Plane, Sum, ϕ-Component, No Radome

APPENDIX D

Antenna Patterns of Small Array with Small (F=1) Radome

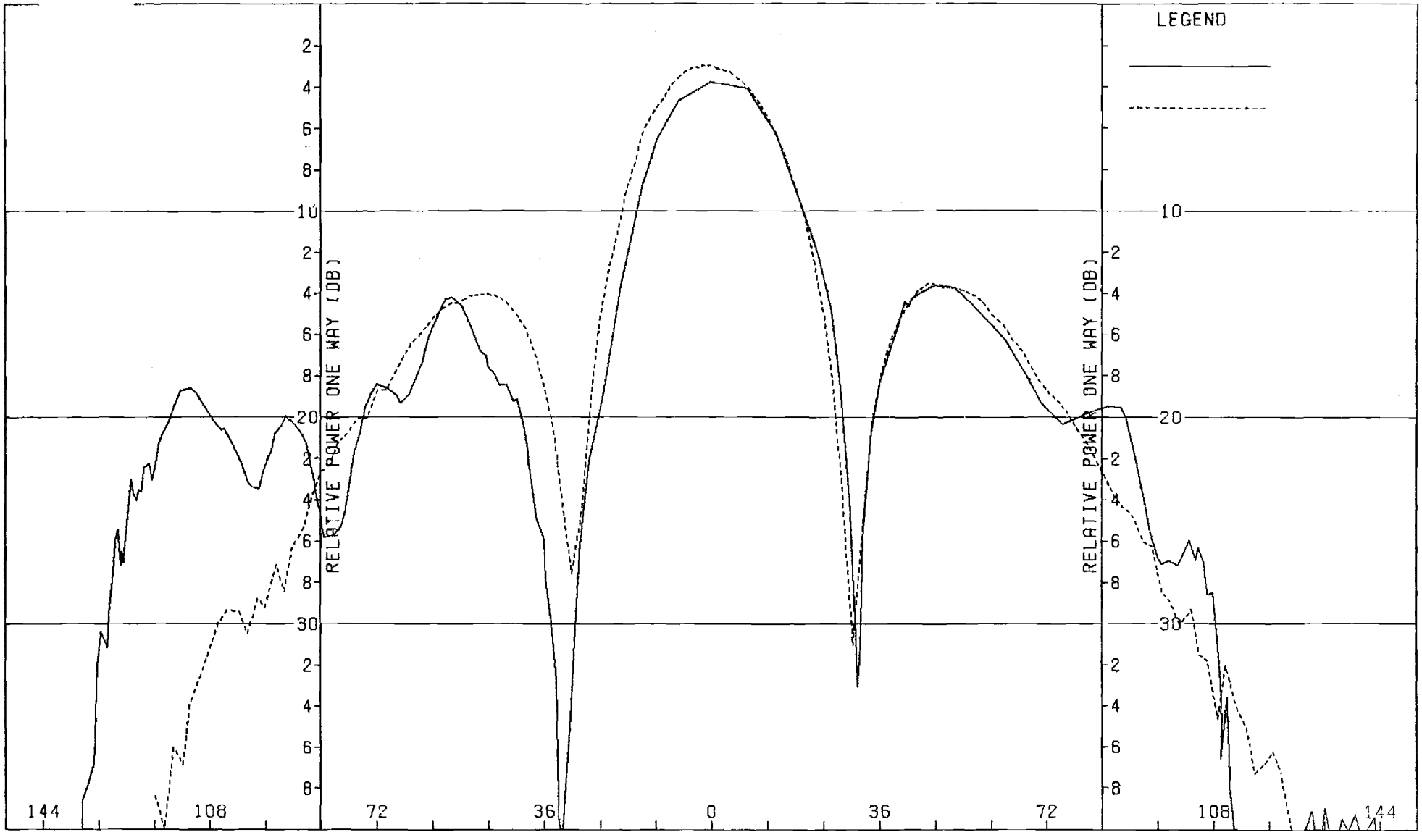

Figure D-1. Pattern of Small Array: H-Plane, Sum, ϕ-Component, Small Radome

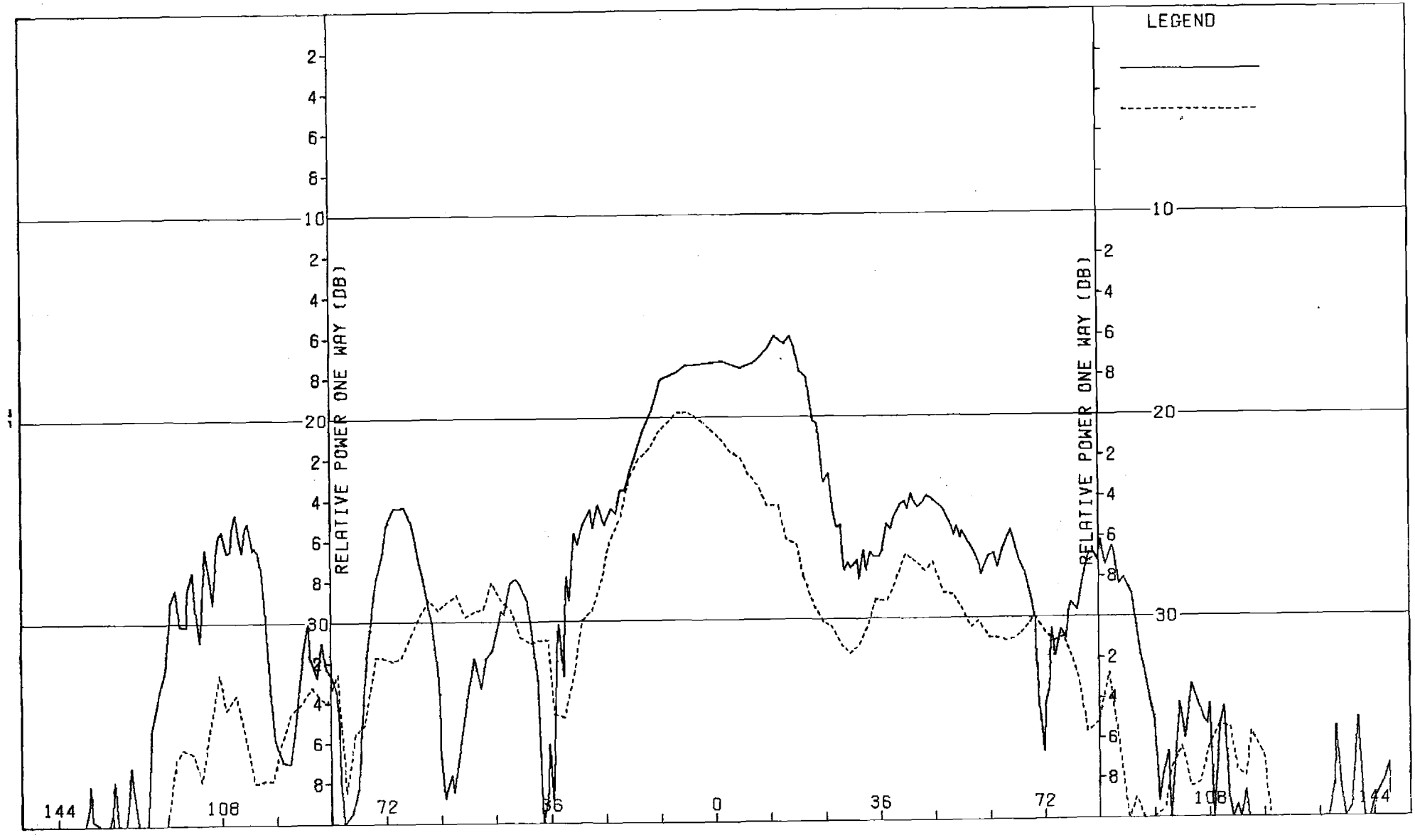

Figure D-2. Pattern of Small Array: H-Plane, Sum, θ-Component, Small Radome

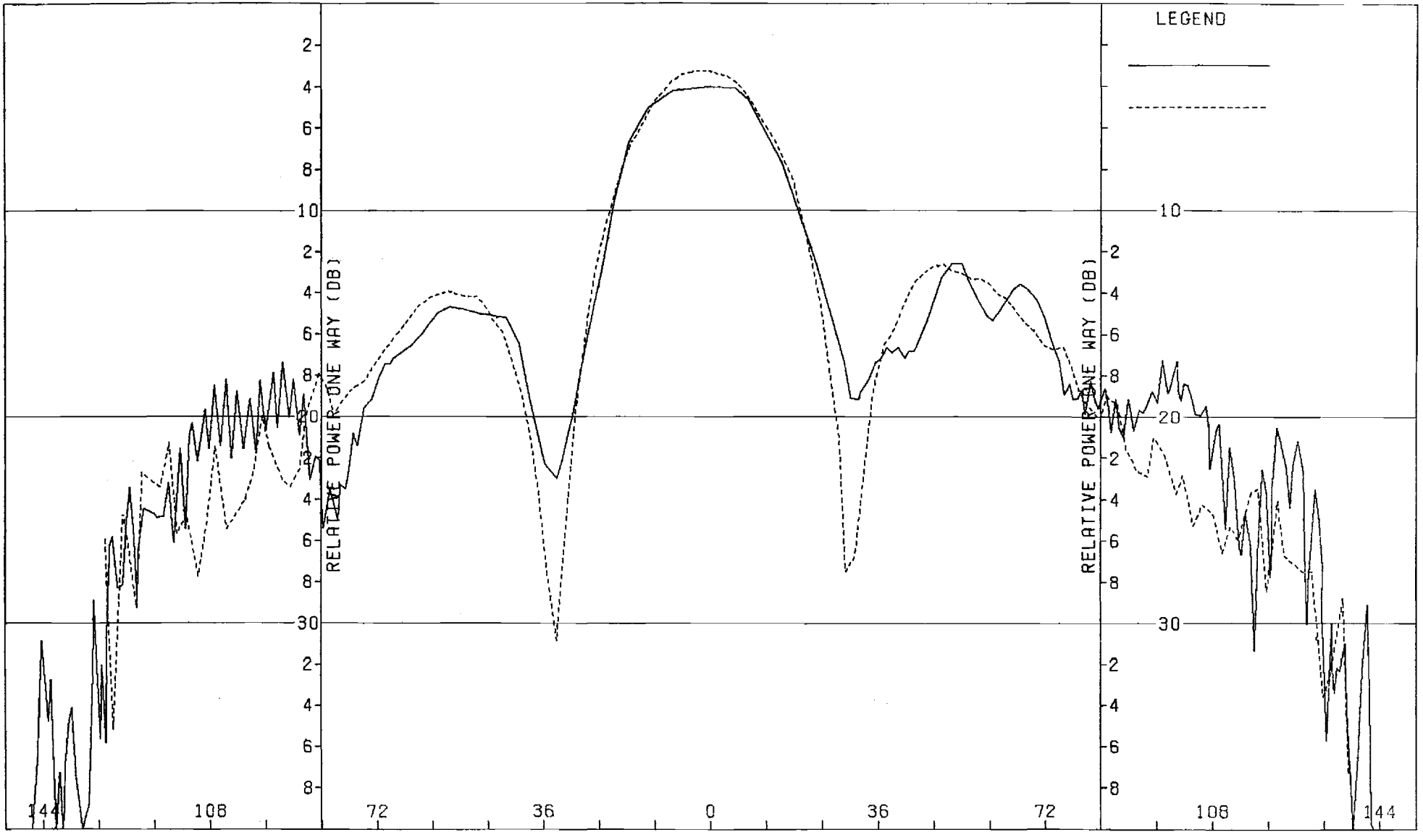

Figure D-3. Pattern of Small Array: E-Plane, Sum, θ-Component, Small Radome.

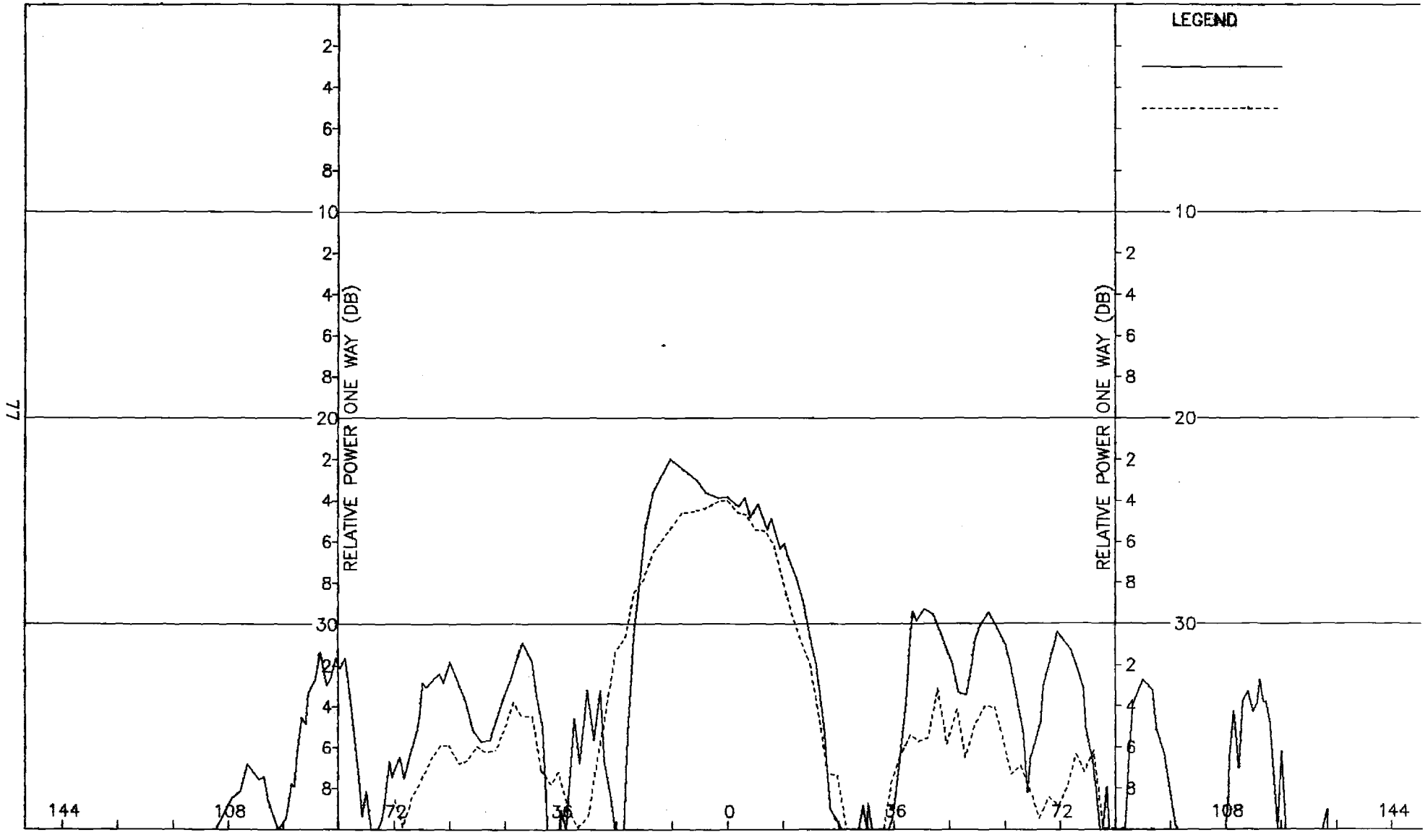

Figure D-4. Pattern of Small Array: E-Plane, Sum, ϕ-Component, Small Radome.

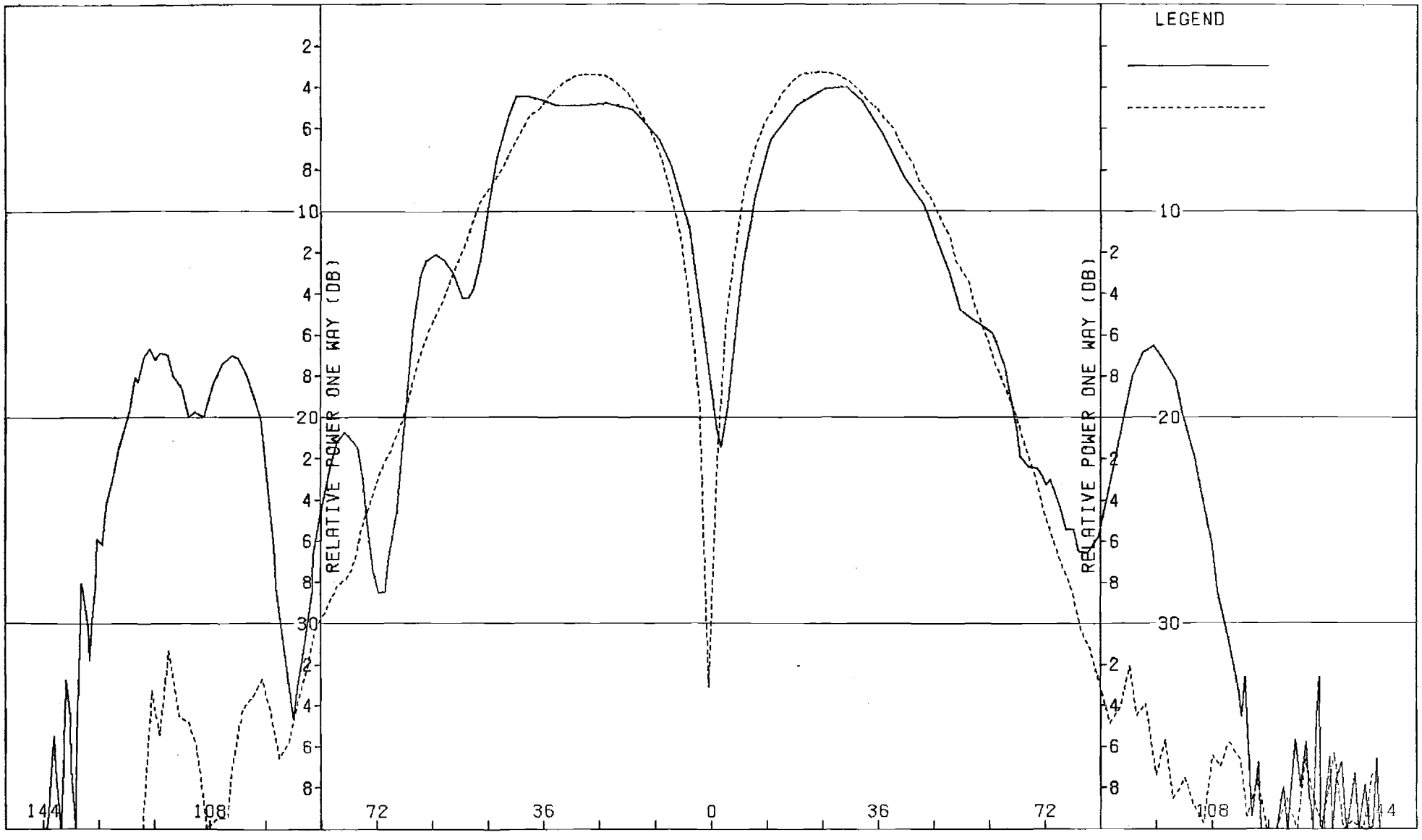

Figure D-5. Pattern of Small Array: H-Plane, Azimuth Difference, ϕ-Component, Small Radome.

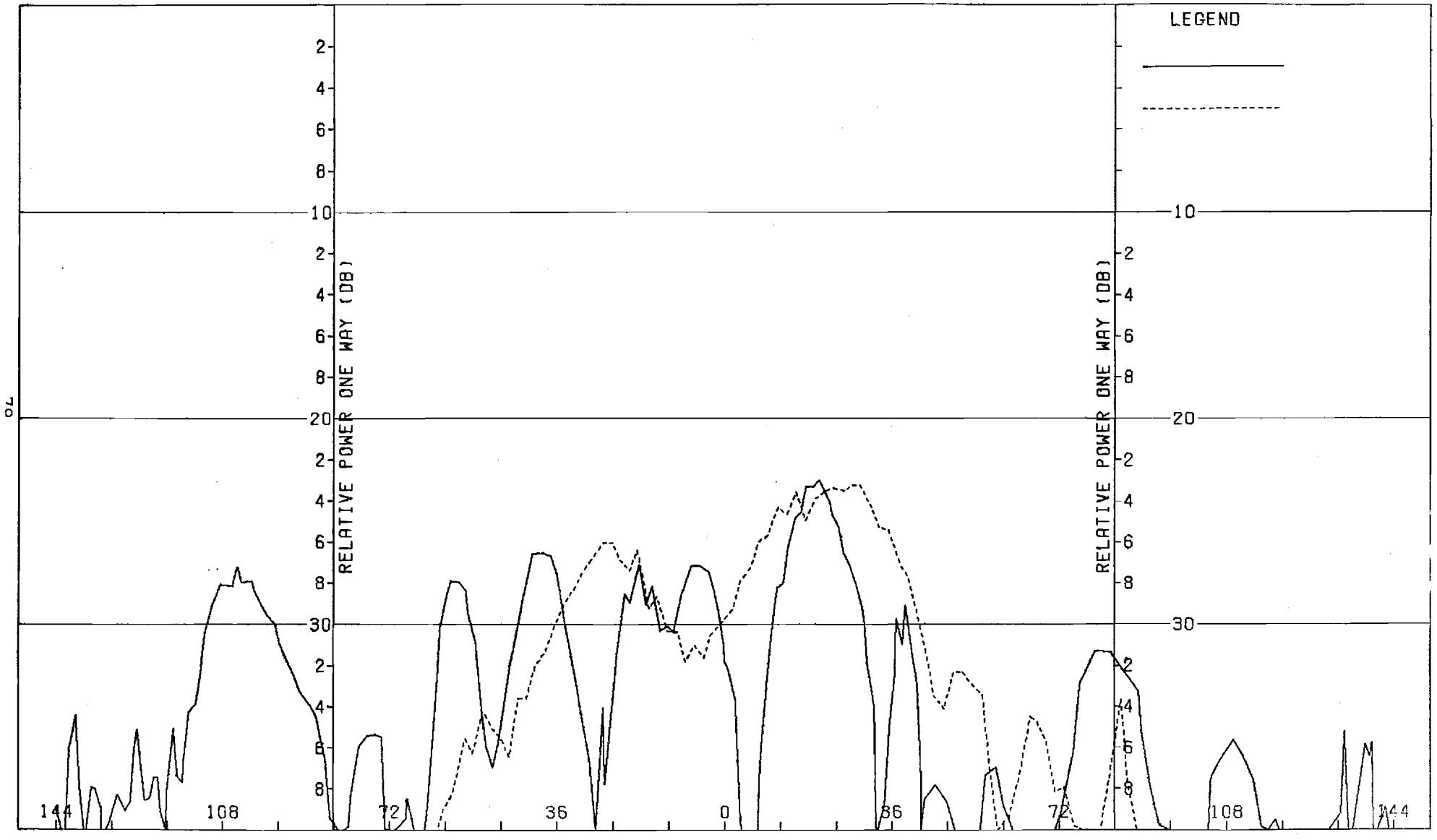

Figure D-6. Pattern of Small Array: H-Plane, Azimuth Difference, θ-Component, Small Radome.

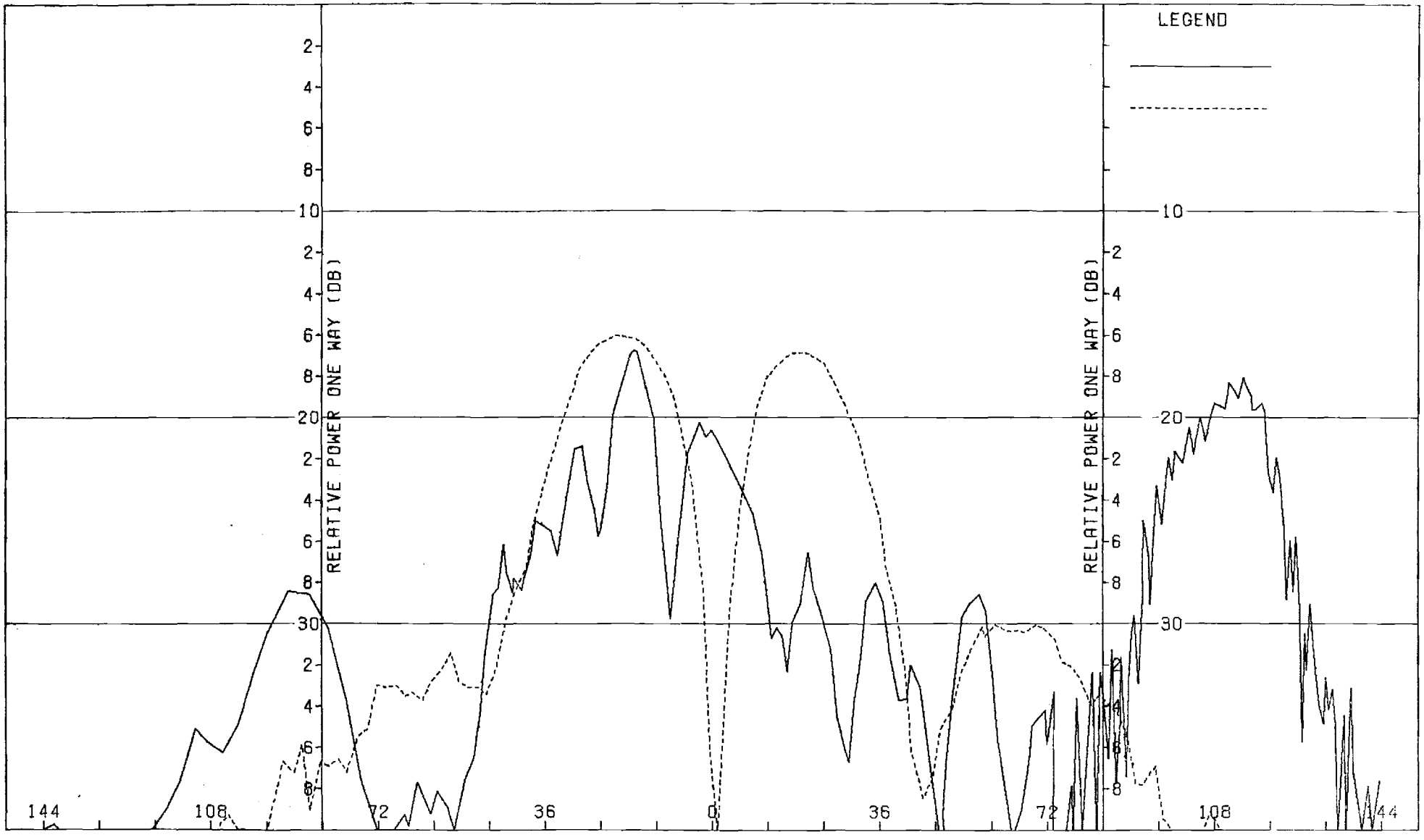

Figure D-7. Pattern of Small Array: E-Plane, Azimuth Difference, θ-Component, Small Radome.

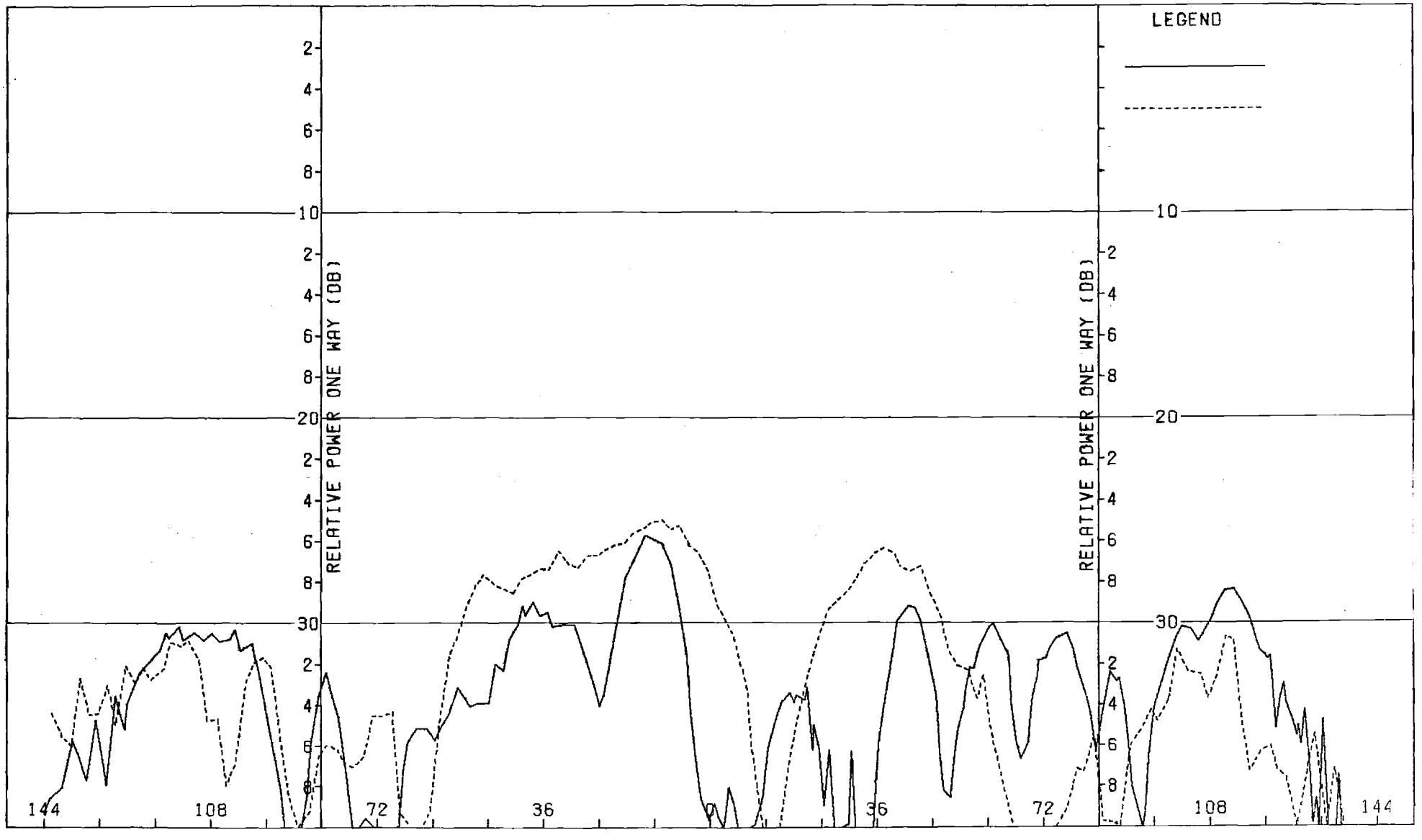

Figure D-8. Pattern of Small Array: E-Plane, Azimuth Difference, ϕ-Component, Small Radome.

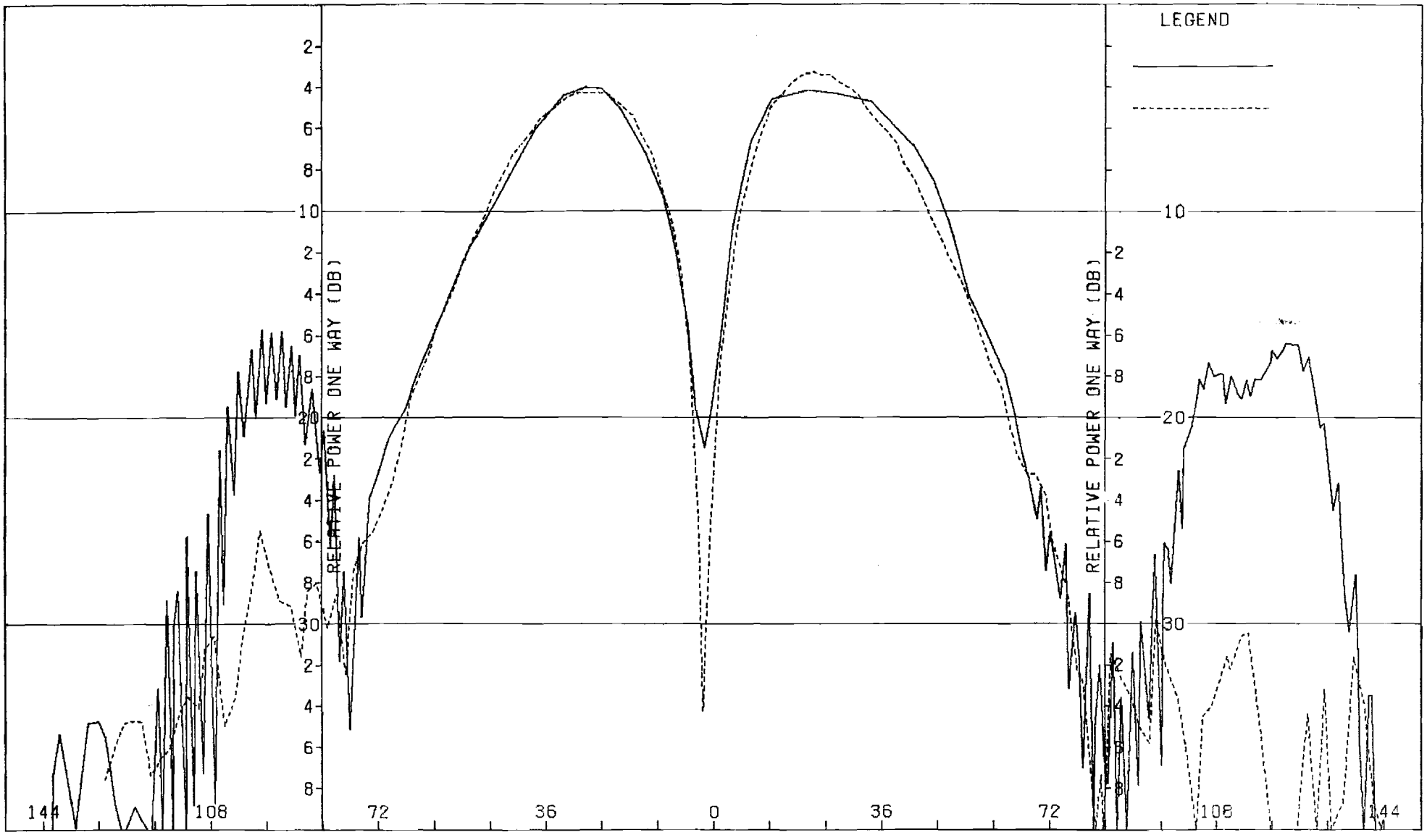

Figure D-9. Pattern of Small Array: E-Plane, Elevation Difference, θ-Component, Small Radome.

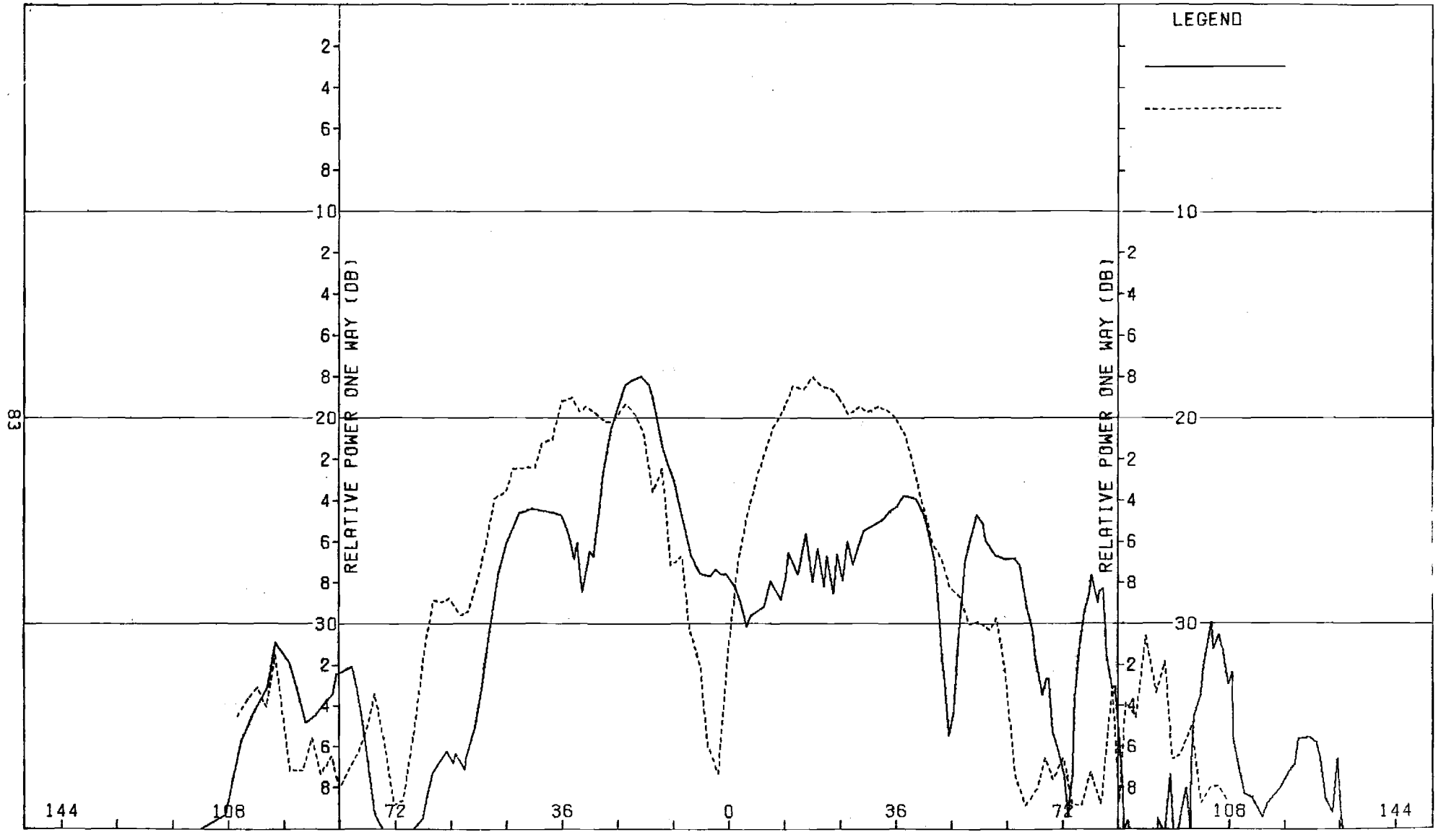

Figure D-10. Pattern of Small Array: E-Plane, Elevation Difference, ϕ-Component, Small Radome.

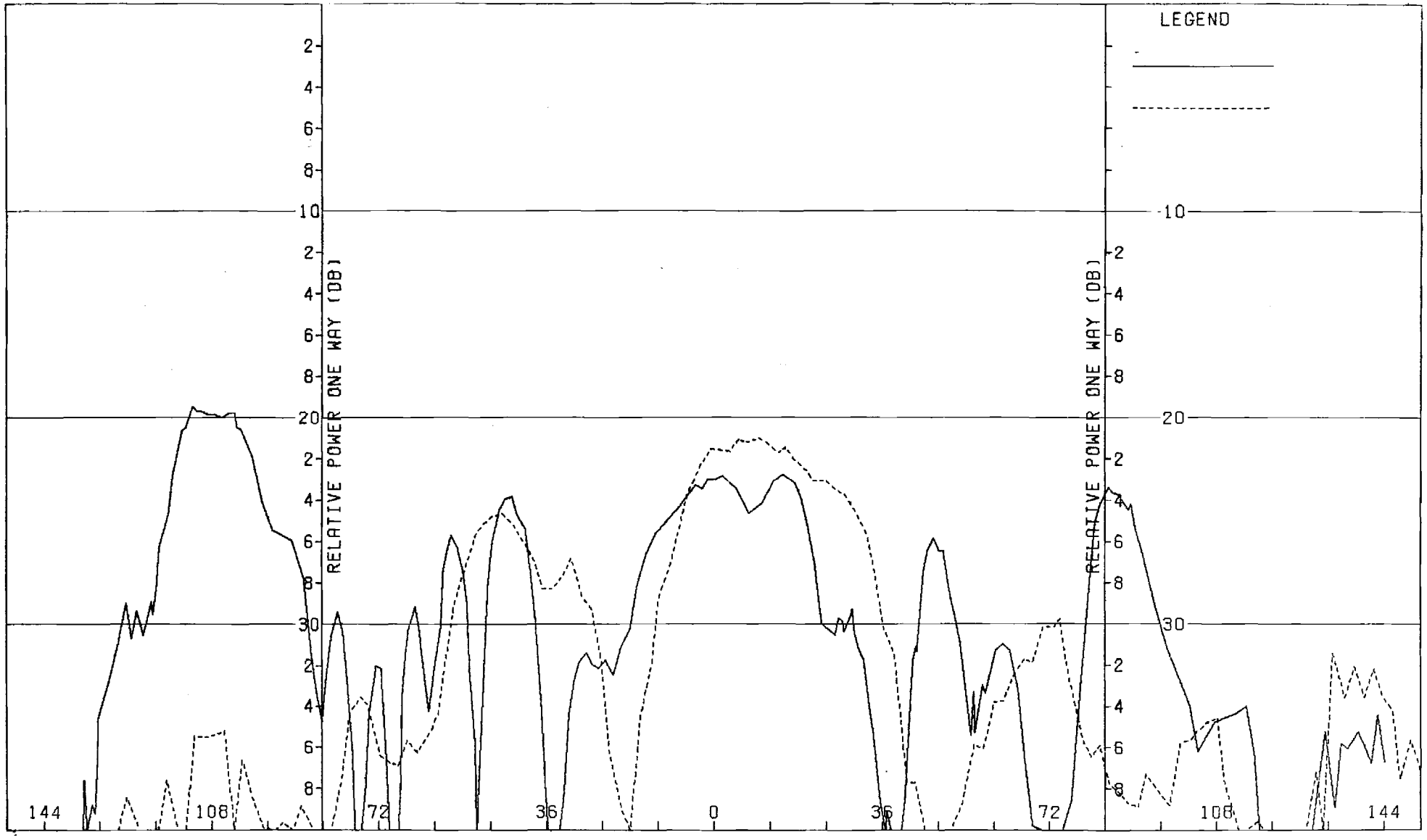

Figure D-11. Pattern of Small Array: H-Plane, Elevation Difference, ϕ-Component, Small Radome.

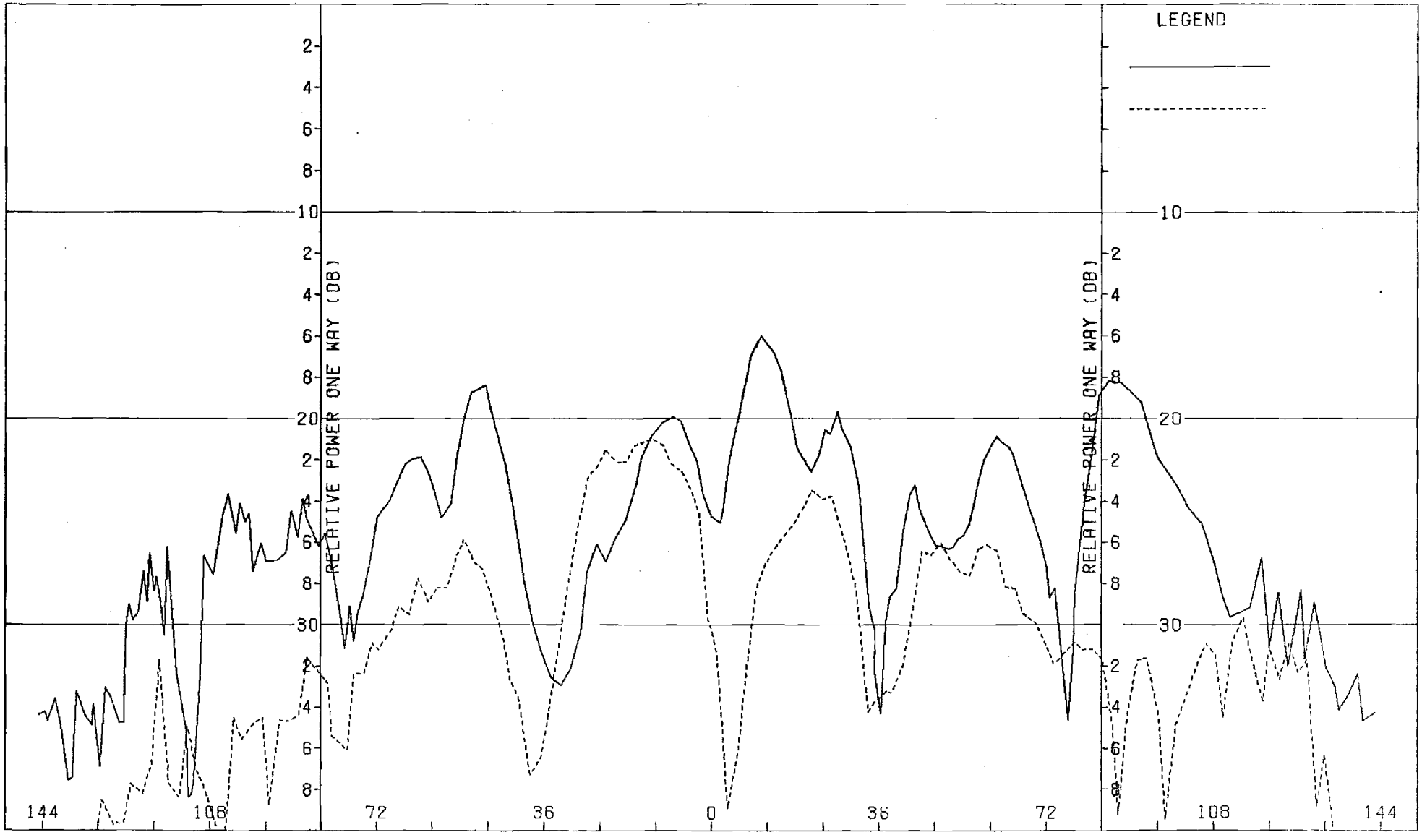

Figure D-12. Pattern of Small Array: H-Plane, Elevation Difference, θ-Component, Small Radome.

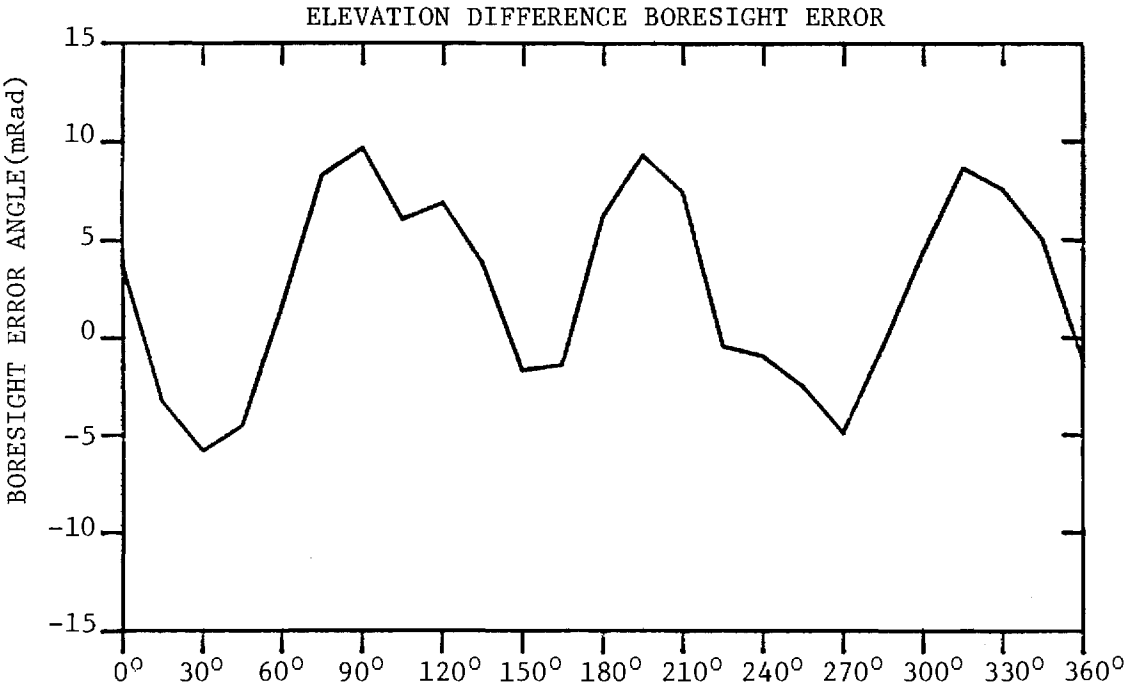

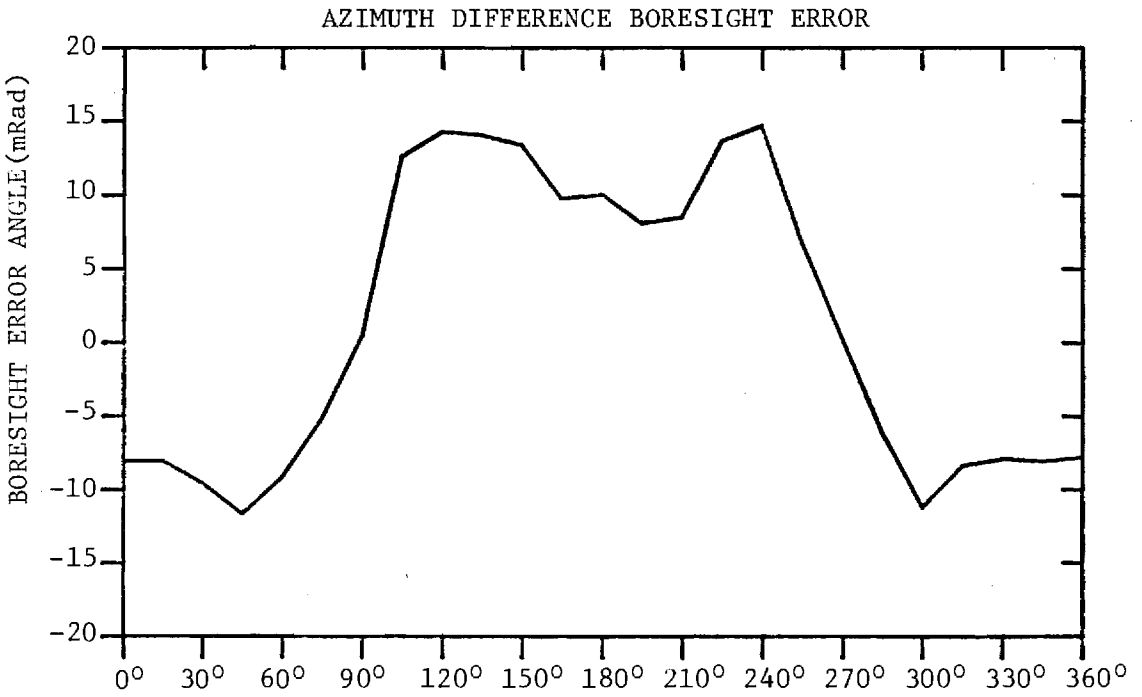

FIGURE D-13. BORESIGHT ERRORS OF SMALL ARRAY AND SMALL (F=1) RADOME.

APPENDIX E

Antenna Patterns of Small Array with Medium (F=1) Radome

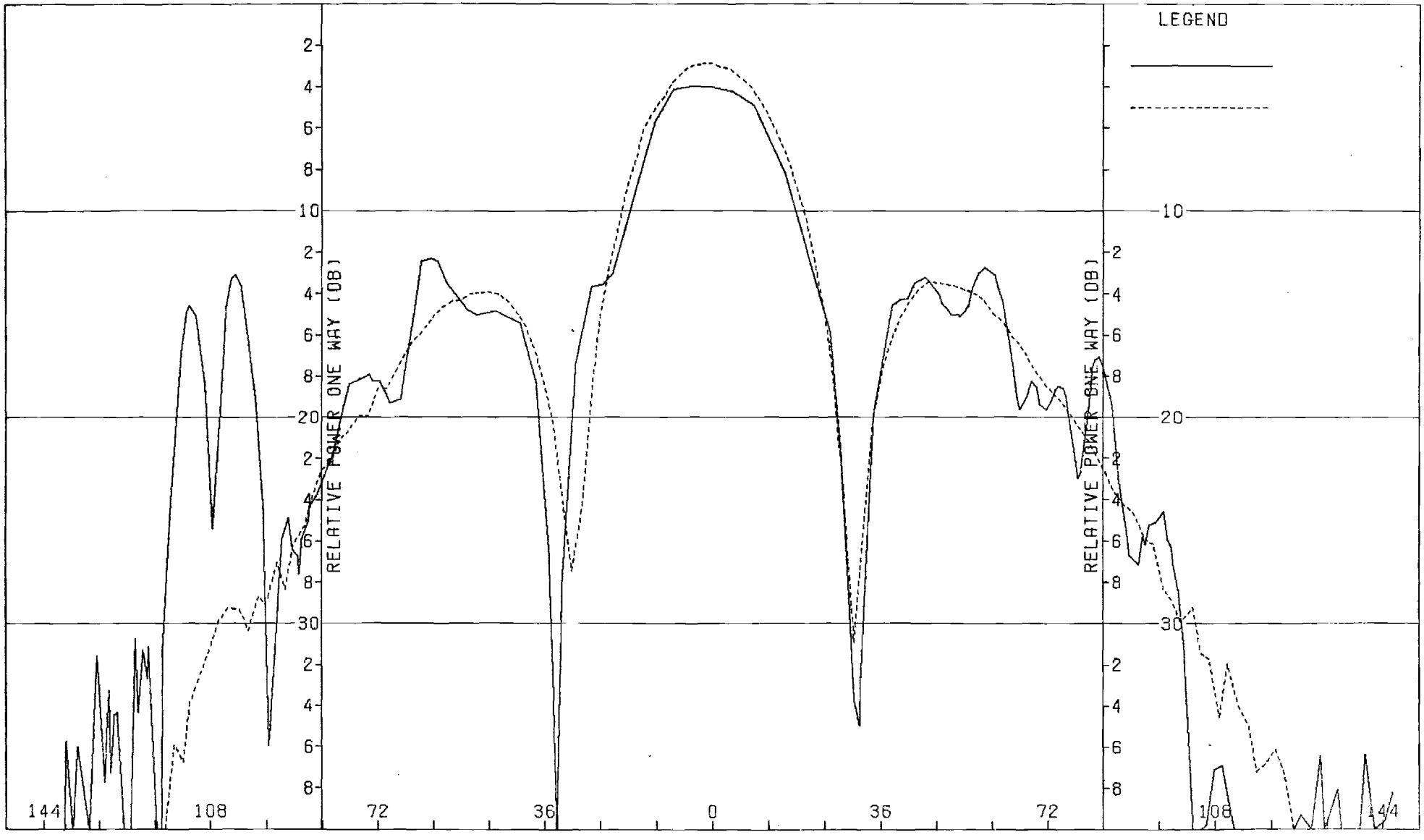

Figure E-1. Pattern of Small Array: H-Plane, Sum, ϕ-Component, Medium (F=1) Radome

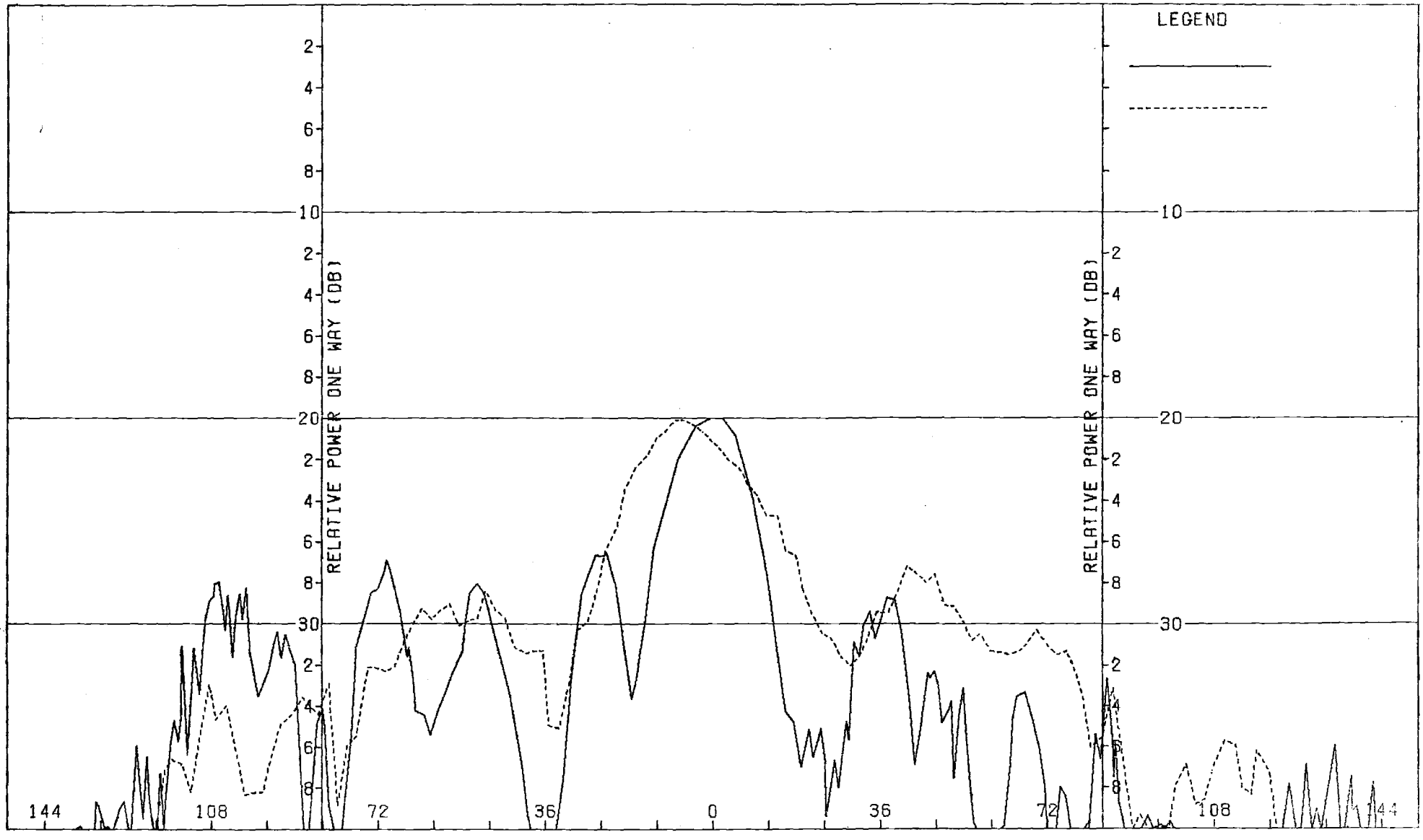

Figure E-2. Pattern of Small Array: H-Plane, Sum, θ—Component, Medium (F=1) Radome

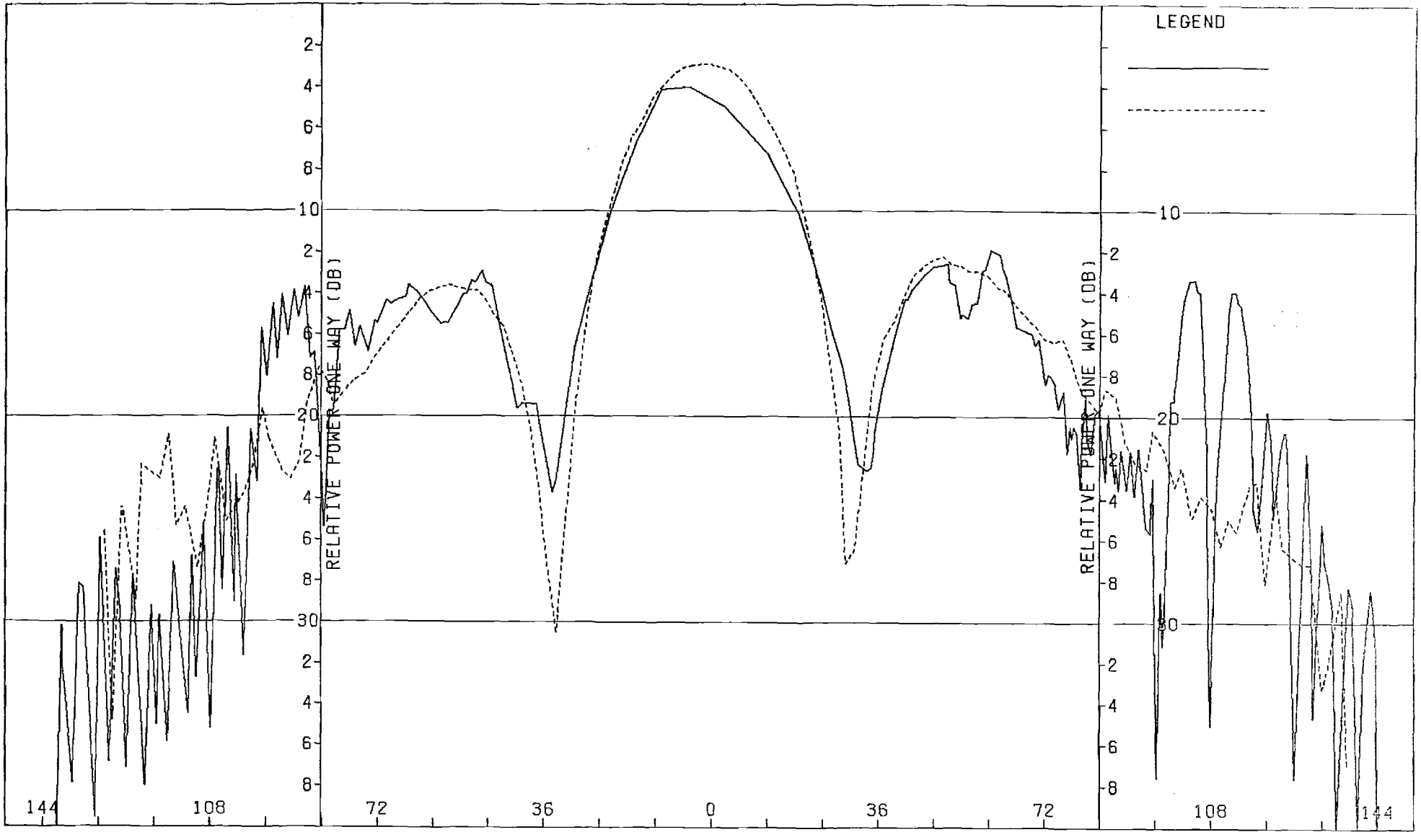

Figure E-3. Pattern of Small Array: E-Plane, Sum, θ-Component, Medium (F=1) Radome

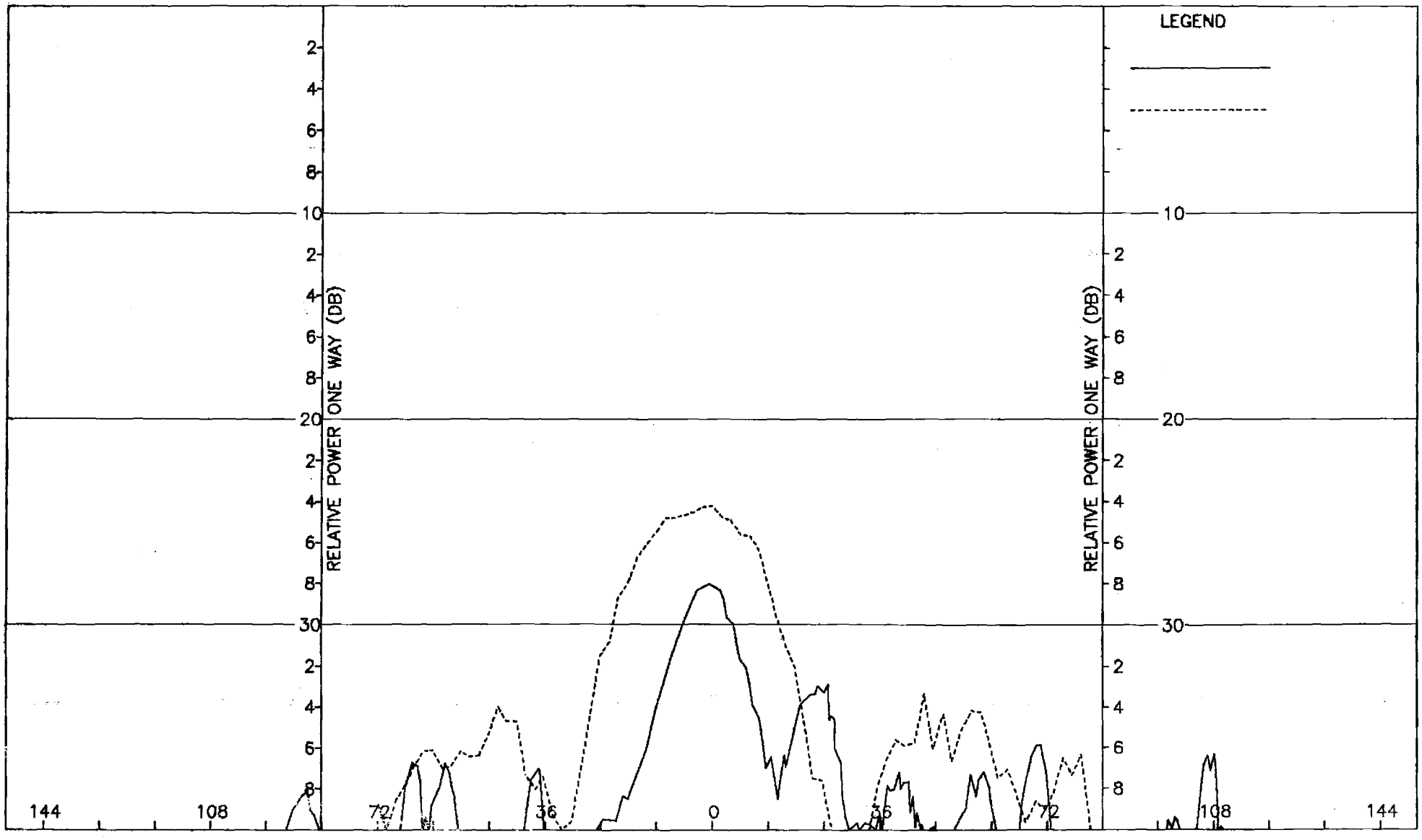

Figure E-4. Pattern of Small Array: E-Plane, Azimuth Difference, ϕ-Component, Medium (F=1) Radome

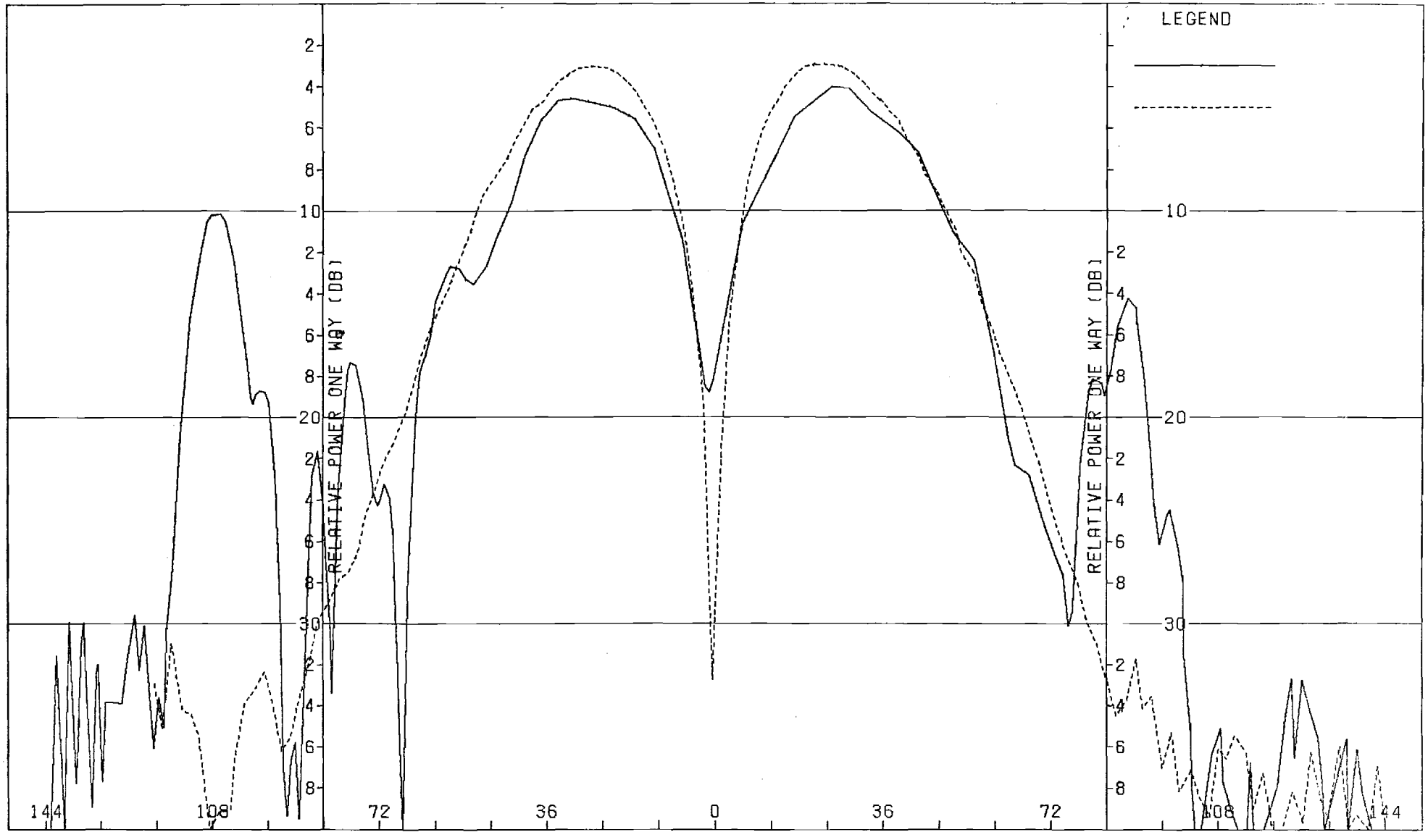

Figure E-5. Pattern of Small Array: H-Plane, Azimuth Difference, ϕ-Component, Medium (F=1) Radome

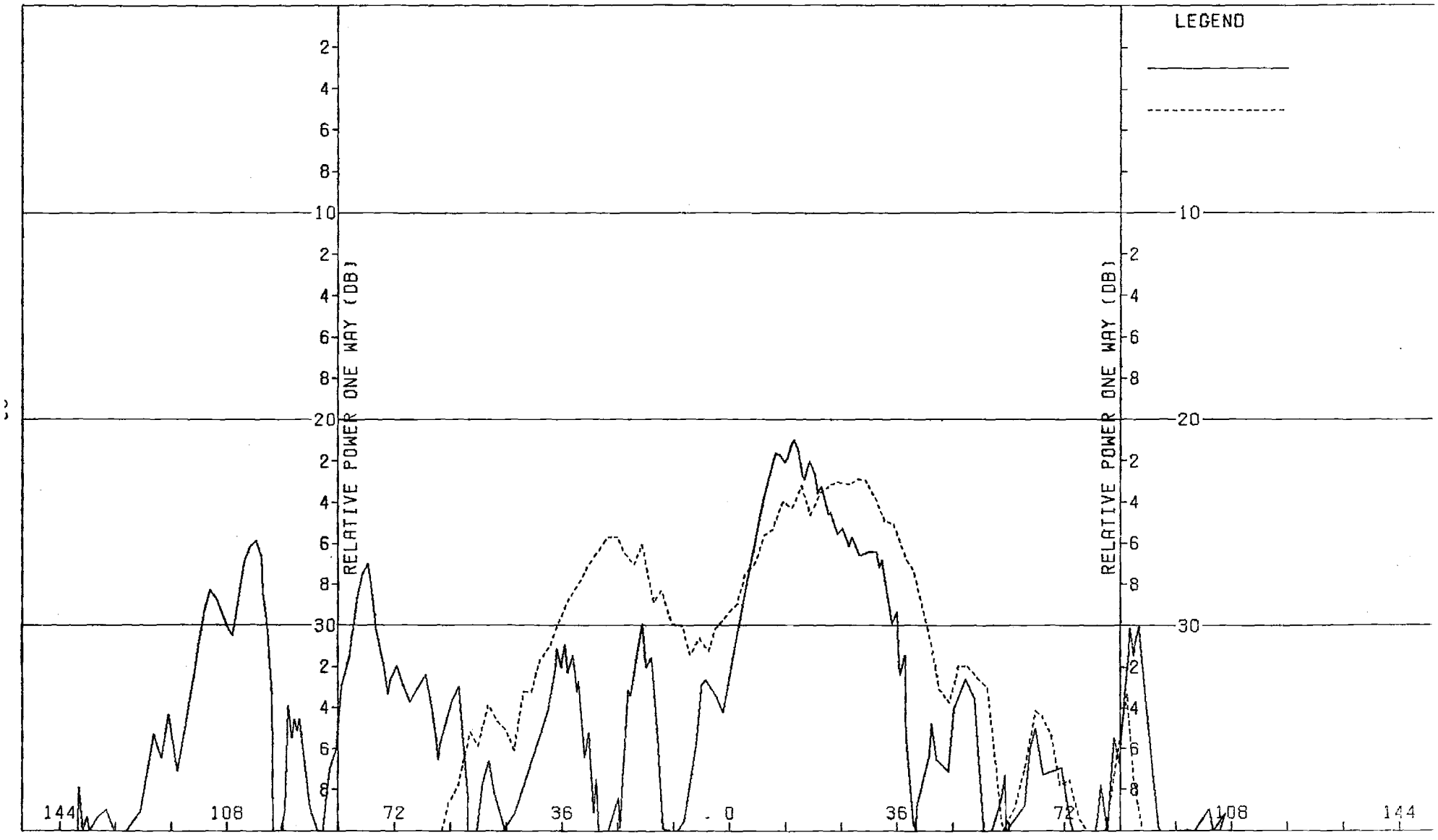

Figure E-6. Pattern of Small Array: H-Plane, Azimuth Difference, θ-Component, Medium (F=1) Radome

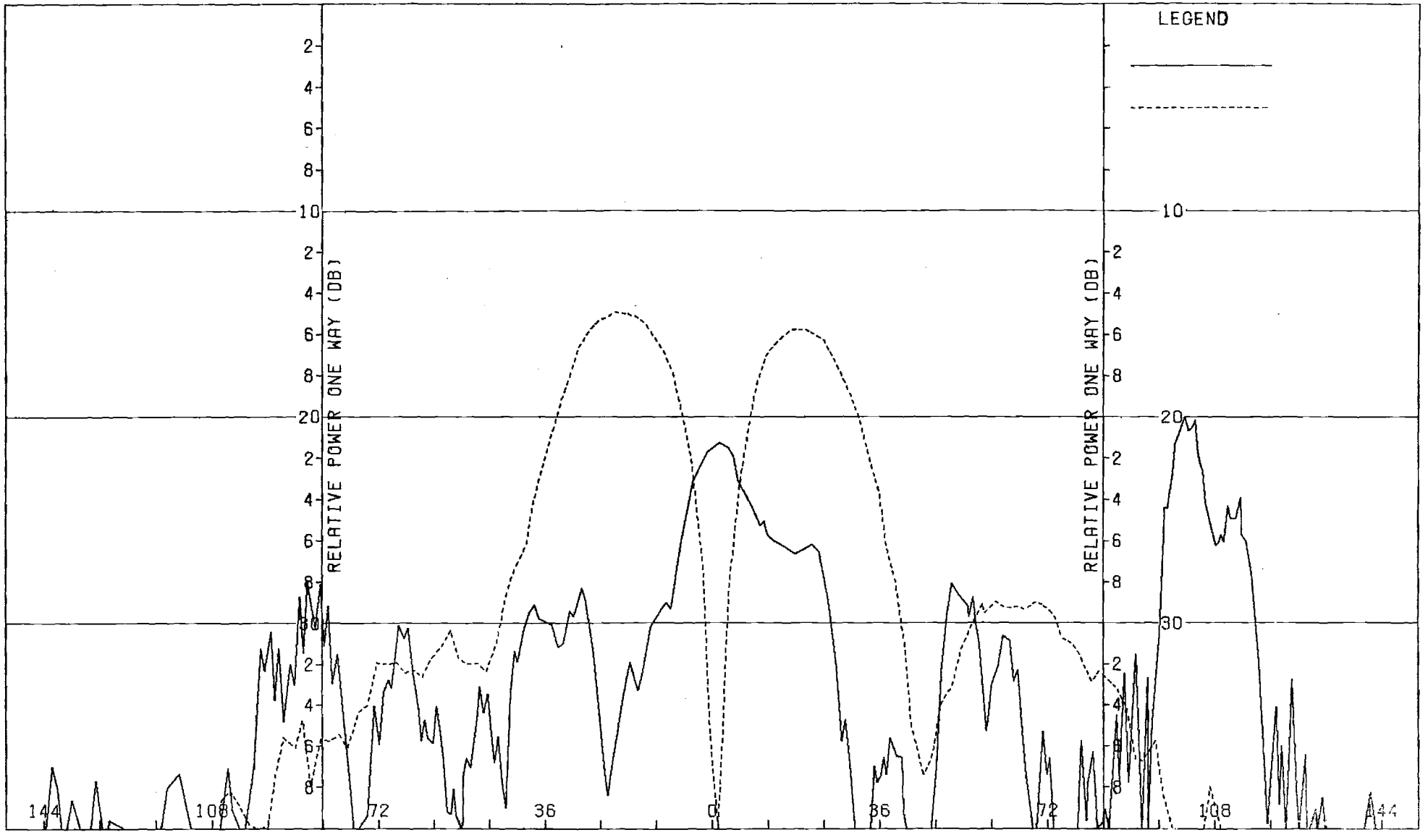

Figure E-7. Pattern of Small Array: E-Plane, Azimuth Difference, θ-Component, Medium (F=1) Radome

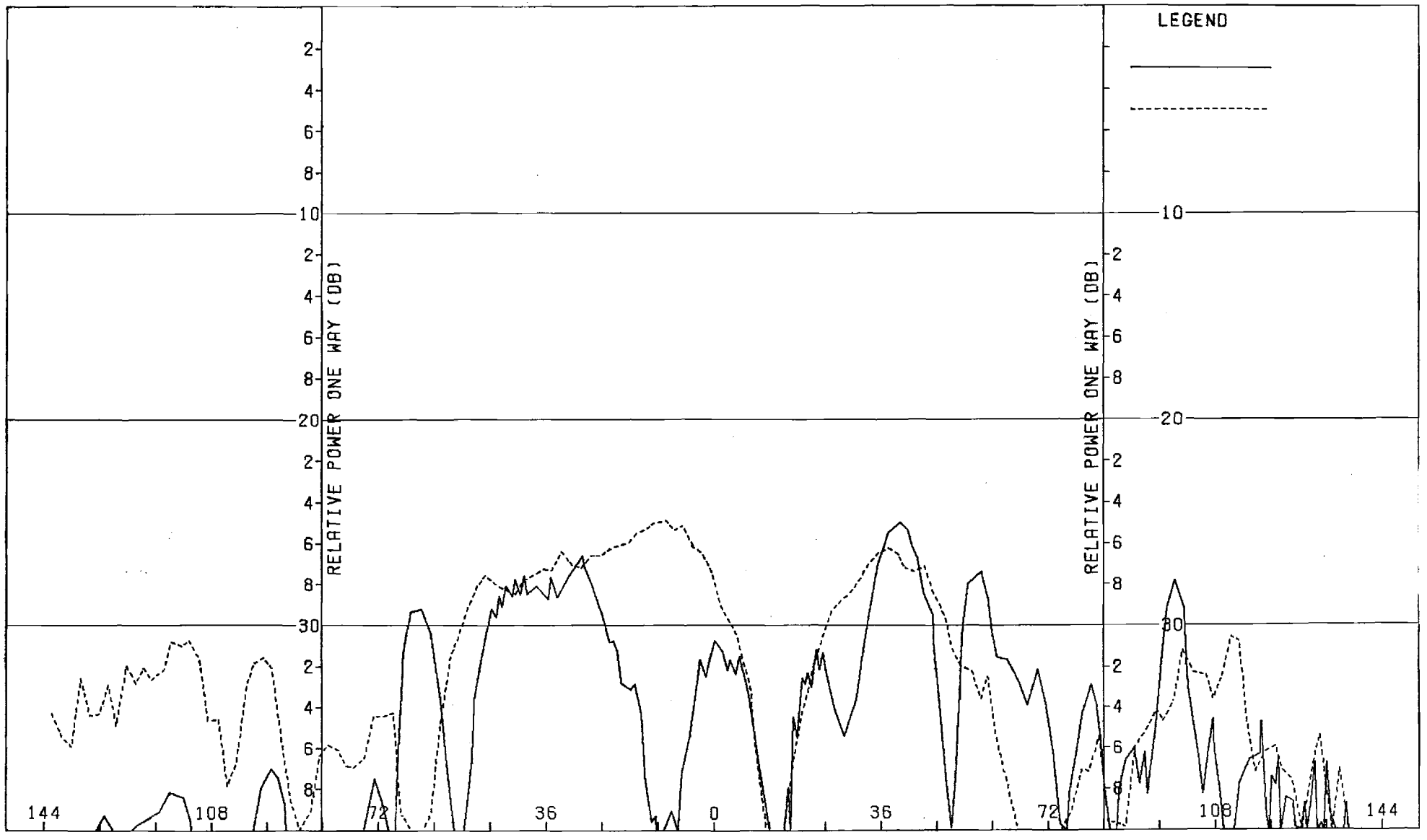

Figure E-8. Pattern of Small Array: E-Plane, Elev. Difference, ϕ-Component, Medium (F=1) Radome

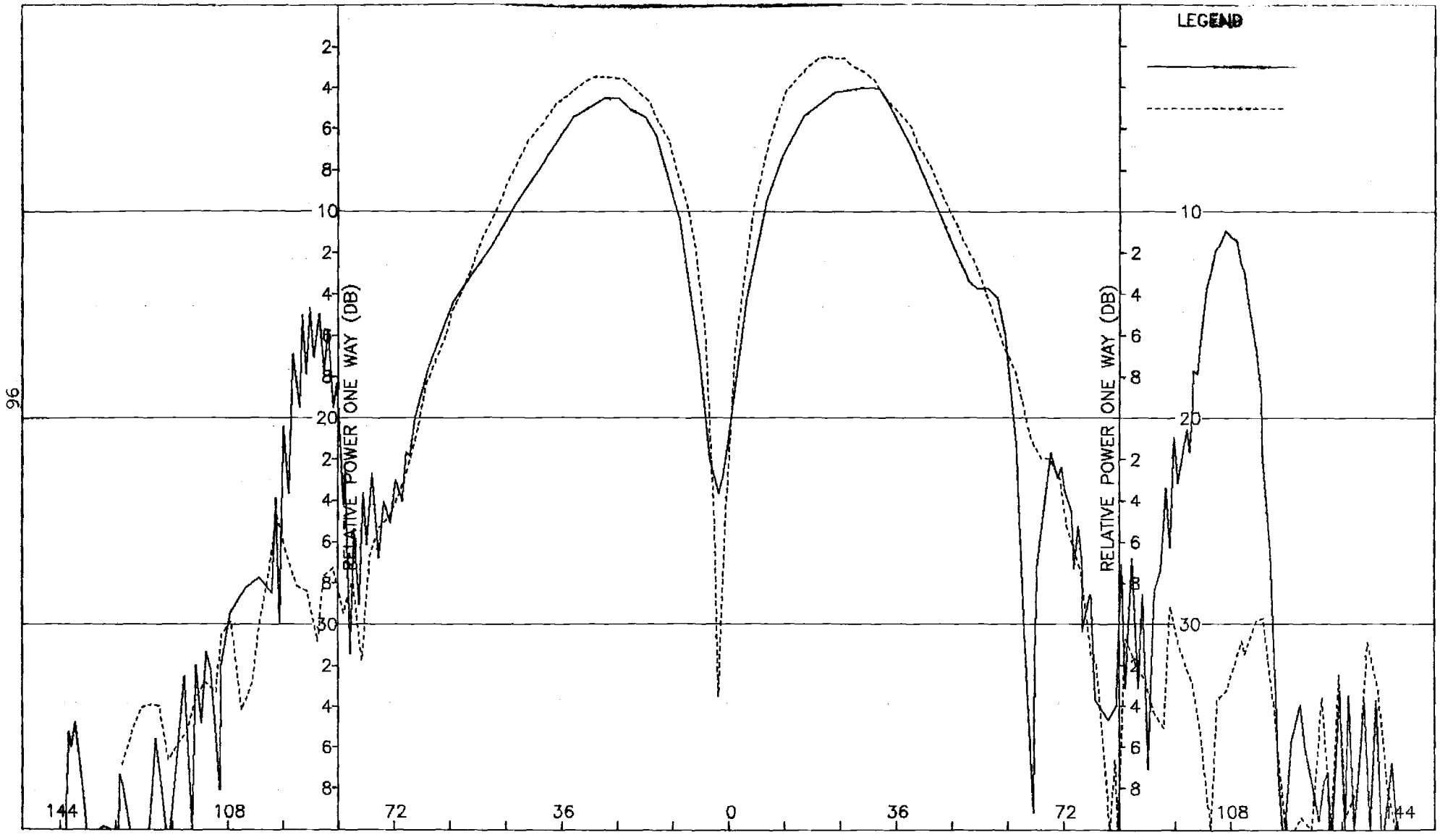

Figure E-9. Pattern of Small Array: E-Plane, Elev. Difference, θ-Component, Medium (F=1) Radome

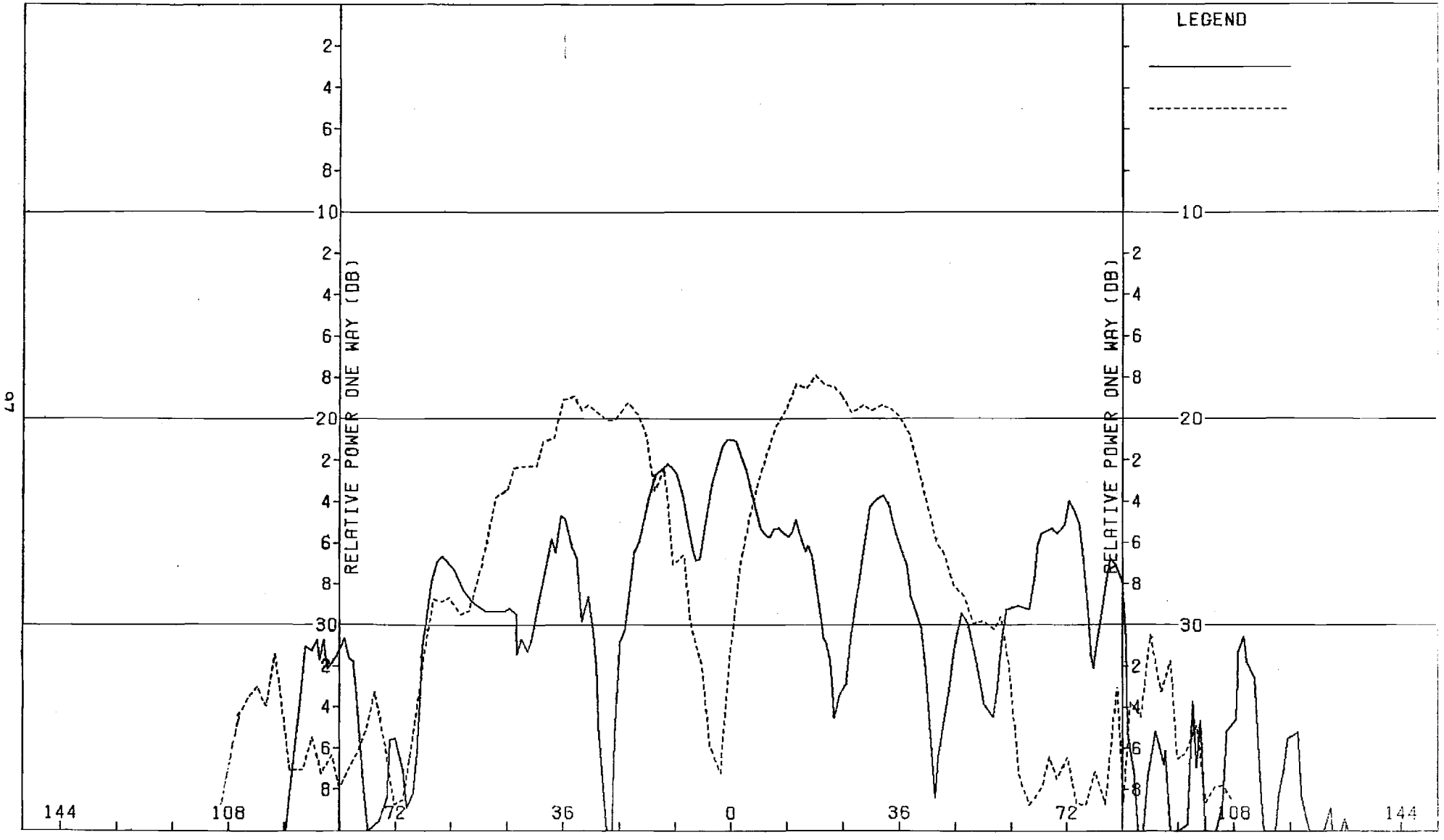

Figure E-10. Pattern of Small Array: E-Plane, Elev. Difference, ϕ-Component, Medium (F=1) Radome

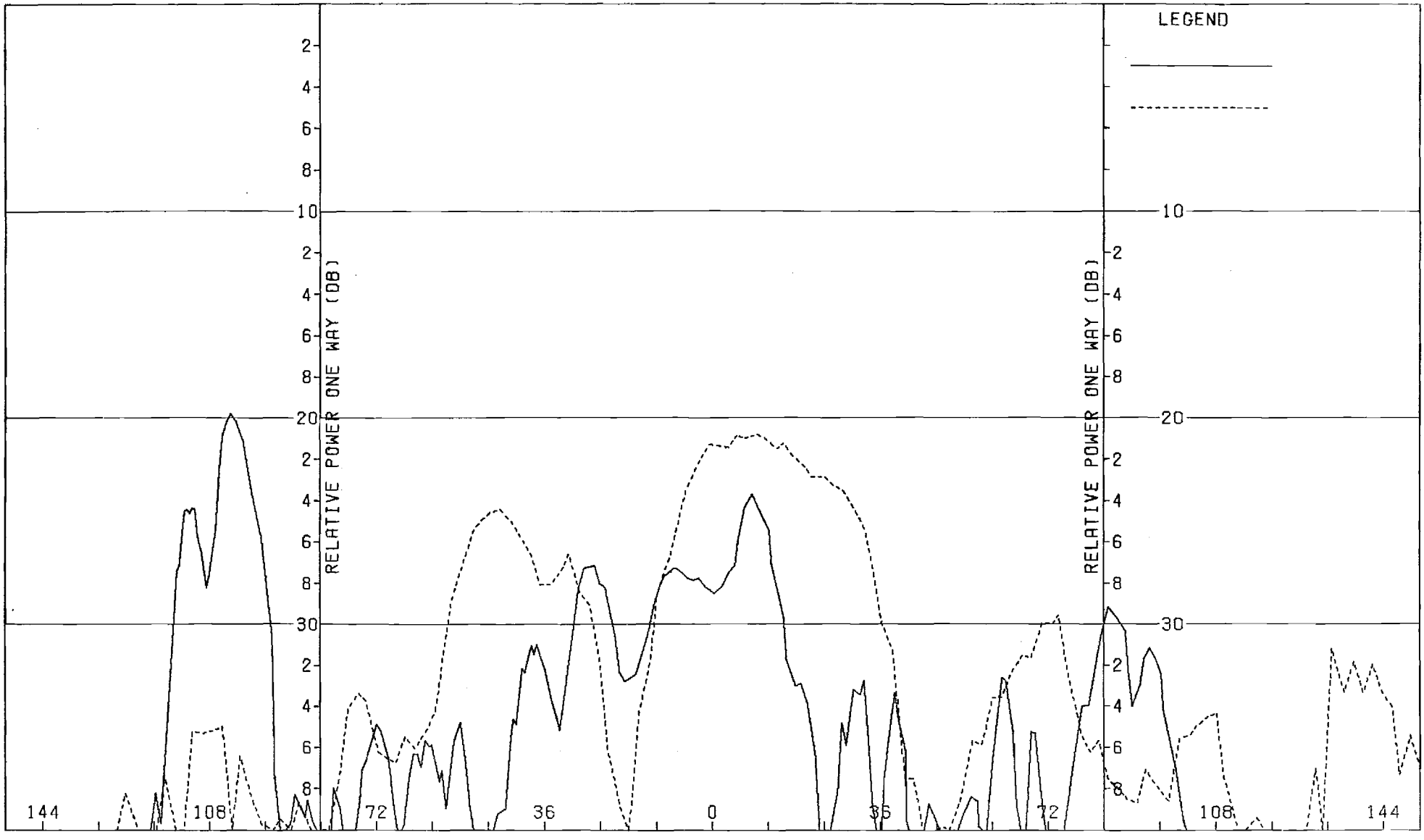

Figure E-11. Pattern of Small Array: H-Plane, Elev. Difference, ϕ-Component, Medium (F=1) Radome

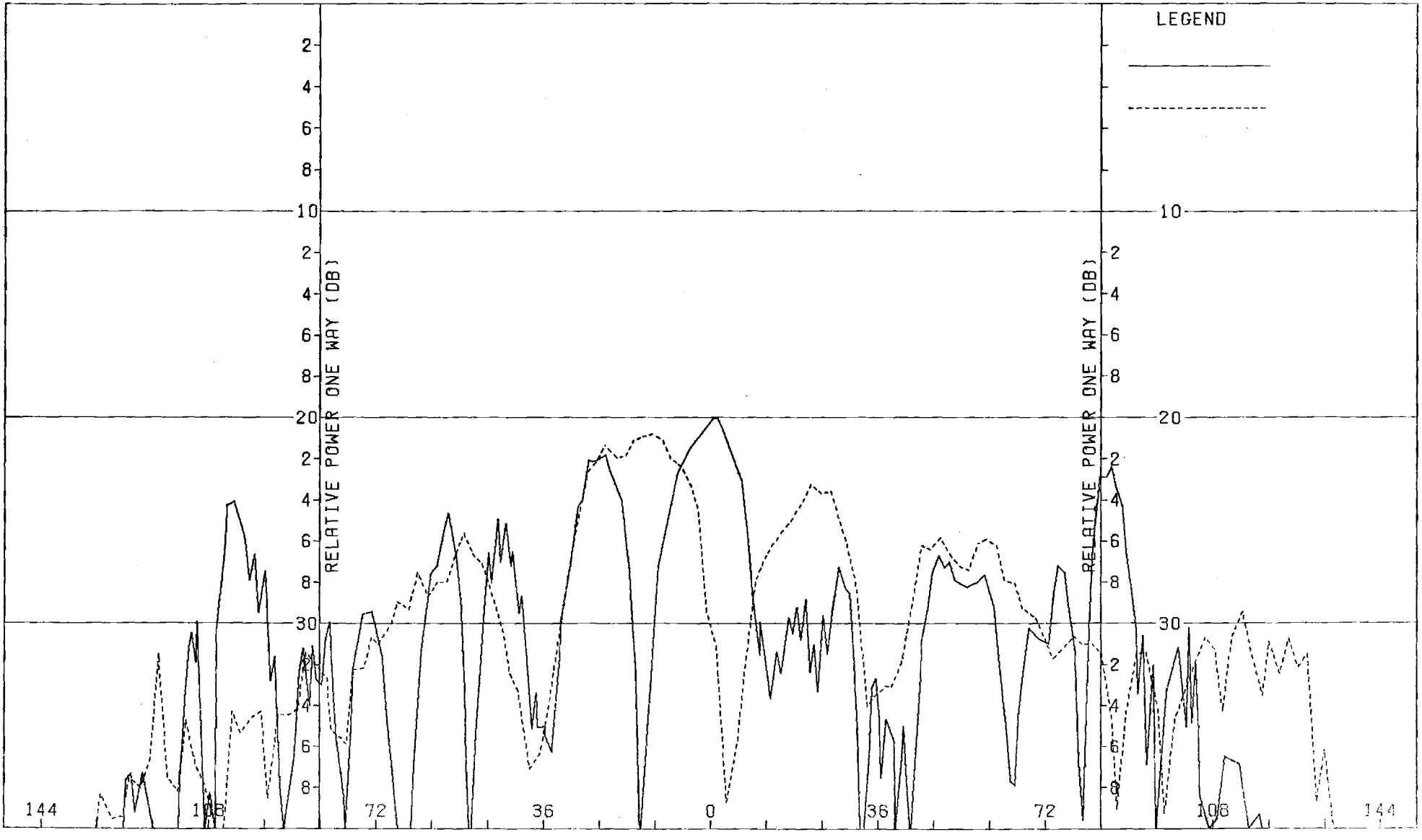

Figure E-12. Pattern of Small Array: H-Plane, Elev. Difference, θ-Component, Medium (F=1) Radome

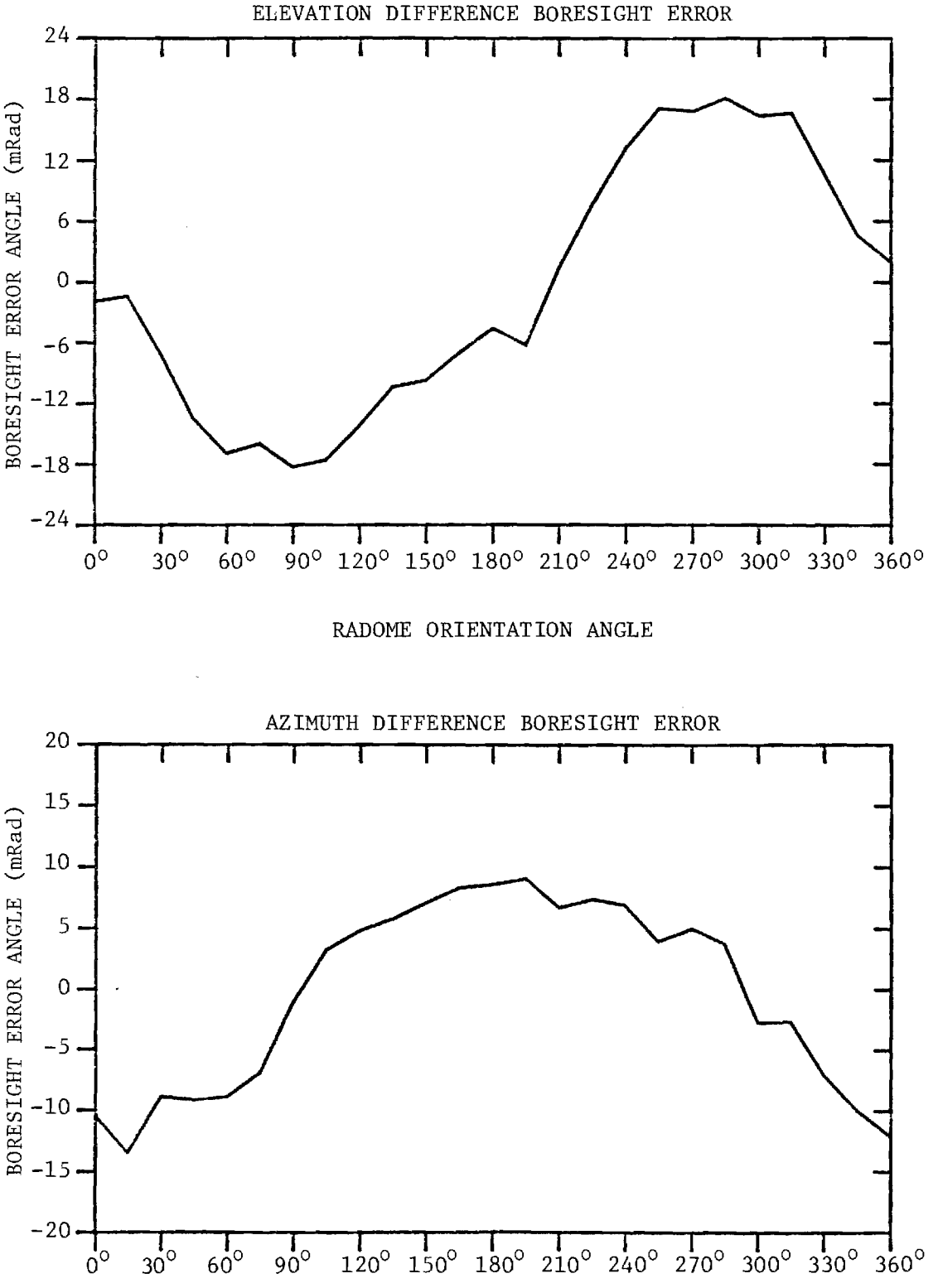

FIGURE E-13. BORESIGHT ERRORS OF SMALL ARRAY AND MEDIUM (F=1) RADOME.

APPENDIX F

Antenna Patterns of Small Array with Large (F=1) Radome

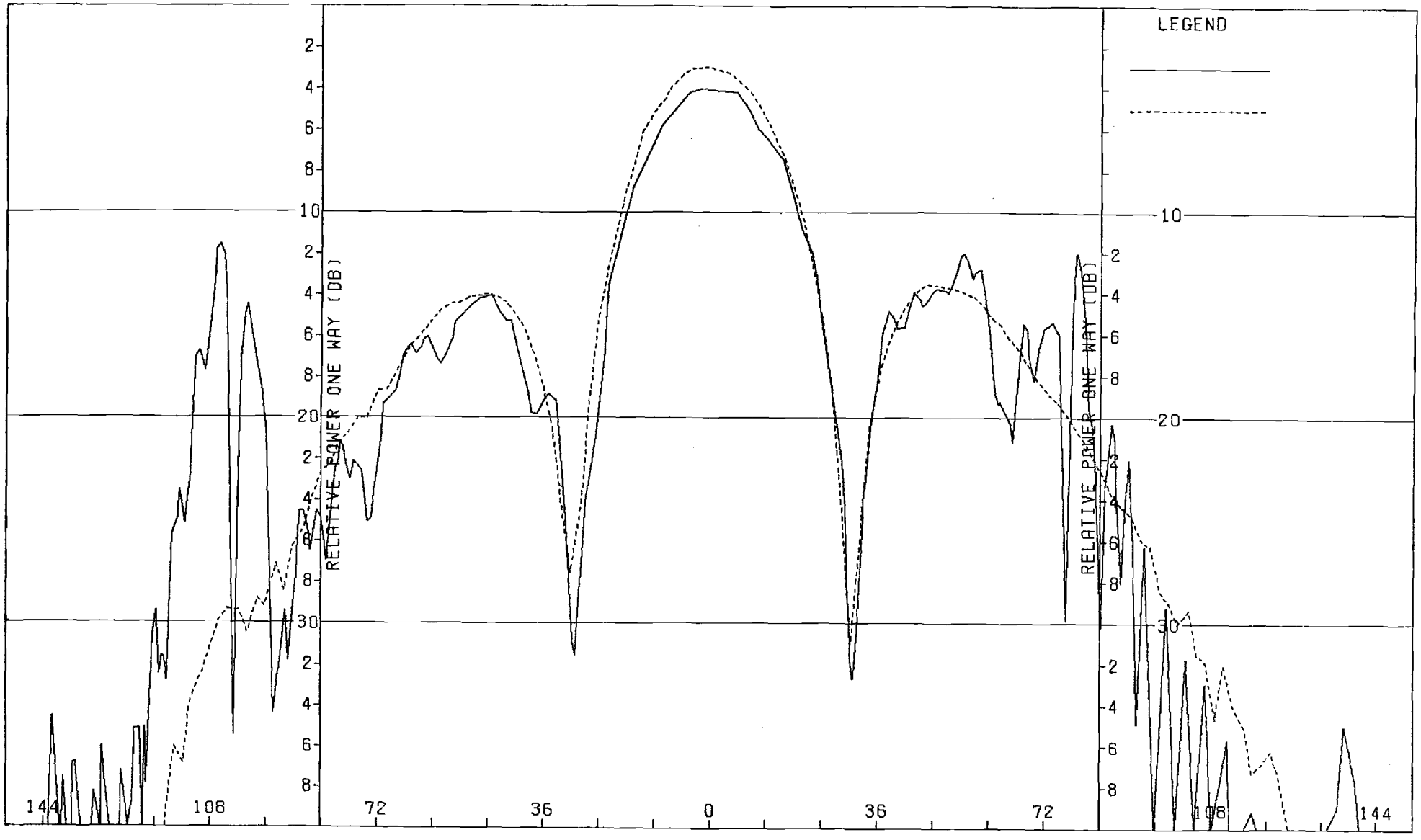

Figure F-1. Pattern of Small Array: H-Plane, Sum, ϕ-Component, Large (F=1) Radome

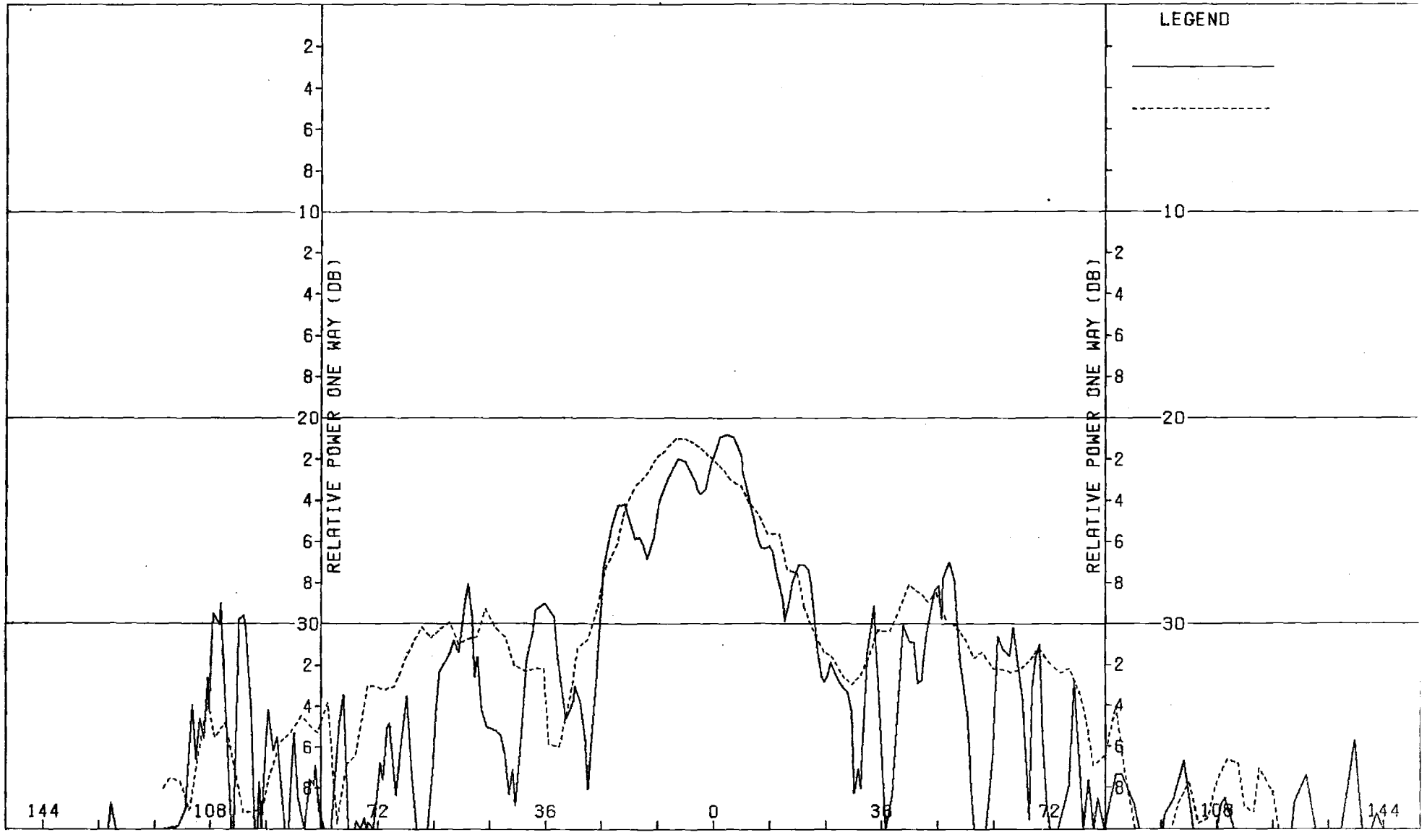

Figure F-2. Pattern of Small Array: H-Plane, Sum, θ-Component, Large (F=1) Radome

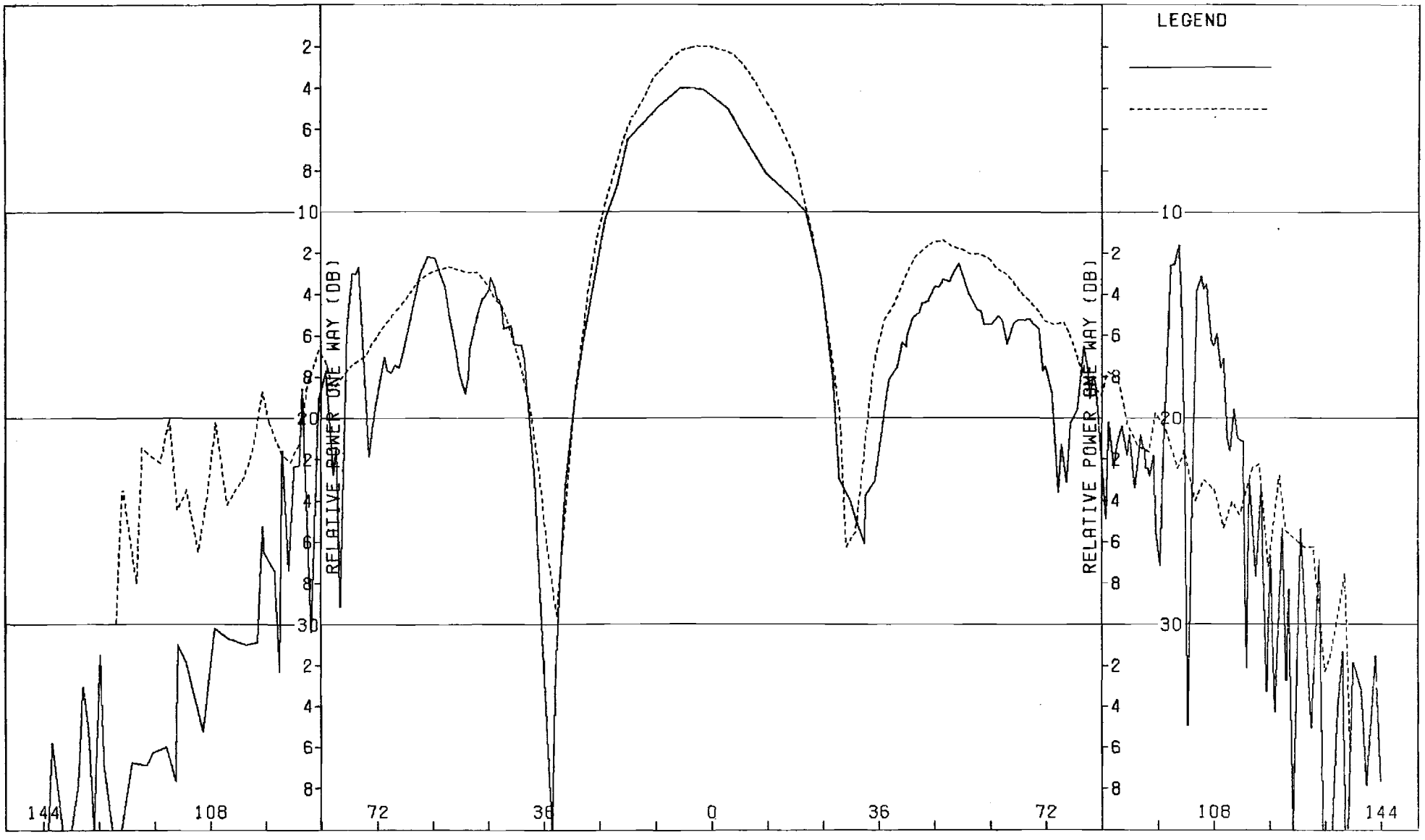

Figure E-3. Pattern of Small Array: E-Plane, Sum, θ-Component, Large (F=1) Radome

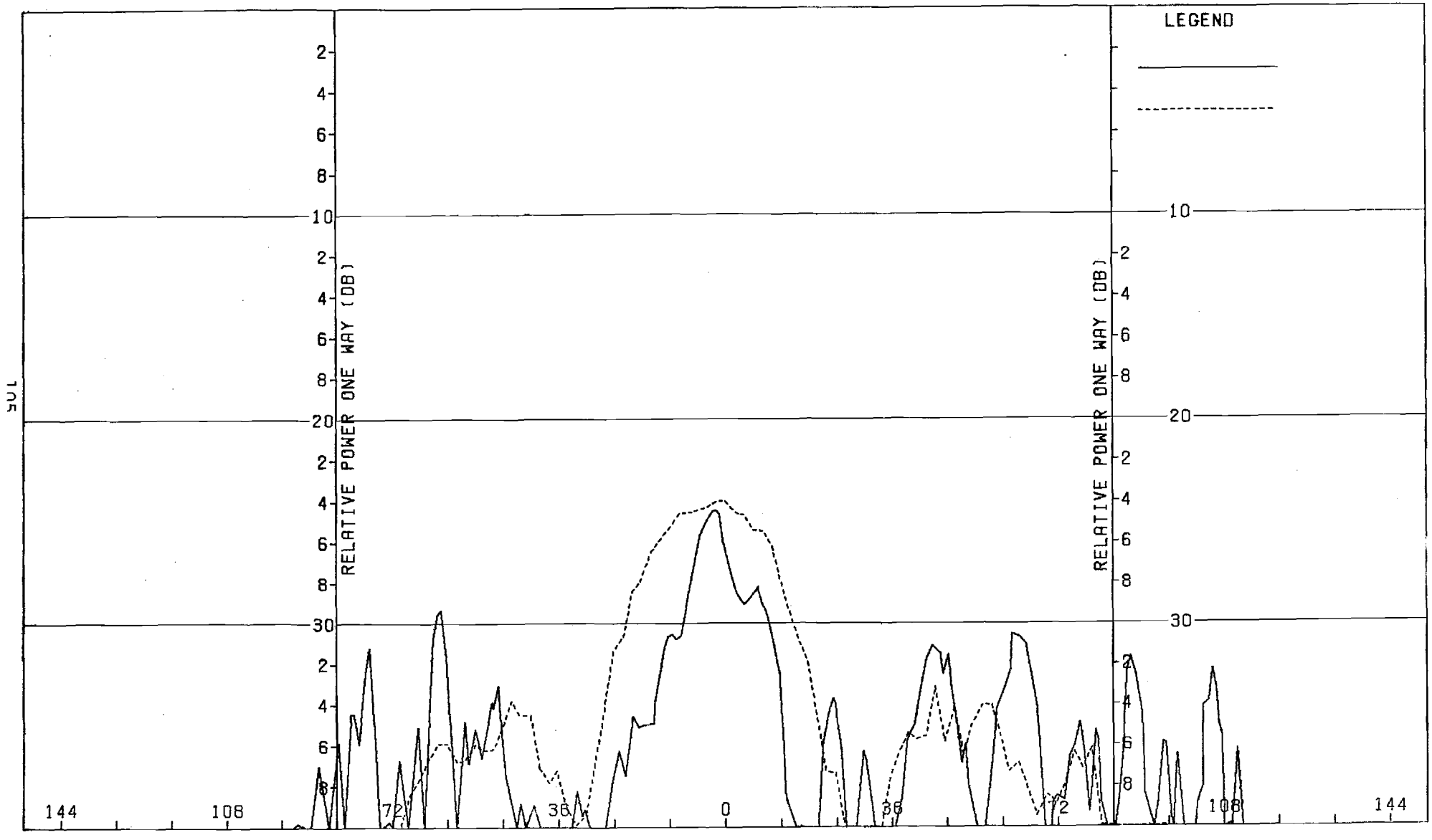

Figure F-4. Pattern of Small Array: E-Plane, Sum, ϕ-Component, Large (F=1) Radome

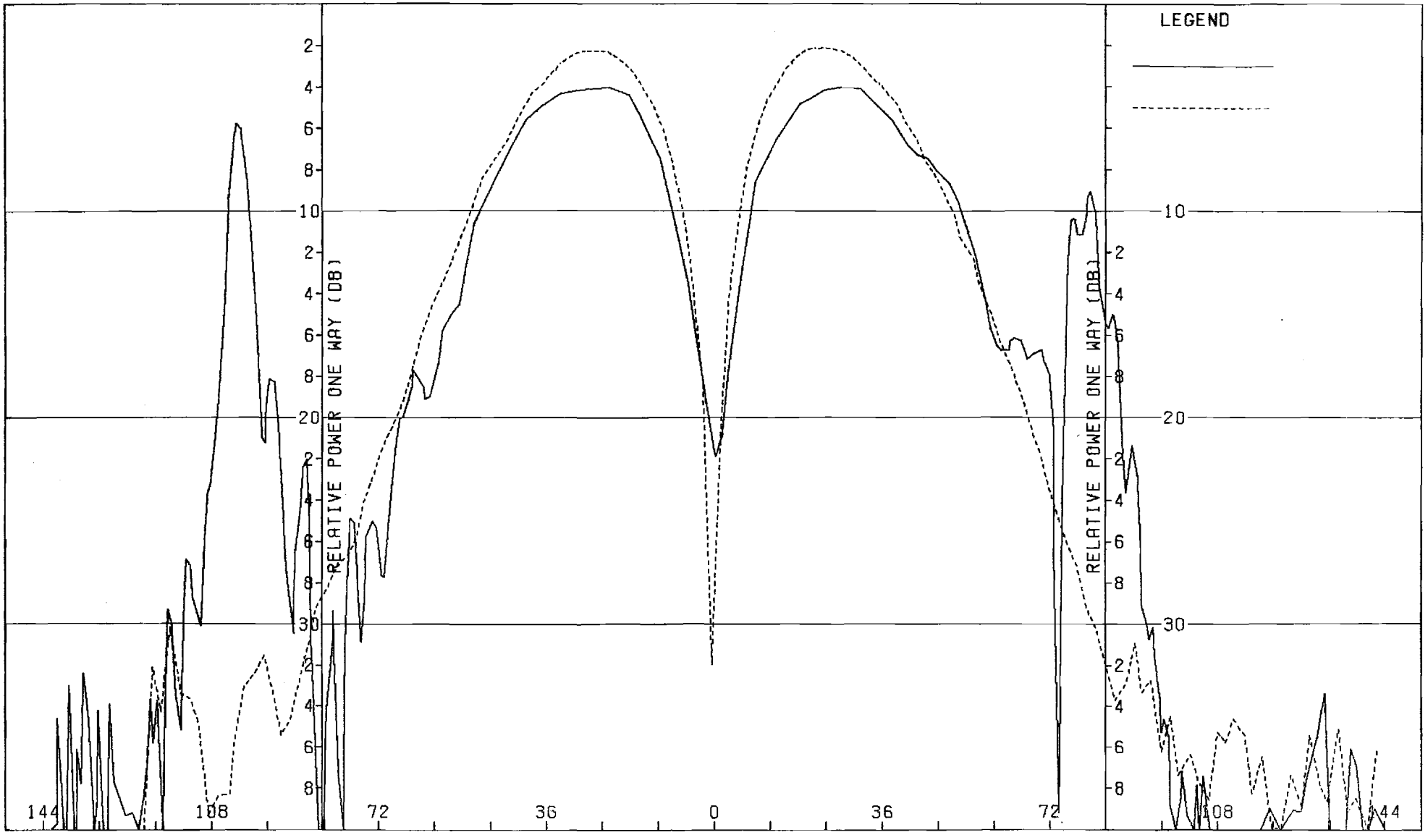

Figure F-5. Pattern of Small Array: H-Plane, Azimuth Diff., ϕ-Component, Large (F=1) Radome

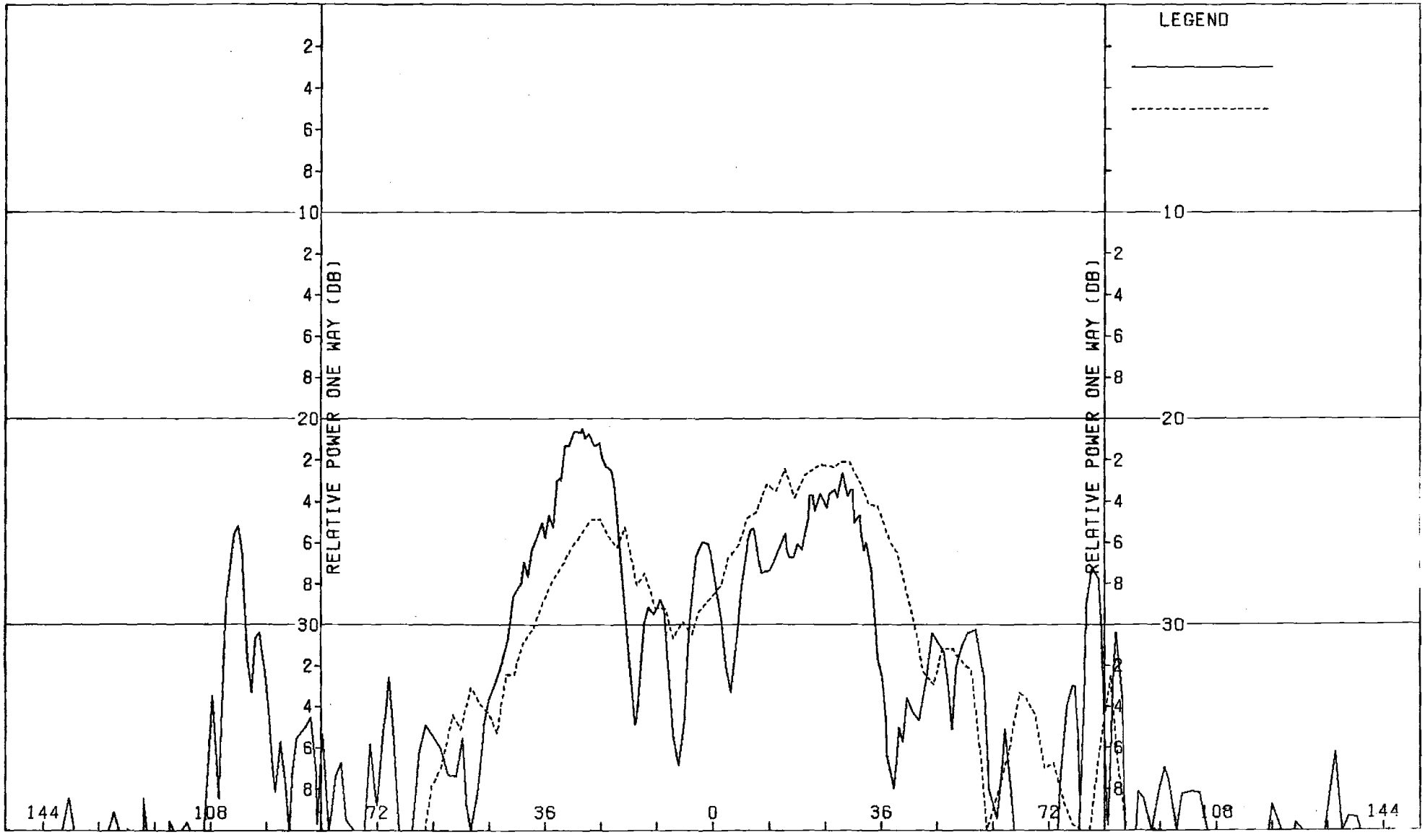

Figure F-6. Pattern of Small Array: H-Plane, Azimuth Diff., θ-Component, Large (F=1) Radome

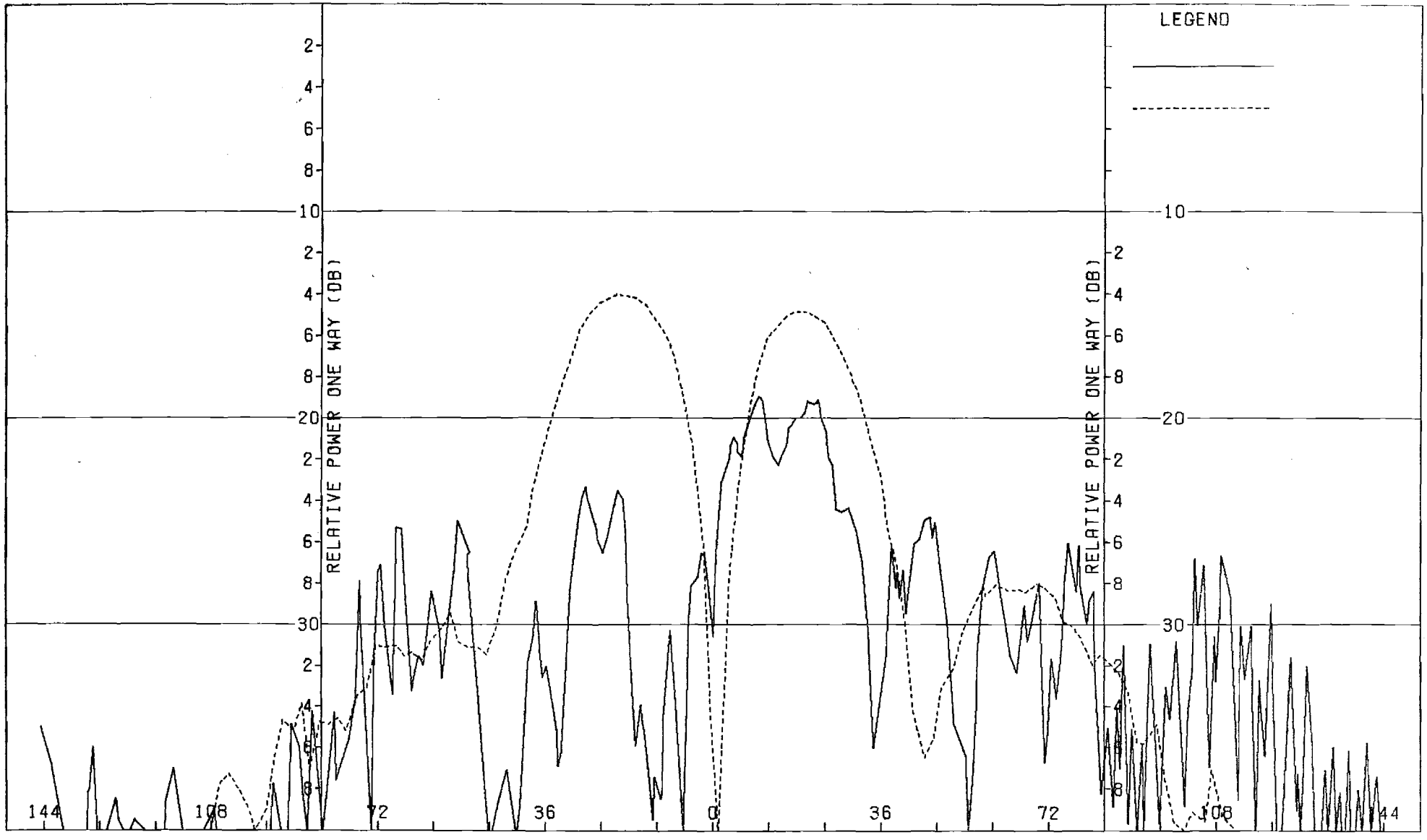

Figure F-7. Pattern of Small Array: E-Plane, Azimuth Diff., θ-Component, Large (F=1) Radome

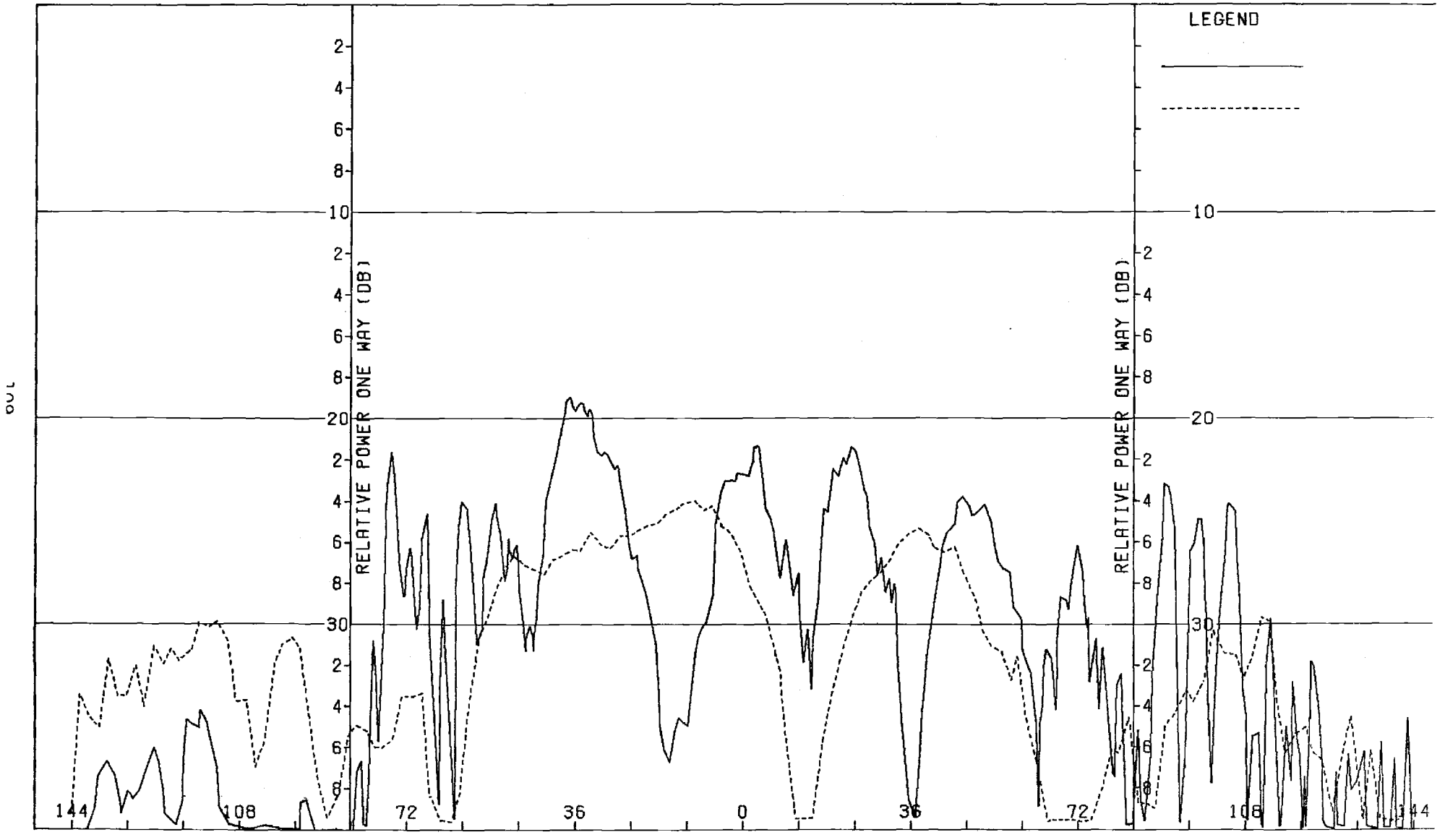

Figure F-8. Pattern of Small Array: E-Plane, Azimuth Diff., ϕ-Component, Large (F=1) Radome

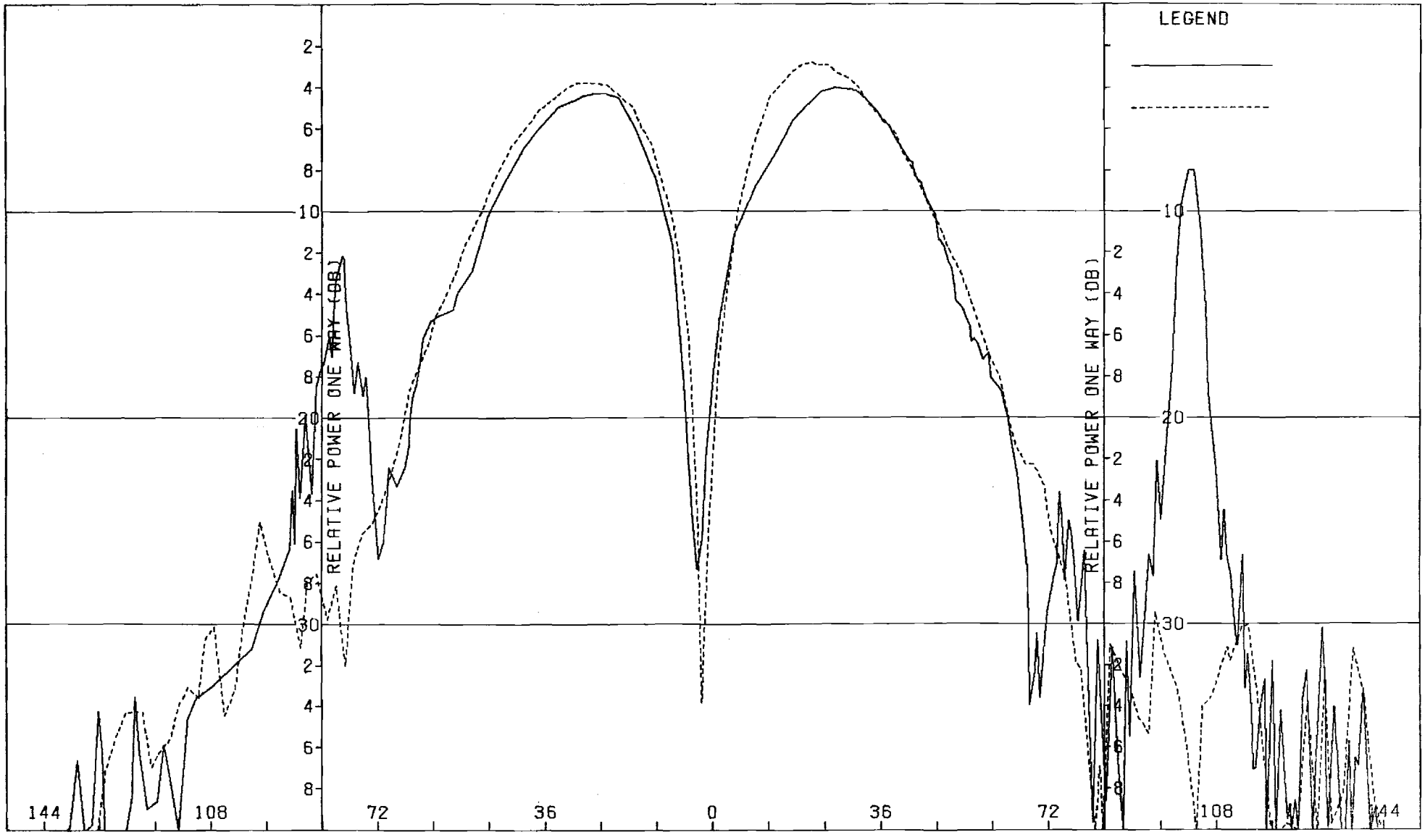

Figure F-9. Pattern of Small Array: E-Plane, Elev. Difference, θ-Component, Large (F=1) Radome

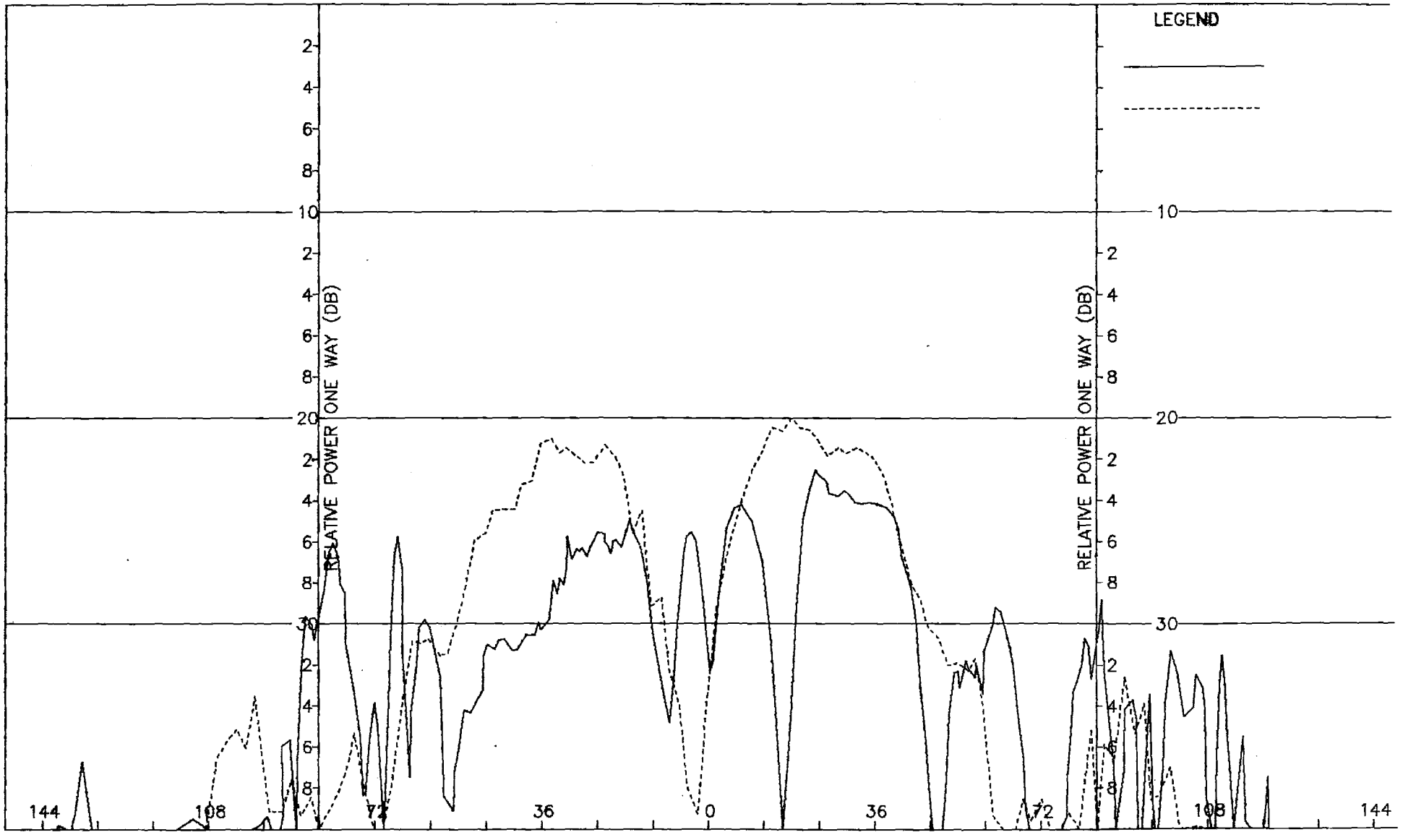

Figure F-10. Pattern of Small Array: E-Plane, Elev. Difference, ϕ-Component, Large (F=1) Radome

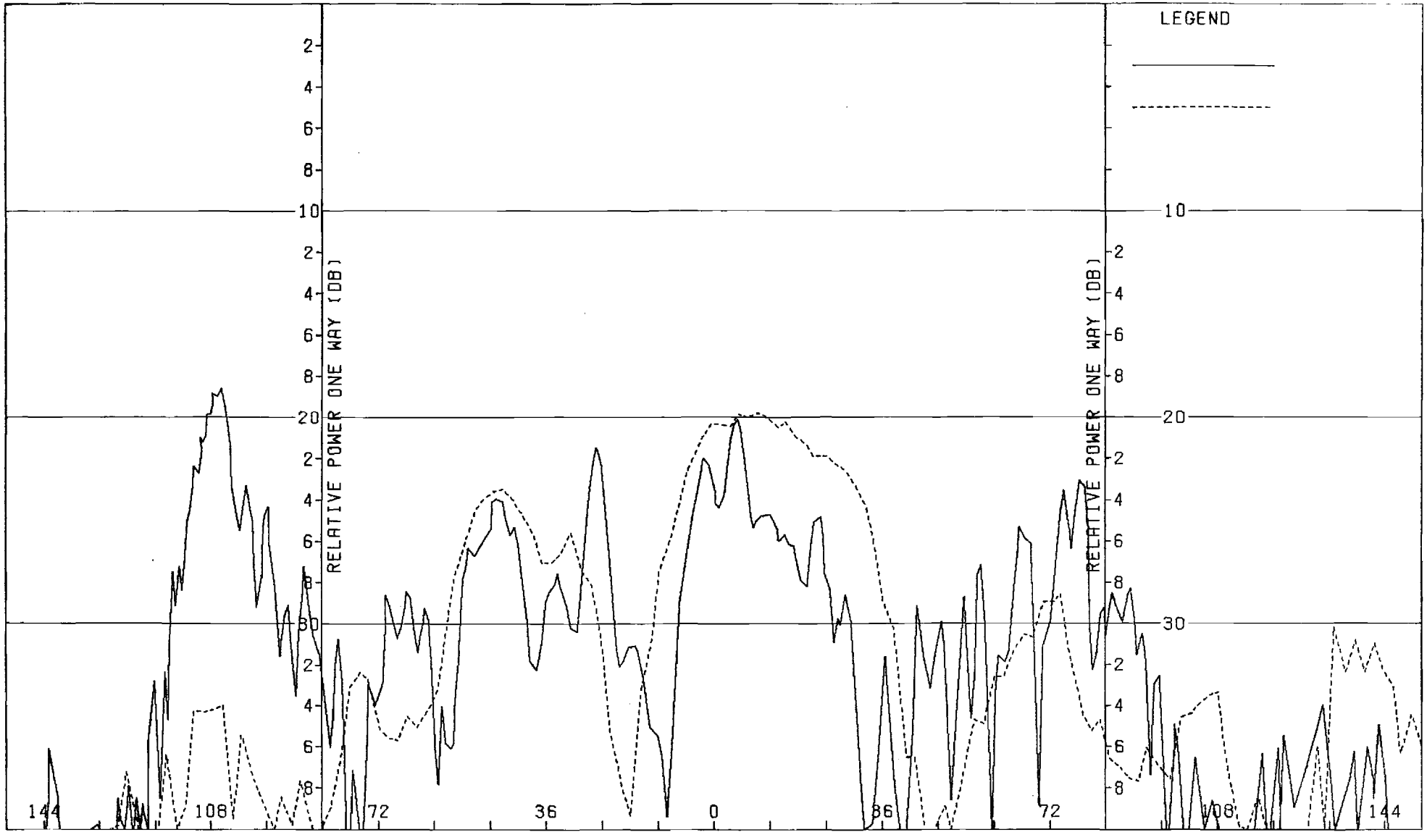

Figure F-11. Pattern of Small Array: H-Plane, Elevation Diff., ϕ-Component, Large (F=1) Radome

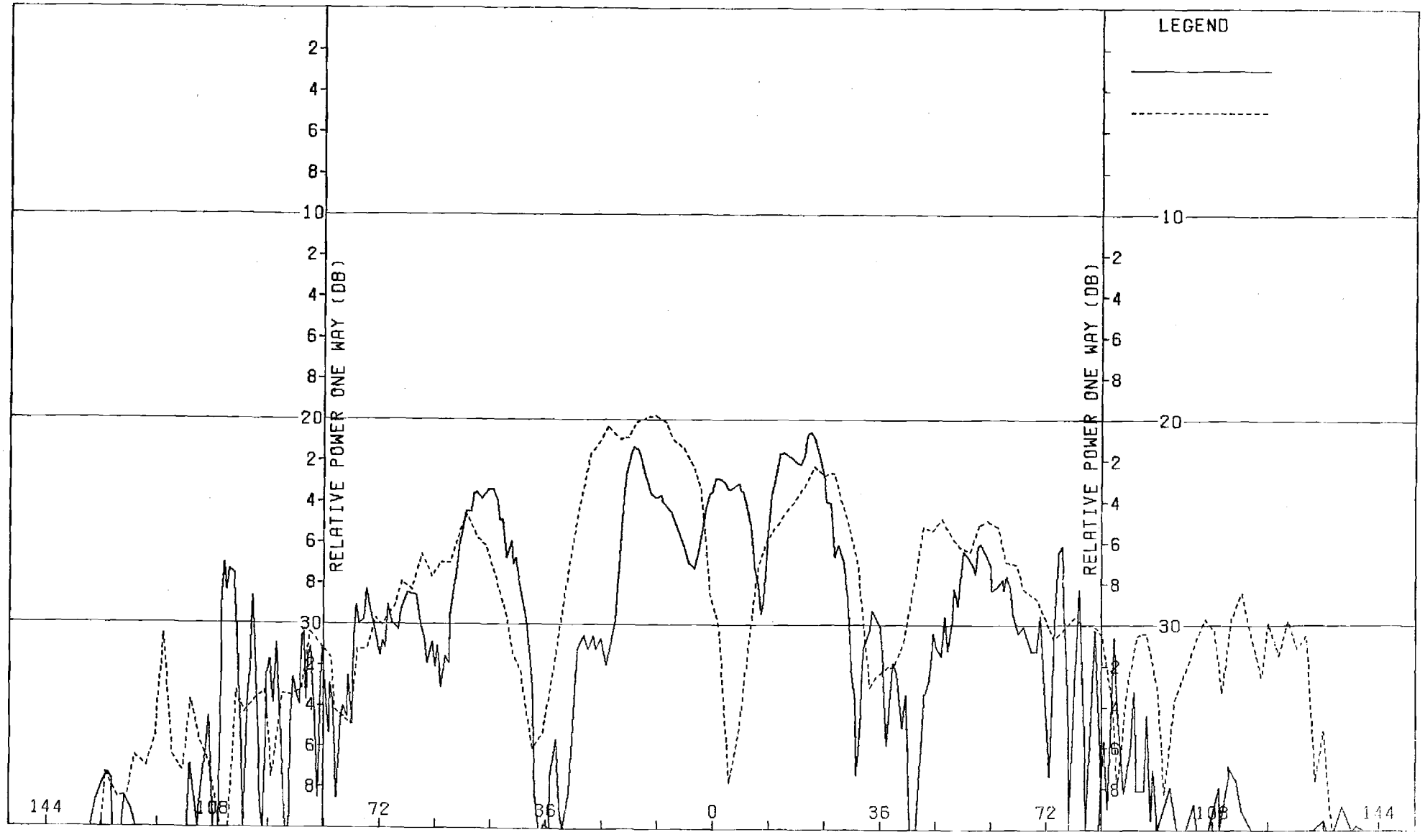

Figure F-12. Pattern of Small Array: H-Plane, Elev. Difference, ϕ-Component, Large (F=1) Radome

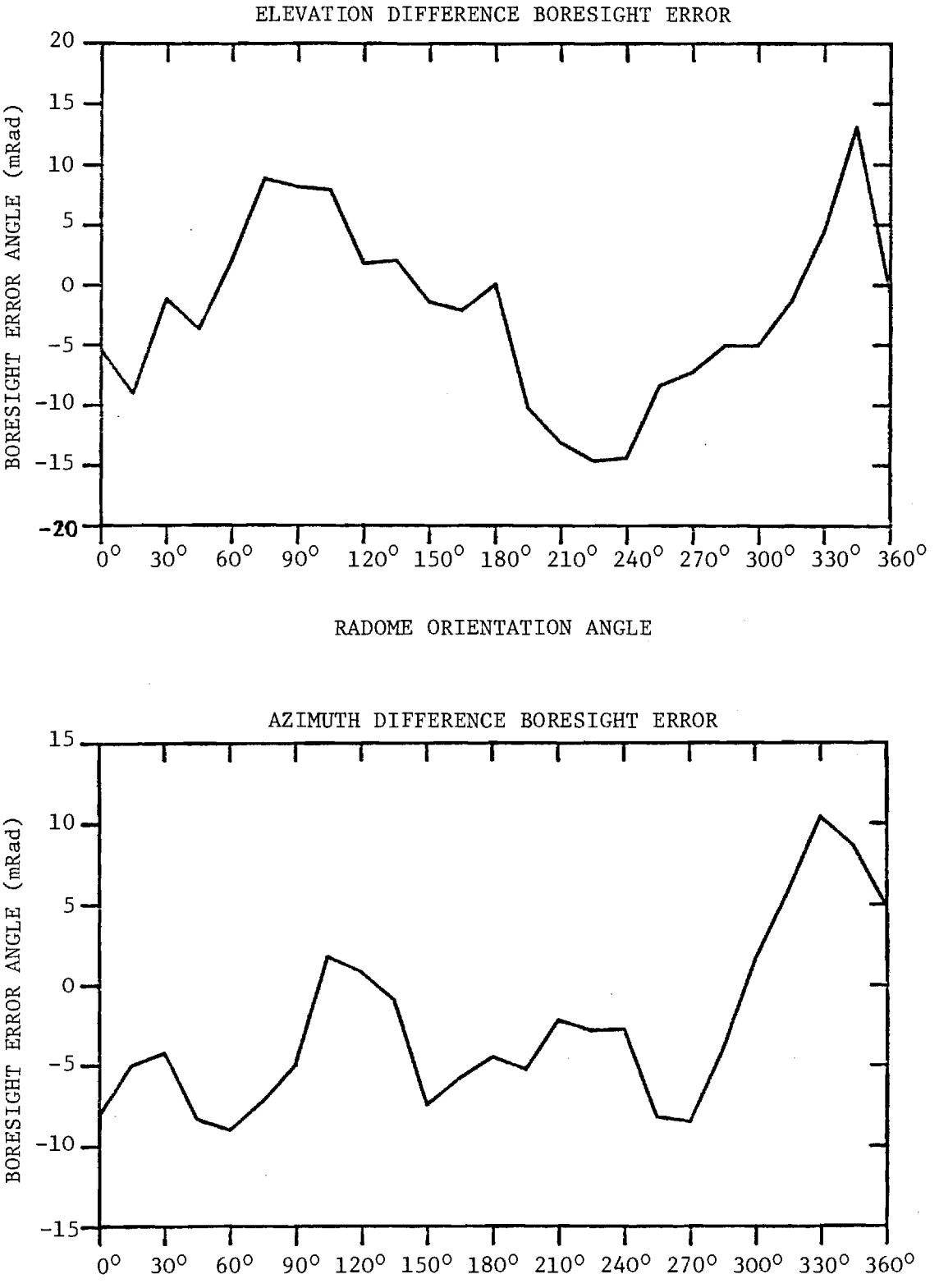

FIGURE F-13. BORESIGHT ERRORS OF SMALL ARRAY AND LARGE RADOME.

APPENDIX G

Antenna Patterns of Medium Array with Medium (F=1) Radome

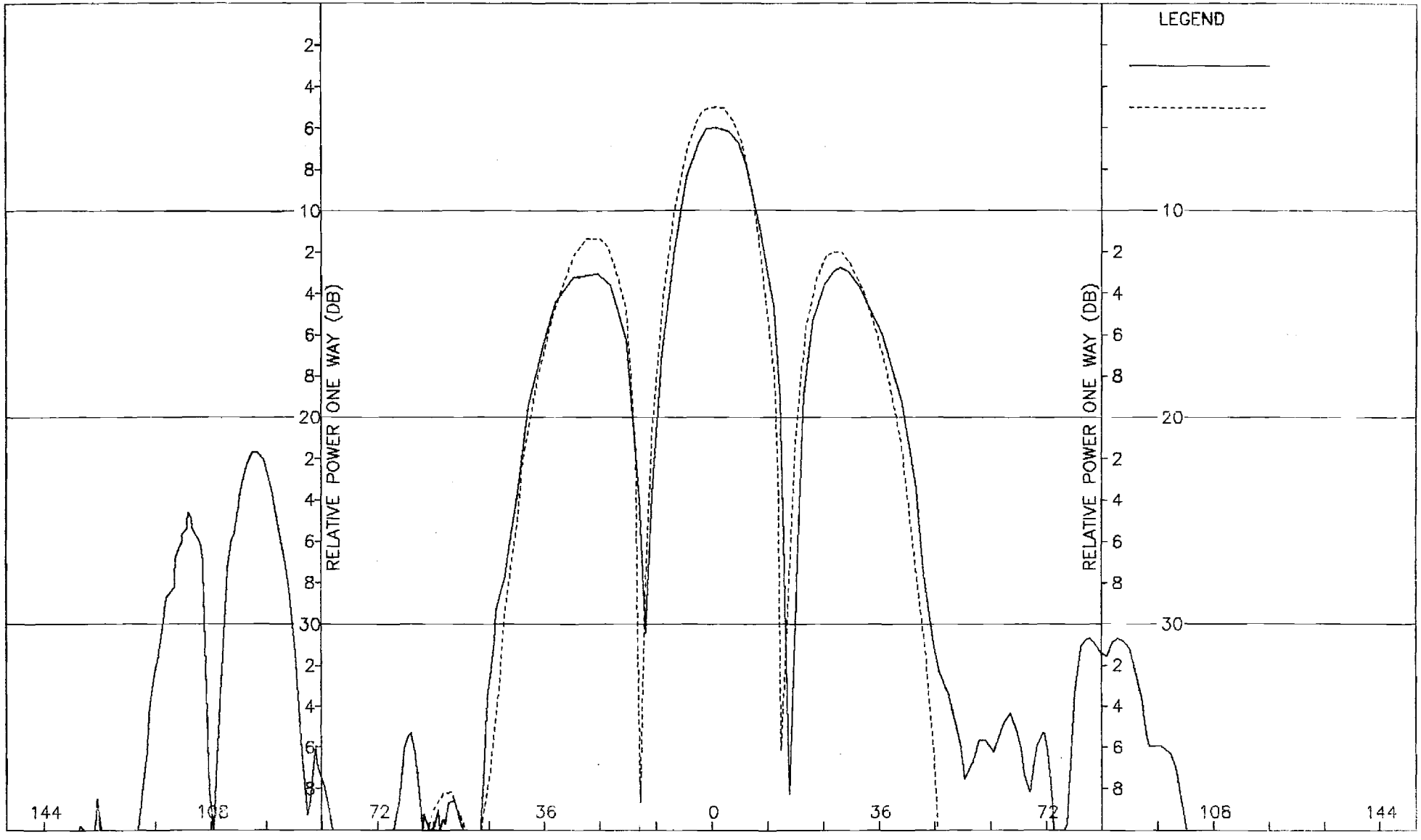

Figure G-1. Pattern of Medium Array: H-Plane, Sum, ϕ-Component, Medium (F=1) Radome

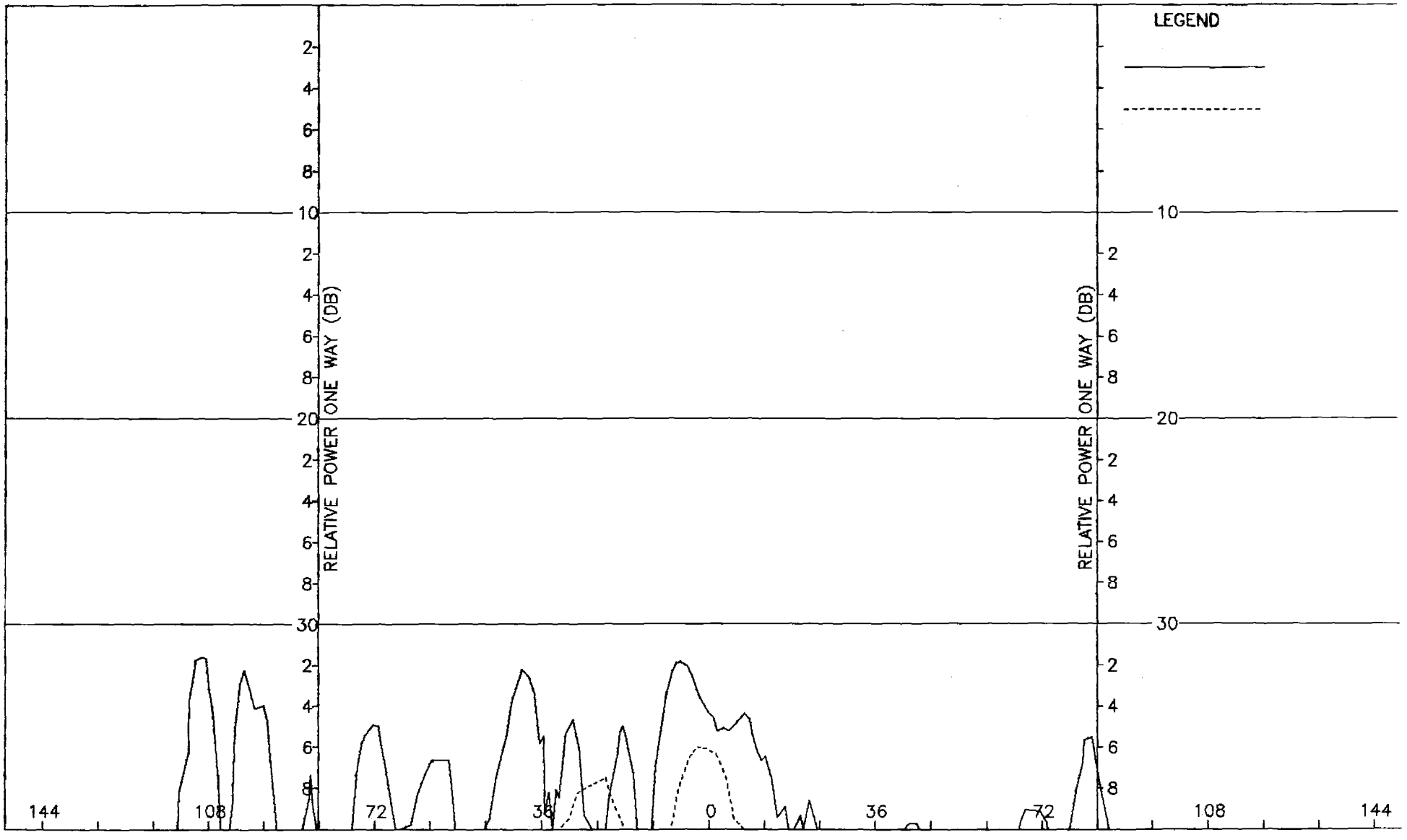

Figure G-2. Pattern of Medium Array: H-Plane, Sum, ϕ-Component, Medium (F=1) Radome

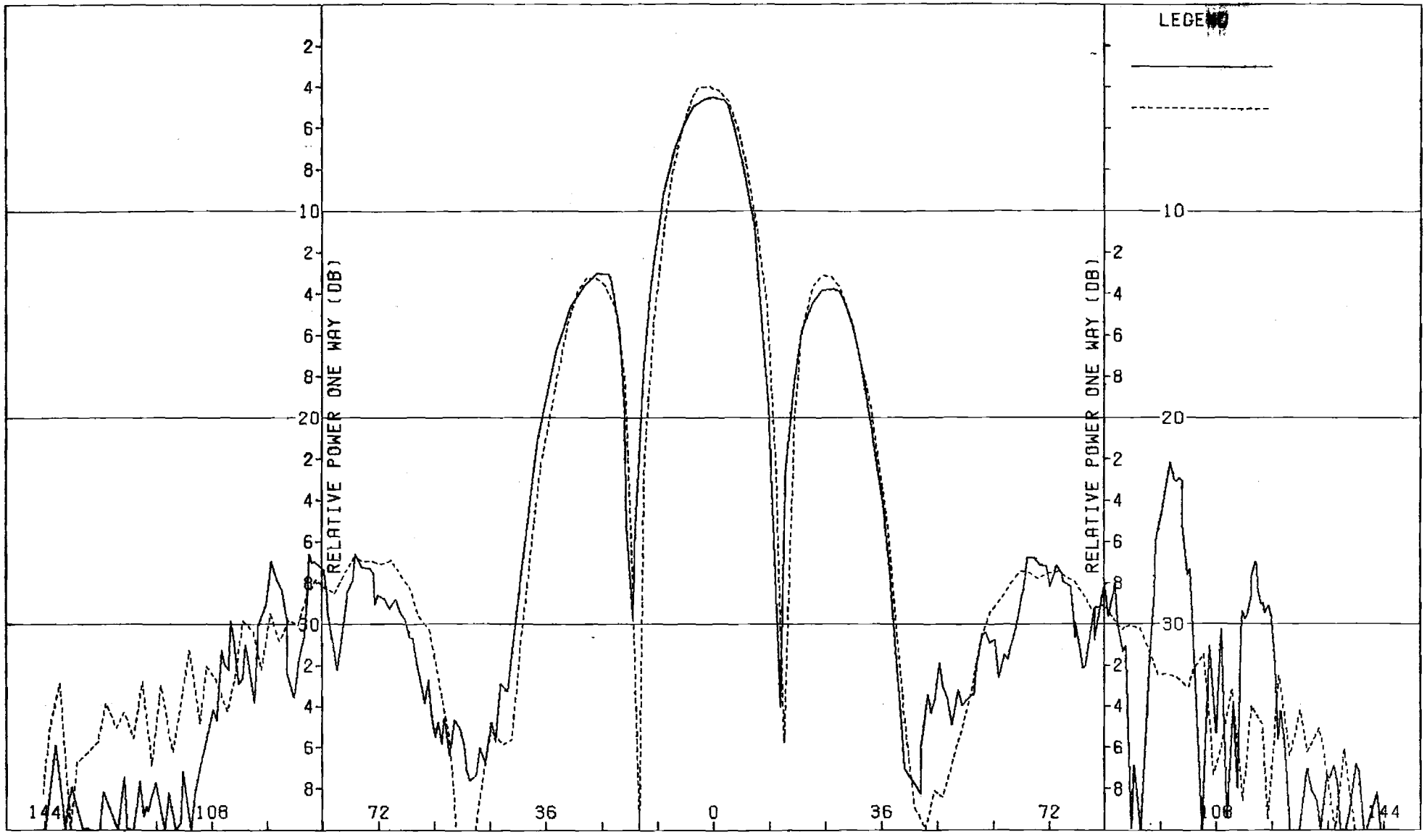

Figure G-3. Pattern of Medium Array: E-Plane, Sum, θ-Component, Medium (F=1) Radome

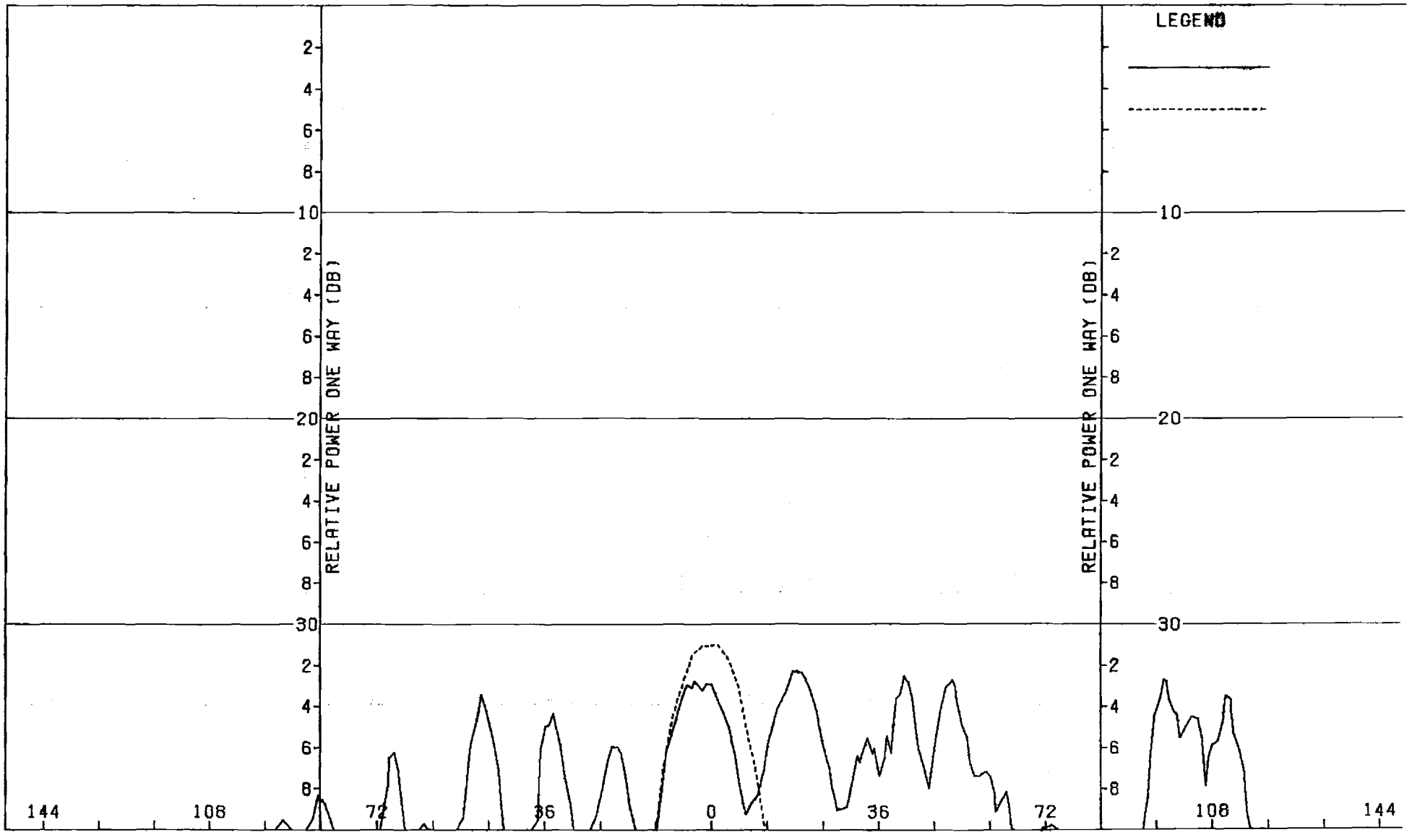

Figure G-4. Pattern of Medium Array: E-Plane Sum, ϕ-Component, Medium (F=1) Radome

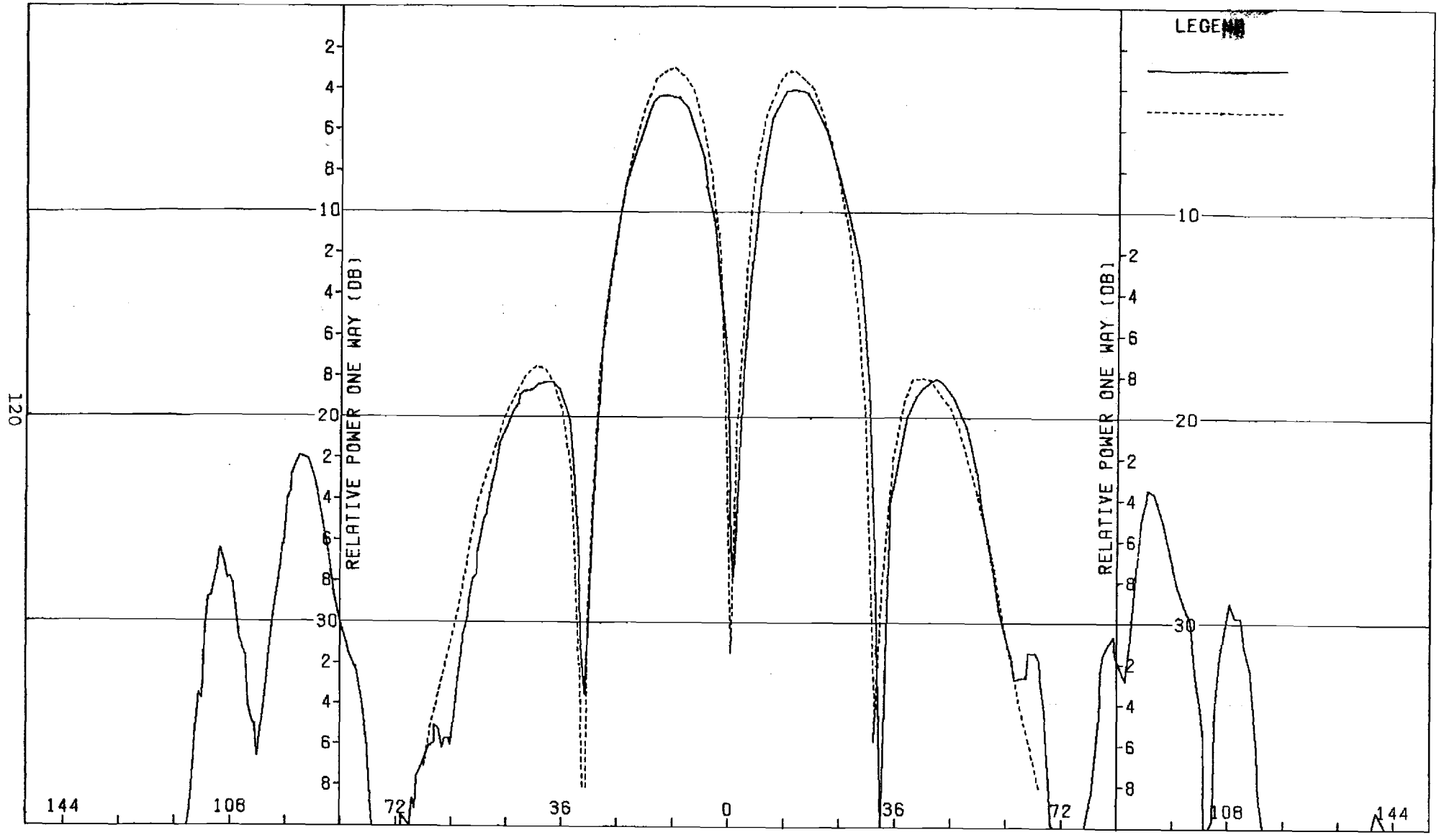

Figure G-5. Pattern of Medium Array: H-Plane, Azimuth Difference, ϕ-Component, Medium (F=1) Radome

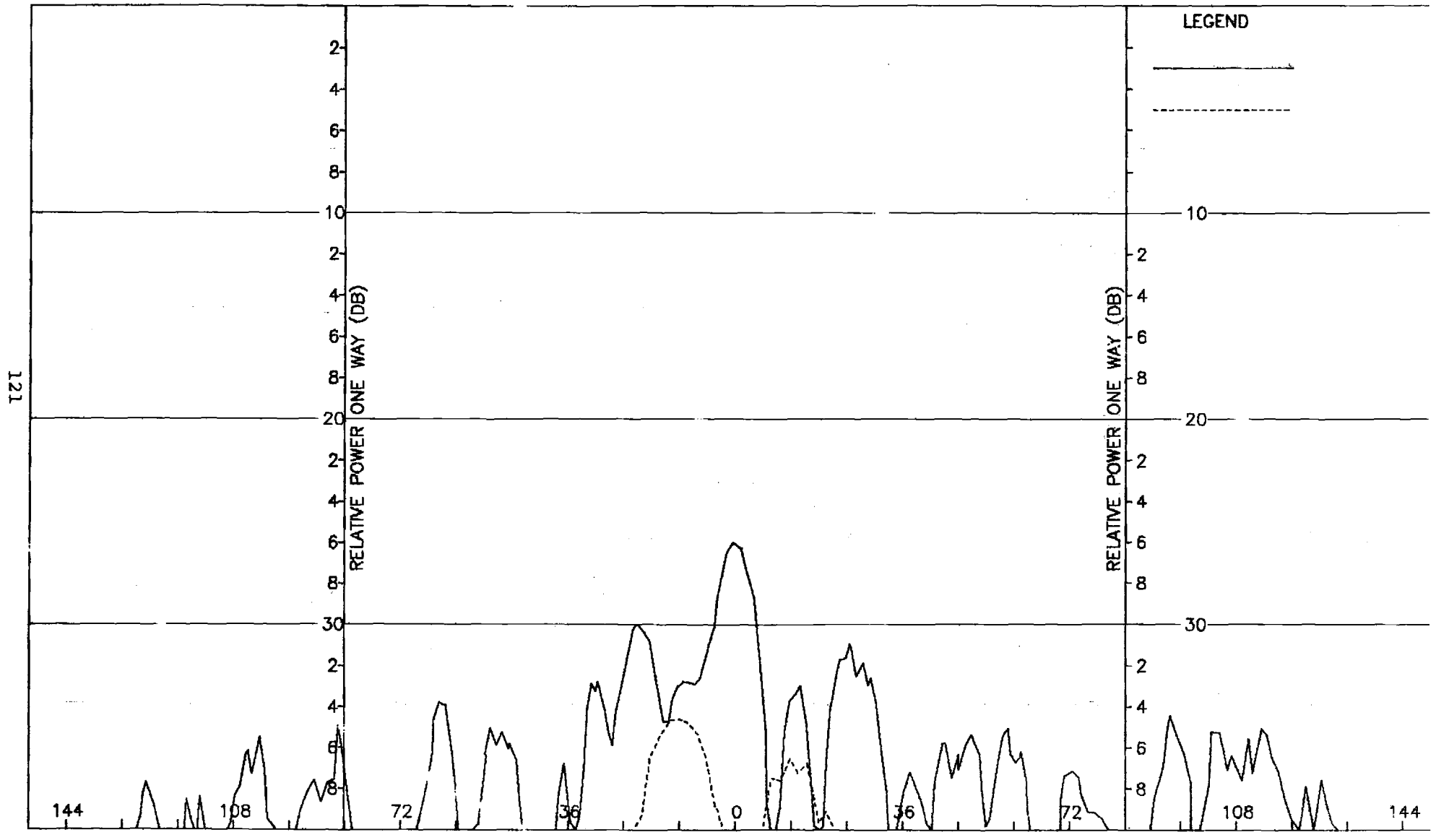

Figure G-6. Pattern of Medium Array: H-Plane, Azimuth Difference, θ-Component, Medium (F=1) Radome

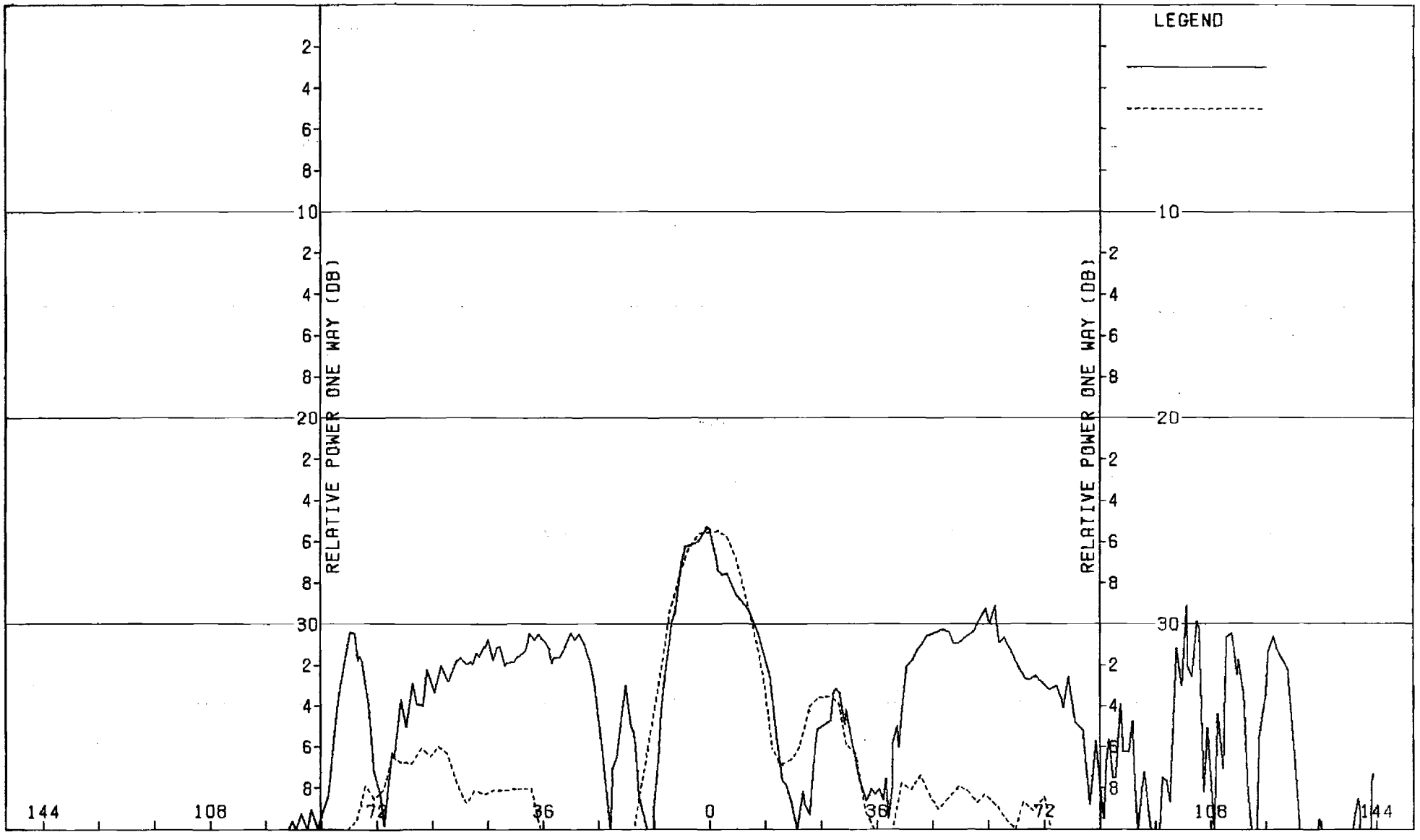

Figure G-7. Pattern of Medium Array: E-Plane, Azimuth Difference, θ-Component, Medium (F=1) Radome

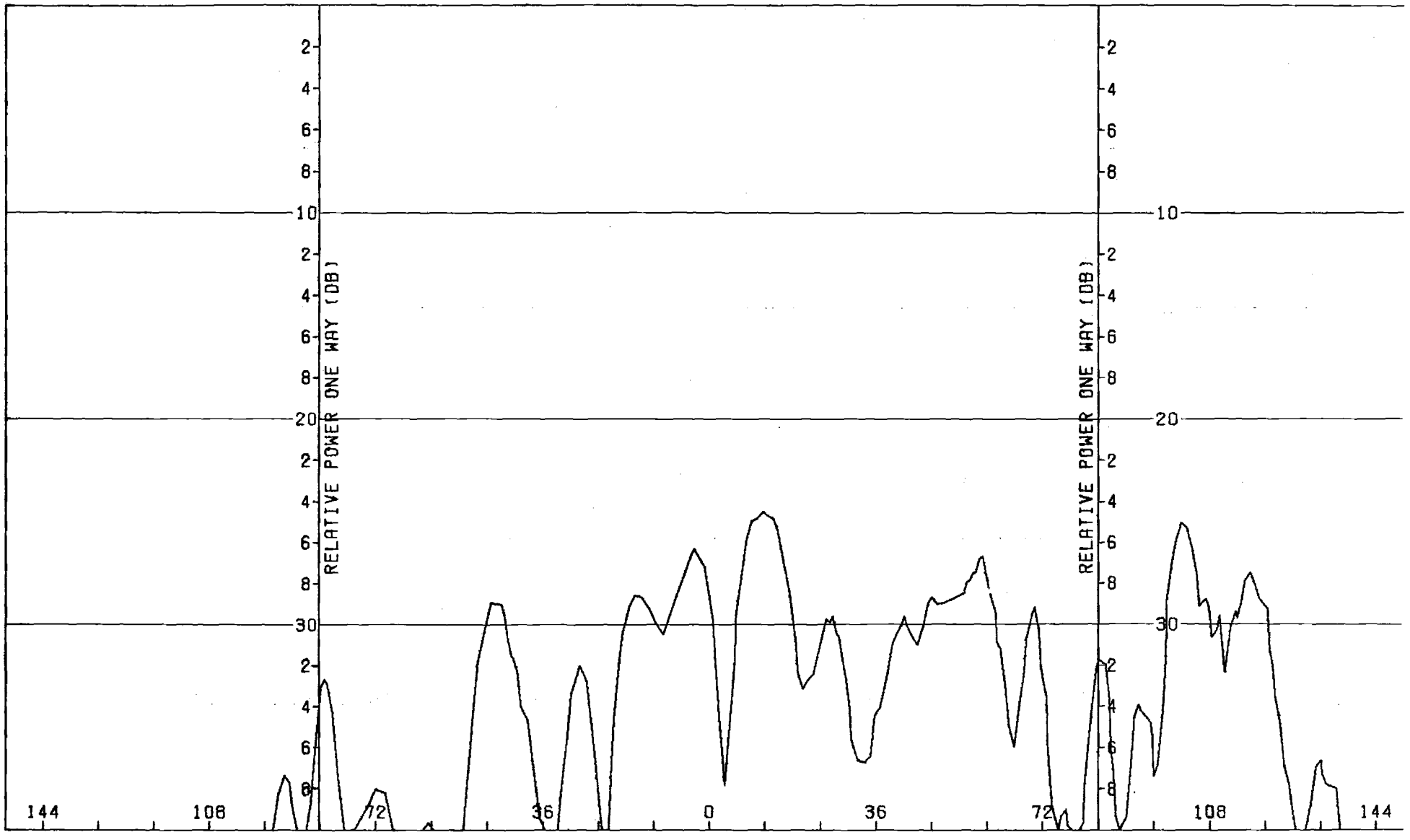

Figure G-8. Pattern of Medium Array: E-Plane, Azimuth Difference, ϕ-Component, Medium (F=1) Radome

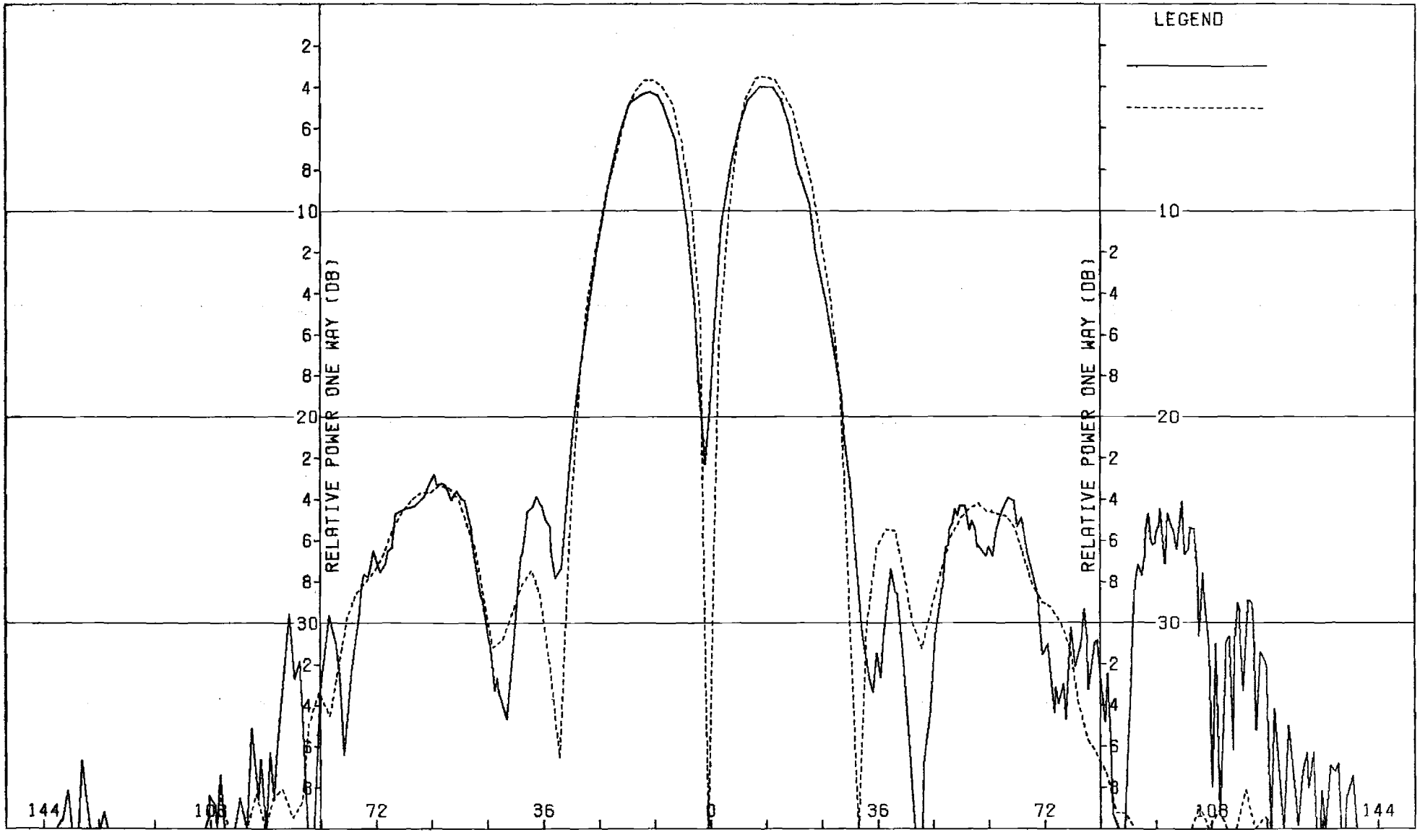

Figure G-9. Pattern of Medium Array: E-Plane, Elevation Difference, θ-Component, Medium (F=1) Radome

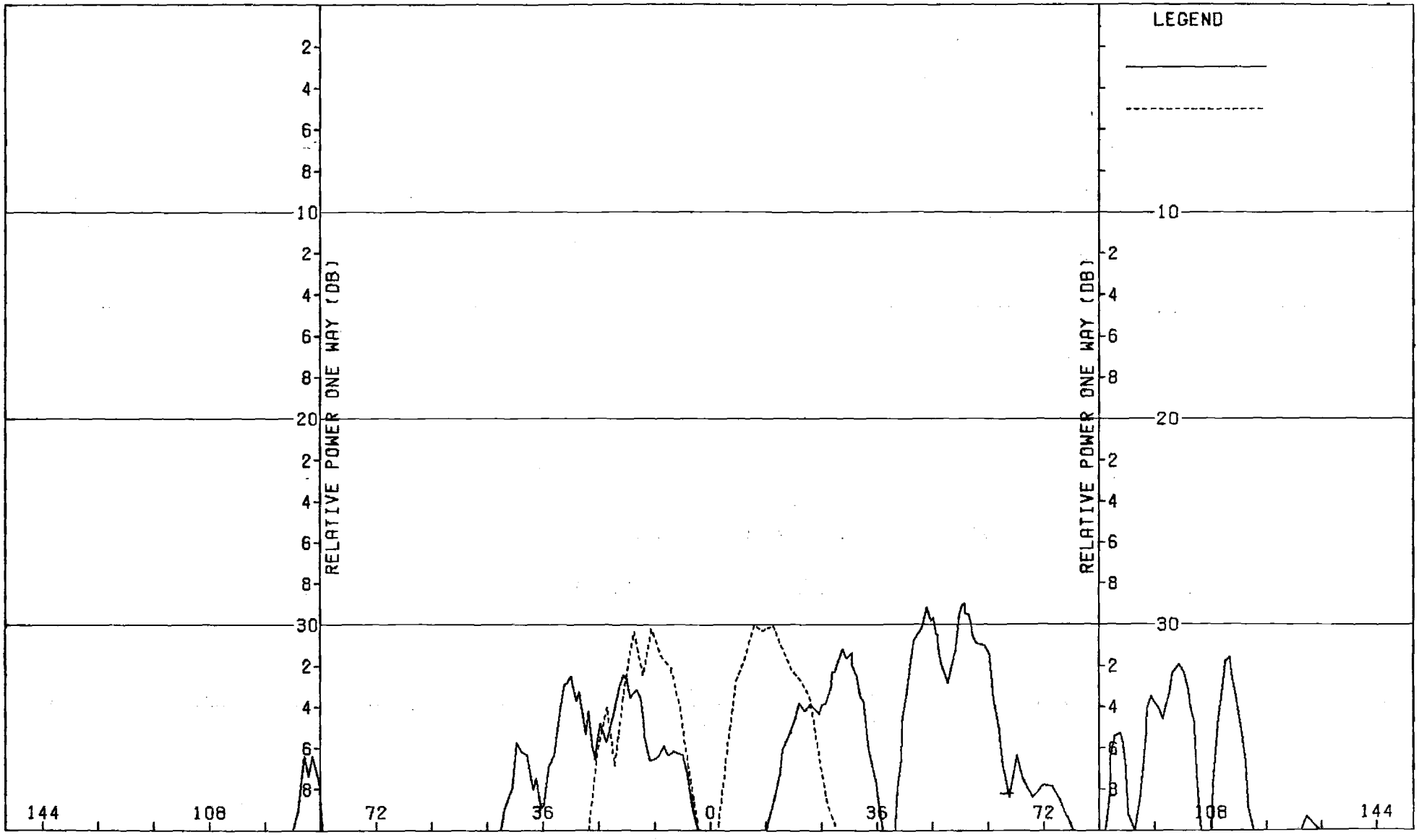

Figure G-10. Pattern of Medium Array: E-Plane, Elevation Difference, ϕ-Component, Medium (F=1) Radome

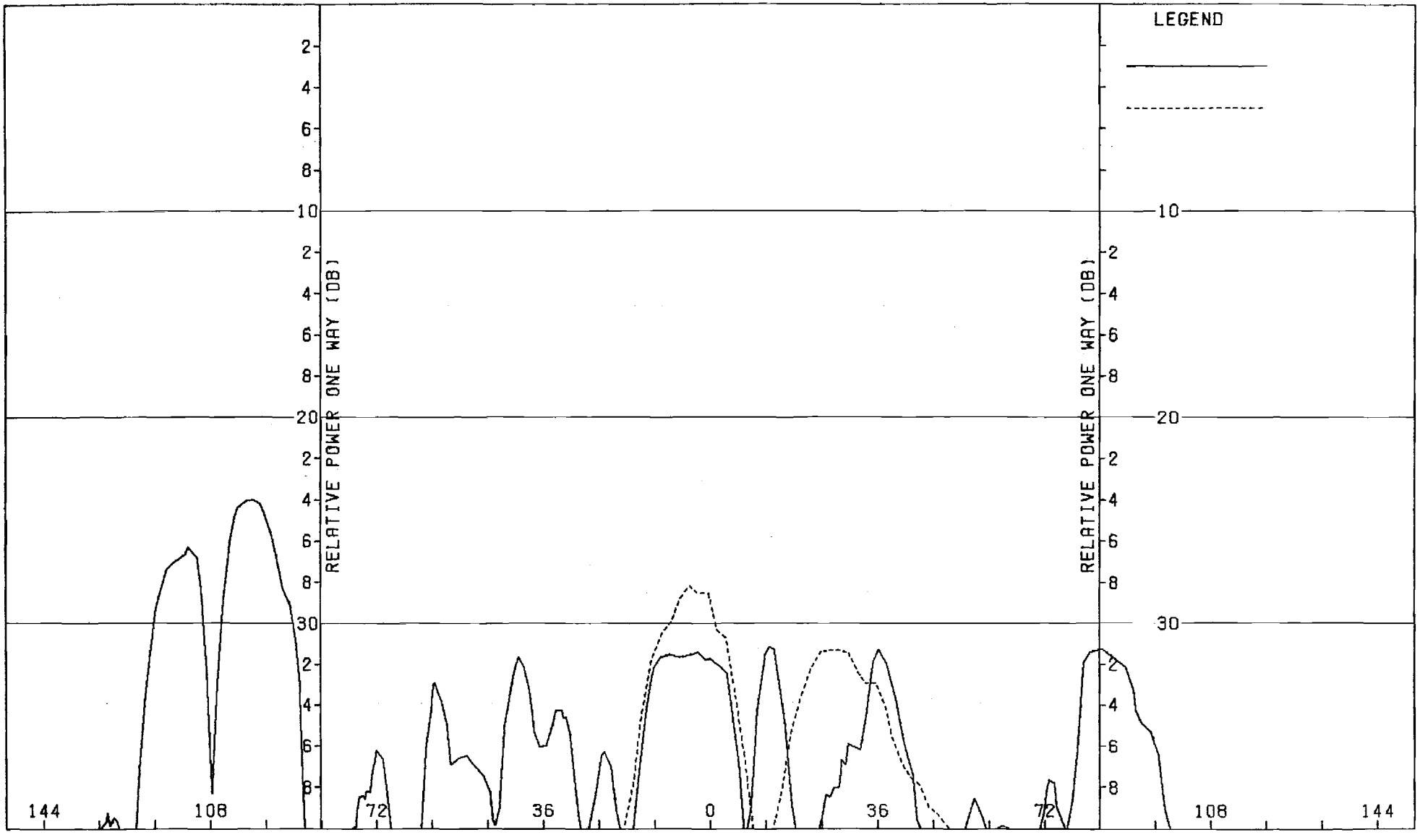

Figure G-11. Pattern of Medium Array: H-Plane, Elevation Difference, ϕ-Component, Medium (F=1) Radome

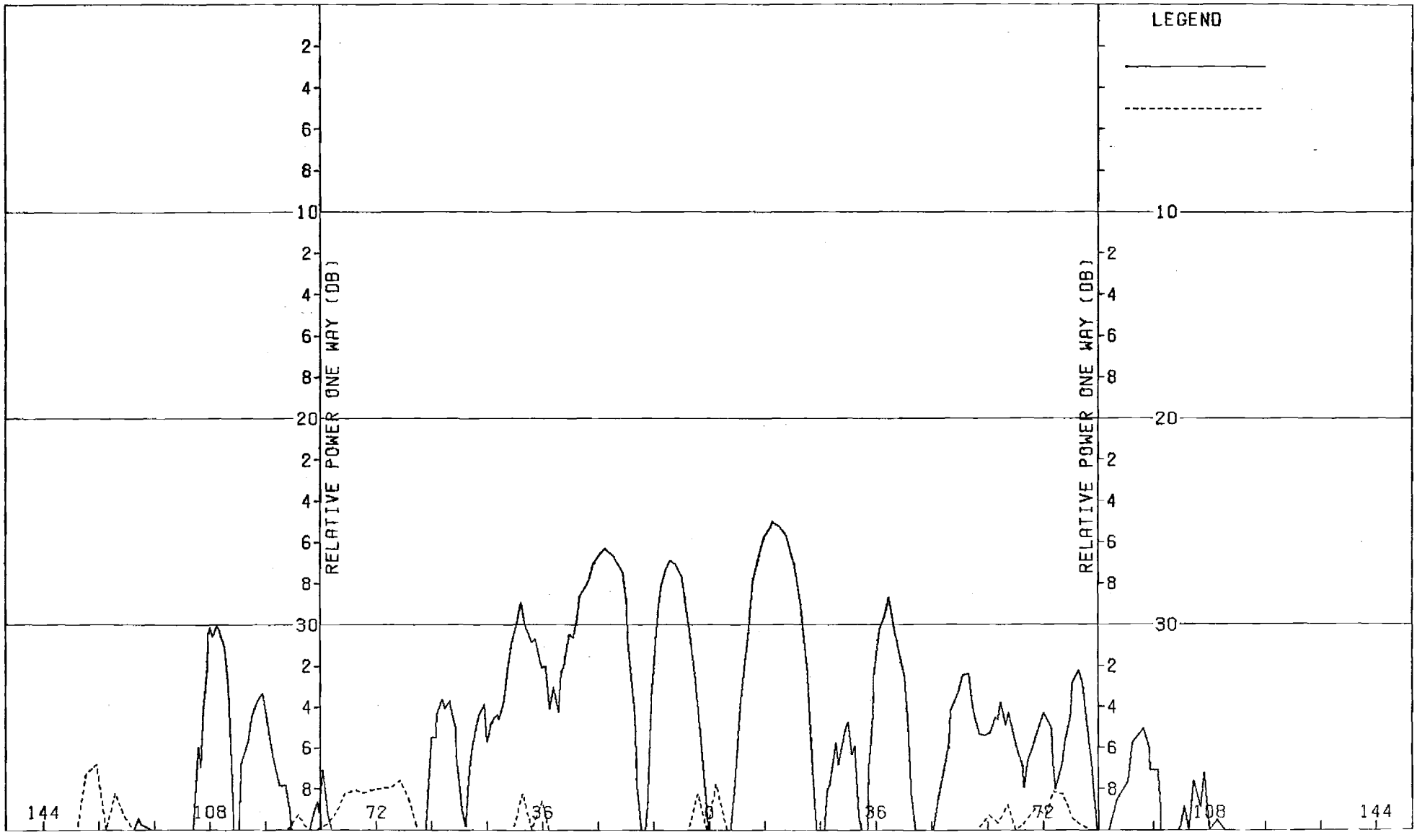

Figure G-12. Pattern of Medium Array: H-Plane, Elevation Difference, θ-Component, Medium (F=1) Radome

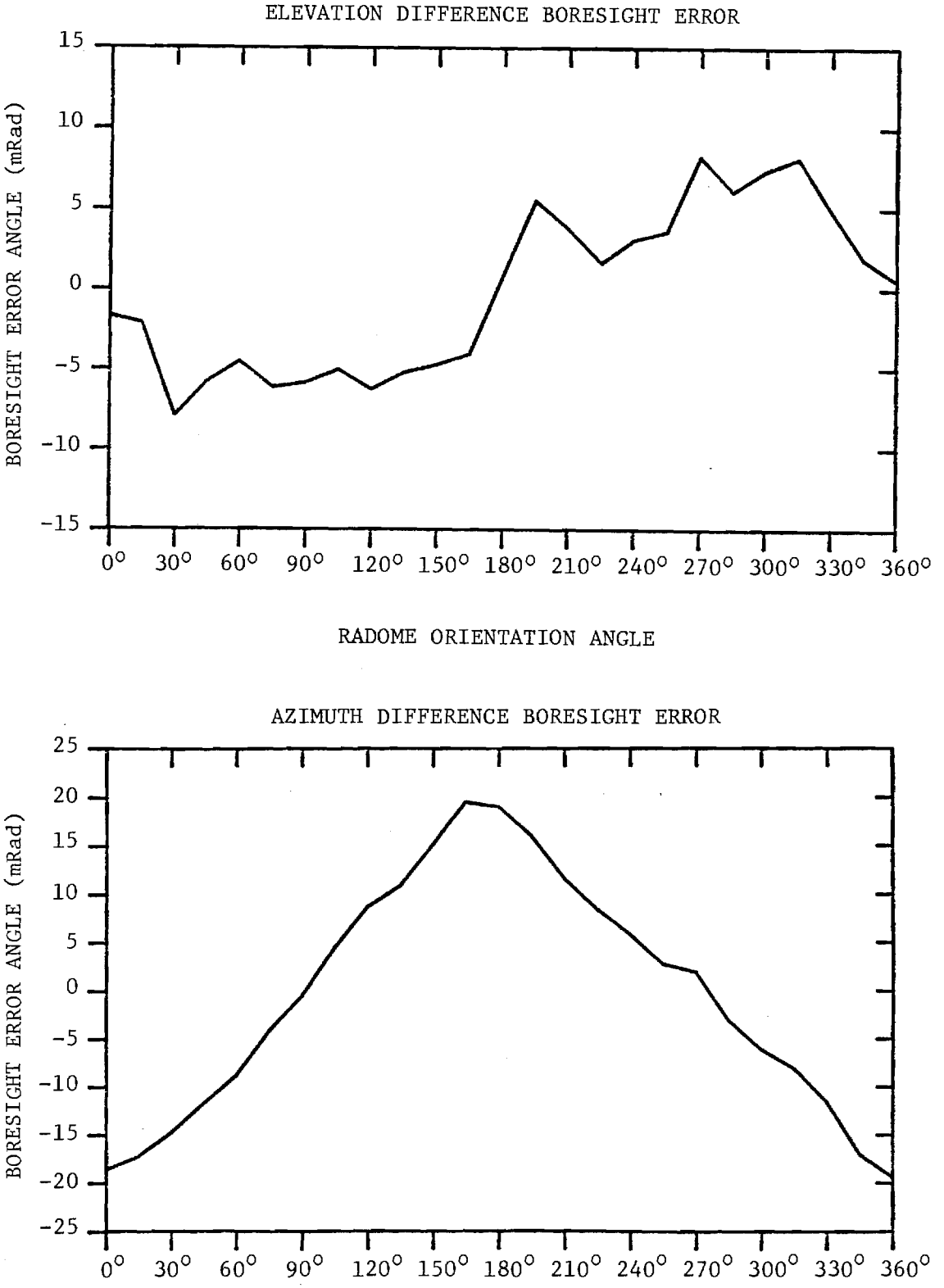

FIGURE G-13. BORESIGHT ERRORS OF MEDIUM ARRAY AND MEDIUM (F=1) RADOME.

APPENDIX H

Antenna Patterns of Medium Array with Medium (F=1.5) Radome

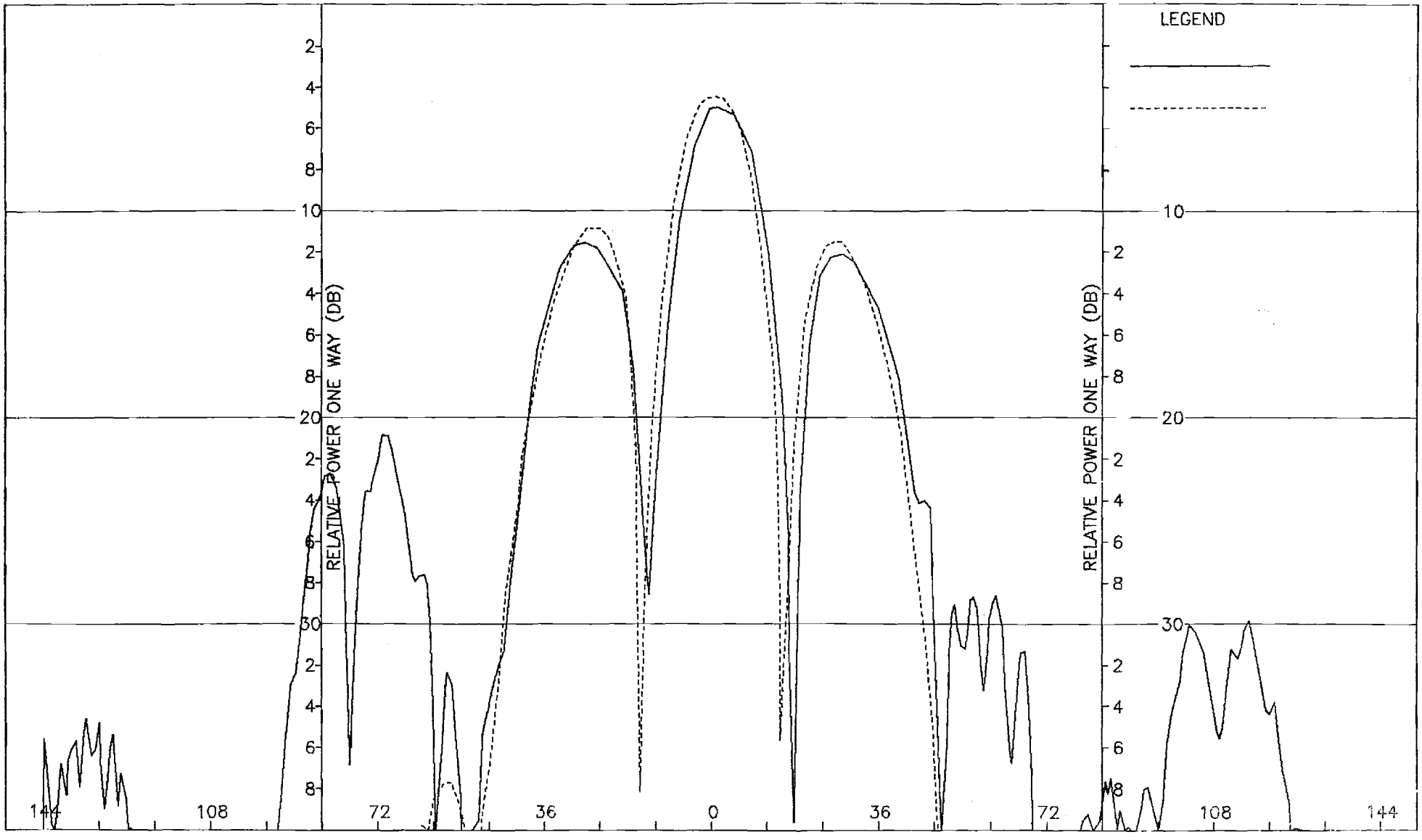

Figure H-1. Pattern of Medium Array: H-Plane, Sum, ϕ-Component, Medium (F=1.5) Radome

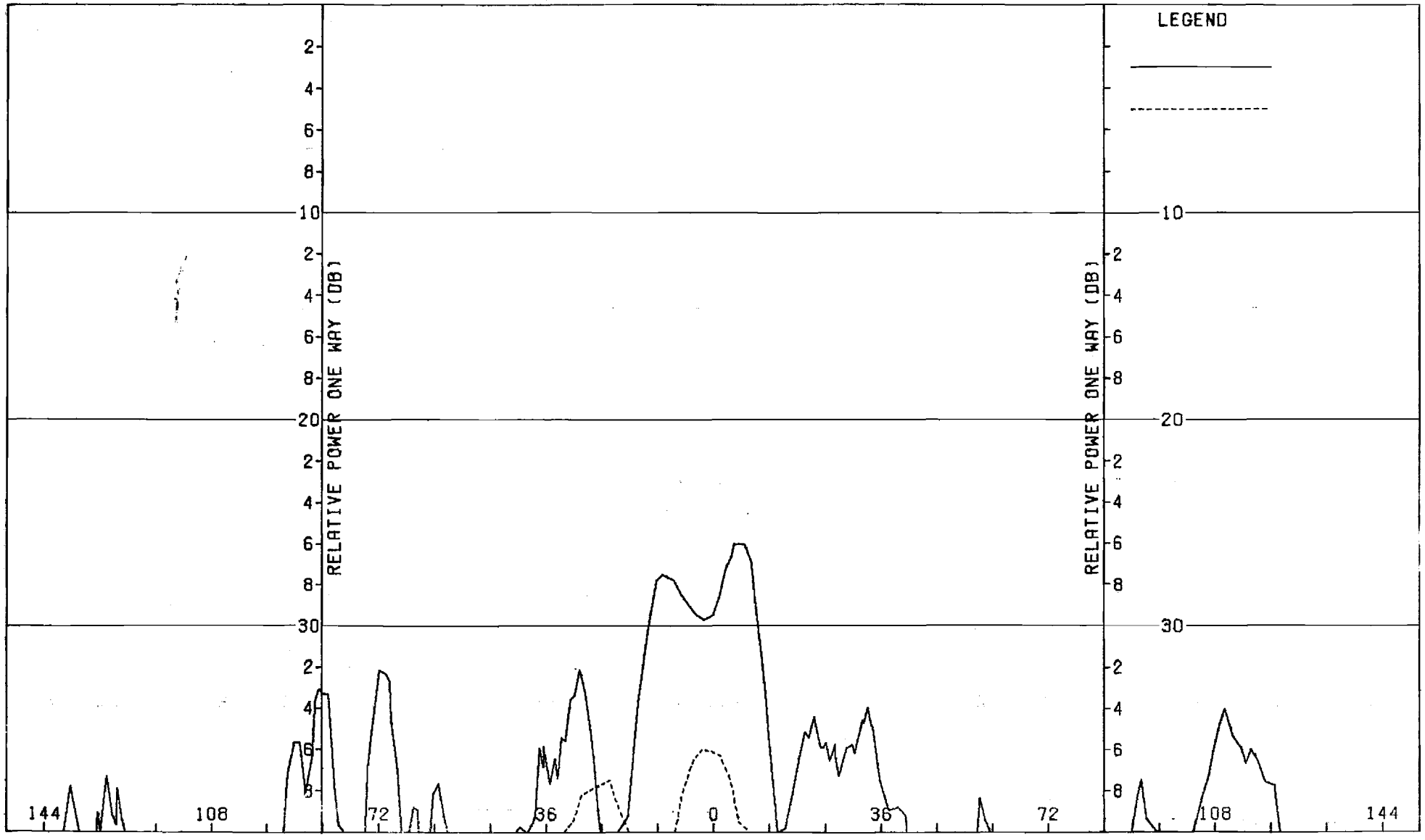

Figure H-2. Pattern of Medium Array: H-Plane, Sum, θ-Component, Medium (F=1.5) Radome

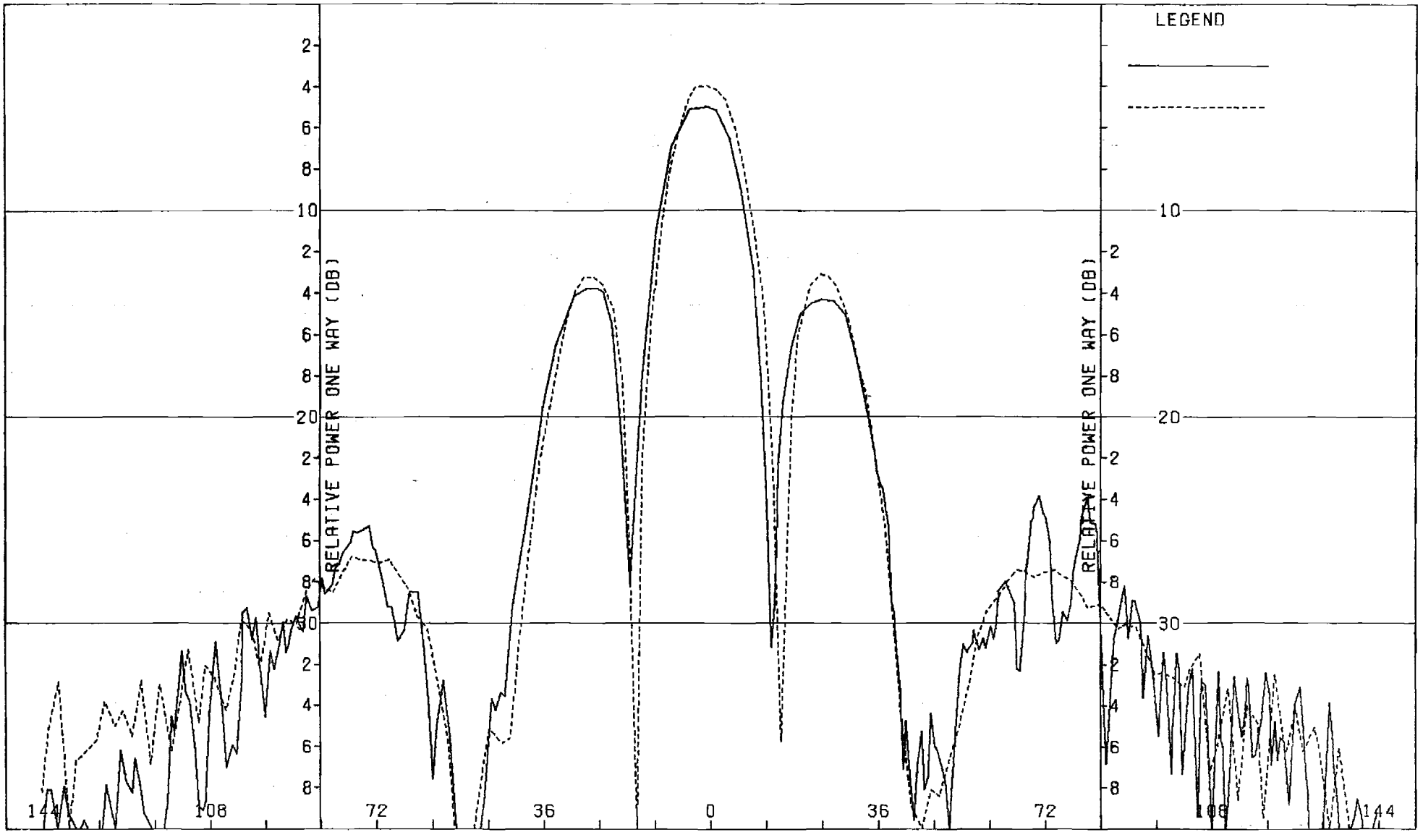

Figure H-3. Pattern of Medium Array: E-Plane, Sum, θ-Component, Medium (F=1.5) Radome

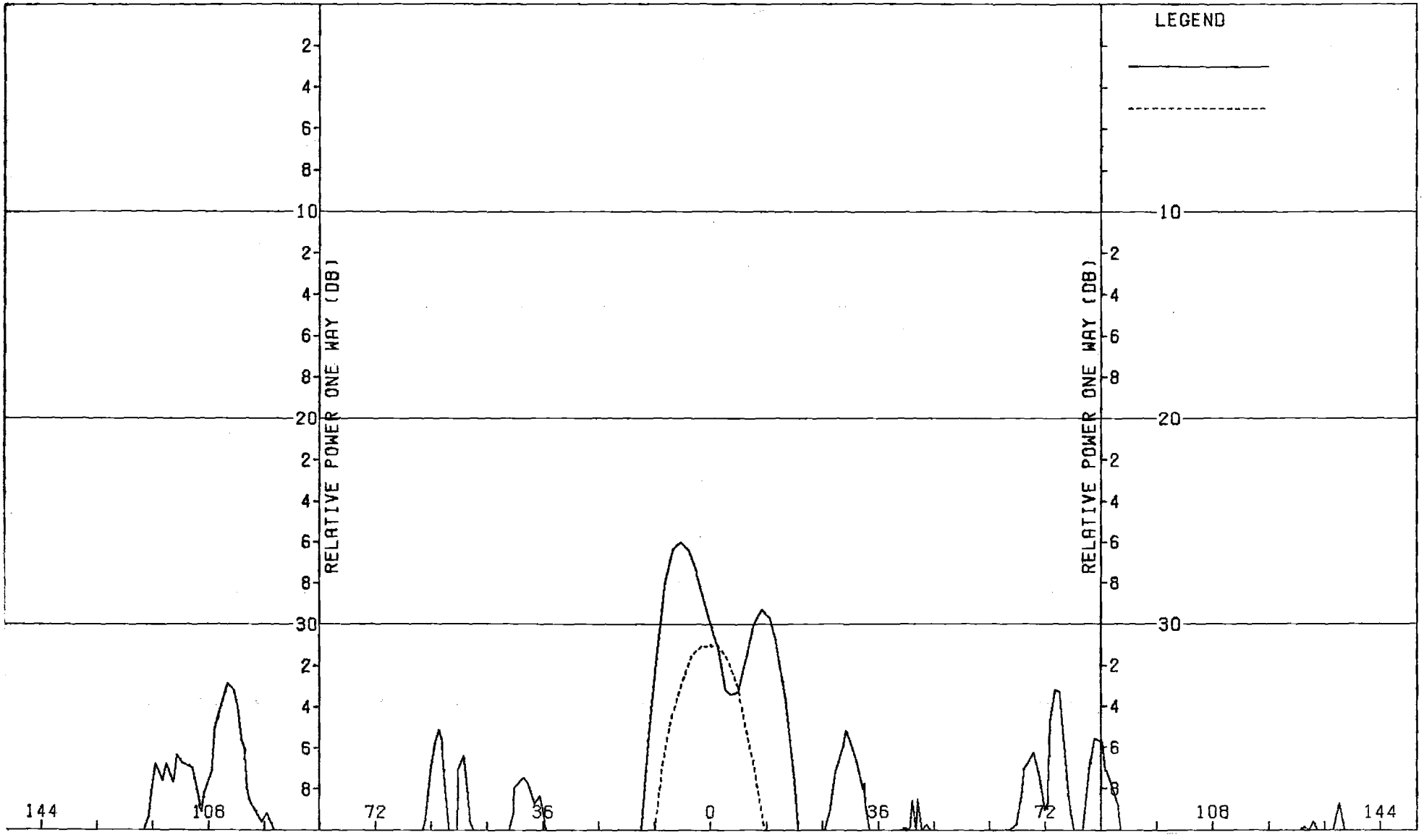

Figure H-4. Pattern of Medium Array: E-Plane, Sum, ϕ-Component, Medium (F=1.5) Radome

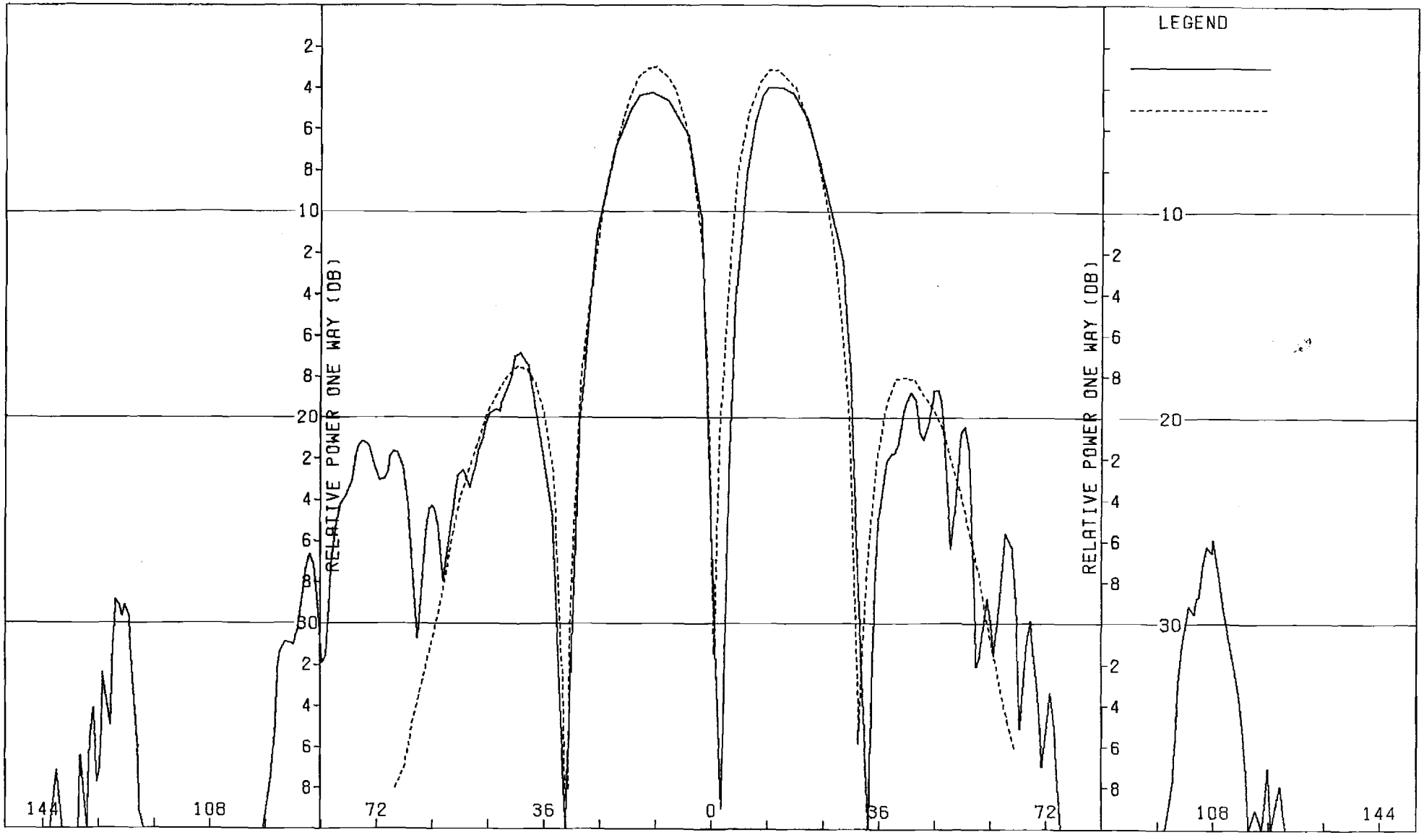

Figure H-5. Pattern of Medium Array: H-Plane, Azimuth Diff., ϕ-Component, Medium (F.1.5) Radome

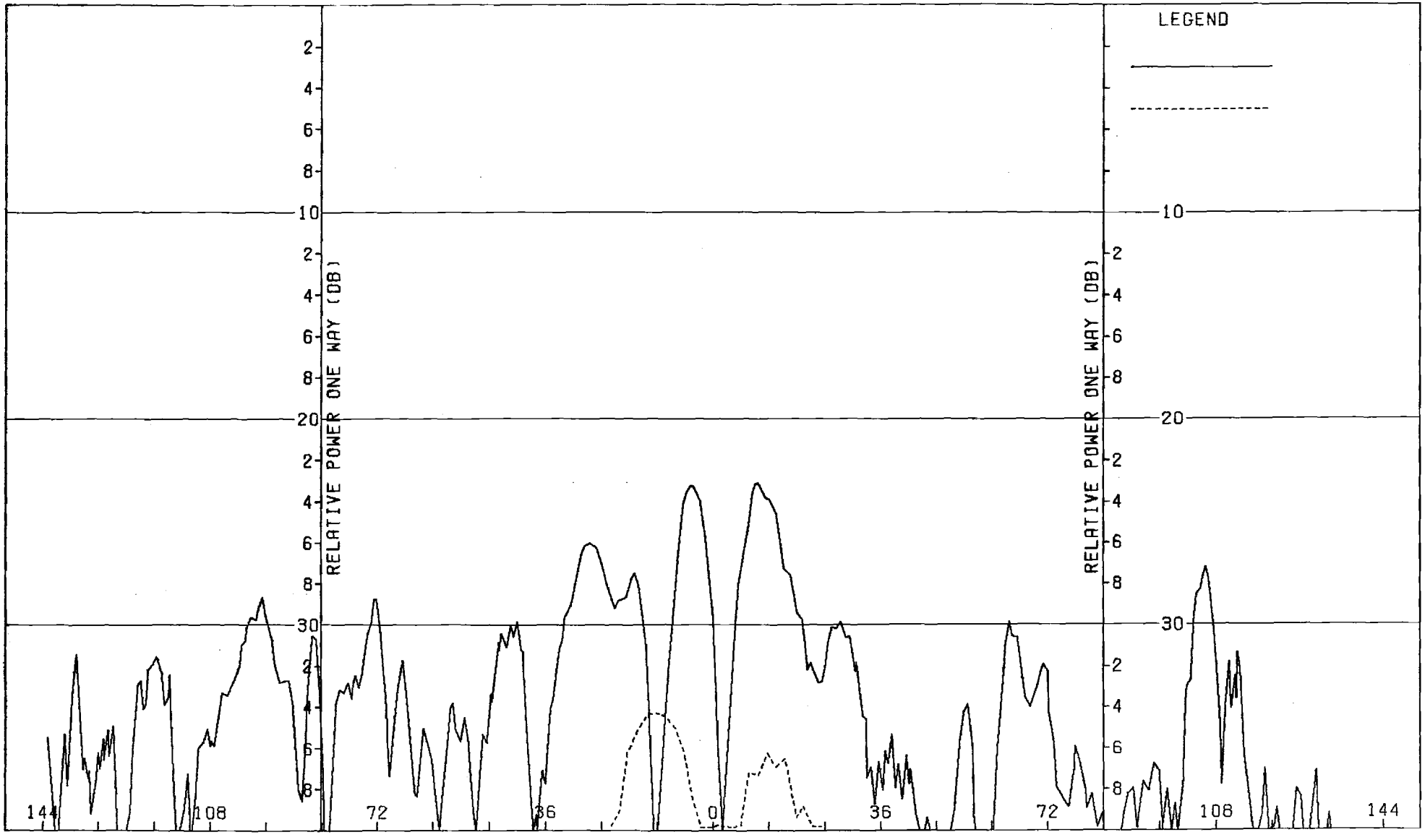

Figure H-6. Pattern of Medium Array: H-Plane, Azimuth Diff., θ-Component, Medium (F=1.5) Radome

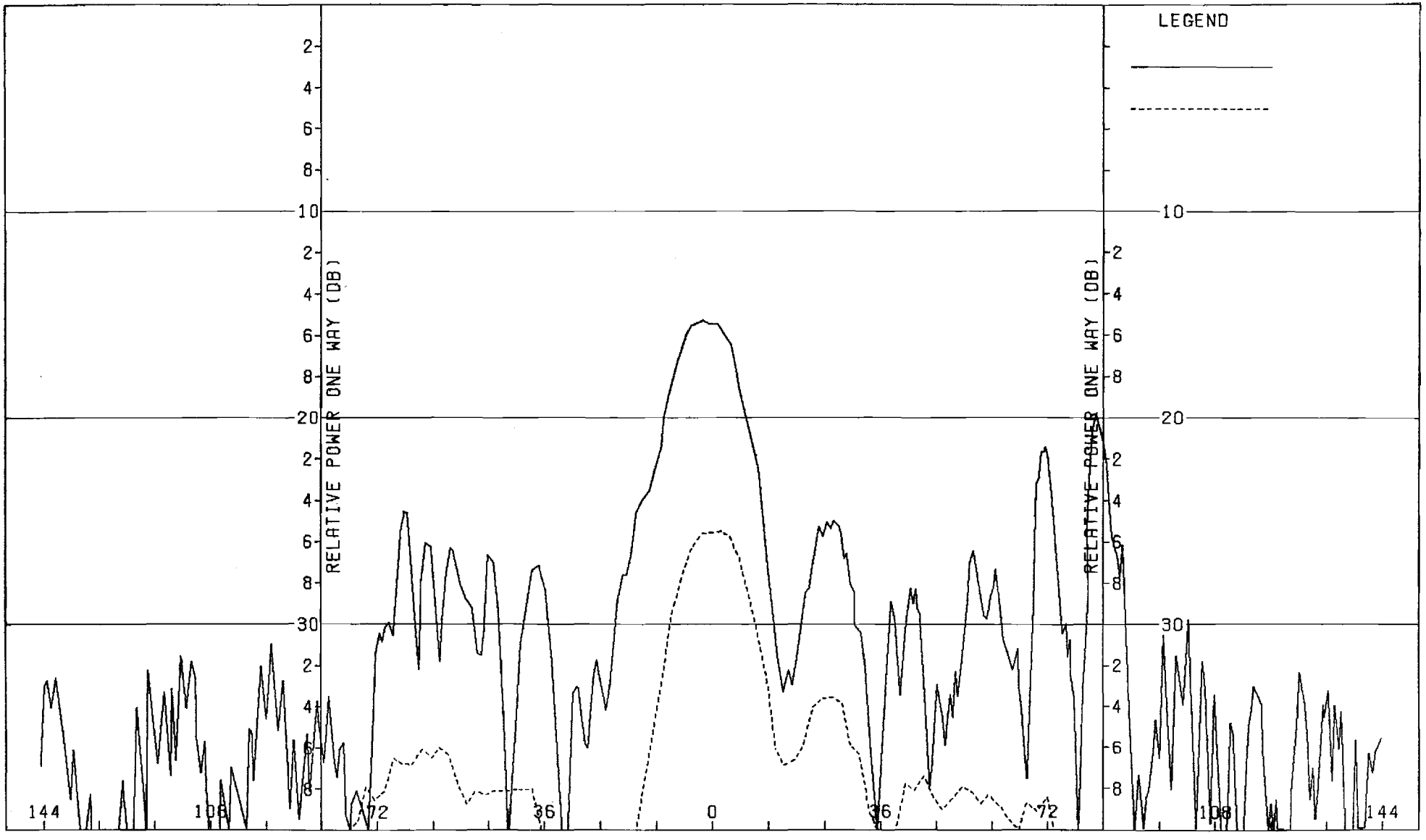

Figure H-7. Pattern of Medium Array: E-Plane, Azimuth Diff., θ-Component, Medium (F=1.5) Radome

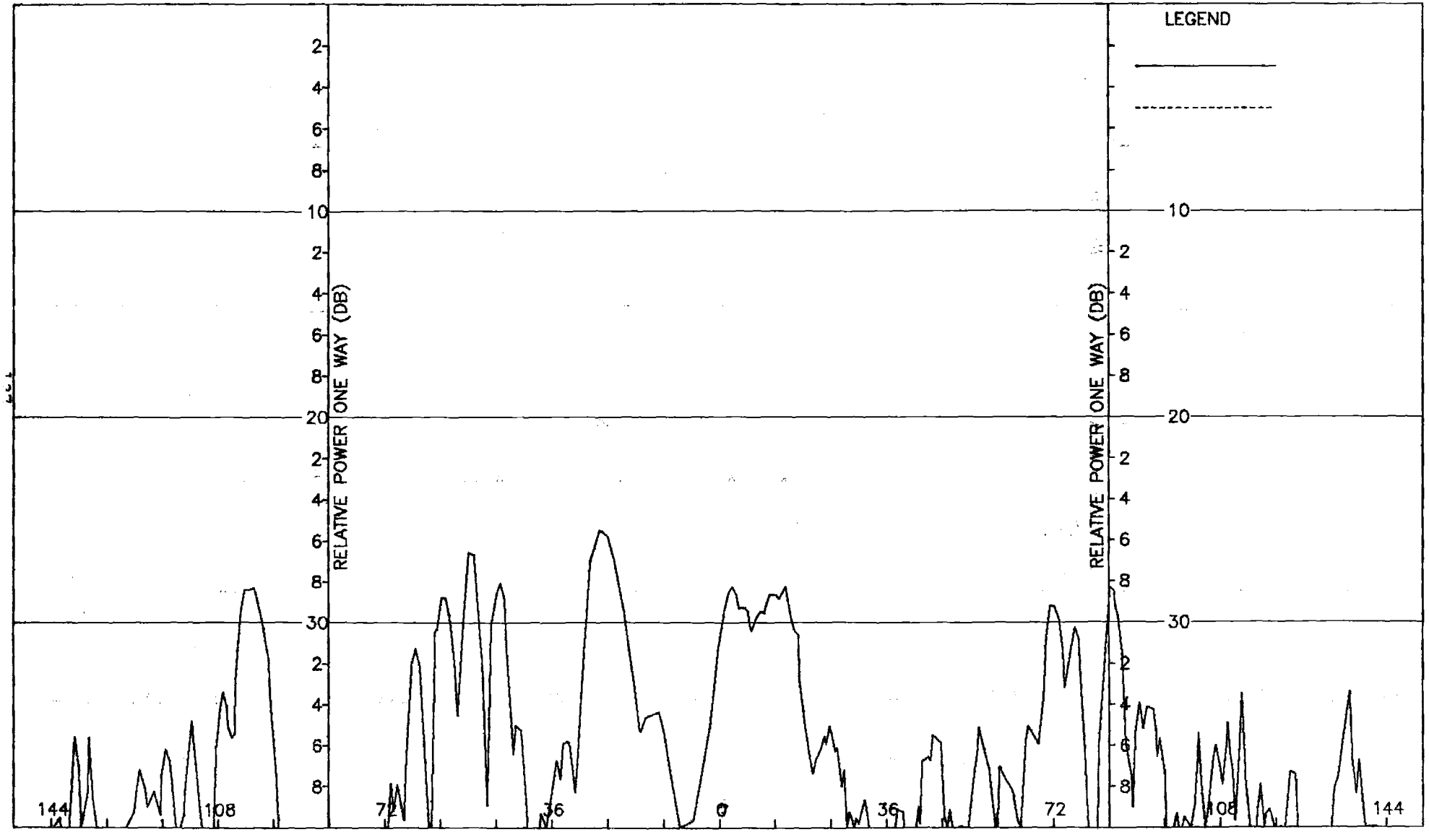

Figure H-8. Pattern of Medium Array: E-Plane, Azimuth Diff., ϕ-Component, Medium (F=1.5) Radome

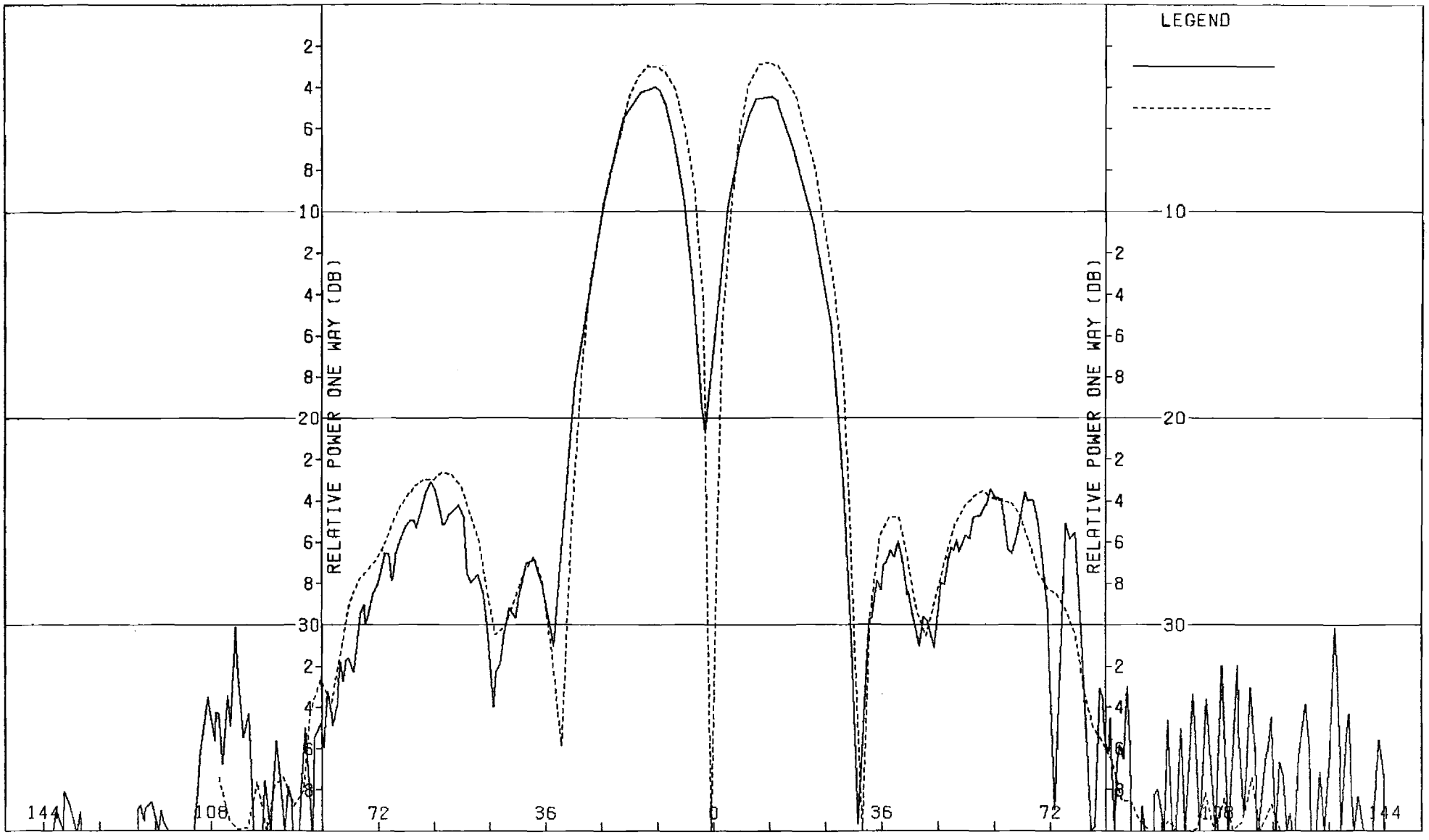

Figure H-9. Pattern of Medium Array: E-Plane, Elevation Diff., θ-Component, Medium (F=1.5) Radome

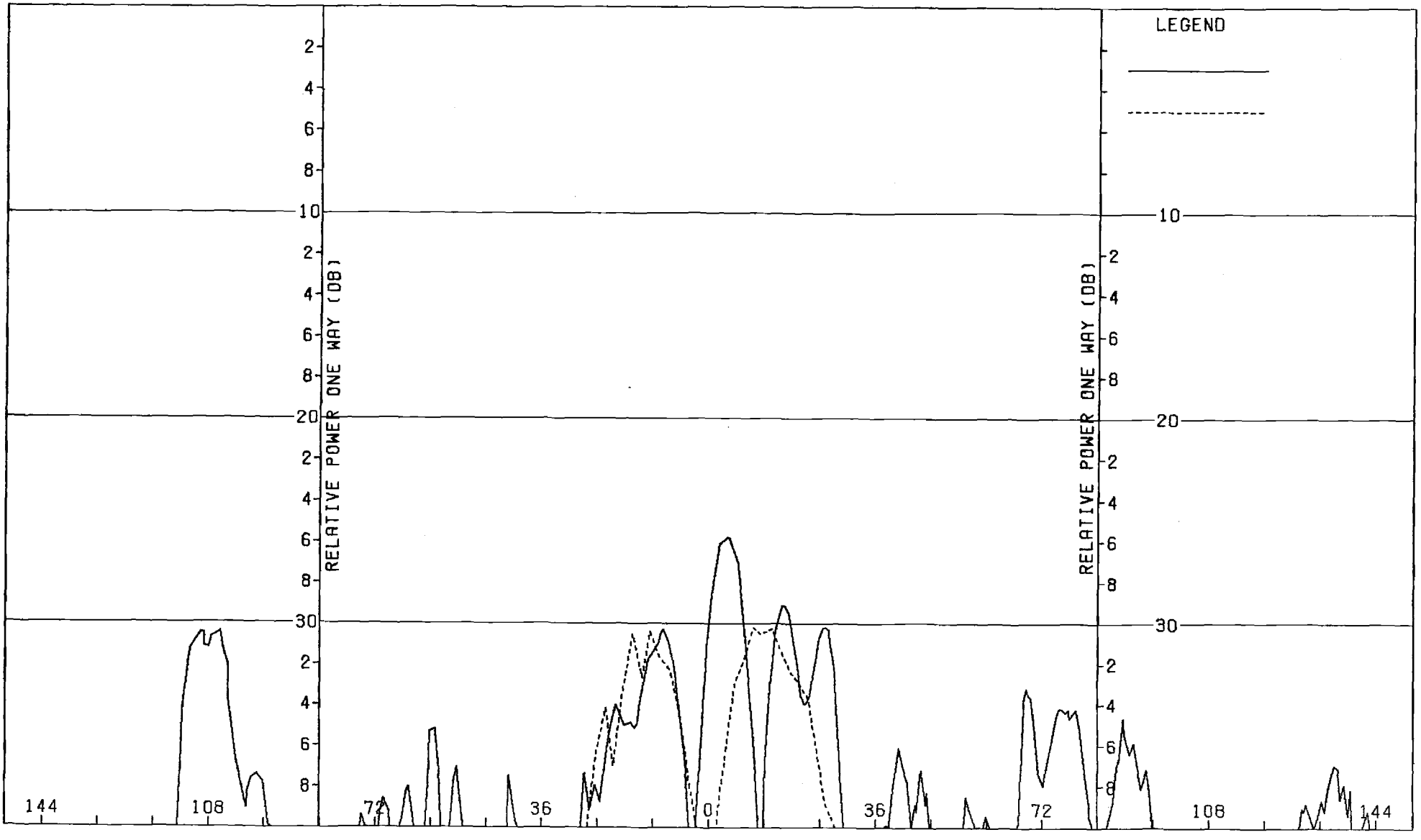

Figure H-10. Pattern of Medium Array: E-Plane, Elevation Diff., ϕ-Component, Medium (F=1) Radome

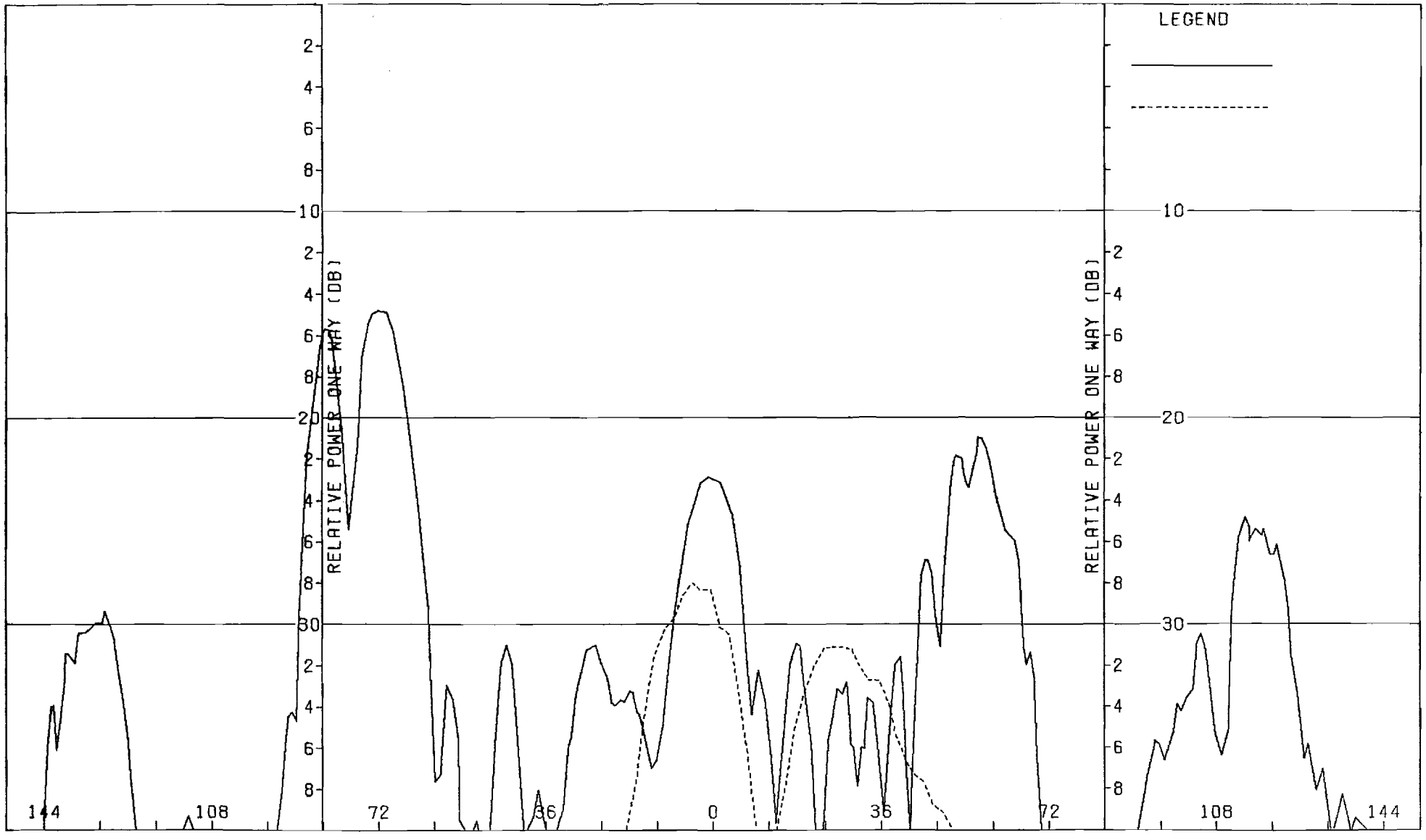

Figure H-11. Pattern of Medium Array: H-Plane, Elevation Diff., ϕ-Component, Medium (F=1.5) Radome

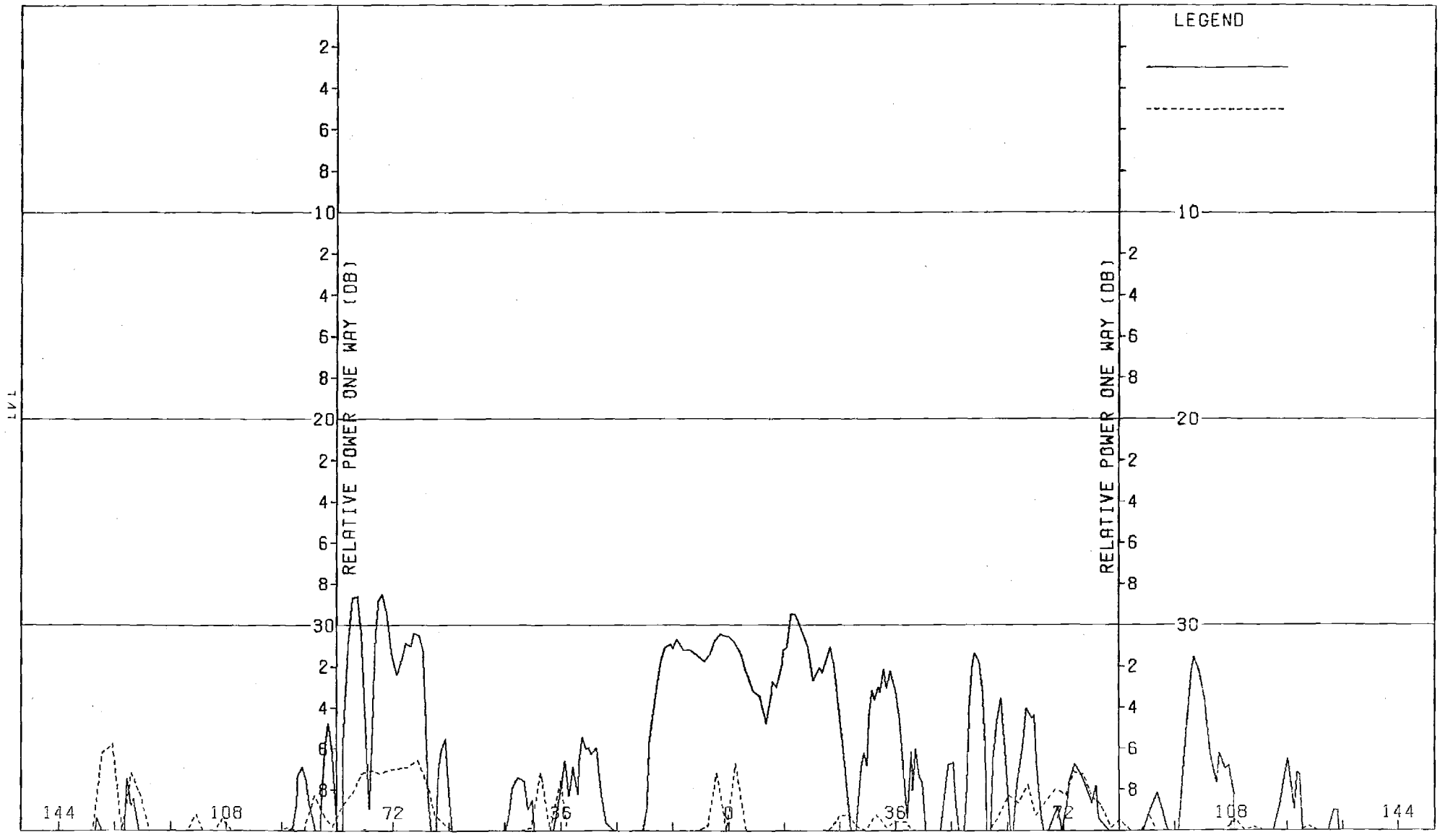

Figure H-12. Pattern of Medium Array: H-Plane, Elevation Diff., θ-Component, Medium (F=1.5) Radome

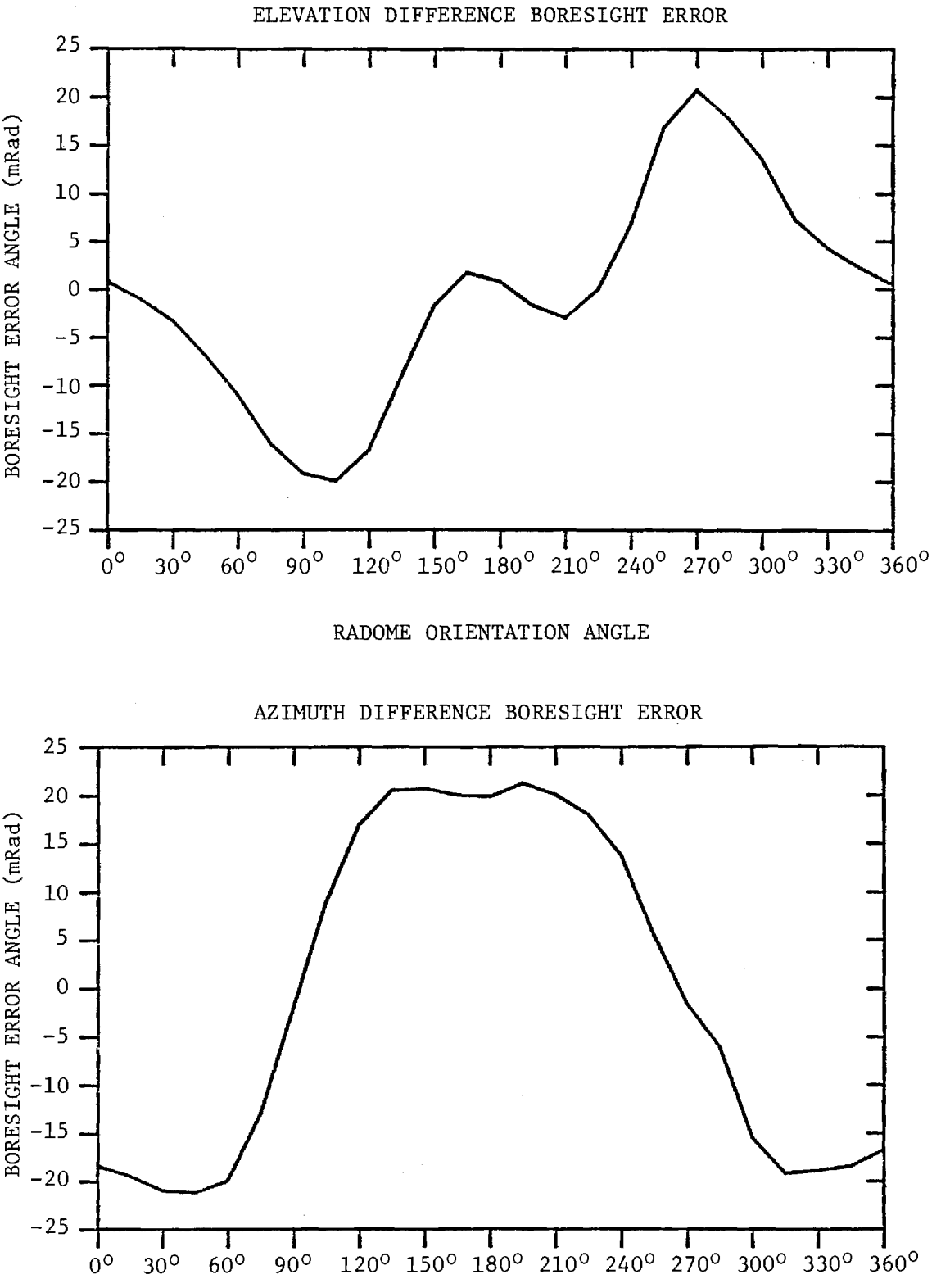

FIGURE H-13. BORESIGHT ERRORS OF MEDIUM ARRAY AND MEDIUM (F=1.5) RADOME.

APPENDIX I

Antenna Patterns of Medium Array with Medium (F=2) Radome

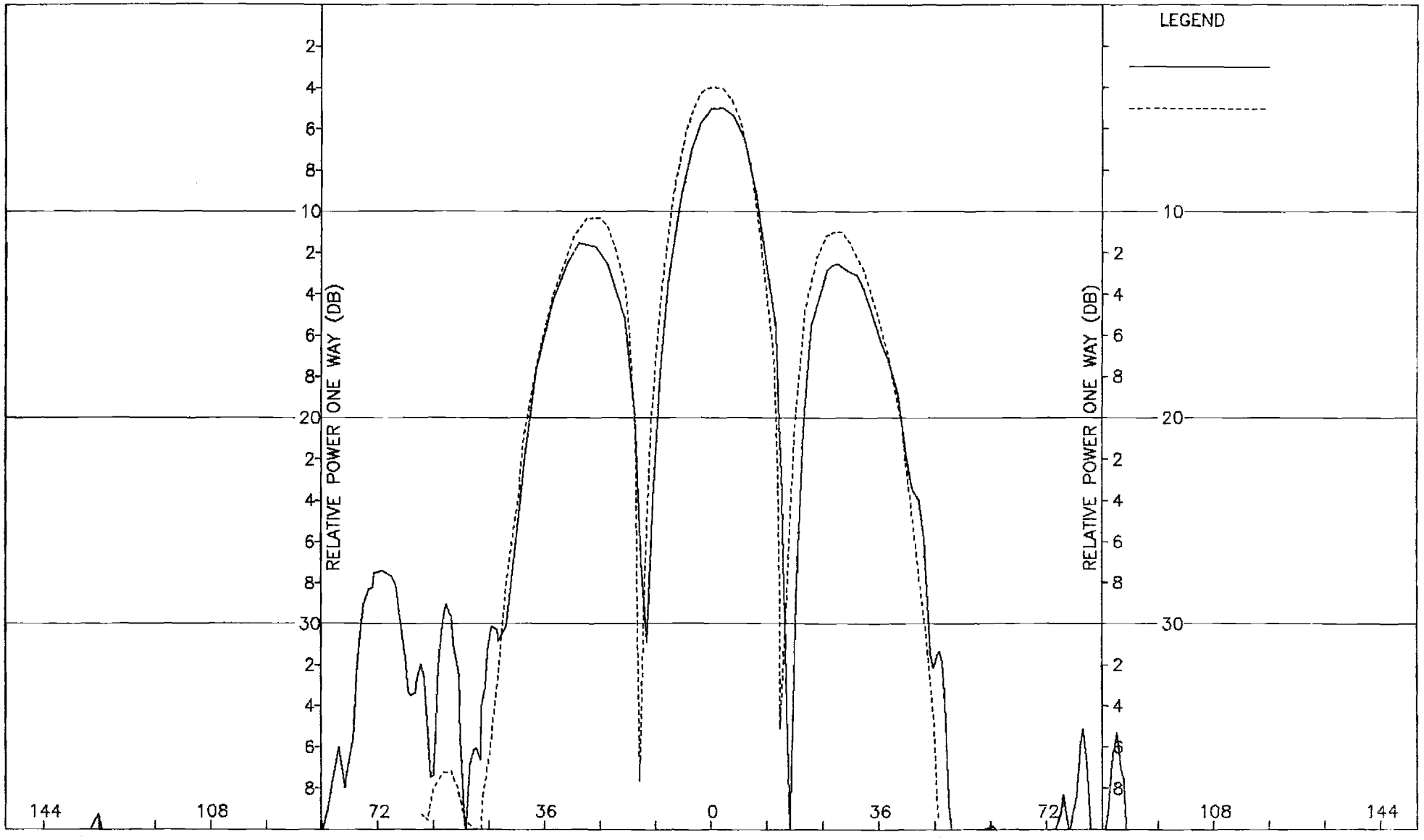

Figure I-1. Pattern of Medium Array: H-Plane, Sum, ϕ-Component, Medium (F=2.0) Radome

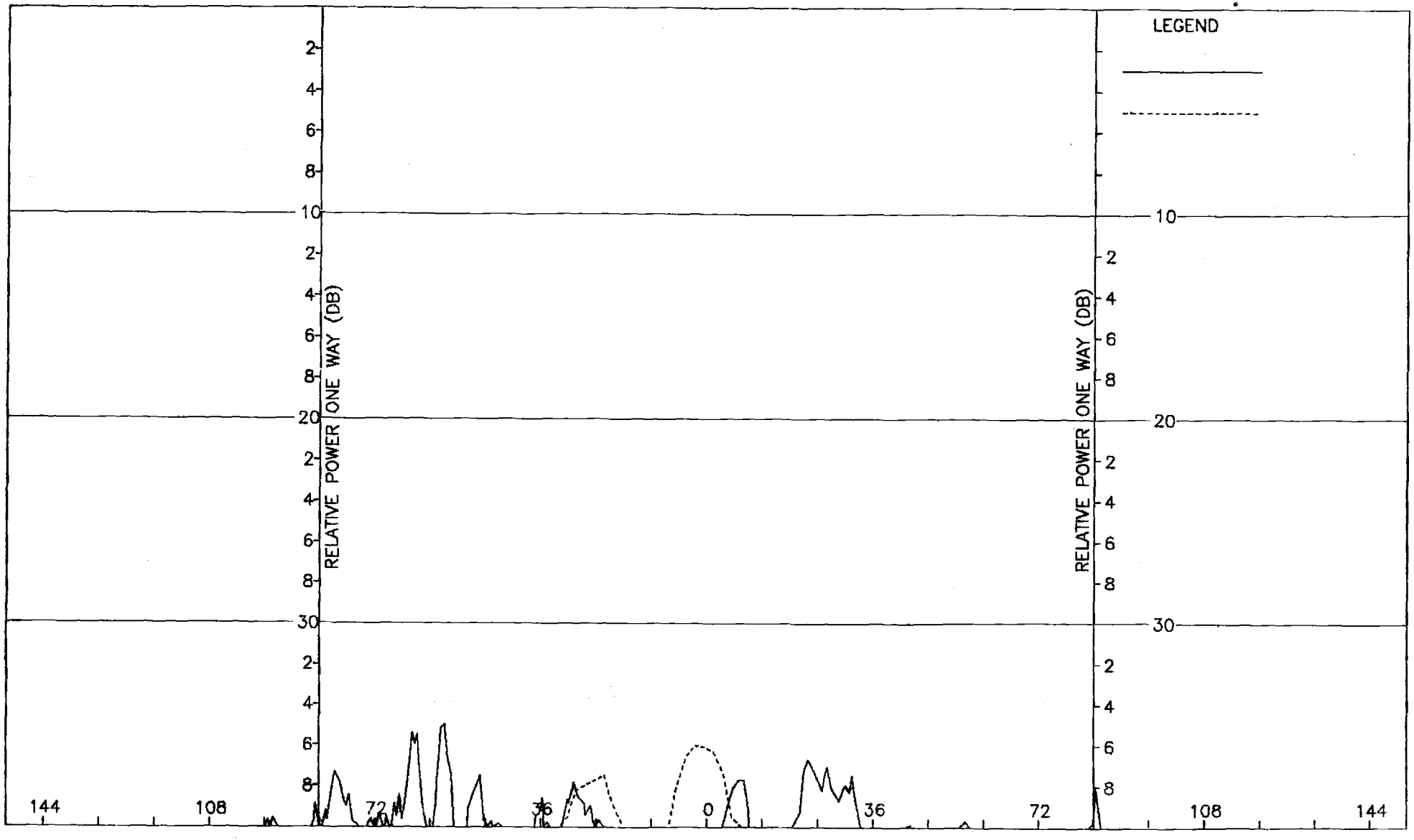

Figure I-2. Pattern of Medium Array: H-Plane, Sum, θ-Component, Medium (F=2.0) Radome

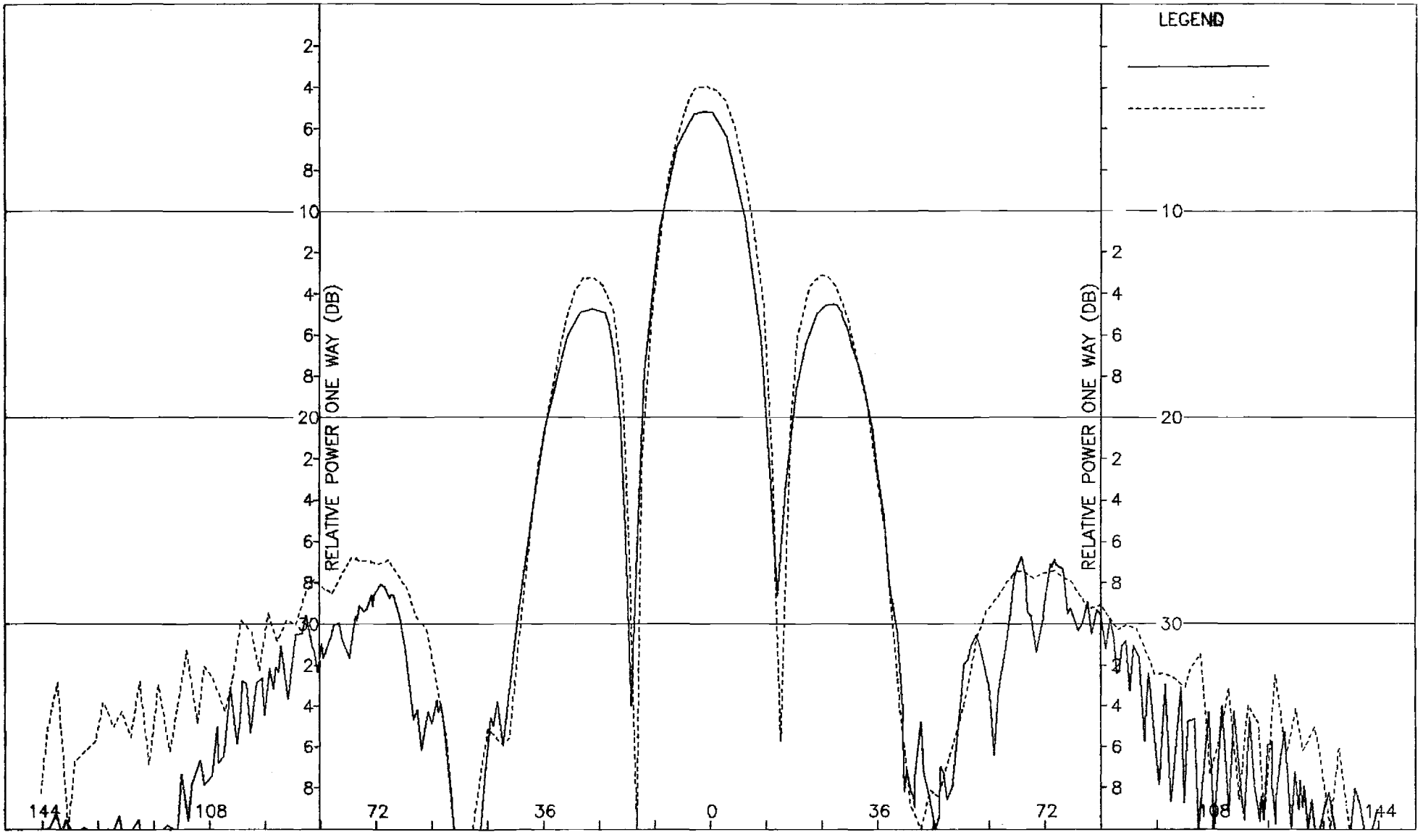

Figure I-3. Pattern of Medium Array: E-Plane, Sum, θ-Component, Medium (F=2.0) Radome

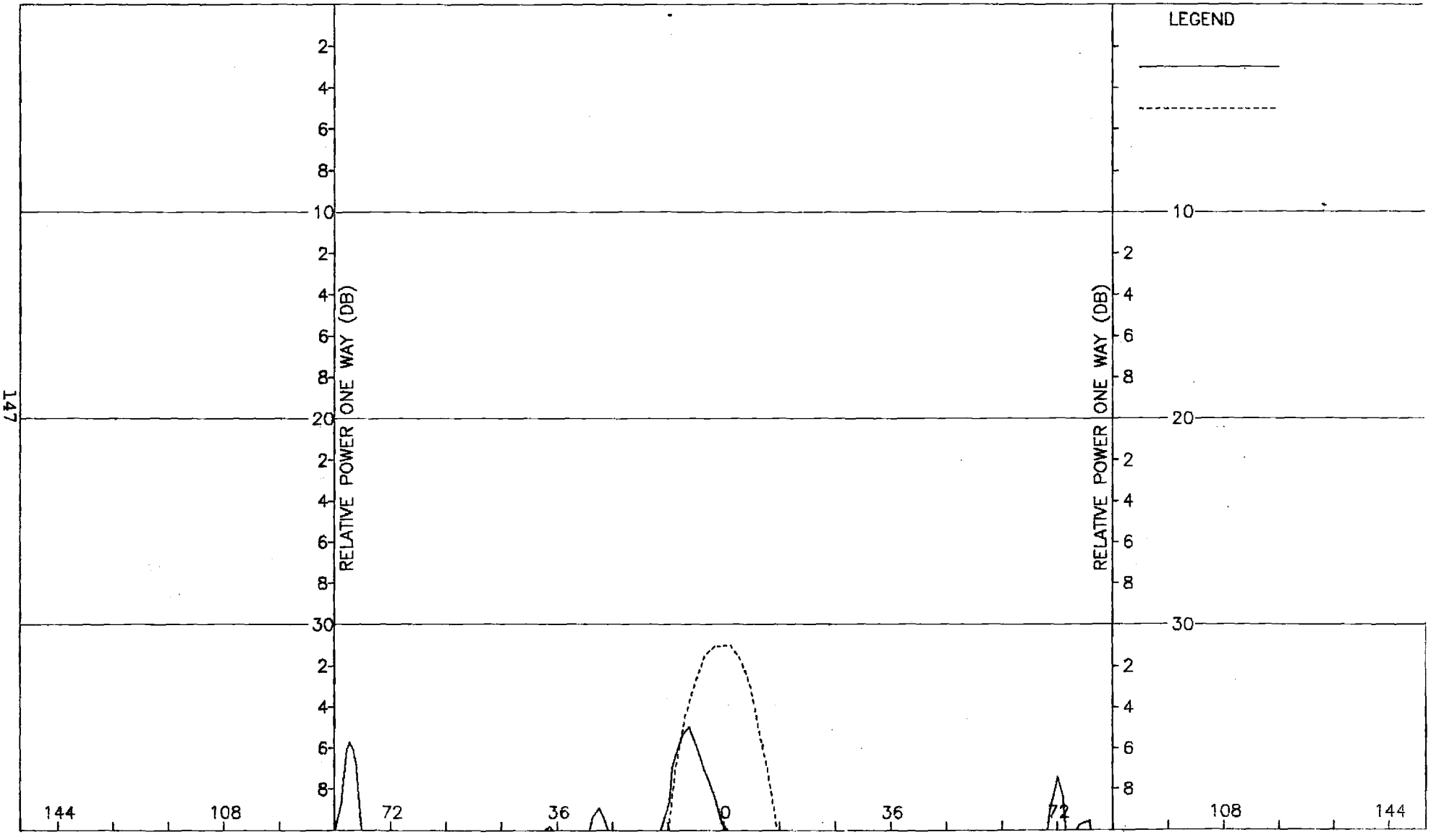

Figure I-4. Pattern of Medium Array: E-Plane, Sum, ϕ-Component, Medium (F=2.0) Radome

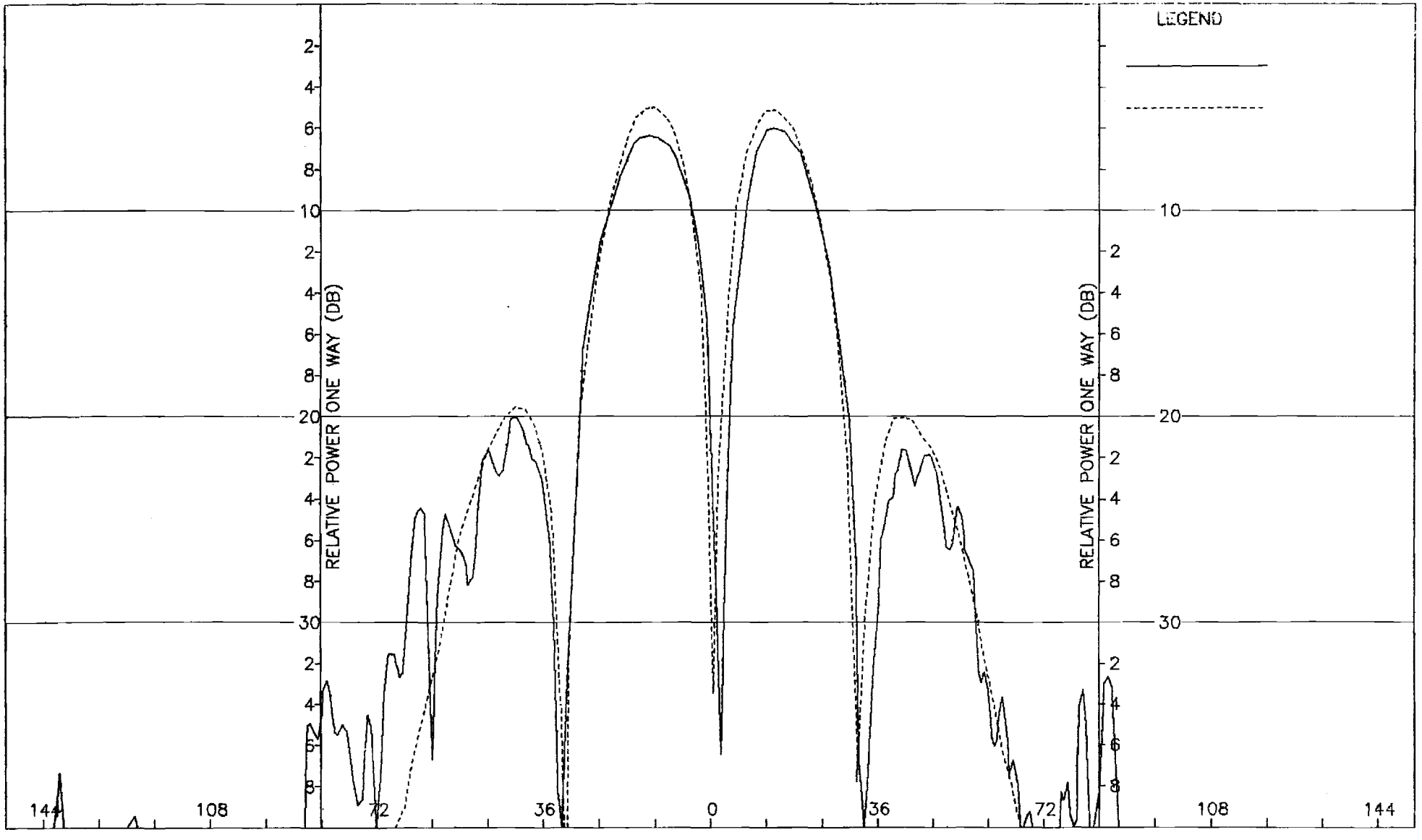

Figure I-5. Pattern of Medium Array: H-Plane, Azimuth Diff., ϕ-Component, Medium (F=2.0) Radome

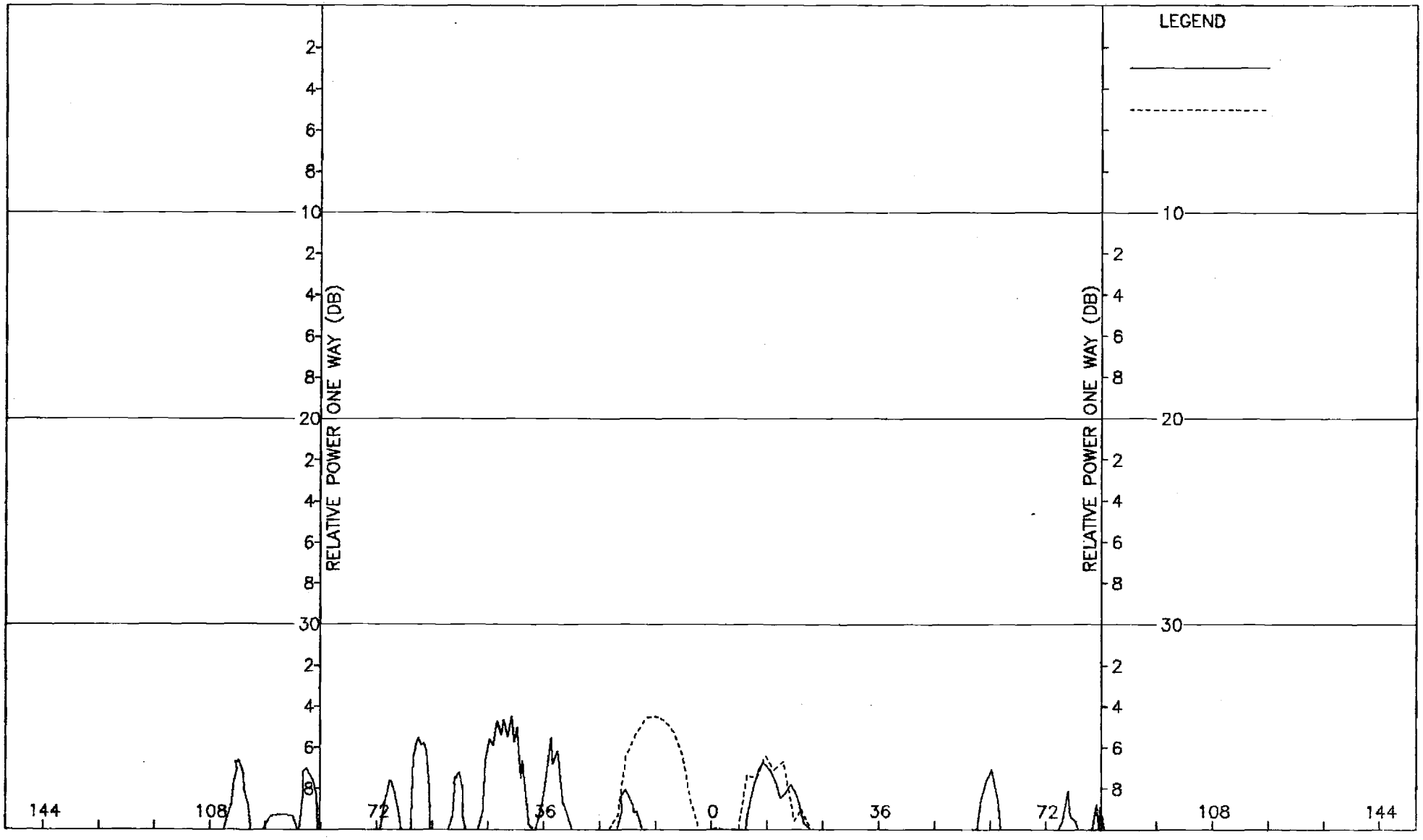

Figure I-6. Pattern of Medium Array: H-Plane, Azimuth Diff., θ-Component, Medium (F=2.0) Radome

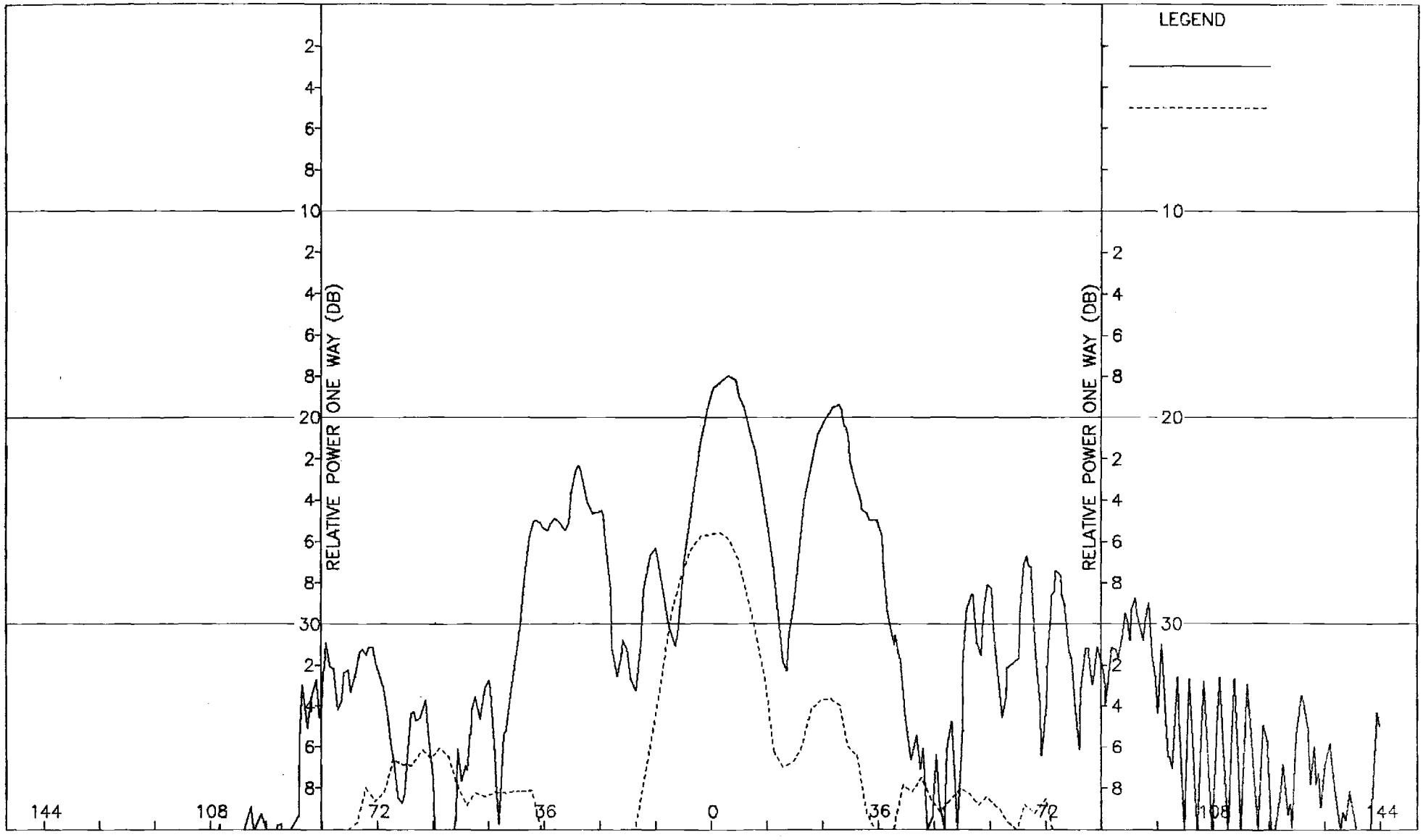

Figure I-7. Pattern of Medium Array: E-Plane, Azimuth Diff., θ-Component, Medium (F=2.0) Radome

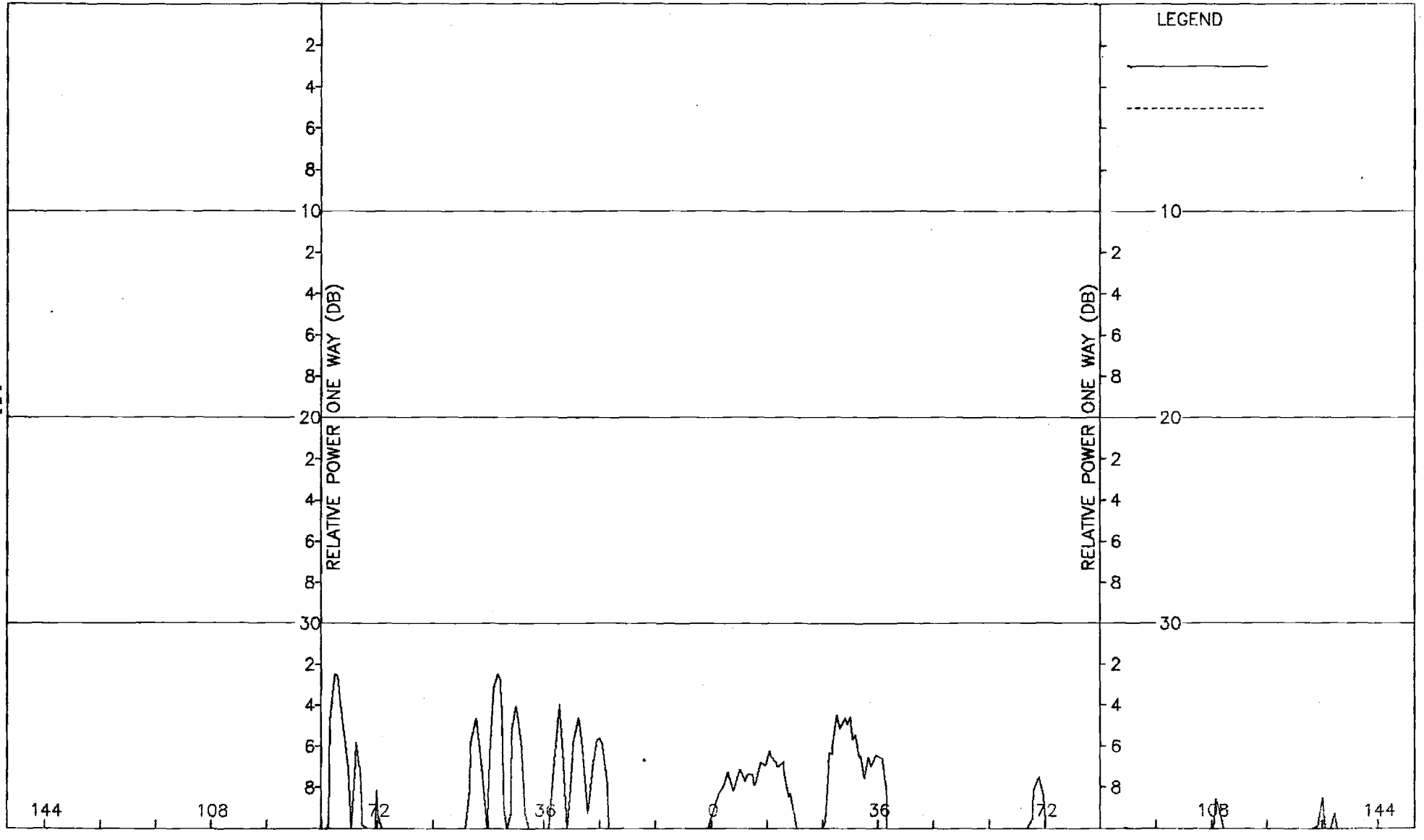

Figure I-8. Pattern of Medium Array: E-Plane, Azimuth Diff., ϕ-Component, Medium (F=2.0) Radome

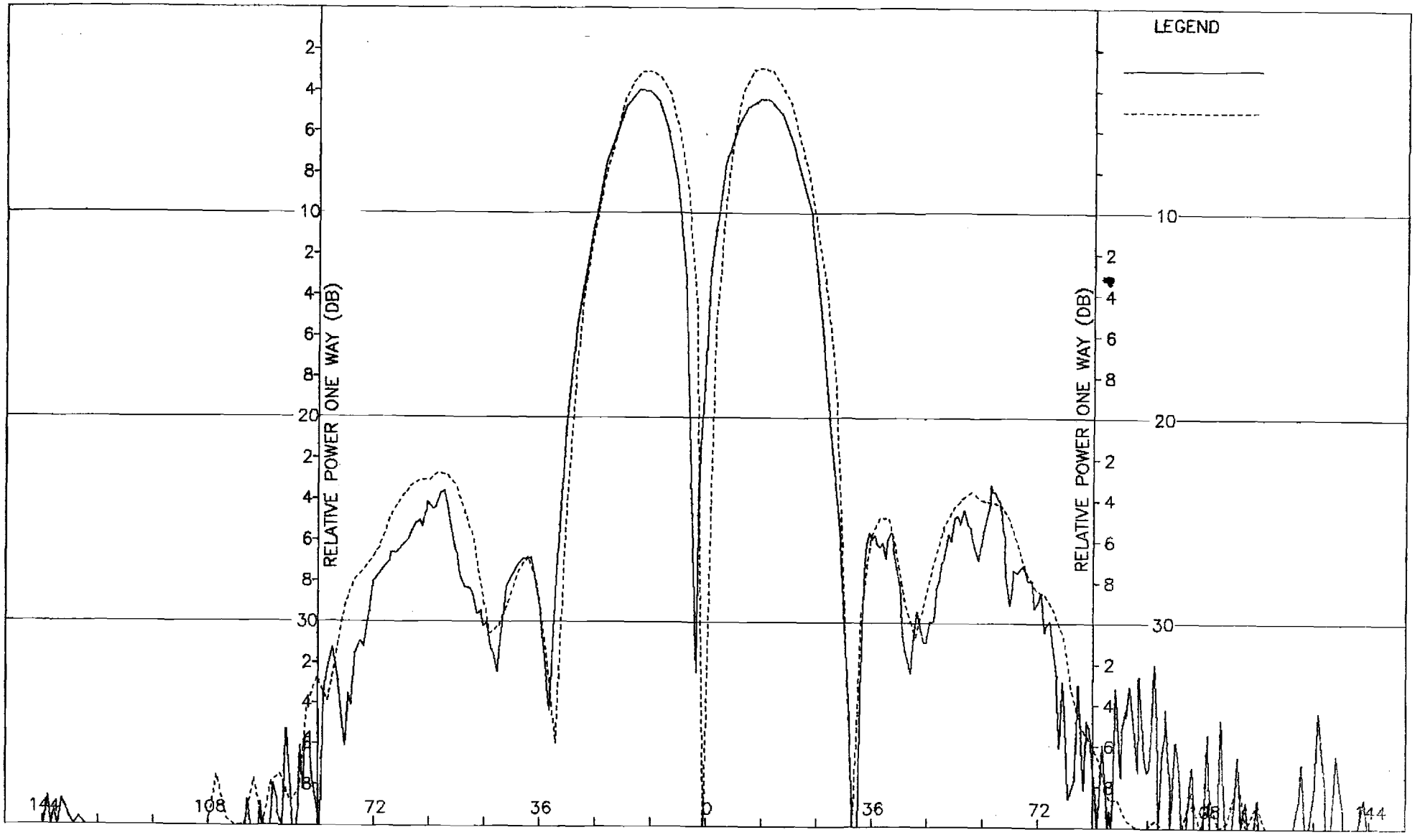

Figure I-9. Pattern of Medium Array: E-Plane, Elevation Diff., θ-Component, Medium (F=2.0) Radome

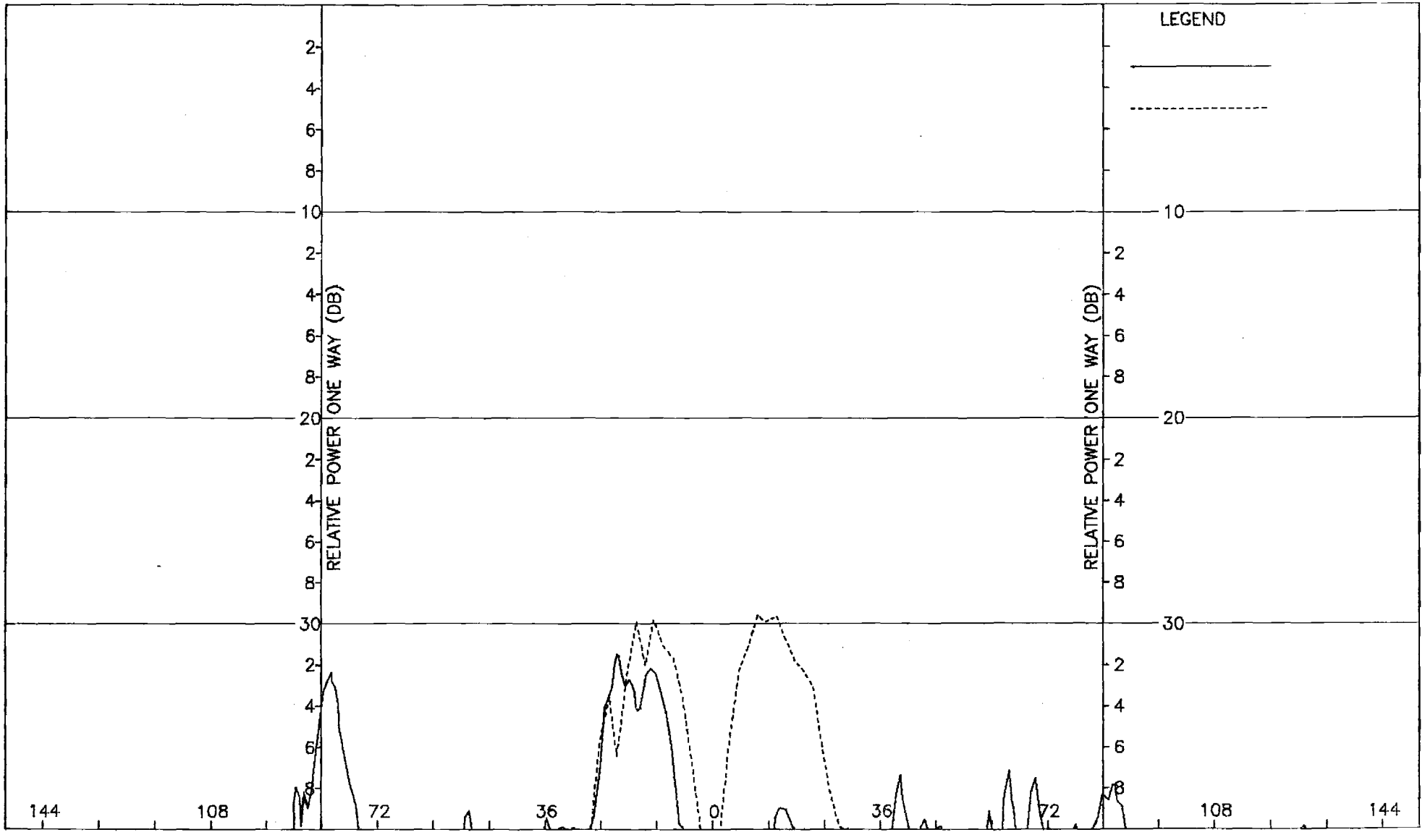

Figure I-10. Pattern of Medium Array: E-Plane, Elevation Diff., ϕ-Component, Medium (F=2.0) Radome

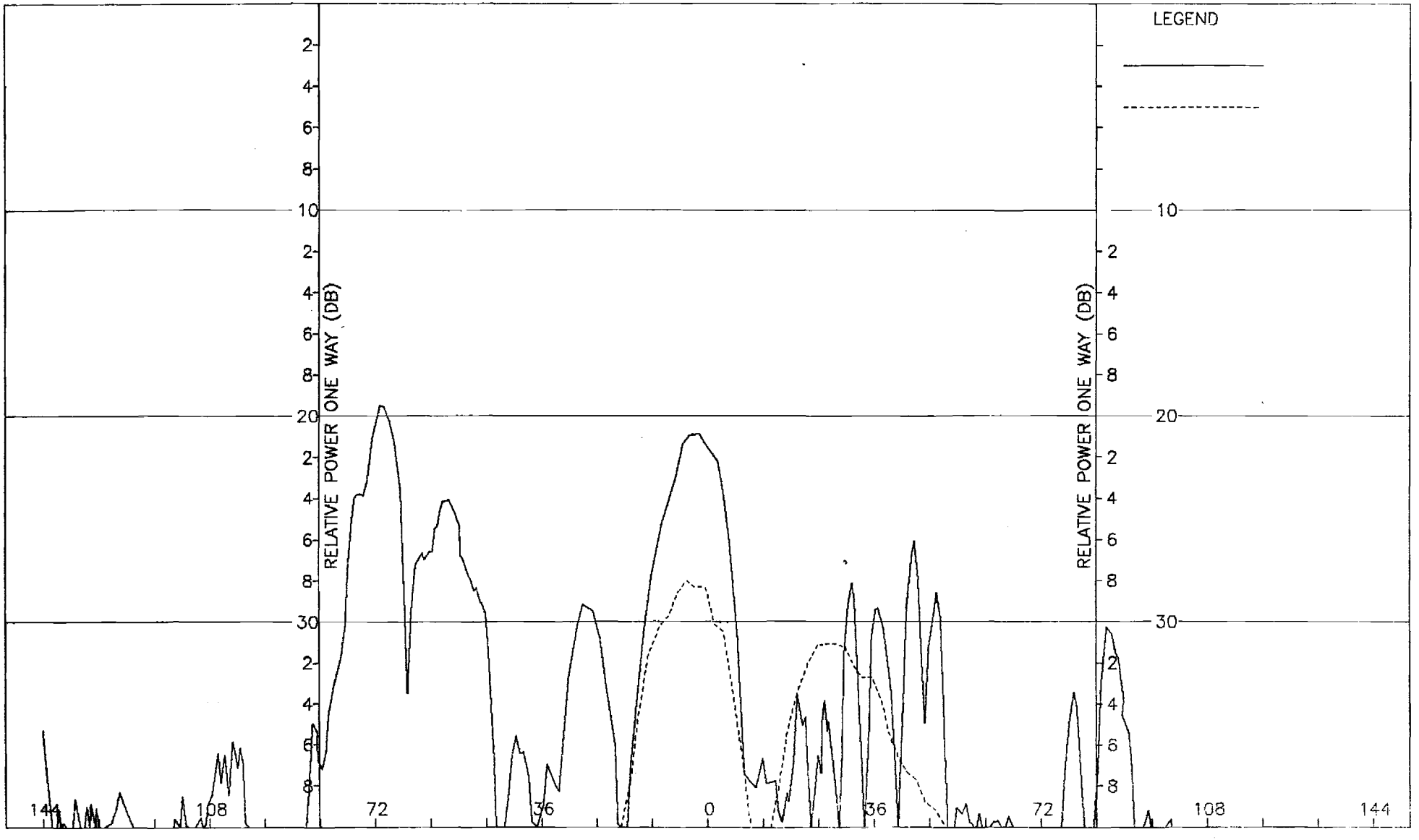

Figure I-11. Pattern of Medium Array: H-Plane, Elevation Diff., ϕ-Component, Medium (F=2.0) Radome

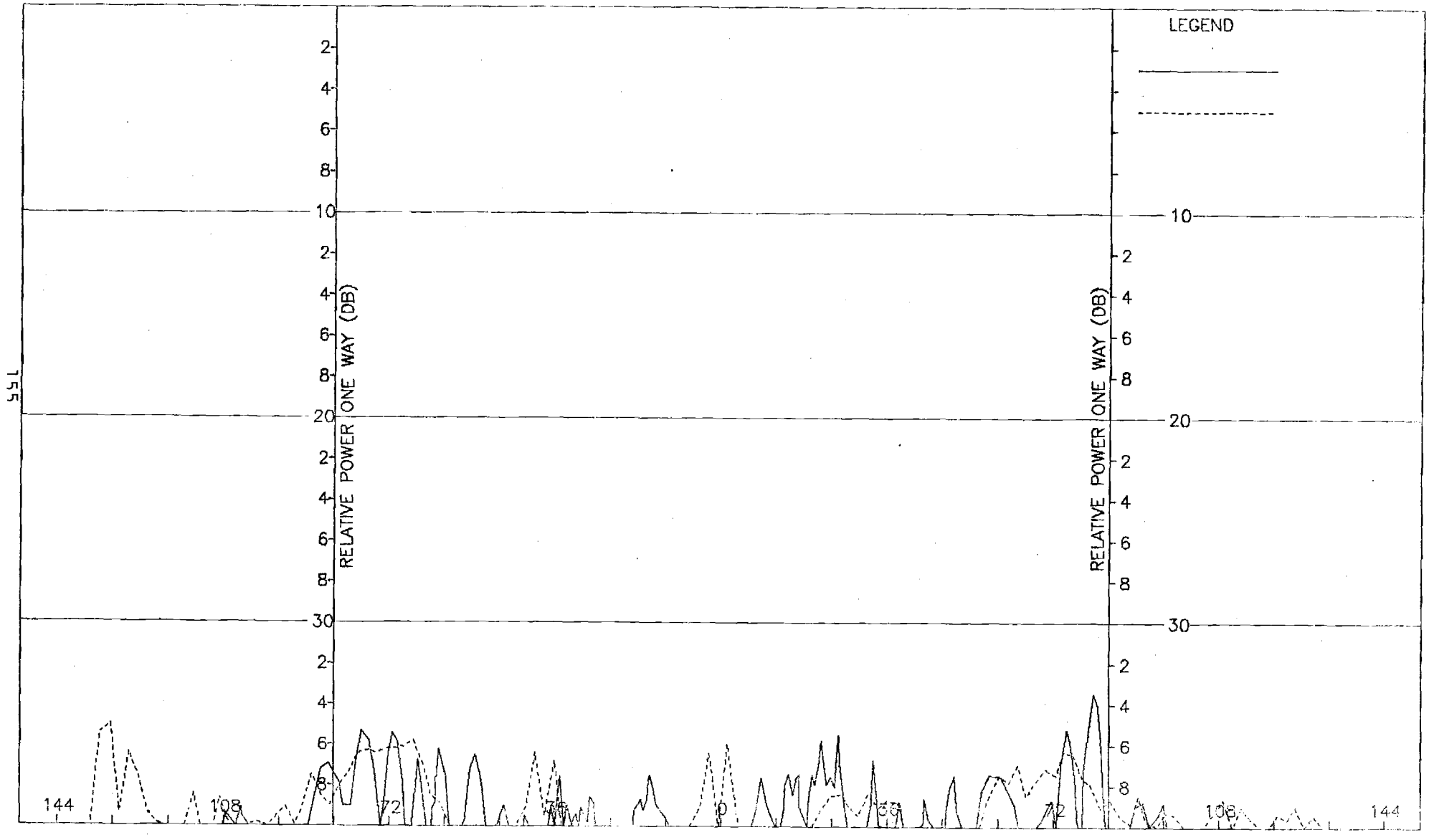

Figure I-12. Pattern of Medium Array: H-Plane, Elevation Diff., θ-Component, Medium (F=2.0) Radome

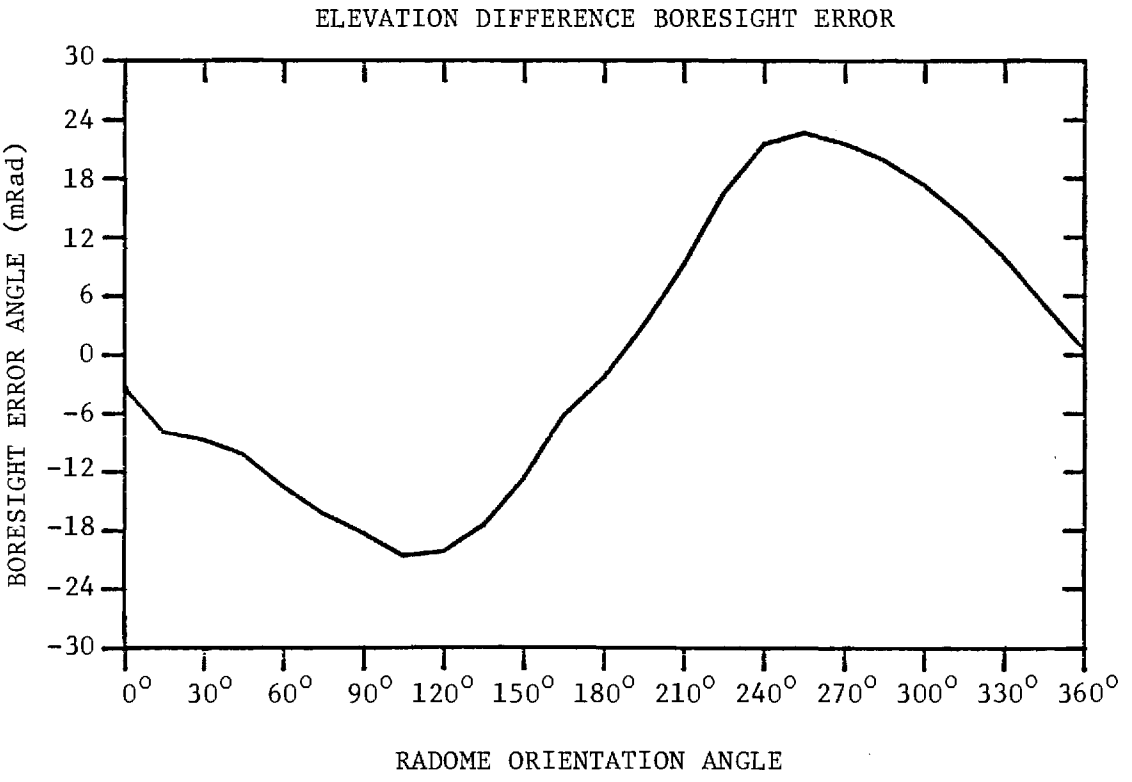

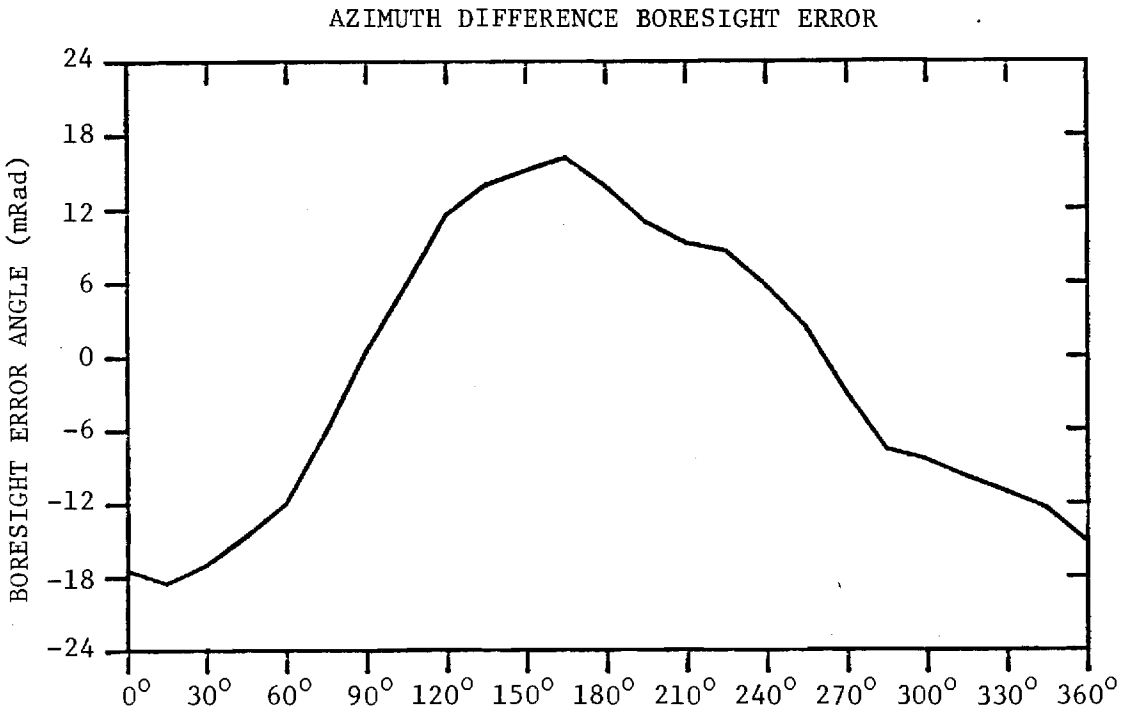

FIGURE I-13. BORESIGHT ERRORS OF MEDIUM ARRAY AND MEDIUM (F=2) RADOME.

APPENDIX J

Antenna Patterns of Medium Array with Large (F=1) Radome

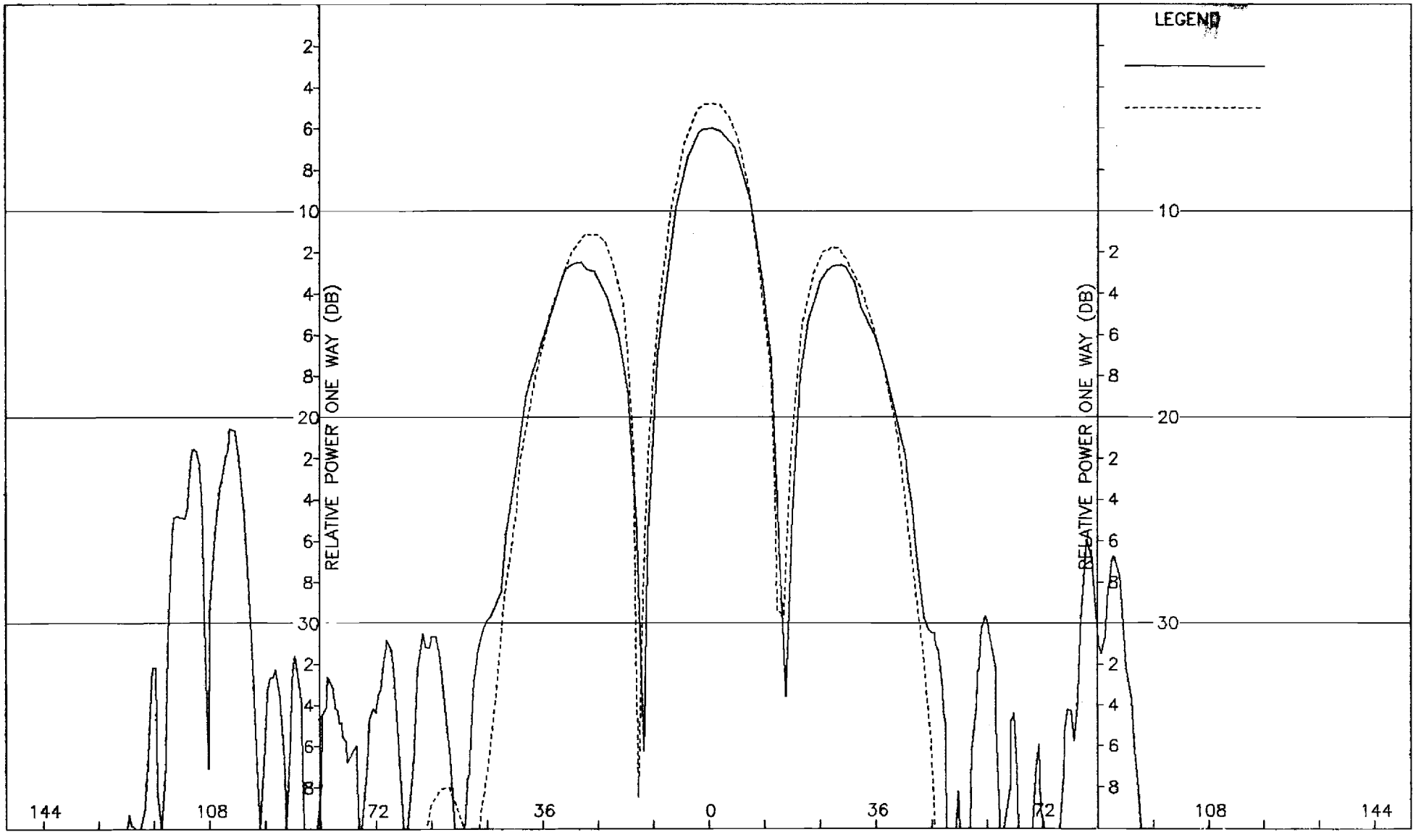

Figure J-1. Pattern of Medium Array: H-Plane, Sum, ϕ-Component, Large (F=1) Radome

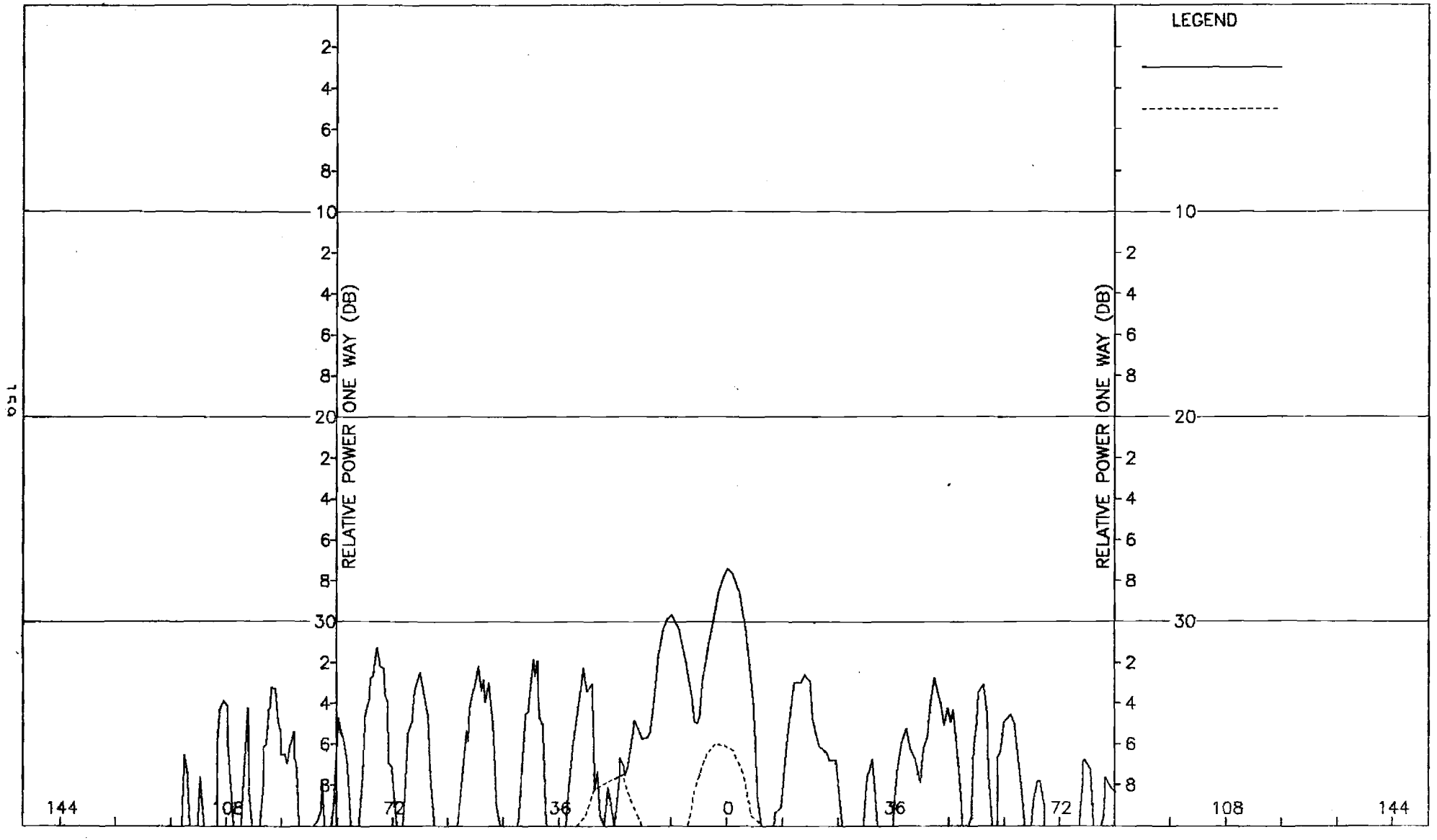

Figure J-2. Pattern of Medium Array: H-Plane, Sum, θ-Component, Large (F=1) Radome

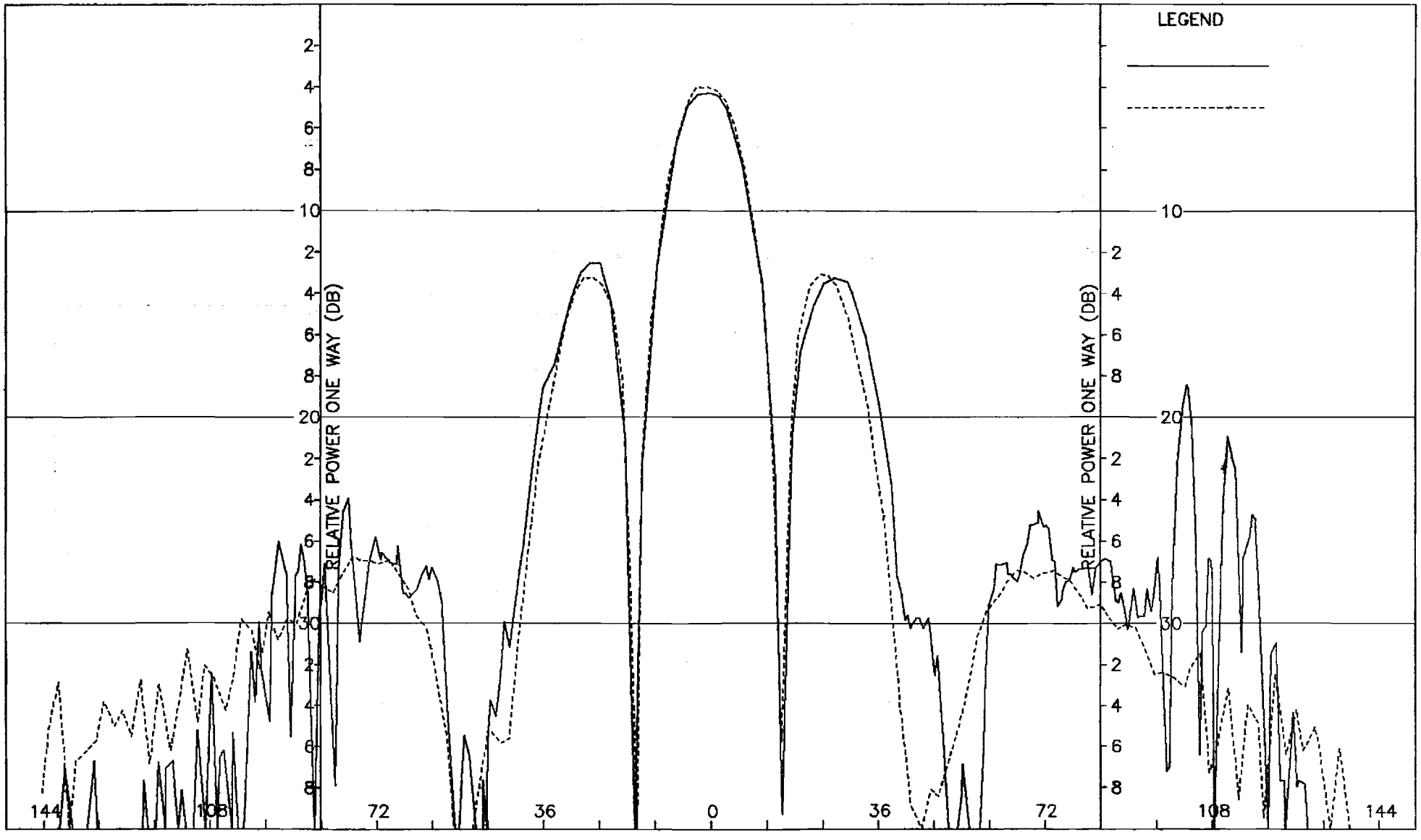

Figure J-3. Pattern of Medium Array: E-Plane, Sum, θ-Component, Large (F=1) Radome

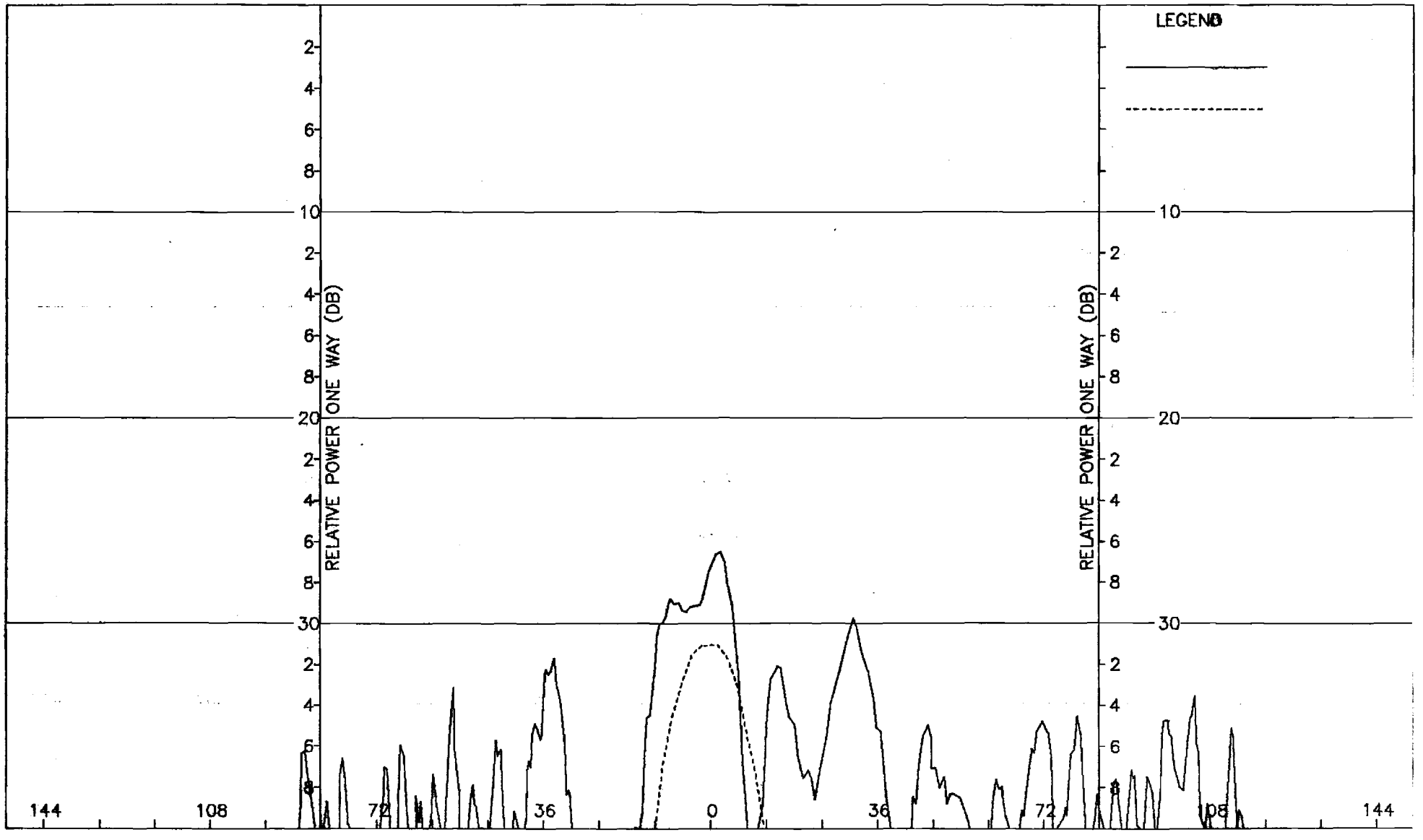

Figure J-4. Pattern of Medium Array: E-Plane, Sum, ϕ-Component, Large (F=1) Radome

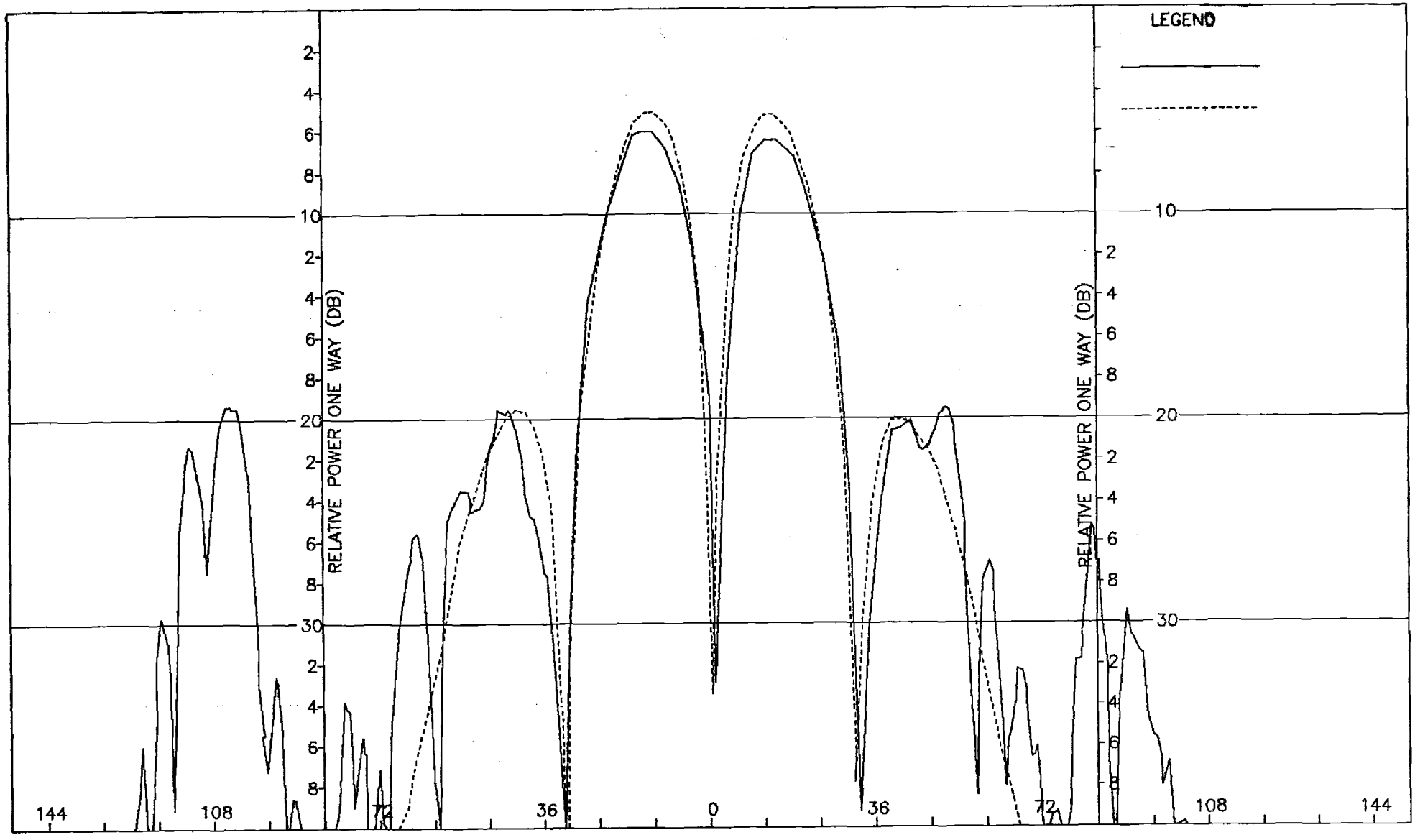

Figure J-5. Pattern of Medium Array: H-Plane, Azimuth Diff., ϕ-Component, Large (F=1) Radome

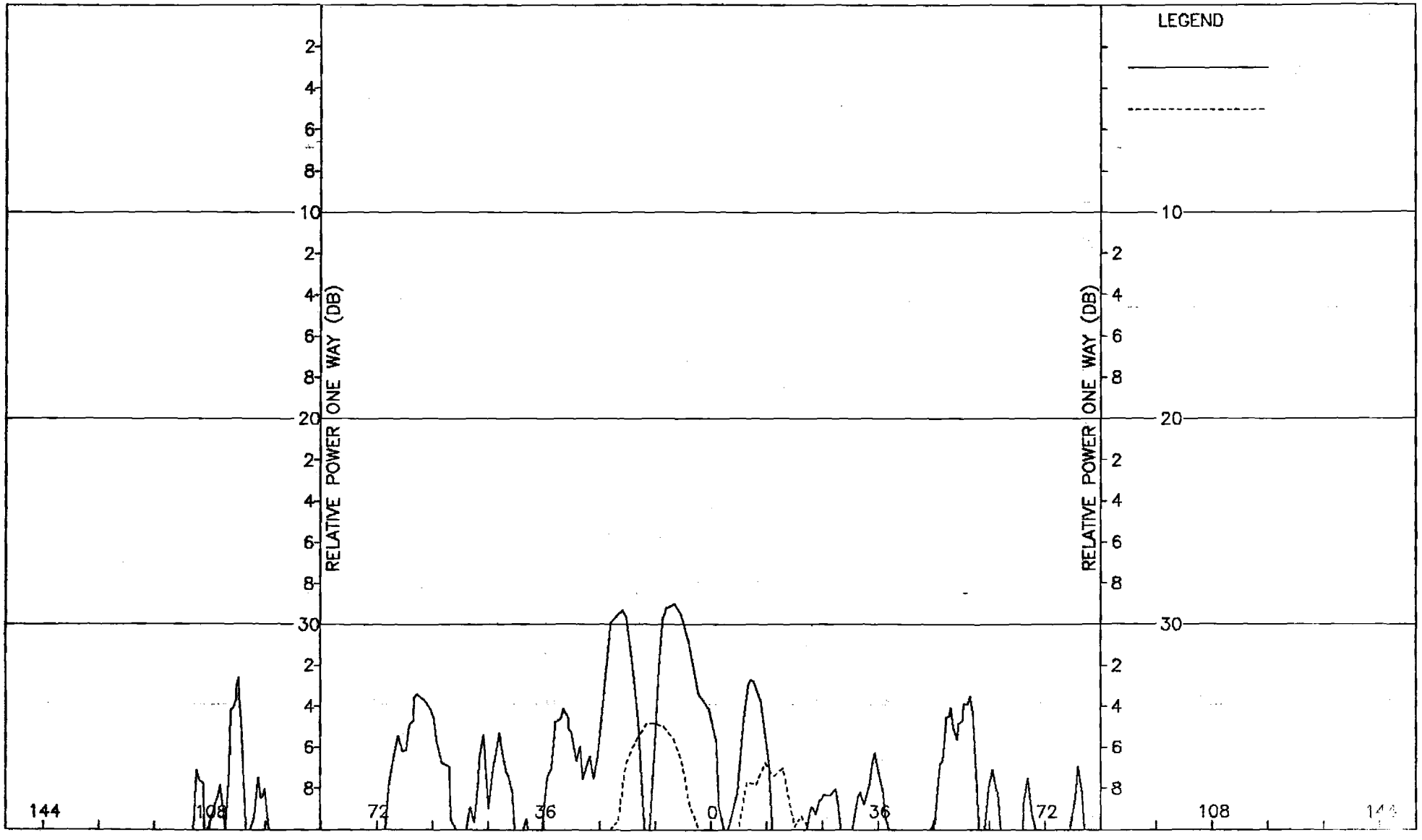

Figure J-6. Pattern of Medum Array: H-Plane, Azimuth Diff., θ -Component, Large (F=1) Radome

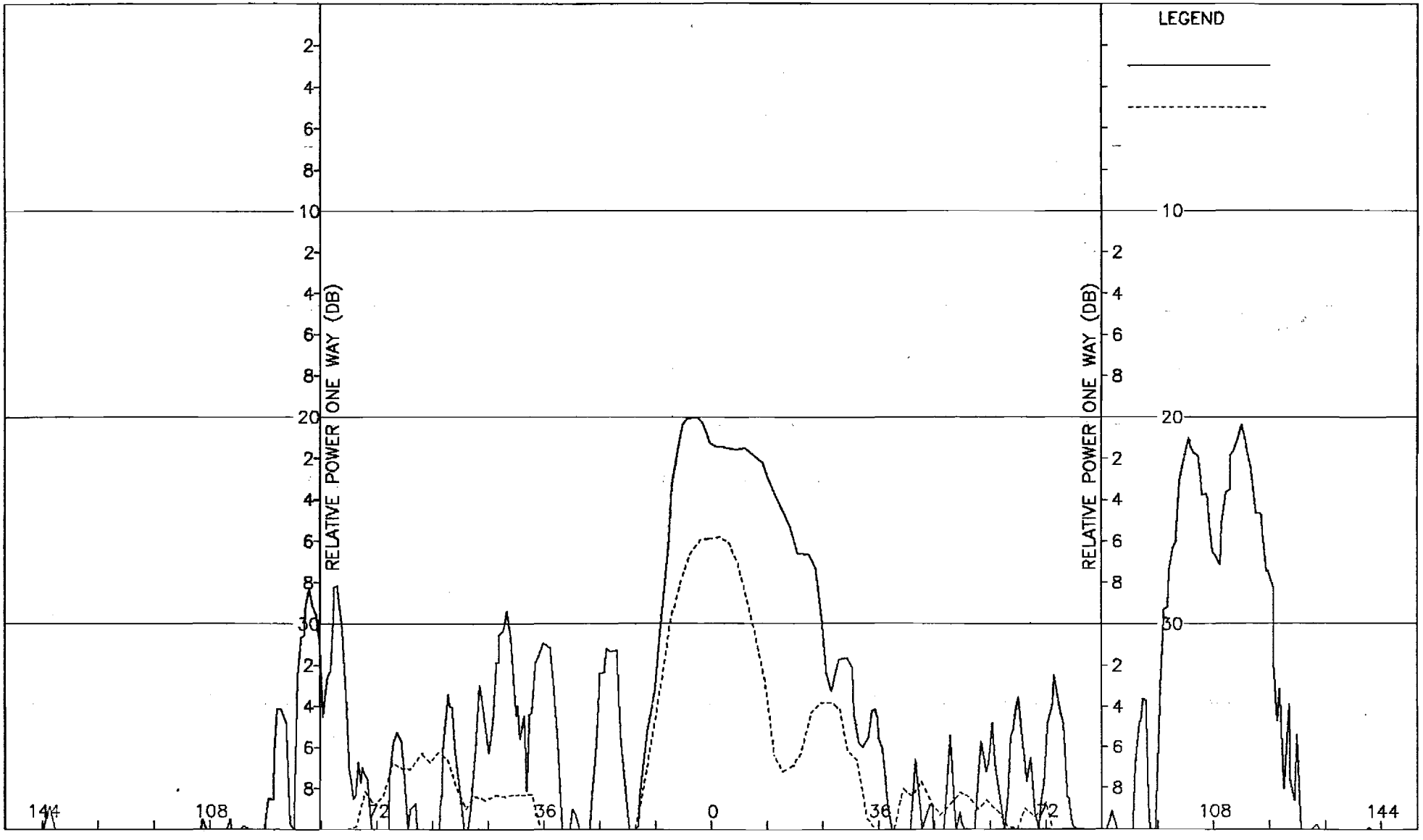

Figure J-7. Pattern of Medium Array: E-Plane, Azimuth Diff., θ -Component, Large (F=1) Radome

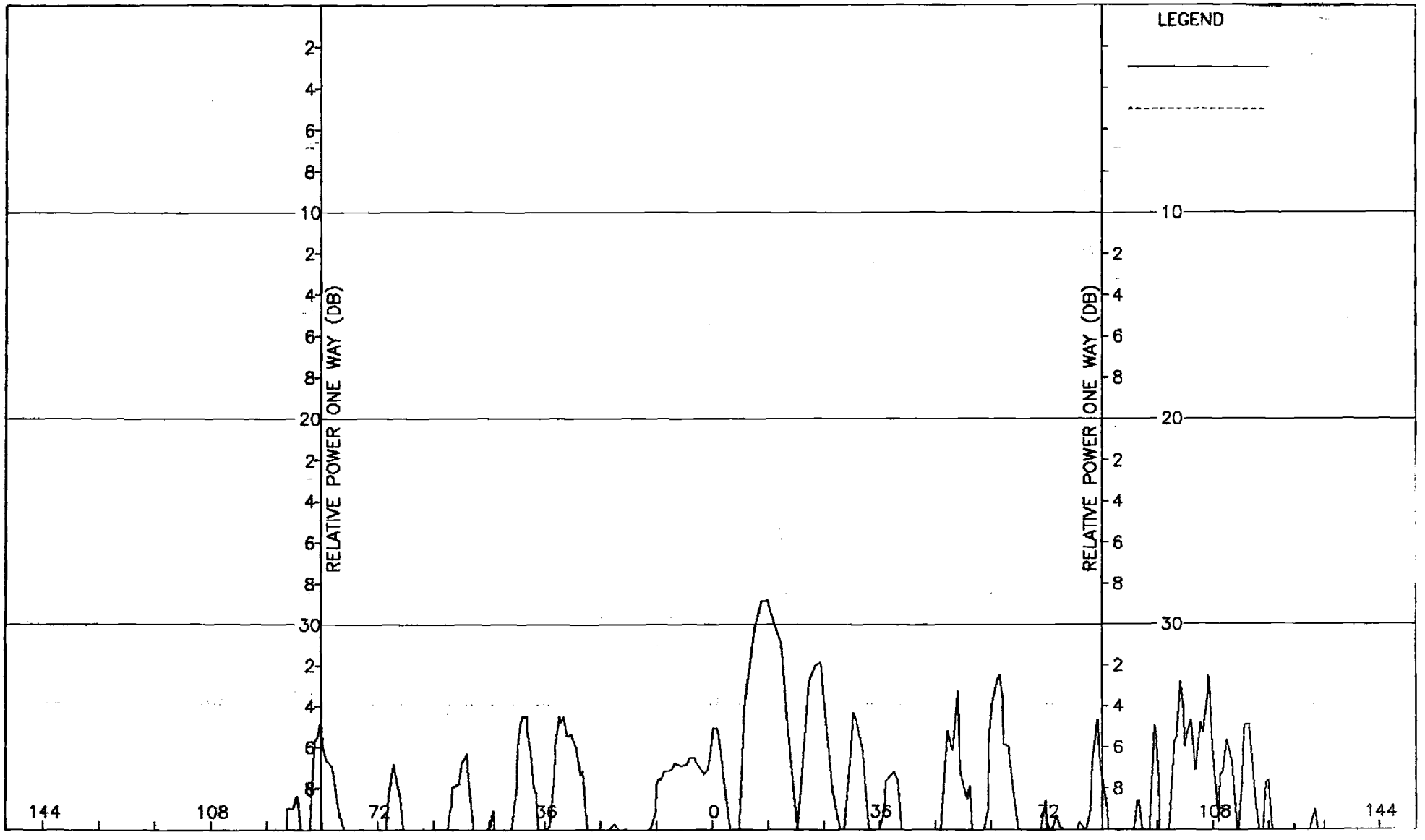

Figure J-8. Pattern of Medium Array: E-Plane, Azimuth Diff., ϕ-Component, Large (F=1) Radome

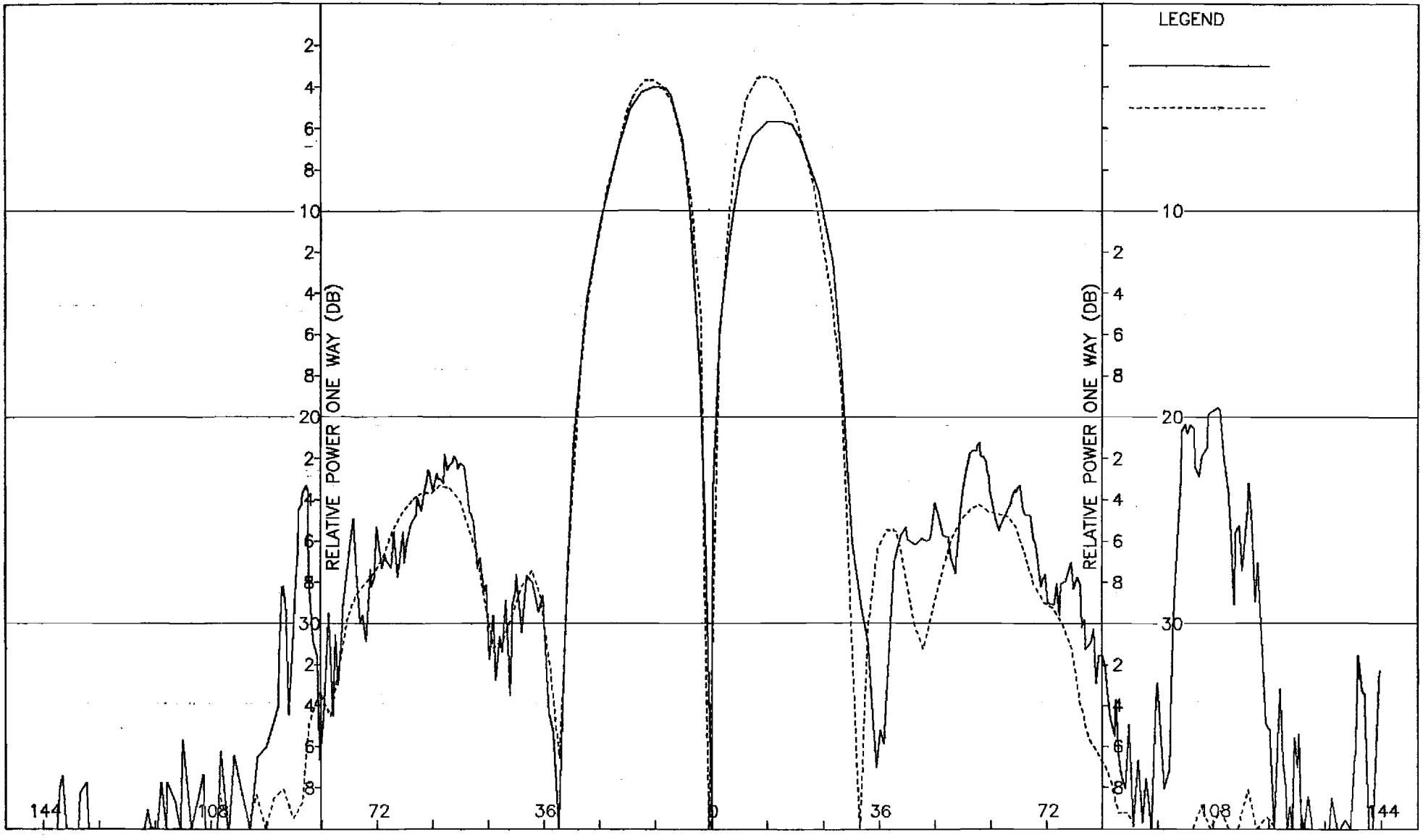

Figure J-9. Pattern of Medium Array: E-Plane, θ-Component, Large (F=1) Radome

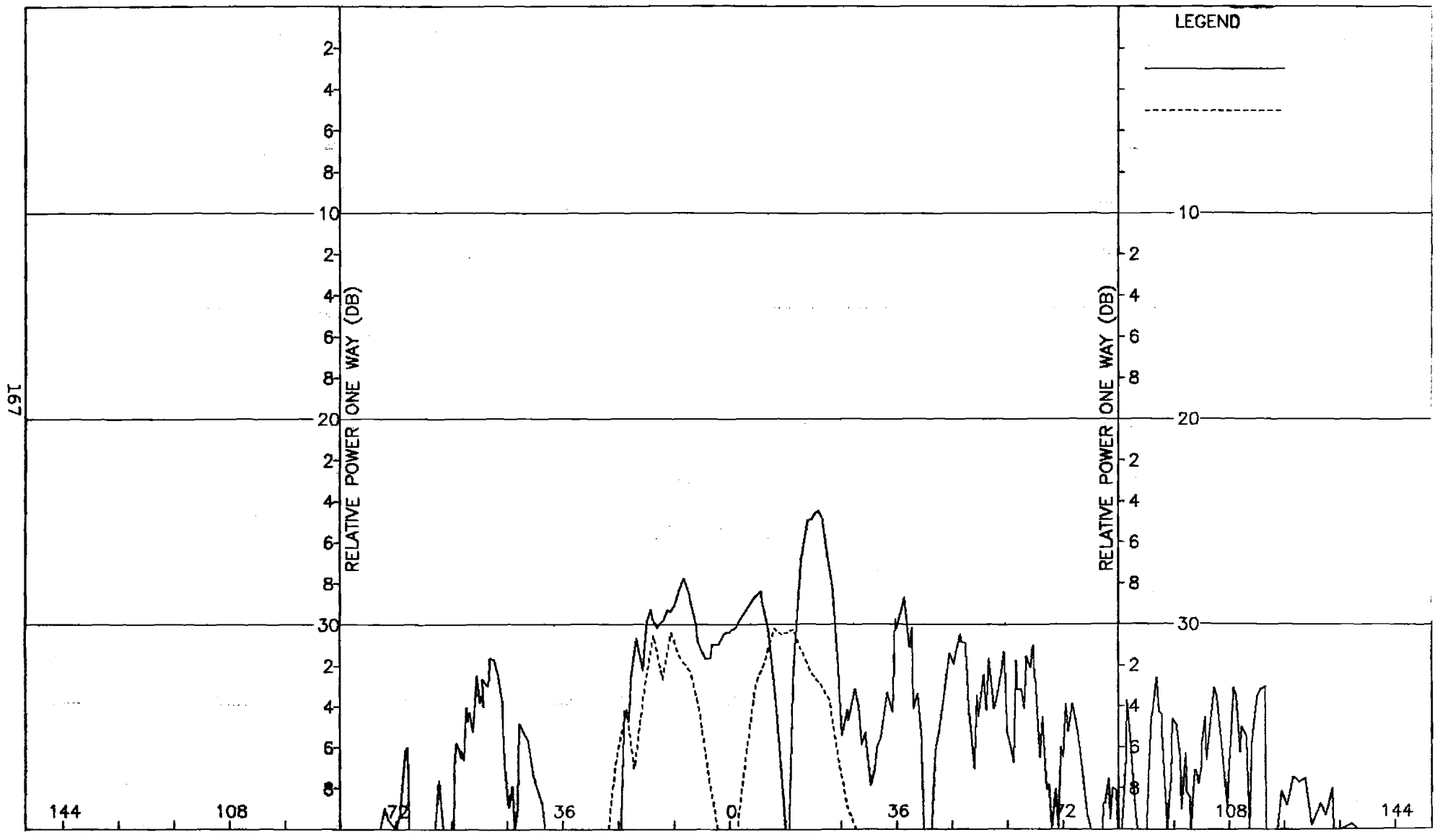

Figure J-10. Pattern of Medium Array: E-Plane, Elevation Diff., ϕ-Component, Large (F=1) Radome

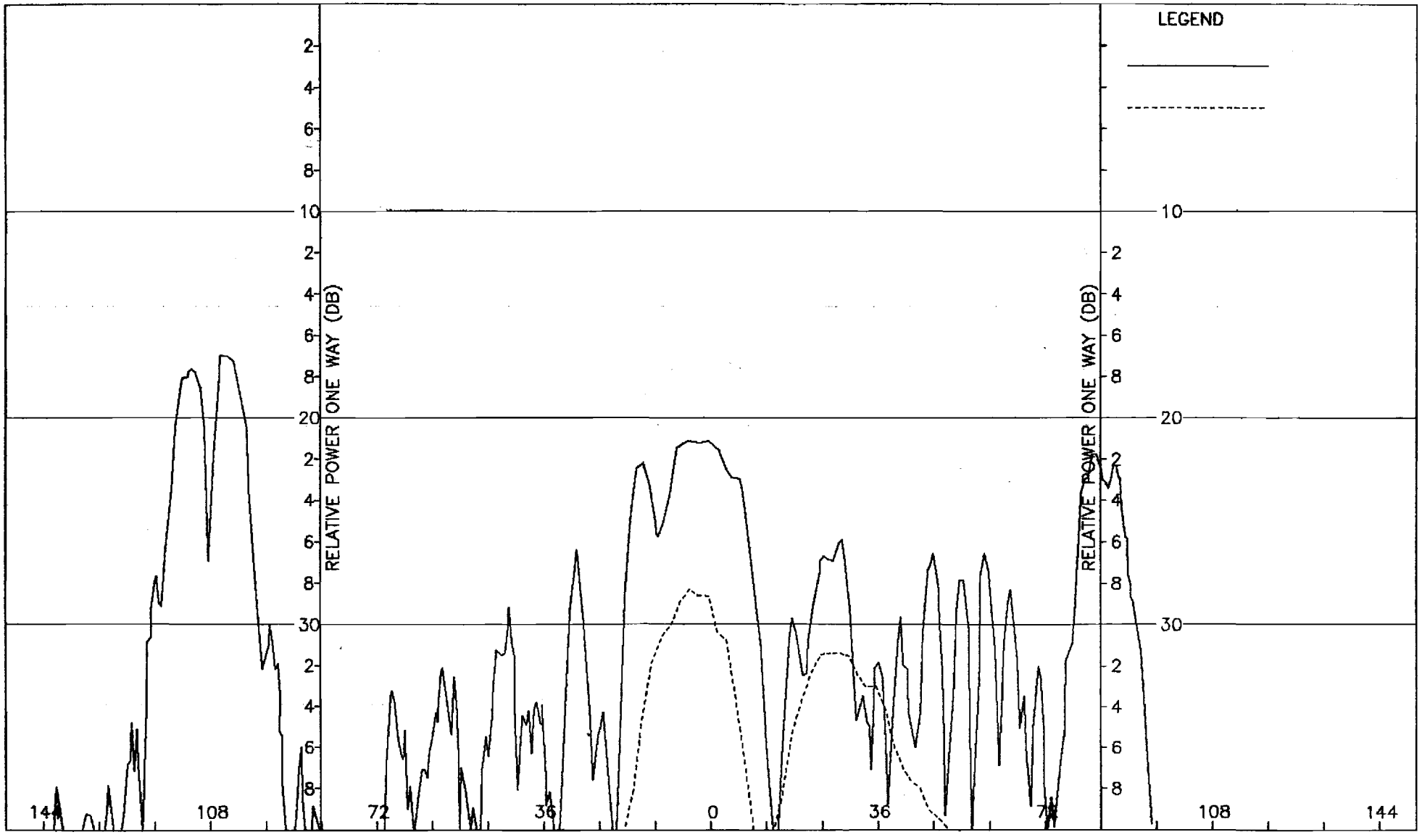

Figure J-11. Pattern of Medium Array: -Plane, Elevation Diff., ϕ-Component, Large (F=1) Radome

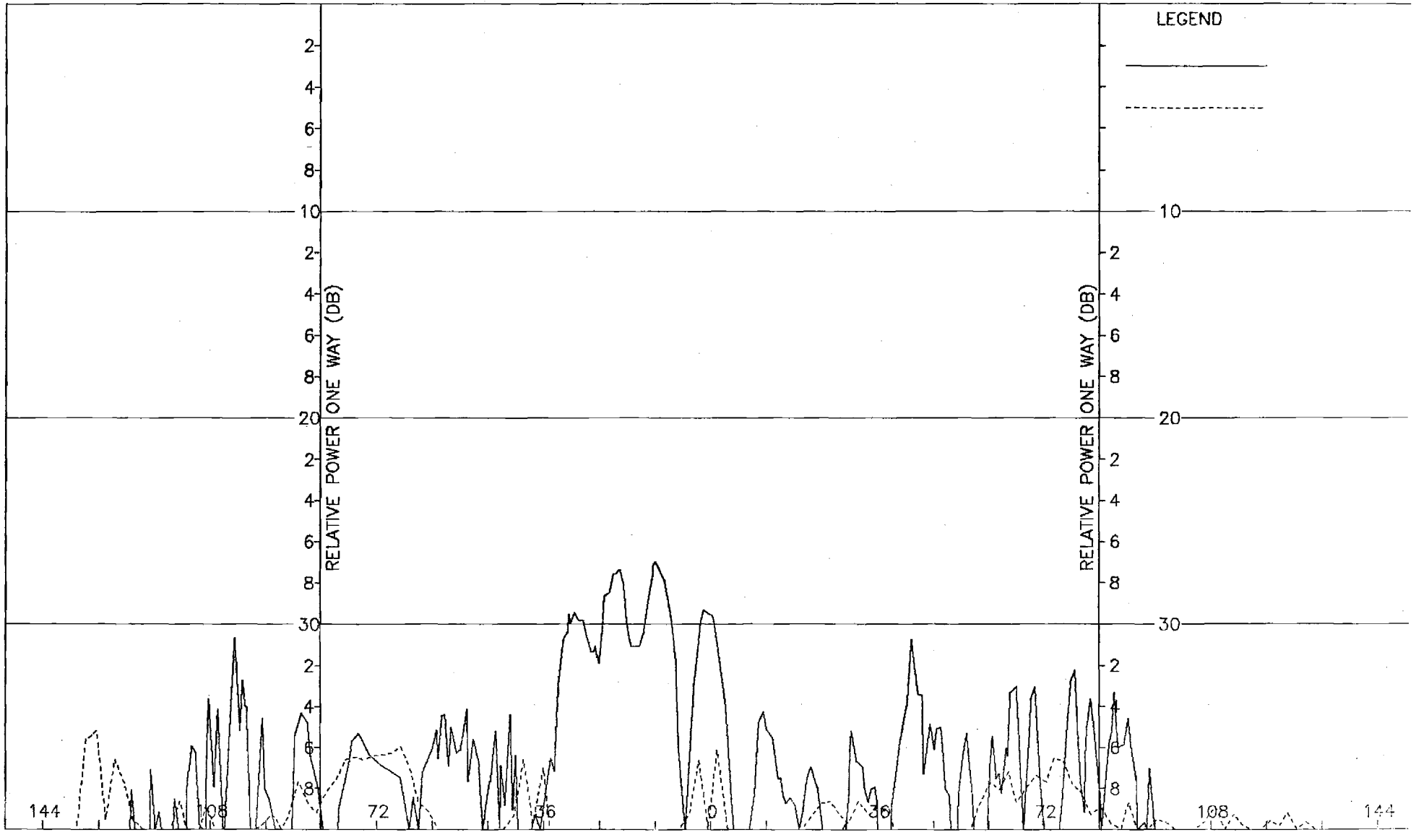

Figure J-12. Pattern of Medium Array: H-Plane, Elevation Diff., θ-Component, Large (F=1) Radome

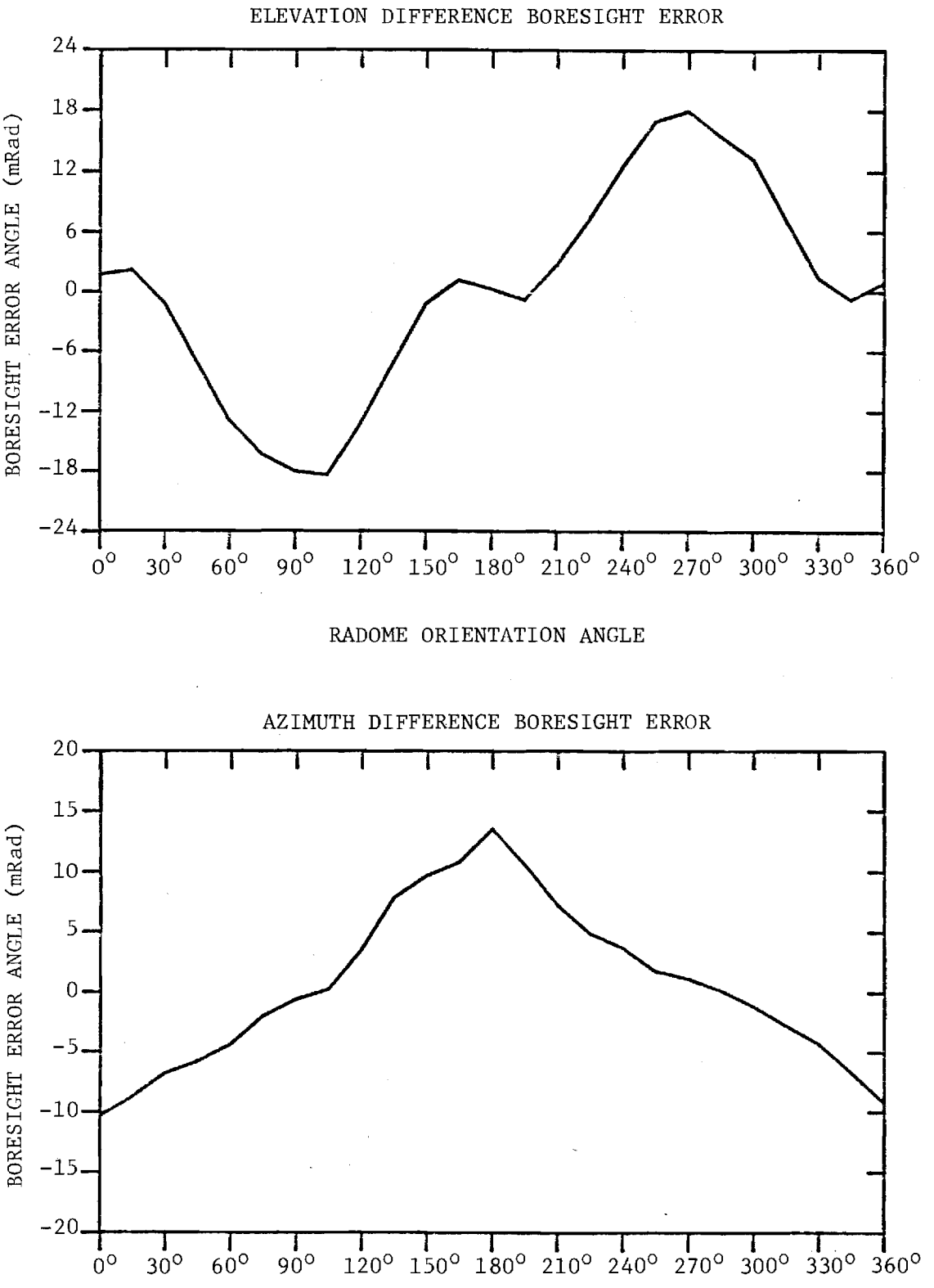

FIGURE J-13. BORESIGHT ERRORS OF MEDIUM ARRAY AND LARGE (F=1) RADOME.

APPENDIX K

Antenna Patterns of Large Array with Large (F=1) Radome

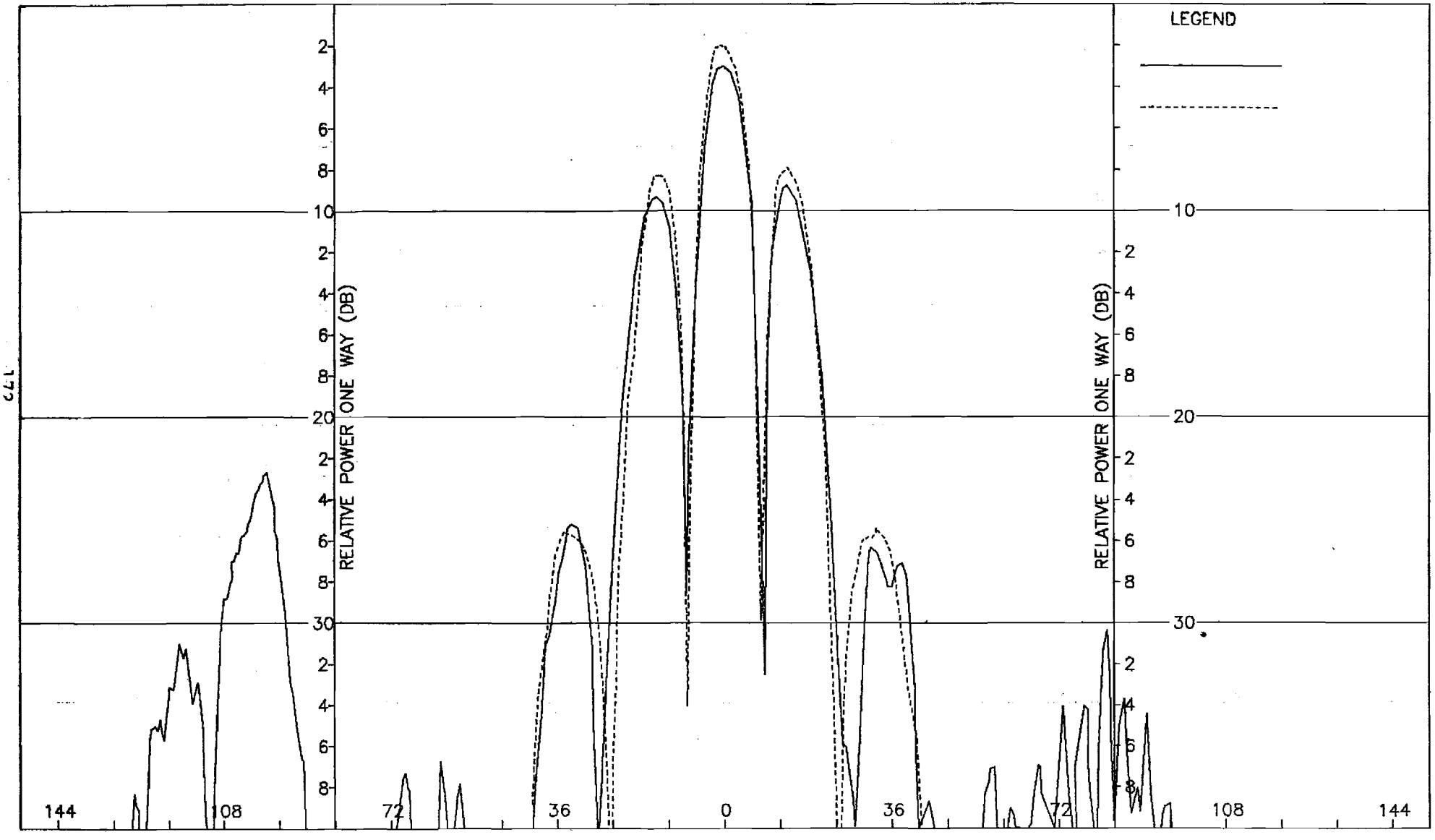

Figure K-1. Pattern of Large Array: H-Plane, Sum, ϕ-Component, Large Radome

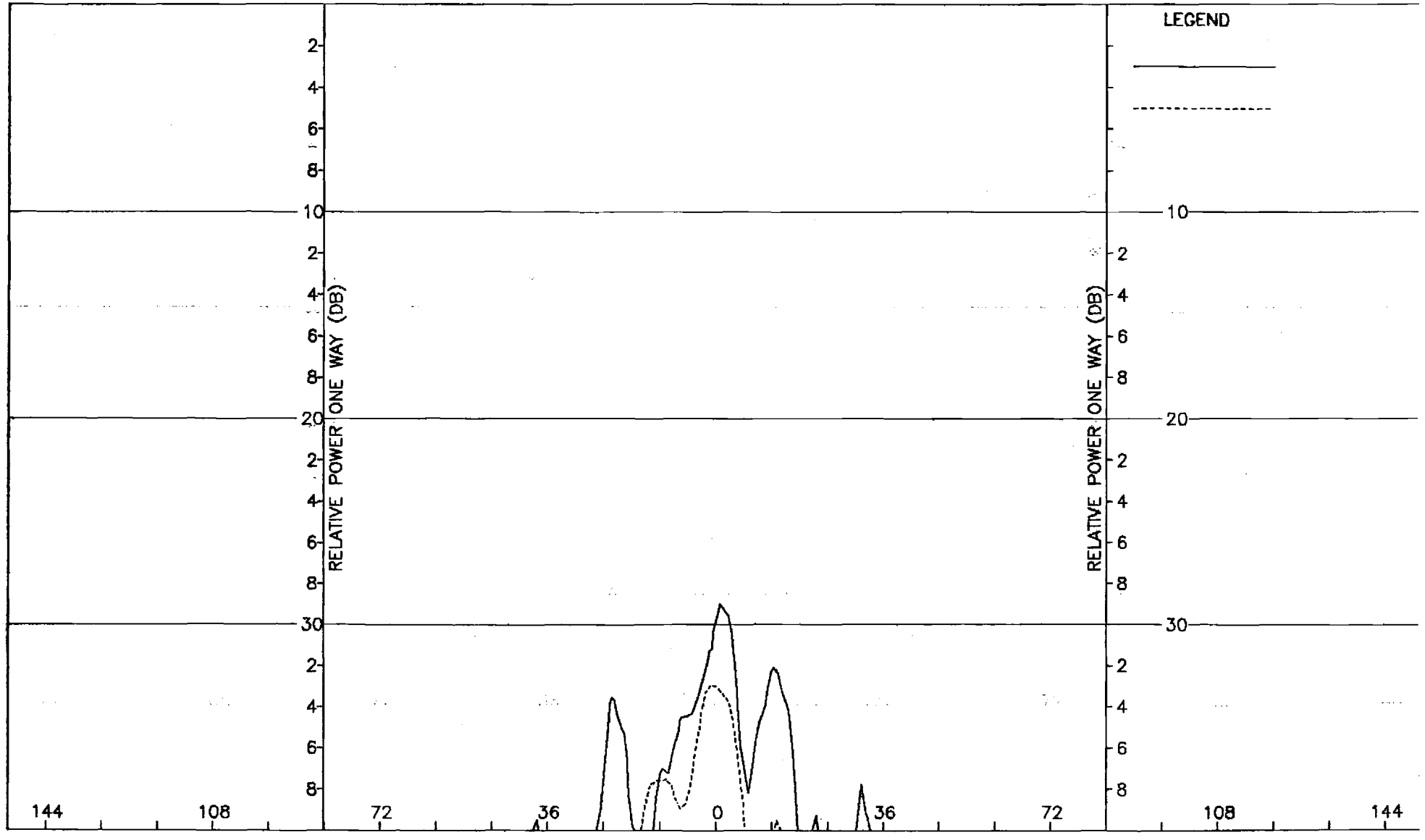

Figure K-2. Pattern of Large Array: H-Plane, Sum, θ-Component, Large Radome

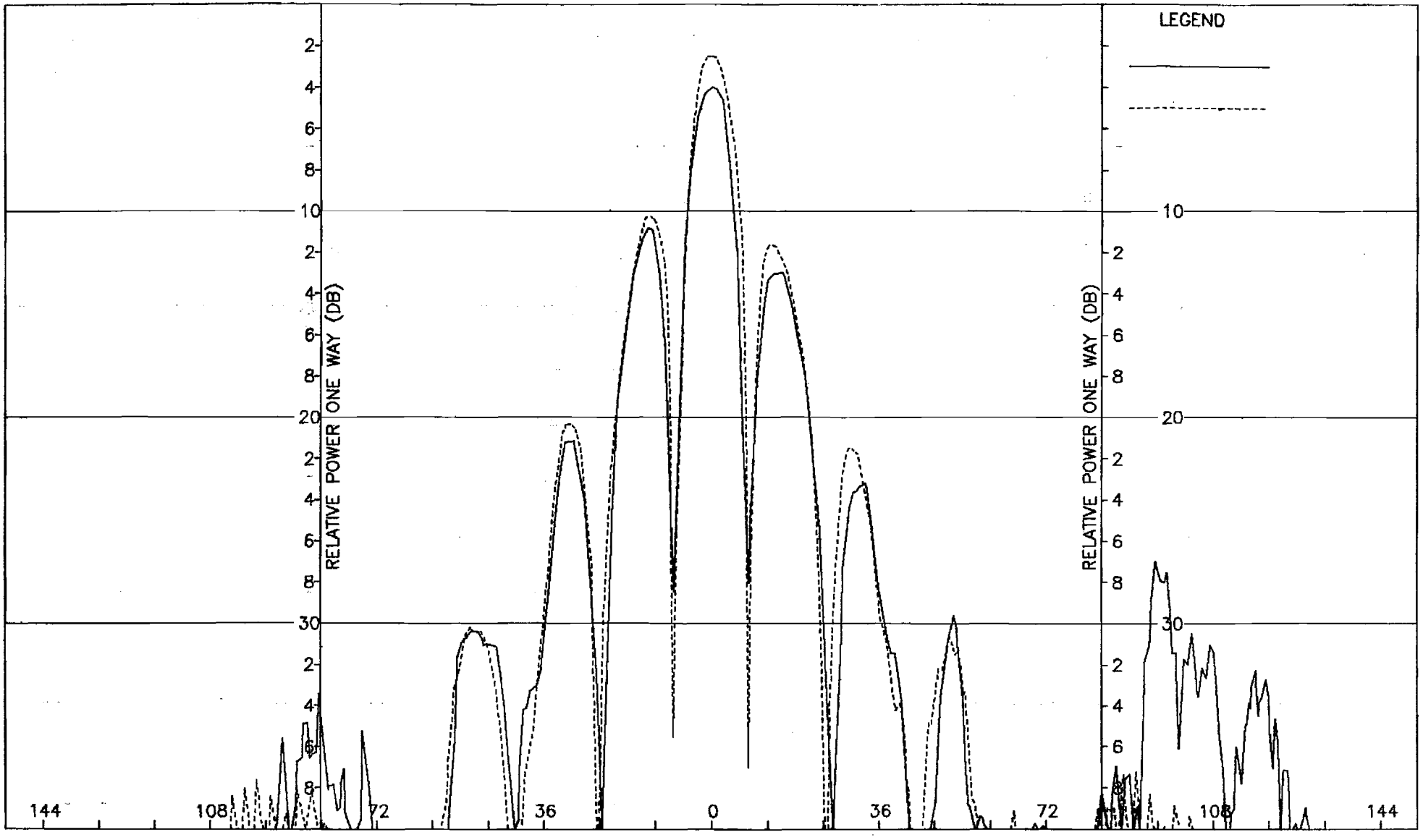

Figure K-3. Pattern of Large Array: E-Plane, Sum, θ-Component, Large Radome

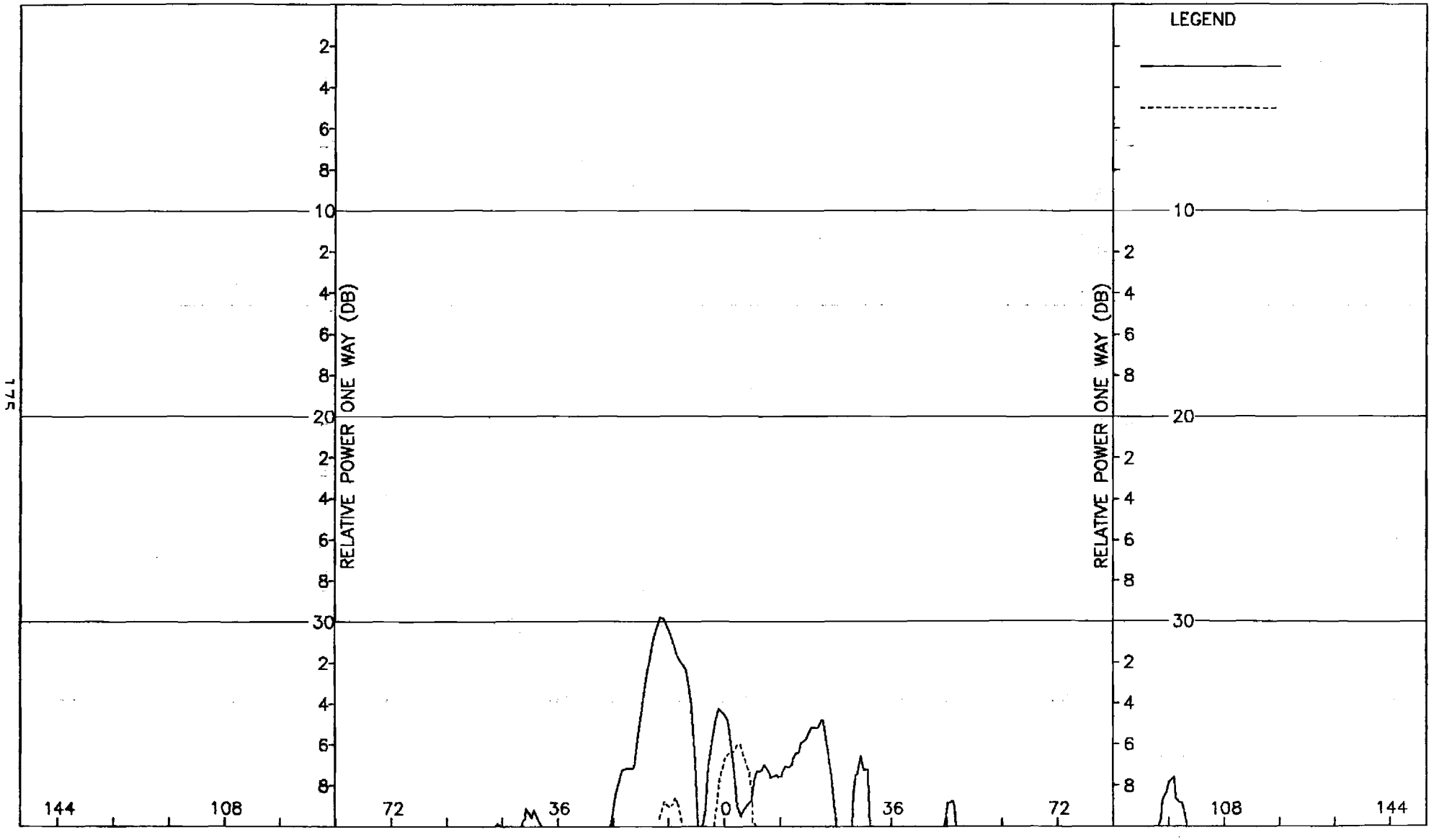

Figure K-4. Pattern of Large Array: E-Plane, Sum, ϕ-Component, Large Radome

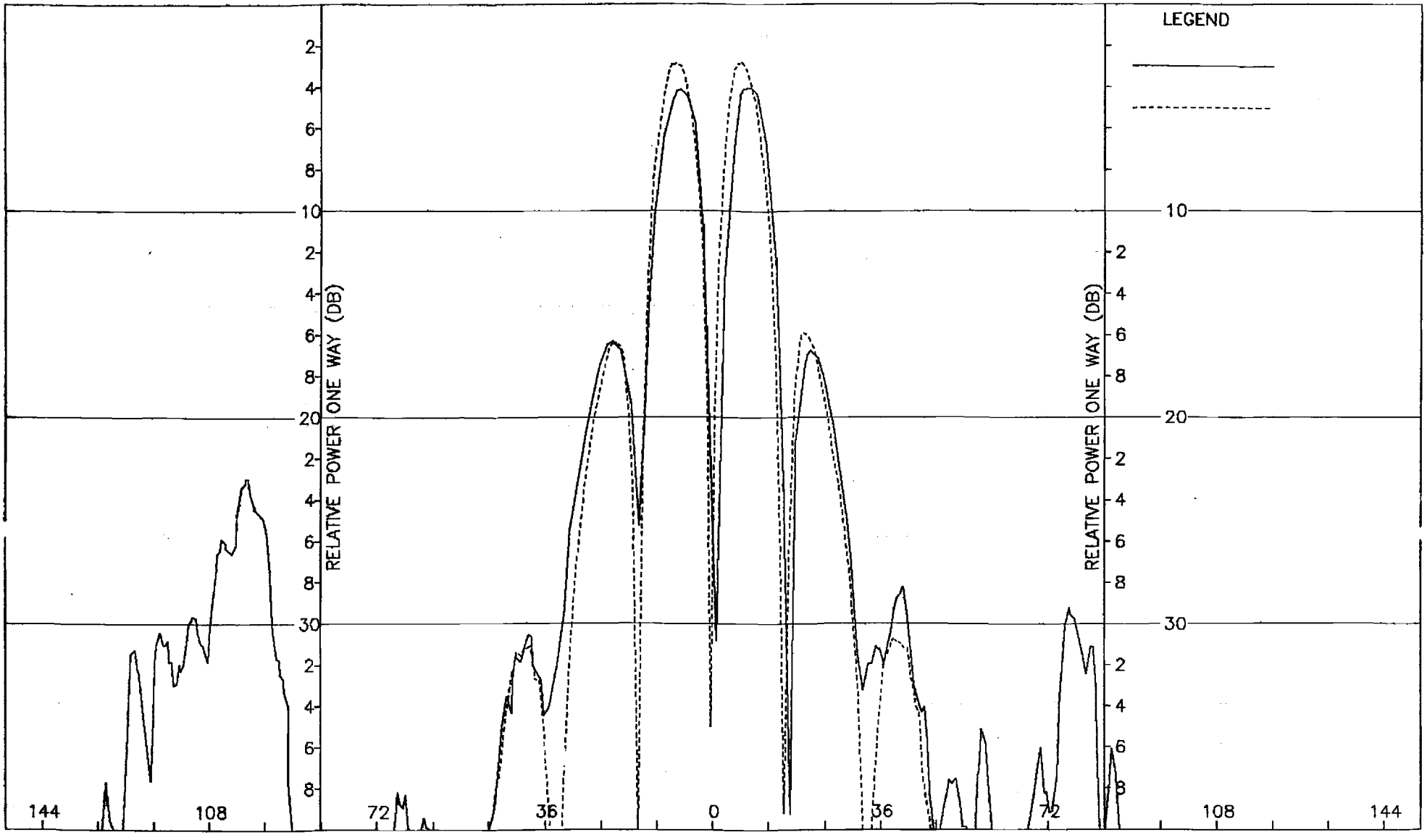

Figure K-5. Pattern of Large Array: H-Plane, Azimuth Diff., ϕ-Component, Large Radome

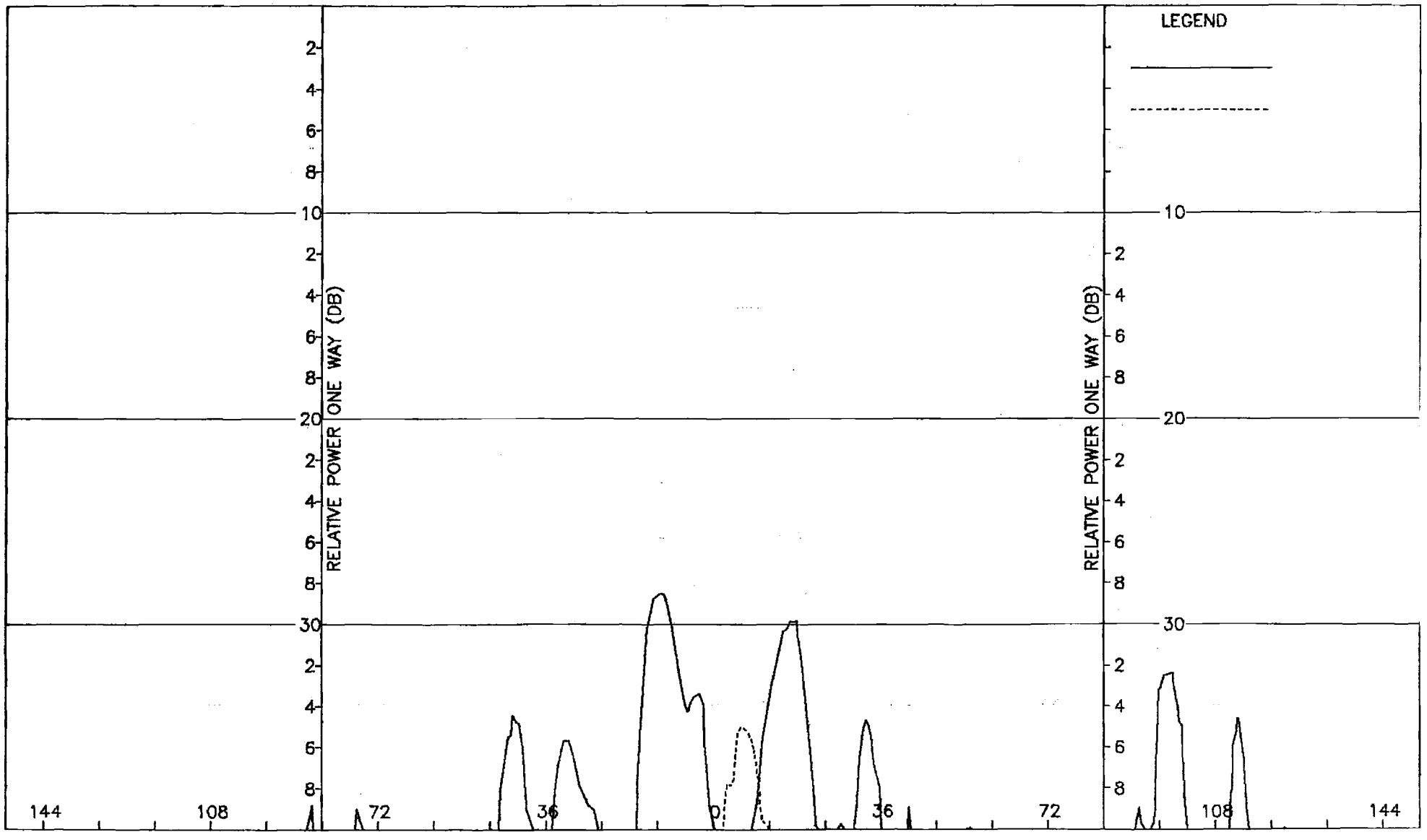

Figure K-6. Pattern of Large Array: H-Plane, Azimuth Diff., θ-Component, Large Radome

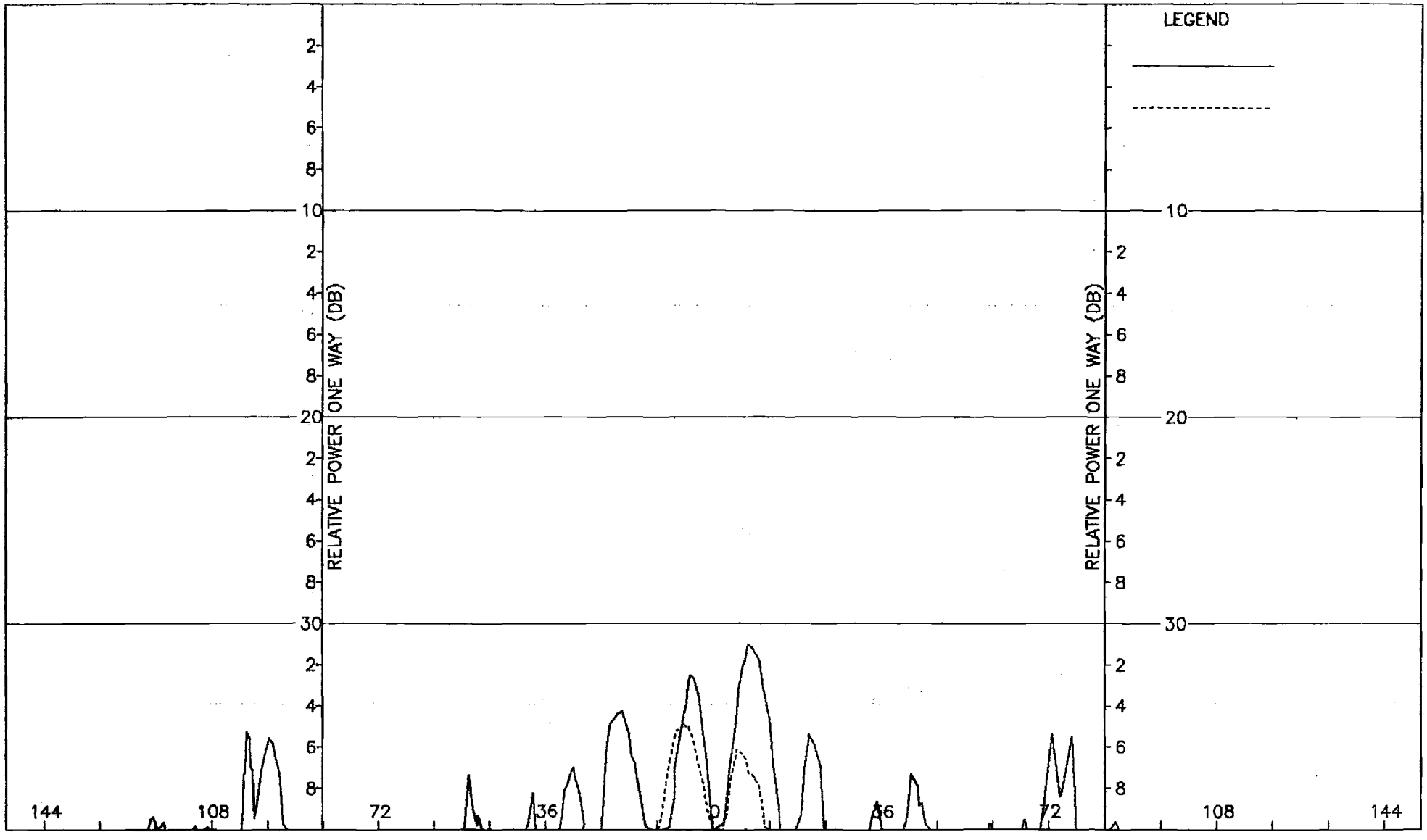

Figure K-7. Pattern of Large Array: E-Plane, Azimuth Diff., θ-Component, Large Radome

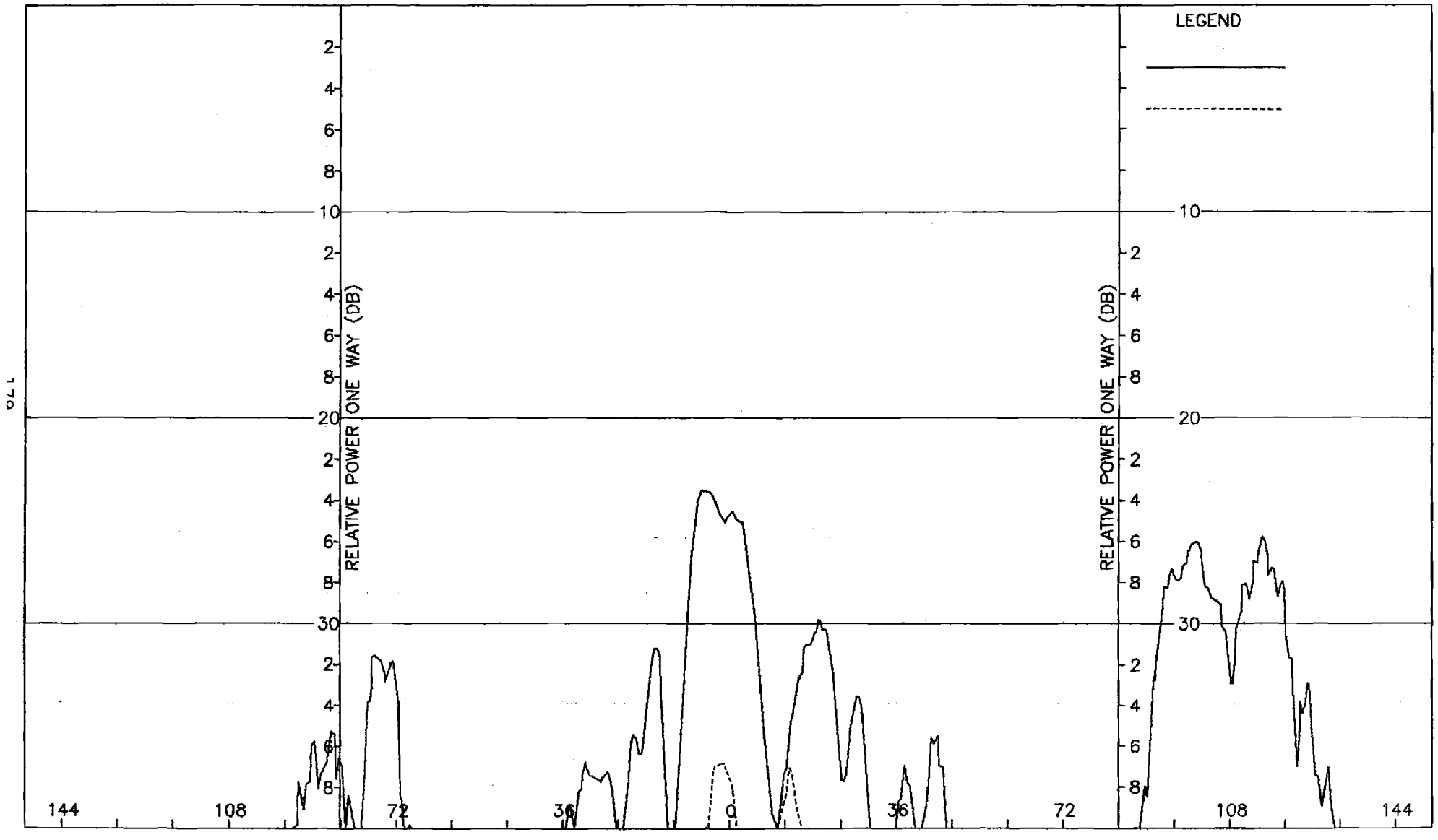

Figure K-8. Pattern of Large Array: E-Plane, Azimuth Diff., ϕ-Component, Large Radome

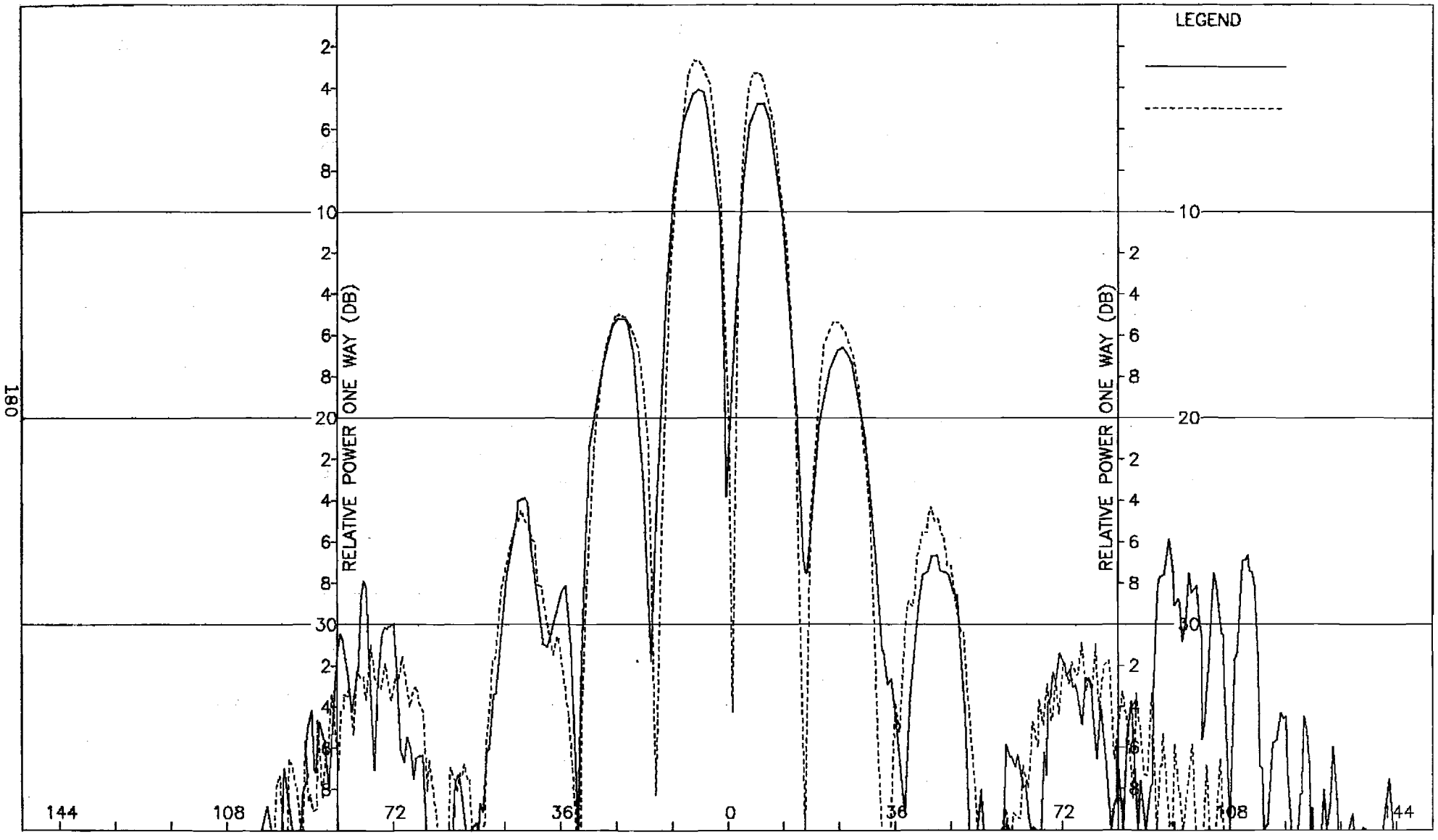

Figure K-9. Pattern of Large Array: E-Plane, Elevation Diff., θ-Component, Large Radome

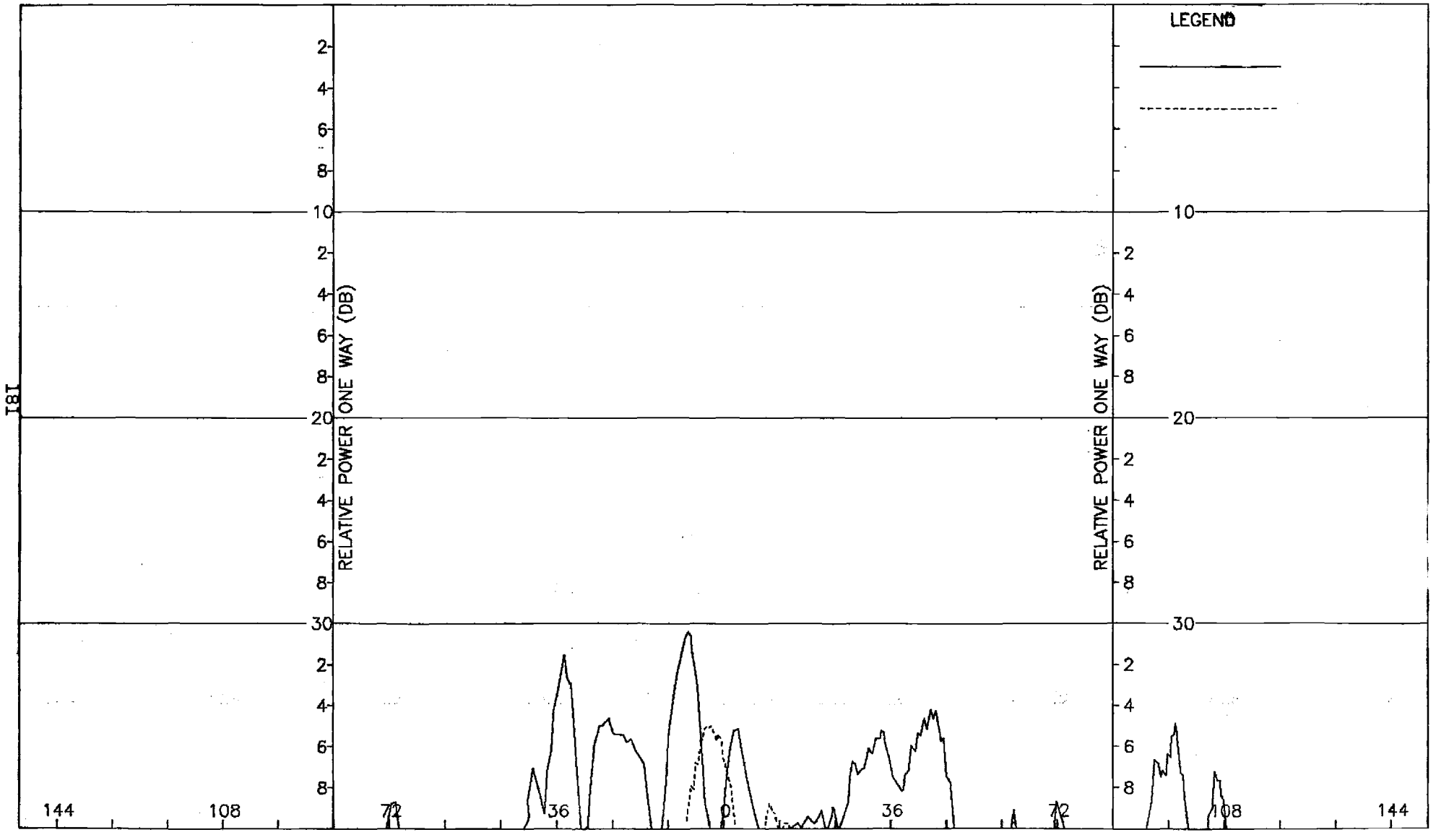

Figure K-10. Pattern of Large Array: E-Plane, Elevation Diff., ϕ-Component, Large Radome

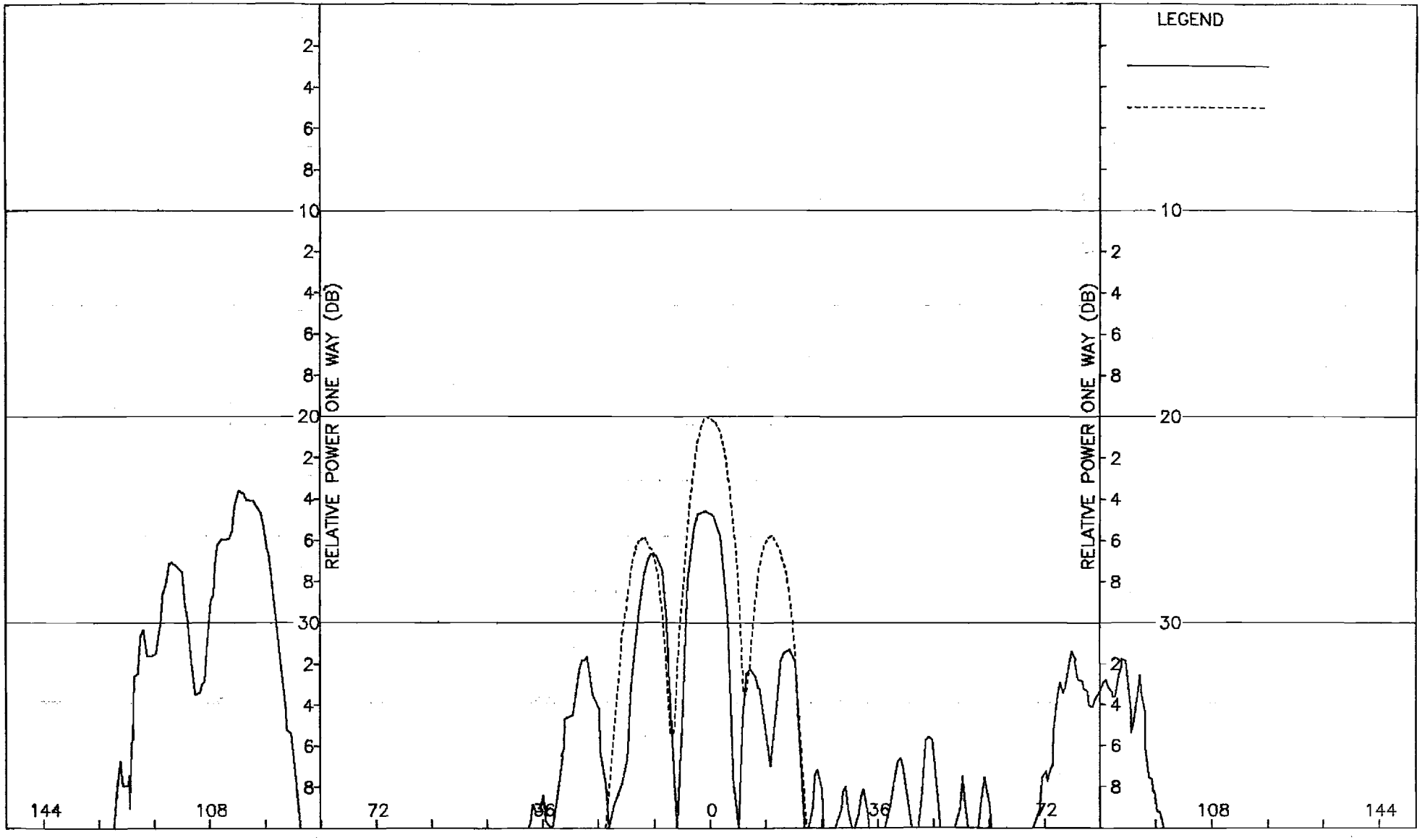

Figure K-11. Pattern of Large Array: H-Plane, Elevation Diff., ϕ-Component, Large Radome

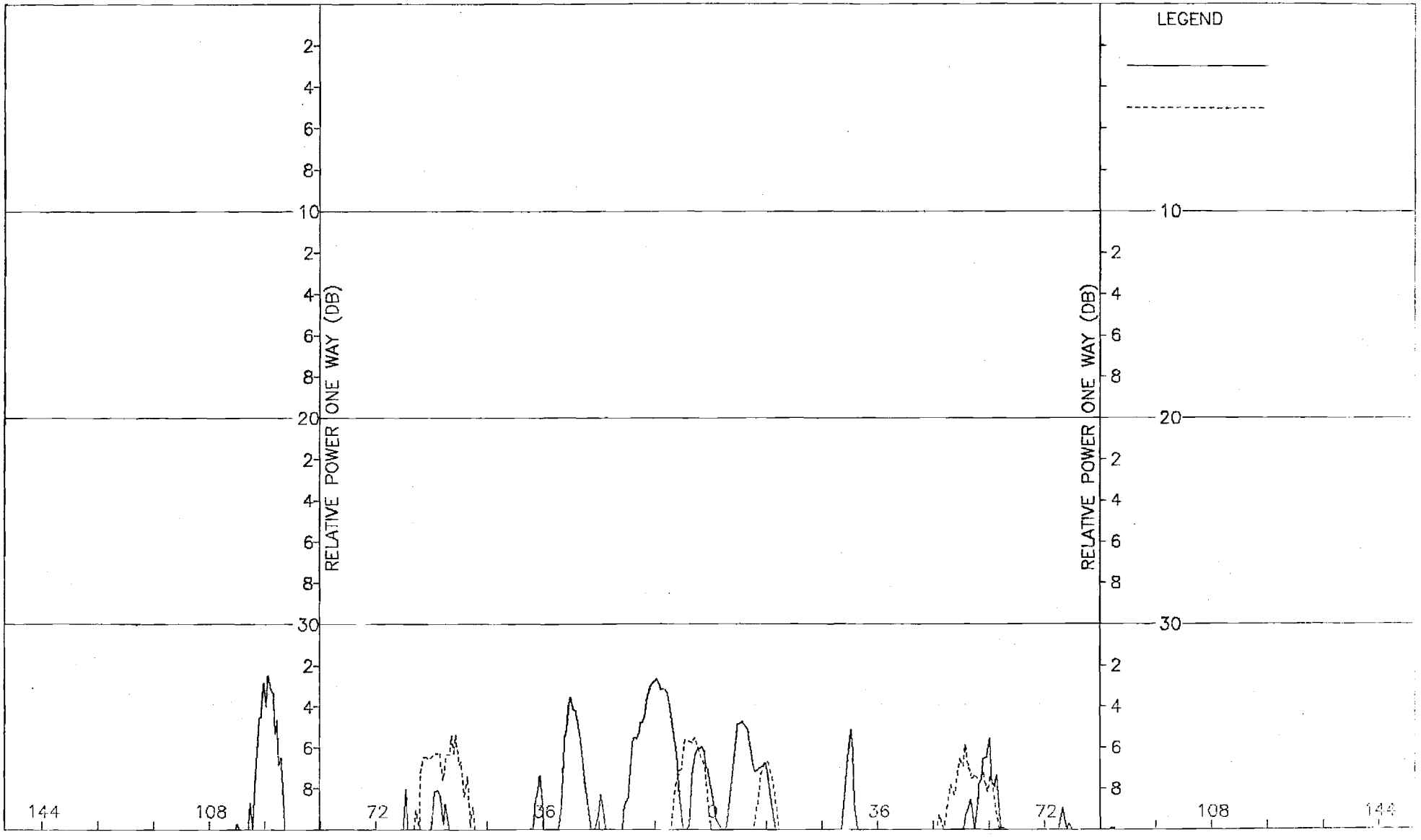

Figure K-12. Pattern of Large Array: H-Plane, Elevation Diff., θ-Component, Large Radome

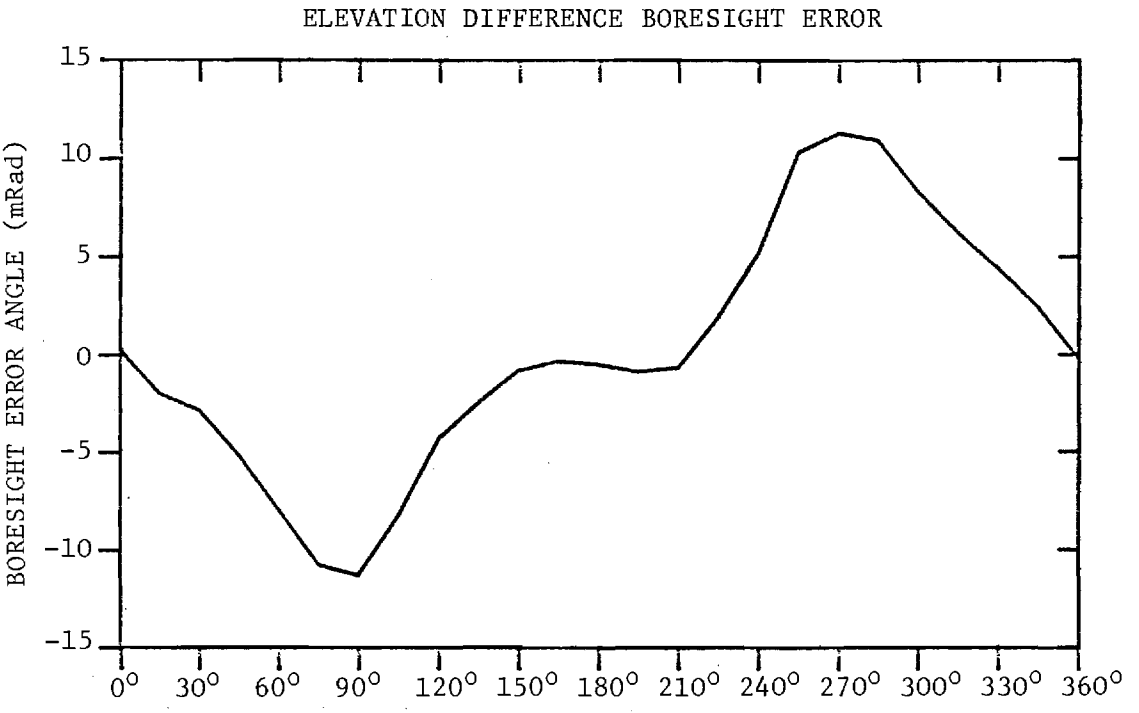

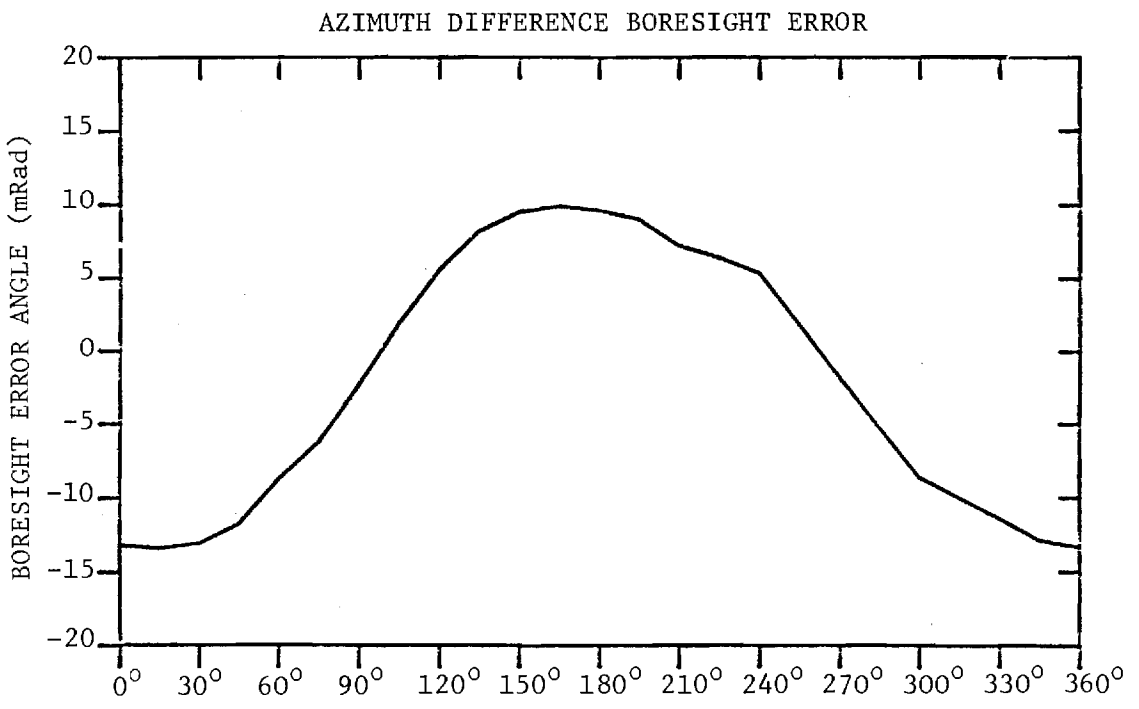

FIGURE K-13. BORESIGHT ERRORS OF LARGE ARRAY AND LARGE (F=1) RADOME.